ABSTRACT

The Design, Synthesis, and Biological Evaluation of Indole-based Anticancer Agents

Matthew T. MacDonough, Ph.D.

Mentor: Kevin G. Pinney, Ph.D.

Solid tumors depend on a vascular network that delivers nutrients and oxygen, thus selectively targeting the developed tumor vasculature represents a feasible strategy for the treatment of cancer. Both small-molecules and biologics that function in this manner are referred to as vascular disrupting agents (VDAs). Two benchmark VDAs, combretastatin A-1 (**CA1**) and combretastatin A-4 (**CA4**), that are both natural products inhibit the dynamic tubulin-microtuble protein system responsible, in part, for the cellular shape of endothelial cells lining tumor blood vessels. This inhibition ultimately results in morphological changes of endothelial cells, from flat to round, and leads to vessel collapse precluding blood flow to the tumor. The success of **CA1P** and **CA4P** (corresponding phosphate salts of **CA1** and **CA4**) as VDAs has inspired the development of inhibitors of tubulin that bear structural similarities and incorporate the indole molecular template.

2-(3′-Hydroxy-4′-methoxyphenyl)-3-(3′′, 4′′, 5′′-trimethoxybenzoyl)-6-methoxyindole (**OXi8006**), prepared as its water-soluble phosphate prodrug salt (**OXi8007**), is a lead VDA discovered by the Pinney Research Group. Scale-up

syntheses were necessary to facilitate planned biological studies. To investigate structure activity relationship considerations, analogues of **OXi8006** were prepared which incorporate functional group modifications of the 3-aroyl ring, the 2-aryl ring, and the indole fused-ring. These derivatives were evaluated for their ability to inhibit tubulin assembly and for their cytotoxicity against three human cancer cell lines (NCI-H460, SK-OV-3, and DU-145) through collaborative studies with the Trawick Research Group. Bioreductively activatable prodrug conjugates (BAPCs) of **OXi8006** that incorporate nitro-thiophenyl bioreductive triggers were synthesized to target tumor hypoxia. The mechanistic pathway for 2-aryl indole formation via the Bischler-Mohlau indole reaction was explored through isotopic labeling of key intermediates. This strategy was also applied to benzo[*b*]furan and benzo[*b*]thiophene analogues. Results suggest formation of an imine intermediate for 2-aryl indoles as evidenced by key ^{13}C NMR signatures. Similar studies suggest the formation of 3-aryl benzo[*b*]furans and benzo[*b*]thiophenes via a pathway in which no aryl shift (2- to 3-position) was observed when hydroxyl substitution is present on the bromoacetophenone starting material. In summary, **OXi8006** and **OXi8007**, a focused library of analogues including BAPCs, as well as isotopically labeled indoles, benzo[*b*]thiophenes, and benzo[*b*]furans were prepared.

The Design, Synthesis, and Biological Evaluation of Indole-based Anticancer Agents

by

Matthew T. MacDonough, B.S.

A Dissertation

Approved by the Department of Chemistry and Biochemistry

_____

Patrick J. Farmer , Ph.D., Chairperson

Submitted to the Graduate Faculty of
Baylor University in Partial Fulfillment of the
Requirements for the Degree
of

Doctor of Philosophy

Approved by the Dissertation Committee

_____

Kevin G. Pinney, Ph.D., Chairperson

_____

Charles M. Garner, Ph.D.

_____

Robert R. Kane, Ph.D.

_____

Mary Lynn Trawick, Ph.D.

_____

William C. Hockaday, Ph.D.

Accepted by the Graduate School

December 2013

_____

J. Larry Lyon, Ph.D., Dean

Page bearing signatures is kept on file in the Graduate School.

TABLE OF CONTENTS

LIST OF FIGURES

CHAPTER FOUR

LIST OF SCHEMES

LIST OF TABLES

ACKNOWLEDGMENTS

I am deeply indebted to my advisor, Dr. Kevin G. Pinney. I am greatly appreciative of the opportunity to work in his research lab. He provided me with guidance and support to be successful both within the lab as well as in life outside the lab. He was always understanding throughout my career both as an undergraduate student and graduate student.

I am also grateful to my committee. Dr. Kane and Dr. Garner have always offered support and have helped extend my knowledge of organic chemistry. Dr. Trawick has been a wonderful collaborator and teacher. I have enjoyed getting to know Dr. Hockaday over my graduate career and sharing our interest in NMR spectroscopy.

I would also like to thank the Department of Chemistry and Biochemistry at Baylor University. Dr. Farmer, Adonna Cook, Nancy Kallus, Barbara Rauls, and Virginia Hynek were all helpful whenever I needed, many times dropping whatever they were working on to help me.

I am thankful to my colleagues in the Pinney Research Group. They provided continued support and advice that allowed me to reach the point I am at now. From understanding basic chemistry mechanisms to ordering chemicals to setting up complex reactions, I could not have done it without them.

I would not be here today if not for my loving family to which I owe everything. Their financial, emotional, and spiritual support and guidance has allowed me to reach the point I am at in life. I love you all and considered myself fortunate for the unconditional love you continue to provide.

DEDICATION

To George Parkman MacDonough III

and the memory of

Marie Caeser MacDonough
Raymond Ignatius Mulligan
Catherine Cecilia Lukasavage Mulligan

CHAPTER ONE

Introduction

The selective targeting of tumor vasculature for the therapeutic treatment of cancer was first suggested by Judah Folkman in 1971.[1] This notion was founded on the fundamental dependence of a vascular network that provides tumors with the necessary blood, oxygen, and nutrients vital for survival.[2] Tumors with a deficiency in vasculature are restricted to a size of 1-2 mm^3 and the capacity to metastasize is constrained.[2] In contrast, tumors with established vascularity can experience exacerbated growth of the primary tumor and enhanced metastatic spread. Healthy tissues and organs also require a vascular network to deliver blood, as well as provide a means of waste removal. However, the vascular architecture within healthy tissues is highly organized and systematic compared to the disorganized and chaotic nature of tumor vasculature, leading to distinct differences between normal healthy tissue vasculature and the vasculature within the tumor microenvironment.[3] Specifically, growth amplification of neoplastic cell population and overexpression of pro-agiogenic factors lead to underdeveloped vasculature deficient in vessel hierarchy, in which arterioles, capillaries, and venules cannot be clearly defined.[4] The immature nature of tumor vasculature results in blood vessels which have an abnormal shape, bulges, inconsistent

---

[1] Folkman J. Tumor Angiogenesis: Therapeutic Implications. *N. Engl. J. Med.* **1971**, *285*, 1182–1186.

[2] Brem, S.; Brem, H.; Folkman, J.; Finkelstein, D.; Patz, A. Prolonged Tumor Dormancy by Prevention of Neovascularization in the Vitreous. *Cancer Res.* **1976**, *36*, 2807-2812.

[3] Siemann, D. W. The Unique Characteristics of Tumor Vasculature and Preclinical Evidence for its Selective Disruption by Tumor-Vascular Disrupting Agents. *Cancer Treatment Reviews*. **2011**, *37*, 63-74.

[4] Konerding, M. A.; Fait, E.; Gaumann, A. 3D Microvascular Architecture of Pre-cancerous Lesions and Invasive Carcinomas of the Colon. *Br. J. Cancer*. **2001**, *84*, 1354-1362.

diameters, blind ends, and arteriolar-venous shunts.[4-6] In addition, lymphatic vessels responsible for waste removal are intermittent, leaky, and result in dilated, swollen vessels.[7-8] Tumor vasculature is also characterized by a diminished presence of smooth muscle cells and asymmetrical lining of endothelial cells which leads to an irregular basement membrane.[9-10] This, in turn, elevates vessel permeability, ultimately increasing interstitial pressure.[11-12] Tumor vessels are also disproportionally distributed throughout the tumor tissue, consequently leading to regions of low oxygen known as hypoxia, a condition that has shown to promote angiogenesis and increased metastatic potential.[11-16] The distinct morphological as well as physiological characteristics of tumor vasculature present a viable target for therapeutic intervention, and two strategies in which to do so have ensued. The first aims to impede new vessel formation and is known as the antiangiogenesis approach, and the second

---

[5] Dewhirst, M. W.; Kimura, H.; Rehmus, S. W.; Braun, R. D.; Papahadjopoulos, D.; Hong, K.; Secomb, T. W. Microvascular Studies on the Origins of Perfusion-limited Hypoxia. *Br. J. Cancer*. **1996**, *27*, S247-S251.

[6] McDonald, D.; Choyke, P. Imaging of Agiogenesis: From Microscope to Clinic. *Nature Med*. **2003**, *9*, 713-725.

[7] Leu, A. J.; Berk, D. A.; Lymboussaki, A.; Alitalo, K.; Jain, R. K. Absence of Functional Lymphatics Within a Murine Sarcoma: a Molecular and Functional Evaluation. *Cancer Res*. **2000**, *60*, 4324-4327.

[8] Padera, T. P.; Kadambi, A.; di Tomaso, E.; Carrerira, C. M.; Brown, E. B.; Boucher, Y.; Choi, N. C.; Mathisen, D.; Wain, J.; Mark, E. J.; Munn, L. L.; Jain, R. K. Lymphatic Metastasis in the Absence of Functional Intratumor Lymphatics. *Scicence*, **2000**, *296*, 1883-1886.

[9] Carmeliet, P.; Jain, R. K.; Angiogenesis in Cancer and Other Diseases. *Nature*, **2000**, *407*, 249-257.

[10] Gee M. S.; Procopio, W. N.; Makonnen, S.; Feldman, M. D.; Yeilding, N. M.; Lee, W. M. Tumor Vessel Development and Maturation Impose Limits on the Effectiveness of Anti-vascular Therapy. *Am. J. Pathol*. **2003**, *162*, 183-193.

[11] Tong, R. T.; Boucher, Y.; Kozin, S. V.; Winkler, F.; Hicklin, D. J.; Jain, R. K. Vascular Normalization by Vascular Endothelial Growth Factor Receptor 2 Blockade Induces a Pressure Gradient Across the Vasculature and Improves Drug Penetration in Tumors. *Cancer Res*. **2004**, *64*, 3731-3736.

[12] Vaupel, P.; Fortmeyer, H. P.; Runkel, S.; Kallinowski, F. Blood Flow, Oxygen Consumption, and Tissue Oxygenation of Human Breast Cancer Xenografts in Nude Rats. *Cancer Res*. **1987**, *47*, 3496-3503.

[13] Vaupel, P.; Schlenger, K.; Knoop, C.; Hockel, M. Oxygenation of Human Tumors: Evaluation of Tissue Oxygen Distribution in Breast Cancers by Computerized O2 Tension Measurements. *Cancer Res*. **1991**, *51*(12), 3316-3322.

[14] Vaupel, P.; Hockel, M. Blood Supply, Oxygenation Status and Metabolic Mircomilieu of Breast Cancers: Characterization and Therapeutic Relevance. *Int. J. Oncol*. **2000**, *17*, 869-879.

[15] Jain, R. K. Determinants of Tumor Blood Flow: A Review. *Cancer Res*. **1988**, *48*, 2641-2658.

[16] Jain, R. K. Normalization of Tumor Vasculature: An Emerging Concept in Antiangiogenic Therapy. *Science*, **2005**, *307*, 58-62.

targets existing vasculature and intents to disrupt established vessels, an approach known as vascular disrupting.[17-18]

Anti-Angiogenic Agents

Angiogenesis refers to the process by which new blood vessels are formed from pre-existing vasculature and is driven by several molecular elements both in healthy tissue and in tumors. However, angiogenesis within the tumor microenvironment is not strictly regulated compared to the methodical systematic processes of healthy tissue. This is a consequence of a prolonged imbalance of pro-angiogenic factors and anti-angiogenic factors in which an excess of pro-angiogenic signaling and an insufficient anti-angiogenic signaling leads to unorthodox tumor vasculature. Some of the established promoters leading to angiogenic signaling include vascular endothelial growth factor (VEGF), angiopoietin (Ang)-1, placental growth factor (P1GF), and cytokines.[19-20] The overexpression of these as well as other angiogenic promoters may occur through a variety of mechanisms such as transcriptional regulation by acidosis, sex hormones, chemokines, oncogene mutations, and hypoxia.[21-22] Antiangiogenic agents are designed to target promoters and factors associated with angiogenesis in an effort to inhibit tumor neovascularization. The first angiogenesis inhibiting agent (AIA) to received approval from the Food and Drug Administration (FDA)

---

[17] Horsman, M. R.; Bohn, A. B.; Busk, M. Vascular Targeting Therapy: Potential Benefit Depends of Tumor and Host Related Effects. Exp. Oncol. 2010, 32(3), 143-148.

[18] Siemann, D. W.; Bibby, M. C.; Dark, G. G.; Dicker, A. P.; Eskens, F. A. L. M.; Horsman, M. R.; Marme, D.; LoRusso, P. M. Differentiation and Definition of Vascular-Targeting Therapies. Clin. Cancer Res. 2005, 11, 416-420.

[19] Carmeliet, P. Angiogenesis in Helath and Disease. Nat. Med. 2003, 9, 653-660.

[20] Carmeliet, P.; Jain, R. K. Molecular Mechanisms and Clinical Applications of Angiogenesis. Nature, 2011, 473, 298-307.

[21] Ferrara, N. Vascular Endothelial Growth Factor. *Arterioscler Thromb. Vasc. Biol.* **2009**, *29*, 789-791.

[22] Vogelstein, B.; Kinzler, K. W.; Cancer Genes and the Pathways They Control. *Nat. Med.* **2004**, *10*, 789-799.

was bevacizumab (Avastin™) in 2004 for the treatment of colorectal cancer.[23] Bevacizumab is a humanized monoclonal antibody that targets VEGF and inhibits the binding of receptors VEGFR1 and VEGFR2, ultimately leading to the normalization of mature vasculature and inhibition of new vessel production.[24] Since initial approval in 2004 Bevacizumab has since been approved for glioblastomas of the brain,[25] lung cancers,[26-27] and renal carsiomas.[24,28] Other strategies associated with AIAs involve targeting the endothelial cell receptor-associated tyrosine kinase activity, basement membrane degradation, tube development, endothelial cell proliferation, and endothelial cell migration.[29-31] AIAs that selectively target pro-angiogenic factors include both antibody-based design, also known as biologics, and small molecules. The complementary approach to targeting tumor vasculature, distinct from inhibiting angiogenesis, involves the direct degradation of the existing vasculature, a process referred to as vascular disruption.

---

[23] Wu, J. M.; Staton, C. A. Anti-angiogenic Drug Discovery: Lessons From the Past and Thoughts for the Furture. *Expert Opin. Drug Discov.* **2012**, *7*(8), 723-743.

[24] Yang, J. C.; Haworth, L.; Sherry, R. M.; Hwu, P.; Schwartzentruber, D. J.; Topalian, S. L.; Steinberg, S. M.; Chen, H. X.; Rosenberg, S. A. A Randomized Trial of Bevacizumab, An Anti-vascular Endothelial Growth Factor Antibody, for Metastatic Renal Cancer. *N. Engl. J. Med.* **2003**, *349*(5), 427-434.

[25] Chamberlain, M. C. Bevacizumab for the Treatment of Recurrent Glioblastoma. *Clin. Med. Insights Oncol.* **2011**, *5*, 117-129.

[26] Sandler, A.; Gray, R.; Perry, M. C.; Brahmer, J.; Schiller, J. H.; Dowiati, A.; Lilenbaum, R.; Johnson, D. H. Paclitaxel-carboplatin Alone or with Bevacizumab for Non-small-cell Lung Cancer. *N. Engl. J. Med.* **2006**, *355*(24), 2542-2550.

[27] Reck, M.; von Pawel, J.; Zatloukal, P.; Ramlau, R.; Gorbounova, V.; Hirsh, V.; Leighl, N.; Mezger, J.; Archer, V.; Moore, N.; Manegold, C. Phase III of Cisplatin Plus Gemcitabine with Either Placebo or Bevacizumab as First-line Therapy For Nonsquamous Non-small-cell Lung Cacner: AVAiL. *J. Clin. Oncol.* **2009**, *27*(8), 1227-1234.

[28] Rini, B. I. Vascular Endothelial Growth Factor-targeted Therapy in Renal Cell Carcinoma: Current Status and Future Directions. *Clin. Cancer Res.* **2007**, *13*, 1098-1106.

[29] Kerbel, R.; Folkman, J. Clinical Translation of Angiogenesis Inhibitors. *Nat. Revs. Cancer,* **2002**, *2*, 727-739.

[30] Boehm, S.; Rothermundt, C.; Hess, D.; Joerger, M. Antiangiogenic Drugs in Oncology: A Focus on Drug Safety and the Elderly- A Mini Review. *Gerontology*, **2010**, *56*, 303-309.

[31] Siemann, D. W.; Warrington, K. H.; Horsman, M. R. Targeting Tumor Blood Vessels: An Adjuvant Strategy for Radiation Therapy. *Radiother. Oncol.* **2000**, *57*, 5-12.

Vascular Disrupting Agents

Vascular disrupting agents (VDAs) seek to selectively destroy the established vascular network within tumor tissue. This concept was developed by Juliana Denekamp and co-workers in 1983 and continues to represent a promising strategy for the therapeutic treatment of cancer.[32] VDAs can be classified into two groups: biological (ligand-directed) and small molecules. Biological or ligand-directed VDAs include peptides and antibodies and are designed to target receptors of up-regulated molecular elements associated with key cell-signaling pathways. Small molecule VDAs have advanced further clinically than their biological counterparts and are further divided into two categories: tubulin-binding agents and the flavonoids. These classes are centered on distinct modes of action and both lead to the ultimate disruption of tumor vasculature. Tubulin-binding small molecule VDAs comprise key binding interactions with tubulin, the key component of microtubules. Microtubules are biopolymers that are responsible for many assorted roles within the cellular environment such as chromosomal segregation, intracellular transport, and are a key component to cytoskeletal shape.[33] Structurally, microtubules are long filamentous hollow tubes that are assembled from 13 parallel profilaments, which are comprised of alternating subunits of α– and β–tubulin heterodimers.[33] Microtubules are assembled through the

[32] Denekamp, J.; Hill, S. A.; Hobson, B. Vascular Occlusion and Tumor Cell Death. *Eur. J. Cancer Clin. Oncl.* **1983**, *19*, 271-275.

[33] Stanton, R. A.; Gernert, K. M.; Nettles, J. H.; Aneja, R. Drugs that Target Dynamic Microtubules: A New Molecular Perspective. *Med. Res. Rev.* **2011**, *31*(3), 443-481.

polymerization of α– and β–tubulin monomers and are disassembled through the depolymerization of α– and β–tubulin monomers, a process known as dynamic instability.[34] The polar nature of this dynamic instability is evident in a plus (+) end that is capable of rapid growth and a sluggish minus (-) end. The growing and shortening of microtubules through this process is regulated by many factors including available GTP, α– and β–tubulin monomer concentrations, and microtubule-stabilizing proteins (MAPs).[33] Efforts to selectively target and disrupt microtubule dynamics have resulted in three classes of tubulin-binding molecules: microtubule stabilizers, microtubule destabilizers, and microtubule modulators.[35] These efforts have also revealed three distinct binding sites on tubulin. The first is referred to as the taxol or taxoid binding site, named for the microtubule stabilizing natural product taxol (paclitaxel) (Fig. 1) and is located on the β–tubulin heterodimer. The second is known as the vinca-alkaloid site, named for the microtubule destabilizing natural products vincristine and vinblastine (Fig. 1), and is located in the αβ–tubulin interface. The third binding site is known as the colchicine site, named after the natural product colchicine (Fig. 1), and is located on β–tubulin heterodimer.

[34] Walker, R. A.; O'Brien, E. T.; Pryer, N. K.; Soboeiro, M. F.; Voter, W. A.; Erickson, H. P.; Salmon, E. D. Dynamic Instability of Individual Microtubules Analyzed by Video Light Microscopy: Rate Constants and Transition Frequencies. *J. Cell Biol.* **1988**, *107*, 1437-1448.

[35] Heidemann, S. Microtubules, Leukemia, and Cough Syrup. *Blood*, **2006**, *107*, 2216-2217.

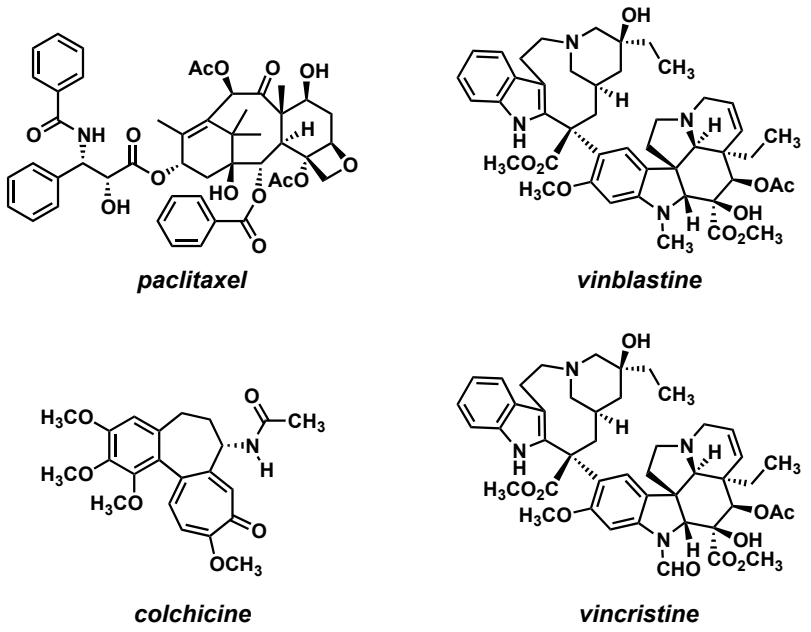

Figure 1.1. Structures of Paclitaxel, Vinblastine, Vincristine, and Colchicine.

The initial success of the taxanes and vinca-alkaloids inspired efforts to develop colchicine-like compounds and lead to the discovery of the combretastatin family of natural products isolated from the South African bush willow tree *Combretum caffrum* by George R. Pettit and co-workers.[36-37] Colchicine itself displays vascular disrupting properties; however, this occurs at doses that exhibit high toxicity.[38] Currently, combretastatin A-4 (CA4) and its phosphate salt prodrug CA4P (Zybrestat™) and combretastatin A-1 (CA1) and its corresponding prodrug CA1P (OXi4503) represent benchmark VDAs that bind at the colchicine site (Fig. 2).

[36] Pettit, G. R.; Cragg, G. M.; Singh, S. B. Antineoplastic Agents, 112. Constituents of Combretum Caffrum. *J. Nat. Prod.* **1987**, *50*, 386-391.

[37] Lin, C. M.; Ho, H. H.; Pettit, G. R.; Hamel, E. The Antimitotic Natural Products Combretastatin A-2 and Combretastatin A-4: Studies on the Mechanism of Their Inhibition of the Binding of Colchicine to Tubulin. *Biochemistry*, **1989**, *28*, 6984-6991.

[38] Boyland, E.; Boyland, M. E. Studies in Tissue Metabolism: The Action of Colchicine and B. Typhosus Extract. *Biochemistry*, **1937**, *31*(3), 454-460.

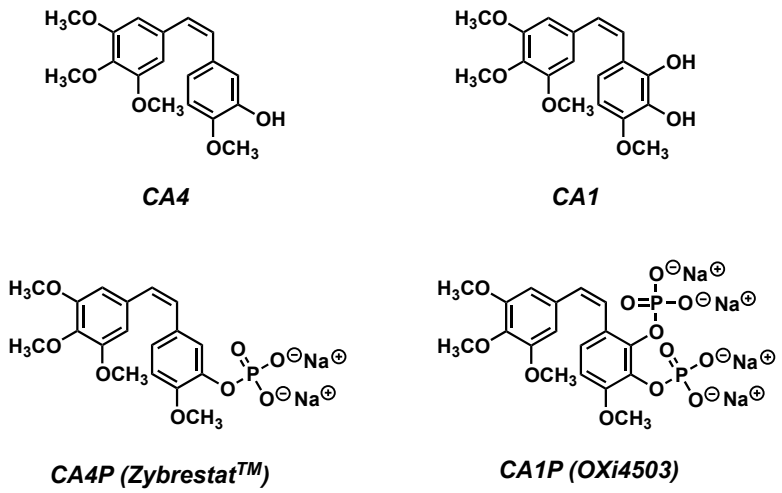

Figure 1.2. Structures of CA4, CA4P, CA1, and CA1P.

CA4P (Zybrestat™) was the first small-molecule, tubulin-binding VDA to enter clinical trails.[39-41] Although several small-molecule VDAs binding to tubulin are currently in clinical trails, there are currently none approved by the FDA.[40-43] The success of the combretastatins has inspired intense research efforts within the Pinney group to develop molecules which incorporate structural similarities to CA4 and CA1 and has resulted in a host of molecular scaffolds, including dihydronaphthalenes,[44-45] benzosuberenes,[44,46-47]

[39] Hasani, A.; Leighl, N. Classification and Toxicities of Vascular Disrupting Agents. *Clin. Lung Cancer*. **2011**, *12*(1), 18-25.

[40] Dowlati, A.; Robertson, K. Cooney, M.; Petros, W. P.; Stratford, M.; Jesberger, J.; Rafie, N.; Overmoyer, B.; Makkar, V.; Stambler, B.; Taylor, A.; Waas, J.; Lewin, J. S.; McCrae, K. R.; Remick, S. C. A Phase I Pharmacokinetic and Translational Study of the Novel Vascular Targeting Agent Combretastatin A-4 Phosphate on a Single-dose Intravenous Schedule in Patients with Advanced Cancer. *Cacner Res*. **2002**, *62*(12), 3408-3416.

[41] Rustin, G. J.; Galbraith, S. M.; Anderson, H.; Stratford, M.; Folkes, L. K.; Sena, L.; Gumbrell, L.; Price, P. M. Phase I Clinical Trial of Weekly Combretastatin A-4 Phosphate: Clinical and Pharmacokinetic Results. *J. Clin. Oncol*. **2003**, *21*(15), 2815-2822.

[42] Lee, R. M.; Gewirtz, D. A. Colchicine Site Inhibitors of Microtubule Integrity as Vascular Disrupting Agents. *Drug Dev. Res*. **2008**, *69*(6), 352-358.

[43] Pinney, K. G. in Vascular-Targeted Therapies in Oncolgy, ed. Siemann, D. John Wiley & Sons, London, UK, **2006**, ch. 6, 95-121.

[44] Sriram, M.; Hall, J. J.; Grohmann, N. C.; Strecker, T. E.; Wootton, T.; Franken, A.; Trawick, M. L.; Pinney, K. G. Design, Synthesis, and Biological Evaluation of Dihydronaphthalene and Benzosuberene Analogs

benzo[*b*]thiophenes,[48-51] benzo[*b*]furans,[52] and indoles[53-54] (Fig. 3). Many of these molecular frameworks aim to mimic the *cis*-stilbenoid arrangement inherent to the combretastatins as well as preserving the 3,4,5-trimethoxyaryl and phenolic functionalities. Further efforts to explore the structural activity relationships essential for the inhibition of tubulin polymerization and cytotoxicity against human cancer cell lines have been explored within a variety of molecular frameworks and the indole scaffold has garnered much attention (see Appendix A for VDA indole stuctures).[55-56] The exploration of tolerable structural

---

of Combretastatins as Inhibitors of Tubulin Polymerization in Cancer Chemotherapy. *Bioorg. Med. Chem.* **2008**, *16*(17), 8161-8171.

[45] Pinney, K. G.; Mocharla, V. P.; Chen, Z.; Garner, C. M.; Ghatak, A.; Hadimani, M.; Kessler, J.; Dorsey, J. Tubulin Binding Ligands and Corresponding Prodrug Constructs. US6593374 B2, **2003**.

[46] Pinney, K. G.; Sriram, M. Combretastatin Analogs with Tubulin Binding Activity. US8394859 B2, **2013**.

[47] Tapure, R. P.; George, C. S.; Sriram, M.; Strecker, T.; Tidmore, J. K.; Hamel, E.; Charlton-Sevcik, A. K.; Chaplin, D. J.; Trawick, M. L.; Pinney, K. G.; *Med. Chem. Comm.* **2012**, *3*, 720-724.

[48] Pinney, K. G.; Bounds, A. D.; Dingeman, K. M.; Mocharla, V. P.; Pettit, G. R.; Bai, R.; Hamel, E. A New Anti-tubulin Agent Containing the Benzo[*b*]thiophene Ring System. *Bioorg. Med. Chem. Lett.* **1999**, *9*, 1081-1086.

[49] Mullica, D. F.; Pinney, K. G.; Mocharla, V. P.; Dingeman, K. M.; Bounds, A. D.; Sappenfield, E. L. Characterization and Structural Analyses of Trimethoxy and Triethoxybenzo[*b*]thiophene. *J. Chem. Crystallogr.* **1998**, *28*, 289-295.

[50] Mullica, D. F.; Pinney, K. G.; Dingeman, K. M.; Bounds, A. D.; Sappenfield, E. L. X-ray Structures of Two Methoxybenzo[*b*]thiophenes. *J. Chem. Crystallogr.* **1996**, *26*, 801-806.

[51] Pinney, K. G.; Pilar, M.; Mocharla, V. P.; Shirali, A.; Pettie, G. R. Anti-mitotic Agents Which Inhibit Tubulin Polymerization. US06162930, **2000**.

[52] Pinney, K. G.; Pettie, G. R.; Mocharla, V. P.; Pilar, M.; Shirali, A. Description Anti-mitotic Agents Which Inhibit Tubulin Polymerization. US6350777 B2, **2002**.

[53] Hadimani, M. B.; Kessler, R. J.; Kautz, J. A.; Ghatak, A.; Shirali, A. R.; O'dell, H.; Garner, C. M.; Pinney, K. G. 2-(3-tert-Butyldimethylsiloxy-4-methoxyphenyl)-6-methoxy-3-(3, 4, 5-trimethoxybenzoyl)indole. *Acta. Cryst.* **2002**, *C58*, 330-332.

[54] Pinney, K. G.; Wang, F.; Hadimani, M. B. Indole-containing and Combretastatin-related Anti-mitotic and Anti-tubulin Polymerization Agents. US6849656 B1, **2005**.

[55] Brancale, A.; Silvestri, R. Indole, A Core Nucleus for Potent Inhibitors of Tubulin Polymerization. *Med. Res. Rev.* **2007**, *27*(2), 209-238.

[56] Patil, S. A.; Patil, R.; Miller, D. D. Indole Molecules as Inhibitors of Tubulin Polymerization: Potential New Anticancer Agents. *Future Med. Chem.* **2012**, *4*(16), 2085-2115.

modifications to VDA scaffolds has also extended into the development of bioreductively activatable prodrug conjugates (BAPCs).

Bioreductive Prodrugs

An established strategy for the delivery of a therapeutic agent involves "masking" the parent agent as an inactive form to later be selectively activated in a desired environment. This approach has been applied to selectively target tumor hypoxia and has resulted in therapeutic agents known as bioreductive prodrugs or bioreductively activatable prodrug conjugates (BAPCs). In general, this is achieved with five chemical classes (nitro groups, quinones, aromatic *N*-oxides, aliphatic *N*-oxides and transition metals) and, upon a one or two electron enzymatic reduction of the prodrug, the resulting superoxide or prodrug radical is strongly cytotoxic.[57] One example of a bioreductive prodrug is tirapazamine, which can undergo a one-electron reduction that results in a free radical species 50-200 fold more toxic than the prodrug under hypoxic conditions.[58-60] A BAPC contains an oxidant moiety that is covalently linked to an active therapeutic agent rendering the BAPC inactive. The oxidant portion of the BAPC is then reduced releasing the parent therapeutic agent in the active form. This method was applied to the development of CA4 BAPCs by Peter Davis and co-workers

[57] Wilson, W. P.; Hay, M. P. Targeting Hypoxia in Cancer Therapy. *Nature Reviews*. **2011**, *11*, 393-410.

[58] Brown, J. M.; SR 4233 (tirapazamine): a new anticancer drug exploiting hypoxia in solid tumours. *Br. J. Cancer* **1993**, *67*, 1163–1170.

[59] Chowdhury, G.; Junnotula, V.; Daniels, J. S.; Greenberg, M. M.; Gates, K. S. DNA strand damage product analysis provides evidence that the tumor cell specific cytotoxin tirapazamine produces hydroxyl radical and acts as a surrogate for O2. *J. Am. Chem. Soc.* **2007**, *129*, 12870–12877.

[60] Shinde, S. S.; Hay, M. P.; Patterson, A. V.; Denny, W. A.; Anderson, R. F. Spin trapping of radicals other than the *OH radical upon reduction of the anticancer agent tirapazamine by cytochrome P450 reductase. *J. Am. Chem. Soc.* **2009**, *131*, 14220–14221.

employing nitrothiophene bioreductive triggers as the oxidant portion and CA4 as the parent VDA (Fig. 4).[61]

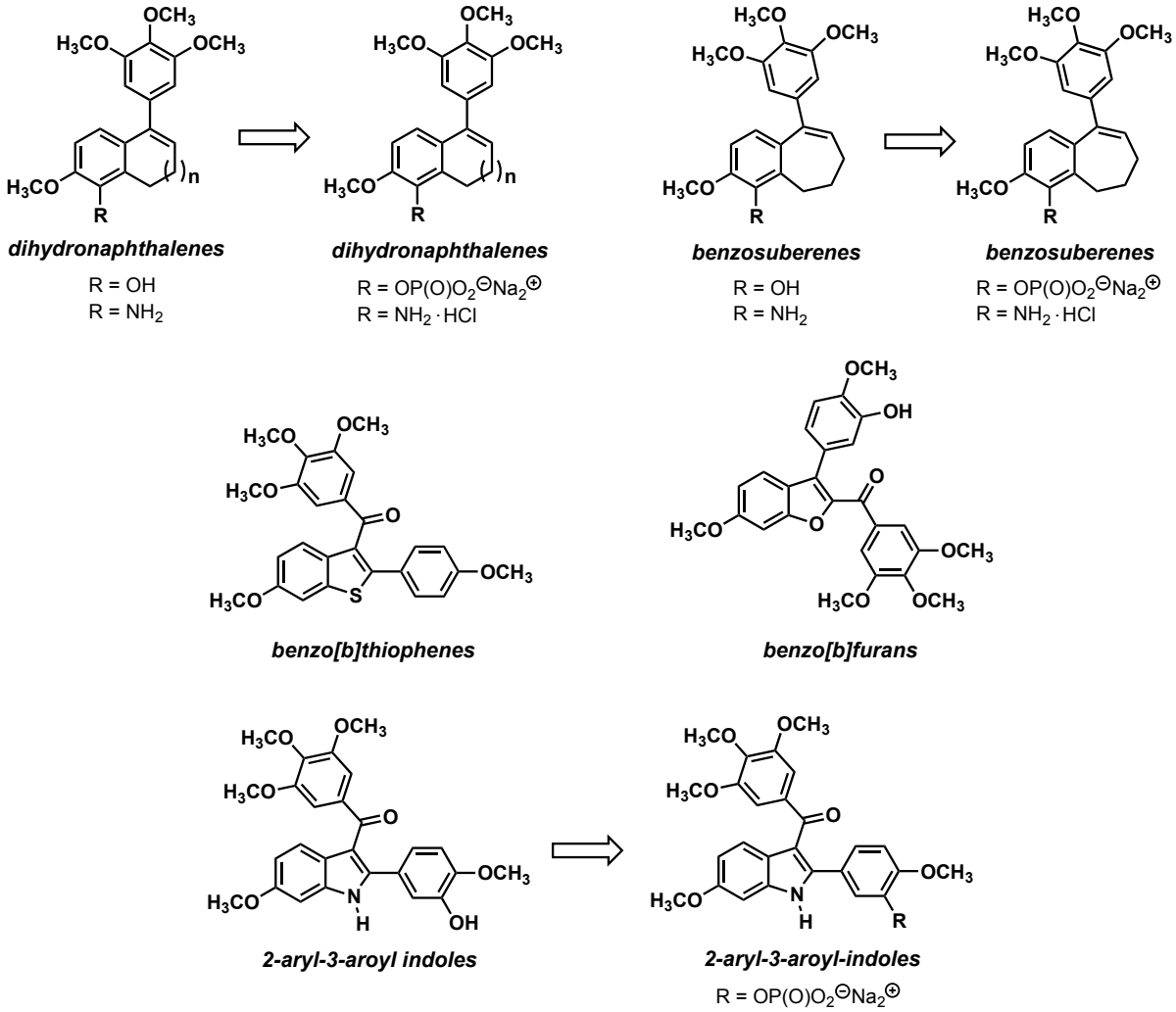

Figure 1.3. Structures of Pinney Group VDAs.

[61] Thompson, P.; Naylor, M. A.; Everett, S. A.; Stratford, M. R. L.; Lewis, G.; Hill, S.; Patel, K. B.; Wardman, P.; Davis, P. D. Synthesis and Biological Properties of Bioreductively Targeted Nitrothienyl Prodrugs of Combretastatin A-4. *Mol. Cancer Ther.* **2006**, *5*(11), 2886-2894.

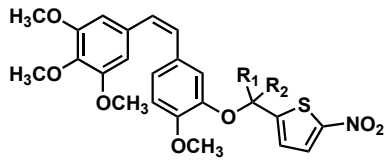

$R_1 = H, R_2 = H$
$R_1 = CH_3, R_2 = H$
$R_1 = CH_3 = R_2 = CH_3$

Figure 1.4. Combretastatin A-4 BAPCs.

These CA4 BACPs showed severe decreases in activity in both the A549 cell line and inhibition of tubulin polymerization in the prodrug form, showing the successful masking of the parent CA4 VDA. It was also determined that *gem*-dimethyl substitution on the ether bridge showed higher susceptibility to cleavage by cytochrome P450 than the *nor*- and *mono*-methyl substitution.

Mechanisms of Heterocyclic Ring Formation

The heterocyclic scaffolding of indoles, benzo[*b*]thiophenes, and benzo[*b*]furans share a prosperous abundance in medical chemistry.[62] The mechanistic pathways and synthetic routes to these platforms are well established and can vary greatly. For instance, the Bischler-Mohlau indole reaction can produce both 2-aryl indoles and 3-aryl indoles from an α-haloketones and appropriate anilines. The indole product (2-aryl or 3-aryl) is determined by the mechanistic pathway that is favored. For the Bischler-Mohlau reaction, Pathway A (Scheme 1) involves initial displacement of a bromine atom by a molecule of aniline. The pathway continues through the intramolecular cyclization and subsequent aromatization resulting in 2-aryl indole **4**. The pathway may stop here, resulting in 2-aryl indole **4**, but, in the presence of acid, can undergo a 1, 2-aryl shift to afford 3-aryl indole **5**.

[62] Roughley, S. D.; Jordan, A. M. The Medicinal Chemist's Toolbox: An Analysis of Reactions Used in the Pursuit of Drug Candidates. *J. Med. Chem.* **2011**, *54*, 3451-3479.

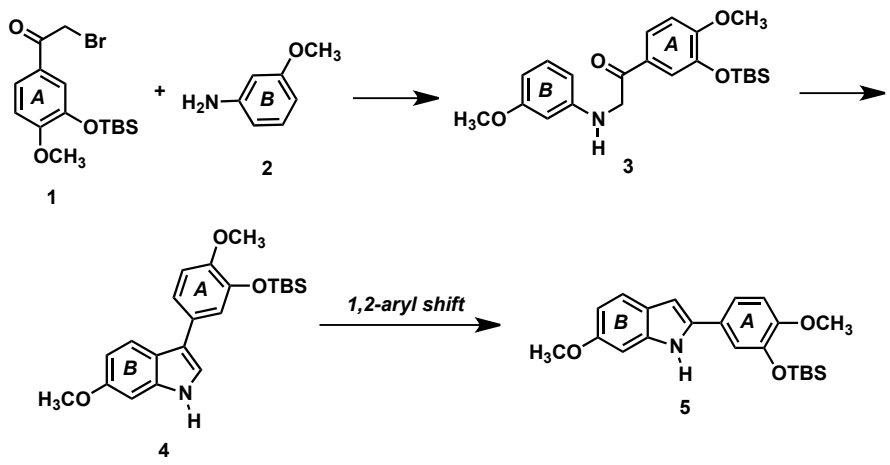

Scheme 1.1. Pathway A of the Bischler-Mohlau Indole Reaction.

The competing Pathway B (Scheme 2) begins in a similar fashion with the initial displacement of bromine by a molecule of aniline, however, pathway B then involves the condensation of a second molecule of aniline, resulting in imine intermediate **6**. Imine **6** then undergoes intramolecular cyclization displacing the initial aniline molecule, and upon tautomerization of 3-aryl **8,** the stable 3-aryl tautomer **9** results.

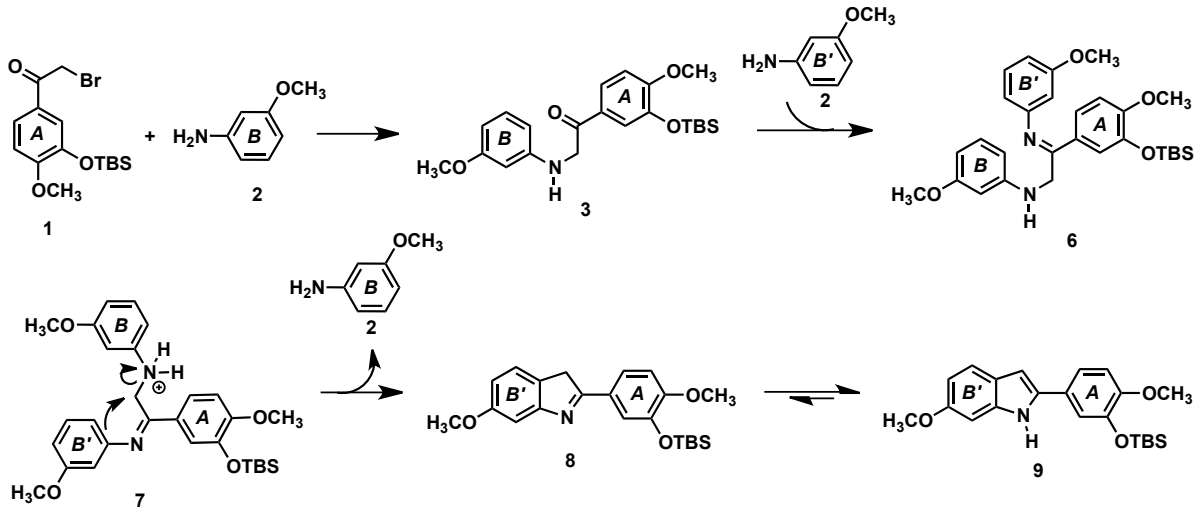

Scheme 1.2. Pathway B of the Bischler-Mohlau Indole Reaction.

Previous computational and experimental studies have suggested that pathway B is preferred when an excess of aniline is used.[63] The synthetic route to benzo[*b*]thiophenes and benzo[*b*]furans also employs α-haloketones with appropriate thiols and phenols, however, the mechanistic pathway is thought to favor a pathway similar to pathway A, resulting in either 1, 2-aryl shifted 2-arylbenzo[*b*]thiophenes and 2-arylbenzo[*b*]furans or non-shifted 3-arylbenzo[*b*]thiophenes and 3-arylbenzo[*b*]furans (Scheme 3).

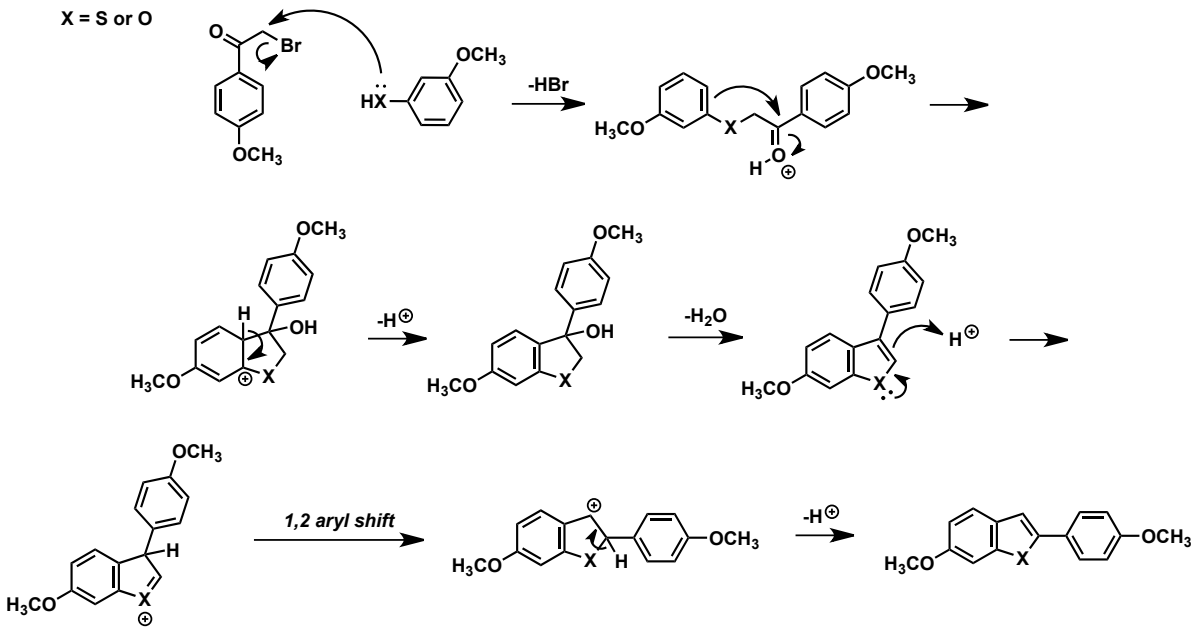

Scheme 1.3. Pathway A for Synthetic Route to Benzo[*b*]thiophenes and Benzo[*b*]furans.

Evidence of the 1, 2-aryl shift was demonstrated in the antiestrogen work of both Eli Lilly[64] and John Katzenellenbogen and co-workers[65] en route to 3-aroyl-2-aryl-

[63] Vara, Y.; Aldaba, E.; Arrieta, A.; Pizarro, J. L.; Arriortua, M. I.; Cossio, F. P. Regiochemistry of the Microwave-assisted Reaction Between Aromatic Amines and a-Bromoketones to Yield Substituted 1*H*-indoles. *Org. Biomol. Chem.* **2008**, *6*, 1763-1772.

[64] Jones, C. D.; Jevnikar, M. G.; Pike, A. J.; Peters, M. K.; Black, L. J.; Thompson, A. R.; Falcone, J. F.; Clemens, J. A. Antiestrogens-2. Structure-activity Studies in a Series of 3-Aroyl-2-arylbenzo[*b*]thiophene Derivatives Leading to [6-Hydroxy-2-(4-hydroxyphenyl)benzo[*b*]thien-3-yl][4-[2-(1-piperidinyl)ethoxy]-phenyl]methanone Hydrochloride (LY156758), a Remarkably Effective Estrogen Antagonist with Only Minimal Intrinsic Estrogenicity. *J. Med. Chem.* **1984**, *27*, 1057-1066.

benzo[*b*]thiophenes. Further evidence of the 1, 2-aryl shift in pathway A was exhibited by the Pinney group and the synthesis of 3-aroyl-2-arylbenzo[*b*]thiophenes as VDAs.[53-54] In contrast, no 1, 2-aryl migration in pathway A was evident in the synthesis of benzo[*b*]furans and resulted in 3-arylbenzo[*b*]furans by Pinney and co-workers.[52]

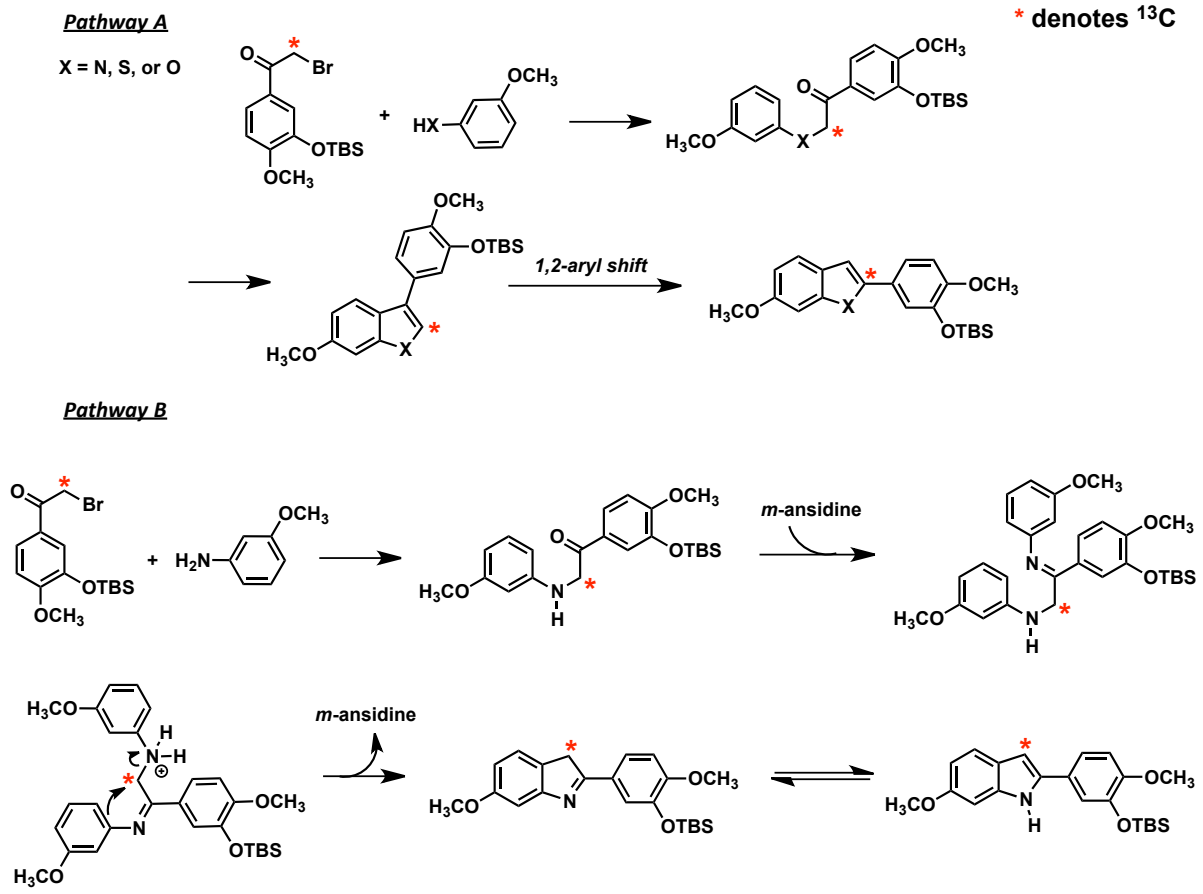

Scheme 1.4. Isotopic Labeling of α-Bromoacetophenone to Determine Mechanstic Pathways of Indole, Benzo[*b*]thiophene, and Benzo[*b*]furan Ring Formation.

In order to evaluate what pathway is operable in our systems, an isotope labeling strategy was engaged where the α-carbon to the carbonyl of the α-bromoacetophenone was

[65] Kym, P. R.; Anstead, G. M.; Pinney, K. G.; Wilson, S. R.; Katzenellenbogen, J. A. Structural and Computational Modeling Studies on 3-aroyl-2-arylbenzo[*b*]thiophene Estrogen Receptor Ligands: LY117018 and Aryl Azide Photoaffinity Labeling Analogs; Investigation of Conformational Preferences, Differential Photoreactivity, and Preferential Modes of Binding. *J. Med. Chem.* **1993**, *36*, 3910-3922.

isotopically labeled with ^{13}C (Scheme 4). The cyclized products could then be evaluated for distinct ^{13}C NMR signatures and provide evidence as to which mechanistic pathway predominates with respect to indoles, benzo[*b*]thiophenes, and benzo[*b*]furans. The mechanistic pathway evidence will provide insight for the rational design of synthetic routes to afford desired functionalized VDAs that incorporate indole, benzo[*b*]thiophene, and benzo[*b*]furan molecular frameworks.

CHAPTER TWO

Synthesis of a 2-Aryl-3-Aroyl-Indole Salt (OXi8007) Resembling Combretastatin A-4 with Application as a Vascular Disrupting Agent

Reprinted (adapted) with permission from Hadimani, M. B.; MacDonough, M. T.; Ghatak, A.; Strecker, T. E.; Lopez, R.; Sriram, M.; Nguyen, B. L.; Hall, J. J.; Kessler, R. J.; Shirali, A. R.; Liu, L.; Garner, C. M.; Pettit, G. R.; Hamel, E.; Chaplin, D. J.; Mason, R. P.; Trawick, M. L.; Pinney, K. G. Synthesis of a 2-Aryl-3-Aroyl-Indole Salt (OXi8007) Resembling Combretastatin A-4 with Application as a Vascular Disrupting Agent. *J. Nat. Prod.* **2013**, http://dx.doi.org/10.1021/np400374w.

ABSTRACT.

The natural products colchicine and combretastatin A-4 (CA4) are potent inhibitors of tubulin assembly, and they have inspired the design and synthesis of a large number of small-molecule, potential anticancer agents. The indole-based molecular scaffold is prominent among these SAR modifications, leading to a rapidly increasing number of agents. The water-soluble phosphate prodrug **33** (OXi8007) of a 2-aryl-3-aroylindole-based phenol **8** (OXi8006) was prepared by chemical synthesis and found to be strongly cytotoxic against selected human cancer cell lines (GI_{50} = 36 nM against DU-145 cells, for example). The free phenol, **8** (OXi8006), was a strong inhibitor (IC_{50} = 1.1 mM) of tubulin assembly. The corresponding phosphate prodrug **33** (OXi8007) also demonstrated pronounced interference with tumor vasculature in a preliminary *in vivo* study utilizing a SCID mouse model bearing an orthotopic PC-3 (prostate) tumor as imaged by color Doppler ultrasound. The combination of these results provides evidence that indole-based phosphate prodrug **33** (OXi8007) functions as a vascular disrupting agent (VDA) that may prove useful for the treatment of cancer.

The vast majority of natural products and synthetic compounds that bind to the tubulin-microtubule protein system and subsequently interfere with the dynamic assembly/disassembly inherent to the a,b-tubulin/microtubule system do so by many variations of this overall mechanism of action. The most thoroughly studied are interactions at the colchicine, vinca alkaloid, and taxoid sites.[1,2] A significant number of antiproliferative, anticancer agents function through this basic mechanism of action. The combretastatin family of natural products consists of a variety of *cis*-stilbenoid compounds isolated from the South African bush willow tree, *Combretum caffrum*.[1] Combretastatin A-4 (CA4) is among the most potent antimitotic agents from this family of compounds and binds to the colchicine site on tubulin (Fig. 1, compound **2**).[3-5] As with many natural products, the challenge of water solubility led to the development of a disodium phosphate prodrug **3**, combretastatin A-4P (CA4P).[6] The discovery of CA4 has led to a diverse library of anti-tubulin agents designed to mimic the simple stilbenoid structure.[1,7]

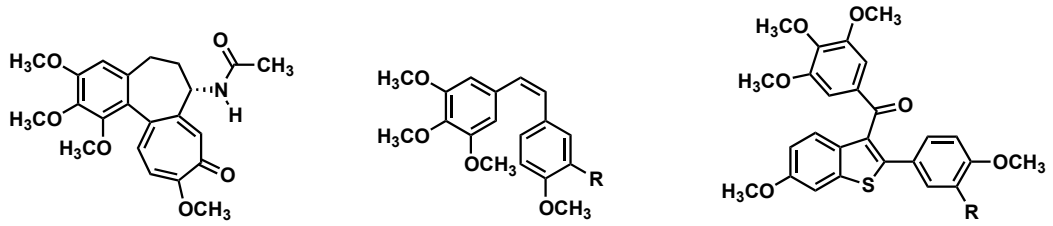

1: Colchicine

2: Combretastatin A-4**:** R = OH
3: Combretastatin A-4P: R = $OP(O)O_2^{\ominus}$ $Na_2^{\oplus}$

4: benzo[*b*]thiophene: R = H
5: benzo[*b*]thiophene: R = OH

Figure 2.1. Representative Small-Molecule Inhibitors of Tubulin Assembly.

The indole structure is prevalent as a core molecular component in a variety of inhibitors of tubulin assembly.[8] As an early example, the vinca alkaloid natural products vinblastine and vincristine, originally isolated from a periwinkle plant (Catharanthus

roseus), both incorporate two key indole ring systems.[9,10] A significant number of compounds that bind to the colchicine site and inhibit microtubule formation are also indole-based (see Fig. 2 for representative molecules). To the best of our knowledge, the first examples of such colchicine site interactive, indole-based compounds were reported by von Angerer *et al*[11] (Fig. 2, compound **6**) and separately by Pinney *et al*[12,13] (Fig. 2, compounds **7-8**) in the middle-to-late 1990s. Our (Pinney and co-workers) 2-aryl-3-aroyl-indole analogues[12-14] were originally inspired, in part, by the combretastatin collection of natural products (pioneered by George R. Pettit)[1,15] and the non-steroidal, selective estrogen receptor modulator (SERM) work of Eli Lilly Inc., featuring benzo[*b*]thiophene templates.[16] A judicious combination of key structural features inherent to both of these molecules led to the preparation of benzo[*b*]thiophene-based analogues (Fig. 1, compounds **4-5**) that proved to be potent inhibitors of tubulin assembly through a binding interaction at the colchicine site.[17-18] A logical course of structure activity relationship (SAR) considerations led to the idea of incorporating a nitrogen atom in the form of an indole-based analogue.

Herein, we report the synthesis of this indole-based compound **8** (OXi8006), along with a water-soluble phosphate salt **33** (OXi8007) and the corresponding *N*-methyl derivatives (**30** and **34**). Cytotoxicity of these compounds against selected human cancer cell lines and their ability to inhibit tubulin polymerization are described. In addition, a preliminary color Doppler ultrasound experiment with a PC-3 tumor in a SCID mouse model is presented, demonstrating a time-progressive disruption of tumor blood flow, thus aiding in the establishment of phosphate prodrug **33** (OXi8007) as among the first indole-based, vascular disrupting agents (VDAs). A structurally similar 3-aroylindole

(Fig. 2, compound **11**, also referred to as BPR0L075)[21,28-29] was recently described by Mason *et al* as a VDA.[30] In addition, *N*-methyl-5,6,7-trimethoxy indole VDAs have been recently reported by Hu *et al*.[31]

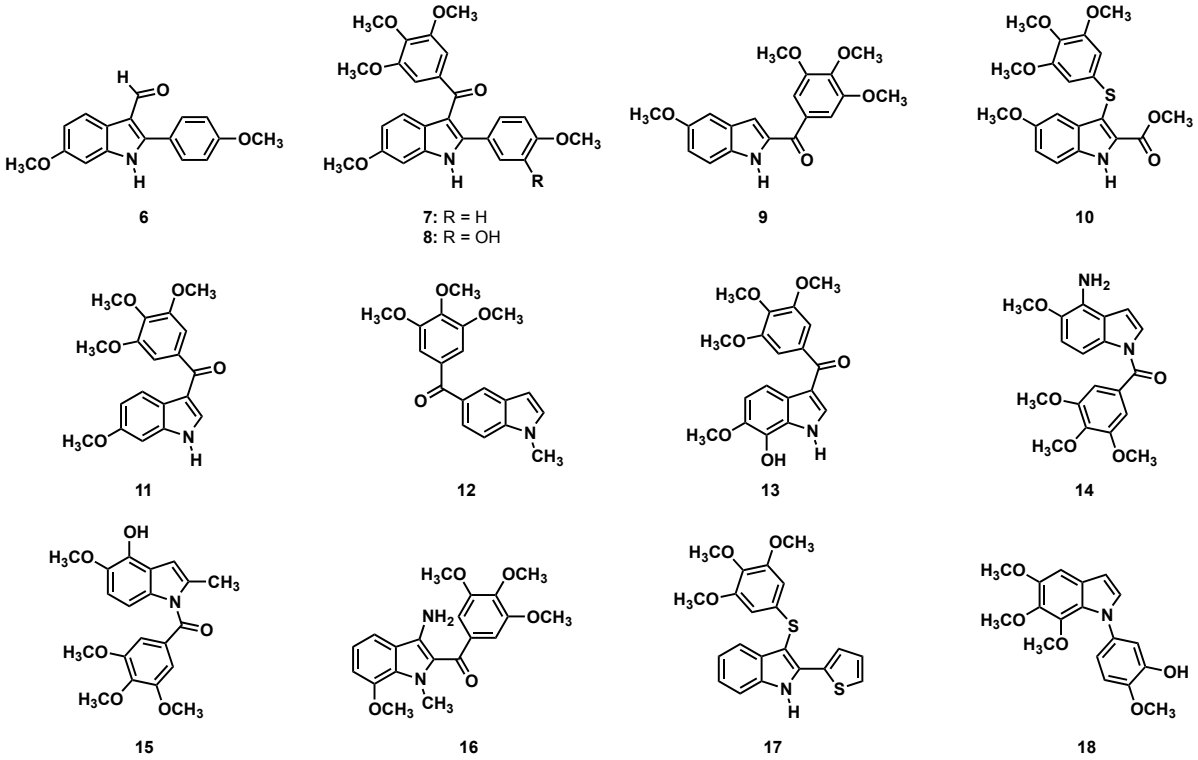

Figure 2.2. Compilation of Indole-Based Inhibitors of Tubulin Assembly (**6**: von Angerer 1998[11] **7-8**: Pinney 2001[12] **9**: Mahboobi and Beckers 2001[19] **10**: Silvestri 2004[20] **11**: Lee and Hsieh 2004[21] **12**: Chang 2007[22] **13**: Cachet 2008[23] **14-15**: Chang 2008[24] **16**: Romagnoli 2008[25] **17**: Silvestri 2011[26] **18**: Liou 2011[27]).

A previous study by Dalal and Burchill in a TC-32 tumor model found minimal necrosis and vessel occlusion with indole salt **33 (**OXi8007) and CA4P as compared with OXi4503.[32] Compounds delineated as VDAs function by disrupting existing tumor vasculature, ultimately leading to oxygen and nutrient deprivation to the tumor. VDAs are a separate class of anticancer agents that are mechanistically distinct from the angiogenesis inhibiting agents (AIAs).[33,34] VDAs cause morphology changes (rounding up) of the endothelial cells lining the microvessels feeding tumors leading to hypoxia,

and ultimately to tumor necrosis.[35] No VDA has been approved by the FDA to date, however several are currently progressing in clinical trials. Our original patent publications inspired Flynn and co-workers to apply their elegant heteroatom ring formation synthetic strategy towards the synthesis of indole **8** (OXi8006).[36] Their important contributions in this area ultimately led to their design and synthesis of BNC105, a benzofuran-based VDA that is currently undergoing clinical trials.[37,38]

RESULTS AND DISCUSSION.

The synthesis of indole analogues **8** and **30** involved substituted bromoacetophenone **24** as a key intermediate, which was prepared from commercially available isovanillin **19** (Scheme 1). After protection of the phenol as its corresponding silyl ether **20**, addition of methyllithium afforded the secondary alcohol **21**, which upon oxidation with PCC furnished the expected acetophenone derivative **22**. Treatment with LDA followed by TMSCl resulted in silyl enol ether **23**, which was converted to its corresponding bromide **24**. The 2-aryl substituted indole derivative **25** was prepared following the Bischler-Mohlau method, by condensation of the substituted bromoacetophenone **24** with 3-methoxyaniline in the high boiling solvent *N*,*N*-dimethyl aniline.[39] Subsequent reaction of indole **25** with 3,4,5-trimethoxybenzoyl chloride yielded the 2-aryl-3-trimethoxybenzoyl substituted indole derivative **27** through a Friedel-Crafts benzoylation reaction. Desilylation of compound **27** with TBAF afforded the desired parent indole-based phenolic ligand **8** (OXi8006). Preparation of the corresponding *N*-methyl indole derivative **30** followed a similar synthetic pathway (Scheme 1) except that the TBS protecting group on intermediate **25** was replaced with an isopropyl group (intermediate **26b**) prior to the benzoylation reaction.

Scheme 2.1. Synthesis of Indole Analogues **8** and **30**.

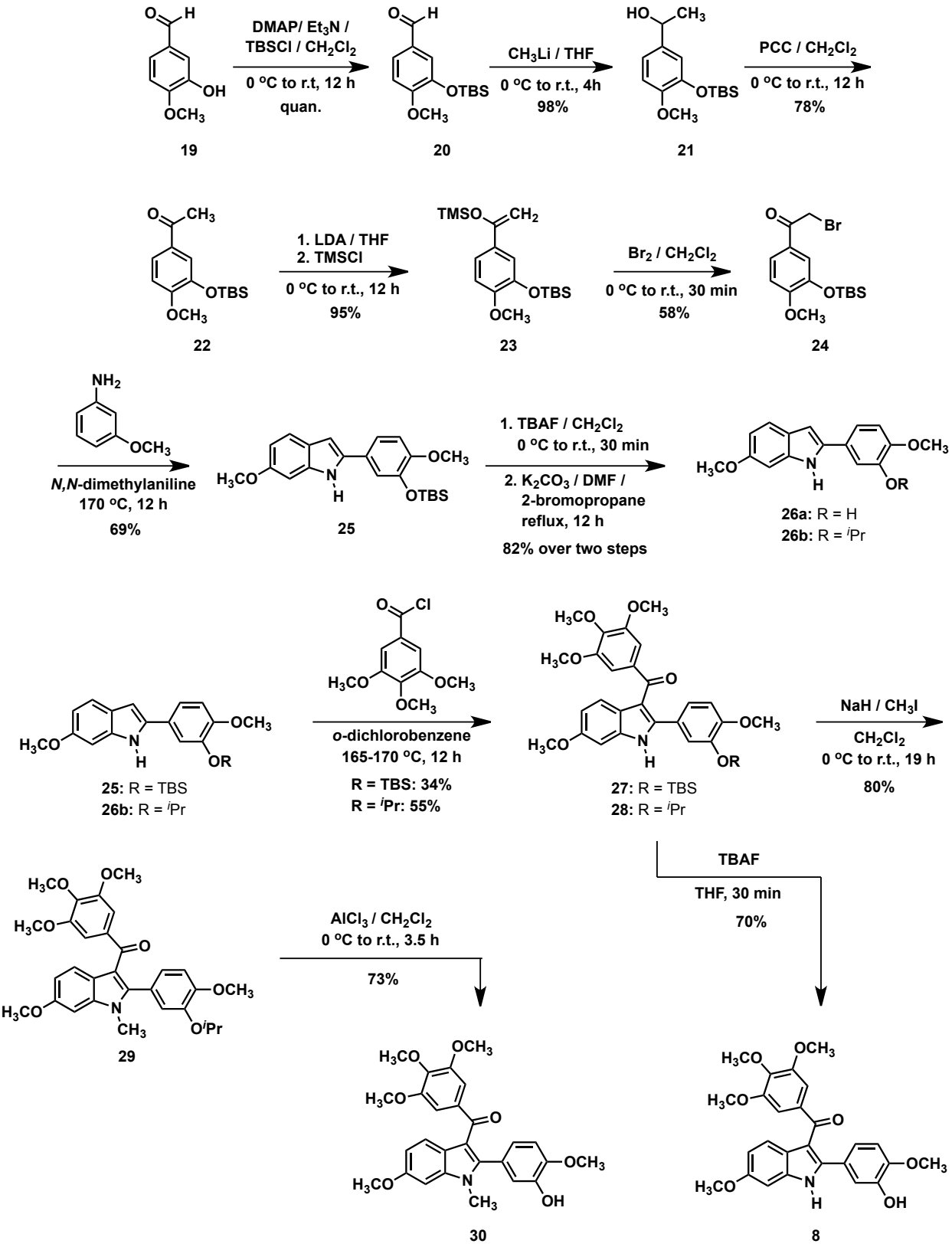

In general, the benzoylation reaction proceeded with higher yields with the isopropyl protecting group rather than with the TBS group. However, the isopropyl group was not used throughout the synthetic sequence since other reactions tended to have higher yields with the TBS group in place, and product purification following deprotection of the isopropyl group was more involved, hence the preference for the TBS group.

Reaction of either phenol (**8** or **30**) with *in situ* generated dibenzyl chlorophosphite resulted in the expected indole-based dibenzyl phosphate ester derivative (**31** or **32**). Catalytic hydrogenolysis of the benzylic carbon-oxygen bonds with hydrogen gas and palladium on activated carbon (10%), followed by an acid-base reaction between the resulting phosphoric acid and sodium methoxide in methanol resulted in the desired disodium phosphate indole prodrug **33** (OXi8007) or the *N*-methyl derivative **34**.[6]

Scheme 2.2. Preparation of Indole-Based Disodium Phosphate Prodrug Salts **33** and **34**.

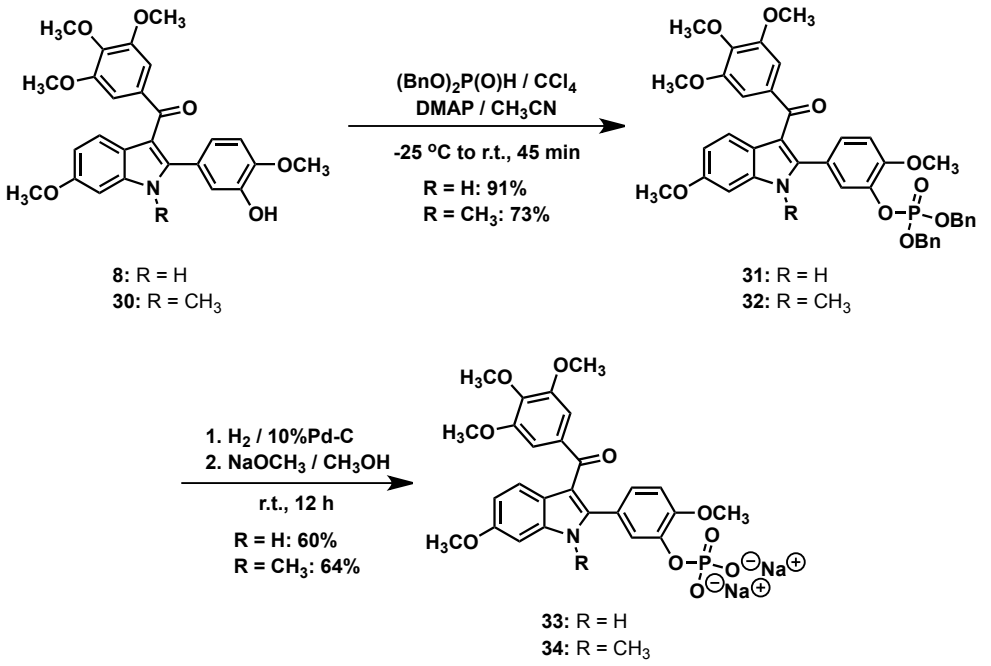

Initial debenzylation attempts involved reaction of the dibenzyl ester with *in situ* generated iodotrimethylsilane, from chlorotrimethylsilane and sodium iodide. The hydrogenolysis reaction offered the advantages of ease of work up and isolation of the product and better yields compared with the iodotrimethylsilane reaction.[6]

The two indole free phenolic analogues **8** (OXi8006) and **30** and their corresponding water-soluble prodrug salts **33** (OXi8007) and **34** were evaluated for their ability to inhibit tubulin polymerization (in a cell-free, pure protein assay). Indole **8** was found to be a potent inhibitor of tubulin assembly (IC_{50} = 1.1 mM) comparable with CA4 (Table 1). While CA4P (containing the bulky phosphate prodrug moiety) is inactive (IC_{50} > 40 mM) as an inhibitor of tubulin assembly,[40] the indole-based phosphate prodrug **33** (OXi8007) was found to be strongly inhibitory (IC_{50} = 4.2 mM). The addition of the *N*-methyl group resulted in a loss of the ability to inhibit tubulin polymerization (IC_{50} > 20 mM) for both the free phenol **30** and its corresponding phosphate prodrug salt **34**. In a binding assay against tritium-labeled colchicine, indole **8** (OXi8006) demonstrated modest inhibition at a concentration of 1 mM (40%) that increased at 5 mM (75%). CA4, as a control, strongly inhibited colchicine binding even at 1 mM (91%). The phosphate prodrug salt, **33** (OXi8007), was only minimally inhibitory (26%) at a concentration of 5 mM.

Both of the *N*-methyl analogues **30** and **34** showed only modest inhibition (34% and 29% respectively) at a high concentration (50 mM). Two possible conclusions can be inferred from these data. First, it seems likely that the non-methylated, free phenol **8** (OXi8006) interacts with the colchicine binding site in an orientation that places the free phenolic moiety outside of the binding pocket. This seems plausible since the

corresponding prodrug **33** (OXi8007), containing the bulky phosphate salt moiety, also demonstrated strong inhibition of tubulin assembly, which is typically not the case for small-molecule phosphate prodrugs of active tubulin binding agents (such as CA4P). Secondly, incorporation of a methyl group on the indole-nitrogen atom severely limited the ability of these analogues to interact with tubulin.

Table 2.1. Inhibition of Tubulin Polymerization and Colchicine Binding.

Compound	Inhibition of tubulin polymerization IC_{50} (mM)	Inhibition of colchicine binding (%)		
		1 mM	5 mM	50 mM
CA4	0.96 ± 0.07	91 ± 1	99 ± 0.8	nd[a]
8 (OXi8006)	1.1 ± 0.04	40 ± 0.2	75 ± 0.2	nd
33 (OXi8007)	4.2 ± 0.1	nd	26 ± 4	nd
30	> 20	nd	nd	34 ± 2
34	> 20	nd	nd	29 ± 2

[a] nd = not determined in this study.

The phenolic indole **8** (OXi8006) and its corresponding prodrug salt **33** (OXi8007) demonstrated consistently strong cytotoxicity (GI_{50} values ranging from 3.5 to 38 nM) against the NCI-H460 (lung), DU-145 (prostate), and SK-OV-3 (ovarian) human cancer cell lines. Cytotoxicity was greatly diminished (IC_{50} approximately 3,000 nM) with the closely related *N*-methyl phenol **30** and prodrug **34**. These data track with the inhibition of tubulin assembly data. Thus, it is instructive to briefly address the question (and subsequent confusion) that occasionally arises in regard to why compounds that are in the nM concentration range in terms of GI_{50} values for cytotoxicity against selected

human cancer cell lines, rarely show lower than micromolar activity in terms of their measured IC_{50} value in the inhibition of tubulin assembly assay. This is commonly noted for many compounds including CA4, for example, as well as indole **8** (OXi8006).

Table 2.2. Cytotoxicity Against Human Cancer Cell Lines NCI-H460, DU-145, and SK-OV-3.

	GI_{50} (mM) SRB assay[a]		
Compound	NCI-H460	DU-145	SK-OV-3
CA4	0.0028[b]	0.00054[b]	0.00042
CA4P	0.066[c]	0.016[c]	nd[d]
8 (OXi8006)	0.0379	0.0356	0.00345
33 (OXi8007)	0.0311	0.0297	0.0223
30	4.14	2.68	2.05
34	3.56	4.67	8.64

[a] Average of $n \geq 3$ independent determinations. [b] For additional data see ref 40. [c] See ref 41. [d] nd = not determined in this study.

Although the reason is not known with certainty, several factors may contribute. For example, the stoichiometry that exists between the concentration of compound and the concentration of tubulin needed to achieve an IC_{50} value in the micromolar range in the pure protein (cell-free) assay may be drastically different from the requisite stoichiometry that exists when inhibiting tubulin in a cell based assay leading to a measured GI_{50} value for cytotoxicity in the nanomolar range. It should be emphasized that the pure protein assay incorporates no cellular components other than tubulin. Importantly, tubulin disassembly (in cells) may release factors that are involved in intramolecular signal transduction leading to a major amplification. In addition, the

amount of tubulin needed in the pure protein assay in order to accurately measure inhibition of microtubule formation (by monitoring absorbance at 350 nm spectrophotometrically) is large enough that the practical lower limit for this assay is around 0.5 to 1 micromolar (IC_{50} value) for even the most active inhibitors of tubulin polymerization.

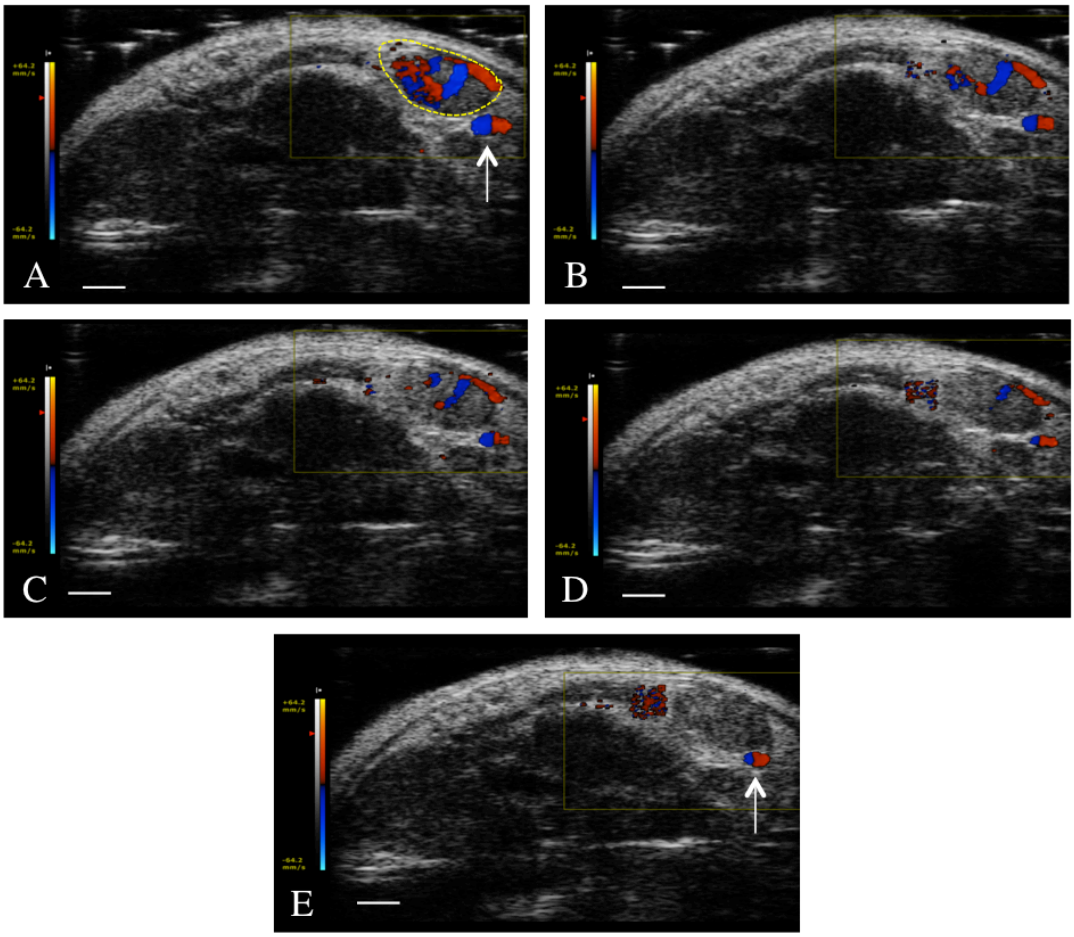

Figure 2.3. Dynamics of Vascular Disruption Caused by OXi8007 in Human Prostate Tumor PC-3 Xenograft Visualized by Doppler Ultrasound. Sequential transaxial images were acquired over a period of 80 min following injection of indole prodrug **33** (OXi8007) (350 mg/kg IP) in a SCID mouse. A) Immediately post injection, B) 20 min, C) 40 min, D) 60 min, E) 80 min. Each image was acquired in color Doppler mode with extensive vasculature initially observed both within the tumor (outline in yellow) and in surrounding tissue. Within 20 min the tumor vascular perfusion had decreased with further progressive decline, so that by 80 min no vascular flow was observed within the tumor. Flow was however still apparent in surrounding normal tissues (white arrow). White scale bar 2 mm. Heat scale bar representing flow ranging from ± 64.2 mm/s.

As a preliminary test of vascular disrupting activity *in vivo*, color Doppler ultrasound was applied to a PC-3 human tumor xenograft growing in a SCID mouse. Images were acquired over a period of 80 min starting immediately after administration of indole prodrug **33** (OXi8007). The tumor was clearly visible (Fig. 3) with extensive bidirectional blood flow displayed in red and blue. Blood flow was also observed in vessels outside the tumor. Blood flow decreased progressively and by 80 min had essentially ceased in the core of the tumor. The extratumoral vessels remained undisrupted throughout. The differential activity in the tumor and animal tissue provides preliminary evidence of selective vascular disruption *in vivo*. Ultrasound has emerged as a valuable imaging technique for VDAs[42] and has recently been validated as a corollary imaging strategy to bioluminescence imaging (BLI)[33] for the assessment of VDAs.[43]

In summary, an indole-based, water-soluble phosphate prodrug salt **33** (OXi8007) was prepared by chemical synthesis and found to be strongly cytotoxic against a selection of human cancer cell lines. Its parent phenolic analogue **8** (OXi8006) was a potent inhibitor of tubulin assembly. A preliminary Doppler ultrasound experiment demonstrated that indole prodrug **33** (OXi8007) has VDA characteristics that are potentially suitable for the treatment of cancer. Additional studies are underway with indole prodrug **33** (OXi8007) and related compounds to further understand the biological mechanism of action and to investigate structure activity relationships within the 2-aryl-3-aroylindole molecular framework.

EXPERIMENTAL SECTION.

General Experimental Methods. Dichloromethane, acetonitrile, dimethylformamide (DMF), methanol, ethanol, and tetrahydrofuran (THF) were used in

their anhydrous forms, as obtained from the chemical suppliers. Reactions were performed under an inert atmosphere using nitrogen gas, unless specified. Thin-layer chromatography (TLC) plates (precoated glass plates with silica gel 60 F_{254}, 0.25 mm thickness) were used to monitor reactions. Purification of intermediates and products was carried out with a Biotage isolera flash purification system using silica gel (200-400 mesh, 60 Å) or RP-18 prepacked columns or manually in glass columns.

Intermediates and products synthesized were characterized on the basis of their ^{1}H NMR (500 or 300 MHz), ^{13}C NMR (125 or 75 MHz), and ^{31}P NMR (200 or 120 MHz) spectroscopic data using a Varian VNMRS 500 MHz or Bruker DPX 300 MHz instrument. Spectra were recorded in $CDCl_3$, D_2O, or CD_3OD. All chemical shifts are expressed in ppm (δ), coupling constants (*J*) are presented in Hz, and peak patterns are reported as broad (br), singlet (s), doublet (d), triplet (t), quartet (q), septet (sept), double doublet, (dd), and multiplet (m).

Purity of the final compounds was further analyzed at 25 °C using an Agilent 1200 HPLC system with a diode-array detector (λ = 190-400 nm), a Zorbax XDB-C18 HPLC column (4.6 mm - 150 mm, 5 μm), and a Zorbax reliance cartridge guard-column; method A: solvent A, acetonitrile, solvent B, 0.1% TFA in H_2O; or method B: solvent A, acetonitrile, solvent B, H_2O; gradient, 10%A / 90%B to 100%A / 0%B over 0 to 40 min; post-time 10 min; flow rate 1.0 mL/min; injection volume 20 μL; monitored at wavelengths of 210, 254, 230, 280, and 360 nm. Mass spectrometry was carried out under positive ESI (electrospray ionization) using a Thermo scientific LTQ Orbitrap Discovery instrument.

*3-(tert-Butyldimethylsilyloxy)-4-methoxybenzaldehyde (**20**).*[44] To a solution of 3-hydroxy-4-methoxybenzaldehyde **19** (25.00 g, 164.4 mmol) dissolved in CH_2Cl_2 (250 mL) at 0 ºC was added triethylamine (Et_3N) (25.2 mL, 180.9 mmol) followed by *N*,*N*-dimethylaminopyridine (DMAP) (2.01 g, 16.4 mmol). The reaction mixture was stirred for 10 min, and *tert*-butyldimethylsilyl chloride (TBSCl) (27.26 g, 180.9 mmol) was then added gradually. The solution was allowed to warm to room temperature over 12 h. Upon completion of the reaction, the reaction mixture was quenched with water (150 mL) and extracted with CH_2Cl_2. The extracted layers were combined, dried over Na_2SO_4, and concentrated under reduced pressure. The TBS benzaldehyde product **20** [47.09 g, 176.9 mmol, R_f = 0.50 (70:30 hexanes:EtOAc)] was isolated quantitatively as a yellow oil and was taken to the next step without further purification. ^{1}H NMR ($CDCl_3$, 500 MHz): δ 9.80 (s, 1H, C<u>H</u>O), 7.45 (dd, *J* = 8.5 Hz, *J* = 2.0 Hz, 1H, Ar<u>H</u>), 7.35 (d, *J* = 2.0 Hz, 1H, Ar<u>H</u>), 6.93 (d, *J* = 8.5 Hz, 1H, Ar<u>H</u>), 3.87 (s, 3H, OC<u>H</u>$_3$), 0.99 (s, 9H, C(C<u>H</u>$_3$)$_3$), 0.16 (s, 6H, Si(C<u>H</u>$_3$)$_2$). ^{13}C NMR ($CDCl_3$, 125 MHz): δ 190.2, 156.2, 145.2, 130.0, 126.0, 119.4, 110.9, 55.1, 25.3, 18.0, -5.0.

*3-tert-Butyldimethylsilyloxy-1-(1'-hydroxyethyl)-4-methoxybenzene (**21**).*[12,44] Crude TBS benzaldehyde **20** (47.09 g, 176.9 mmol) dissolved in tetrahydrofuran (THF, 500 mL) at 0 ºC was treated with CH_3Li (144 mL, 230 mmol) dropwise. The solution was allowed to reach room temperature over 12 h. Upon completion of the reaction, the reaction mixture was slowly quenched with water (200 mL) and extracted with EtOAc. The organic extract was dried over Na_2SO_4 and concentrated under reduced pressure, resulting in secondary alcohol **21** [48.97 g, 173.4 mmol, 98%, R_f = 0.40 (70:30 hexanes:EtOAc)] as a yellow oil, which was taken to the next step without further

purification. ^{1}H NMR ($CDCl_3$, 500 MHz): δ 6.88 (m, 2H, Ar<u>H</u>), 6.83 (d, *J* = 8.1 Hz, 1H, Ar<u>H</u>), 4.81 (q, *J* = 6.3 Hz, 1H, C<u>H</u>), 3.79 (s, 3H, OC<u>H</u>$_3$), 1.82 (s, 1H, O<u>H</u>), 1.45 (d, *J* = 6.3 Hz, 3H, C<u>H</u>$_3$), 0.99 (s, 9H, (C<u>H</u>$_3$)$_3$), 0.15 (s, 6H, Si(C<u>H</u>$_3$)$_2$). ^{13}C NMR ($CDCl_3$, 125 MHz): δ 149.7, 144.5, 138.9, 118.4, 118.0, 111.7, 69.1, 55.1, 25.5, 24.9, 18.2, -4.8.

*3-tert-Butyldimethylsilylox)-4-methoxyacetophenone (**22**)*.[17,44] To a solution of crude alcohol **21** (48.97 g, 173.4 mmol) and Celite® (35 g) in CH_2Cl_2 (500 mL) at 0 ºC was added pyridinium chlorochromate (PCC, 41.12 g, 190.7 mmol) in small increments (1-3 g), allowing 10 min of stirring between each addition. The reaction mixture was allowed to warm to room temperature over 12 h. Upon completion of the reaction, the reaction mixture was filtered through a 50/50 plug of silica gel/Celite®, and the plug was rinsed well with CH_2Cl_2. The filtrate was concentrated under reduced pressure providing the desired acetophenone derivative **22** [37.94 g, 135.3 mmol, 78%, R_f = 0.50 (70:30 hexanes:EtOAc)] as a pale yellow solid. ^{1}H NMR ($CDCl_3$, 500 MHz): δ 7.57 (dd, *J* = 8.5 Hz, 2.0 Hz, 1H, Ar<u>H</u>), 7.46 (d, *J* = 2.0 Hz, 1H, Ar<u>H</u>), 6.86 (d, *J* = 8.5 Hz, 1H, Ar<u>H</u>), 3.86 (s, 3H, OC<u>H</u>$_3$), 2.52 (s, 3H, C<u>H</u>$_3$), 1.00 (s, 9H, C(C<u>H</u>$_3$)$_3$), 0.16 (s, 6H, Si(C<u>H</u>$_3$)$_2$). ^{13}C NMR ($CDCl_3$, 125 MHz): δ 196.7, 155.3, 144.8, 130.5, 123.5, 120.4, 110.7, 55.4, 26.2, 25.6, 18.4, -4.7.

*1-(3-tert-Butyldimethylsilyloxy-4-methoxyphenyl)-1-trimethylsilylethene (**23**)*.[17] To a solution of diisopropylamine (16.6 mL, 117 mmol) in THF (300 mL) at 0 ºC was added *n*-butyllithium (47.04 mL, 117.4 mmol) dropwise. The LDA solution was allowed to stir for 15 min, and then a solution of TBS-acetophenone **22** (21.95 g, 78.27 mmol) in THF (100 mL) was added dropwise. The solution was stirred for 10 min, and trimethylsilyl chloride (TMSCl) (14.9 mL, 117.4 mmol) was added dropwise. The

reaction mixture was allowed to reach room temperature over 12 h. Upon completion of the reaction, the solution was diluted with $NaHCO_3$ (10%, 200 mL). The reaction mixture was extracted with diethyl ether. Next the extract was dried over Na_2SO_4, and the organic phase was concentrated under reduced pressure to provide crude TMS-enol ether **23** (30.45 g, 86.12 mmol) as a dark yellow oil, which was taken to the next step without purification. ^{1}HNMR ($CDCl_3$, 500 MHz): δ 7.18 (dd, *J* = 8.5 Hz, 2.5 Hz, 1H Ar<u>H</u>), 7.12 (d, *J* = 2.5 Hz, 1H, Ar<u>H</u>), 6.80 (d, *J* = 8.5 Hz, 1H, Ar<u>H</u>), 4.78 (d, *J* = 1.5 Hz, 1H, C<u>H</u>$_2$), 4.34 (d, *J* = 1.5 Hz, 1H, C<u>H</u>$_2$), 3.81 (s, 3H, OC<u>H</u>$_3$), 1.03 (s, 9H, C(C<u>H</u>$_3$)$_3$), 0.27 (s, 9H, Si(C<u>H</u>$_3$)$_3$), 0.18 (s, 6H, Si(C<u>H</u>$_3$)$_2$). ^{13}C NMR ($CDCl_3$, 125 MHz): δ 155.3, 151.1, 144.4, 130.6, 118.8, 118.1, 111.2, 89.5, 55.4, 25.7, 18.4, 0.03, -4.7.

*3'-(tert-Butyldimethylsilyloxy)-4'-methoxy-2-bromoacetophenone (**24**)*.[17] To a solution of crude **23** (30.45 g, 86.12 mmol) and anhydrous K_2CO_3 (0.51 g, 3.7 mmol) in CH_2Cl_2 (250 mL) at 0 ºC was added bromine (2.66 mL, 51.7 mmol) dropwise. The solution was allowed to stir for 30 min, diluted with sodium thiosulfate (10%) and extracted with CH_2Cl_2. The extract was dried over Na_2SO_4 and concentrated under reduced pressure. Purification by flash chromatography using a prepacked 25 g silica column [solvent A: EtOAc; solvent B: hexanes; gradient: 2%A / 98%B (4 CV), 2%A / 98%B → 20%A / 80%B (10 CV), 20%A / 80%B (1.2 CV); flow rate: 25 mL/min; monitored at 254 and 280 nm] afforded bromoacetophenone analogue **24** [18.10 g, 50.38 mmol, 58%, R_f = 0.37 (90:10 hexanes:EtOAc)] as a tan red solid. ^{1}H NMR ($CDCl_3$, 500 MHz): δ 7.61 (dd, *J* = 8.5 Hz, 2.5 Hz, 1H, Ar<u>H</u>), 7.48 (d, *J* = 2.5 Hz, 1H, Ar<u>H</u>), 6.88 (d, *J* = 8.5 Hz, 1H, Ar<u>H</u>), 4.37 (s, 2H, C<u>H</u>$_2$), 3.88 (s, 3H, OC<u>H</u>$_3$), 1.00 (s, 9H, C(C<u>H</u>$_3$)$_3$), 0.17 (s, 6H, Si(C<u>H</u>$_3$)$_2$). ^{13}C NMR ($CDCl_3$, 125 MHz): δ 189.8, 156.1, 145.1, 127.1, 124.2,

121.0, 111.0, 55.5, 30.7, 25.6, 18.4, -4.6. HPLC: method B, 9.10 min. HRMS (ESI^+): *m/z* calculated for $C_{15}H_{23}BrNaO_3Si$ $[M+Na]^+$ 381.0492, found 381.0496.

*2-(3'-tert-Butyldimethylsilyloxy-4'-methoxyphenyl)-6-methoxyindole (**25**)*.[45] To a solution of *m*-anisidine (2.05 mL, 18.4 mmol) dissolved in *N*,*N*-dimethylaniline (20 mL) at 170 ºC was added dropwise bromoacetophenone **24** (2.0 g, 5.6 mmol) in EtOAc (5 mL). The reaction mixture was stirred at 170 ºC for 12 h. Upon completion of the reaction, the reaction mixture was cooled to room temperature and extracted with EtOAc (3 x 50 mL). The combined organic extract was dried over Na_2SO_4 and concentrated under reduced pressure. Purification by flash chromatography using a prepacked 25 g silica column [solvent A: EtOAc; solvent B: hexanes; gradient: 12%A / 88%B (4 CV), 12%A / 88%B → 100%A / 0%B (10 CV), 100%A / 0%B (2.6 CV); flow rate: 25 mL/min; monitored at 254 and 280 nm] resulted in the desired 2-phenylindole derivative **25** [1.49 g, 3.88 mmol, 69%, R_f = 0.48 (50:50 hexanes:EtOAc)] as light tan crystals. ^1H NMR ($CDCl_3$, 500 MHz): δ 8.11 (br s, 1H, NH), 7.47 (d, *J* = 8.5 Hz, 1H, ArH), 7.16 (dd, *J* = 8.5 Hz, 2.0 Hz 1H, ArH), 7.13 (d, *J* = 2.5 Hz, 1H, ArH), 6.90 (d, *J* = 8.5 Hz, 1H, ArH), 6.89 (d, *J* = 2.5 Hz, 1H, ArH), 6.79 (dd, *J* = 8.5 Hz, 2.5 Hz, 1H, ArH), 6.64 (dd, *J* = 2.0 Hz, 1.0 Hz 1H, ArH), 3.86 (s, 3H, OCH_3), 3.84 (s, 3H, OCH_3), 1.04 (s, 9H, $C(CH_3)_3$), 0.21 (s, 6H, $Si(CH_3)_2$). ^{13}C NMR ($CDCl_3$, 125 MHz): δ 156.3, 150.5, 145.4, 137.4, 136.9, 125.8, 123.7, 120.9, 118.2, 117.8, 112.4, 109.9, 98.6, 94.5, 55.6, 55.4, 25.7, 18.5, -4.6. HPLC: method B, 21.09 min. HRMS (ESI^+): *m/z* calculated for $C_{22}H_{30}NO_3Si$ $[M+H]^+$ 384.1989, found 384.1989.

*2-(3'-Hydroxy-4'-methoxyphenyl)-6-methoxyindole (**26a**)*.[46] To a solution of TBS-protected phenol **25** (0.10 g, 0.26 mmol) in THF (10 mL) at 0 ºC was added

tetrabutylammonium fluoride (TBAF, 0.4 mL, 0.4 mmol, 1 M in THF) dropwise. The reaction mixture was stirred for 30 min and then allowed to reach room temperature. The reaction mixture was quenched with water (10 mL) and extracted with EtOAc (3 x 10 mL). The combined organic layers were dried over Na_2SO_4 and concentrated under reduced pressure. Purification by flash column chromatography using a prepacked 25 g silica column [solvent A: EtOAc; solvent B: hexanes; gradient: 7%A / 93%B (4 CV), 7%A / 93%B → 60%A / 40%B (10 CV), 60%A / 40%B (5.2 CV); flow rate: 25 mL/min; monitored at 254 and 280 nm] afforded the desired free phenol indole **26a** [0.72 g, 0.27 mmol, R_f = 0.22 (70:30 hexanes:EtOAc)] as a yellow powder. ^{1}H NMR ($CDCl_3$, 500 MHz): δ 8.12 (br s, 1H, NH), 7.47 (d, *J* = 8.6 Hz, 1H, ArH), 7.20 (d, *J* = 2.1 Hz, 1H, ArH), 7.11 (dd, *J* = 8.3 Hz, 2.1 Hz, 1H, ArH), 6.90 (m, 1H, ArH), 6.78 (dd, *J* = 8.6 Hz, 2.2 Hz, 1H, ArH), 6.64 (d, *J* = 1.6 Hz, 1H, ArH), 5.67 (br s, 1H, OH), 3.93 (s, 3H, OCH_3), 3.86 (s, 3H, OCH_3). ^{13}C NMR ($CDCl_3$, 125 MHz): δ 156.6, 146.20, 146.15, 137.6, 136.9, 126.5, 123.8, 121.2, 116.8, 111.4, 111.2, 110.1, 99.1, 94.6, 56.2, 55.9. HPLC: method B, 12.33 min. HRMS (ESI^+): *m/z* calculated for $C_{16}H_{16}NO_3$ $[M+H]^+$ 270.1125, found 270.1128.

*2-(3'-Isopropoxy-4'-methoxyphenyl)-6-methoxyindole (**26b**)*.[45] To a well-stirred solution of free phenol **26a** (0.07 g, 0.27 mmol) and K_2CO_3 (0.12 g, 0.89 mmol) in DMF (10 mL) at 100 ºC was added 2-bromopropane (0.05 mL, 0.54 mmol) dropwise. The reaction mixture was stirred for 12 h at 100 ºC. The mixture was cooled to room temperature and extracted with EtOAc (3 x 10 mL). The combined organic extract was dried over Na_2SO_4 and concentrated under reduced pressure to afford the desired isopropyl protected indole **26b** [0.05 g, 0.27 mmol, 60%, R_f = 0.50 (60:40

hexanes:EtOAc)] as a tan solid which was carried to the next step without further purification. ^{1}H NMR ($CDCl_3$, 500 MHz): δ 8.43 (br s, 1H, N<u>H</u>), 7.47 (d, *J* = 8.6 Hz, 1H, Ar<u>H</u>), 7.21 (d, *J* = 2.1 Hz, 1H, Ar<u>H</u>), 7.16 (dd, *J* = 8.3 Hz, 2.1 Hz, 1H, Ar<u>H</u>), 6.90 (d, *J* = 8.4 Hz, 1H, Ar<u>H</u>), 6.86 (d, *J* = 2.1 Hz, 1H, Ar<u>H</u>), 6.79 (dd, *J* = 8.6 Hz, 2.3 Hz, 1H, Ar<u>H</u>), 6.67 (m, 1H, Ar<u>H</u>), 4.61 (sept, *J* = 6.0 Hz, 1H, C<u>H</u>), 3.87 (s, 3H, OC<u>H</u>$_3$), 3.83 (s, 3H, OC<u>H</u>$_3$), 1.39 (d, *J* = 6.1 Hz, 6H, (C<u>H</u>$_3$)$_2$). ^{13}C NMR ($CDCl_3$, 125 MHz): δ 156.5, 150.2, 147.7, 137.6, 137.2, 125.9, 123.8, 121.0, 117.9, 113.4, 112.5, 110.0, 98.7, 94.7, 71.9, 56.1, 55.8, 22.3. HRMS (ESI^+): *m/z* calculated for $C_{19}H_{22}NO_3$ $[M+H]^+$ 312.1594, found 312.1596.

*2-(3'-tert-Butyldimethylsiloxy-4'-methoxyphenyl)-3-(3",4",5"-trimethoxybenzoyl)-6-methoxyindole (**27**)*.[13] To a solution of compound **25** (3.12 g, 8.14 mmol) in *o*-dichlorobenzene (30 mL) was added 3,4,5-trimethoxybenzoylchloride (2.82 g, 12.2 mmol). The reaction mixture was heated to reflux at 170 ºC for 12 h. The *o*-dichlorobenzene was removed by simple distillation, and the resulting dark colored crude oil was subjected to flash chromatography using a prepacked 100 g silica column [solvent A: EtOAc; solvent B: hexanes; gradient: 10%A / 90%B (4 CV), 10%A / 90%B → 80%A / 20%B (10 CV), 80%A / 20%B (2.8 CV); flow rate: 40 mL/min; monitored at 254 and 280 nm] resulting in TBS-indole analogue **27** [1.60 g, 2.77 mmol, 34%, R_f = 0.38 (60:40 hexanes:EtOAc)] as a yellow powder. ^{1}H NMR ($CDCl_3$, 500 MHz): δ 8.42 (br s, 1H, N<u>H</u>), 7.93 (d, *J* = 9.5 Hz, 1H, Ar<u>H</u>), 6.99 (s, 2H, Ar<u>H</u>) 6.94 (dd, *J* = 8.0 Hz, 2.0 Hz 1H, Ar<u>H</u>), 6.91 (dd, *J* = 9.0 Hz, 2.0 Hz, 1H, Ar<u>H</u>), 6.91 (d, *J* = 2.0 Hz, 1H, Ar<u>H</u>), 6.77 (d, *J* = 2.0 Hz, 1H, Ar<u>H</u>), 6.70 (d, *J* = 8.5 Hz, 1H, Ar<u>H</u>), 3.87 (s, 3H, OC<u>H</u>$_3$), 3.79 (s, 3H, OC<u>H</u>$_3$), 3.74 (s, 3H, OC<u>H</u>$_3$), 3.69 (s, 6H, OC<u>H</u>$_3$), 0.94 (s, 9H, C(C<u>H</u>$_3$)$_3$), 0.04 (s, 6H, Si(C<u>H</u>$_3$)$_2$).

^{13}C NMR ($CDCl_3$, 125 MHz): δ 191.9, 157.4, 152.6, 151.6, 145.2, 142.1, 141.3, 136.5, 134.6, 125.2, 123.4, 122.6, 122.3, 121.9, 112.9, 111.8, 111.7, 107.4, 94.6, 60.9, 56.1, 55.9, 55.5, 25.8, 18.5, -4.7.

*2-(3'-Isopropoxy-4'-methoxyphenyl)-3-(3",4",5"-trimethoxybenzoyl)-6-methoxyindole (**28**)*.[36] To a well-stirred solution of compound **26b** (1.07 g, 3.45 mmol) in *o*-dichlorobenzene (20 mL) was added 3,4,5-trimethoxybenzoylchloride (1.39 g, 6.04 mmol). The reaction mixture was heated to reflux at 160 ºC for 16 h. The excess *o*-dichlorobenzene was removed by simple distillation, and the resulting dark colored solid was subjected to glass column flash chromatography (silica gel, hexanes/EtOAc: 50/50), yielding the desired isopropyl-indole analogue **28** [0.96 g, 1.90 mmol, 55%, R_f = 0.29 (hexanes/EtOAc: 50/50)] as a yellow solid. ^{1}H NMR ($CDCl_3$, 300 MHz): δ 8.79 (br s, 1H, N<u>H</u>), 7.94 (d, *J* = 9.4 Hz, 1H, Ar<u>H</u>), 6.99 (dd, *J* = 8.2 Hz, *J* = 2.1 Hz, 1H, Ar<u>H</u>), 6.98 (s, 2H, Ar<u>H</u>), 6.92 (dd, *J* = 6.1 Hz, 2.3 Hz, 1H, Ar<u>H</u>), 6.90 (d, *J* = 2.3 Hz, 1H, Ar<u>H</u>), 6.74 (d, *J* = 2.1 Hz, 1H, Ar<u>H</u>), 6.73 (d, *J* = 8.4 Hz, 1H, Ar<u>H</u>), 4.16 (m, 1H, C<u>H</u>), 3.85 (s, 3H, OC<u>H</u>$_3$), 3.79 (s, 3H, OC<u>H</u>$_3$), 3.78 (s, 3H, OC<u>H</u>$_3$), 3.66 (s, 6H, OC<u>H</u>$_3$), 1.21 (d, *J* = 5.6 Hz, 3H, C<u>H</u>$_3$), 1.19 (d, *J* = 5.6 Hz, 3H, C<u>H</u>$_3$). ^{13}C NMR ($CDCl_3$, 75 MHz): δ 191.8, 157.3, 152.5, 150.9, 147.1, 142.3, 141.2, 136.4, 134.5, 124.8, 123.2, 122.4, 121.0, 117.3, 112.6, 111.6, 111.5, 107.2, 94.5, 71.7, 64.4, 60.8, 55.9, 55.6, 25.3, 21.9.

2-(3'-Isopropoxy-4'-methoxyphenyl)-3-(3",4",5"-trimethoxybenzoyl)-N-methyl-*6-methoxyindole (**29**)*.[45] To a solution of compound **28** (0.52 g, 1.03 mmol) in CH_2Cl_2 (20 mL) at 0 ºC was added sodium hydride (0.04 g, 1.75 mmol) slowly and carefully. The solution was stirred for 5 min, and methyl iodide (0.13 mL, 2.16 mmol) was added dropwise. The reaction mixture was allowed to warm to room temperature over 19 h.

Upon completion of the reaction, the solution was diluted with water (15 mL) and extracted with CH_2Cl_2 (2 x 15 mL). The combined organic phases were dried over Na_2SO_4 and concentrated under reduced pressure. Purification by column flash column chromatography (silica gel, hexanes/EtOAc: 70/30) afforded methyl indole analogue **29** (0.43 g, 0.82 mmol, 80%, R_f = 0.18 (hexanes/EtOAc: 60/40)) as a white solid. ^{1}H NMR ($CDCl_3$, 300 MHz): d 8.00 (d, *J* = 8.7 Hz, 1H, Ar<u>H</u>), 6.97 (dd, *J* = 8.7 Hz, 2.3 Hz, 1H, Ar<u>H</u>), 6.88 (dd, *J* = 7.9 Hz, 1.9 Hz, 1H, Ar<u>H</u>), 6.87 (d, *J* = 2.4 Hz, 1H, Ar<u>H</u>), 6.84 (s, 2H, Ar<u>H</u>), 6.81 (d, *J* = 8.3 Hz, 1H, Ar<u>H</u>), 6.66 (d, *J* = 1.9 Hz, 1H, Ar<u>H</u>), 4.28 (m, 1H, C<u>H</u>), 3.93 (s, 3H, C<u>H</u>$_3$), 3.82 (s, 3H, OC<u>H</u>$_3$), 3.78 (s, 3H, OC<u>H</u>$_3$), 3.73 (s, 6H, OC<u>H</u>$_3$), 3.66 (s, 3H, OC<u>H</u>$_3$), 1.27 (d, *J* = 6.1 Hz, 6H, (C<u>H</u>$_3$)$_2$). ^{13}C NMR ($CDCl_3$, 75 MHz): d 191.8, 157.2, 152.2, 150.6, 146.7, 145.2, 140.5, 138.1, 135.3, 123.5, 123.3, 122.5, 121.8, 118.4, 114.0, 111.5, 111.2, 106.7, 93.6, 71.4, 60.7, 55.90, 55.86, 55.7, 31.4, 21.9. HPLC: method B, 15.14 min. HRMS (ESI$^+$): *m/z* calculated for $C_{30}H_{33}NNaO_7$ $[M+Na]^+$ 542.2149, found 542.2150.

*2-(3'-Hydroxy-4'-methoxyphenyl)-3-(3",4",5"-trimethoxybenzoyl)-6-methoxyindole (**8**) (OXi8006)*.[12] To a well-stirred solution of compound **27** (4.45 g, 7.70 mmol) in THF (15 mL) at 0 ºC was added tetrabutylammonium fluoride (TBAF, 11.55 mL, 11.55 mmol, 1 M in THF) dropwise. The reaction mixture was stirred for 30 min while warming to room temperature. The reaction mixture was quenched with water (10 mL) and extracted with EtOAc (3 x 10 mL). The combined organic extract was dried over Na_2SO_4 and concentrated under reduced pressure. Purification by flash column chromatography using a prepacked 50 g silica column [solvent A: EtOAc; solvent B: hexanes; gradient: 12%A / 88%B (1 CV), 12%A / 88%B → 100%A / 0%B (10 CV),

100%A / 0%B (5 CV); flow rate: 40 mL/min; monitored at 254 and 280 nm] afforded the desired phenolic indole **8** (OXi8006) [2.49 g, 5.37 mmol, 70%, R_f = 0.28 (50:50 hexanes:EtOAc)] as a yellow powder. ^{1}H NMR ($CDCl_3$, 500 MHz): δ 8.30 (br s, 1H, NH), 7.93 (d, *J* = 9.5 Hz, 1H, ArH), 6.96 (s, 2H, ArH) 6.95 (d, *J* = 2.0 Hz, 1H, ArH), 6.93 (dd, *J* = 9.5 Hz, 2.5 Hz, 1H, ArH), 6.92 (d, *J* = 2.5 Hz, 1H, ArH), 6.78 (dd, *J* = 8.0 Hz, 2.0 Hz, 1H, ArH), 6.65 (d, *J* = 8.5 Hz, 1H, ArH), 5.55 (s, 1H, OH) 3.89 (s, 3H, OCH_3), 3.84 (s, 3H, OCH_3), 3.80 (s, 3H, OCH_3), 3.71 (s, 6H, OCH_3). ^{13}C NMR ($CDCl_3$, 125 MHz): δ 192.7, 157.1, 152.5, 147.0, 145.3, 143.3, 141.0, 136.6, 135.0, 125.1, 123.0, 122.1, 121.5, 115.1, 112.6, 111.6, 110.3, 107.4, 94.8, 60.8, 56.0, 55.8, 55.6. HPLC: method B, 11.43 min. HRMS (ESI^+): *m/z* calculated for $C_{26}H_{26}NO_7$ $[M+H]^+$ 464.1704, found 464.1706.

2-(3'-Hydroxy-4'-methoxyphenyl)-3-(3",4",5"-trimethoxybenzoyl)-N-methyl-*6-methoxyindole (**30**)*.[45] To a solution of isopropyl ether **29** (0.426 g, 0.819 mmol) in CH_2Cl_2 (15 mL) at 0 ºC was added $AlCl_3$ (0.33 g, 2.46 mmol). The reaction mixture was allowed to warm to room temperature and stirring at room temperature continued for 2 h. Examination by TLC indicated the presence of starting material so an additional 3 molar equivalents (0.33 g, 2.46 mmol) of $AlCl_3$ was added, and the reaction mixture was stirred for an additional 1.5 h. Upon completion of the reaction, the reaction mixture was quenched with water (15 mL) and extracted with CH_2Cl_2 (2 x 10 mL). The combined organic extract was dried over Na_2SO_4 and concentrated under reduced pressure. Purification by flash column chromatography (silica gel, hexanes/EtOAc: 60/40) afforded the free phenolic *N*-methyl indole analogue **30** [0.286 g, 0.599 mmol, 73%, R_f = 0.17 (hexanes/EtOAc: 50/50)] as a colorless solid. ^{1}H NMR ($CDCl_3$, 500 MHz): d 8.02 (d, *J* =

8.7 Hz, 1H, Ar<u>H</u>), 6.96 (dd, *J* = 8.7 Hz, 2.2 Hz, 1H, Ar<u>H</u>), 6.86 (d, *J* = 2.1 Hz, 1H, Ar<u>H</u>), 6.79 (d, *J* = 8.0 Hz, 1H, Ar<u>H</u>), 6.78 (s, 2H, Ar<u>H</u>), 6.65 (m, 2H, Ar<u>H</u>), 5.77 (s, 1H, O<u>H</u>), 3.92 (s, 3H, C<u>H</u>$_3$), 3.82 (s, 3H, OC<u>H</u>$_3$), 3.77 (s, 3H, OC<u>H</u>$_3$), 3.74 (s, 6H, OC<u>H</u>$_3$), 3.65 (s, 3H, OC<u>H</u>$_3$). ^{13}C NMR ($CDCl_3$, 75 MHz): d 192.2, 157.3, 152.3, 147.0, 145.4, 145.2, 140.2, 138.2, 135.8, 124.0, 123.6, 122.7, 121.9, 117.0, 114.4, 111.7, 110.2, 106.6, 93.7, 60.8, 56.1, 56.0, 55.9, 31.5. HPLC: method B, 12.38 min. HRMS (ESI$^+$): *m/z* calculated for $C_{27}H_{28}NO_7$ $[M+H]^+$ 478.1860, found 478.1857.

*2-(3'-Dibenzylphosphate-4'-methoxyphenyl)-3-(3",4",5"-trimethoxybenzoyl)-6-methoxyindole (**31**)*.[45] To a solution of compound **8** (1.90 g, 4.09 mmol) in acetonitrile (70 mL) at -25 ºC was added CCl_4 (3.50 mL, 35.98 mmol). The solution was stirred for 10 min, and ethyldiisopropylamine (1.50 mL, 8.63 mmol) and DMAP (0.05 g, 0.41 mmol) were added. After 5 min of stirring, dibenzyl phosphite (1.36 mL, 6.17 mmol) was added, and the reaction mixture was stirred for 2 h while allowing the solution to reach room temperature. Upon completion of the reaction, the reaction was terminated by adding a solution of KH_2PO_4 (15 mL, 0.5 M) and extracted with EtOAc (3 x 50 mL). The combined organic extract was dried over Na_2SO_4 and concentrated under reduced pressure. Purification by flash column chromatography using a prepacked 25 g silica column [solvent A: EtOAc; solvent B: hexanes; gradient: 12%A / 88%B (4 CV), 12%A / 88%B → 100%A / 0%B (10 CV), 100%A / 0%B (5.2 CV); flow rate: 25 mL/min; monitored at 254 and 280 nm] afforded the desired phosphate ester **31** [2.71 g 3.75 mmol, 91 %, R_f = 0.57 (50:50 (hexanes:EtOAc)] as a yellow powder. ^{1}H NMR ($CDCl_3$, 500 MHz): δ 9.20 (br s, 1H, N<u>H</u>), 7.78 (d, *J* = 8.5 Hz, 1H, Ar<u>H</u>), 7.35 (m, 10H, Ar<u>H</u>), 7.25 (m, 1H, Ar<u>H</u>), 6.96 (dd, *J* = 9.0 Hz, 2.5 Hz, 1H, Ar<u>H</u>), 6.93 (s, 2H, Ar<u>H</u>), 6.91 (d, *J* = 2.0

Hz, 1H, Ar<u>H</u>), 6.86 (dd, *J* = 9.0 Hz, 2.5 Hz, 1H, Ar<u>H</u>), 6.51 (d, *J* = 8.5 Hz, 1H, Ar<u>H</u>) 5.17 (d, 4H, *J* = 8.0 Hz, C<u>H</u>$_2$), 3.82 (s, 3H, OC<u>H</u>$_3$), 3.79 (s, 3H, OC<u>H</u>$_3$), 3.65 (s, 6H, OC<u>H</u>$_3$), 3.54 (s, 3H, OC<u>H</u>$_3$). ^{13}C NMR ($CDCl_3$, 125 MHz): δ 192.1, 157.3, 152.7, 150.73, 150.69, 141.3, 141.2, 136.7, 135.6 (d, *J* = 7.3 Hz), 135.0, 128.84, 128.78, 128.1, 127.8, 124.6, 123.1, 122.3, 121.4, 112.8, 112.0, 111.7, 107.4, 94.9, 70.3 (d, *J* = 6.0 Hz), 60.9, 56.2, 55.8, 55.7. ^{31}P NMR ($CDCl_3$, 200 MHz): δ -6.1. HPLC: method B, 16.40 min. HRMS (ESI$^+$): *m/z* calculated for $C_{40}H_{38}NNaO_{10}P$ $[M+Na]^+$ 746.2126, found 746.2126.

*2-(3'-Dibenzylphosphate-4'-methoxyphenyl)-3-(3",4",5"-trimethoxybenzoyl)-N-methyl-6-methoxyindole (**32**).*[45] To a well-stirred solution of compound **30** (0.312 g, 0.653 mmol) dissolved in acetonitrile (15 mL) at -25 °C was added CCl_4 (0.56 mL, 5.75 mmol). The reaction mixture was stirred for 10 min and ethyldiisopropylamine (0.24 mL, 1.37 mmol) and DMAP (0.01 g, 0.06 mmol) were added. After 5 min, dibenzyl phosphite (0.22 mL, 0.99 mmol) was added, and the reaction mixture was allowed to reach room temperature over 1.5 h. A solution of KH_2PO_4 (20 mL, 0.5 M) was added, and the reaction mixture was extracted with EtOAc (3 x 50 mL). The combined organic extract was dried over Na_2SO_4 and concentrated under reduced pressure. Purification by flash column chromatography (silica gel, hexanes/EtOAc: 50/50) yielded the desired phosphate ester **32** [0.35 g, 0.47 mmol, 73%, R_f = 0.52 (hexanes/EtOAc: 30/70)] as a colorless solid. ^{1}H NMR ($CDCl_3$, 300 MHz): d 7.88 (d, *J* = 8.7 Hz, 1H, Ar<u>H</u>), 7.31 (m, 10H, Ar<u>H</u>), 7.17 (m, 1H, Ar<u>H</u>), 7.03 (m, 1H, Ar<u>H</u>), 6.93 (dd, *J* = 8.8 Hz, 2.2 Hz, 1H, Ar<u>H</u>), 6.84 (d, *J* = 2.2 Hz, 1H, Ar<u>H</u>), 6.83 (s, 2H, Ar<u>H</u>), 6.78 (d, *J* = 8.5 Hz, 1H, Ar<u>H</u>), 5.14 (d, *J* = 8.1 Hz, 4H, C<u>H</u>$_2$), 3.91 (s, 3H, C<u>H</u>$_3$), 3.79 (s, 3H, OC<u>H</u>$_3$), 3.76 (s, 3H, OC<u>H</u>$_3$), 3.70 (s, 6H, OC<u>H</u>$_3$), 3.54 (s, 3H, OC<u>H</u>$_3$). ^{13}C NMR ($CDCl_3$, 125 MHz): δ 191.7, 157.4,

152.5, 150.99, 150.95, 144.1, 140.7, 138.2, 135.7 (d, J = 6.8 Hz), 135.6, 129.0, 128.74, 128.70, 128.1, 123.84, 123.82, 122.8, 121.7, 114.5, 112.2, 111.7, 106.9, 93.7, 70.1 (d, J = 5.8 Hz), 60.9, 56.2, 56.1, 55.9, 31.4. ^{31}P NMR ($CDCl_3$, 120MHz): d 5.95. HPLC: method B, 16.84 min. HRMS (ESI^+): m/z calculated for $C_{41}H_{40}NNaO_{10}P$ $[M+Na]^+$ 760.2282, found 760.2280.

*2-(3'-Disodiumphosphate-4'-methoxyphenyl)-3-(3",4",5"-trimethoxybenzoyl)-6-methoxyindole (**33**) (OXi8007).*[12] To a solution of dibenzyl ester **31** (2.71 g, 3.74 mmol) in methanol (70 mL) was added 10% palladium-carbon (1.2 g). The flask was evacuated under vacuum, and H_2 gas was introduced via a balloon. The reaction proceeded for 30 min, and the solution was filtered using Celite® with EtOAc. The filtrate was concentrated under reduced pressure to give the crude phosphoric acid derivative as a greenish-yellow oil (2.29 g, 4.22 mmol). The oil was dissolved in methanol (20 mL), and a solution of sodium methoxide (2.0 mL, 25% w/v in methanol) was added. The reaction mixture was stirred at room temperature for 12 h, and the methanol was removed under reduced pressure. Purification by flash chromatography using a prepacked 25 g reversed phase silica column [solvent A: water; solvent B: acetonitrile; gradient: 100%A / 0%B (3 CV), 100%A / 0%B → 20%A / 80%B (10 CV), 0%A / 100%B (7.3 CV); flow rate: 25 mL/min; monitored at 254 and 280 nm] resulted in the desired disodium phosphate salt **33** (OXi8007) (1.49 g, 2.54 mmol, 60%) as a yellow powder. ^{1}H NMR (D_2O, 500 MHz): δ 8.03 (d, J = 9.0 Hz, 1H, Ar<u>H</u>), 7.71 (m, 1H, Ar<u>H</u>), 7.21 (d, J = 2.0 Hz, 1H, Ar<u>H</u>) 7.03 (dd, J = 9.0 Hz, 2.5 Hz, 1H, Ar<u>H</u>), 6.93 (s, 2H, Ar<u>H</u>), 6.67 (d, J = 8.5 Hz, 1H, Ar<u>H</u>), 6.63 (dd, J = 9.0 Hz, 2.0 Hz 1H, Ar<u>H</u>), 3.95 (s, 3H, OC<u>H</u>$_3$), 3.77 (s, 3H, OC<u>H</u>$_3$), 3.75 (s, 6H, OC<u>H</u>$_3$), 3.72 (s, 3H, OC<u>H</u>$_3$). ^{13}C NMR (D_2O, 125 MHz): δ 195.1, 156.3, 151.7, 150.5,

150.4, 147.7, 142.8 (d, J = 5.6 Hz), 139.7, 136.6, 135.4, 125.8, 123.8, 122.2, 121.5, 120.4, 111.7, 111.2, 107.8, 94.5, 60.8, 56.1, 55.8, 55.7. ^{31}P NMR (D_2O, 200 MHz): δ 0.57. HPLC: method A, 8.32 min. HRMS (ESI^+): *m/z* calculated for $C_{26}H_{25}NNa_2O_{10}P$ $[M+H]^+$ 588.1006, found 588.1008.

*2-(3'-Disodiumphosphate-4'-methoxyphenyl)-3-(3",4",5"-trimethoxybenzoyl)-N-*methyl-*6-methoxyindole (**34**)*.[45] To a solution of dibenzyl ester **32** (0.32 g, 0.43 mmol) in ethanol (10 mL) was added 5% palladium-carbon (0.10 g). The flask was evacuated by aspirator vacuum, and H_2 gas was introduced into the solution via balloon. The reaction proceeded for 30 min, and the solution was filtered through Celite® in EtOAc. The filtrate was concentrated under reduced pressure to afford the crude phosphoric acid derivative as a yellow foam (0.223 g, 0.400 mmol). The foam product was dissolved in methanol (15 mL), and a solution of sodium methoxide (0.18 mL, 0.80 mmol, 4.37 M solution in methanol) was added. The reaction mixture was stirred at room temperature for 12 h. Next, the methanol was removed under reduced pressure. Purification by recrystallization from water-acetone afforded the desired salt **34** (0.168 g, 0.279 mmol, 64%) as a yellow solid. ^{1}H NMR (CD_3OD, 500 MHz): δ 7.89 (d, J = 8.8 Hz, 1H, Ar<u>H</u>), 7.79 (m, 1H, Ar<u>H</u>), 7.02 (d, J = 2.0 Hz, 1H, Ar<u>H</u>), 6.88 (dd, J = 8.8 Hz, 2.2 Hz, 1H, Ar<u>H</u>), 6.76 (s, 2H, Ar<u>H</u>), 6.62 (d, J = 8.3 Hz, 1H, Ar<u>H</u>), 6.58 (dd, J = 8.4 Hz, 2.1 Hz, 1H, Ar<u>H</u>), 3.90 (s, 3H, C<u>H</u>$_3$), 3.77 (s, 3H, OC<u>H</u>$_3$), 3.76 (s, 3H, OC<u>H</u>$_3$), 3.74 (s, 6H, OC<u>H</u>$_3$), 3.69 (s, 3H, OC<u>H</u>$_3$). ^{13}C NMR (CD_3OD, 75 MHz): δ 194.9, 158.8, 153.7, 152.2, 149.1, 148.9, 145.6 (d, J = 5.5 Hz), 141.5, 139.9, 137.4, 126.5, 124.3, 124.0, 123.2, 114.6, 112.9, 112.6, 108.0, 94.8, 61.1, 56.8, 56.6, 56.2, 32.4. ^{31}P NMR (CD_3OD, 120 MHz): δ

1.84. HPLC: method B, 8.74 minutes. HRMS (ESI^+): *m/z* calculated for $C_{27}H_{27}NNa_2O_{10}P$ $[M+H]^+$ 602.1162, found 602.1180.

Effects on Tubulin Polymerization. Bovine brain tubulin was purified using methods previously described.[47] The effect of compounds on tubulin assembly in vitro was determined by using a series of concentrations that were preincubated with 10 μM tubulin (1.0 mg/mL) in glutamate buffer at 30 °C, followed by cooling to 0 °C. After GTP was added, the samples were mixed and transferred to cuvettes at 0 °C in a recording spectrophotometer and warmed to 30 °C to initiate polymerization. Tubulin assembly was observed turbidimetrically at 350 nm.[48] Polymer disassembly was confirmed by cooling to 0 °C. The calculated compound concentration that inhibited the extent of tubulin assembly by 50% after a 20 min incubation was defined as the IC_{50} value.

Colchicine Binding Assay. Colchicine binding was measured as previously described.[49,50] Solutions containing 1 μM tubulin, 5.0 μM [^{3}H]colchicine, and inhibitor at either 50 μM, 5 μM, and/or 1 μM (as specified) were used.

Cell Lines and Sulforhodamine B (SRB) Assay. Cancer cell lines were obtained from ATCC (DU-145 (prostate), SK-OV-3 (ovarian), and NCI-H460 (lung)) and maintained as recommended. Media included gentamicin and amphotericin B. The National Cancer Institute's standard SRB assay assessed cancer cell line growth inhibition, as previously described, with the GI_{50} being the drug concentrations calculated to cause a 50% reduction in net protein increase relative to untreated cells.[51-53] Results reported are averages of at least three separate experiments, each of which was carried out in triplicate.

Color Doppler Ultrasound Imaging with indole 33 (OXi8007). PC-3-luc cells were grown in culture and harvested, as described previously.[43] Cells (2 x 10^6) were implanted orthotopically in the prostate of a SCID mice (NIH, Frederick, MD), and the tumor was allowed to grow to approximately 5-7 mm in diameter. At this stage NAIR® Lotion (Church and Dwight, Princeton, NJ) was applied to ensure complete local hair removal. The mouse was anesthetized (2% isoflurane in oxygen), and gel was applied to ensure effective ultrasound coupling to the solid-state transducers: MS400 (24 MHz). Data were acquired using a Vevo 2100 (Visual Sonics Inc, Toronto, Ontario, Canada) in both B and color Doppler modes. Compound **33** (OXi8007) (350 mg/kg in saline) was injected IP, and ultrasound images were acquired over the next 80 min.

SUPPORTING INFORMATION. Characterization data for selected intermediates and the final compounds are available free of charge via the Internet at http://pubs.acs.org.

AUTHOR INFORMATION. Corresponding Author: *Tel: 1-254-710-4117. Fax: 1-254-710-4272. Email: Kevin_Pinney@baylor.edu

ACKNOWLEDGMENTS. The authors are grateful to the Cancer Prevention and Research Institute of Texas (CPRIT (RP100406), to K.G.P. and M.L.T.), Oxigene Inc. (to K.G.P. and M.L.T), the Welch Foundation (grant no. AA-1278 to K.G.P.), the Baylor University Research Committee (URC grant to K.G.P) and the National Cancer Institute Award Number 5R01CA140674 (to K.G.P and M.L.T with subcontract to R.P.M.) for their financial support of this project. The content is solely the responsibility of the authors and does not necessarily represent the official views of the National Cancer Institute or the National Institutes of Health. The authors also thank Dr. Alejandro

Ramirez (Mass Spectrometry Core Facility, Baylor University) and Dr. James Karban and Dr. Michelle Nemec (Director) for use of the shared Molecular Biosciences Center at Baylor University. Imaging was facilitated with the assistance of the Southwestern Small Animal Imaging Resource (SW-SAIRP), which is supported in part by NCI U24 CA126608, the Harold C. Simmons Cancer Center through an NCI Cancer Center Support Grant, 1P30 CA142543, and the Department of Radiology. We are grateful to Professor J. Hill (Cardiology, UTSW) for providing access to the Vevo 2100, which was acquired thanks to the NIH Shared Instrumentation Grant S10 RR031859.

REFERENCES.

1) Pinney, K. G.; Pettit, G. R.; Trawick, M. L.; Jelinek, C.; Chaplin, D. J. The Discovery and Development of the Combretastatins. In Antitumor Agents from Natural Products, 2nd ed.; Kingston, D., Newman, D., Cragg, G., Eds.; CRC Press, Taylor and Francis Group: Boca Raton, Florida, 2011; pp 27-64.

2) Hamel, E. An Overview of Compounds and their Effects on Microtubule Assembly. In *Microtubule Targets in Cancer Therapy,* Fojo, A. T., Ed.; Humana Press: Towota, New Jersey, 2008; pp. 1-20.

3) Pettit, G. R.; Cragg, G. M.; Herald, D. L.; Schmidt, J. M.; Lohavanijaya, P. Antineoplastic agents. 84. Isolation and Structure of Combretastatin. *Can. J. Chem.* **1982**, *60*, 1374-1376.

4) Pettit, G. R.; Cragg, G. M.; Singh, S. B. Antineoplastic Agents, 122. Constituents of Combretum caffrum. *J. Nat. Prod.* **1987**, *50*, 386-391.

5) Lin, C. M.; Ho, H. H.; Pettit, G. R.; Hamel, E. The Antimitotic Natural Products Combretastatin A-2 and Combretastatin A-4: Studies on the Mechanism of Their Inhibition of the Binding of Colchicine to Tubulin. *Biochemistry* **1989**, *28*, 6984-6991.

6) Pettit, G. R.; Rhodes, M. R. Antineoplastic Agents 389. New Syntheses of the Combretastatin A-4 Prodrug. *Anticancer Drug. Des.* **1998**, *13*, 183-191.

7) Chaudhary, A.; Pandeya, S. N.; Kumar, P.; Sharma, P. P.; Gupta, S.; Soni, N.; Verma, K. K.; Bhardwaj, G. Combretastatin A-4 Analogs as Anticancer Agents. *Mini-Rev. Med. Chem.* **2007**, *7*, 1186-1205.

8) Patil, S. A.; Patil, R.; Miller, D. D. Indole Moleceules as Inhibitors of Tubulin Polymerization: Potential New Anitcancer Agents. *Future Med. Chem.* **2012**, *4*(16), 2085-2115.

9) Owellen, R. J.; Hartke, C. A.; Dickerson, R. M.; Hains, F. O. Inhibition of Tubulin-microtubule Polymerization by Drugs of the Vinca Alkaloid Class. *Cancer Res.* **1976**, *36*, 1499-1502.

10) Cragg, G. M.; Newman, D. J. Plants as a Source of Anti-cancer Agents. *J. Ethnopharmacol.* **2005**, *100*, 72-79.

11) Gastpar, R.; Goldbrunner, M.; Marko, D.; von Angerer, E. Methoxy-Substituted 3-Formyl-2-phenylindoles Inhibit Tubulin Polymerization. *J. Med. Chem.* **1998**, *41*, 4965-4972.

12) Pinney, K. G.; Wang, F.; Del Pilar Mejia, M. Preparation of Indole-containing and Combretastatin-related Anti-mitotic and Anti-tubulin Polymerization Agents. From PCT Int. Appl. **2001**, WO 2001019794 A2 20010322.

13) Note: The X-ray structure and a brief synthetic description of compound **27** were reported by Pinney and co-workers in: Hadimani, M.; Kessler, R. J.; Kautz, J. A.; Ghatak, A.; Shirali, A. R.; O'Dell, H.; Garner, C. M.; Pinney, K. G. 2-(3-*tert*-Butyldimethylsilyloxy-4-methoxyphenyl)-6-methoxy-3-(3,4,5-trimethoxybenzoyl)indole. *Acta Cryst*. **2002**, *C58*, 330-332.

14) Note: The structures of **8** (OXi8006) and **33** (OXi8007), along with a brief summary of their biological activity, were presented as a portion of a book chapter: Pinney, K. G. Molecular Recognition of the Colchicine Binding Site as a Design Paradigm for the Discovery and Development of Vascular Disrupting Agents. In *Vascular-targeted Therapies in Oncology*; Siemann, D. W., Ed.; John Wiley & Sons: London. 2006; pp 95-121.

15) Pettit G. R.; Pinney, K. G. Major Milestones. In *American Society of Pharmacognosy History*. Cragg, G., Ed.; 2009.

16) Jones, C. D.; Jevnikar, M. G.; Pike, A. J.; Peters, M. K.; Black, L. J.; Thompson, A. R.; Falcone, J. F.; Clemens, J. A. Antiestrogens. 2. Structure-Activity Studies in a Series of 3-Aroyl-2-arylbenzo[*b*]thiophene Derivatives Leading to [6-Hydroxy-2-(4-hydroxyphenyl)benzo[*b*]thien-3-yl]-[4-[2-(1-piperidinyl)ethoxy]phenyl]methanone Hydrochloride (LY 156758), a Remarkably Effective Estrogen Antagonist with Only Minimal Intrinsic Estrogenicity. *J. Med. Chem*. **1984**, *27*, 1057-1066.

17) Pinney, K. G.; Mocharla, V. P.; Chen, Z.; Garner, C. M.; Ghatak, A.; Hadimani, M.; Kessler, J.; Dorsey, J. M. Preparation of Trimethoxyphenyl-containing Tubulin Binding Ligands and Corresponding Prodrug Constructs as Inhibitors of Tubulin Polymerization and Antimitotic Agents. From PCT Int. Appl. **2001**, WO 2001068654 A2 20010920.

18) Pinney, K. G.; Dingeman, K. M.; Bounds, A. D.; Mocharla, V. P.; Pettit, G. R.; Bai, R.; Hamel, E. A New Anti-tubulin Agent Containing the Benzo[*b*]thiophene Ring System. *Bioorg. Med. Chem. Lett.* **1999**, *9*, 1081-1086.

19) Mahboobi, S.; Pongratz, H.; Hufsky, H.; Hockemeyer, J.; Frieser, M.; Lyssenko, A.; Paper, D. H.; Burgermeister, J.; Bohmer, F.-D.; Fiebig, H.-H.; Burger, A. M.; Baasner, S.; Beckers, T. Synthetic 2-Aroylindole Derivatives as a New Class of Potent Tubulin-Inhibitory, Antimitotic Agents. *J. Med. Chem.* **2001**, *44*, 4535-4553.

20) Martino, G. D.; La Regina, G.; Coluccia, A.; Edler, M. C.; Barbera, M. C.; Brancale, A.; Wilcox, E.; Hamel, E.; Artico, M.; Silvestri, R. Arylthioindoles, Potent Inhibitors of Tubulin Polymerization. *J. Med. Chem.* **2004**, *47*, 6120-6123.

21) Liou, J.-P.; Chang, Y.-L.; Kuo, F.-M.; Chang, C.-W.; Tseng, H.-Y.; Wang, C.-C.; Yang, Y.-N.; Chang, J.-Y.; Lee, S.-J.; Hsieh, H.-P. Concise Synthesis and Structure-Activity Relationships of Combretastatin A-4 Analogues, 1-Aroylindoles and 3-Aroylindoles, as Novel Classes of Potent Antitubulin Agents. *J. Med. Chem.* **2004**, *47*, 4247-4257.

22) Liou, J.-P.; Wu, C.-Y.; Hsieh, H.-P.; Chang, C.-Y.; Chen, C.-M.; Kuo, C.-C.; Chang, J.-Y. 4- and 5-Aroylindoles as Novel Classes of Potent Antitubulin Agents. *J. Med. Chem.* **2007**, *50*, 4548-4552.

23) Ty, N.; Dupeyre, G.; Chabot, G. G.; Seguin, J.; Tillequin, F.; Scherman, D.; Michel, S.; Cachet, X. Synthesis and Biological Evaluation of New Disubstituted Analogues of 6-Methoxy-3-(3,4,5-trimethoxybenzoyl)-1*H*-indole (BPR0L075), as Potential Antivascular Agents. *Bioorg. Med. Chem.* **2008**, *16*, 7494–7503.

24) Liou, J.-P.; Wu, Z.-Y.; Kuo, C.-C.; Chang, C.-Y.; Lu, P.-Y.; Chen, C.-M.; Hsieh, H.-P.; Chang, J.-Y. Discovery of 4-Amino and 4-Hydroxy-1-aroylindoles as Potent Tubulin Polymerization Inhibitors. *J. Med. Chem.* **2008**, *51*, 4351–4355.

25) Romagnoli, R.; Baraldi, P. G.; Sarkar, T.; Carrion, M. D.; Cara, C. L.; Cruz-Lopez, O.; Preti, D.; Tabrizi, M. A.; Tolomeo, M.; Grimaudo, S.; Cristina, A. D.; Zonta, N.; Balzarini, J.; Brancale, A.; Hsieh, H.-P.; Hamel, E. Synthesis and Biological Evaluation of 1-Methyl-2-(3',4',5'-trimethoxybenzoyl)-3-aminoindoles as a New Class of Antimitotic Agents and Tubulin Inhibitors. *J. Med. Chem.* **2008**, *51*, 1464–1468.

26) Regina, G. L.; Bai, R.; Rensen, W.; Coluccia, A.; Piscitelli, F.; Gatti, V.; Bolognesi, A.; Lavecchia, A.; Granata, I.; Porta, A.; Maresca, B.; Soriani, A.; Iannitto, M. L.; Mariani, M.; Santoni, A.; Brancale, A.; Ferlini, C.; Dondio, G.; Varasi, M.; Mercurio, C.; Hamel, E.; Lavia, P.; Novellino, E.; Silvestri, R. Design and Synthesis of 2-Heterocyclyl-3-arylthio-1*H*-indoles as Potent Tubulin Polymerization and Cell Growth Inhibitors with Improved Metabolic Stability. *J. Med. Chem.* **2011**, *54*, 8394-8406.

27) Lee, H.-Y.; Chang, J.-Y.; Chang, L.-Y.; Lai, W.-Y.; Lai, M.-J.; Shih, K.-H.; Kuo, C.-C.; Chang, C.-Y.; Liou, J.-P. Concise Syntheses of *N*-Aryl-5,6,7-trimethoxyindoles as Antimitotic and Vascular Disrupting Agents: Application of the Copper-Mediated Ullmann-Type Arylation. *Org. Biomol. Chem.* **2011**, *9*, 3154-3157.

28) Kuo, C.-C.; Hsieh, H.-P.; Pan, W.-Y.; Chen, C.-P.; Liou, J.-P.; Lee, S.-J.; Chang, L.-Y.; Chen, L.-T.; Chen, C.-T.; Chang, J.-Y. BPR0L075, A Novel Synthetic Indole Compound with Antimitotic Activity in Human Cancer Cells, Exerts Effective Antitumoral Activity *in Vivo*. *Cancer Res.* **2004**, *64*, 4621-4628.

29) Wu, Y.-S.; Coumar, M. S.; Chang, J.-Y.; Sun, H.-Y.; Kuo, F.-M.; Kuo, C.-C.; Chen, Y.-J.; Chang, C.-Y.; Hsiao, C.-L.; Liou, J.-P.; Chen, C.-P.; Yao, H.-T.; Chiang, Y.-K.; Tan, U.-K.; Chen, C.-T.; Chu, C.-Y.; Wu, S.-Y.; Yeh, T.-K.; Lin, C.-Y.; Hsieh, H.-P. *J. Med. Chem.* **2009**, *52*, 4941-4945.

30) Liu, L.; Beck, H.; Wang, X.; Hsieh, H.-P.; Mason, R. P.; Liu, X. Tubulin-Destabilizing Agent BPR0L075 Induces Vascular-Disruption in Human Breast Cancer Mammary Fat Pad Xenografts. *PLoS ONE,* published online August 24, **2012**; DOI: 10.1371/journal.pone.0043314.

31) Zhao, D.-G.; Chen, J. J.; Du, Y.-R.; Ma, Y.-Y.; Chen, Y.-X.; Gao, K.; Hu, B.-R. Synthesis and Structure-Activity Relationships of *N*-Methyl-5,6,7-trimethoxyindoles as Novel Antimitotic and Vascular Disrupting Agents. *J. Med. Chem.* **2013**, *56*, 1467-1477.

32) Dalal, S.; Burchill, S. A. Preclinical Evaluation of Vascular-disrupting Agents in Ewing's Sarcoma Family of Tumours. *Eur. J. Cancer* **2009**, *45*, 713-722.

33) Mason, R. P.; Zhao, D.; Liu, L.; Trawick, M. L.; Pinney, K. G. A Perspective on Vascular Disrupting Agents that Interact with Tubulin: Preclinical Tumor Imaging and Biological Assessment. *Integr. Biol.*, **2011**, *3*, 375-387.

34) Tozer, G. M.; Kanthou, C.; Baguley, B. C. Disrupting Tumour Blood Vessels. *Nat. Rev. Cancer* **2005**, *5*, 423-435.

35) Chaplin, D. J.; Pettit, G. R.; Hill, S. A. Anti-vascular Approaches to Solid Tumour Therapy: Evaluation of Combretastatin A4 Phosphate. *Anticancer Res.* **1999**, *19*, 189-195.

36) Flynn, B. L.; Hamel, E.; Jung, M. K. One-Pot Synthesis of Benzo[*b*]furan and Indole Inhibitors of Tubulin Polymerization. *J. Med. Chem.* **2002**, *45*, 2670-2673.

37) Flynn, B. L.; Gill, G. S.; Grobelny, D. W.; Chaplin, J. H.; Paul, D.; Leske, A. F.; Lavranos, T. C.; Chalmers, D. K.; Charman, S. A.; Kostewicz, E.; Shackleford, D. M.; Morizzi, J.; Hamel, E.; Jung, M. K.; Kremmidiotis, G. Discovery of 7-Hydroxy-6-methoxy-2-methyl-3-(3,4,5-trimethoxybenzoyl)benzo[*b*]furan (BNC105), a Tubulin Polymerization Inhibitor with Potent Antiproliferative and Tumor Vascular Disrupting Properties. *J. Med. Chem.* **2011**, *54*, 6014-6027.

38) Kremmidiotis, G.; Leske, A. F.; Lavranos, T. C.; Beaumont, D.; Gasic, J.; Hall, A.; O'Callaghan, M.; Matthews, C. A.; Flynn, B. BNC105: A Novel Tubulin Polymerization Inhibitor that Selectively Disrupts Tumor Vasculature and Displays Single-Agent Antitumor Efficacy. *Mol. Cancer Ther.* **2010**, *9*, 1562-1573.

39) von Angerer, E.; Prekajac, J.; Strohmeier, J. 2-Phenylindoles. Relationship between Structure, Estrogen Receptor Affinity, and Mammary Tumor Inhibiting Activity in the Rat. *J. Med. Chem.* **1984**, *27*, 1439-1447.

40) Pettit, G. R.; Grealish, M. P.; Herald, D. L.; Boyd, M. R.; Hamel, E.; Pettit, R. K. Antineoplastic Agents. 443. Synthesis of the Cancer Cell Growth Inhibitor Hydroxyphenstatin and Its Sodium Diphosphate Prodrug. *J. Med. Chem.* **2000**, *43*, 2731-2737.

41) Pettit, G. R.; Rosenberg, H. J.; Dixon, R.; Knight, J. C.; Hamel, E.; Chapuis, J.-C.; Pettit, R. K.; Hogan, F.; Sumner, B.; Ain, K. B.; Trickey-Platt, B. Antineoplastic Agents. 548. Synthesis of Iodo- and Diiodocombstatin Phosphate Prodrugs. *J. Nat. Prod.* **2012**, *75*, 385-393.

42) Goertz, D. E.; Yu, J. L.; Kerbel, R. S.; Burns, P. N.; Foster, F. S. High-frequency Doppler Ultrasound Monitors the Effects of Antivascular Therapy on Tumor Blood Flow. *Cancer Res.* **2002**, *62*, 6371-6375.

43) Alhasan, M. K.; Liu, L.; Lewis, M. A.; Magnusson, J.; Mason, R. P. Comparison of Optical and Power Doppler Ultrasound Imaging for Non-Invasive Evaluation of Arsenic Trioxide as a Vascular Disrupting Agent in Tumors. *PLoS ONE* **2012**, *7*, e46106.

44) Tanpure, R. P.; Harkrider, A. R.; Strecker, T. E.; Hamel, E.; Trawick, M. L.; Pinney, K. G. Application of the McMurry Coupling Reaction in the Synthesis of Tri- and Tetra-arylethylene Analogues as Potential Cancer Chemotherapeutic Agents. *Bioorg. Med. Chem.* **2009**, *17*, 6993-7001.

45) Pinney, K.; Wang, F.; Hadimani, M.; Del Pilar Mejia, M.; Preparation of Trimethoxyphenyl-substituted Indoles with Anti-tubulin and Vascular Targeting Activity for Treatment of Cancer. From PCT Int. Appl. **2004**, WO 2004099139 A1 20041118.

46) Kaufmann, D.; Pojarova, M.; Vogel, S.; Liebl, R.; Gastpar, R.; Gross, D.; Nishino, T.; Pfaller, T.; von Angerer, E.; Antimitotic Activities of 2-Phenylindole-3-carbaldehydes in Human Breast Cancer Cells. *Bioorg. Med. Chem.* **2007**, *15*, 5122-5136.

47) Hamel, E.; Lin, C. M. Separation of Active Tubulin and Microtubule-associated Proteins by Ultracentrifugation and Isolation of a Component Causing the Formation of Microtubule Bundles. *Biochemistry* **1984**, *23*, 4173-4184.

48) Hamel, E. Evaluation of Antimitotic Agents by Quantitative Comparisons of Their Effects on the Polymerization of Purified Tubulin. *Cell Biochem. Biophys.* **2003**, *38*, 1-21.

49) Verdier-Pinard, P.; Lai, J. Y.; Yoo, H. D.; Yu, J.; Marquez, B.; Nagle, D. G.; Nambu, M.; White, J. D.; Falck, J. R.; Gerwick, W. H.; Day, B. W.; Hamel, E. Structure-activity Analysis of the Interaction of Curacin A, The Potent Colchicine Site Antimitotic Agent, with Tubulin and Effects of Analogs on the Growth of MCF-7 Breast Cancer Cells. *Mol. Pharmacol.* **1998**, *53*, 62-76.

50) Hamel, E.; Lin, C. M. Stabilization of the Colchicine Binding Activity of Tubulin by Organic Acids. *Biochim. Biophys. Acta* **1981**, *675*, 226-231.

51) Vichai, V.; Kirtikara, K. Sulforhodamine B Colorimetric Assay for Cytotoxicity Screening. *Nat. Protocols* **2006**, *1*, 1112-1116.

52) Monks, A.; Scudiero, D.; Skehan, P.; Shoemaker, R.; Paull, K.; Vistica, D.; Hose, C.; Langley, J.; Cronise, P.; Vaigro-Wolff, A.; Gray-Goodrich, M.; Campbell, H.; Mayo, J.; Boyd, M. Feasibility of a High-flux Anticancer Drug Screen Using a Diverse Panel of Cultured Human Tumor Cell Lines. *J. Natl. Cancer Inst.* **1991**, *83*, 757-766.

53) Siles, R.; Ackley, J. F.; Hadimani, M. B.; Hall, J. J.; Mugabe, B. E.; Guddneppanavar, R.; Monk, K. A.; Chapuis, J.; Pettit, G. R.; Chaplin, D. J.; Edvardsen, K.; Trawick, M. L.; Garner, C. M.; Pinney, K. G. Combretastatin Dinitrogen-substituted Stilbene Analogues as Tubulin-binding and Vascular-disrupting Agents. *J. Nat. Prod.* **2008**, *71*, 313-320.

CHAPTER THREE

Synthesis and Biological Evaluation of Indole-based, Anti-cancer Agents Inspired by the Vascular Disrupting Agent 2-(3′-Hydroxy-4′-methoxyphenyl)-3-(3′′, 4′′, 5′′-trimethoxybenzoyl)-6-methoxyindole (OXi8006)

Reprinted from Synthesis and Biological Evaluation of Indole-based, Anti-cancer Agents Inspired by the Vascular Disrupting Agent 2-(3 ′-Hydroxy-4 ′-methoxyphenyl)-3-(3 ′ ′, 4 ′ ′, 5 ′ ′-trimethoxybenzoyl)-6-methoxyindole (OXi8006), MacDonough, M. T.; Strecker, T. E.; Hamel, E.; Hall, J. J.; Chaplin, D. J.; Trawick, M. L.; Pinney, K. G. Copyright 2013, with permission from from Elsevier.

ABSTRACT.

The discovery of a 2-aryl-3-aroyl indole-based small-molecule inhibitor of tubulin assembly (referred to as **OXi8006**) inspired the design, synthesis, and biological evaluation of a series of diversely functionalized analogues. In the majority of examples, the pendant 2-aryl ring contained a 3-hydroxy-4-methoxy substitution pattern, and the fused aryl ring featured a 6-methoxy group. Most of the variability was in the 3-aroyl moiety, which was modified to incorporate methoxy (**33-36**), nitro (**25-27**), halogen (**28-29**), trifluoromethyl (**30**), or trifluoromethoxy (**31-32**) functionalities. In two analogues (**34** and **36**), the methoxy substitution pattern in the fused aryl ring varied, while in another derivative (**35**) the phenolic moiety was translocated from the pendant 2-aryl ring to position-7 of the fused aryl ring. Each of the compounds were evaluated for their cytotoxicity (*in vitro*) against the SK-OV-3 (ovarian), NCI-H460 (lung), and DU-145 (prostate) human cancer cell lines and for their ability to inhibit tubulin assembly. Four of the compounds (**30**, **31**, **35**, **36**) proved to be potent inhibitors of tubulin assembly (IC_{50} < 5 mM), and three of these compounds (**31**, **35**, **36**) were strongly cytotoxic against the

three cancer cell lines. The most active compound (**36**) in this series, which incorporated a methoxy group at position-7, was comparable in terms of inhibition of tubulin assembly and cytotoxicity to the lead compound **OXi8006**.

Keywords: Vascular disrupting agent (VDA), inhibitor of tubulin assembly, functionalized indole, combretastatin.

1. Introduction

The exploration and assessment of the tumor microenvironment and its physiology have revealed a number of prospective molecular targets for selective therapeutic intervention by small-molecule anti-cancer agents. A well-established target is the dynamic tubulin-microtubule protein system. Microtubules are structurally characterized as biopolymers composed of αβ-tubulin heterodimers.[1-5] The dynamic assembly and disassembly of microtubules is linked to a variety of cellular functions, including cell shape, intracellular motility, cellular division, and apoptosis.[1-5] More recently, certain small-molecule inhibitors of tubulin assembly have been identified as vascular disrupting agents (VDAs).[6] These compounds selectively disrupt tumor vasculature by interfering with the tubulin-microtubule protein system of the endothelial cells lining tumor microvessels, which sets in motion a cascade of cell signaling events leading to morphology changes (rounding up) of these endothelial cells. This results in the occlusion of the vessels, which limits tumor blood flow. This in turn restricts the oxygen and nutrients vital for tumor survival. The vascular network feeding tumors is distinct from normal tissue vasculature and incorporates branching that is often unsystematic and convoluted.[7-9] In addition, increased rates of tumor cell proliferation coupled with underdeveloped endothelium, in contrast to normal tissue vasculature, has

established tumor vasculature as a selective therapeutic target for anti-cancer agents.[9] This approach has led to the development of a class of therapeutics referred to as vascular targeting agents (VTAs). This class is further subdivided into two discrete sub-classes centered upon distinct mechanism(s) of action: vascular disrupting agents (VDAs) and angiogenesis inhibiting agents (AIAs).[10] VDAs damage existing tumor vasculature while AIAs impede new tumor vessel formation.[10-12] VDAs can be further divided into two distinct groups: biologics and small-molecules. One strategy focuses on the development of indole-based small-molecule VDAs that bind at the colchicine site, named after the natural product originally described as binding at the site (Figure 1)[13] and whose interaction with tubulin led to the original isolation of the protein.[14] Synthetic and biological studies with indole-based, colchicine site VDAs were originally prompted by the discovery of the potent natural products combretastatin A-4 (**CA4**) and combretastatin A-1 (**CA1**) that were isolated from the African bush willow tree, *Combretum caffrum*, by Pettit and co-workers (Figure 1).[15-16] **CA4** emerged as a benchmark VDA, and its corresponding prodrug salt **CA4P** (Zybrestat™) was the first small-molecule tubulin binding VDA to enter clinical trials.[17-19] Although no VDA is yet in routine clinical use, several small-molecule VDAs interacting at the colchicine site are in clinical trials.[17-21]

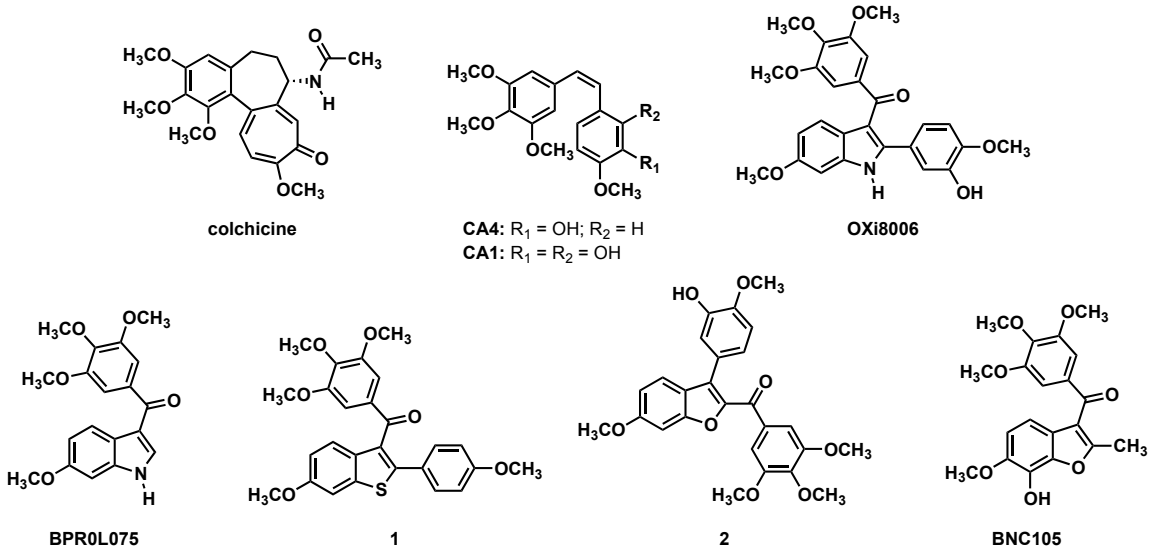

Figure 3.1. Selected colchicine site tubulin binding agents.

VDAs derived from the combretastatin family demonstrate potent antiproliferative activity in various human cancer cell lines *in vitro* through the inhibition of tubulin polymerization.[22-31] These findings led us and others to explore indole-based compounds for potential VDA and antitubulin activities by incorporating into their design structural similarities to the combretastatin series. Our work led to the potent compound 2-(3′-hydroxy-4′-methoxyphenyl)-3-(3′′,4′′,5′′-trimethoxybenzoyl)-6-methoxyindole (referred to as **OXi8006**),[21,32-34] and Flynn[35] has subsequently pursued this compound (through a separate synthetic route) and structurally similar, highly active compounds. Because **OXi8006** potently inhibits tubulin assembly (IC_{50} = 1.1 mM) and cell growth (for example, GI_{50} = 3.45 nM against SK-OV-3 cells), we initiated further structural studies. As an initial finding, a water-soluble, disodium phosphate prodrug salt, **OXi8007**, demonstrated distinct *in vivo* VDA activity in a study employing a SCID

mouse model bearing an orthotopic PC-3 (prostate) tumor as imaged by color Doppler ultrasound.[36]

Herein, we report the synthesis and biological evaluation of a series of functionalized analogues of **OXi8006** in an effort to further explore the molecular space inherent to 2-aryl-3-aroyl indole-based anti-cancer agents. Our finding[21,32-34] that **OXi8006** is a potent tubulin binding agent combined with the work of Hseih[37] with **BPR0L075** (Figure 1) provided preliminary structural parallels defining distinct associations between the stilbene aryl rings of **CA4** and the aryl and aroyl rings of **OXi8006** and **BPR0L075**. These correlations were further expanded by our previous identification of benzo[*b*]thiophene **1** and benzo[*b*]furan **2** as tubulin interacting compounds[38-41] and the subsequent studies by Flynn leading to the benzofuran-based **BNC105** (Figure 1), a VDA currently undergoing clinical trials.[42-44] A narrow but focused literature survey of inhibitors of tubulin assembly that incorporate the indole molecular template confirms the importance of the 3-(3′, 4′, 5′-trimethoxybenzoyl)indole functionality while allowing for structural diversity within the indole core (Figure 2). This is exemplified by structures that include variation in alkoxy substitution (structure **I**, Fig. 2),[37] halogen incorporation (structures **I** and **III**),[37,45] heterocyclic substitution at the 2-position (structure **IV**),[46] and derivatives of **BRP0L075** (such as compound **II**).[47]

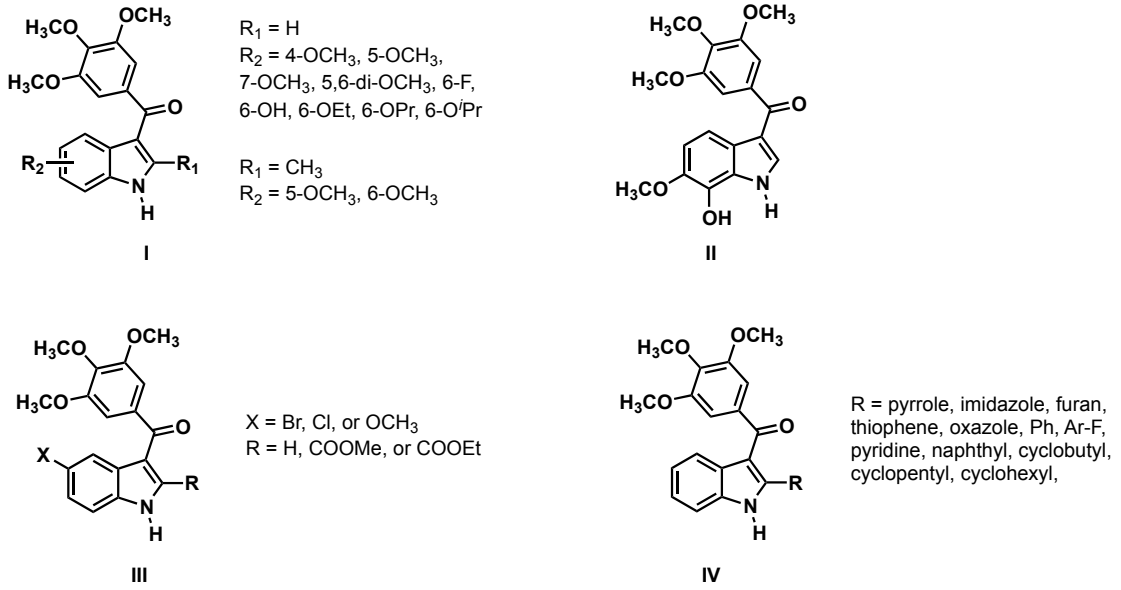

Figure 3.2. Structural diversity within the 3-(3′, 4′, 5′-trimethoxybenzoyl)indole molecular space.

The potent inhibition of tubulin assembly and cytotoxicity of **OXi8006** and **BPR0L075**, in addition to the previous studies with benzo[*b*]thiophene and benzo[*b*]furan derivatives, led to the present study, which investigates a small collection of diversely modified 2-aryl-3-aroyl indole-based analogues to gain further insight into the structural features of **OXi8006** that are most important for biological activity (inhibition of tubulin assembly and cytotoxicity).

2. Results and discussion

2.1 Chemistry

The synthetic route to derivatized **OXi8006** analogues **25**-**36** involved the previously described bromoacetophenone **3**[36] and commercially available bromoacetophenone **4** as key intermediates. 2-Aryl substituted indoles **5**-**11** were prepared by condensation of bromoacetophenone **3** or **4** with suitable anilines under Bischler-Mohlau conditions[48-49] (Scheme 1). Further modification of 2-aryl indole **8** by

selective demethoxylation in the presence of ionic liquid [TMAH][Al_2Cl_7][50] (generated from $AlCl_3$ and trimethylamine hydrochloride (TMAH)) and microwave irradiation yielded the phenolic 2-aryl indole **9**, which was subsequently protected as its corresponding TBS derivative **10** (Scheme 2). The regioselectivity of the demethylation reaction was confirmed by X-ray crystallographic analysis of TBS indole **10** (see Supplementary data). Treatment of 2-aryl indoles **5**-**11** with appropriate functionalized benzoyl chloride derivatives resulted in 2-aryl-3-aroyl indole analogues **12**-**24** through a benzoylation reaction. Final desilylation with TBAF provided the parent 2-aryl-3-aroyl free phenol indole analogues **25**-**36**.

Scheme 3.1. Synthetic route to OXi8006 analogues from bromoacetophenones 3 and 4.

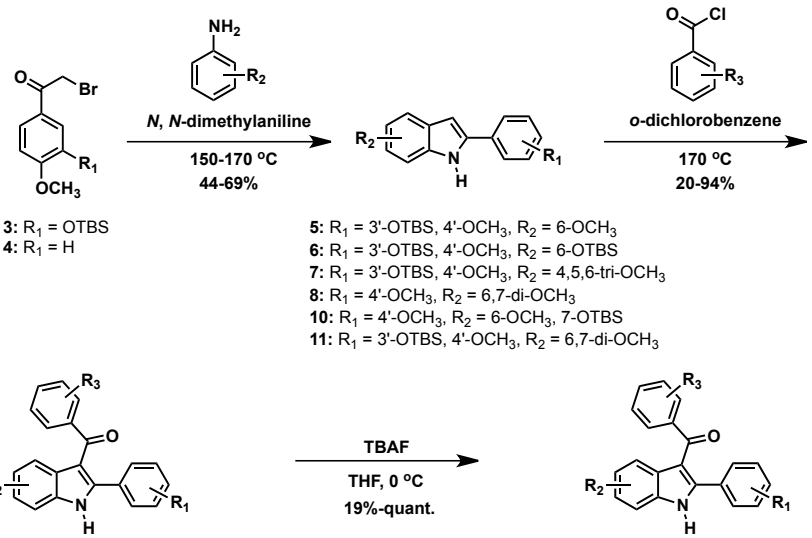

3: R_1 = OTBS
4: R_1 = H

5: R_1 = 3'-OTBS, 4'-OCH_3, R_2 = 6-OCH_3
6: R_1 = 3'-OTBS, 4'-OCH_3, R_2 = 6-OTBS
7: R_1 = 3'-OTBS, 4'-OCH_3, R_2 = 4,5,6-tri-OCH_3
8: R_1 = 4'-OCH_3, R_2 = 6,7-di-OCH_3
10: R_1 = 4'-OCH_3, R_2 = 6-OCH_3, 7-OTBS
11: R_1 = 3'-OTBS, 4'-OCH_3, R_2 = 6,7-di-OCH_3

12: R_1 = 3'-OTBS, 4'-OCH_3, R_2 = 6-OCH_3, R_3 = 3",4",5"-tri-OCH_3
13: R_1 = 3'-OTBS, 4'-OCH_3, R_2 = 6-OCH_3, R_3 = 3",5"-di-NO_2
14: R_1 = 3'-OTBS, 4'-OCH_3, R_2 = 6-OCH_3, R_3 = 4"-NO_2
15: R_1 = 3'-OTBS, 4'-OCH_3, R_2 = 6-OCH_3, R_3 = 3"-NO_2
16: R_1 = 3'-OTBS, 4'-OCH_3, R_2 = 6-OCH_3, R_3 = 3",4",5"-tri-F
17: R_1 = 3'-OTBS, 4'-OCH_3, R_2 = 6-OCH_3, R_3 = 4"-F
18: R_1 = 3'-OTBS, 4'-OCH_3, R_2 = 6-OCH_3, R_3 = 3",5"-di-CF_3
19: R_1 = 3'-OTBS, 4'-OCH_3, R_2 = 6-OCH_3, R_3 = 3"-OCF_3
20: R_1 = 3'-OTBS, 4'-OCH_3, R_2 = 6-OCH_3, R_3 = 4"-OCF_3
21: R_1 = 3'-OTBS, 4'-OCH_3, R_2 = 6-OTBS, R_3 = 3",4",5"-tri-OCH_3
22: R_1 = 3'-OTBS, 4'-OCH_3, R_2 = 4,5,6-tri-OCH_3, R_3 = 3",4",5"-tri-OCH_3
23: R_1 = 4'-OCH_3, R_2 = 6-OCH_3, 7-OTBS, R_3 = 3",4",5"-tri-OCH_3
24: R_1 = 3'-OTBS, 4'-OCH_3, R_2 = 6,7-di-OCH_3, R_3 = 3",4",5"-tri-OCH_3

OXi8006: R_1 = 3'-OH, 4'-OCH_3, R_2 = 6-OCH_3, R_3 = 3",4",5"-tri-OCH_3
25: R_1 = 3'-OH, 4'-OCH_3, R_2 = 6-OCH_3, R_3 = 3",5"-di-NO_2
26: R_1 = 3'-OH, 4'-OCH_3, R_2 = 6-OCH_3, R_3 = 4"-NO_2
27: R_1 = 3'-OH, 4'-OCH_3, R_2 = 6-OCH_3, R_3 = 3"-NO_2
28: R_1 = 3'-OH, 4'-OCH_3, R_2 = 6-OCH_3, R_3 = 3",4",5"-tri-F
29: R_1 = 3'-OH, 4'-OCH_3, R_2 = 6-OCH_3, R_3 = 4"-F
30: R_1 = 3'-OH, 4'-OCH_3, R_2 = 6-OCH_3, R_3 = 3",5"-di-CF_3
31: R_1 = 3'-OH, 4'-OCH_3, R_2 = 6-OCH_3, R_3 = 3"-OCF_3
32: R_1 = 3'-OH, 4'-OCH_3, R_2 = 6-OCH_3, R_3 = 4"-OCF_3
33: R_1 = 3'-OH, 4'-OCH_3, R_2 = 6-OH, R_3 = 3",4",5"-tri-OCH_3
34: R_1 = 3'-OH, 4'-OCH_3, R_2 = 4,5,6-tri-OCH_3, R_3 = 3",4",5"-tri-OCH_3
35: R_1 = 4'-OCH_3, R_2 = 6-OCH_3, 7-OH, R_3 = 3",4",5"-tri-OCH_3
36: R_1 = 3'-OH, 4'-OCH_3, R_2 = 6,7-di-OCH_3, R_3 = 3",4",5"-tri-OCH_3

Scheme 3.2. Synthetic route to modified indole 10.

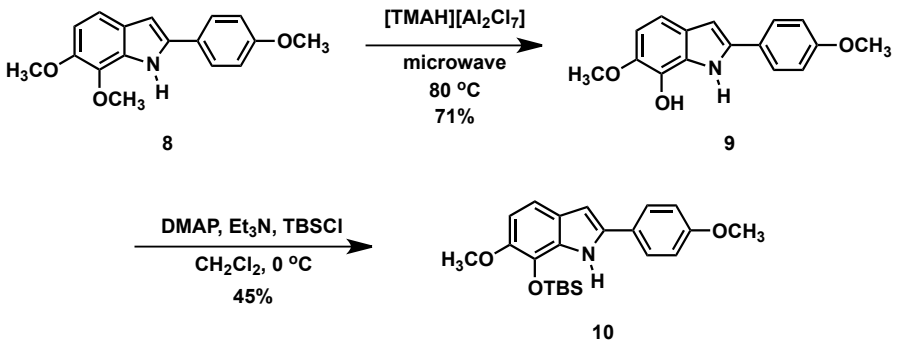

2.2 Biological Evaluation

The series of 2-aryl-3-aroyl indole analogues (Fig. 3) were evaluated for their cytotoxicity against the SK-OV-3, NCI-H460, and DU-145 human cancer cell lines (Table 1) and for their ability to inhibit tubulin assembly (Table 2). The two most active compounds (**35** and **36**) in the series featured substitution at position-7 in the fused aryl ring. Compound **36** (7-methoxy) was comparable to **OXi8006** in terms of both cytotoxicity (sub-micromolar) and inhibition of tubulin assembly (IC_{50} = 1.1 μM), and analogue **35**, in which the hydroxyl group was transposed from the pendant 2-aryl ring to position-7 of the fused aryl ring, was nearly equipotent. Replacement of the 6-methoxy group with a 6-hydroxy moiety (analogue **33**) resulted in a loss of antitubulin activity (> 20 μM) and a significant decrease in cytotoxicity. All structural modifications in the 3-aroyl moiety that replaced the 3,4,5-trimethoxy motif (inherent to **OXi8006**) with a different functionality resulted in a decrease in cytotoxicity (compared to **OXi8006** and the reference stilbene compound, **CA4**). However, the 3,5-*bis*-trifluoromethyl analogue (**30**) and the 3-trifluoromethoxy derivative (**31**) remained relatively good inhibitors of tubulin assembly (3.1 and 3.7 μM, respectively). Although selective fluorine substitution

in **CA4** analogues has been generally well-tolerated,[51] this trend did not carry forward to this indole series of compounds. A 3,4,5-trifluoro analogue (**28**) demonstrated only modest inhibition of tubulin assembly (7.5 μM), while a 3-fluoro derivative (**29**) was inactive (> 20 μM) in this assay. Nitro-bearing analogues (**25**-**27**) were similarly inactive. These results suggest the importance of the 3,4,5-trimethoxy substitution pattern in the 3-aroyl moiety and appropriate substitution at positions 6 and 7 of the fused aryl ring for maintaining potent cytotoxicity and inhibition of tubulin assembly in this series of compounds.

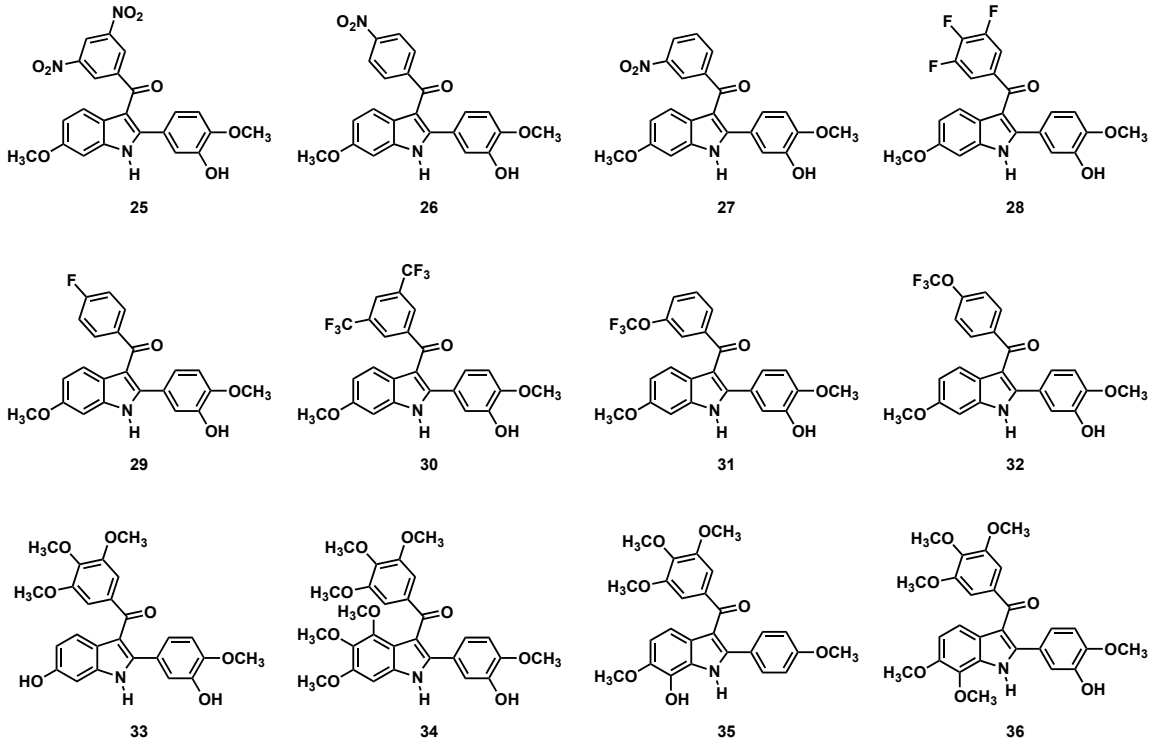

Figure 3.3. Molecular structures of synthesized 2-aryl-3-aroylindole analogues **25-36**.

Table 3.1. Cytotoxicity against human cancer cell lines SK-OV-3, NCI-H460, and DU-145

	GI_{50} (μM) ± SD Sulforhodamine B assay[a]		
Compound	SK-OV-3	NCI-H460	DU-145
CA4	0.00533 ± 0.00180	0.00449 ± 0.0000648[b]	0.00484 ± 0.000848[b]
OXi8006	0.00345 ± 0.000409	0.0379 ± 0.00182	0.0356 ± 0.00107
25	4.35 ± 0.290	4.08 ± 0.119	5.52 ± 0.106
26	21.1 ± 2.45	16.8 ± 2.13	8.16 ± 4.41
27	2.65 ± 1.94	15.7 ± 1.64	7.11 ± 2.16
28	19.8 ± 3.95	5.54 ± 0.505	10.0 ± 9.83
29	15.0 ± 9.60	49.6 ± 3.20	10.0 ± 4.21
30	1.45 ± 0.365	2.86 ± 0.104	3.01 ± 0.0829
31	0.283 ± 0.0395	3.57 ± 0.508	2.99 ± 0.235
32	3.05 ± 0.895	2.35 ± 0.159	3.21 ± 0.294
33	2.167 ± 0.3657	2.910 ± 0.4833	3.401 ± 1.471
34	25.1 ± 0.262	41.8 ± 2.52	28.3 ± 18.0
35	0.264 ± 0.0418	0.177 ± 0.0245	0.309 ± 0.0143
36	0.0119 ± 0.00422	0.992 ± 0.320	0.0181 ± 0.000772

[a] Average of $n \geq 3$ independent determinations. [b] For additional data see refs. 15-16.

Table 3.2. Inhibition of tubulin polymerization and colchicine binding

Compound	Inhibition of tubulin polymerization IC_{50} (μM) ± SD	Inhibition of colchicine binding (%) ± SD	
		1 μM	5 μM
CA4	1.3 ± 0.07	88 ± 2	98 ± 0.5
OXi8006	1.1 ± 0.04	40 ± 0.2	75 ± 0.2
25	> 20	nd[a]	nd
26	> 20	nd	nd
27	19 ± 0.8	nd	21 ± 1
28	7.5 ± 2	nd	26 ± 2
29	> 20	nd	nd
30	3.1 ± 0.2	nd	26 ± 2
31	3.7 ± 0.4	nd	19 ± 4
32	> 20	nd	nd
33	> 20	nd	nd
34	> 20	nd	nd
35	1.0 ± 0.1	51 ± 0.4	85 ± 0.7
36	1.1 ± 0.4	31 ± 4	67 ± 3

[a] nd = not determined in this study.

3. Conclusion

In summary, the results of this study have significantly extended our knowledge of functional group tolerability for 2-aryl-3-aroyl indole analogues. The most promising new analogues (**35**, **36**) demonstrated inhibition of tubulin assembly comparable to the reference compounds **OXi8006** and **CA4**, and future studies will evaluate these

compounds (as their corresponding water-soluble phosphate prodrug salts) for their potential to function as VDAs.

4. Experimental

4.1 Chemistry

4.1.1 Materials and instrumentation

CH_2Cl_2 and tetrahydrofuran (THF) were used in their anhydrous forms, as obtained from the chemical suppliers. Reactions were performed under an inert atmosphere using nitrogen gas, unless specified otherwise. Thin-layer chromatography (TLC) plates (precoated glass plates with silica gel 60 F254, 0.25 mm thickness) were used to monitor reactions. Purification of intermediates and products was carried out with a flash purification system (Biotage Isolera 1 or 4) using silica gel (200-400 mesh, 60 Å) prepacked columns. Reactions carried out under microwave irradiation were performed with a Biotage Initiator Microwave Synthesizer. Intermediates and products synthesized were characterized on the basis of their ^{1}H NMR (500 MHz), ^{13}C NMR (125 MHz), and ^{19}F NMR (470 MHz) spectroscopic data using a Varian VNMRS 500 MHz instrument. Spectra were recorded in $CDCl_3$, $(CD_3)_2SO$, or $(CD_3)_2CO$. All of the chemical shifts are expressed in ppm (δ), coupling constants (*J*) are presented in Hz, and peak patterns are reported as broad (br), singlet (s), doublet (d), triplet (t), double doublet (dd), double triplet (dt), triplet of triplets (tt), doublet of doublets of doublets (ddd), and multiplet (m). Purity of the final compounds was further analyzed at 25 °C using an Agilent 1200 HPLC system with a diode-array detector (λ = 190-400 nm), a Zorbax XDB-C18 HPLC column (4.6 mm - 150 mm, 5 μm), and a Zorbax reliance cartridge guard-column; solvent A: acetonitrile, solvent B: H_2O; gradient: 10%A / 90%B to 100%A / 0%B over 0 to 40 min;

post-time 10 min; flow rate 1.0 mL/min; injection volume 20 μL; monitored at wavelengths of 210, 254, 230, 280, and 360 nm. Mass spectrometry was carried out under positive ESI (electrospray ionization) using a Thermo scientific LTQ Orbitrap Discovery instrument.

4.1.2. 2-(3′-*tert*-Butyldimethylsilyloxy-4′-methoxyphenyl)-6-methoxyindole (5)[37]

To a solution of *m*-anisidine (2.05 mL, 18.4 mmol) dissolved in *N,N*-dimethylaniline (20 mL) at 170 ºC was added dropwise bromoacetophenone **3** (2.0 g, 5.6 mmol) in EtOAc (5 mL). The reaction mixture was stirred at 170 ºC for 12 h. Upon completion of the reaction, the reaction mixture was cooled to room temperature and extracted with EtOAc (3 x 50 mL). The combined organic extract was dried over Na_2SO_4 and concentrated under reduced pressure. Purification by flash chromatography using a prepacked 25 g silica column [solvent A: EtOAc; solvent B: hexanes; gradient: 12%A / 88%B (4 CV), 12%A / 88%B → 100%A / 0%B (10 CV), 100%A / 0%B (2.6 CV); flow rate: 25 mL/min; monitored at 254 and 280 nm] resulted in the desired 2-phenylindole derivative **5** (1.49 g, 3.88 mmol, 69%, R_f = 0.48 (50:50 hexanes:EtOAc)) as light tan crystals. **^{1}H NMR** ($CDCl_3$, 500 MHz): δ 8.11 (br s, 1H, NH), 7.47 (d, *J* = 8.5 Hz, 1H, ArH), 7.16 (dd, *J* = 8.5 Hz, 2.0 Hz 1H, ArH), 7.13 (d, *J* = 2.5 Hz, 1H, ArH), 6.90 (d, *J* = 8.5 Hz, 1H, ArH), 6.89 (d, *J* = 2.5 Hz, 1H, ArH), 6.79 (dd, *J* = 8.5 Hz, 2.5 Hz, 1H, ArH), 6.64 (dd, *J* = 2.0 Hz, 1.0 Hz 1H, ArH), 3.86 (s, 3H, OCH_3), 3.84 (s, 3H, OCH_3), 1.04 (s, 9H, $C(CH_3)_3$), 0.21 (s, 6H, $Si(CH_3)_2$). **^{13}C NMR** ($CDCl_3$, 125 MHz): δ 156.3, 150.5, 145.4, 137.4, 136.9, 125.8, 123.7, 120.9, 118.2, 117.8, 112.4, 109.9, 98.6, 94.5, 55.6, 55.4, 25.7, 18.5, -4.6.

4.1.3. 2-(3′-*tert*-Butyldimethylsilyloxy-4′-methoxyphenyl)-6-*tert*-butyldimethylsilyloxyindole (6)

To a solution of 3-(*tert*-butyldimethylsilyloxy)aniline (2.06 g, 9.21 mmol) in *N*,*N*-dimethylaniline (20 mL) at 170 ºC was added compound **3** (1.00 g, 2.79 mmol) dropwise in EtOAc (5 mL). The reaction mixture was stirred at 170 ºC for 12 h. Upon completion of the reaction, the reaction mixture was cooled to room temperature and extracted with EtOAc (3 x 50 mL). The combined organic extract was dried over Na_2SO_4 and concentrated under reduced pressure. Purification by flash chromatography using a prepacked 100 g silica column [solvent A: EtOAc; solvent B: hexanes; gradient: 2%A / 98%B (4 CV), 2%A / 98%B → 20%A / 80%B (10 CV), 20%A / 80%B (2 CV); flow rate: 40 mL/min; monitored at 254 and 280 nm] resulted in the desired 2-phenylindole **6** (0.59 g, 1.23 mmol, 44%, R_f = 0.39 (90:10 hexanes:EtOAc)) as a brown solid. **^{1}H NMR** ($CDCl_3$, 500 MHz): δ 8.09 (br s, 1H, NH), 7.37 (d, *J* = 8.5 Hz, 1H, ArH), 7.10 (d, *J* = 1.5 Hz, 1H, ArH), 7.01 (dd, *J* = 8.5 Hz, 1.5 Hz, 1H, ArH), 6.82 (s, 1H, ArH), 6.72 (d, *J* = 8.5 Hz, 1H, ArH), 6.67 (dd, *J* = 8.5 Hz, 1.5 Hz, 1H, ArH), 6.54 (s, 1H, ArH), 3.70 (s, 3H, OCH_3), 1.02 (s, 9H, $C(CH_3)_3$), 1.01 (s, 9H, $C(CH_3)_3$), 0.20 (s, 6H, $Si(CH_3)_2$), 0.18 (s, 6H, $Si(CH_3)_2$). **^{13}C NMR** ($CDCl_3$, 125 MHz): δ 150.7, 150.6, 145.4, 137.7, 137.3, 126.0, 124.5, 120.6, 118.5, 118.0, 114.6, 112.4, 101.8, 98.7, 55.4, 25.93, 25.89, 18.6, 18.4, -4.3, -4.5. **HPLC**: 25.45 min., purity at 254 nm >99%. **HRMS (ESI$^+$)**: *m/z* calculated for $C_{27}H_{42}NO_3Si_2$ $[M+H]^+$ 484.2698, found 484.2698.

4.1.4. 2-(3′-*tert*-Butyldimethylsilyloxy-4′-methoxyphenyl)-4,5,6-trimethoxyindole (7)

To a solution of 3,4,5-trimethoxyaniline (0.336 g, 1.84 mmol) in *N*,*N*-dimethylaniline (20 mL) at 170 ºC was added compound **3** (0.20 g, 0.56 mmol) dropwise

in EtOAc (5 mL). The reaction mixture was stirred at 170 ºC for 12 h. Upon completion of the reaction, the reaction mixture was cooled to room temperature and extracted with EtOAc (3 x 50 mL). The combined organic extract was dried over Na_2SO_4 and concentrated under reduced pressure. Purification by flash chromatography using a prepacked 50 g silica column [solvent A: EtOAc; solvent B: hexanes; gradient: 7%A / 93%B (4 CV), 7%A / 93%B → 60%A / 40%B (10 CV), 60%A / 40%B (2 CV); flow rate: 40 mL/min; monitored at 254 and 280 nm] resulted in the desired 2-phenylindole **7** (0.14 g, 0.32 mmol, 58%, R_f = 0.31 (70:30 hexanes:EtOAc)) as colorless crystals. **^{1}H NMR** ($CDCl_3$, 500 MHz): δ 8.06 (br s, 1H, NH), 7.15 (dd, *J* = 8.5 Hz, 2.0 Hz, 1H, ArH), 7.10 (d, *J* = 2.0 Hz, 1H, ArH), 6.90 (d, *J* = 8.5 Hz, 1H, ArH), 6.70 (dd, *J* = 2.0 Hz, 1.0 Hz, 1H, ArH), 6.66 (d, *J* = 0.5 Hz, 1H, ArH), 4.13 (s, 3H, OCH_3), 3.90 (s, 3H, OCH_3), 3.88 (s, 3H, OCH_3), 3.84 (s, 3H, OCH_3), 1.03 (s, 9H, $C(CH_3)_3$), 0.19 (s, 6H, $Si(CH_3)_2$). **^{13}C NMR** ($CDCl_3$, 125 MHz): δ 151.0, 150.6, 145.6, 145.5, 136.4, 135.8, 133.9, 125.8, 118.3, 117.9, 116.6, 112.5, 96.3, 89.8, 61.6, 60.9, 56.2, 55.2, 25.9, 18.5, -4.6. **HPLC**: 20.17 min., purity at 254 nm 94.2%. **HRMS (ESI$^+$)**: *m/z* calculated for $C_{24}H_{34}NO_5Si$ $[M+H]^+$ 444.2201, found 443.2200.

4.1.5. 2-(4′-Methoxyphenyl)-6,7-dimethoxyindole (8)

To a solution of 2,3-dimethoxyaniline (0.92 mL, 6.85 mmol) dissolved in *N*,*N*-dimethylaniline (10 mL) was added 4-methoxybromoacetophenone **4** (0.79 g, 3.43 mmol). The solution was heated to reflux and stirred at 150 ºC for 12 h. Upon completion of the reaction, the reaction mixture was cooled to room temperature and extracted with EtOAc (3 x 50 mL). The combined organic extract was dried over Na_2SO_4 and concentrated under reduced pressure. Purification by flash chromatography using a

prepacked 100 g silica column [solvent A: EtOAc; solvent B: hexanes; gradient: 5%A / 95%B (4 CV), 5%A / 95%B → 40%A / 60%B (10 CV), 40%A / 60%B (4 CV); flow rate: 40 mL/min; monitored at 254 and 280 nm] resulted in the desired 6,7-dimethoxy-2-phenylindole **8** (0.50 g, 1.76 mmol, 51%, R_f = 0.35 (80:20 hexanes:EtOAc)) as a tan solid. **^{1}H NMR** ($CDCl_3$, 500 MHz): δ 8.61 (br s, 1H, NH), 7.61 (d, *J* = 8.7 Hz, 2H, ArH), 7.28 (d, *J* = 8.5 Hz, 1H, ArH), 6.97 (d, *J* = 8.7 Hz, 2H, ArH), 6.87 (d, *J* = 8.6 Hz, 1H, ArH), 6.66 (d, *J* = 2.1 Hz, 1H, ArH), 4.09 (s, 3H, OCH_3), 3.97 (s, 3H, OCH_3), 3.85 (s, 3H, OCH_3). **^{13}C NMR** ($CDCl_3$, 125 MHz): δ 159.2, 147.1, 138.0, 134.2, 131.3, 126.4, 126.0, 125.3, 115.3, 114.5, 108.5, 98.8, 61.1, 57.4, 55.4. **HPLC**: 15.30 min., purity at 254 nm 90.6%. **HRMS (ESI$^+$)**: *m/z* calculated for $C_{17}H_{18}NO_3$ $[M+H]^+$ 284.1281, found 284.1282.

4.1.6. 2-(4′-Methoxyphenyl)-6-methoxy-7-hydroxyindole (9)

Trimethoxyindole **8** (0.61 g, 2.16 mmol) was dissolved in a solution of $[Al_2Cl_7][TMAH]$ (6.3 mL, 3.13 mmol, 0.496 M in CH_2Cl_2). The reaction mixture was sealed and subjected to microwave irradiation at 80 ºC for 1 h. Upon completion of the reaction, the reaction mixture was diluted with $NaHCO_3$ and extracted with CH_2Cl_2 (3 x 20 mL). The combined organic extract was dried over Na_2SO_4 and concentrated under reduced pressure. Purification by flash chromatography using a prepacked 100 g silica column [solvent A: EtOAc; solvent B: hexanes; gradient: 7%A / 93%B (4 CV), 7%A / 93%B → 60%A / 40%B (10 CV), 60%A / 40%B (2 CV); flow rate: 40 mL/min; monitored at 254 and 280 nm] resulted in the desired 6-methoxy-7-hydroxy-2-phenylindole **9** (0.42 g, 1.55 mmol, 71%, R_f = 0.36 (70:30 hexanes:EtOAc)) as a tan solid. **^{1}H NMR** ($(CD_3)_2CO$, 500 MHz): δ 10.11 (br s, 1H, NH), 7.85 (d, *J* = 8.7 Hz, 2H,

Ar<u>H</u>), 7.66 (s, 1H, O<u>H</u>), 6.98 (m, 3H, Ar<u>H</u>), 6.81 (d, *J* = 8.5 Hz, 1H, Ar<u>H</u>), 6.66 (d, *J* = 2.2 Hz, 1H, Ar<u>H</u>), 3.83 (s, 3H, OC<u>H</u>$_3$), 3.81 (s, 3H, OC<u>H</u>$_3$). **^{13}C NMR** ((CD$_3$)$_2$CO, 125 MHz): δ 159.9, 142.5, 138.8, 133.1, 128.4, 127.2, 127.1, 126.5, 115.0, 111.3, 108.9, 99.0, 58.3, 55.7. **HPLC**: 13.47 min., purity at 254 nm 85.8%. **HRMS (ESI$^+$)**: *m/z* calculated for $C_{16}H_{16}NO_3$ $[M+H]^+$ 270.1125, found 270.1129.

4.1.7. 2-(4′-Methoxyphenyl)-6-methoxy-7-*tert*-butyldimethylsilyloxyindole (10)

To a solution of free phenol indole **9** (0.08 g, 0.28 mmol) in CH_2Cl_2 (5 mL) at 0 ºC was added Et_3N (0.04 mL, 0.31 mmol) and DMAP (0.01 g, 0.11 mmol). The reaction mixture was stirred for 10 min, and TBSCl (0.05 g, 0.31 mmol) was added gradually. The solution was allowed to warm to room temperature over 12 h. Upon completion of the reaction, water (10 mL) was added, and the reaction mixture was extracted with CH_2Cl_2 (3 x 50 mL). The combined organic extract was dried over Na_2SO_4 and concentrated under reduced pressure. Purification by flash chromatography using a prepacked 25 g silica column [solvent A: EtOAc; solvent B: hexanes; gradient: 2%A / 98%B (4 CV), 2%A / 98%B → 20%A / 80%B (10 CV), 20%A / 80%B (5.2 CV); flow rate: 35 mL/min; monitored at 254 and 280 nm] resulted in the TBS indole product **10** (0.05 g, 0.02 mmol, 45%, R_f = 0.64 (70:30 hexanes:EtOAc))) as a light tan solid. **^{1}H NMR** ($CDCl_3$, 500 MHz): δ 8.03 (br s, 1H, N<u>H</u>), 7.53 (d, *J* = 8.7, 2H, Ar<u>H</u>), 7.13 (d, *J* = 8.5 Hz, 1H, Ar<u>H</u>), 6.98 (d, *J* = 8.7 Hz, 2H, Ar<u>H</u>), 6.80 (d, *J* = 8.5 Hz, 1H, Ar<u>H</u>), 6.61 (d, *J* = 2.2 Hz, 1H, Ar<u>H</u>), 3.86 (s, 6H, OC<u>H</u>$_3$), 1.11 (s, 9H, C(C<u>H</u>$_3$)$_3$), 0.24 (s, 6H, Si(C<u>H</u>$_3$)$_2$). **^{13}C NMR** ($CDCl_3$, 125 MHz): δ 159.3, 145.2, 137.5, 131.2, 130.2, 126.2, 125.9, 125.6, 114.6, 112.9, 108.5, 99.0, 57.0, 55.5, 26.3, 18.8, -4.2. **HPLC**: 21.73 min., purity at 254

nm 93.7%. **HRMS (ESI$^+$)**: *m/z* calculated for $C_{22}H_{30}NO_3Si$ $[M+H]^+$ 384.1989, found 384.1990.

4.1.8. 2-(3′-*tert*-Butyldimethylsilyloxy-4′-methoxyphenyl)-6,7-dimethoxyindole (11)

To a solution of 2,3-dimethoxyaniline (2.19 mL, 16.3 mmol) dissolved in *N*,*N*-dimethylaniline (20 mL) was added bromoacetophenone **3** (2.93 g, 8.16 mmol). The solution was heated to reflux and stirred at 150 ºC for 12 h. Upon completion of the reaction, the reaction mixture was cooled to room temperature and extracted with EtOAc (3 x 50 mL). The combined organic extract was dried over Na_2SO_4 and concentrated under reduced pressure. Purification by flash chromatography using a prepacked 50 g silica column [solvent A: EtOAc; solvent B: hexanes; gradient: 5%A / 95%B (4 CV), 5%A / 95%B → 40%A / 60%B (10 CV), 40%A / 60%B (2 CV); flow rate: 50 mL/min; monitored at 254 and 280 nm] resulted in the desired 6,7-dimethoxy-2-phenylindole **11** (1.43 g, 3.47 mmol, 43%, R_f = 0.40 (80:20 hexanes:EtOAc)) as a tan solid. **^{1}H NMR** ($CDCl_3$, 500 MHz): δ 8.63 (br s, 1H, NH), 7.33 (d, *J* = 8.5 Hz, 1H, ArH), 7.28 (d, *J* = 2.2 Hz, 1H, ArH), 7.26 (dd, *J* = 8.5 Hz, 2.2 Hz 1H, ArH), 6.92 (dd, *J* = 8.4 Hz, 1.4 Hz, 2H, ArH), 6.71 (d, *J* = 2.2 Hz, 1H, ArH), 4.15 (s, 3H, OCH_3), 4.01 (s, 3H, OCH_3), 3.88 (s, 3H, OCH_3), 1.15 (s, 9H, $C(CH_3)_3$), 0.31 (s, 6H, $Si(CH_3)_2$). **^{13}C NMR** ($CDCl_3$, 125 MHz): δ 150.7, 147.1, 145.4, 137.9, 134.2, 131.2, 126.0, 125.7, 118.4, 118.1, 115.2, 112.3, 108.7, 99.0, 60.9, 57.3, 55.4, 25.8, 18.5, -4.5. **HPLC**: 21.28 min., purity at 254 nm >99%. **HRMS (ESI$^+$)**: *m/z* calculated for $C_{23}H_{32}NO_4Si$ $[M+H]^+$ 414.2095, found 414.2095.

4.1.9. 2-(3′-*tert*-Butyldimethylsiloxy-4′-methoxyphenyl)-3-(3′′,5′′dinitrobenzoyl)-6-methoxyindole (13)

To a solution of compound **5** (0.50 g, 1.30 mmol) in *o*-dichlorobenzene (20 mL) was added 3,5-dinitrobenzoylchloride (0.45 g, 1.90 mmol). The reaction mixture was heated to reflux at 160 ºC for 12 h. The *o*-dichlorobenzene was removed by simple distillation, and the resulting dark colored solid was subjected to flash chromatography using a prepacked 50 g silica column [solvent A: EtOAc; solvent B: hexanes; gradient: 7%A / 93%B (4 CV), 7%A / 93%B → 60%A / 40%B (11 CV), 60%A / 40%B (2 CV); flow rate: 40 mL/min; monitored at 254 and 280 nm] resulting in TBS-indole **13** as a pale yellow powder (0.40 g, 0.69 mmol, 53%, R_f = 0.59 (70:30 hexanes:EtOAc)). **^{1}H NMR** ($CDCl_3$, 500 MHz): δ 8.85 (t, *J* = 2.0 Hz, 1H, Ar<u>H</u>), 8.62 (d, *J* = 2.0 Hz, 2H, Ar<u>H</u>), 8.60 (br s, 1H, N<u>H</u>) 8.15 (d, *J* = 8.5 Hz, 1H, Ar<u>H</u>), 7.00 (dd, *J* = 8.5 Hz, 2.0 Hz, 1H, Ar<u>H</u>), 6.95 (d, 2.0 Hz, 1H, Ar<u>H</u>), 6.87 (dd, *J* = 8.0 Hz, 2.0 Hz, 1H, Ar<u>H</u>), 6.61 (d, *J* = 8.5 Hz, 1H, Ar<u>H</u>), 6.56 (d, *J* = 2.5 Hz, 1H, Ar<u>H</u>), 3.90 (s, 3H, OC<u>H</u>$_3$), 3.70 (s, 3H, OC<u>H</u>$_3$), 0.89 (s, 9H, C(C<u>H</u>$_3$)$_3$), 0.00 (s, 6H, Si(C<u>H</u>$_3$)$_2$). **^{13}C NMR** ($CDCl_3$, 125 MHz): δ 187.3, 158.1, 152.1, 147.8, 145.3, 145.1, 143.1, 136.5, 129.1, 123.5, 123.4, 122.7, 122.4, 122.3, 120.1, 112.8, 112.5, 111.8, 95.0, 55.9, 55.5, 25.6, 18.4, -4.8. **HPLC**: 20.28 min., purity at 254 nm 93.1%. **HRMS (ESI$^+$)**: *m/z* calculated for $C_{29}H_{32}N_3O_8Si$ $[M+H]^+$ 578.1953, found 578.1950.

4.1.10. 2-(3′-*tert*-Butyldimethylsiloxy-4′-methoxyphenyl)-3-(4′′-nitrobenzoyl)-6-methoxyindole (14)

To a solution of compound **5** (0.20 g, 0.52 mmol) in *o*-dichlorobenzene (10 mL) was added 3-nitrobenzoylchloride (0.15 g, 0.78 mmol). The reaction mixture was heated

to reflux at 160 ºC for 12 h. The *o*-dichlorobenzene was removed by simple distillation, and the resulting dark colored solid was subjected to flash chromatography using a prepacked 100 g silica column [solvent A: EtOAc; solvent B: hexanes; gradient: 7%A / 93%B (4 CV), 7%A / 93%B → 60%A / 40%B (10 CV), 60%A / 40%B (8.8 CV); flow rate: 40 mL/min; monitored at 254 and 280 nm] resulting in TBS-indole **14** as a yellow powder (0.14 g, 0.28 mmol, 51%, R_f = 0.36 (70:30 hexanes:EtOAc)). **^{1}H NMR** ($CDCl_3$, 500 MHz): δ 8.37 (br s, 1H, NH), 8.06 (d, *J* = 8.5 Hz, 1H, ArH), 7.97 (d, *J* = 8.5 Hz, 2H, ArH) 7.69 (d, *J* = 8.5 Hz, 2H, ArH), 6.97 (dd, *J* = 8.5 Hz, 2.0 Hz, 1H, ArH), 6.93 (d, *J* = 2.5 Hz, 1H, ArH), 6.75 (m, 2H, ArH), 6.58 (d, *J* = 8.0 Hz, 1H, ArH), 3.89 (s, 3H, OCH_3), 3.71 (s, 3H, OCH_3), 0.97 (s, 9H, $C(CH_3)_3$), 0.07 (s, 6H, $Si(CH_3)_2$). **^{13}C NMR** ($CDCl_3$, 125 MHz): δ 190.9, 157.8, 152.1, 148.9, 145.6, 145.2, 144.4, 136.5, 130.3, 124.1, 123.7, 123.0, 122.69, 122.67, 121.7, 113.0, 112.3, 111.7, 94.9, 55.9, 55.6, 25.8, 18.6, -4.6. **HPLC**: 20.23 min., purity at 254 nm >99%. **HRMS (ESI$^+$)**: *m/z* calculated for $C_{29}H_{33}N_2O_6Si$ $[M+H]^+$ 533.2102, found 533.2100.

4.1.11. 2-(3′-*tert*-Butyldimethylsiloxy-4′-methoxyphenyl)-3-(3′′-nitrobenzoyl)-6-methoxyindole (15)

To a solution of compound **5** (0.10 g, 0.26 mmol) in *o*-dichlorobenzene (10 mL) was added 3-nitrobenzoylchloride (0.07 g, 0.39 mmol). The reaction mixture was heated to reflux at 160 ºC for 12 h. The *o*-dichlorobenzene was removed by simple distillation, and the resulting dark colored solid was subjected to flash chromatography using a prepacked 25 g silica column [solvent A: EtOAc; solvent B: hexanes; gradient: 12%A / 88%B (4 CV), 12%A / 88%B → 100%A / 0%B (10 CV), 100%A / 0%B (2.8 CV); flow rate: 25 mL/min; monitored at 254 and 280 nm] resulting in TBS-indole **15** as pale

yellow crystals (0.13 g, 0.25 mmol, 94%, R_f = 0.63 (50:50 hexanes:EtOAc)). **^{1}H NMR** ($CDCl_3$, 500 MHz): δ 9.15 (br s, 1H, NH), 8.30 (t, *J* = 2.0 Hz, 1H, ArH), 8.06 (ddd, *J* = 8.0 Hz, 2.0 Hz, 1.0 Hz, 1H, ArH) 8.03 (d *J* = 9.5 Hz, 1H, ArH), 7.88 (dt, *J* = 8.0 Hz, 1.0 Hz, 1H, ArH), 7.29 (t, *J* = 8.0 Hz, 1H, ArH), 6.92 (dd, *J* = 7.0 Hz, 2.0 Hz, 1H, ArH), 6.91 (d, *J* = 2.0 Hz, 1H, ArH), 6.78 (dd, *J* = 8.0 Hz, 2.0 Hz, 1H, ArH), 6.66 (d, *J* = 2.5 Hz, 1H, ArH), 6.50 (d, *J* = 8.5 Hz, 1H, ArH), 3.82 (s, 3H, OCH_3), 3.65 (s, 3H, OCH_3), 0.91 (s, 9H, $C(CH_3)_3$), 0.00 (s, 6H, $Si(CH_3)_2$). **^{13}C NMR** ($CDCl_3$, 125 MHz): δ 190.4, 157.6, 151.7, 147.4, 144.9, 144.6, 141.3, 136.6, 135.0, 128.9, 125.4, 124.7, 124.1, 123.4, 122.7, 122.3, 122.0, 112.4, 112.3, 111.6, 94.9, 55.7, 55.4, 25.7, 18.4, -4.7. **HPLC**: 20.13 min., purity at 254 nm >99%. **HRMS (ESI$^+$)**: *m/z* calculated for $C_{29}H_{33}N_2O_6Si$ $[M+H]^+$ 533.2102, found 533.2100.

4.1.12. 2-(3′-*tert*-Butyldimethylsiloxy-4′-methoxyphenyl)-3-(3′′,4′′,5′′-trifluorobenzoyl)-6-methoxyindole (16)

To a solution of compound **5** (0.61 g, 1.59 mmol) in *o*-dichlorobenzene (10 mL) was added 3,4,5-trifluorobenzoylchloride (3.12 mL, 2.38 mmol). The reaction mixture was heated to reflux at 160 °C for 12 h. The *o*-dichlorobenzene was removed by simple distillation, and the resulting dark colored solid was subjected to flash chromatography using a prepacked 100 g silica column [solvent A: EtOAc; solvent B: hexanes; gradient: 7%A / 93%B (4 CV), 7%A / 97%B → 60%A / 40%B (10 CV), 60%A / 40%B (5.5 CV); flow rate: 40 mL/min; monitored at 254 and 280 nm] resulting in TBS-indole **16** as a white powder (0.70 g, 1.29 mmol, 81%, R_f = 0.48 (50:50 hexanes:EtOAc)). **^{1}H NMR** ($CDCl_3$, 500 MHz): δ 8.44 (br s, 1H, NH), 7.95 (d, *J* = 9.0 Hz, 1H, ArH), 7.25 (m, 2H, ArH) 6.94 (dd, *J* = 8.5 Hz, 2.5 Hz, 1H, ArH), 6.91 (d, *J* = 2.0 Hz, 1H, ArH), 6.83 (dd, *J* =

8.0 Hz, 2.0 Hz, 1H, Ar<u>H</u>), 6.79 (d, J = 2.0 Hz, 1H, Ar<u>H</u>), 6.70 (d, J = 8.5 Hz, 1H, Ar<u>H</u>), 3.87 (s, 3H, OC<u>H</u>$_3$), 3.78 (s, 3H, OC<u>H</u>$_3$), 0.97 (s, 9H, C(C<u>H</u>$_3$)$_3$), 0.09 (s, 6H, Si(C<u>H</u>$_3$)$_2$). **^{13}C NMR** ($CDCl_3$, 125 MHz): δ 189.1, 157.7, 152.1, 150.6 (ddd, $J_{C\text{-}F}$ = 250.0 Hz, 10.0 Hz, 3.1 Hz), 145.4, 143.5, 141.8 (dt, $J_{C\text{-}F}$ = 255.9 Hz, 15.5 Hz), 136.5, 135.6 (d, $J_{C\text{-}F}$ = 3.9 Hz), 124.4, 123.2, 122.8, 121.4, 121.6, 114.1 (dd, $J_{C\text{-}F}$ = 16.9 Hz, 5.1 Hz), 112.3, 112.2, 112.0, 94.8, 55.9, 55.6, 25.7, 18.5, -4.8. **^{19}F NMR** ($CDCl_3$, 470 MHz): δ -134.0 (dd, J = 21.2 Hz, 7.5 Hz, 2F, Ar<u>F</u>), -155.6 (tt, J = 20.2 Hz, 6.6 Hz, 1F, Ar<u>F</u>). **HPLC**: 21.32 min., purity at 254 nm >99%. **HRMS (ESI$^+$)**: m/z calculated for $C_{29}H_{30}F_3NNaO_4Si$ $[M+Na]^+$ 564.1788, found 564.1786.

4.1.13. 2-(3′-*tert*-Butyldimethylsiloxy-4′-methoxyphenyl)-3-(4′′-fluorobenzoyl)-6-methoxyindole (17)

To a solution of compound **5** (0.10 g, 0.26 mmol) in *o*-dichlorobenzene (10 mL) was added 4-fluorobenzoylchloride (0.05 mL, 0.39 mmol). The reaction mixture was heated to reflux at 160 ºC for 12 h. The *o*-dichlorobenzene was removed by simple distillation, and the resulting dark colored solid was subjected to flash chromatography using a prepacked 25 g silica column [solvent A: EtOAc; solvent B: hexanes; gradient: 12%A / 88%B (4 CV), 12%A / 88%B → 100%A / 0%B (10 CV), 100%A / 0%B (2 CV); flow rate: 25 mL/min; monitored at 254 and 280 nm] resulting in TBS-indole **17** as pale yellow crystals (0.09 g, 0.18 mmol, 69%, R_f = 0.73 (50:50 hexanes:EtOAc)). **^{1}H NMR** ($CDCl_3$, 500 MHz): δ 8.59 (br s, 1H, N<u>H</u>), 7.88 (d, J = 9.5 Hz, 1H, Ar<u>H</u>), 7.65 (m, 2H, Ar<u>H</u>), 6.89 (m, 2H, Ar<u>H</u>), 6.82 (m, 4H, Ar<u>H</u>), 6.60 (d, J = 8.0 Hz, 1H, Ar<u>H</u>), 3.84 (s, 3H, OC<u>H</u>$_3$), 3.73 (s, 3H, OC<u>H</u>$_3$), 0.96 (s, 9H, C(C<u>H</u>$_3$)$_3$), 0.08 (s, 6H, Si(C<u>H</u>$_3$)$_2$). **^{13}C NMR** ($CDCl_3$, 125 MHz): δ 191.7, 164.8 (d, $J_{C\text{-}F}$ = 251 Hz), 157.4, 151.7, 145.1, 142.8, 136.4,

136.09, 136.06, 132.2 (d, $J_{C\text{-}F}$ = 9 Hz), 124.6, 123.4, 123.1, 122.4, 121.6, 114.9 (d, $J_{C\text{-}F}$ = 22 Hz), 113.0, 111.8, 94.7, 55.8, 55.5, 25.8, 18.6, -4.6. **^{19}F NMR** ($CDCl_3$, 470 MHz): δ -108.1 (m, 1F, ArF). **HPLC**: 20.59 min., purity at 254 nm >99%. **HRMS (ESI$^+$)**: *m/z* calculated for $C_{29}H_{33}FNO_4Si$ $[M+H]^+$ 506.2157, found 506.2155.

4.1.14. 2-(3′-*tert*-Butyldimethylsiloxy-4′-methoxyphenyl)-3-(3′′,5′′-*bis*-trifluoromethylbenzoyl)-6-methoxyindole (18)

To a solution of compound **5** (0.20 g, 0.52 mmol) in *o*-dichlorobenzene (15 mL) was added 3,5-*bis*-trifluoromethylbenzoyl chloride (0.14 mL, 0.78 mmol). The reaction mixture was heated to reflux at 160 ºC for 12 h. The *o*-dichlorobenzene was removed by simple distillation, and the resulting dark colored solid was subjected to flash chromatography using a prepacked 50 g silica column [solvent A: EtOAc; solvent B: hexanes; gradient: 7%A / 93%B (4 CV), 7%A / 93%B → 60%A / 40%B (10 CV), 60%A / 40%B (2 CV); flow rate: 40 mL/min; monitored at 254 and 280 nm] resulting in TBS-indole **18** as pale orange crystals (0.26 g, 0.42 mmol, 81%, R_f = 0.47 (70:30 hexanes:EtOAc)). **^{1}H NMR** ($CDCl_3$, 500 MHz): δ 8.70 (br s, 1H, NH), 8.07 (d, *J* = 9.0 Hz, 1H, ArH), 8.03 (s, 2H, ArH) 7.74 (s, 1H, ArH), 6.96 (dd, *J* = 9.0 Hz, 2.5 Hz, 1H, ArH), 6.92 (d, *J* = 2.0 Hz, 1H, ArH), 6.85 (dd, *J* = 8.0 Hz, 2.0 Hz, 1H, ArH), 6.65 (d, *J* = 8.5 Hz, 1H, ArH), 6.62 (d, *J* = 2.5 Hz, 1H, ArH), 3.86 (s, 3H, OCH_3), 3.71 (s, 3H, OCH_3), 0.91 (s, 9H, $C(CH_3)_3$), 0.00 (s, 6H, $Si(CH_3)_2$). **^{13}C NMR** ($CDCl_3$, 125 MHz): δ 189.5, 157.8, 152.0, 145.3, 144.5, 141.5, 136.6, 131.3 (q, $J_{C\text{-}F}$ = 33 Hz), 129.7 (m), 124.47 (q, $J_{C\text{-}F}$ = 7 Hz), 124.46, 124.0, 123.1 (q, $J_{C\text{-}F}$ = 275 Hz), 122.9, 122.7, 122.5, 122.2, 112.4, 112.1, 94.9, 55.8, 55.5, 25.6, 18.4, -4.8. **^{19}F NMR** ($CDCl_3$, 470 MHz): δ -62.8 (s, 6F,

C$\underline{F}_3$). **HPLC**: 22.22 min., purity at 254 nm 96.3%. **HRMS (ESI$^+$)**: *m/z* calculated for $C_{31}H_{32}F_6NO_4Si$ $[M+H]^+$ 624.1999, found 624.1997.

4.1.15. (2-(3′-*tert*-Butyldimethylsilyloxy-4′-methoxyphenyl)-3-(3′′-trifluoromethoxybenzoyl)-6-methoxyindole (19)

To a solution of compound **5** (1.14 g, 2.97 mmol) in *o*-dichlorobenzene (15 mL) was added 3-trifluoromethoxybenzoylchloride (0.70 mL, 4.45 mmol). The reaction mixture was heated to reflux at 170 ºC for 12 h. The *o*-dichlorobenzene was removed by simple distillation, and the resulting dark green colored solid was subjected to flash chromatography using a prepacked 50 g silica column [solvent A: EtOAc; solvent B: hexanes; gradient: 7%A / 93%B (4 CV), 7%A / 93%B → 60%A / 40%B (10 CV), 60%A / 40%B (2 CV); flow rate: 40 mL/min; monitored at 254 and 280 nm] resulting in TBS-indole **19** as a yellow powder (1.21 g, 2.11 mmol, 71%, R_f = 0.43 (70:30 hexanes:EtOAc)). **^{1}H NMR** ($CDCl_3$, 500 MHz): δ 8.31 (br s, 1H, N$\underline{H}$), 7.96 (d, *J* = 8.4 Hz, 1H, Ar$\underline{H}$), 7.52 (dt, *J* = 7.5 Hz, 1.3 Hz, 1H, Ar$\underline{H}$) 7.48 (s, 1H, Ar$\underline{H}$), 7.17 (t, *J* = 7.8 Hz, 1H, Ar$\underline{H}$), 7.13 (d, *J* = 8.2 Hz, 1H, Ar$\underline{H}$), 6.93 (m, 2H, Ar$\underline{H}$), 6.81 (m, 2H, Ar$\underline{H}$), 6.62 (d, *J* = 9.0 Hz, 1H, Ar$\underline{H}$), 3.88 (s, 3H, OC$\underline{H}_3$), 3.73 (s, 3H, OC$\underline{H}_3$), 0.97 (s, 9H, C(C$\underline{H}_3$)$_3$), 0.08 (s, 6H, Si(C$\underline{H}_3$)$_2$). **^{13}C NMR** ($CDCl_3$, 125 MHz): δ 191.8, 157.4, 151.6, 148.8, 144.9, 144.1, 142.1, 136.6, 129.2, 128.0, 124.3, 123.6, 123.5, 122.9, 122.2, 122.0, 121.4, 120.4 (q, $J_{C\text{-}F}$ = 256 Hz), 112.6, 112.0, 111.6, 94.8, 55.7, 55.3, 25.7, 18.4, -4.7. **^{19}F NMR** ($CDCl_3$, 470 MHz): δ -57.8 (s, 3F, OC$\underline{F}_3$). **HPLC**: 21.53 min., purity at 254 nm >99%. **HRMS (ESI$^+$)**: *m/z* calculated for $C_{30}H_{33}F_3NO_5Si$ $[M+H]^+$ 572.2075, found 572.2071.

4.1.16. (2-(3′-*tert*-Butyldimethylsilyloxy-4′-methoxyphenyl)-3-(4′′-trifluoromethoxybenzoyl)-6-methoxyindole (20)

To a solution of compound **5** (1.14 g, 2.97 mmol) in *o*-dichlorobenzene (15 mL) was added 3-trifluoromethylbenzoylchloride (0.70 mL, 4.45 mmol). The reaction mixture was heated to reflux at 170 ºC for 12 h. The *o*-dichlorobenzene was removed by simple distillation, and the resulting dark green colored solid was subjected to flash chromatography using a prepacked 50 g silica column [solvent A: EtOAc; solvent B: hexanes; gradient: 7%A / 93%B (4 CV), 7%A / 93%B → 60%A / 40%B (10 CV), 60%A / 40%B (1.1 CV); flow rate: 40 mL/min; monitored at 254 and 280 nm] resulting in TBS-indole **20** as a yellow powder (0.92 g, 1.61 mmol, 54%, R_f = 0.43 (70:30 hexanes:EtOAc)). **^{1}H NMR** ($CDCl_3$, 500 MHz): δ 8.29 (br s, 1H, NH), 8.00 (d, *J* = 8.6 Hz, 1H, ArH), 7.64 (d, *J* = 8.7 Hz, 2H, ArH) 6.97 (d, *J* = 8.0 Hz, 2H, ArH), 6.93 (m, 2H, ArH), 6.83 (d, *J* = 2.2 Hz, 1H, ArH), 6.73 (dd, *J* = 8.3 Hz, 2.2 Hz, 1H, ArH), 6.58 (d, *J* = 8.4 Hz, 1H, ArH), 3.88 (s, 3H, OCH_3), 3.73 (s, 3H, OCH_3), 0.98 (s, 9H, $C(CH_3)_3$), 0.10 (s, 6H, $Si(CH_3)_2$). **^{13}C NMR** ($CDCl_3$, 125 MHz): δ 191.9, 157.3, 151.6, 151.0, 144.8, 144.1, 138.4, 136.6, 131.3, 124.2, 123.8, 122.8, 122.2, 121.4, 120.3 (q, $J_{C\text{-}F}$ = 256 Hz), 119.7, 112.6, 111.9, 111.3, 94.8, 55.6, 55.1, 25.6, 18.4, -4.8. **^{19}F NMR** ($CDCl_3$, 470 MHz): δ -57.7 (s, 3F, OCF_3). **HPLC**: 21.61 min., purity at 254 nm >99%. **HRMS (ESI$^+$)**: *m/z* calculated for $C_{30}H_{33}F_3NO_5Si$ $[M+H]^+$ 572.2075, found 572.2075.

4.1.17. 2-(3′-*tert*-Butyldimethylsiloxy-4′-methoxyphenyl)-3-(3′′,4′′,5′′-trimethoxybenzoyl)-6-*tert*-butyldimethylsiloxyindole (21)

To a solution of compound **6** (0.19 g, 0.39 mmol) in *o*-dichlorobenzene (20 mL) was added 3,4,5-trimethoxybenzoylchloride (0.13 g, 0.58 mmol). The reaction mixture

was heated to reflux at 160 ºC for 12 h. The *o*-dichlorobenzene was removed by simple distillation, and the resulting dark colored solid was subjected to flash chromatography using a prepacked 50 g silica column [solvent A: EtOAc; solvent B: hexanes; gradient: 7%A / 93%B (4 CV), 7%A / 93%B → 60%A / 40%B (10 CV), 60%A / 40%B (2 CV); flow rate: 40 mL/min; monitored at 254 and 280 nm] resulting in di-TBS-indole **21** as a pale yellow powder (0.04 g, 0.59 mmol, 20%, R_f = 0.33 (70:30 hexanes:EtOAc)). **^{1}H NMR** ($CDCl_3$, 500 MHz): δ 8.31 (br s, 1H, NH), 7.90 (d, *J* = 8.5 Hz, 1H, ArH), 6.99 (s, 2H, ArH) 6.94 (dd, *J* = 8.5 Hz, 2.0 Hz, 1H, ArH), 6.89 (d, *J* = 2.0 Hz, 1H, ArH), 6.82 (dd, *J* = 8.5 Hz, 2.0 Hz, 1H, ArH), 6.76 (d, *J* = 2.5 Hz, 1H, ArH), 6.70 (d, *J* = 8.0 Hz, 1H, ArH), 3.79 (s, 3H, OCH$_3$), 3.75 (s, 3H, OCH$_3$), 3.69 (s, 6H, OCH$_3$), 1.01 (s, 9H, C(CH$_3$)$_3$), 0.94 (s, 9H, C(CH$_3$)$_3$), 0.22 (s, 6H, Si(CH$_3$)$_2$), 0.04 (s, 6H, Si(CH$_3$)$_2$). **^{13}C NMR** ($CDCl_3$, 125 MHz): δ 191.8, 153.0, 152.6, 151.7, 145.2, 142.3, 141.3, 136.5, 134.6, 125.2, 123.9, 122.3, 121.9, 116.7, 112.9, 111.8, 107.4, 105.1, 101.6, 60.9, 56.1, 55.5, 25.9, 25.8, 18.46, 18.45, -4.2, -4.8. **HPLC**: 23.31 min., purity at 254 nm 90.6%. **HRMS (ESI$^+$)**: *m/z* calculated for $C_{37}H_{52}NO_7Si_2$ $[M+H]^+$ 678.3277, found 678.3279.

4.1.18. 2-(3′-*tert*-Butyldimethylsiloxy-4′-methoxyphenyl)-3-(3′′,4′′,5′′-trimethoxybenzoyl)-4,5,6-trimethoxyindole (22)

To a solution of compound **7** (0.05 g, 0.11 mmol) in *o*-dichlorobenzene (10 mL) was added 3,4,5-trimethoxybenzoylchloride (0.04 g, 0.17 mmol). The reaction mixture was heated to reflux at 160 ºC for 12 h. The *o*-dichlorobenzene was removed by simple distillation, and the resulting dark green colored solid was subjected to flash chromatography using a prepacked 25 g silica column [solvent A: EtOAc; solvent B: hexanes; gradient: 12%A / 88%B (4 CV), 12%A / 88%B → 100%A / 0%B (10 CV),

100%A / 0%B (2 CV); flow rate: 25 mL/min; monitored at 254 and 280 nm] resulting in TBS-indole **22** as a pale yellow powder (0.03 g, 0.05 mmol, 46%, R_f = 0.50 (50:50 hexanes:EtOAc)). **^{1}H NMR** ($CDCl_3$, 500 MHz): δ 8.25 (br s, 1H, NH), 7.19 (s, 2H, ArH), 6.99 (dd, *J* = 8.5 Hz, 2.5 Hz, 1H, ArH) 6.88 (d, *J* = 2.5 Hz, 1H, ArH), 6.75 (d, *J* = 8.0 Hz, 1H, ArH), 6.69 (s, 1H, ArH), 3.90 (s, 3H, OCH_3), 3.85 (s, 3H, OCH_3), 3.82 (s, 3H, OCH_3), 3.76 (s, 3H, OCH_3), 3.74 (s, 6H, OCH_3), 3.72 (s, 3H, OCH_3), 0.93 (s, 9H, $C(CH_3)_3$), 0.04 (s, 6H, $Si(CH_3)_2$). **^{13}C NMR** ($CDCl_3$, 125 MHz): δ 193.4, 152.9, 152.1, 151.4, 146.4, 145.3, 142.2, 137.8, 136.6, 134.2, 132.4, 124.7, 121.1, 120.5, 116.7, 114.4, 112.3, 107.6, 89.8, 61.4, 61.0, 60.8, 56.4, 56.3, 55.6, 25.8, 18.5, -4.7. **HPLC**: 18.60 min., purity at 254 nm 90.7%. **HRMS (ESI$^+$)**: *m/z* calculated for $C_{34}H_{44}NO_9Si$ $[M+H]^+$ 638.2780, found 638.2780.

4.1.19. 2-(4′-Methoxyphenyl)-3-(3′′,4′′,5′′-trimethoxybenzoyl)-6-methoxy-7-*tert*-butyldimethylsilyloxyindole (23)

To a solution of compound **10** (0.05 g, 0.13 mmol) in *o*-dichlorobenzene (10 mL) was added 3,4,5-trimethoxybenzoylchloride (0.05 g, 0.20 mmol). The reaction mixture was heated to reflux at 160 °C for 12 h. The *o*-dichlorobenzene was removed by simple distillation, and the resulting dark green colored solid was subjected to flash chromatography using a prepacked 25 g silica column [solvent A: EtOAc; solvent B: hexanes; gradient: 10%A / 90%B (4 CV), 10%A / 90%B → 80%A / 20%B (10 CV), 80%A / 20%B (2 CV); flow rate: 25 mL/min; monitored at 254 and 280 nm] resulting in TBS-indole **23** as a yellow powder (0.06 g, 0.10 mmol, 76%, R_f = 0.36 (60:40 hexanes:EtOAc)). **^{1}H NMR** ($CDCl_3$, 500 MHz): δ 8.20 (br s, 1H, NH), 7.56 (d, *J* = 8.7 Hz, 1H, ArH), 7.26 (d, *J* = 9.0 Hz, 2H, ArH), 6.96 (s, 2H, ArH), 6.94 (d, *J* = 8.7 Hz, 1H,

Ar$\underline{H}$), 6.78 (d, J = 8.6 Hz, 2H, Ar$\underline{H}$), 3.88 (s, 3H, OC$\underline{H}_3$), 3.80 (s, 3H, OC$\underline{H}_3$), 3.76 (s, 3H, OC$\underline{H}_3$), 3.70 (s, 6H, OC$\underline{H}_3$), 1.09 (s, 9H, C(C$\underline{H}_3$)$_3$), 0.26 (s, 6H, Si(C$\underline{H}_3$)$_2$). **^{13}C NMR** ($CDCl_3$, 125 MHz): δ 192.0, 160.2, 152.6, 146.0, 142.8, 141.3, 134.9, 130.3, 129.99, 129.95, 125.0, 124.8, 114.4, 114.2, 113.4, 109.9, 107.5, 61.0, 56.7, 56.2, 55.5, 26.3, 18.8, -4.1. **HPLC**: 20.21 min., purity at 254 nm >99%. **HRMS (ESI$^+$)**: *m/z* calculated for $C_{32}H_{39}NNaO_7Si$ $[M+Na]^+$ 600.2388, found 600.2383.

4.1.20. 2-(3′-*tert*-Butyldimethylsiloxy-4′-methoxyphenyl)-3-(3′′,4′′,5′′-trimethoxybenzoyl)-6,7-dimethoxyindole (24)

To a solution of compound **11** (0.25 g, 0.60 mmol) in *o*-dichlorobenzene (10 mL) was added 3,4,5-trimethoxybenzoylchloride (0.15 g, 0.66 mmol). The reaction mixture was heated to reflux at 160 ºC for 12 h. The *o*-dichlorobenzene was removed by simple distillation, and the resulting dark green colored solid was subjected to flash chromatography using a prepacked 50 g silica column [solvent A: EtOAc; solvent B: hexanes; gradient: 7%A / 93%B (4 CV), 7%A / 93%B → 60%A / 40%B (10 CV), 60%A / 40%B (5.2 CV); flow rate: 50 mL/min; monitored at 254 and 280 nm] resulting in TBS-indole **24** as a yellow powder (0.08 g, 0.14 mmol, 23%, R_f = 0.17 (70:30 hexanes:EtOAc)). **^{1}H NMR** ($CDCl_3$, 500 MHz): δ 8.53 (br s, 1H, N$\underline{H}$), 7.71 (d, J = 8.5 Hz, 1H, Ar$\underline{H}$), 6.98 (m, 4H, Ar$\underline{H}$), 6.77 (d, J = 2.0 Hz, 1H, Ar$\underline{H}$), 6.73 (d, J = 8.5 Hz, 1H, Ar$\underline{H}$), 4.06 (s, 3H, OC$\underline{H}_3$), 3.96 (s, 3H, OC$\underline{H}_3$), 3.79 (s, 3H, OC$\underline{H}_3$), 3.76 (s, 3H, OC$\underline{H}_3$), 3.69 (s, 6H, OC$\underline{H}_3$), 0.94 (s, 9H, C(C$\underline{H}_3$)$_3$), 0.03 (s, 6H, Si(C$\underline{H}_3$)$_2$). **^{13}C NMR** ($CDCl_3$, 125 MHz): δ 191.8, 152.6, 151.8, 148.0, 145.2, 142.8, 141.3, 134.6, 134.0, 130.2, 125.2, 125.1, 122.3, 122.2, 116.8, 113.1, 111.8, 110.4, 107.4, 61.3, 60.9, 57.3, 56.1, 55.5, 25.8,

18.5, -4.7. **HPLC**: 19.24 min., purity at 254 nm >99%. **HRMS (ESI$^+$)**: *m/z* calculated for $C_{33}H_{41}NNaO_8Si$ $[M+Na]^+$ 630.2494, found 630.2491.

4.1.21. 2-(3′-Hydroxy-4′-methoxyphenyl)-3-(3′′,5′′-dinitrobenzoyl)-6-methoxyindole (25)

To a well-stirred solution of compound **13** (0.40 g, 0.69 mmol) in THF (10 mL) at 0 ºC was added tetrabutylammonium fluoride (TBAF) (1.03 mL, 1.03 mmol, 1 M in THF) dropwise. The reaction mixture was stirred for 30 min while warming to room temperature. The reaction mixture was quenched with water (10 mL) and extracted with EtOAc (3 x 10 mL). The combined organic extract was dried over Na_2SO_4 and concentrated under reduced pressure. Purification by flash column chromatography using a prepacked 50 g silica column [solvent A: EtOAc; solvent B: hexanes; gradient: 7%A / 93%B (4 CV), 7%A / 93%B → 60%A / 40%B (10 CV), 60%A / 40%B (2 CV); flow rate: 40 mL/min; monitored at 254 and 280 nm] afforded the desired indole free phenol ligand **25** (0.15 g, 0.33 mmol, 47%, R_f = 0.12 (70:30 hexanes:EtOAc)) as a yellow powder. **^{1}H NMR** ($(CD_3)_2SO$, 500 MHz): δ 12.21 (br s, 1H, NH), 9.06 (br s, 1H, OH), 8.68 (t, *J* = 2.0 Hz, 1H, ArH), 8.41 (d, *J* = 2.0 Hz, 2H, ArH), 8.05 (d, *J* = 8.5 Hz, 1H, ArH), 6.97 (d, *J* = 2.0 Hz, 1H, ArH), 6.92 (dd, *J* = 8.5 Hz, 2.0 Hz, 1H, ArH), 6.71 (dd, *J* = 8.0 Hz, 2.0 Hz, 1H, ArH), 6.68 (d, *J* = 8.5 Hz, 1H, ArH), 6.54 (d, *J* = 2.0 Hz, 1H, ArH), 3.83 (s, 3H, OCH_3), 3.65 (s, 3H, OCH_3. **^{13}C NMR** ($(CD_3)_2SO$, 125 MHz): δ 186.7, 156.8, 148.2, 147.1, 146.7, 146.1, 142.8, 136.7, 128.5, 123.3, 121.77, 121.75, 121.7, 119.3, 117.2, 112.0, 111.7, 111.1, 95.0, 55.7, 55.3. **HPLC**: 13.87 min., purity at 254 nm 93.4%. **HRMS (ESI$^+$)**: *m/z* calculated for $C_{23}H_{18}N_3O_8$ $[M+H]^+$ 464.1088, found 464.1087.

4.1.22. 2-(3′-Hydroxy-4′-methoxyphenyl)-3-(4′′-nitrobenzoyl)-6-methoxyindole (26)

To a well-stirred solution of compound **14** (0.14 g, 0.27 mmol) in THF (10 mL) at 0 ºC was added TBAF (0.40 mL, 0.40 mmol, 1 M in THF) dropwise. The reaction mixture was stirred for 30 min while warming to room temperature. The reaction mixture was quenched with water (10 mL) and extracted with EtOAc (3 x 10 mL). The combined organic extract was dried over Na_2SO_4 and concentrated under reduced pressure. Purification by flash column chromatography using a prepacked 50 g silica column [solvent A: EtOAc; solvent B: hexanes; gradient: 12%A / 88%B (3 CV), 12%A / 88%B → 100%A / 0%B (11 CV), 100%A / 0%B (2 CV); flow rate: 40 mL/min; monitored at 254 and 280 nm] afforded the desired indole phenol ligand **26** (0.02 g, 0.05 mmol, 19%, R_f 0.23 (50:50 hexanes:EtOAc)) as a yellow powder. **^{1}H NMR** ($(CD_3)_2SO$, 500 MHz): δ 12.04 (br s, 1H, NH), 9.05 (s, 1H, OH), 7.98 (d, *J* = 8.0 Hz, 2H, ArH), 7.83 (d, *J* = 8.5 Hz, 1H, ArH), 7.61 (d, *J* = 8.5 Hz, 2H, ArH), 6.95 (d, *J* = 1.0 Hz, 1H, ArH), 6.85 (dd, *J* = 8.5 Hz, 1.5 Hz, 1H, ArH), 6.71 (s, 1H, ArH), 6.68 (d, *J* = 8.5 Hz, 1H, ArH), 6.63 (d, *J* = 8.5 Hz, 1H, ArH), 3.81 (s, 3H, OCH_3), 3.65 (s, 3H, OCH_3). **^{13}C NMR** ($(CD_3)_2SO$, 125 MHz): δ 190.1, 156.6, 148.3, 148.0, 146.1, 146.0, 145.6, 136.6, 129.8, 123.9, 122.6, 122.0, 121.47, 121.45, 116.8, 111.62, 111.55, 111.4, 94.9, 55.7, 55.3. **HPLC**: 13.19 min., purity at 254 nm >99%. **HRMS (ESI$^+$)**: *m/z* calculated for $C_{23}H_{19}N_2O_6$ $[M+H]^+$ 419.1238, found 419.1237.

4.1.23. 2-(3′-Hydroxy-4′-methoxyphenyl)-3-(3′′-nitrobenzoyl)-6-methoxyindole (27)

To a well-stirred solution of compound **15** (0.13 g, 0.25 mmol) in THF (10 mL) at 0 ºC was added TBAF (0.38 mL, 0.38 mmol, 1 M in THF) dropwise. The reaction mixture was stirred for 30 min while warming to room temperature. The reaction

mixture was quenched with water (10 mL) and extracted with EtOAc (3 x 10 mL). The combined organic extract was dried over Na_2SO_4 and concentrated under reduced pressure. Purification by flash column chromatography using a prepacked 50 g silica column [solvent A: EtOAc; solvent B: hexanes; gradient: 15%A / 85%B (4.5 CV), 40%A / 60%B (16 CV), 40%A / 60%B → 100%A / 0%B (2 CV), 100%A / 0%B (10.5 CV); flow rate: 40 mL/min; monitored at 254 and 280 nm] afforded the desired indole phenol ligand **27** (0.10 g, 0.25 mmol, R_f = 0.28 (50:50 hexanes:EtOAc)) quantitatively as a yellow powder. **^{1}H NMR** ($(CD_3)_2CO$, 500 MHz): δ 10.95 (br s, 1H, NH), 8.25 (t, *J* = 2.0 Hz, 1H, ArH), 8.13 (ddd, *J* = 8.0 Hz, 2.0 Hz, 1.0 Hz, 1H, ArH), 8.02 (d, *J* = 8.5 Hz, 1H, ArH), 7.93 (dt, *J* = 7.5 Hz, 1.0 Hz, 1H, ArH), 7.69 (s, 1H, OH), 7.49 (t, *J* = 8.0 Hz, 1H, ArH), 7.06 (d, *J* = 2.0 Hz, 1H, ArH), 6.91 (dd, *J* = 9.0 Hz, 2.5 Hz, 1H, ArH), 6.81 (d, *J* = 2.0 Hz, 1H, ArH), 6.78 (dd, *J* = 8.5 Hz, 2.0 Hz, 1H, ArH), 6.73 (d, *J* = 8.0 Hz, 1H, ArH), 3.86 (s, 3H, OCH_3), 3.75 (s, 3H, OCH_3). **^{13}C NMR** ($(CD_3)_2CO$, 125 MHz): δ 190.5, 158.5, 149.2, 148.5, 147.4, 146.0, 143.1, 138.0, 135.9, 130.1, 125.8, 125.7, 124.8, 123.7, 123.0, 122.9, 117.5, 113.0, 112.7, 112.3, 95.8, 56.5, 56.0. **HPLC**: 12.97 min., purity at 254 nm >99%. **HRMS (ESI$^+$)**: *m/z* calculated for $C_{23}H_{19}N_2O_6$ $[M+H]^+$ 419.1238, found 419.1236.

4.1.24. 2-(3′-Hydroxy-4′-methoxyphenyl)-3-(3′′,4′′,5′′-trifluorobenzoyl)-6-methoxyindole (28)

To a well-stirred solution of compound **16** (0.70 g, 1.29 mmol) in THF (10 mL) at 0 ºC was added TBAF (1.94 mL, 1.94 mmol, 1 M in THF) dropwise. The reaction mixture was stirred for 30 min while warming to room temperature. The reaction mixture was quenched with water (10 mL) and extracted with EtOAc (3 x 10 mL). The

combined organic extract was dried over Na_2SO_4 and concentrated under reduced pressure. Purification by flash column chromatography using a prepacked 50 g silica column [solvent A: EtOAc; solvent B: hexanes; gradient: 12%A / 88%B (4 CV), 12%A / 88%B → 100%A / 0%B (10 CV), 100%A / 0%B (2 CV); flow rate: 40 mL/min; monitored at 254 and 280 nm] afforded the desired indole free phenol ligand **28** (0.35 g, 0.41 mmol, 64%, R_f = 0.18 (50:50 hexanes:EtOAc)) as a tan powder. **^{1}H NMR** ((CD_3)$_2$SO, 500 MHz): δ 12.02 (br s, 1H, NH), 9.12 (br s, 1H, OH), 7.85 (d, *J* = 8.5 Hz, 1H, ArH), 7.28 (m, 2H, ArH), 6.94 (d, *J* = 2.0 Hz, 1H, ArH), 6.86 (dd, *J* = 9.0 Hz, 2.0 Hz, 1H, ArH), 6.80 (d, *J* = 8.0 Hz, 1H, ArH), 6.71 (d, *J* = 2.0 Hz, 1H, ArH), 6.69 (dd, *J* = 8.0 Hz, 2.0 Hz, 1H, ArH), 3.81 (s, 3H, OCH_3), 3.73 (s, 3H, OCH_3). **^{13}C NMR** ((CD_3)$_2$SO, 125 MHz): δ 188.0, 156.6, 149.5 (ddd, $J_{C\text{-}F}$ = 247.6 Hz, 10.2 Hz, 3.0 Hz), 148.2, 146.1, 145.5, 140.0 (dt, $J_{C\text{-}F}$ = 251.4 Hz, 15.5 Hz), 136.71 (d, $J_{C\text{-}F}$ = 5.6 Hz), 136.65, 124.2, 122.0, 121.4, 121.2, 116.8, 113.5 (dd, $J_{C\text{-}F}$ = 16.6 Hz, 4.8 Hz), 111.8, 111.5, 110.8, 94.9, 55.8, 55.3. **^{19}F NMR** ((CD_3)$_2$SO, 470 MHz): δ -135.5 (dd, *J* = 21.6 Hz, 8.5 Hz, 2F, ArF), -158.6 (tt, *J* = 21.2 Hz, 6.6 Hz, 1F, ArF). **HPLC**: 14.33 min., purity at 254 nm >99%. **HRMS (ESI$^+$)**: *m/z* calculated for $C_{23}H_{17}F_3NO_4$ $[M+H]^+$ 428.1104, found 428.1104.

4.1.25. 2-(3′-Hydroxy-4′-methoxyphenyl)-3-(4′′-fluorobenzoyl)-6-methoxyindole (29)

To a well-stirred solution of compound **17** (0.09 g, 0.18 mmol) in THF (10 mL) at 0 ºC was added TBAF (0.30 mL, 0.38 mmol, 1 M in THF) dropwise. The reaction mixture was stirred for 30 min while warming to room temperature. The reaction mixture was quenched with water (10 mL) and extracted with EtOAc (3 x 10 mL). The combined organic extract was dried over Na_2SO_4 and concentrated under reduced

pressure. Purification by flash column chromatography using a prepacked 50 g silica column [solvent A: EtOAc; solvent B: hexanes; gradient: 35%A / 65%B (5 CV), 35%A / 65%B → 50%A / 50%B (17.5 CV), 100%A / 0%B (7 CV); flow rate: 40 mL/min; monitored at 254 and 280 nm] afforded the desired indole phenol ligand **29** (0.05 g, 0.12 mmol, 64%, R_f = 0.31 (50:50 hexanes:EtOAc)) as a tan powder. **^{1}H NMR** ($(CD_3)_2CO$, 500 MHz): δ 10.78 (br s, 1H, NH), 7.77 (d, *J* = 8.5 Hz, 1H, ArH), 7.66 (m, 3H, 2 ArH, 1 OH), 7.03 (d, *J* = 2.5 Hz, 1H, ArH), 6.96 (m, 2H, ArH), 6.92 (d, *J* = 2.0 Hz, 1H, ArH), 6.84 (dd, *J* = 9.0 Hz, 2.5 Hz, 1H, ArH), 6.81 (dd, *J* = 8.0 Hz, 2.0 Hz, 1H, ArH), 6.78 (d, *J* = 8.5 Hz, 1H, ArH), 3.84 (s, 3H, OCH_3), 3.79 (s, 3H, OCH_3. **^{13}C NMR** ($(CD_3)_2CO$, 125 MHz): δ 190.6, 164.3 (d, $J_{C\text{-}F}$ = 248 Hz), 157.2, 147.9, 146.3, 143.0, 137.00, 136.98, 136.9, 131.8 (d, $J_{C\text{-}F}$ = 9 Hz), 125.1, 123.0, 121.7, 121.5, 116.0, 114.4 (d, $J_{C\text{-}F}$ = 22 Hz), 111.17, 111.15, 94.5, 55.4, 55.9. **^{19}F NMR** ($(CD_3)_2CO$, 470 MHz): δ -110.8 (m, 1F, ArF). **HPLC**: 12.91 min., purity at 254 nm >99%. **HRMS (ESI$^+$)**: *m/z* calculated for $C_{23}H_{19}FNO_4$ $[M+H]^+$ 392.1293, found 392.1291.

4.1.26. 2-(3′-Hydroxy-4′-methoxyphenyl)-3-(3′′,5′′-*bis*-trifluoromethylbenzoyl)-6-methoxyindole (30)

To a well-stirred solution of compound **18** (0.26 g, 0.42 mmol) in THF (10 mL) at 0 ºC was added TBAF (0.63 mL, 0.63 mmol, 1 M in THF) dropwise. The reaction mixture was stirred for 30 min while warming to room temperature. The reaction mixture was quenched with water (10 mL) and extracted with EtOAc (3 x 10 mL). The combined organic extract was dried over Na_2SO_4 and concentrated under reduced pressure. Purification by flash column chromatography using a prepacked 50 g silica column [solvent A: EtOAc; solvent B: hexanes; gradient: 7%A / 93%B (4 CV), 7%A /

93%B → 60%A / 40%B (10 CV), 60%A / 40%B (5.2 CV); flow rate: 40 mL/min; monitored at 254 and 280 nm] afforded the desired indole free phenol ligand **30** (0.22 g, 0.42 mmol, R_f = 0.21 (70:30 hexanes:EtOAc)) quantitatively as an orange powder. **^{1}H NMR** ($(CD_3)_2SO$, 500 MHz): δ 12.10 (br s, 1H, NH), 9.00 (br s, 1H, OH), 7.99 (m, 2H, 1 ArH, 1 OH), 7.90 (s, 2H, ArH), 6.96 (d, J = 2.0 Hz, 1H, ArH), 6.89 (dd, J = 9.0 Hz, 2.5 Hz, 1H, ArH), 6.64 (m, 3H, ArH), 3.82 (s, 3H, OCH_3), 3.66 (s, 3H, OCH_3). **^{13}C NMR** ($(CD_3)_2SO$, 125 MHz): δ 188.4, 156.7, 148.2, 146.3, 146.2, 142.2, 136.7, 129.7 (q, $J_{C\text{-}F}$ = 33 Hz), 128.9 (m), 123.7 (m), 123.5, 123.0 (q, $J_{C\text{-}F}$ = 272 Hz), 122.0, 121.6, 121.4, 116.9, 111.7, 111.6, 111.0, 94.9, 55.6, 55.3. **^{19}F NMR** ($(CD_3)_2SO$, 470 MHz): δ -61.4 (s, 6F, CF_3). **HPLC**: 16.17 min., purity at 254 nm >99%. **HRMS (ESI$^+$)**: *m/z* calculated for $C_{25}H_{18}F_6NO_4$ $[M+H]^+$ 510.1135, found 510.1134.

4.1.27. 2-(3′-Hydroxy-4′-methoxyphenyl)-3-(3′′-trifluoromethoxybenzoyl)-6-methoxyindole (31)

To a well-stirred solution of compound **19** (1.21 g, 2.11 mmol) in THF (10 mL) at 0 ºC was added TBAF (3.20 mL, 3.17 mmol, 1 M in THF) dropwise. The reaction mixture was stirred for 30 min while warming to room temperature. The reaction mixture was quenched with water (10 mL) and extracted with EtOAc (3 x 10 mL). The combined organic extract was dried over Na_2SO_4 and concentrated under reduced pressure. Purification by flash column chromatography using a prepacked 50 g silica column [solvent A: EtOAc; solvent B: hexanes; gradient: 12%A / 88%B (4 CV), 12%A / 88%B → 100%A / 0%B (10 CV), 100%A / 0%B (4 CV); flow rate: 50 mL/min; monitored at 254 and 280 nm] afforded the desired indole free phenol ligand **31** (0.67 g, 1.51 mmol, 71%, R_f = 0.33 (50:50 hexanes:EtOAc)) as an orange powder. **^{1}H NMR**

($(CD_3)_2CO$, 500 MHz): δ 10.89 (br s, 1H, NH), 7.89 (d, *J* = 8.7 Hz, 1H, ArH), 7.72 (s, 1H, OH), 7.55 (d, *J* = 7.4 Hz, 1H, ArH), 7.47 (s, 1H, ArH), 7.30 (t, *J* = 7.8 Hz, 1H, ArH), 7.26 (d, *J* = 8.3 Hz, 1H, ArH), 7.04 (d, *J* = 2.2 Hz, 1H, ArH), 6.93 (d, *J* = 2.0 Hz, 1H, ArH), 6.88 (dd, *J* = 8.7, 2.3 Hz, 1H, ArH), 6.78 (dd, *J* = 8.3, 2.0 Hz, 1H, ArH), 6.72 (d, *J* = 8.3 Hz, 1H, ArH), 3.84 (s, 3H, OCH_3), 3.76 (s, 3H, OCH_3). **^{13}C NMR** ($(CD_3)_2CO$, 125 MHz): δ 191.4, 158.1, 149.4 (q, $J_{C\text{-}F}$ = 2 Hz), 148.9, 147.2, 145.2, 143.8, 137.8, 130.3, 128.9, 125.6, 123.9, 123.7, 122.63, 122.59, 122.2, 121.3 (q, $J_{C\text{-}F}$ = 254.75 Hz), 116.9, 112.8, 112.3, 112.0, 95.6, 56.2, 55.8. **^{19}F NMR** ($(CD_3)_2CO$, 470 MHz): δ -58.5 (s, 6F, OCF_3). **HPLC**: 14.71 min., purity at 254 nm >99%. **HRMS (ESI$^+$)**: *m/z* calculated for $C_{24}H_{19}F_3NO_5$ $[M+H]^+$ 458.1210, found 458.1210.

4.1.28. 2-(3′-Hydroxy-4′-methoxyphenyl)-3-(4′′-trifluoromethoxybenzoyl)-6-methoxyindole (32)

To a well-stirred solution of compound **20** (0.92 g, 1.60 mmol) in THF (5 mL) at 0 ºC was added TBAF (2.5 mL, 2.40 mmol, 1 M in THF) dropwise. The reaction mixture was stirred for 30 min while warming to room temperature. The reaction mixture was quenched with water (10 mL) and extracted with EtOAc (3 x 10 mL). The combined organic extract was dried over Na_2SO_4 and concentrated under reduced pressure. Purification by flash column chromatography using a prepacked 50 g silica column [solvent A: EtOAc; solvent B: hexanes; gradient: 12%A / 88%B (4 CV), 12%A / 88%B → 100%A / 0%B (10 CV), 100%A / 0%B (4 CV); flow rate: 50 mL/min; monitored at 254 and 280 nm] afforded the desired indole free phenol ligand **32** (0.43 g, 0.96 mmol, 60%, R_f = 0.33 (50:50 hexanes:EtOAc)) as a yellow powder. **^{1}H NMR** ($(CD_3)_2CO$, 500 MHz): δ 10.86 (br s, 1H, NH), 7.91 (d, *J* = 8.8 Hz, 1H, ArH), 7.69 (s, 1H, OH), 7.65 (d, *J*

= 8.5 Hz, 2H, ArH), 7.10 (d, *J* = 8.5 Hz, 2H, ArH), 7.03 (d, *J* = 2.2 Hz, 1H, ArH), 6.90 (s, 1H, ArH), 6.87 (dd, *J* = 8.8 Hz, 2.2 Hz, 1H, ArH), 6.71 (m, 2H, ArH), 3.84 (s, 3H, OCH_3), 3.77 (s, 3H, OCH_3). **^{13}C NMR** ($(CD_3)_2CO$, 125 MHz): δ 191.6, 158.1, 151.3 (q, $J_{C\text{-}F}$ = 2 Hz), 148.9, 147.2, 145.1, 140.5, 137.8, 132.0, 125.7, 123.7, 122.72, 122.67, 121.7 (q, $J_{C\text{-}F}$ = 254.75 Hz), 120.7, 116.9, 113.0, 112.3, 111.8, 95.5, 55.1, 55.8. **^{19}F NMR** ($(CD_3)_2CO$, 470 MHz): δ -58.5 (s, 6F, OCF_3). **HPLC**: 14.80 min., purity at 254 nm >99%. **HRMS (ESI$^+$)**: *m/z* calculated for $C_{24}H_{19}F_3NO_5$ $[M+H]^+$ 458.1210, found 458.1210.

4.1.29. 2-(3′-Hydroxy-4′-methoxyphenyl)-3-(3′′,4′′,5′′-trimethoxybenzoyl)-6-hydroxyindole (33)

To a well-stirred solution of compound **21** (0.40 g, 0.59 mmol) in THF (10 mL) at 0 ºC was added TBAF (1.00 mL, 0.89 mmol, 1 M in THF) dropwise. The reaction mixture was stirred for 30 min while warming to room temperature. The reaction mixture was quenched with water (10 mL) and extracted using EtOAc (3 x 10 mL). The combined organic extract was dried over Na_2SO_4 and concentrated under reduced pressure. Purification by flash column chromatography using a prepacked 50 g silica column [solvent A: EtOAc; solvent B: hexanes; gradient: 12%A / 88%B (4 CV), 12%A / 88%B → 100%A / 0%B (10 CV), 100%A / 0%B (1.4 CV); flow rate: 40 mL/min; monitored at 254 and 280 nm] afforded the desired indole free phenol ligand **33** (0.11 g, 0.25 mmol, 42%, R_f = 0.03 (70:30 hexanes:EtOAc)) as a yellow powder. **^{1}H NMR** ($(CD_3)_2SO$, 500 MHz): δ 11.62 (br s, 1H, NH), 9.19 (br s, 1H, OH), 9.00 (br s, 1H, OH), 7.66 (d, *J* = 8.5 Hz, 1H, ArH), 6.82 (d, *J* = 2.0 Hz, 1H, ArH), 6.78 (s, 2H, ArH), 6.74 (d, *J* = 9.0 Hz, 2H, ArH), 6.67 (t, *J* = 2.5 Hz, 1H, ArH), 6.65 (t, *J* = 3.0 Hz, 1H, ArH), 3.69

(s, 3H, OC$\underline{H}_3$), 3.61 (s, 6H, OC$\underline{H}_3$), 3.59 (s, 3H, OC$\underline{H}_3$). **^{13}C NMR** ($(CD_3)_2SO$, 125 MHz): δ 192.0, 155.2, 153.4, 148.5, 147.0, 143.7, 141.8, 138.0, 136.4, 126.5, 123.4, 122.7, 122.0, 116.9, 113.1, 112.3, 111.8, 106.0, 97.4, 60.4, 56.18, 56.17. **HPLC**: 8.95 min., purity at 254 nm 90.7%. **HRMS (ESI$^+$)**: *m/z* calculated for $C_{25}H_{24}NO_7$ $[M+H]^+$ 450.1547, found 450.1547.

4.1.30. 2-(3′-Hydroxy-4′-methoxyphenyl)-3-(3′′,4′′,5′′-trimethoxybenzoyl)-4,5,6-methoxyindole (34)

To a well-stirred solution of compound **22** (0.03 g, 0.05 mmol) in THF (10 mL) at 0 °C was added TBAF (0.1 mL, 0.08 mmol, 1 M in THF) dropwise. The reaction mixture was stirred for 30 min while warming to room temperature. The reaction mixture was quenched with water (10 mL) and extracted with EtOAc (3 x 10 mL). The combined organic extract was dried over Na_2SO_4 and concentrated under reduced pressure. Purification by flash column chromatography using a prepacked 100 g silica column [solvent A: EtOAc; solvent B: hexanes; gradient: 12%A / 88%B (4 CV), 12%A / 88%B → 100%A / 0%B (10 CV), 100%A / 0%B (2 CV); flow rate: 40 mL/min; monitored at 254 and 280 nm] afforded the desired indole phenol ligand **34** (0.02 g, 0.03 mmol, 60%, R_f = 0.10 (50:50 hexanes:EtOAc)) as a yellow powder. **^{1}H NMR** ($CDCl_3$, 500 MHz): δ 8.30 (br s, 1H, N$\underline{H}$), 7.15 (s, 2H, Ar$\underline{H}$), 6.99 (d, *J* = 2.0 Hz, 1H, Ar$\underline{H}$), 6.89 (dd, *J* = 8.0 Hz, 2.0 Hz, 1H, Ar$\underline{H}$), 6.71 (d, *J* = 8.5 Hz, 1H, Ar$\underline{H}$), 6.68 (s, 1H, Ar$\underline{H}$), 5.62 (s, 1H, O$\underline{H}$), 3.90 (s, 3H, OC$\underline{H}_3$), 3.85 (s, 3H, OC$\underline{H}_3$), 3.84 (s, 3H, OC$\underline{H}_3$), 3.82 (s, 3H, OC$\underline{H}_3$), 3.74 (s, 6H, OC$\underline{H}_3$), 3.69 (s, 3H, OC$\underline{H}_3$). **^{13}C NMR** ($CDCl_3$, 125 MHz): δ 193.4, 152.8, 152.2, 146.8, 146.5, 145.8, 142.1, 137.8, 137.0, 134.6, 132.4, 125.1, 120.5, 116.1, 113.7, 112.6, 110.9, 107.5, 89.7, 61.4, 61.0, 60.8, 56.4, 56.3, 56.1. **HPLC**: 11.13 min., purity at

254 nm >99%. **HRMS (ESI$^+$)**: *m/z* calculated for $C_{28}H_{30}NO_9$ $[M+H]^+$ 524.1915, found 524.1912.

4.1.31. 2-(4′-Methoxyphenyl)-3-(3′′,4′′,5′′-trimethoxybenzoyl)-6-methoxy-7-hydroxyindole (35)

To a well-stirred solution of compound **23** (0.008 g, 0.014 mmol) in THF (10 mL) at 0 °C was added TBAF (0.01 mL, 0.01 mmol, 1 M in THF) dropwise. The reaction mixture was stirred for 30 min while warming to room temperature. The reaction mixture was quenched with water (10 mL) and extracted with EtOAc (3 x 10 mL). The combined organic extract was dried over Na_2SO_4 and concentrated under reduced pressure. Purification by flash column chromatography using a prepacked 10 g silica column [solvent A: EtOAc; solvent B: hexanes; gradient: 7%A / 93%B (4 CV), 7%A / 93%B → 60%A / 40%B (10 CV), 60%A / 40%B (5 CV); flow rate: 12 mL/min; monitored at 254 and 280 nm] resulting in free phenol indole **35** as a dark brown powder (0.006 g, 0.013 mmol, 90%, R_f = 0.22 (50:50 hexanes:EtOAc)). **^{1}H NMR** ($CDCl_3$, 500 MHz): δ 8.57 (br s, 1H, NH), 7.52 (d, *J* = 8.4 Hz, 1H, ArH), 7.29 (d, *J* = 8.1 Hz, 2H, ArH), 6.95 (br s, 3H, ArH), 6.74 (d, *J* = 8.1 Hz, 2H, ArH), 5.76 (br s, 1H, OH), 3.97 (s, 3H, OCH_3), 3.80 (s, 3H, OCH_3), 3.75 (s, 3H, OCH_3), 3.69 (s, 6H, OCH_3). **^{13}C NMR** ($CDCl_3$, 125 MHz): δ 192.2, 160.1, 152.6, 143.7, 142.3, 141.3, 134.8, 131.0, 130.4, 125.5, 125.3, 124.5, 114.0, 113.0, 112.8, 108.7, 107.5, 61.0, 57.6, 56.2, 55.4. **HPLC**: 11.67 min., purity at 254 nm 96.9%. **HRMS (ESI$^+$)**: *m/z* calculated for $C_{26}H_{26}NO_7$ $[M+H]^+$ 464.1704, found 464.1704.

4.1.32. 2-(3′-Hydroxy-4′-methoxyphenyl)-3-(3′′,4′′,5′′-trimethoxybenzoyl)-6,7-dimethoxyindole (36)

To a well-stirred solution of compound **24** (0.08 g, 0.14 mmol) in THF (10 mL) at 0 ºC was added TBAF (0.21 mL, 0.21 mmol, 1 M in THF) dropwise. The reaction mixture was stirred for 30 min while warming to room temperature. The reaction mixture was quenched with water (10 mL) and extracted with EtOAc (3 x 10 mL). The combined organic extract was dried over Na_2SO_4 and concentrated under reduced pressure. Purification by flash column chromatography using a prepacked 25 g silica column [solvent A: EtOAc; solvent B: hexanes; gradient: 12%A / 88%B (4 CV), 12%A / 88%B → 100%A / 0%B (10 CV), 100%A / 0%B (2 CV); flow rate: 25 mL/min; monitored at 254 and 280 nm] resulting in free phenol indole **36** as a dark brown powder (0.02 g, 0.04 mmol, 27%, R_f = 0.14 (50:50 hexanes:EtOAc)). **^{1}H NMR** ($CDCl_3$, 500 MHz): δ 8.57 (br s, 1H, NH), 7.71 (d, *J* = 9.0 Hz, 1H, ArH), 6.972 (d, *J* = 9.0 Hz, 1H, ArH), 6.971 (d, *J* = 2.0 Hz, 1H, ArH), 6.94 (s, 2H, ArH), 6.79 (dd, *J* = 8.3 Hz, 2.0 Hz, 1H, ArH), 6.64 (d, *J* = 8.3 Hz, 1H, ArH), 5.63 (br s, 1H, OH), 4.06 (s, 3H, OCH_3), 3.96 (s, 3H, OCH_3), 3.83 (s, 3H, OCH_3), 3.79 (s, 3H, OCH_3), 3.71 (s, 6H, OCH_3). **^{13}C NMR** ($CDCl_3$, 125 MHz): δ 192.0, 152.6, 148.1, 147.2, 145.7, 143.2, 141.1, 135.0, 134.0, 130.2, 125.4, 125.0, 122.0, 116.8, 114.8, 113.4, 110.52, 110.45, 107.3, 61.3, 60.9, 57.4, 56.17, 56.15. **HPLC**: 11.45 min., purity at 254 nm >99%. **HRMS (ESI$^+$)**: *m/z* calculated for $C_{27}H_{27}NNaO_8$ $[M+Na]^+$ 516.1629, found 516.1626.

4.2 Biological evaluation

4.2.1. SRB Assay[52-53]

We assessed inhibition of human cancer cell growth using the National Cancer Institute's standard sulforhodamine B assay, as previously described.[52] Briefly, cancer cell lines in a 5% fetal bovine serum/RPMI1640 medium, 1% gentamicin solution were plated in 96-well plates and incubated for 24 h. Serial dilutions of the compounds were then added. After 48 h, the cells were fixed with trichloroacetic acid, stained with sulforhodamine B, and read with an automated Biotek plate reader. A growth inhibition of 50% (GI_{50} or the drug concentration causing a 50% reduction in the net protein increase) was calculated from optical density data.

4.2.2. Colchicine Binding Assay

Inhibition of [^{3}H]colchicine binding was determined using 100 mL reaction mixtures containing 1.0 mM tubulin, 5.0 μM [^{3}H]colchicine (from Perkin-Elmer), 5% (v/v) dimethyl sulfoxide, and potential inhibitors at 1.0 or 5.0 μM. Reaction mixtures also contained components shown to potently stabilize the colchicine binding activity of tubulin:[54] 1.0 M monosodium glutamate (pH 6.6 as above), 0.5 mg/mL bovine serum albumin, 0.1 M glucose-1-phosphate, 1.0 mM $MgCl_2$, and 1.0 mM GTP. Incubation was for 10 min at 37 ºC, a time point at which the reaction in the control is 40-60% complete. Reactions were stopped by adding 2.0 mL of ice-cold water and placing the samples on ice prior to filtration. Each sample was poured onto a stack of two DEAE-cellulose filters, followed immediately by 6 mL of ice-cold water, and the water was aspirated under reduced vacuum. The filters were washed with additional water and placed into vials containing 5 mL of Biosafe II scintillation cocktail. The samples were counted the

next day in a Beckman scintillation counter. Samples with potential inhibitors were compared to controls with no inhibitor to determine percent inhibition.

4.2.3. Inhibition of Tubulin Polymerization

Tubulin assembly experiments were performed with 0.25 mL reaction mixtures (final volume). The mixtures contained 1 mg/mL (10 μM) purified bovine brain tubulin, 0.8 M tubulin monosodium glutamate (adjusted to pH 6.6 with HCl in 2.0 M stock solution), 4% (v/v) dimethyl sulfoxide, 0.4 mM GTP, and varying concentrations of compound. Initially, all components except GTP were preincubated for 15 min at 30 ºC in a 0.24 mL volume. After chilling the mixtures on ice, 10 μL of 10 mM GTP was added to each sample. The reaction mixtures were then transferred to cuvettes held at 0 ºC in Beckman DU-7400 and DU-7500 spectrophotometers equipped with electronic temperature controllers. The temperature was jumped to 30 ºC over about 30 s, and polymerization was followed turbidimetrically at 350 nM for 30 min. Each reaction set included a reaction mixture without compound, and the IC_{50} was defined as the concentration of compound that inhibited the extent of assembly versus the control after 20 min at 30 ºC. These values were obtained by interpolation between the actual experimental values.

Supplementary Data.

Characterization data (^{1}H NMR, ^{13}C NMR, ^{19}F NMR, HPLC, and HRMS) for final compounds and X-ray crystallography for compound **10** are available free of charge via the internet at http://pubs.acs.org.

Acknowledgements.

The authors are grateful to the National Cancer Institute of the National Institutes

of Health (grant no. 5R01CA140674 to K.G.P. and M.L.T.) and Oxigene Inc. (grant to K.G.P. and M.L.T.) for their financial support of this project, and to the NSF for funding the Varian 500 MHz NMR spectrometer (grant no. CHE- 0420802). The content is solely the responsibility of the authors and does not necessarily reflect the official views of the National Institutes of Health. The authors also thank Dr. James Karban and Dr. Michelle Nemec (Director) for the use of the shared Molecular Biosciences Center at Baylor University, Dr. Alejandro Ramirez (Mass Spectrometry Core Facility, Baylor University), and Dr. Kevin Klausmeyer (X-ray analysis). The authors are grateful to Mr. Robert Harris, Ms. Priscilla Hor, and Ms. Siri Ancha for their valuable contributions to the synthesis of certain analogues.

References and notes.

1. Jordan, M. A.; Wilson, L. *Nat. Rev. Cancer* **2004**, *4*, 253–265.

2. Lopus, M.; Yenjerle, M.; Wilson, L. In Wiley Encyclopedia of Chemical Biology; Begley, T. P.; Eds.; John Wiley and Sons, Inc.: Hoboken, NJ, **2008**; 3, 153-160.

3. Etienne-Manneville, S. *Curr. Opin. Cell Biol.* **2010**, *22*, 104–111.

4. Wade, R. H. *Mol. Biotechnol.* **2009**, *43*, 177–191.

5. Valiron, O.; Caudron, N.; Job, D. *Cell. Mol. Life Sci.* **2001**, *58*, 2069–2084.

6. Mason, R. P.; Zhao, D.; Liu, L.; Trawick, M. L.; Pinney, K. G. *Integr. Biol.* **2011**, *3*, 375-387.

7. Tozer, G. M.; Kanthou, C.; Baguley, B. C. *Nat. Rev. Cancer* **2005**, *5*, 423-435.

8. Hida, K.; Hida, Y.; Shindoh, M. *Cancer Sci.* **2008**, *99*(3), 459-466.

9. Kanthou, C.; Tozer, G. M. *Exp. Opin. Ther. Targets* **2007**, *11*(11), 1443-1457.

10. Siemann, D. W.; Bibby, M. C.; Dark, G. G.; Dicker, A. P.; Eskens, F. A.; Horsman, M. R.; Marme, D.; Lorusso, P. M. *Clin. Cancer Res.* **2005**, *11*, 416-420.

11. Dougherty, G. J.; Chaplin, D. J. in Vascular Disruptive Agents for the Treatment of Cancer, ed. T. Meyer, Springer, New York, **2010**, ch. 1, 1-27.

12. Siemann, D. W. in Vascular-Targeted Therapies in Oncology, ed. Siemann, D. John Wiley & Sons, London, UK, **2006**, ch. 1, 1-8.

13. Patil, S. A.; Patil, R.; Miller, D. D. *Future Med. Chem.* **2012**, *4*(16), 2085-2115.

14. Weisenberg, R. C.; Borisy, G. G.; Taylor, W. *Biochemistry* **1968**, *7*, 4466-4477.

15. Pettit, G. R.; Singh, S. B.; Hamel, E.; Lin, C. M.; Alberts, D. S.; Garcia-Kendall, D. *Experientia* **1989**, *45*(2), 209-211.

16. Pettit, G. R.; Singh, S. B.; Niven, M. L.; Hamel, E.; Schmidt, J. M. *J. Nat. Prod.* **1987**, *50*(1), 119-131.

17. Hasani, A.; Leighl, N. *Clinical Lung Cancer* **2011**, *12*(1), 18-25.

18. Dowlati, A.; Robertson, K.; Cooney, M.; Petros, W. P.; Stratford, M.; Jesberger, J.; Rafie, N.; Overmoyer, B.; Makkar, V.; Stambler, B.; Taylor, A.; Waas, J.; Lewin, J. S.; McCrae, K. R.; Remick, S. C. *J. Clin. Oncol.* **2003**, *62*(12), 3408-3416.

19. Rustin, G. J.; Galbraith, S. M.; Anderson, H.; Stratford, M.; Folkes, L. K.; Sena, L.; Gumbrell, L.; Price, P. M. *J. Clin. Oncol.* **2003**, *21*(15), 2815-2822.

20. Lee, R. M.; Gewirtz, D. A. *Drug Dev. Res.* **2008**, *69*(6), 352-358.

21. Pinney, K. G. in Vascular-Targeted Therapies in Oncology, ed. Siemann, D. John Wiley & Sons, London, UK, **2006**, ch. 6, 95-121.

22. Pettit, G. R.; Singh, S. B.; Boyd, M. R. *J. Med. Chem.* **1995**, *38*, 1666-1672.

23. Oshumi, K.; Nakagawa, R.; Fukuda, Y. *J. Med. Chem.* **1998**, *41*, 3022-3032.

24. McGowan, A. T.; Fox, B. W. *Cancer Chemother. Pharmacol.* **1990**, *26*, 79-81.

25. El-Zayat, A. A. E.; Degan, D.; Drabek, S. *Anticancer Drugs* **1993**, *4*, 19-25.

26. Oshumi, K.; Hatanaka, R.; Nakagawa, R. *Anticancer Drug Des.* **1999**, *14*, 539-548.

27. Pettit, G. R.; Minardi, M. D.; Boyd, M. R.; Pettit, R. K. *Anticancer Drug Des.* **2000**, *15*, 397-403.

28. Pettit, G. R.; Lippert, J. W. III. *Anticancer Drug Des.* **2000**, *15*, 203-216.

29. Boehle, A. S.; Sipos, B.; Kliche, U.; Kalthoff, H.; Dohrmann, P. *Ann. Thorac. Surg.* **2001**, *71*, 1657-1665.

30. Pettit, G. R.; Moser, B. R.; Boyd, M. R. *Anticancer Drug Des.* **2001**, *16*, 185-193.

31. Ohno, T.; Kawano, K.; Tahara, K. *Gastroenterology* **2001**, *120*, 2831.

32. Pinney, K. G.; Wang, F.; Hadimani, M. **2005**, US Patent 6849656.

33. Hadimani, M. B.; Kessler, R. J.; Kautz, J. A.; Ghatak, A.; Shirali, R.; O'Dell, H.; Garner, C. M.; Pinney, K. G. *Acta Crystallogr.* **2002**, C58, 330;

34. Pinney, K.; Wang, F.; Del Pilar Mejia, M. **2001**, From PCT Int. Appl. WO 0119794 A2.

35. Flynn, B. L.; Hamel, E.; Jung, M. K. *J. Med. Chem.* **2002**, *45*, 2670-2673.

36. Hadimani, M. B.; MacDonough, M. T.; Strecker, T. E.; Lopez, R.; Sriram, M.; Nguyen, B. L.; Kessler, R. J.; Ghatak, A.; Shirali, A. R.; Liu, L.; Garner, C. M.; Pettit, G. R.; Hamel, H.; Chaplin, D. J.; Mason, R. P.; Trawick, M. L.; Pinney, K. G. *J. Nat. Prod.* http://dx.doi.org/10.1021/np400374w.

37. Liou, J.-P.; Chang, Y.-C.; Kuo, F.-M.; Chang, C-.W.; Tseng, H.-Y.; Wang, C.-C.; Yang, Y.-N.; Chang, J.-Y.; Lee, S.-J.; Hsieh, H. P. *J. Med. Chem.* **2004**, *47*, 4247–4257.

38. Pinney, K. G.; Bounds, A. D.; Dingeman, K. M.; Mocharla, V. P.; Pettit, G. R.; Bai, R.; Hamel, E. *Bioorg. Med. Chem. Lett.* **1999**, *9*, 1081–1086.

39. Mullica, D. F.; Pinney, K. G.; Mocharla, V. P.; Dingeman, K. M.; Bounds, A. D.; Sappenfield, E. L. *J. Chem. Crystallogr.* **1998**, *28*, 289–295.

40. Kessler, R. J.; Hadimani, B.; Pinney, K. G.; Edvardsen, K. (Poster). 38th National Organic Symposium Indiana University, Bloomington IN, June 8-12, **2003**.

41. Kessler, R. J. Synthesis and Evaluation of New Inhibitors of Tubulin Polymerization and Their Corresponding Prodrugs as Potential Vascular Targeting Agents. M.S. Thesis, Baylor University, Waco, TX, 2002.42.

42. Flynn, B. L.; Flynn, G. P.; Hamel, E.; Jung, M. K. *Bioorg. Med. Chem. Lett.* **2001**, *11*, 2341–2343.

43. Flynn, B. L.; Gill, G. S.; Grobelny, D. W.; Chaplin, J. H.; Paul, D.; Leske, A. F.; Lavranos, T. C.; Chalmers, D. K.; Charman, S. A.; Kostewicz, E.; Shackleford, D. M.; Morizzi, J.; Hamel, E.; Jung, M. K.; Kremmidiotis, G. *J. Med. Chem.* **2011**, *54*, 6014-6027.

44. Kremmidiotis, G.; Leske, A. F.; Lavranos, T. C.; Beaumont D.; Hall, A.; O'Callaghan, M.; Matthews, C. A.; Flynn, B. L. *Mol. Cancer Ther.* **2010**, *6*, 1562-1573.

45. La Regina, G.; Sarkar, T.; Bai, R.; Edler, M. C.; Saletti, R.; Coluccia, A.; Piscitelli, F.; Minelli, L.; Gatti, V.; Mazzoccoli, C.; Palermo, V.; Mazzoni, C.; Falcone, C.; Scovassi, A. I.; Giansanti, V.; Campiglia, P.; Porta, A.; Maresca, B.; Hamel, E.; Brancale, A.; Novellino, E.; Silvestri, R. *J. Med. Chem.* **2009**, *52*, 7512-7527.

46. La Regina, Bai, R.; Rensen, W. M.; Cesare, E. D.; Coluccia, A.; Piscitelli, F.; Famiglini, V.; Reggio, A.; Nalli, M.; Pelliccia, S.; Pozza, E. D.; Costa, B.; Granata, I.;

Porta, A.; Maresca, B.; Soriani, A.; Iannitto, M. L.; Santoni, A.; Li, J.; Cona, M. M.; Chen, F.; Ni, Y.; Brancale, A.; Dondio, G.; Vultaggio, S.; Varasi, M.; Mercurio, C.; Martini, C.; Hamel, E.; Lavia, P.; Novellino, E.; Silvestri, R. *J. Med. Chem.* **2013**, *56*, 123-149.

47. Ty, N.; Dupeyre, G.; Chabot, G. G.; Seguin, J.; Tillequin, F.; Scherman, D.; Michel, S.; Cachet, X. *Bioorg. Med. Chem.* **2008**, *16*(15), 7494-7503.

48. Bischler, A.; Brion, H. *Chem. Ber.* **1892**, *25*, 2860.

49. Mohlau, H. *Chem. Ber.* **1881**, *14*, 173.

50. Kemperman, G. J.; Roeters, T. A.; Hilberink, P. W. *Eur. J. Org. Chem.* **2003**, 1681-1686.

51. Hall, J. J.; Sriram, M.; Strecker, T. E.; Tidmore, J. K.; Jelinek, C. J.; Kumar, G. D. K.; Hadimani, M. B.; Pettit, G. R.; Chaplin, D. J.; Trawick, M. L.; Pinney, K. G. *Bioorg. Med. Chem. Lett.* **2008**, *18*, 5146-5149.

52. Monks, A.; Scudiero, D.; Skehan, P.; Shoemaker, R.; Paul, K.; Vestica, D.; Hose, C.; Langley, J.; Cronise, P.; Vaigro-Wolf, A. *J. Natl. Cancer Inst.* **1991**, *83*, 767-766.

53. Vichai, V.; Kirtikara, K. *Nature Protocols*. **2006**, *1*(3), 1112-1116.

54. Hamel, E.; Lin, C. M. *Biochim. Biophys. Acta*. **1981**, *675*, 226-231.

CHAPTER FOUR

Indole-based Bioreductively Activatable Prodrug Conjugates

Synthesis of Bioreductive Prodrugs

As described in more detail, the selective targeting of tumor hypoxia is a useful strategy for the treatment of cancer. The selective cleavage of the parent VDA from the bioreductive trigger is achieved by upregulated reductase enzymes such as cyctochrome P450 and is depicted in figure 1.

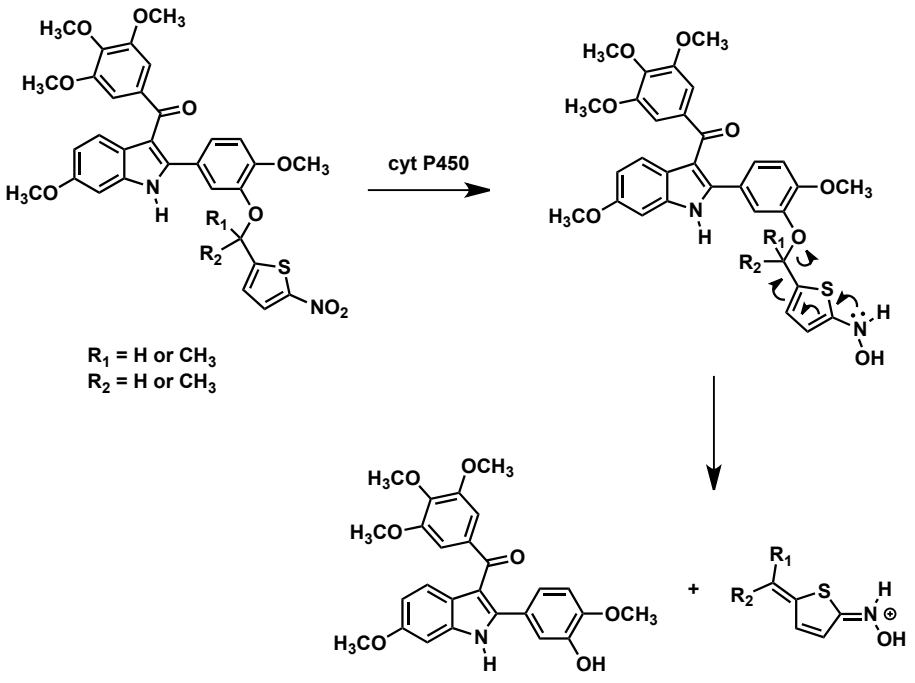

Figure 4.1. Reductive Cleavage of Indole-based BAPCs.

The synthetic route to bioreductively activatable prodrug conjugates (BACPs) **8-10** was achieved through the coupling of the parent indole-based VDA **OXi8006** and bioreductive nitrothiophene triggers **2**, **4**, or **7** under Mitsunobu conditions. This required

both the scale up synthesis of **OXi8006** (Chapter 2) and generation of the *nor*-methyl-, *mono*-methyl-, and *gem*-dimethyl-nitrothiophenes **2**, **4**, and **7** (Scheme 1). The *nor*-methyl- and *mono*-methyl-nitrothiophenes **2** and **4** were attained by the selective reduction of their commercially available carbonyl precursors (aldehyde **1** for the *nor*-methyl and ketone **3** for the *mono*-methyl) with $NaBH_4$ in MeOH at 0 ºC for 2 h and resulted in the reduced alcohol nitrothiophene triggers **2** and **4** in good yield. Additional synthetic modification was necessary to obtain *gem*-dimethyl-nitrothiophene bioreductive trigger **7** from commercially available 2-acetylthiophene **5** and entailed the initial methylation with CH_3Li in THF at 0 ºC for 12 h to yield tertiary alcohol **6**. Tertiary alcohol **6** was subjected to nitration conditions in acetic anhydride and fuming nitric acid at -70 ºC to afford *gem*-dimethyl-nitrothiophene **7**. The nitration reaction proceeded in low yields and was therefore repeated several times in small scale portions in order to obtain a sufficient quantity for subsequent Mitsunobu coupling as well as limit the safety concerns associated with large scale nitration reactions of aromatic compounds.

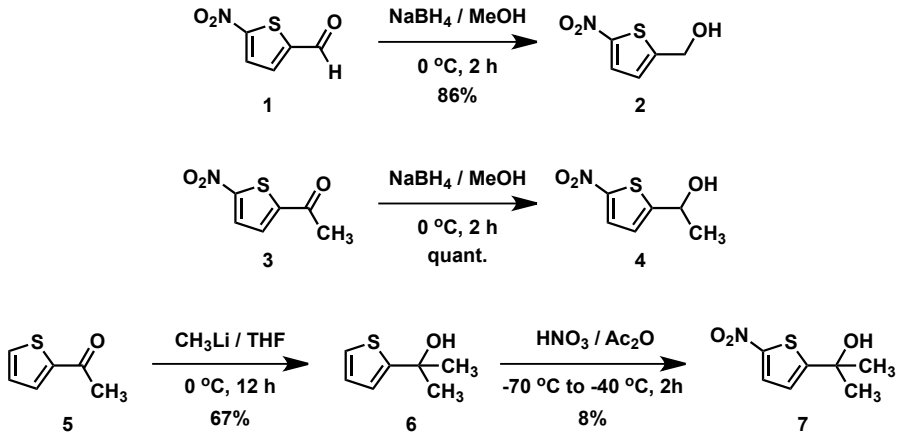

Scheme 4.1. Synthesis of nitrothiophene bioreductive triggers.

The coupling between nitrothiophene triggers **2**, **4**, and **7** and **OXi8006** was accomplished with representative Mitsunobu reagents which included the two requisite alcohols (a nitrothiophene and the parent VDA **OXi8006**), a tertiary phosphine, and an azodicarboxylate (Scheme 2). BAPC **8** was obtained from *nor*-methyl-nitrothiophene **2** and **OXi8006** upon the addition of DIAD to a solution of PPh_3, **OXi8006**, and thiophene **2** in CH_2Cl_2. The synthesis of BAPC **9** involved a similar sequence in which DIAD was added to a solution of **OXi8006**, *mono*-methyl-nitrothiophene **4**, and PPh_3 in CH_2Cl_2 to yield BAPC **9**. The *gem*-dimethyl coupled BAPC **10** involved analogous Mitsunobu conditions as the *nor*-methyl- and *mono*-methyl- derivatives, however, PBu_3 was added to a solution of **OXi8006**, tertiary thiophene alcohol **7**, and ADDP in benzene and resulted in the desired BAPC **10**. Although all three Mitsunobu couplings were successful, it should be noted that all proceeded with low yields 5-32% and required a total of 1.5 grams of non-commercially available **OXi8006** (0.5 g per reaction) in order to isolate sufficient quantities of BAPCs **8-10** for biological evaluation in addition to arduous purifications that each compound demanded. BACPs **8-10** will be evaluated through an established collaboration with the Trawick Research Group at Baylor University to determine their hypoxic cytotoxicity ratio (HCR), which is described as the IC_{50} of the prodrug under oxic conditions divided by the IC_{50} of the prodrug under anoxic conditions. A larger HCR value suggests an increase in the enzymatic cleavage that releases the parent anticancer agent under anoxic conditions (as anticipated) evidenced by an increase in cytotoxicity (decrease in IC_{50} value under anoxia).

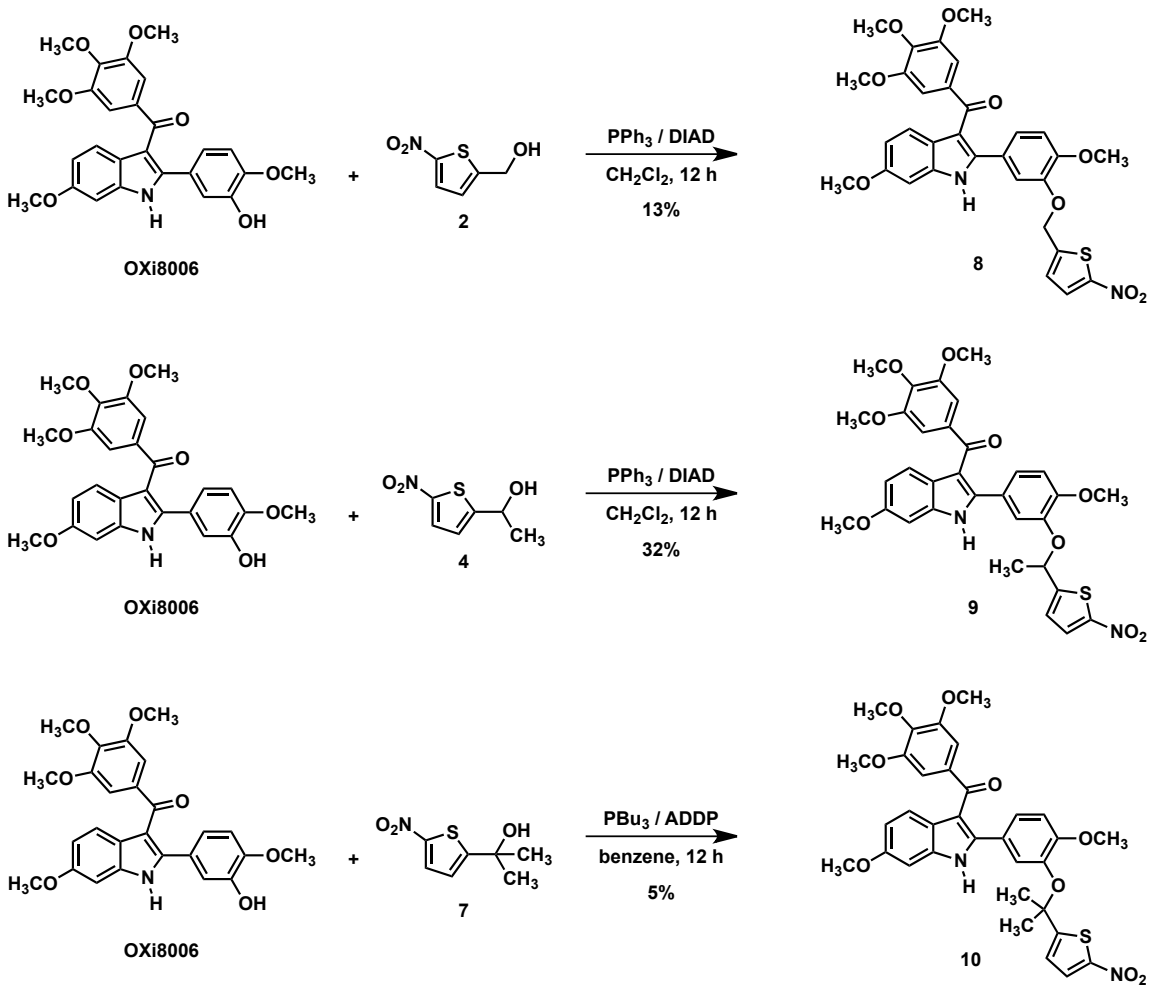

Scheme 4.2. Synthesis of bioreductively activatable prodrug conjugates (BAPCs).

Materials and Methods

General Section

CH_2Cl_2, THF, MeOH, and benzene were used in their anhydrous forms as obtained from the chemical suppliers. Reactions were performed under an inert atmosphere using nitrogen gas, unless specified otherwise. Thin-layer chromatography (TLC) plates (precoated glass plates with silica gel 60 F254, 0.25 mm thickness) were used to monitor reactions. Purification of intermediates and products was carried out

with a flash purification system (Biotage Isolera 4) using silica gel (200-400 mesh, 60 Å) prepacked columns. Intermediates and products synthesized were characterized on the basis of their ^{1}H NMR (500 MHz) and ^{13}C NMR (125 MHz) spectroscopic data using a Varian VNMRS 500 MHz instrument. Spectra were recorded in $CDCl_3$. All of the chemical shifts are expressed in ppm (δ), coupling constants (*J*) are presented in Hz, and peak patterns are reported as broad (br), singlet (s), doublet (d), double doublet (dd), quartet (q), and multiplet (m). Purity of the final compounds was further analyzed at 25 °C using an Agilent 1200 HPLC system with a diode-array detector (λ = 190-400 nm), a Zorbax XDB-C18 HPLC column (4.6 mm - 150 mm, 5 μm), and a Zorbax reliance cartridge guard-column; solvent A: acetonitrile, solvent B: H_2O; gradient: 10%A / 90%B to 100%A / 0%B over 0 to 40 min; post-time 10 min; flow rate 1.0 mL/min; injection volume 20 μL; monitored at wavelengths of 210, 254, 230, 280, and 360 nm. Mass spectrometry was carried out under positive ESI (electrospray ionization) using a Thermo scientific LTQ Orbitrap Discovery instrument.

1-(5′-Nitrothiophen-2′-yl)ethanol ***4***[1]

To a clean dry round bottom flask 1-(5-nitrothiophe-2-yl)ethanone **3** (1.00 g, 5.84 mmol) was dissolved in MeOH (20 mL). The solution was cooled to 0 °C and $NaBH_4$ (0.33 g, 8.76 mmol) was added. The reaction mixture was stirred for 2 h. Upon completion, the reaction was quenched with water (10 mL), transferred to a separatory funnel, and extracted with EtOAc. The organic extracts were combined, dried over

[1] Thompson, P.; Naylor, M. A.; Everett, S. A.; Stratford, M. R. L.; Lewis, G.; Hill, S.; Patel, K. B.; Wardman, P.; Davis, P. D. Synthesis and Biological Properties of Bioreductively Targeted Nitrothienyl Prodrugs of Combretastatin A-4. *Mol. Cancer Ther.* **2006**, *5*(11), 2886-2894.

Na_2SO_4, filtered, and concentrated under reduced pressure. The alcohol product **4** (1.01 g, 5.84 mmol) was isolated quantitatively as a brown oil.

^{1}H NMR ($CDCl_3$, 500 MHz): δ 7.72 (d, *J* = 4.5 Hz, 1H, ArH), 6.84 (d, *J* = 4.5 Hz, 1H, ArH), 5.07 (q, *J* = 6.5 Hz, 1H, CH), 3.71 (br s, 1H, OH), 1.54 (d, *J* = 6.5 Hz, 3H, CH_3.

^{13}C NMR ($CDCl_3$, 125 MHz): δ 159.9, 149.9, 129.1, 122.2, 66.3, 25.0.

2-(Thiophen-2-yl)propan-2-ol ***6***[1]

To a clean, dry round-bottom flask, 1-(2-thiophenyl)ethanone **5** (20.0 g, 157 mmol) was dissolved in THF (500 mL). The solution was cooled to 0 ºC and CH_3Li (129 mL, 206 mmol) was added drop wise. The reaction mixture was stirred for 12 h allowing the reaction mixture to warm to room temperature. Upon completion, the reaction was quenched with water (150 mL), transferred to a separatory funnel, and extracted with EtOAc. The organic extracts were combined, dried over Na_2SO_4, filtered, and concentrated under reduced pressure. The alcohol product **6** (15.1 g, 106 mmol, 67%) was isolated as a colorless oil.

^{1}H NMR ($CDCl_3$, 500 MHz): δ 7.15 (dd, *J* = 4.9, 1.4 Hz, 1H, ArH), 6.93 – 6.89 (m, 2H, ArH), 2.53 (s, 1H, OH), 1.63 (s, 9H, CH_3).

^{13}C NMR ($CDCl_3$, 125 MHz): δ 154.5, 126.6, 123.8, 122.0, 71.3, 32.2.

2-(5'-Nitrothiophen-2-yl)propan-2-ol ***7***[1]

To a clean, dry round-bottom flask, 2-(thiophen-2-yl)propan-2-ol **6** (3.0 g, 21.1 mmol) was dissolved in Ac_2O (70 mL). The solution was cooled to -70 ºC and fuming nitric acid (0.96 mL, 21.1 mmol) was added drop wise. The reaction mixture was stirred for 2 h allowing the reaction mixture to warm to -40 ºC. Ice (20 g) was added to the

solution and was stirred for 45 min. The reaction mixture was transferred to a separatory funnel and extracted with EtOAc. The organic extracts were combined, dried over Na_2SO_4, filtered, and concentrated under reduced pressure. The alcohol product **7** (0.16 g, 0.85 mmol, 8%) was isolated as an orange wax.

^{1}H NMR ($CDCl_3$, 500 MHz): δ 7.75 (d, *J* = 4.2 Hz, 1H, Ar<u>H</u>), 6.85 (d, *J* = 4.2 Hz, 1H, Ar<u>H</u>), 1.64 (s, 6H, C<u>H</u>$_3$).

^{13}C NMR ($CDCl_3$, 125 MHz): δ 164.1, 129.1, 121.4, 72.0, 32.0.

*(6-methoxy-2-(4-methoxy-3-((5-nitrothiophen-2-yl)methoxy)phenyl)-1H-indol-3-yl)(3,4,5-trimethoxyphenyl)methanone **8***

To a clean, dry round-bottom flask, nitrothiophenyl alcohol **2** (0.14 g, 0.90 mmol) obtained from pervious Pinney group member Dr. Clinton George, was dissolved in CH_2Cl_2 (10 mL). **OXi8006** (0.47 g, 1.01 mmol) and PPh_3 (0.46 g, 1.75 mmol) were added and the solution was stirred for 5 min. Diisopropylazodicarboxylate (DIAD) (0.24 mL, 1.22 mmol) was added drop wise and the reaction mixture was stirred for 12 h. The CH_2Cl_2 was removed under reduced pressure and the crude mixture was subjected to flash column chromatography using a pre-packed 50 g silica gel column [solvent A, EtOAc, solvent B, hexanes; gradient 15%A / 85%B (4 CV), 15%A / 85%B → 100%A / 0%B (8 CV), 100%A / 0%B (7.2 CV); flow rate, 40 mL/min; monitored at 254 and 280 nm]. BAPC **8** (0.08 g, 0.13 mmol, 13%) was isolated as a yellow solid.

^{1}H NMR ($CDCl_3$, 500 MHz): δ 8.62 (br s, 1H, N<u>H</u>), 7.81 (d, *J* = 9.5 Hz, 1H, Ar<u>H</u>), 7.78 (d, *J* = 4.0 Hz, 1H, Ar<u>H</u>), 7.10 (dd, *J* = 8.0 Hz, *J* = 2.0 Hz, 1H, Ar<u>H</u>), 6.99 (s, 2H, Ar<u>H</u>), 6.95 (d, *J* = 4.0 Hz, 1H, Ar<u>H</u>), 6.89 (m, 2H, Ar<u>H</u>), 6.85 (d, *J* = 2.0 Hz, 1H, Ar<u>H</u>), 6.81 (d,

J = 8.0 Hz, 1H, ArH), 4.91 (s, 2H, CH_2), 3.85 (s, 3H, OCH_3), 3.83 (s, 3H, OCH_3), 3.82 (s, 3H, OCH_3), 3.67 (s, 6H, OCH_3).

^{13}C NMR ($CDCl_3$, 125 MHz): δ 192.0, 157.5, 152.8, 151.8, 150.6, 148.1, 147.0, 141.8, 141.6, 136.5, 134.9, 128.5, 125.1, 124.9, 123.1, 122.9, 122.5, 117.3, 113.0, 111.94, 111.87, 107.5, 94.7, 66.9, 61.1, 56.2, 56.1, 55.8.

HPLC: 15.21 min.

HRMS (ESI$^+$): *m/z* calculated for $C_{31}H_{29}N_2O_9S$ $[M+H]^+$ 605.1588, found 605.1587.

*(6-methoxy-2-(4-methoxy-3-(1-(5-nitrothiophen-2-yl)ethoxy)phenyl)-1H-indol-3-yl)(3,4,5-trimethoxyphenyl)methanone **9***

To a clean, dry round-bottom flask, nitrothiophenyl alcohol **4** (0.17 g, 0.96 mmol) was dissolved in CH_2Cl_2 (10 mL). **OXi8006** (0.50 g, 1.08 mmol) and PPh_3 (0.49 g, 1.86 mmol) were added and the solution was stirred for 5 min. Diisopropylazodi-carboxylate (DIAD) (0.26 mL, 1.30 mmol) was added drop wise and the reaction mixture was stirred for 12 h. The CH_2Cl_2 was removed under reduced pressure, and the crude mixture was subjected to flash column chromatography using a pre-packed 50 g silica gel column [solvent A, EtOAc, solvent B, hexanes; gradient 15%A / 85%B (4 CV), 15%A / 85%B → 100%A / 0%B (8 CV), 100%A / 0%B (4 CV); flow rate, 40 mL/min; monitored at 254 and 280 nm]. BAPC **9** (0.19 g, 0.31 mmol, 32 %) was isolated as a yellow solid.

^{1}H NMR ($CDCl_3$, 500 MHz): δ 8.97 (br s, 1H, NH), 7.75 (d, *J* = 9.5 Hz, 1H, ArH), 7.68 (d, *J* = 4.0 Hz, 1H, ArH), 7.05 (dd, *J* = 8.0 Hz, *J* = 2.0 Hz, 1H, ArH), 6.99 (s, 2H, ArH), 6.86 (d, *J* = 2.0 Hz, 1H, ArH), 6.84 (m, 2H, ArH), 6.79 (dd, *J* = 4.0 Hz, *J* = 1.0 Hz, 1H, ArH), 6.71 (d, *J* = 8.0 Hz, 1H, ArH), 5.13 (q, *J* = 6.0 Hz, 1H, CH), 3.82 (s, 3H, OCH_3),

3.80 (s, 3H, OC$\underline{H}_3$), 3.78 (s, 3H, OC$\underline{H}_3$), 3.66 (s, 6H, OC$\underline{H}_3$), 1.53 (d, *J* = 6.0 Hz, 3H, C$\underline{H}_3$).

^{13}C NMR ($CDCl_3$, 125 MHz): δ 191.9, 157.4, 155.3, 152.7, 151.4, 150.9, 146.1, 141.7, 141.5, 136.5, 134.7, 128.6, 124.8, 123.4, 123.13, 123.09, 122.4, 119.7, 112.9, 112.1, 111.8, 107.4, 94.6, 74.5, 61.0, 56.2, 56.0, 55.7, 22.9.

HPLC: 15.73 min.

HRMS (ESI$^+$): *m/z* calculated for $C_{32}H_{31}N_2O_9S$ $[M+H]^+$ 619.1745, found 619.1742.

*(6-methoxy-2-(4-methoxy-3-((2-(5-nitrothiophen-2-yl)propan-2-yl)oxy)phenyl)-1H-indol-3-yl)(3,4,5-trimethoxyphenyl)methanone **10***

To a clean, dry round-bottom flask was dissolved nitrothiophenyl alcohol **7** (0.22 g, 1.15 mmol), **OXi8006** (0.50 g, 1.08 mmol), and 1,1′-(azodicarbonyl)-dipiperidine (ADDP) (0.27 g, 1.08 mmol) in benzene (10 mL). PBu_3 (0.27 mL, 1.08 mmol) was added drop wise and the reaction mixture was stirred for 24 h. The benzene was removed under reduced pressure, and the crude mixture was subjected to flash column chromatography using a pre-packed 50 g silica gel column [solvent A, EtOAc, solvent B, hexanes; gradient 5%A / 95%B (1 CV), 5%A / 95%B → 40%A / 60%B (12 CV), 40%A / 60%B (1 CV); flow rate, 25 mL/min; monitored at 254 and 280 nm]. BAPC **10** (0.03 g, 0.05 mmol, 5%) was isolated as a yellow solid.

^{1}H NMR ($CDCl_3$, 500 MHz): δ 8.68 (br s, 1H, N$\underline{H}$), 7.67 (d, *J* = 9.0 Hz, 1H, Ar$\underline{H}$), 7.65 (d, *J* = 4.0 Hz, 1H, Ar$\underline{H}$), 7.16 (dd, *J* = 8.5 Hz, *J* = 2.0 Hz, 1H, Ar$\underline{H}$), 7.03 (s, 2H, Ar$\underline{H}$), 6.87 (d, *J* = 2.0 Hz, 1H, Ar$\underline{H}$), 6.84 (m, 2H, Ar$\underline{H}$), 6.78 (d, *J* = 8.5 Hz, 1H, Ar$\underline{H}$), 6.76 (d, *J* = 4.5 Hz, 1H, Ar$\underline{H}$), 3.85 (s, 3H, OC$\underline{H}_3$), 3.83 (s, 3H, OC$\underline{H}_3$), 3.74 (s, 3H, OC$\underline{H}_3$), 3.71 (s, 6H, OC$\underline{H}_3$), 1.51 (s, 6H, C$\underline{H}_3$).

^{13}C NMR ($CDCl_3$, 125 MHz): δ 191.5, 161.1, 157.4, 154.1, 152.8, 150.7, 143.4, 141.6, 141.3, 136.4, 134.5, 128.4, 125.4, 124.83, 124.76, 123.1, 122.4, 122.2, 112.9, 112.2, 111.8, 107.6, 94.6, 80.7, 61.0, 55.3, 55.84, 55.79, 28.7.

HPLC: 16.37 min.

HRMS (ESI$^+$): *m/z* calculated for $C_{33}H_{33}N_2O_9S$ $[M+H]^+$ 633.1901, found 633.1899.

CHAPTER FIVE

Mechanisms of Heterocyclic Ring Formation

Synthesis of ^{13}C labeled indoles

To further explore the mechanistic pathway of the Bischler-Mohlau indole formation reaction the key bromoacetophenone intermediate **6** was isotopically labeled with the carbon-13 isotope at the alpha position to the carbonyl (Scheme 1). This carbon then provides evidence for which mechanistic pathway is predominating within our system according to the key distinct ^{13}C NMR signature. A similar approach utilizing deuterium atoms at the same position proved to be inconclusive presumably due to proton transfer during tautomerization (see Appendix F for NMR results).

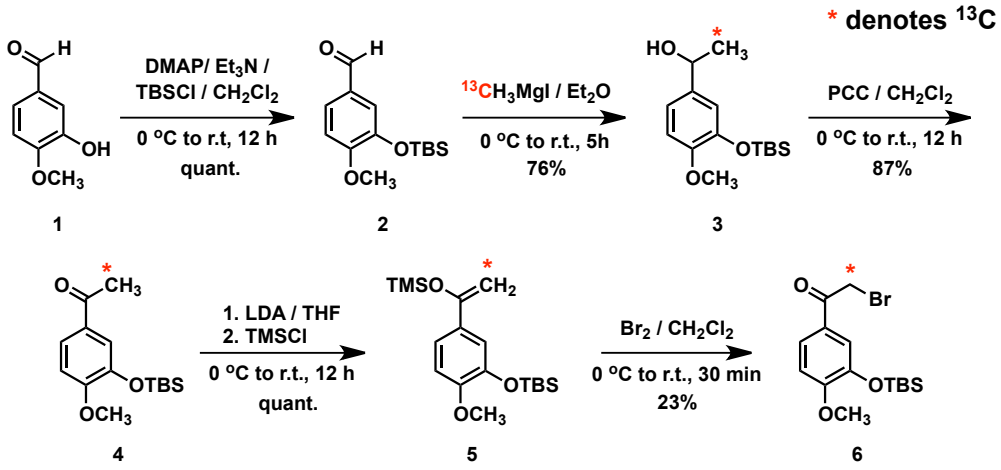

Scheme 5.1. Synthetic route to ^{13}C-labeled bromoacetophenone intermediate **6**.

The synthetic route to ^{13}C-labeled bromoacetophenone intermediate **6** followed a similar sequence as the non-labeled bromoacetophenone intermediate en route to **OXi8006** (Chapter 2) and simply replaces the transitional methylation step reagents to

install the ^{13}C carbon atom at the alpha position. The first step of the synthesis was the phenolic protection of 3-hydroxy-4-methoxybenzaldehyde (also known as *iso*vanillin) with TBSCl in the presence of Et_3N and catalytic DMAP to afford TBS-aldehyde **2** in good yield. TBS-aldehyde **2** was treated with *in situ* generated $^{13}CH_3MgI$ (from commercially available $^{13}CH_3I$) to yield ^{13}C-labeled secondary alcohol **3**, which was oxidized with PCC to generated ^{13}C-labeled acetophenone **4**. Acetophenone **4** was treated with a solution of LDA and the resulting enolate was trapped as the enol ether with TMSCl to provide ^{13}C-labled enol ether **5** which was subjected to bromination with Br_2 to afford key ^{13}C-labeled bromoacetophenone intermediate **6**. The synthetic pathway to ^{13}C-labeled indole **8** employed the ^{13}C-labeled bromoacetophenone intermediate **6** and *m*-anisidine under Bishler-Mohlau conditions to generated ^{13}C-labeled indole **8** (Scheme 2). The ^{13}C-labeled bromoacetophenone **6** and 3 equivalents of 3-methoxyaniline (*m*-anisidine) **7** were dissolved in *N*,*N*-dimethylaniline and heated to 170 ºC (Bishler-Mohlau conditions) for 12 h to afford ^{13}C-labeled indole **8** in which the ^{13}C atom was located at the 3 position of the indole core, suggesting the system moves through pathway B (imine intermediate formation, see chapter one for scheme).

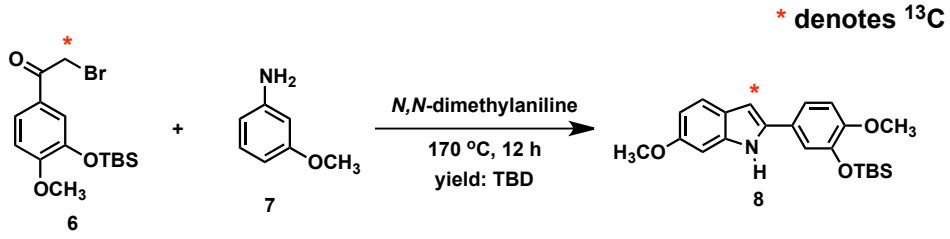

Scheme 5.2. Synthesis of ^{13}C-labeled indole **8**.

These preliminary results were established by ^{1}H NMR, ^{13}C NMR, and DEPT ^{13}C NMR analysis of intermediate **8** (see Appendix E).

Synthesis of ^{13}C labeled benzo[b]furans

A similar labeling strategy was applied to the cyclization of benzo[*b*]furans to explore the mechanistic pathways of formation. The same sequence was employed to generate bromoacetophenone **6** (Scheme 1) and once achieved **6** was treated with KOH in the presence of 3-methoxyphenol **9** to afford ^{13}C-labeled ether intermediate **10** which was then cyclized to ^{13}C-labeled benzo[*b*]furan **11** by treatment with PPA. Preliminary ^{1}H NMR, ^{13}C NMR, and DEPT ^{13}C NMR results (Appendix E), suggest the mechanism moves through pathway A, without migration of the aryl ring to the two position, which is consistent with previously synthesized non-labeled benzo[*b*]furans within the Pinney group for which the structures were determined by X-ray crystallographic diffraction analysis.

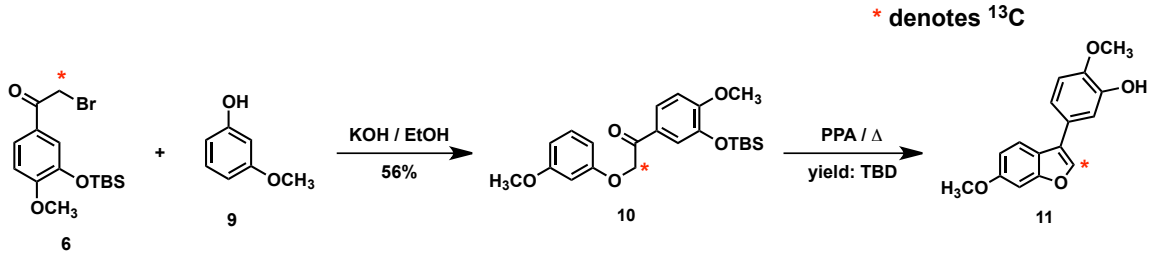

Scheme 5.3. Synthesis of benzo[*b*]furan **11**.

Synthesis of ^{13}C labeled benzo[b]thiophenes

A paralleled approach was employed to examine the cyclization pathway of benzo[*b*]thiophenes. Key ^{13}C-labeled bromoacetophenone **6** was added to a solution of 3-methoxybenzenethiol **12** and KOH in EtOH to afford the intermediate thio-ester **13**. ^{13}C-

labeled thio-ester intermediate **13** was cyclized with PPA resulting in ^{13}C-labeled benzo[*b*]thiophene **14**. Preliminary ^{1}H NMR, ^{13}C NMR, and DEPT ^{13}C NMR results (Appendix E), suggest the mechanic pathway is the same as the benzo[*b*]furan (pathway A), without migration of the aryl ring to the two position, this contradicts previously synthesized non-labeled benzo[*b*]thiophenes within the Pinney group for these specific substrates. Previous work in the Pinney group has established aryl migration to the 2-position as determined by X-ray crystallographic diffraction analysis however this migration was observed for a substrate that lacked the protected 3-phenolic moiety of the bromoacetophenone intermediate. In addition, previous work in the Pinney group employing the same substrates includes the aryl ring migration to the 2-position however this was not confirmed by X-ray crystallographic diffraction analysis and further studies are now underway to determine the structural evidence for the previously observed aryl ring migration.

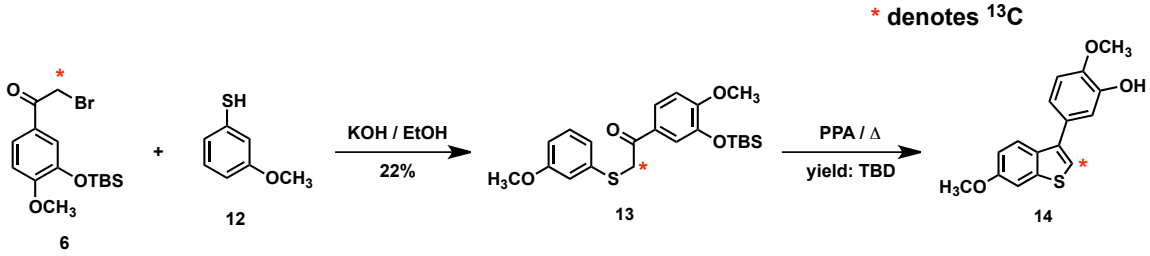

Scheme 5.4. Synthesis of benzo[*b*]thiophene **14**.

Materials and Methods

General Section

CH_2Cl_2, THF, EtOH, and Et_2O were used in their anhydrous forms as obtained from the chemical suppliers. Reactions were performed under an inert atmosphere using

nitrogen gas, unless specified otherwise. Thin-layer chromatography (TLC) plates (precoated glass plates with silica gel 60 F254, 0.25 mm thickness) were used to monitor reactions. Purification of intermediates and products was carried out with a flash purification system (Biotage Isolera 1 or 4) using silica gel (200-400 mesh, 60 Å) prepacked columns. Intermediates and products synthesized were characterized on the basis of their ^{1}H NMR (500 MHz), ^{13}C NMR (125 MHz), and DEPT ^{13}C NMR (125 MHz) spectroscopic data using a Varian VNMRS 500 MHz instrument. Spectra were recorded in $CDCl_3$. All of the chemical shifts are expressed in ppm (δ), coupling constants (*J*) are presented in Hz, and peak patterns are reported as broad (br), singlet (s), doublet (d), double doublet (dd), doublet of quartets (dq), quartet (q), and multiplet (m).

3-(tert-Butyldimethylsilyloxy)-4-methoxybenzaldehyde ***2***

To a clean dry round bottom flask 3-hydroxy-4-methoxybenaldehyde **1** (25.0 g, 164 mmol) was dissolved in CH_2Cl_2 (250 mL). The solution was cooled to 0 ºC and Et_3N (25.2 mL, 181 mmol) was added followed by the addition of *N*,*N*-dimethylaminopyridine (DMAP) (2.01 g, 16.4 mmol). The reaction mixture was stirred for 10 min and *tert*-butyldimethylsilyl chloride (TBSCl) (27.3 g, 181 mmol) was added gradually. The solution was allowed to warm to room temperature and was stirred for 12 hrs. The reaction was diluted with water (150 mL), transferred to a separatory funnel, and was extracted with CH_2Cl_2. The organic extracts were combined, dried over Na_2SO_4, filtered, and concentrated under reduced pressure. The TBS benzaldehyde product **2** (47.1 g, 177 mmol) was isolated quantitatively as a yellow oil and was taken to the next step without further purification.

^{1}H NMR ($CDCl_3$, 500 MHz): δ 9.80 (s, 1H, C<u>H</u>O), 7.45 (dd, *J* = 8.5 Hz, *J* = 2.0 Hz, 1H, Ar<u>H</u>), 7.35 (d, *J* = 2.0 Hz, 1H, Ar<u>H</u>), 6.93 (d, *J* = 8.5 Hz, 1H, Ar<u>H</u>), 3.87 (s, 3H, OC<u>H_3</u>), 0.99 (s, 9H, C(C<u>H_3</u>)$_3$), 0.16 (s, 6H, Si(C<u>H_3</u>)$_2$).

^{13}C NMR ($CDCl_3$, 125 MHz): δ 190.2, 156.2, 145.2, 130.0, 126.0, 119.4, 110.9, 55.1, 25.3, 18.0, -5.0.

*3-tert-Butyldimethylsilyloxy-1-(1'-hydroxyethyl)-4-methoxybenzene **3***

To a solution of magnesium turnings (0.40 g, 16.7 mmol) in diethyl ether (Et_2O) was added ^{13}C-labeled methyl iodide (1.00 mL, 16.0 mmol). The solution was refluxed until the turnings were dissolved. The solution was cooled to room temperature and TBS benzaldehyde **2** (1.94 g, 7.28 mmol) in Et_2O was added drop wise. The reaction mixture was stirred for 5 hours. Upon completion the reaction mixture was slowly quenched with water and extracted with Et_2O. The organic extracts were dried over Na_2SO_4, filtered, and concentrated under reduced pressure resulting in ^{13}C-labeled alcohol **3** (1.57 g, 5.54 mmol, 76%, R_f = 0.47 (70:30 hexanes:EtOAc)) as a yellow oil which was taken to the next step without further purification.

^{1}H NMR ($CDCl_3$, 500 MHz): δ 6.85 (m, 2H, Ar<u>H</u>), 6.76 (m, 1H, Ar<u>H</u>), 4.70 (dq, *J* = 1.5 Hz, 6.5 Hz, 1H, C<u>H</u>), 3.75 (s, 3H, OC<u>H_3</u>), 2.75 (s, 1H, O<u>H</u>), 1.39 (dd, *J* = 6.5 Hz, $J_{C\text{-}H}$ = 126.4 Hz, 3H, C<u>H_3</u>), 1.01 (s, 9H, (C<u>H_3</u>)$_3$), 0.16 (s, 6H, Si(C<u>H_3</u>)$_2$).

^{13}C NMR ($CDCl_3$, 125 MHz): δ 150.1, 144.8, 138.9, 118.5 (d, *J* = 1.8 Hz), 118.3 (d, *J* = 1.6 Hz), 111.9, 69.6 (d, 38.4 Hz), 55.5, 25.7, **25.0**, 18.4, -4.6.

*3-tert-Butyldimethylsilylox)-4-methoxyacetophenone **4***

The crude alcohol **3** (1.50 g, 5.29 mmol) was dissolved in CH_2Cl_2 (50 mL). Celite (5 g) was added and the solution was cooled to 0 ºC. Pyridiniumchlorochromate (PCC) (1.25 g, 5.82 mmol) was added in small increments allowing 10 minutes of stirring between each addition. The reaction was allowed to warm to room temperature and stirred for 12 hrs. The reaction mixture was filtered through a 50/50 mixture of silica gel/celite rinsing well with CH_2Cl_2. The filtrate was concentrated under reduced pressure providing the desired ^{13}C-labeled acetophenone **4** (1.30 g, 4.62 mmol, 87%) as a pale yellow solid.

^{1}H NMR ($CDCl_3$, 500 MHz): δ 7.51 (dd, *J* = 8.5 Hz, *J* = 2.0 Hz, 1H, Ar<u>H</u>), 7.43 (d, *J* = 2.0 Hz, 1H, Ar<u>H</u>), 6.81 (d, *J* = 8.5 Hz, 1H, Ar<u>H</u>), 3.80 (s, 3H, OC<u>H</u>$_3$), 2.46 (d, $J_{C\text{-}H}$ = 127.2 Hz, 3H, C<u>H</u>$_3$), 0.96 (s, 9H, C(C<u>H</u>$_3$)$_3$), 0.12 (s, 6H, Si(C<u>H</u>$_3$)$_2$).

^{13}C NMR ($CDCl_3$, 125 MHz): δ 196.2 (d, *J* = 42.5 Hz), 155.1, 144.7, 130.4 (d, *J* = 13.8 Hz), 123.4, 120.1, 110.6, 55.2, **26.0**, 25.5, 18.2, -4.8.

*1-(3-tert-Butyldimethylsilyloxy-4-methoxyphenyl)-1-trimethylsilylethene **5***

To a solution of diisopropylamine (0.9 mL, 6.39 mmol) in THF (50 mL) at 0 ºC was added *n*-butyllithium (2.56 mL, 6.39 mmol) drop wise. The LDA solution was allowed to stir for 15 and a solution of TBS acetophenone **4** (1.20 g, 4.26 mmol) in THF (5 mL) was added drop wise. The solution was stirred for 10 min and TMSCl (0.81 mL, 6.39 mmol) was added drop wise and the reaction was allowed to warm to room temperature. The solution was stirred for 12 hrs and was quenched using 10% $NaHCO_3$ (100 mL). The reaction mixture was extracted with Et_2O, dried over Na_2SO_4, and concentrated under reduced pressure resulting in ^{13}C-labeled TMS enol ether **5** (1.55 g,

4.39 mmol) quantitatively as a dark yellow oil which was taken to the next step without purification.

^{1}HNMR ($CDCl_3$, 500 MHz): δ 7.23 (dd, *J* = 8.5 Hz, *J* = 2.0 Hz, 1H Ar<u>H</u>), 7.18 (d, *J* = 2.0 Hz, 1H, Ar<u>H</u>), 6.82 (d, *J* = 8.5 Hz, 1H, Ar<u>H</u>), 4.83 (dd, *J* = 1.5 Hz, $J_{C\text{-}H}$ = 159.5 Hz, 1H, C<u>H</u>$_2$), 4.38 (dd, *J* = 1.5 Hz, $J_{C\text{-}H}$ = 159.0 Hz, 1H, C<u>H</u>$_2$), 3.83 (s, 3H, OC<u>H</u>$_3$), 1.08 (s, 9H, C(C<u>H</u>$_3$)$_3$), 0.32 (s, 9H, Si(C<u>H</u>$_3$)$_3$), 0.23 (s, 6H, Si(C<u>H</u>$_3$)$_2$).

^{13}C NMR ($CDCl_3$, 125 MHz): δ 155.4 (d, *J* = 82.0 Hz), 151.3, 144.6, 130.8 (d, *J* = 6.9 Hz), 118.9 (d, *J* = 2.4 Hz), 118.2 (d, *J* = 2.3 Hz), 111.3 (d, *J* = 42.6 Hz), **89.6**, 55.5, 25.9, 18.6, 0.2, -4.5.

*3'-(tert-Butyldimethylsilyloxy)-4'-methoxy-2-bromoacetophenone **6***

A solution of crude **5** (1.56 g, 4.39 mmol) in CH_2Cl_2 (50 mL) and K_2CO_3 (0.03 g, 0.19 mmol) was cooled to 0º C. Bromine (0.14 mL, 2.6 mmol) was added drop wise and the solution was allowed to stir for 30 minutes. The reaction was quenched with10 % sodium thiosulfate solution, transferred to separatory funnel, and extracted with CH_2Cl_2. The organic extracts were dried over Na_2SO_4 and concentrated under reduced pressure. The crude mixture was subjected to flash chromatography using a prepacked 50 g silica column [solvent A, EtOAc, solvent B, hexanes; gradient, 5%A / 95%B (4 CV), 5%A / 95%B → 10%A / 90%B (12 CV), 45%A / 55%B (3.7 CV); flow rate, 40 mL/min; monitored at 254 and 280 nm] to yield ^{13}C-labeled bromoacetophenone **6** as a tan solid (0.36 g, 1.01 mmol, 23%, R_f = 0.29 (80:20 hexanes:EtOAc)).

^{1}H NMR ($CDCl_3$, 500 MHz): δ 7.61 (dd, *J* = 2.5 Hz, 8.5 Hz, 1H, Ar<u>H</u>), 7.48 (d, *J* = 2.0 Hz, 1H, Ar<u>H</u>), 6.89 (d, *J* = 9.0 Hz, 1H, Ar<u>H</u>), 4.37 (d, $J_{C\text{-}H}$ = 151.2 Hz, 2H, C<u>H</u>$_2$), 3.88 (s, 3H, OC<u>H</u>$_3$), 1.00 (s, 9H, C(C<u>H</u>$_3$)$_3$), 0.17 (s, 6H, Si(C<u>H</u>$_3$)$_2$).

^{13}C NMR ($CDCl_3$, 125 MHz): δ 190.0 (d, *J* = 48.5 Hz), 156.2, 145.2, 127.2 (d, *J* = 17.3 Hz), 124.4, 121.2, 111.1, 55.7, **30.8**, 25.6, 18.6, -4.6.

*2-(3'-tert-Butyldimethylsilyloxy-4'-methoxyphenyl)-6-methoxyindole **8***

A solution of *m*-anisidine (0.24 mL, 2.10 mmol) was dissolved in N,N-dimethylaniline (20 mL) and was heated to reflux at 170° C. A solution of **6** (0.23 g, 0.64 mmol) in EtOAc (5 mL) was added drop wise. The reaction mixture was stirred at 170° C for 12 hours. The reaction mixture was allowed to cool to room temperature and was extracted with EtOAc (3 x 50 mL). The combined organic extracts were dried over Na_2SO_4 and concentrated under reduced pressure. Purification by flash chromatography using a prepacked 25 g silica column [solvent A, EtOAc, solvent B, hexanes; gradient, 12%A / 88%B (4 CV), 12%A / 88%B → 100%A / 0%B (10 CV), 100%A / 0%B (2.6 CV); flow rate, 25 mL/min; monitored at 254 and 280 nm] resulted in the desired ^{13}C-labeled phenylindole **8** (R_f = 0.48 (50:50 hexanes:EtOAc)) as a light tan solid.

^{1}H NMR ($CDCl_3$, 500 MHz): δ 8.13 (br s, 1H, N<u>H</u>), 7.47 (dd, *J* = 2.5 Hz, 8.5 Hz, 1H, Ar<u>H</u>), 7.15 (m, 2H, Ar<u>H</u>), 6.89 (m, 2H, Ar<u>H</u>), 6.79 (dd, *J* = 2.5 Hz, 8.5 Hz, 1H, Ar<u>H</u>), 6.79-6.44 (d, *J* = 1.5 Hz, J_{C-H} = 171 Hz 1H, Ar<u>H</u>), 3.86 (s, 3H, OC<u>H</u>$_3$), 3.84 (s, 3H, OC<u>H</u>$_3$), 1.04 (s, 9H, C(C<u>H</u>$_3$)$_3$), 0.21 (s, 6H, Si(C<u>H</u>$_3$)$_2$).

^{13}C NMR ($CDCl_3$, 125 MHz): δ **98.3**.

*1-(3-(((tert-Butyldimethylsilyl)oxy)-4-methoxyphenyl)-2-(3-methoxyphenoxy)ethanone **10***

To a solution of KOH (0.02 g, 0.28 mmol) in EtOH:H_2O (2.5:1) (2 mL) at 5 °C was added ^{13}C-labeled bromoacetonphenone **6** (0.10 g, 0.28 mmol) drop wise. The reaction mixture was allowed to warm to room temperature over 12 h. The reaction

mixture was extracted with EtOAc (3 x 50 mL). The combined organic extracts were dried over Na_2SO_4 and concentrated under reduced pressure. Purification by flash chromatography using a prepacked 25 g silica column [solvent A, EtOAc, solvent B, hexanes; gradient, 2%A / 98%B (4 CV), 2%A / 98%B → 20%A / 80%B (10 CV), 20%A / 80%B (2 CV); flow rate, 25 mL/min; monitored at 254 and 280 nm] resulted in the desired ^{13}C-labeled ether **10** (R_f = 0.31 (90:10 hexanes:EtOAc)) as a yellow oil.

^{1}H NMR ($CDCl_3$, 500 MHz): δ 7.64 (dd, *J* = 2.0 Hz, 8.5 Hz, 1H, Ar<u>H</u>), 7.52 (d, *J* = 2.0 Hz, 2H, Ar<u>H</u>), 7.17 (m, 1H, Ar<u>H</u>), 6.89 (d, *J* = 8.5 Hz, 1H, Ar<u>H</u>), 6.53 (m, 3H, Ar<u>H</u>), 5.17 (d, $J_{C\text{-}H}$ = 143.5 Hz), 3.88 (s, 3H, OC<u>H</u>$_3$), 3.77 (s, 3H, OC<u>H</u>$_3$), 1.00 (s, 9H, C(C<u>H</u>$_3$)$_3$), 0.17 (s, 6H, Si(C<u>H</u>$_3$)$_2$).

^{13}C NMR ($CDCl_3$, 125 MHz): δ 193.0 (d, *J* = 44.8 Hz), 160.9, 159.4, 156.1, 145.2, 130.1, 127.9 (d, *J* = 15.9 Hz), 123.4, 120.5, 111.1, 107.3, 106.7 (d, *J* = 3.6 Hz), 101.6 (d, *J* = 3.6 Hz), **70.8**, 55.6, 55.4, 25.8, 18.6, -4.5.

*2-methoxy-5-(6-methoxybenzofuran-3-yl)phenol **11***

^{13}C-labeled ether intermediate **10** (0.06 g, 0.15 mmol) was added to PPA (0.38 g, 0.93 mmol) and the reaction was heated to 50 ºC. The reaction was stirred for 12 h and cooled to room temperature. The reaction mixture was extracted with EtOAc (3 x 50 mL). The combined organic extracts were dried over Na_2SO_4 and concentrated under reduced pressure. Purification by flash chromatography using a prepacked 25 g silica column [solvent A, EtOAc, solvent B, hexanes; gradient, 7%A / 93%B (4 CV), 7%A / 93%B → 60%A / 40%B (10 CV), 60%A / 40%B (5.2 CV); flow rate, 25 mL/min; monitored at 254 and 280 nm] resulted in the desired ^{13}C-labeled benzo[*b*]furan **11** (R_f = 0.53 (70:30 hexanes:EtOAc)) as a yellow oil.

^{1}H NMR ($CDCl_3$, 500 MHz): δ 7.64 (d, $J_{C\text{-}H}$ = 201.0 Hz, 1H, Ar<u>H</u>), 7.64 (d, *J* = 8.5 Hz, 1H, Ar<u>H</u>), 7.46 (d, *J* = 8.5 Hz, 1H, Ar<u>H</u>), 7.30 (s, 1H, Ar<u>H</u>), 7.06 (m, 2H, Ar<u>H</u>), 6.93 (d, *J* = 8.0 Hz), 3.89 (s, 3H, OC<u>H</u>$_3$), 3.78 (s, 3H, OC<u>H</u>$_3$).

^{13}C NMR ($CDCl_3$, 125 MHz): δ **140.1**.

1-(3-(((tert-Butyldimethylsilyl)oxy)-4-methoxyphenyl)-2-(3-methoxyphenyl)thio)ethanone ***13***

To a solution of KOH (0.02 g, 0.28 mmol) in EtOH:H_2O (2.5:1) (2 mL) at 5 ºC was added ^{13}C-labeled bromoacetonphenone **6** (0.10 g, 0.28 mmol) drop wise. The reaction mixture was allowed to warm to room temperature over 12 h. The reaction mixture was extracted with EtOAc (3 x 50 mL). The combined organic extracts were dried over Na_2SO_4 and concentrated under reduced pressure. Purification by flash chromatography using a prepacked 25 g silica column [solvent A, EtOAc, solvent B, hexanes; gradient, 2%A / 98%B (4 CV), 2%A / 98%B → 20%A / 80%B (10 CV), 20%A / 80%B (2 CV); flow rate, 25 mL/min; monitored at 254 and 280 nm] resulted in the desired ^{13}C-labeled thio-ether **13** (R_f = 0.34 (90:10 hexanes:EtOAc)) as a colorless oil.

^{1}H NMR ($CDCl_3$, 500 MHz): δ 7.57 (dd, *J* = 2.5 Hz, 8.5 Hz, 1H, Ar<u>H</u>), 7.47 (d, *J* = 2.0 Hz, 1H, Ar<u>H</u>), 7.18 (m, 1H, Ar<u>H</u>), 6.96 (m, 1H, Ar<u>H</u>), 6.94 (ddd, *J* = 1.0 Hz, 1.5 Hz, 8.0 Hz, 1H, Ar<u>H</u>), 6.74 (ddd, *J* = 1.0 Hz, 2.5 Hz, 8.0 Hz, 1H, Ar<u>H</u>), 4.22 (d, $J_{C\text{-}H}$ = 139.5 Hz), 3.87 (s, 3H, OC<u>H</u>$_3$), 3.76 (s, 3H, OC<u>H</u>$_3$), 1.00 (s, 9H, C(C<u>H</u>$_3$)$_3$), 0.16 (s, 6H, Si(C<u>H</u>$_3$)$_2$).

^{13}C NMR ($CDCl_3$, 125 MHz): δ 192.8 (d, *J* = 42.3 Hz), 159.9, 155.8, 145.1, 136.6, 129.3, 128.7 (d, *J* = 15.3 Hz), 124.0, 122.1 (d, *J* = 2.5 Hz), 121.0, 115.2 (d, *J* = 2.5 Hz), 112.8, 111.0, 55.6, 55.4, **40.6**, 25.8, 18.6, -4.5.

*2-methoxy-5-(6-methoxybenzo[b]thiophen-3-yl)phenol **14***

^{13}C-labeled thio-ether intermediate **13** (0.02 g, 0.06 mmol) was added to PPA (0.15 g, 0.37 mmol) and the reaction was heated to 50 ºC. The reaction was stirred for 12 h and cooled to room temperature. The reaction mixture was extracted with EtOAc (3 x 50 mL). The combined organic extracts were dried over Na_2SO_4 and concentrated under reduced pressure. Purification by flash chromatography using a prepacked 25 g silica column [solvent A, EtOAc, solvent B, hexanes; gradient, 2%A / 98%B (4 CV), 2%A / 98%B → 20%A / 60%B (10 CV), 20%A / 60%B (4 CV); flow rate, 25 mL/min; monitored at 254 and 280 nm] resulted in the desired ^{13}C-labeled benzo[*b*]thiophene **14** (R_f = 0.61 (90:10 hexanes:EtOAc)) as a colorless oil.

^{1}H NMR ($CDCl_3$, 500 MHz): δ 7.80 (d, *J* = 9.0 Hz, 1H, Ar<u>H</u>), 7.36 (d, *J* = 2.5 Hz, 1H, Ar<u>H</u>), 7.34-6.97 (d, $J_{C\text{-}H}$ = 195.5 Hz, 1H, Ar<u>H</u>), 7.16 (d, *J* = 2.0 Hz, 1H, Ar<u>H</u>), 7.07 (dd, *J* = 2.0 Hz, 8.0 Hz, 1H, Ar<u>H</u>), 7.01 (dd, *J* = 2.5 Hz, 9.0 Hz, 1H, Ar<u>H</u>), 6.95 (d, *J* = 8.0 Hz, 1H, Ar<u>H</u>), 5.69 (s, 1H, O<u>H</u>), 3.96 (s, 3H, OC<u>H</u>$_3$), 3.89 (s, 3H, OC<u>H</u>$_3$).

^{13}C NMR ($CDCl_3$, 125 MHz): δ **120.2**.

CHAPTER SIX

Conclusions

Functionalized indole ring systems have a rich history as either the pharmacophore itself or a key molecular component of numerous drugs and drug candidates. A significant portion of the studies described herein involve small-molecule anticancer agents that feature indole-based molecular templates. For example, a scale up synthesis of the lead indole-based vascular disrupting agent (VDA) **OXi8006** and its corresponding water-soluble phosphate prodrug salt **OXi8007** was achieved in order to supply sufficient quantities of each of these compounds for further biological evaluation, including color doppler ultrasound to assess blood-flow disruption in real time using a mouse model (collaboration with Ralph Mason, University of Texas Southwestern Medical Center).

In addition, a small library of **OXi8006** analogues was synthesized in which functional group modifications were explored at the 2-aryl position, the 3-aroyl position, and within the indole core. These analogues provide a foundation for advancing our understanding of salient structure-activity relationship (SAR) consideration with respect to 2-aryl-3-aroyl indole-based VDAs and related anticancer agents.

In an effort to target tumor hypoxia for selective drug delivery and release, three **OXi8006** bioreductively activatable prodrug conjugates (BAPCs) were prepared by chemical synthesis in which the ether bridge between the nitrophenyl trigger and the parent VDA, **OXi8006**, was functionalized to incorporate *nor*-methyl, mono-methyl, and *gem*-dimethyl substitution patterns.

Finally, an isotopic labeling strategy was used to explore the mechanistic pathway of the Bischler-Mohlau indole reaction. A similar method was also applied to the formation of benzo[*b*]thiophenes and benzo[*b*]furans. Key ^{13}C NMR signatures of the final products provided insight into the mechanistic pathways of indole formation via the Bischler-Mohlau reaction as well as formation of benzo[*b*]thiophene and benzo[*b*]furan derivatives.

APPENDICES

APPENDIX A

Indole-based Vascular Disrupting Agents

This appendix represents a comprehensive literature review of indole-based tubulin binding agents from 2007 to present. It is organized by publication with the structures of each derivative from each publication depicted in addition to the corresponding biological data. Each publication also depicts the structures and biological data of the standards for which the indole-based analogues are compared to.

3-Substitued indoles: One-pot synthesis and evaluation of anticancer and Src kinase inhibitory activities

V. Kameshwara Rao, Bhupender S. Chhikara, Amir Nasrolahi Shirazi, Rakesh Tiwari, Keykavous Parang, Anil Kumar

Bioorganic & Medicinal Chemistry Letters 21 (2011) 3511–3514

HT-29: colon- % inhibition cell proliferation
SK-OV-3: ovarian- % inhibition cell proliferation

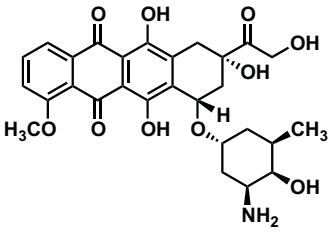

adriamycin / doxorubicin

HT-29: 75
SK-OV-3: 77

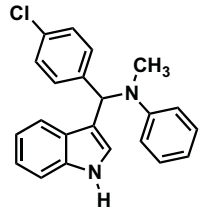

HT-29: 0
SK-OV-3: 70

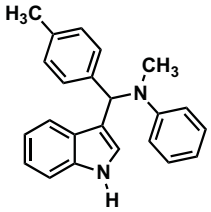

HT-29: -10
SK-OV-3: 30

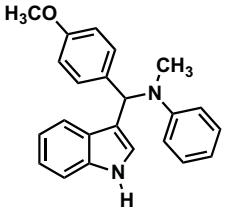

HT-29: -9
SK-OV-3: 42

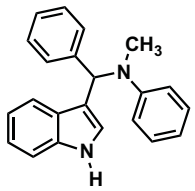

HT-29: -10
SK-OV-3: 55

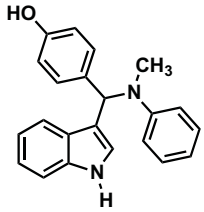

HT-29: -10
SK-OV-3: 44

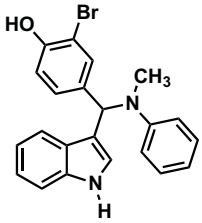

HT-29: -10
SK-OV-3: 10

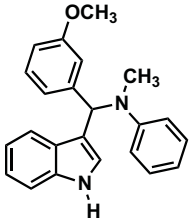

HT-29: 38
SK-OV-3: 22

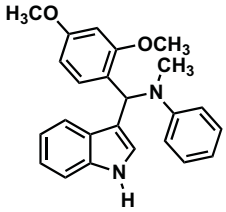

HT-29: 23
SK-OV-3: 20

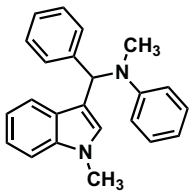

HT-29: 18
SK-OV-3: 25

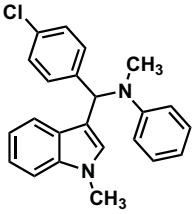

HT-29: 10
SK-OV-3: 26

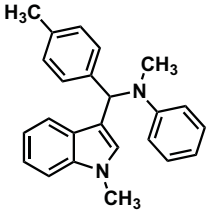

HT-29: 10
SK-OV-3: 12

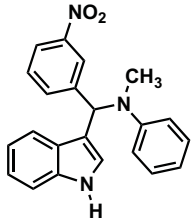

HT-29: 45
SK-OV-3: 25

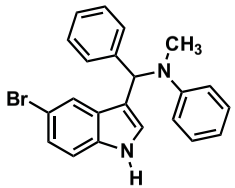

HT-29: 50
SK-OV-3: 30

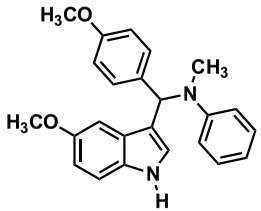

HT-29: 10
SK-OV-3: 30

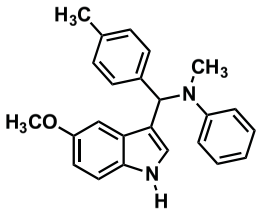

HT-29: 72
SK-OV-3: 73

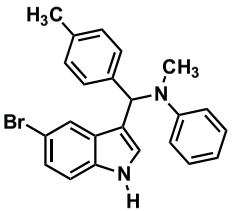

HT-29: 70
SK-OV-3: 77

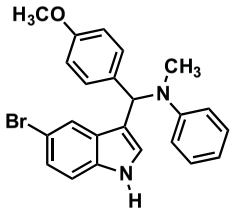

HT-29: 71
SK-OV-3: 77

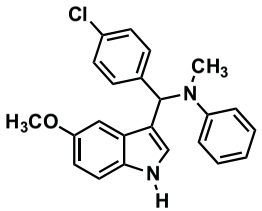

HT-29: 65
SK-OV-3: 77

4- and 5-Aroylindoles as Novel Classes of Potent Antitubulin Agents

Jing-Ping Liou, Chang-Ying Wu, Hsing-Pang Hsieh, Chi-Yen Chang, Chi-Ming Chen, Ching-Chuan Kuo, and Jang-Yang Chang

J. Med. Chem. 2007, 50, 4548-4552

KB: oral epidermoid carcinoma
KB-vin10: MDR-positive
H460: non small cell lung carcinoma
HT29: colorectal carcinoma
TSGH: stomach carcinoma
MKN45: stomach carcinoma

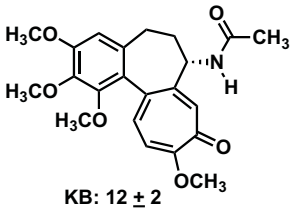

KB: 12 ± 2
KB-vin10: 120 ± 4
H460: 19 ± 3
HT29: nd
TSGH: nd
MKN45: 13 ± 1

Tubulin: 2.9 ± 0.4 μM

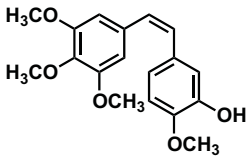

Tubulin: 1.3 ± 0.2 μM

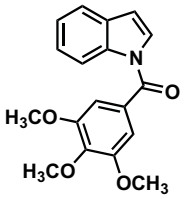

KB: >10,000
KB-vin10: >10,000
H460: > 10,000
HT29: 9600 ± 510
TSGH: 8400 ± 350
MKN45: 5200 ± 420

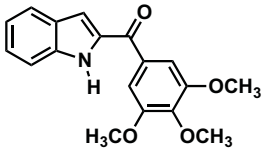

KB: 2900 ± 150
KB-vin10: 2800 ± 120
H460: 2100 ± 250
HT29: 1700 ± 280
TSGH: 1800 ± 320
MKN45: 1500 ± 80

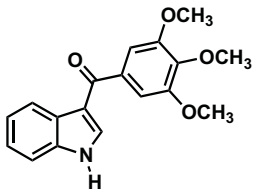

KB: 1600 ± 110
KB-vin10: 1500 ± 70
H460: 1700 ± 70
HT29: 1000 ± 120
TSGH: 1100 ± 130
MKN45: 980 ± 90

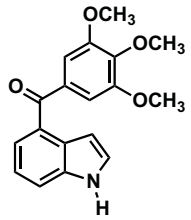

KB: 50.7 ± 8
KB-vin10: 51.4 ± 2
H460: 53.8 ± 7
HT29: 46.4 ± 4
TSGH: 54.4 ± 6
MKN45: 49.1 ± 8

Tubulin: 2.0 ± 0.2 μM

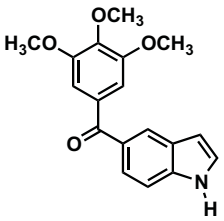

KB: 104 ± 15
KB-vin10: 111 ± 6
H460: 112 ± 12
HT29: 100 ± 7
TSGH: 103 ± 8
MKN45: 88 ± 11

Tubulin: 2.2 ± 0.3 μM

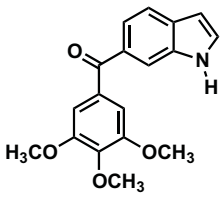

KB: 510 ± 21
KB-vin10: 452 ± 8
H460: 520 ± 120
HT29: 330 ± 18
TSGH: 430 ± 31
MKN45: 480 ± 22

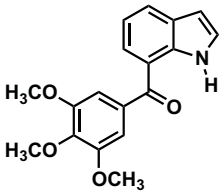

KB: 310 ± 25
KB-vin10: 284 ± 12
H460: 295 ± 19
HT29: 250 ± 24
TSGH: 310 ± 18
MKN45: 210 ± 11

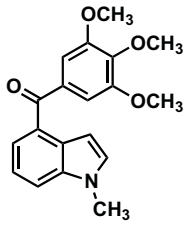

KB: 22.1 ± 6
KB-vin10: 26.1 ± 2
H460: 28.8 ± 3
HT29: 22.4 ± 4
TSGH: 26.9 ± 3
MKN45: 21.6 ± 4

Tubulin: 1.9 ± 0.2 μM

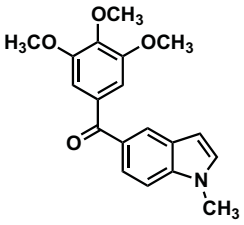

KB: 13.6 ± 1
KB-vin10: 12.5 ± 3
H460: 14.1 ± 1
HT29: 10.5 ± 2
TSGH: 13.4 ± 2
MKN45: 11.2 ± 3

Tubulin: 1.1 ± 0.1 μM

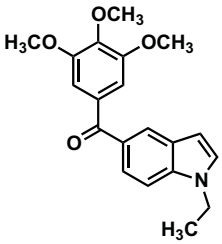

KB: 36 ± 1
KB-vin10: 40 ± 2
H460: 38 ± 4
HT29: 32 ± 6
TSGH: 41 ± 3
MKN45: 31 ± 4

Tubulin: 1.2 ± 0.3 μM

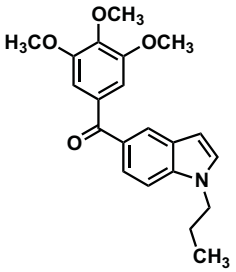

KB: 1900 ± 120
KB-vin10: 2100 ± 480
H460: 2000 ± 520
HT29: 1800 ± 350
TSGH: 1500 ± 180
MKN45: 680 ± 33

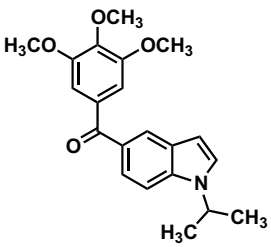

KB: 1800 ± 240
KB-vin10: 1600 ± 150
H460: 1600 ± 120
HT29: 1200 ± 210
TSGH: 1100 ± 320
MKN45: 470 ± 51

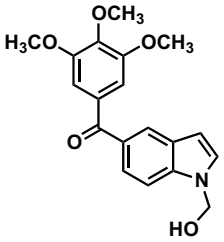

KB: 39 ± 7
KB-vin10: 35 ± 4
H460: 39 ± 6
HT29: 34 ± 3
TSGH: 43 ± 8
MKN45: 33 ± 4

Tubulin: 1.8 ± 0.2 μM

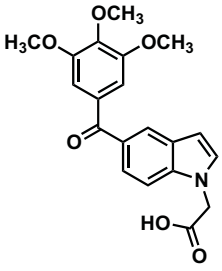

KB: 520 ± 69
KB-vin10: 476 ± 16
H460: 530 ± 77
HT29: 460 ± 58
TSGH: 548 ± 81
MKN45: 396 ± 38

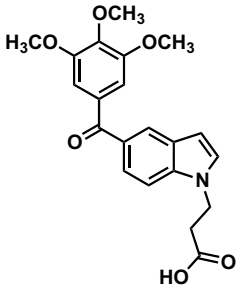

KB: >10,000
KB-vin10: >10,000
H460: >10,000
HT29: >10,000
TSGH: >10,000
MKN45: >10,000

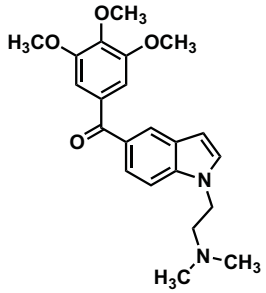

KB: 5200 ± 380
KB-vin10: 4900 ± 210
H460: 5100 ± 620
HT29: 4600 ± 310
TSGH: 4900 ± 610
MKN45: 2900 ± 320

9-Benzylidene-naphtho[2,3-b]thiophen-4-ones as Novel Antimicrotubule AgentssSynthesis, Antiproliferative Activity, and Inhibition of Tubulin Polymerization

Anne Zuse, Peter Schmidt, Silke Baasner, Konrad J. Bohm, Klaus Muller, Matthias Gerlach, Eckhard G. Gunther, Eberhard Unger, and Helge Prinz

J. Med. Chem. 2006, 49, 7816-7825

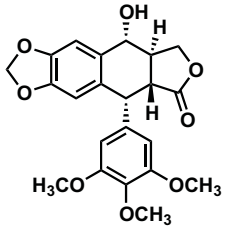

podophyllotoxin

K562: nd
ITP: 0.35

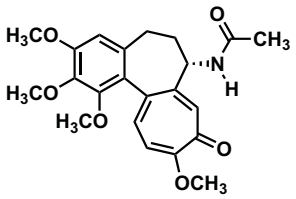

colchicine

K562: 0.2
ITP: 1.4

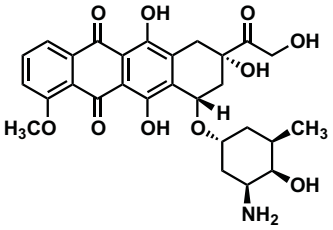

adriamycin/doxorubicin

K562: 0.01
ITP: nd

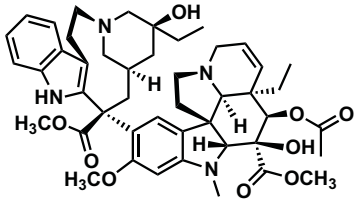

vinblastine

K562: 0.001
ITP: 0.13

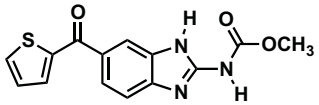

nocodazole

K562: nd
ITP: 0.76

K562: myelogenous leukemia-μM
ITP: inhibit tubulin poly-μM

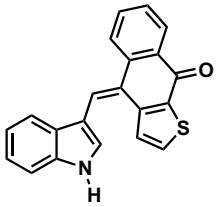

K562: 0.72
ITP: 2.80

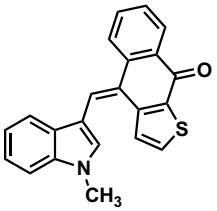

K562: 0.25
ITP: nd

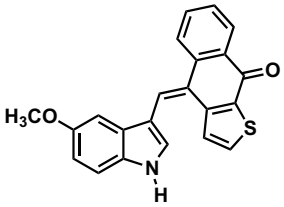

K562: 0.24
ITP: nd

A DC-81-indole conjugate agent suppresses melanoma A375 cell migration partially via interrupting VEGF production and stromal cell-derived factor-1á mediated signaling

Ming-Chu Hsieh, Wan-Ping Hu, Hsin-Su Yu, Wen-Chuan Wu, Long-Sen Chang, Ying Hsien Kao, Jeh-Jeng Wang

Toxicology and Applied Pharmacology 255 (2011) 150–159

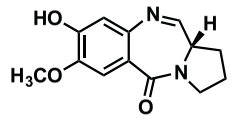

DC-81

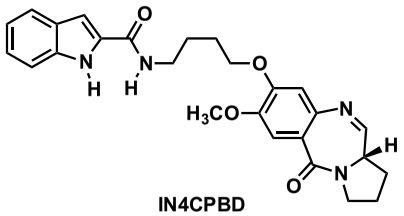

IN4CPBD

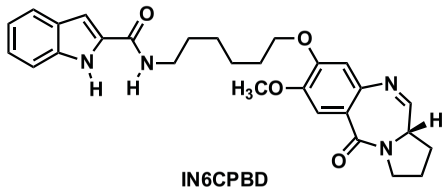

IN6CPBD

Effect of DC-81 and IN4CPBD on cell cycle distribution of A375 melanoma cells a.
Groups (dose) % G1/G0 % S % G2/M
Control 67.4±1.0 b 18.9±3.9 13.7±3.0
DC-81 (5 iM) 69.4±1.5 13.5±0.9. 17.1±0.6
IN4CPBD (0.1 iM) 81.0±1.0. 11.6±1.6. 7.4±1.2.
IN4CPBD (0.5 iM) 74.5±1.9. 14.7±0.4. 10.9±1.8
a Human A375 melanoma cells were treated with DC-81 or its indole conjugate, IN4CPBD, in triplicate at indicated concentrations for 12 h. Cells were harvested for cell cycle analysis by using flow cytometer.
b Values are represented as mean±SD.
. Pb0.05 (n=3) compared to control.

Antiangiogenic Effects of Indole-3-Carbinol and 3,3'-Diindolylmethane Are Associated with Their Differential Regulation of ERK1/2 and Akt in Tube-Forming HUVEC

Kazuhiro Kunimasa, Tomomi Kobayashi, Kazuhiko Kaji, and Toshiro Ohta

J. Nutr. 140: 1–6, 2010

HUVEC
tube area: 31 ± 1 %
apoptosis: 15 ± 2 %

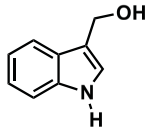

indole-3-carbinol (I3C)

tube area: 12.5 μM: 24 ± 2
25 μM: 21 ± 1
apoptosis: 12.5 μM: 19 ± 3
25 μM: 22 ± 2

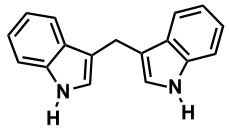

3,3'-diindolylmethane (DIM)

tube area: 12.5 μM: 14 ± 4
25 μM: 10 ± 2
apoptosis: 12.5 μM: 30 ± 3
25 μM: 40 ± 3

Arylthioindole Inhibitors of Tubulin Polymerization. 3. Biological Evaluation, Structure-Activity Relationships and Molecular Modeling Studies

Giuseppe La Regina, Michael C. Edler, Andrea Brancale, Sahar Kandil, Antonio Coluccia, Francesco Piscitelli, Ernest Hamel, Gabriella De Martino, Ruth Matesanz, Jose Fernando Dıaz, Anna Ivana Scovassi, Ennio Prosperi, Antonio Lavecchia, Ettore Novellino, Marino Artico, and Romano Silvestri

J. Med. Chem. 2007, 50, 2865-2874

tubulin: μM
MCF-7: breast cancer-nM
ICB: inibition of colchicine-%

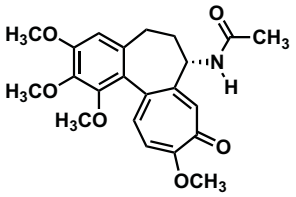

tubulin: 3.2 ± 0.4
MCF-7: 13 ± 3
ICB:

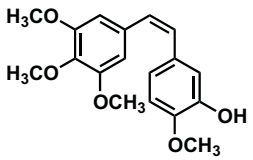

tubulin: 2.2 ± 0.2
MCF-7: 17 ± 10
ICB: 99 ± 1

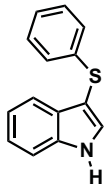

tubulin: 15 ± 0.7
MCF-7: >2500
ICB: nd

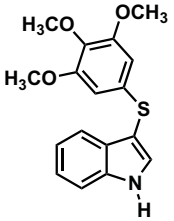

tubulin: 2.6 ± 0.2
MCF-7: 34 ± 9
ICB: 68 ± 0.8

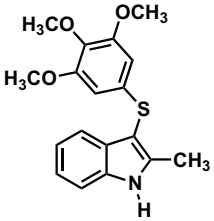

tubulin: 6.8 ± 0.6
MCF-7: 46 ± 4
ICB: 61 ± 4

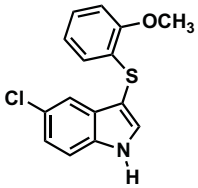

tubulin: 11 ± 2
MCF-7: >2500
ICB: nd

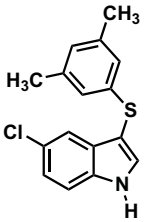

tubulin: 9.4 ± 0.3
MCF-7: 1200 ± 100
ICB: 33 ± 3

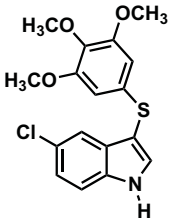

tubulin: 2.6 ± 0.2
MCF-7: 77 ± 7
ICB: 51 ± 4

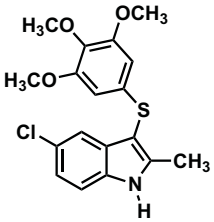

tubulin: 2.7 ± 0.5
MCF-7: 82 ± 10
ICB: 59 ± 5

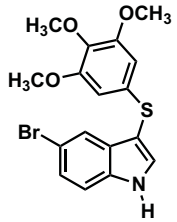

tubulin: 1.6 ± 0.3
MCF-7: 43 ± 7
ICB: 65 ± 3

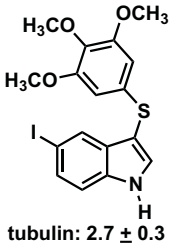

tubulin: 2.7 ± 0.3
MCF-7: 68 ± 7
ICB: 61 ± 2

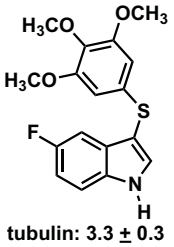

tubulin: 3.3 ± 0.3
MCF-7: 160 ± 50
ICB: 39 ± 6

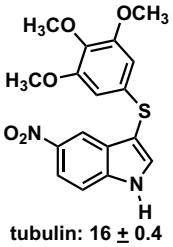

tubulin: 16 ± 0.4
MCF-7: 560 ± 70
ICB: nd

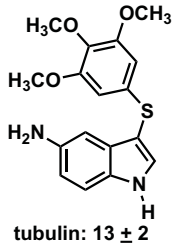

tubulin: 13 ± 2
MCF-7: 260 ± 30
ICB: nd

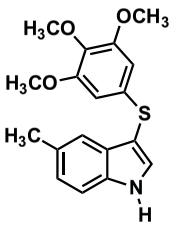

tubulin: 2.7 ± 0.2
MCF-7: 16 ± 6
ICB: 56 ± 3

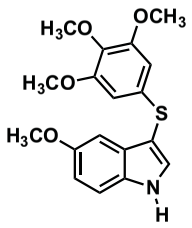

tubulin: 4.1 ± 0.6
MCF-7: 22 ± 2
ICB: 61 ± 4

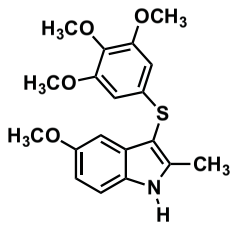

tubulin: 3.3 ± 0.2
MCF-7: 18 ± 4
ICB: 69 ± 0.2

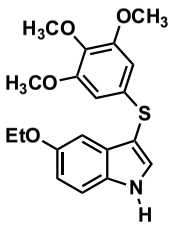

tubulin: 2.1 ± 0.1
MCF-7: 16 ± 5
ICB: 76 ± 5

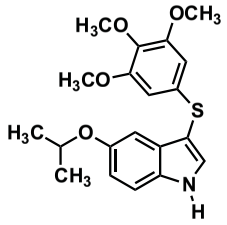

tubulin: 19 ± 0.6
MCF-7: 1500 ± 700
ICB: nd

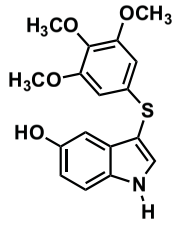

tubulin: 6.3 ± 0.8
MCF-7: 190 ± 40
ICB: 26 ± 0.5

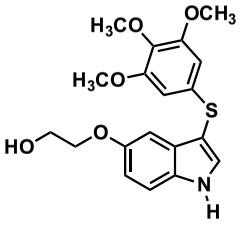

tubulin: 6.8 ± 0.8
MCF-7: 95 ± 8
ICB: 31 ± 2

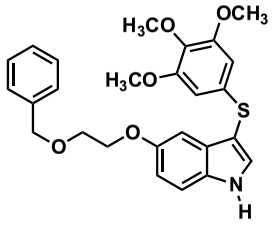

tubulin: >40
MCF-7: 260 ± 20
ICB: nd

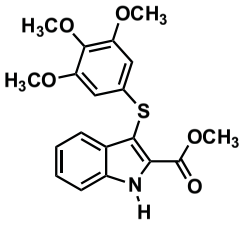

tubulin: 2.9 ± 0.1
MCF-7: 25 ± 1
ICB: 74 ± 2

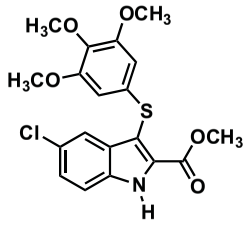

tubulin: 2.3 ± 0.3
MCF-7: 42 ± 1
ICB: 57 ± 2

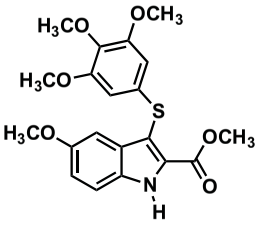

tubulin: 2.0 ± 0.2
MCF-7: 13 ± 3
ICB: 90 ± 1

Arylthioindoles, Potent Inhibitors of Tubulin Polymerization

Gabriella De Martino, Giuseppe La Regina, Antonio Coluccia, Michael C. Edler, Maria Chiara Barbera, Andrea Brancale, Elizabeth Wilcox, Ernest Hamel, Marino Artico, and Romano Silvestri

J. Med. Chem. 2004, 47, 6120-6123

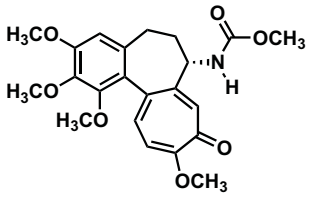

tubulin: 3.2 ± 0.4
MCF-7: 13 ± 3

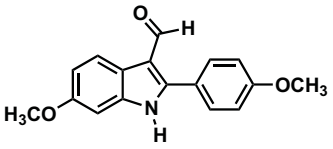

tubulin: nd
colchicine binding: nd
MCF-7: 160

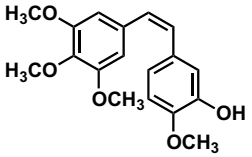

tubulin: 2.2 ± 0.2
colchicine binding: 100 ± 0.9
MCF-7: 17 ± 10

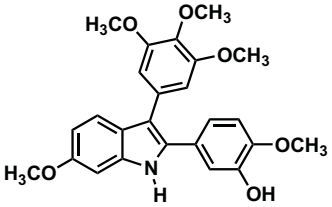

tubulin: 4.1 ± 0.6
colchicine binding: 28 ± 8
MCF-7: 370 ± 2

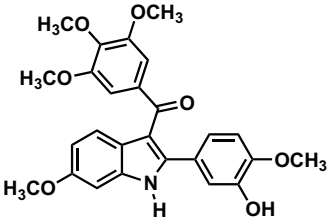

tubulin: 1.6
colchicine binding: 54 ± 0.7
MCF-7: 45 ± 5

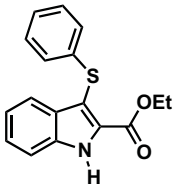

tubulin: 4.4 ± 0.3
colchicine binding: 19 ± 7
MCF-7: >1250

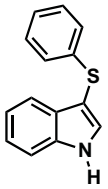

tubulin: 15 ± 0.7
colchicine binding: 13 ± 5
MCF-7: >2500

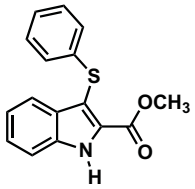

tubulin: 8.3 ± 0.6
colchicine binding: 21 ± 7
MCF-7: >2500

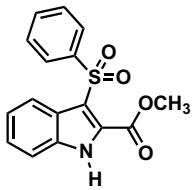

tubulin: >40
colchicine binding: 5.1 ± 1
MCF-7: >2500

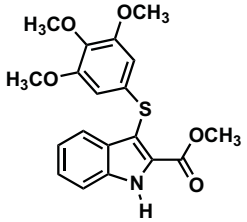

tubulin: 2.9 ± 0.1
colchicine binding: 81 ± 1
MCF-7: 25 ± 1

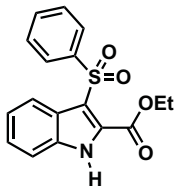

tubulin: 4.4 ± 0.2
colchicine binding: 33 ± 0.6
MCF-7: >1000

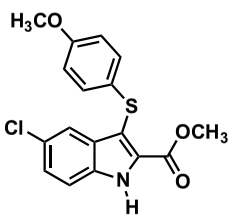

tubulin: >40
colchicine binding: 3.6 ± 8
MCF-7: >2500

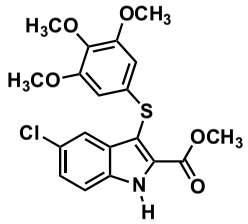

tubulin: 2.5 ± 0.3
colchicine binding: 76 ± 0.2
MCF-7: 42 ± 10

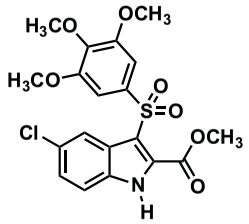

tubulin: >40
colchicine binding: 1.6 ± 2
MCF-7: >2500

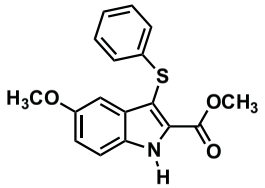

tubulin: 6.2 ± 0.3
colchicine binding: 31 ± 8
MCF-7: >2500

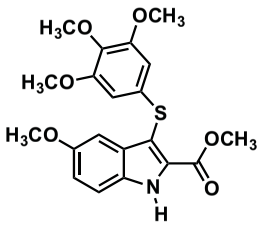

tubulin: 2.0 ± 0.2
colchicine binding: 93 ± 0.8
MCF-7: 13 ± 3

BPR0L075, a Novel Synthetic Indole Compound with Antimitotic Activity in Human Cancer Cells, Exerts Effective Antitumoral Activity *in Vivo*

Ching-Chuan Kuo, Hsing-Pang Hsieh, Wen-Yu Pan, Ching-Ping Chen, Jing-Ping Liou, Shiow-Ju Lee, Yi-Ling Chang, Li-Tzong Chen, Chiung-Tong Chen, and Jang-Yang Chang

CANCER RESEARCH 64, 4621–4628, July 1, 2004

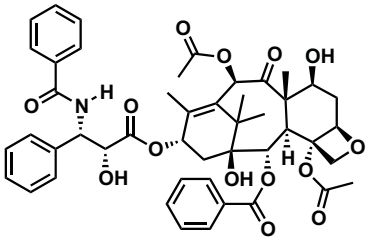

paclitaxel

KB: 4.1 ± 1.6
KB-VIN10 (P-gp170/MDR): 16500 ± 707
KB-TAX50 (P-gp170/MDR): 130 ± 6.9
KB-7D (MRP): 7.9 ± 0.5

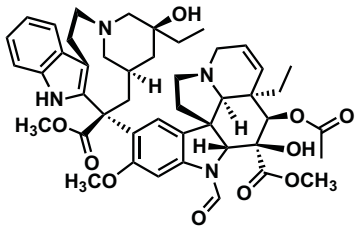

vincristine

KB: 0.6 ± 0.2
KB-VIN10 (P-gp170/MDR): 90 ± 7.4
KB-TAX50 (P-gp170/MDR): 1.8 ± 0.5
KB-7D (MRP): 1.2 ± 0.4

Growth inhibition IC_{50} - nM

KB: human cervical
KB-VIN10 (P-gp170/MDR):
KB-TAX50 (P-gp170/MDR):
KB-7D (MRP):

P-gp170/MDR and MRP: overexpression of efflux pump

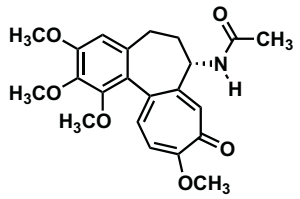

colchicine

KB: 10.5 ± 2.2
KB-VIN10 (P-gp170/MDR): 115 ± 7.2
KB-TAX50 (P-gp170/MDR): 31.9 ± 2.4
KB-7D (MRP): 55.2 ± 7.8

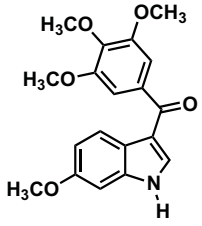

BPR0L075

KB: 3.6 ± 1.8
KB-VIN10 (P-gp170/MDR): 2.9 ± 1.5
KB-TAX50 (P-gp170/MDR): 3.1 ± 0.3
KB-7D (MRP): 4.2 ± 1.9

COMPARATIVE MOLECULAR FIELD ANALYSIS OF ANTI-TUBULIN AGENTS WITH INDOLE RING BINDING AT THE COLCHICINE BINDING SITE

I-HUNG LIN, CHENG-CHANG HSU, SHIH-HONG WANG,
HSING-PANG HSIEH, and YING-CHIEH SUN

Journal of Theoretical and Computational Chemistry Vol. 9, No. 1 (2010) 279–291

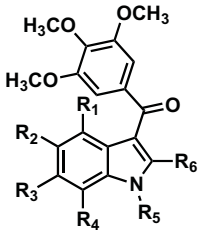

IC_{50} : 1.3 - >10,000

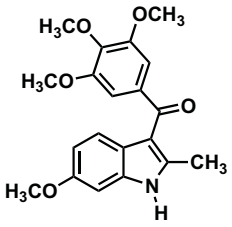

IC_{50} : 1.4

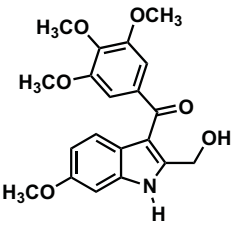

IC_{50} : 1.3

built training set of 42 known compounds then test set of 17 known compounds
IC_{50} experimental vs. IC_{50} predecited: $R^2 = 0.714$
IC_{50} values in nM inhibition of MKN-45 gastric cancer cells

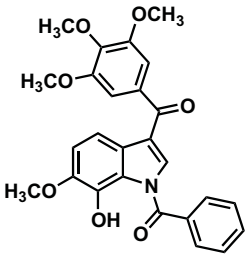

pIC_{50} : 9.04711

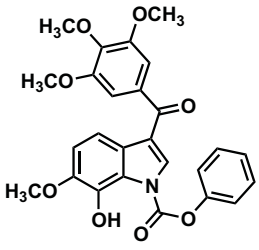

pIC_{50} : 8.99303

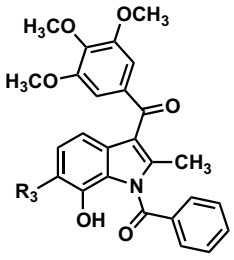

pIC_{50} : 9.52103

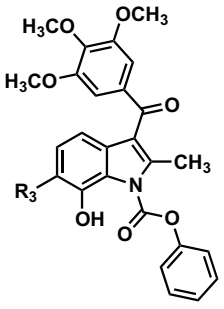

pIC_{50} : 9.4287

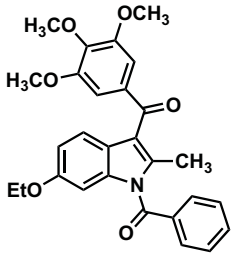

pIC_{50} : 9.48207

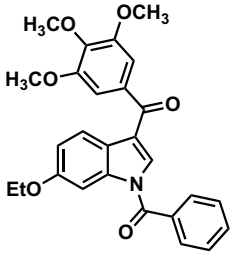

pIC_{50} : 9.30451

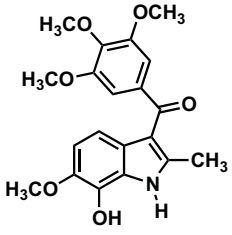

pIC_{50} : 9.00536

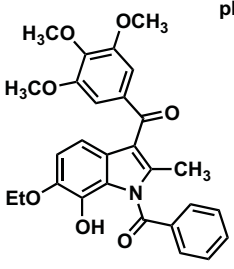

pIC_{50} : 9.64992

Concise syntheses of N-aryl-5,6,7-trimethoxyindoles as antimitotic and vascular disrupting agents: application of the copper-mediated Ullmann-type arylation

Hsueh-Yun Lee, Jang-Yang Chang, Ling-Yin Chang, Wen-Yang Lai, Mei-Jung Lai, Kuang-Hsing Shih, Ching-Chuan Kuo, Chi-Yen Chang and Jing-Ping Liou

Org. Biomol. Chem., 2011, 9, 3154

KB: cervical- nM
HT29: colon-nM
MKN45: stomach-nM
H460: non-small lung-nM
tubulin: μM
col bind: % inhibition

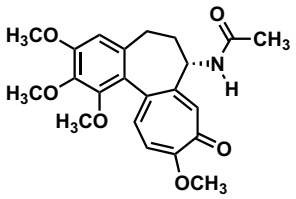

KB: 10.3 ± 0.9
HT29: 15.9 ± 4.9
MKN45: 17.9 ± 1.8
H460: 17.0 ± 5.1
tubulin: 3.9 ± 0.4
col bind:

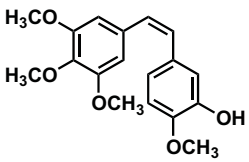

KB: 2.0 ± 0.4
HT29: 715.1 ± 32.6
MKN45: 8.5 ± 2.5
H460: 19.0 ± 3.5
tubulin: 1.7 ± 0.7
col bind: 95 ± 2

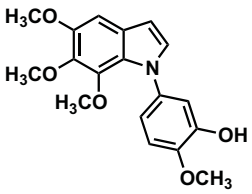

KB: 13.7 ± 4.8
HT29: 10 ± 3.1
MKN45: 11.1 ± 3.6
H460: 12.9 ± 5.2
tubulin: 2.5 ± 0.2
col bind: 82 ± 2

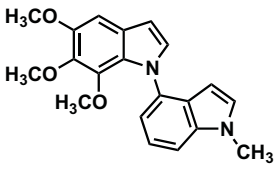

KB: 1226.5 ± 125.2
HT29: 3120 ± 959.5
MKN45: 1718.0 ± 816.0
H460: 4250.0 ± 458.7
tubulin: >10
col bind: nd

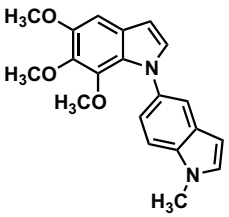

KB: 48.9 ± 45.0
HT29: 40.1 ± 2.1
MKN45: 35.4 ± 7.6
H460: 38.5 ± 5.5
tubulin: 2.5 ± 0.3
col bind: 77 ± 3

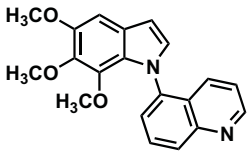

KB: >5000
HT29: >5000
MKN45: >5000
H460: >5000
tubulin: >10
col bind: nd

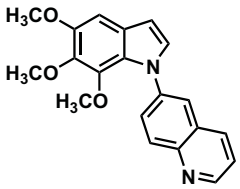

KB: 31.6 ± 10.9
HT29: 50.1 ± 10.6
MKN45: 38.6 ± 9.5
H460: 38.3 ± 8.4
tubulin: 3.2 ± 0.2
col bind: 78 ± 5

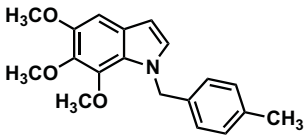

KB: 946.3 ± 234.0
HT29: 964.0 ± 62.2
MKN45: 1005.0 ± 24.0
H460: 1096.2 ± 316.5
tubulin: nd
col bind: nd

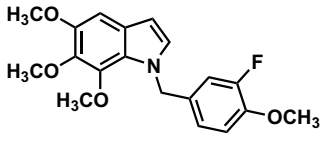

KB: 751.7 ± 31.8
HT29: 770.5 ± 35.1
MKN45: 490.5 ± 46.6
H460: 870.0 ± 89.1
tubulin: nd
col bind: nd

Concise Synthesis and Structure-Activity Relationships of Combretastatin A-4 Analogues, 1-Aroylindoles and 3-Aroylindoles, as Novel Classes of Potent Antitubulin Agents

Jing-Ping Liou, Yi-Ling Chang, Fu-Ming Kuo, Chun-Wei Chang, Huan-Yi Tseng, Chiung-Chiu Wang, Yung-Ning Yang, Jang-Yang Chang, Shiow-Ju Lee, and Hsing-Pang Hsieh

J. Med. Chem. 2004, 47, 4247-4257

Cells: nM
Tubulin: μM

NUGC3: stomach
MKN45: stomach
MESSA: uterine
A549: lung
MCF-7: breast

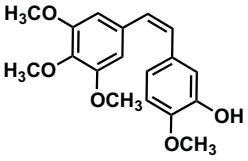

CA4

NUGC3: >10,000
MKN45: 82 ± 8
MESSA: 13 ± 14
A549: 117 ± 86
MCF-7: 8 ± 1
Tubulin: 2.03 ± 0.41

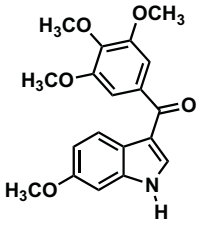

BPR0L075

NUGC3: 1 ± 0
MKN45: 4 ± 2
MESSA: 4 ± 1
A549: 23 ± 6
MCF-7: 7 ± 1
Tubulin: 2.18 ± 0.16

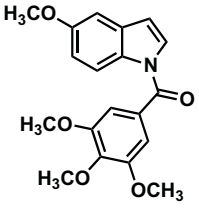

BPR0L081

NUGC3: 368 ± 210
MKN45: 34 ± 11
MESSA: 1687 ± 151
A549: 671 ± 326
MCF-7: 590 ± 154
Tubulin: 3.76 ± 0.51

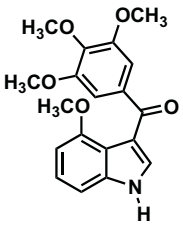

NUGC3: 3359 ± 1263
MKN45: 487 ± 148
MESSA: 9393 ± 1052
A549: 6499 ± 230
MCF-7: 9057 ± 1633

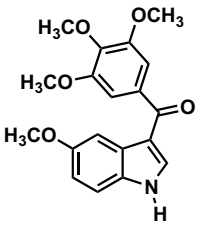

NUGC3: 360 ± 140
MKN45: 326 ± 84
MESSA: 884 ± 246
A549: 614 ± 282
MCF-7: 639 ± 46

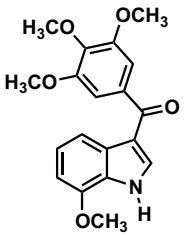

NUGC3: 474 ± 134
MKN45: 323 ± 28
MESSA: 3524 ± 805
A549: 729 ± 157
MCF-7: 4772 ± 1697

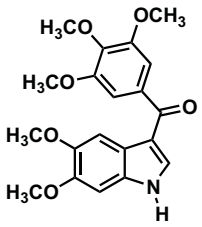

NUGC3: >10,000
MKN45: 3708 ± 953
MESSA: >10,000
A549: >10,000
MCF-7: 9242 ± 1313

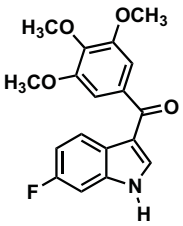

NUGC3: >10,000
MKN45: 669 ± 108
MESSA: >10,000
A549: >10,000
MCF-7: >10,000

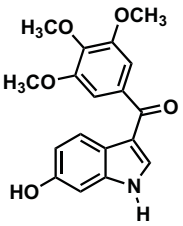

NUGC3: 585 ± 180
MKN45: 43 ± 7
MESSA: 889 ± 268
A549: 815 ± 368
MCF-7: 728 ± 74

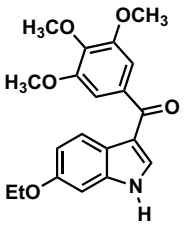

NUGC3: 1 ± 0
MKN45: 2 ± 2
MESSA: 3 ± 3
A549: 26 ± 21
MCF-7: 1 ± 0

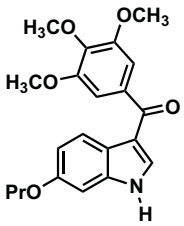

NUGC3: 47 ± 1
MKN45: 11 ± 8
MESSA: 56 ± 15
A549: 230 ± 103
MCF-7: 52 ± 18

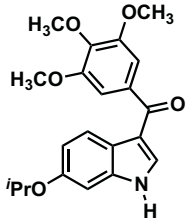

NUGC3: 41 ± 14
MKN45: 3 ± 2
MESSA: 10 ± 3
A549: 121 ± 15
MCF-7: 40 ± 1

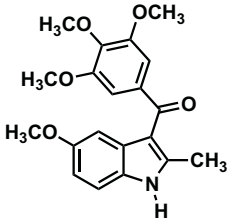

NUGC3: 42 ± 5
MKN45: 111 ± 54
MESSA: 160 ± 93
A549: 596 ± 294
MCF-7: 50 ± 18

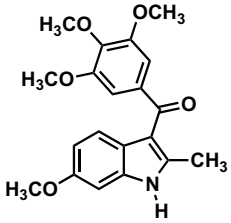

NUGC3: 4 ± 1
MKN45: 3 ± 2
MESSA: 4 ± 1
A549: 6 ± 2
MCF-7: 0.9 ± 0.1
Tubulin: 0.90 ± 0.10

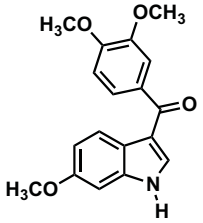

NUGC3: >10,000
MKN45: >10,000
MESSA: >10,000
A549: >10,000
MCF-7: >10,000

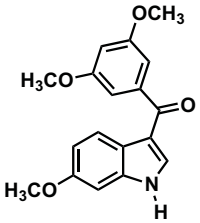

NUGC3: >10,000
MKN45: 1 ± 0
MESSA: 24 ± 9
A549: 23 ± 7
MCF-7: 20 ± 8
Tubulin: 2.69 ± 0.43

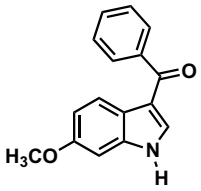

NUGC3: >10,000
MKN45: 3939 ± 689
MESSA: 8064 ± 2037
A549: 8562 ± 2491
MCF-7: >10,000

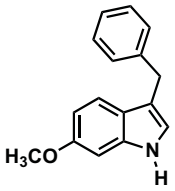

NUGC3: 2 ± 2
MKN45: 38 ± 4
MESSA: 50 ± 13
A549: 52 ± 14
MCF-7: 6 ± 0

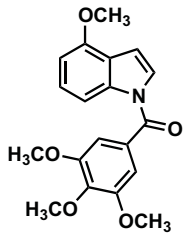

NUGC3: >10,000
MKN45: 3924 ± 1219
MESSA: >10,000
A549: >10,000
MCF-7: >10,000

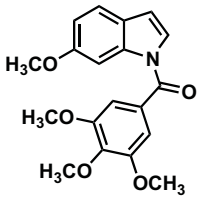

NUGC3: >10,000
MKN45: 3615 ± 859
MESSA: >10,000
A549: >10,000
MCF-7: >10,000

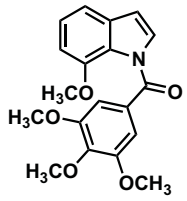

NUGC3: >10,000
MKN45: 4074 ± 1100
MESSA: >10,000
A549: >10,000
MCF-7: >10,000

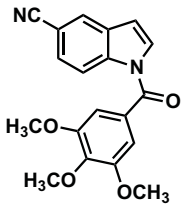

NUGC3: >10,000
MKN45: >10,000
MESSA: >10,000
A549: >10,000
MCF-7: >10,000

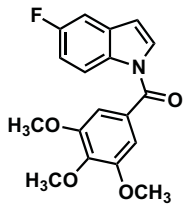

NUGC3: >10,000
MKN45: 5050 ± 1709
MESSA: >10,000
A549: >10,000
MCF-7: >10,000

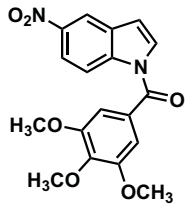

NUGC3: >10,000
MKN45: >10,000
MESSA: >10,000
A549: >10,000
MCF-7: >10,000

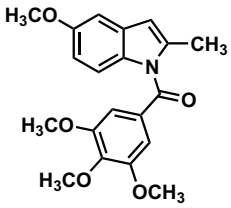

NUGC3: 75 ± 17
MKN45: 39 ± 40
MESSA: 102 ± 72
A549: 62 ± 25
MCF-7: 28 ± 28
Tubulin: 3.31 ± 0.09

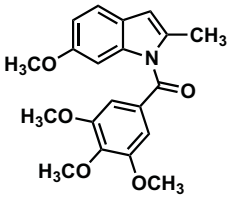

NUGC3: >10,000
MKN45: 432 ± 101
MESSA: >10,000
A549: 7533 ± 2932
MCF-7: 7908 ± 1087

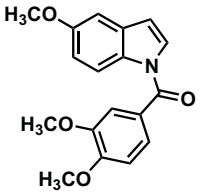

NUGC3: 9625 ± 867
MKN45: 4488 ± 528
MESSA: >10,000
A549: >10,000
MCF-7: >10,000

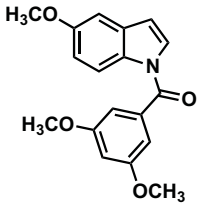

NUGC3: >10,000
MKN45: 319 ± 73
MESSA: 9279 ± 1248
A549: 4486 ± 1043
MCF-7: 9429 ± 990

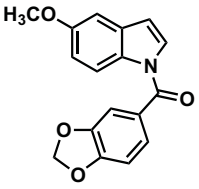

NUGC3: >10,000
MKN45: >10,000
MESSA: >10,000
A549: >10,000
MCF-7: >10,000

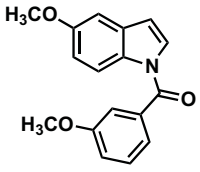

NUGC3: >10,000
MKN45: >10,000
MESSA: >10,000
A549: >10,000
MCF-7: >10,000

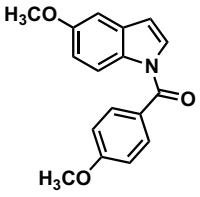

NUGC3: >10,000
MKN45: >10,000
MESSA: >10,000
A549: >10,000
MCF-7: >10,000

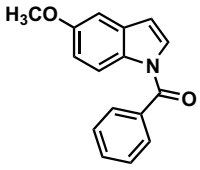

NUGC3: >10,000
MKN45: 7610 ± 2368
MESSA: >10,000
A549: >10,000
MCF-7: >10,000

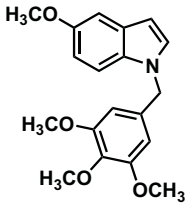

NUGC3: 2907 ± 185
MKN45: 649 ± 128
MESSA: 9297 ± 1217
A549: 9212 ± 1365
MCF-7: 8723 ± 2212

D-24851, a Novel Synthetic Microtubule Inhibitor, Exerts Curative Antitumoral Activity *in Vivo*, Shows Efficacy toward Multidrug-resistant Tumor Cells, and Lacks Neurotoxicity

Gerald Bacher, Bernd Nickel, Peter Emig, Udo Vanhoefer, Siegfried Seeber, Alexei Shandra, Thomas Klenner, and Thomas Beckers

CANCER RESEARCH 61, 392–399, January 1, 2001

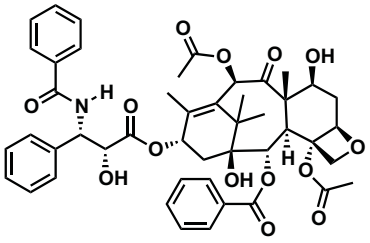

paclitaxel

SKOV3: 0.007
KB/HeLa: 0.007
HT 29: 0.010
A549: 0.013
PC-3: 0.012
DU145: 0.012
AsPC-1: 0.012
C6: 0.047
U 87: 0.013
MDA-MB 231: 0.011
L1210: 0.140

MDR1
L1210: 0.14
L1210/VCR: 15.7
MDR1
LT12: 0.012
LT12/mdr: 0.22
MDR1
MCF-7: 0.003
MCF-7/adr: 2.1
MDR1
A2780: 0.005
A2780/Dx5: 0.145
MRP
HT1080: 0.003
HT1080/DR4: 0.005

Cisplatin
A2780: 0.005
A2790/CP2: 0.007
5-FU
HT29: 0.007
Bolus
HT29-R1: 0.006
Continous
HT29-R24: 0.006
Raltitrexed
HT29/ICID: 0.016
Topoisomerase-I
HT29/SN38: 0.008
Topoisomerase-I
HCT-8: 0.033
HCT-8/SN38: 0.133

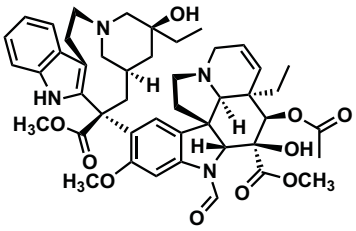

vincristine

SKOV3: 0.002
KB/HeLa: 0.001
HT 29: 0.005
A549: 0.027
PC-3: 0.004
DU145: 0.010
AsPC-1: 0.017
C6: 0.007
U 87: 0.003
MDA-MB 231: 0.008
L1210: 0.021

MDR1
L1210: 0.021
L1210/VCR: 1.575
MDR1
LT12: 0.001
LT12/mdr: 0.014
MDR1
MCF-7: 0.001
MCF-7/adr: 1.2
MDR1
A2780: 0.0006
A2780/Dx5: 0.024
MRP
HT1080: 0.0008
HT1080/DR4: 0.018

Cisplatin
A2780: 0.0006
A2790/CP2: 0.003
5-FU
HT29: 0.003
Bolus
HT29-R1: 0.002
Continous
HT29-R24: 0.003
Raltitrexed
HT29/ICID: 0.006
Topoisomerase-I
HT29/SN38: 0.003
Topoisomerase-I
HCT-8: 0.013
HCT-8/SN38: 0.020

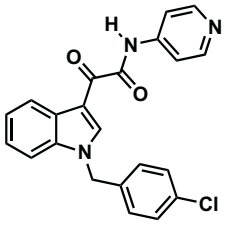

SKOV3: 0.036
KB/HeLa: 0.115
HT 29: 0.072
A549: 0.164
PC-3: 0.064
DU145: 0.148
AsPC-1: 0.285
C6: 0.200
U 87: 0.077
MDA-MB 231: 0.074
L1210: 0.089

MDR1
L1210: 0.089
L1210/VCR: 0.080
MDR1
LT12: 0.035
LT12/mdr: 0.042
MDR1
MCF-7: 0.057
MCF-7/adr: 0.083
MDR1
A2780: 0.026
A2780/Dx5: 0.041
MRP
HT1080: 0.031
HT1080/DR4: 0.030

Cisplatin
A2780: 0.026
A2790/CP2: 0.048
5-FU
HT29: 0.059
Bolus
HT29-R1: 0.057
Continous
HT29-R24: 0.065
Raltitrexed
HT29/ICID: 0.064
Topoisomerase-I
HT29/SN38: 0.070
Topoisomerase-I
HCT-8: 0.037
HCT-8/SN38: 0.037

growth inhibition IC_{50} - μM

SKOV3: human ovary
KB/HeLa: human cervix
HT 29: human colon
A549: human lung
PC-3: human prostate
DU145: human prostate
AsPC-1: human pacreas
C6: rat brain
U 87: human brain
MDA-MB 231: human breast
L1210: mouse leukemia

growth inibition constant rF- μM

different resistance phenotypes

MDR1
L1210: (parental)
L1210/VCR:
MDR1
LT12: (parental)
LT12/mdr:
MDR1
MCF-7: (parental)
MCF-7/adr: 2.1
MDR1
A2780: (parental)
A2780/Dx5:
MRP
HT1080: (parental)
HT1080/DR4: 0.005

Cisplatin
A2780: (parental)
A2790/CP2:
5-FU
HT29: (parental)
Bolus
HT29-R1:
Continous
HT29-R24:
Raltitrexed
HT29/ICID:
Topoisomerase-I
HT29/SN38:
Topoisomerase-I
HCT-8: (parental)
HCT-8/SN38:

For synthesis see:

Synthesis and Characterization of the Biologically Active 2-[1-(4-Chlorobenzyl)-1*H*-indol-3-yl]-2-oxo-*N*-pyridin-4-yl Acetamide

Martin Knaack, Peter Emig, Jan W. Bats, Michael Kiesel, Arndt Müller, and Eckhard Günther

Eur. J. Org. Chem. 2001, 384323847

Design and Synthesis of 2-Heterocyclyl-3-arylthio-1H-indoles as Potent Tubulin Polymerization and Cell Growth Inhibitors with Improved Metabolic Stability

Giuseppe La Regina, Ruoli Bai, Willeke Rensen, Antonio Coluccia, Francesco Piscitelli, Valerio Gatti, Alessio Bolognesi, Antonio Lavecchia, Ilaria Granata, Amalia Porta, Bruno Maresca, Alessandra Soriani, Maria Luisa Iannitto, Marisa Mariani,› Angela Santoni,,˜ Andrea Brancale, Cristiano Ferlini, Giulio Dondio, Mario Varasi, Ciro Mercurio, Ernest Hamel, Patrizia Lavia, Ettore Novellino, and Romano Silvestri

J. Med. Chem. 2011, 54, 8394-8406

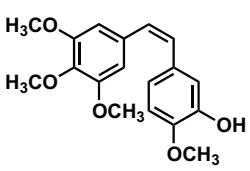

CA4

Tubulin: 1.0 ± 0.1 μM
MCF-7: 13 ± 3 nM
HeLa: 0.2 ± 0.005 μM
PC3: 0.4 ± 0.02 μM
HT-29: >10 μM
A549: >10 μM
OVCAR-8: 1.3 ± 0.6 nM
NCI/ADR-RES: 1.3 ± 0.6 nM
HAOSMC: 5 ± 3 nM
A10: 1 ± 1 nM
PtK2: 3 ± 1 nM
HUVEC: 1 ± 1 nM

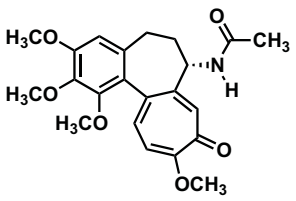

colchicine

Tubulin: 3.2 ± 0.4 μM
MCF-7: 5 ± 1 nM

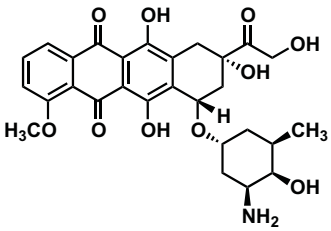

DOX

HeLa: 1.5 ± 0.03 μM
PC3: 1.7 ± 0.02 μM
HT-29: 1.0 ± 0.04 μM
A549: 1.0 ± 0.08 μM

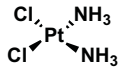

cisplatin

A2780wt: 48.5 ± 60 nM
A2780-CIS: 8980 ± 565 nM
OVCAR-3: 1816 ± 254 nM

MCF-7: human breast carcinoma
HeLa: cervix
PC3: prostate
HT-29: colon
A549: nonsmall cell lung
A2780wt: ovarian cancer model with high drug sensitivity
A2780-CIS: cisplatin-resistant
OVCAR-3: cell line derived from a cisplatin-resistant patient
OVCAR-8: ovarian tumor cell line
NCI/ADR-RES: DOX-resistant cell line derived from OVCAR-8
HAOSMC: human aortic smooth muscle cells
A10: rat embryonic aortic smooth muscle cells
PtK2: Potorous tridactylis kidney epithelial cells
HUVEC: human umbilical vein endothelial cells

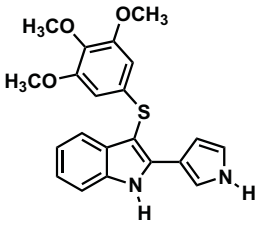

Tubulin: 1.2 ± 0.2 μM
MCF-7: 20 ± 0 nM
HeLa: 0.4 ± 0.02 μM
PC3: 0.5 ± 0.1 μM
HT-29: 0.1 ± 0.03 μM
A549: 0.08 ± 0.02 μM
A2780wt: 21.5 ± 1.2 nM
A2780-CIS: 6.3 ± 1.8 nM
OVCAR-3: 81 ± 21 nM
OVCAR-8: 70 ± 30 nM
NCI/ADR-RES: 25 ± 7 nM
HAOSMC: 33 ± 10 nM
A10: 40 ± 30 nM
PtK2: 60 ± 0 nM
HUVEC: 30 ± 0 nM

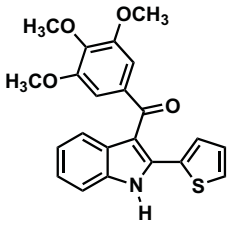

Tubulin: 1.1 ± 0.1 μM
MCF-7: 36 ± 6 nM
HeLa: 0.07 ± 0.004 μM
PC3: 0.1 ± 0.08 μM
HT-29: 0.08 ± 0.01 μM
A549: 0.08 ± 0.01 μM
A2780wt: 30.5 ± 0.7 nM
A2780-CIS: 29.3 ± 3.2 nM
OVCAR-3: 117 ± 18 nM
OVCAR-8: 20 ± 10 nM
NCI/ADR-RES: 15 ± 7 nM

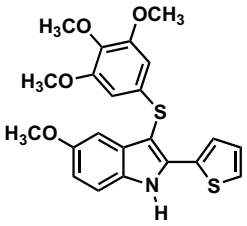

Tubulin: 0.98 ± 0.08 μM
MCF-7: 58 ± 4 nM
HeLa: 0.4 ± 0.02 μM
PC3: 0.8 ± 0.08 μM
HT-29: 0.4 ± 0.02 μM
A549: 0.3 ± 0.09 μM

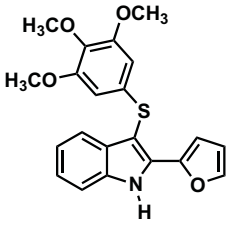

Tubulin: 1.0 ± 0.1 μM
MCF-7: 45 ± 4 nM

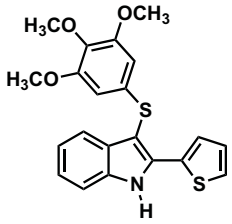

Tubulin: 0.74 ± 0.05 μM
MCF-7: 39 ± 10 nM
HeLa: 0.09 ± 0.002 μM
PC3: 0.2 ± 0.05 μM
HT-29: 0.15 ± 0.03 μM
A549: 0.09 ± 0.02 μM
OVCAR-8: 45 ± 20 nM
NCI/ADR-RES: 25 ± 7 nM

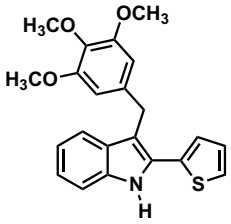

Tubulin: 1.9 ± 0.2 μM
MCF-7: 200 nM
HeLa: 1 ± 0.03 μM
PC3: 2 ± 0.1 μM
HT-29: 1 ± 0.05 μM
A549: 2 ± 0.08 μM
HAOSMC: 250 ± 90 nM
A10: 150 ± 90 nM
PtK2: 300 ± 0 nM
HUVEC: 180 ± 40 nM

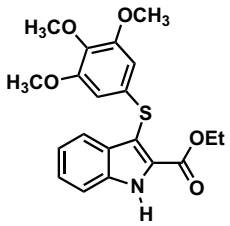

Tubulin: 2.9 ± 0.1 μM
MCF-7: 40 ± 2 nM

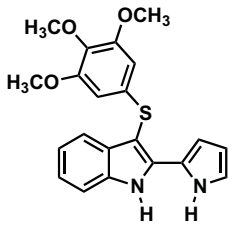

Tubulin: 1.1 ± 0.05 μM
MCF-7: 18 ± 6 nM

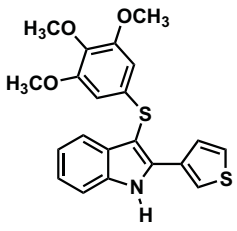

Tubulin: 0.91 ± 0.2 μM
MCF-7: 60 ± 20 nM

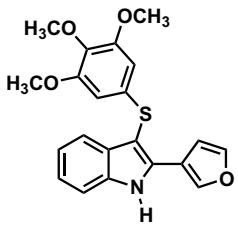

Tubulin: 1.0 ± 0.1 μM
MCF-7: 33 ± 5 nM

Discovery and SAR of indole-2-carboxylic acid benzylidenehydrazides as a new series of potent apoptosis inducers using a cellbased HTS assay

Han-Zhong Zhang, John Drewe, Ben Tseng, Shailaja Kasibhatla and Sui Xiong Cai

Bioorganic & Medicinal Chemistry 12 (2004) 3649–3655

screening hit (commerical)

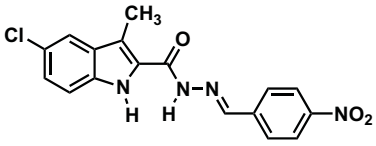

T47D: 2.2 ± 0.2
H-1299: 1.4 ± 0.14
DLD: 2.0 ± 0.3

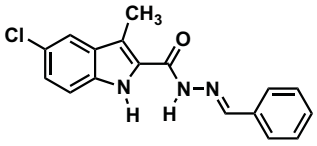

T47D: 4.0 ± 0.4
H-1299: 3.5 ± 0.3
DLD: 4.3 ± 0.5

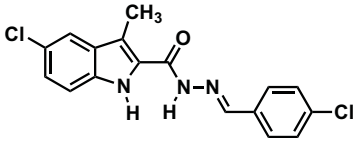

T47D: 2.5 ± 0.07
H-1299: 2.0 ± 0.4
DLD: 1.5 ± 0.07

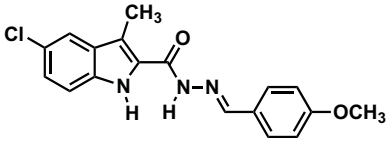

T47D: 2.4 ± 0.3
H-1299: 0.98 ± 0.3
DLD: 2.7 ± 0.09

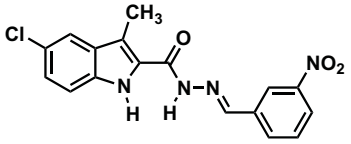

T47D: >10
H-1299: >10
DLD: >10

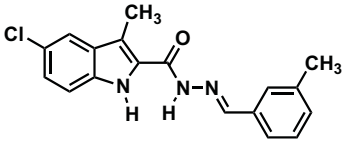

T47D: >10
H-1299: >10
DLD: >10

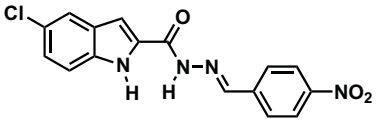

T47D: 5.8 ± 0.4
H-1299: 4.9 ± 0.4
DLD: >10

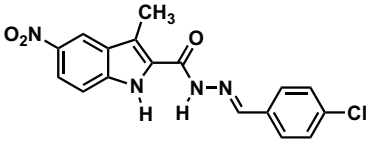

T47D: 2.1 ± 0.4
H-1299: 2.6 ± 0.07
DLD: 2.7 ± 0.1

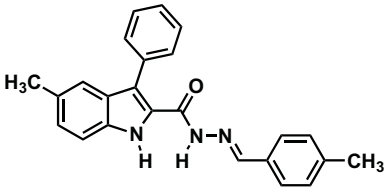

T47D: 0.1 ± 0.03
H-1299: 0.5 ± 0.07
DLD: 0.4 ± 0.1

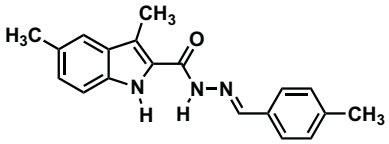

T47D: 1.04 ± 0.1
H-1299: 0.7 ± 0.1
DLD: 0.7 ± 0.4

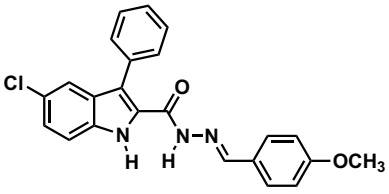

T47D: 0.2 ± 0.03
H-1299: 0.2 ± 0.03
DLD: 0.4 ± 0.07

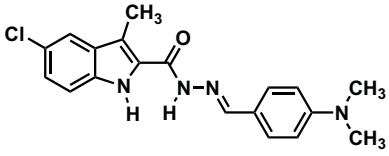

T47D: 1.3 ± 0.1
H-1299: 2.8 ± 0.4
DLD: 1.6 ± 0.2

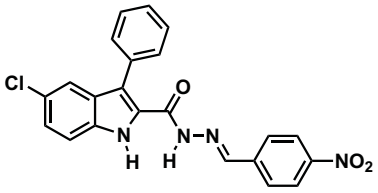

T47D: 0.1 ± 0.06
H-1299: 0.2 ± 0.07
DLD: 0.6 ± 0.1

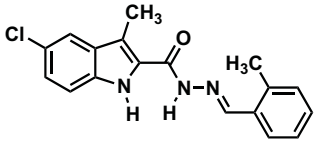

T47D: >10
H-1299: >10
DLD: >10

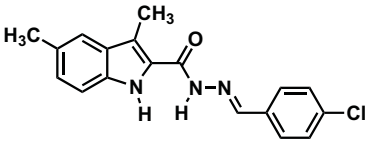

T47D: 0.5 ± 0.08
H-1299: 1.5 ± 0.1
DLD: 2.2 ± 0.5

Discovery of 4-Amino and 4-Hydroxy-1-aroylindoles as Potent Tubulin Polymerization Inhibitors

Jing-Ping Liou, Zi-Yi Wu, Ching-Chuan Kuo, Chi-Yen Chang, Pei-Yi Lu, Chi-Ming Chen, Hsing-Pang Hsieh, and Jang-Yang Chang

J. Med. Chem. 2008, 51, 4351–4355

KB: oral epidermoid carcinoma-nM
H460: non-small liung-nM
MKN45: stomach carcinoma-nM
KB-vin10: MDR-positive-nM
tubulin: μM

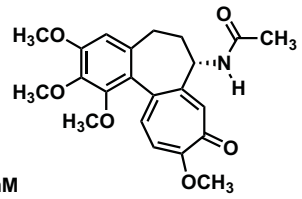

KB: 11.4 ± 1
H460: 20 ± 2
MKN45: 11 ± 1
KB-vin10: 125 ± 10
tubulin: 3.0 ± 0.4

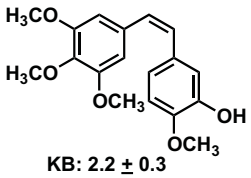

KB: 2.2 ± 0.3
H460: 2.8 ± 0.8
MKN45: 5.6 ± 0.2
KB-vin10: 1.8 ± 0.4
tubulin: 1.1 ± 0.3

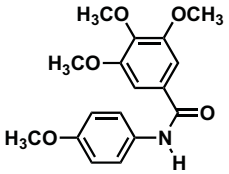

KB: >5000
H460: >5000
MKN45: >5000
KB-vin10: >5000
tubulin: nd

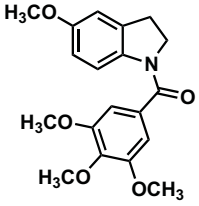

KB: 89 ± 2.9
H460: 98 ± 1
MKN45: 53 ± 1.4
KB-vin10: 84 ± 11
tubulin: 2.6 ± 0.3

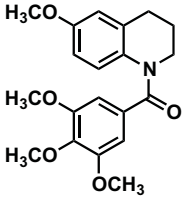

KB: 596 ± 123
H460: 652 ± 32
MKN45: 395 ± 51
KB-vin10: 586 ± 82
tubulin: >5

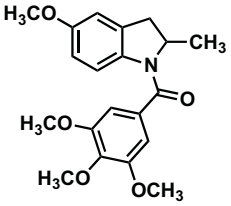

KB: 370 ± 33
H460: 413 ± 6
MKN45: 257 ± 30
KB-vin10: 372 ± 18
tubulin: nd

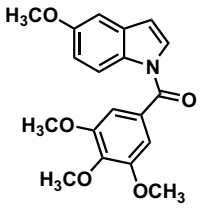

KB: 208 ± 58
H460: 232 ± 21
MKN45: 198 ± 13
KB-vin10: 197 ± 20
tubulin: 2.5 ± 0.6

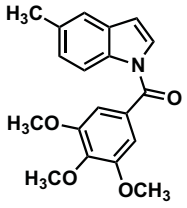

KB: 371 ± 111
H460: 353 ± 75
MKN45: 314 ± 35
KB-vin10: 400 ± 80
tubulin: nd

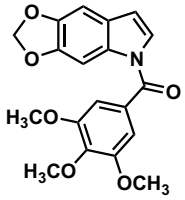

KB: 575 ± 55
H460: 559 ± 81
MKN45: 521 ± 51
KB-vin10: 587 ± 42
tubulin: nd

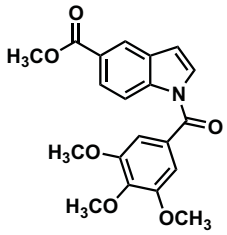

KB: >5000
H460: >5000
MKN45: >5000
KB-vin10: >5000
tubulin: nd

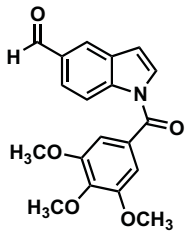

KB: >5000
H460: >5000
MKN45: >5000
KB-vin10: >5000
tubulin: nd

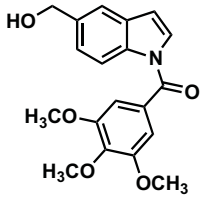

KB: >5000
H460: >5000
MKN45: >5000
KB-vin10: >5000
tubulin: nd

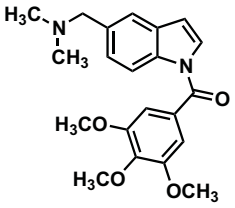

KB: >5000
H460: >5000
MKN45: >5000
KB-vin10: >5000
tubulin: nd

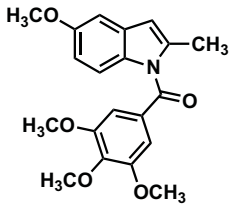

KB: 18 ± 6
H460: 23 ± 7
MKN45: 17 ± 3
KB-vin10: 11 ± 4
tubulin: nd

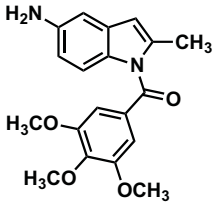

KB: 345 ± 17
H460: 334 ± 84
MKN45: 156 ± 54
KB-vin10: 312 ± 20
tubulin: nd

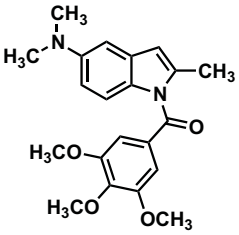

KB: 42 ± 21
H460: 52 ± 7
MKN45: 41 ± 13
KB-vin10: 38 ± 14
tubulin: 1.5 ± 0.5

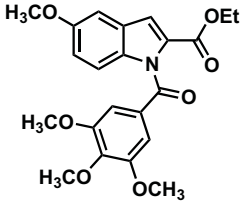

KB: 230 ± 71
H460: 198 ± 1.4
MKN45: 101 ± 19
KB-vin10: 185 ± 21
tubulin: nd

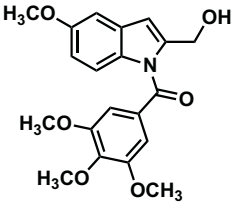

KB: >5000
H460: >5000
MKN45: >5000
KB-vin10: >5000
tubulin: nd

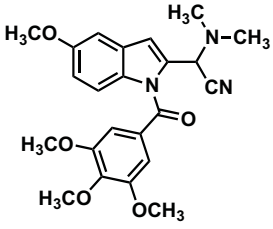

KB: >5000
H460: >5000
MKN45: >5000
KB-vin10: >5000
tubulin: nd

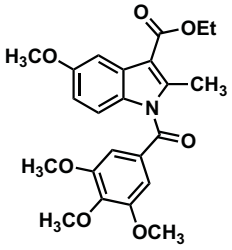

KB: >5000
H460: >5000
MKN45: >5000
KB-vin10: >5000
tubulin: nd

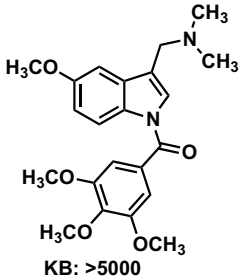

KB: >5000
H460: >5000
MKN45: >5000
KB-vin10: >5000
tubulin: nd

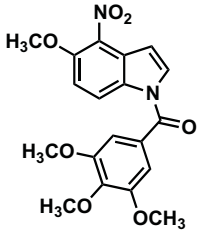

KB: >5000
H460: >5000
MKN45: >5000
KB-vin10: >5000
tubulin: nd

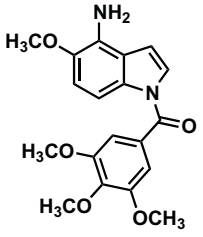

KB: 1.2 ± 0.4
H460: 5.4 ± 1.2
MKN45: 3.1 ± 2.3
KB-vin10: 2.4 ± 1.3
tubulin: 0.9 ± 0.2

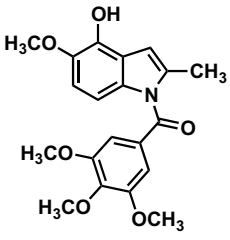

KB: 0.3 ± 0.3
H460: 0.5 ± 0.4
MKN45: 0.6 ± 0.8
KB-vin10: 0.3 ± 0.2
tubulin: 0.6 ± 0.1

Domino approach to 2-aroyltrimethoxyindoles as novel heterocyclic combretastatin A4 analogues

Martin Arthuis, Renée Pontikis, Guy G. Chabot, Lionel Quentin, Daniel Scherman, Jean-Claude Florent

European Journal of Medicinal Chemistry 46 (2011) 95-100

B16: murine melanoma-μM
tubulin: μM
HCT-116: human colon-μM
HCT-15: human colon-μM
HT-29: human colon-μM

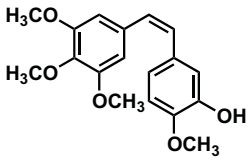

B16: 0.005
tubulin: 0.27
HCT-116: 0.001
HCT-15: 0.001
HT-29: 0.013

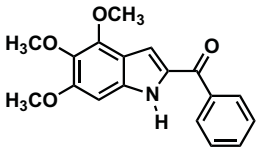

B16: 45
tubulin: >20

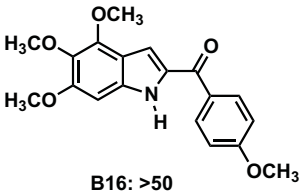

B16: >50
tubulin: 9
HCT-116: 4.2
HCT-15: 0.45
HT-29: 1.24

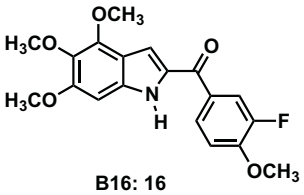

B16: 16
tubulin: >20

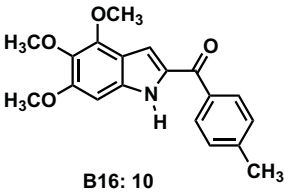

B16: 10
tubulin: 4
HCT-116: 2.8
HCT-15: 0.61
HT-29: 1.09

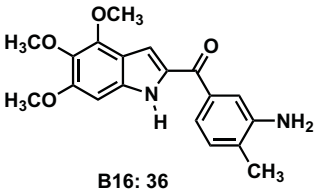

B16: 36
tubulin: 10
HCT-116: 2.0
HCT-15: 0.32
HT-29: 0.99

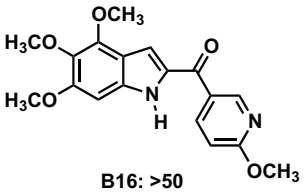

B16: >50
tubulin: 15

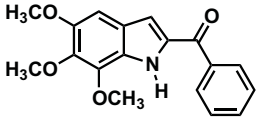

B16: >50
tubulin: 9
HCT-116: >50
HCT-15: >50
HT-29: >50

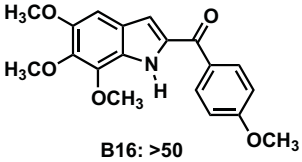

B16: >50
tubulin: 12

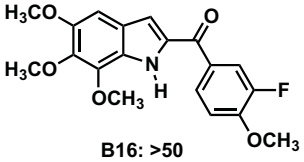

B16: >50
tubulin: 20

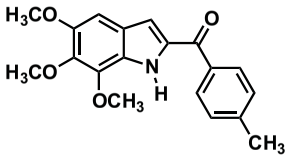

B16: 10
tubulin: >20
HCT-116: >50
HCT-15: >50
HT-29: >50

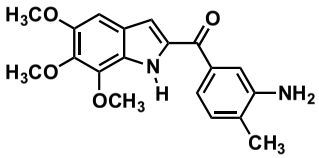

B16: nd
tubulin: nd

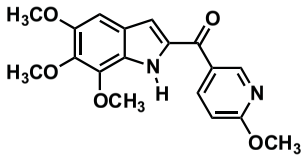

B16: >50
tubulin: 18

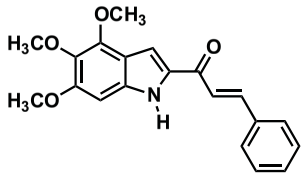

B16: 16
tubulin: >20

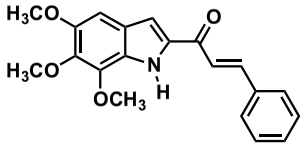

B16: 33
tubulin: 18

Exploring the effect of 2,3,4-trimethoxy-phenyl moiety as a component of indolephenstatins

Concepcion A Ivarez, Raquel A Ivarez, Purificacion Corchete, Concepcion Perez-Melero, Rafael Pelaez, Manuel Medarde

European Journal of Medicinal Chemistry 45 (2010) 588–597

TPI: tubulin inhib.
HeLa: cervix
HL-60: leukemia
A-549: lung
HT-29: colon

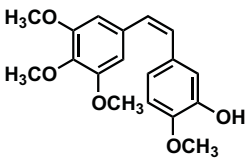

TPI: 3.0
HeLa: 0.003
HL-60: 0.002
A-549: 0.003
HT-29: 0.032

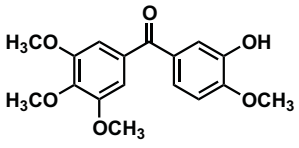

TPI: 2.5
HeLa: 0.03
HL-60: 0.03
A-549: 0.3
HT-29: 1.8

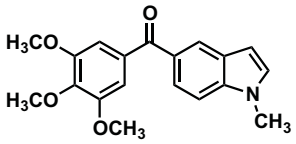

TPI: 6.9
HeLa: 0.034
HL-60: nd
A-549: 0.12
HT-29: nd

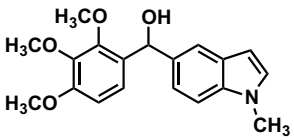

TPI: nd
HeLa: 2.4
HL-60: nd
A-549: >10
HT-29: nd

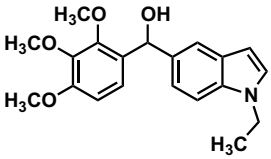

TPI: nd
HeLa: <1.0
HL-60: >10
A-549: >10
HT-29: >10

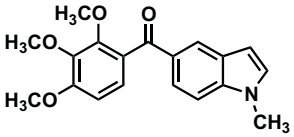

TPI: 0.4
HeLa: 0.017
HL-60: nd
A-549: 0.51
HT-29: 0.021

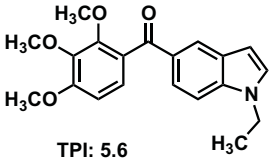

TPI: 5.6
HeLa: 0.42
HL-60: 5.0
A-549: >10
HT-29: 2.0

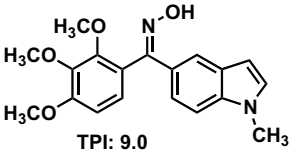

TPI: 9.0
HeLa: 0.076
HL-60: nd
A-549: 1.0
HT-29: 0.27

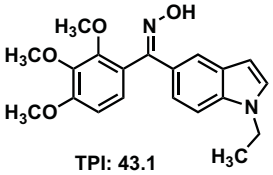

TPI: 43.1
HeLa: 2.0
HL-60: 2.0
A-549: >10
HT-29: 2.0

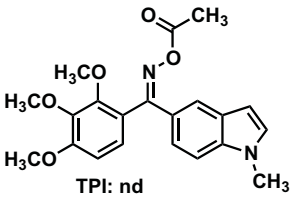

TPI: nd
HeLa: 1.0
HL-60: 0.58
A-549: >10
HT-29: 1.5

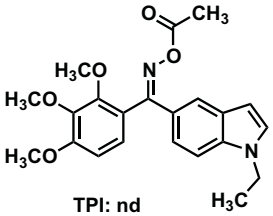

TPI: nd
HeLa: nd
HL-60: nd
A-549: nd
HT-29: nd

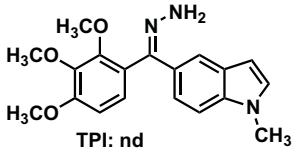

TPI: nd
HeLa: 2.0
HL-60: 2.0
A-549: >10
HT-29: 2.0

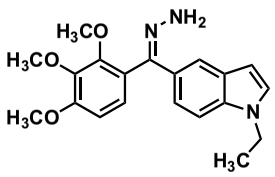

TPI: nd
HeLa: nd
HL-60: 2.0
A-549: >10
HT-29: >10

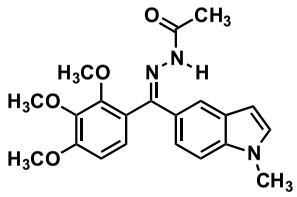

TPI: nd
HeLa: 1.0
HL-60: 2.0
A-549: >10
HT-29: 2.0

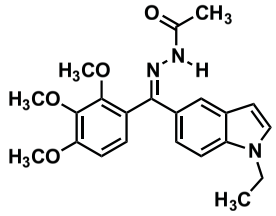

TPI: nd
HeLa: nd
HL-60: nd
A-549: nd
HT-29: nd

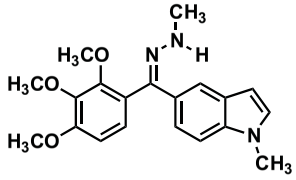

TPI: nd
HeLa: 1.0
HL-60: 1.0
A-549: >10
HT-29: 2.0

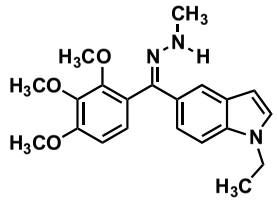

TPI: nd
HeLa: 0.29
HL-60: nd
A-549: 1.9
HT-29: 1.2

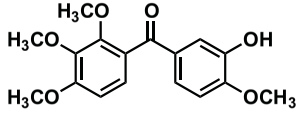

TPI: nd
HeLa: nd
HL-60: nd
A-549: nd
HT-29: nd

Generation of Ligand-Based Pharmacophore Model and Virtual Screening for Identification of Novel Tubulin Inhibitors with Potent Anticancer Activity

Yi-Kun Chiang, Ching-Chuan Kuo, Yu-Shan Wu, Chung-Tong Chen, Mohane Selvaraj Coumar, Jian-Sung Wu, Hsing-Pang Hsieh, Chi-Yen Chang, Huan-Yi Jseng, Ming-Hsine Wu, Jiun-Shyang Leou, Jen-Shin Song, Jang-Yang Chang, Ping-Chiang Lyu, Yu-Sheng Chao, and Su-Ying Wu

J. Med. Chem. 2009, 52, 4221–4233

KB: human oral squamous carcinoma

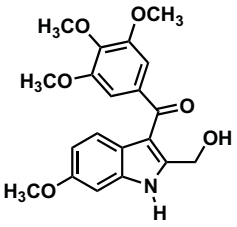

1.2 nM

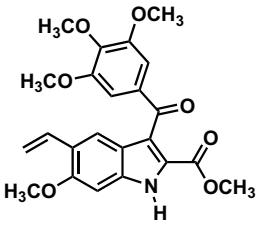

5.5 nM

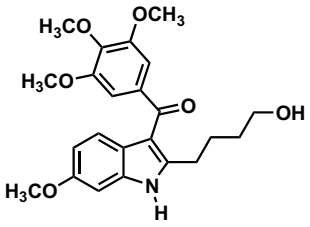

6.6 nM

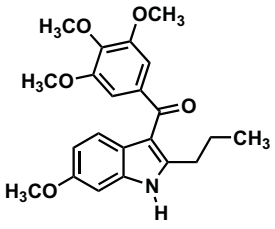

11 nM

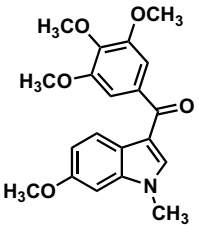

34 nM

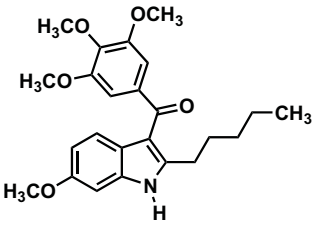

38 nM

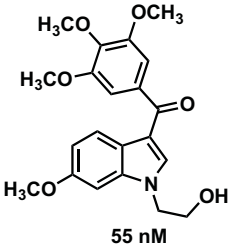

55 nM

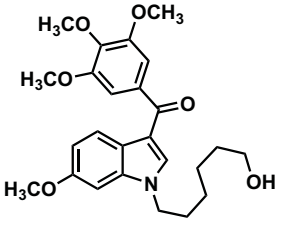

70 nM

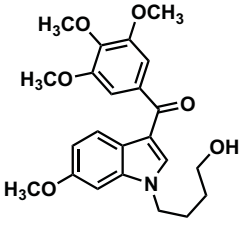

75 nM

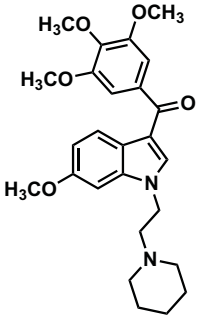

93 nM

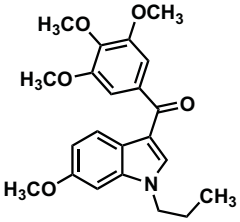

180 nM

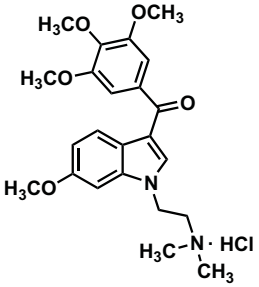

200 nM

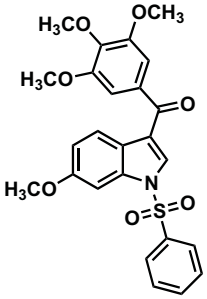

200 nM

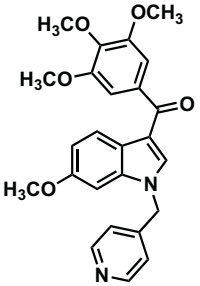

210 nM

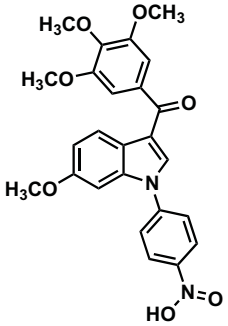

290 nM

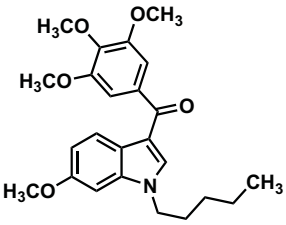

350 nM

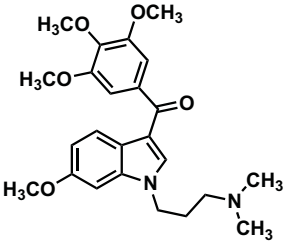

1700 nM

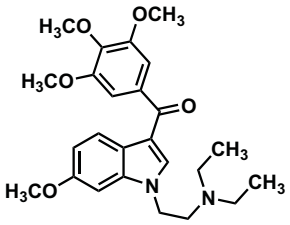

1800 nM

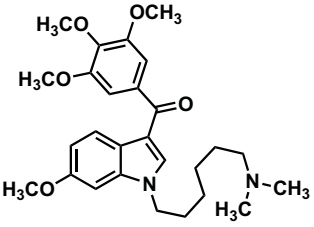

2100 nM

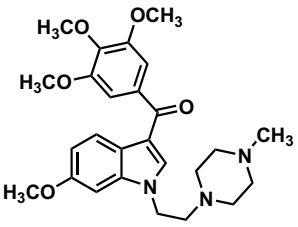

4100 nM

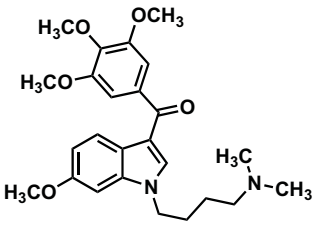

6000 nM

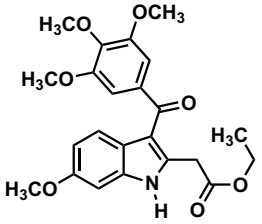

3.9 nM

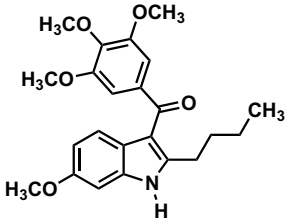

14.3 nM

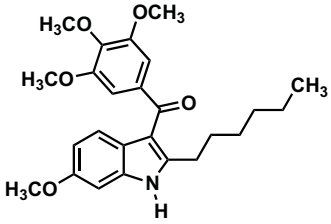

37.8 nM

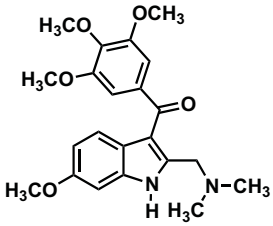

49.75 nM

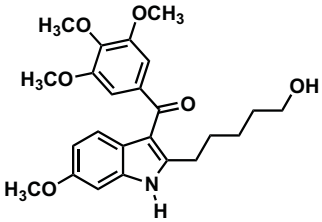

57.3 nM

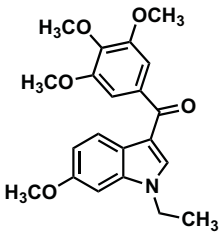

64 nM

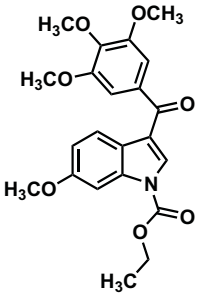

73 nM

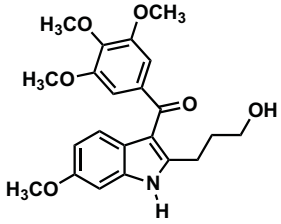

92 nM

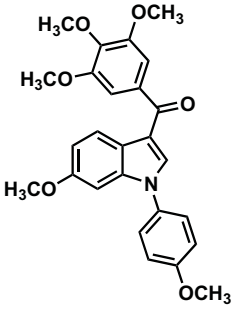

207 nM

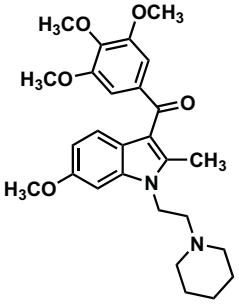

222 nM

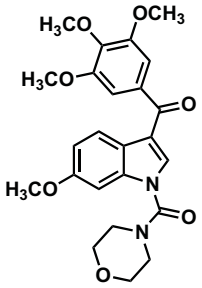

237 nM

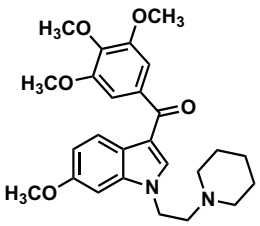

279.8 nM

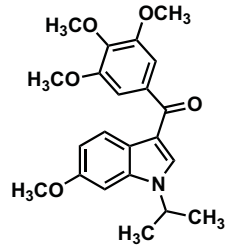

287 nM

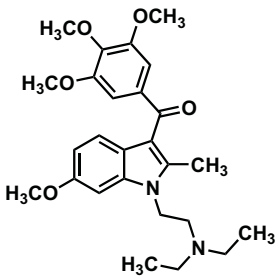

288.1 nM

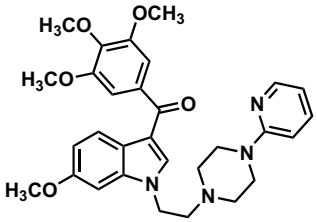

292.5 nM

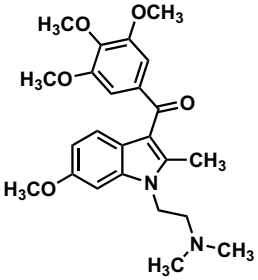

331.6 nM

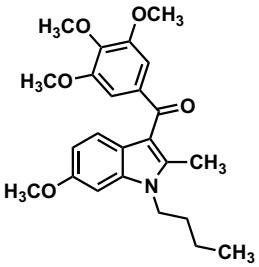

346 nM

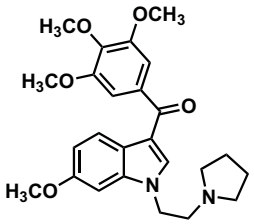

406.5 nM

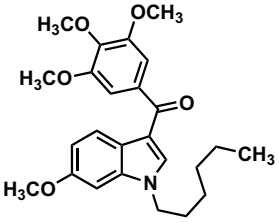

455 nM

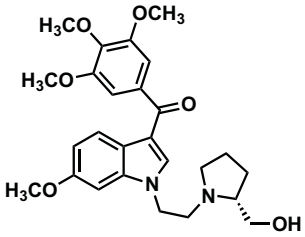

500 nM

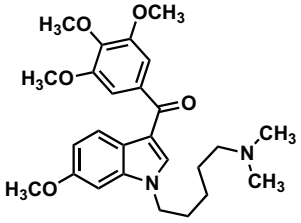

1800 nM

Inhibition of Tubulin Polymerization by 5,6-Dihydroindolo[2,1-a]isoquinoline Derivatives

Michael Goldbrunner, Gunther Loidl, Thomas Polossek, Albrecht Mannschreck, and Erwin von Angerer

J. Med. Chem. 1997, 40, 3524-3533

ITP: inhibit tubulin poly %
MDA: MDA-MB 231 breast μM
MCF-7: estrogen-sens breast μM
ITP: inhibit tubulin poly μM
ICB: inhibt of colchicine %

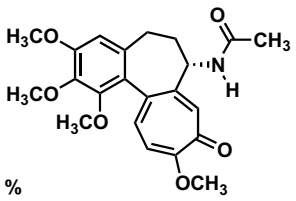

ITP: 100
MDA: 0.03
MCF-7: nd
ITP: 2.1 ± 0.1
ICB:

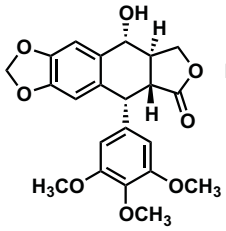

podophyllotoxin
MDA: 0.026
MCF-7: nd
ITP: 1.2 ± 0.1
ICB: 89

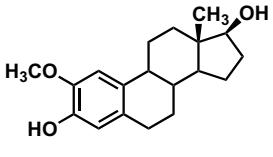

2-methoxyestradiol
MDA: 0.25
MCF-7: nd
ITP: 60 ± 2
ICB: 44

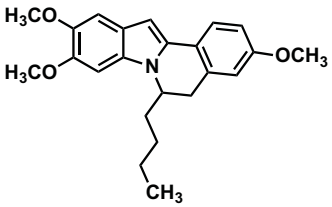

ITP: 41
MDA: >10
MCF-7: nd

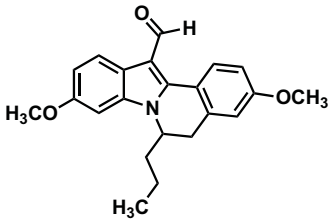

ITP: 17
MDA: >10
MCF-7: nd

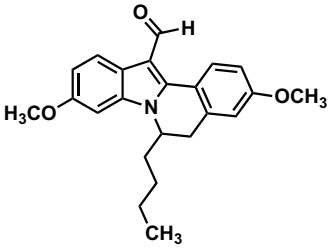

ITP: 11
MDA: 8.7
MCF-7: nd

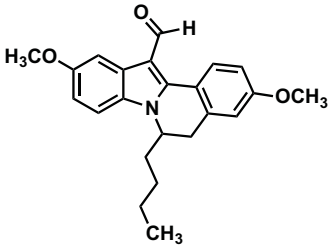

ITP: 10
MDA: >10
MCF-7: nd

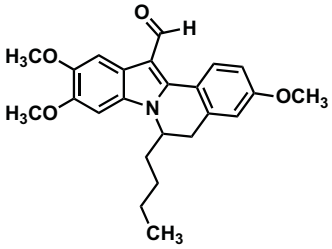

ITP: 1
MDA: 9.0
MCF-7: nd

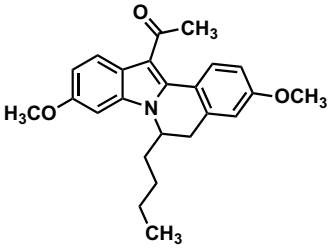

ITP: 5
MDA: >10
MCF-7: nd

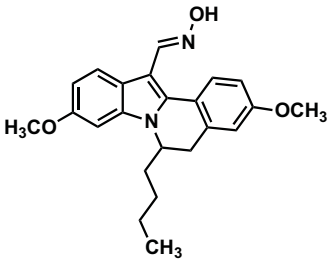

ITP: 17
MDA: >10
MCF-7: nd

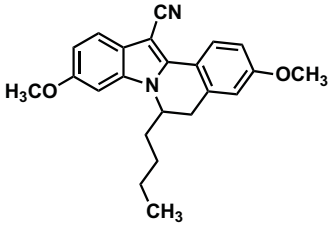

ITP: 16
MDA: 3.1
MCF-7: nd

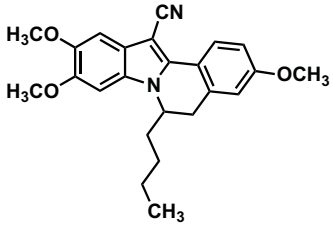

ITP: 32
MDA: 2.7
MCF-7: nd

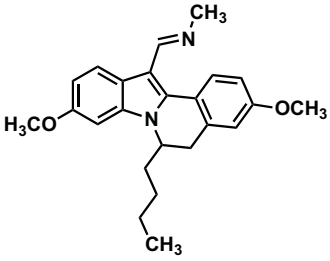

ITP: 3
MDA: 7.8
MCF-7: nd

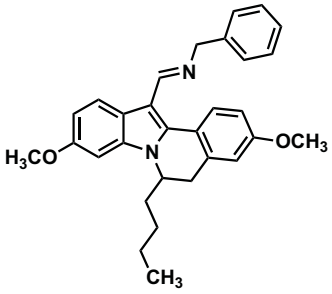

ITP: 16
MDA: 5.7
MCF-7: nd

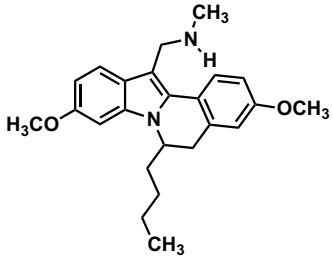

ITP: 9
MDA: 2.1
MCF-7: nd

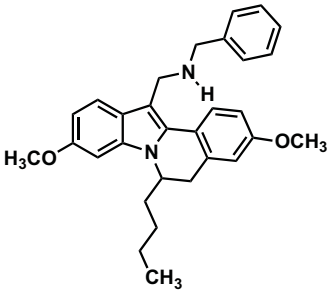

ITP: 27
MDA: 7.0
MCF-7: nd

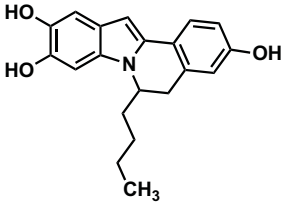

ITP: 33
MDA: >10
MCF-7: >10

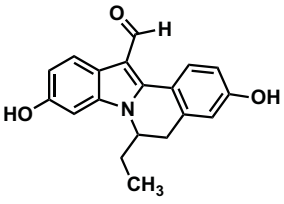

TP: 11
MDA: 2.8
MCF-7: 2.5

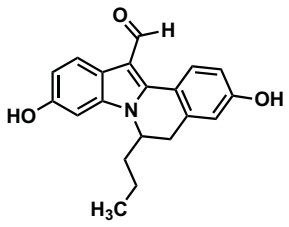

TP: 93
MDA: 0.3
MCF-7: 0.29

(±)
ITP: 19 ± 1
ICB: 40
ICG: 0.35; 0.45 (OAc)

(-)
ITP: >70
ICB: 27
ICG: nd; 5.5 (OAc)

(+)
ITP: 11 ± 0.4
ICB: 53
ICG: nd; 0.35 (OAc)

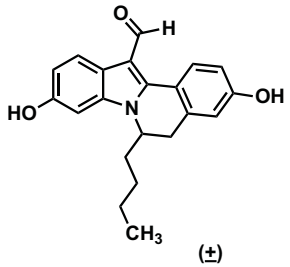

TP: 100
MDA: 1.4
MCF-7: 0.22

(±)
ITP: 8.9 ± 0.3
ICB: 67
ICG: 1.4; 0.32 (OAc)

(-)
ITP: >60
ICB: 22
ICG: nd; 0.78 (OAc)

(+)
ITP: 3.1 ± 0.4
ICB: 69
ICG: nd; 0.15 (OAc)

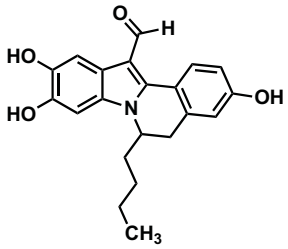

TP: 100
MDA: 3.2
MCF-7: >10

(±)
ITP: 19 ± 1
ICB: 57

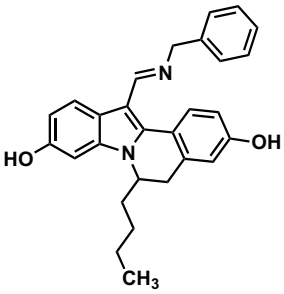

TP: 93
MDA: 2.1
MCF-7: 0.26

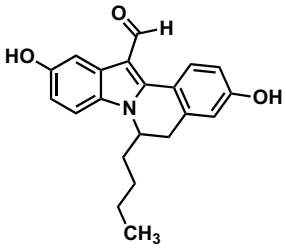

TP: 81
MDA: 0.2
MCF-7: 0.65

(±)
ITP: 19 ± 3
ICB: nd

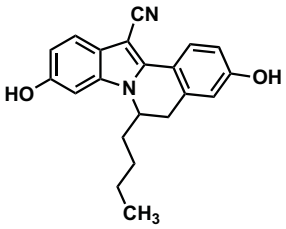

TP: 100
MDA: 0.3
MCF-7: 0.54

(±)
ITP: 13 ± 2
ICB: 48

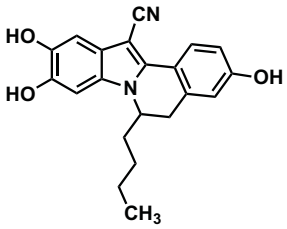

TP: 79
MDA: 3.4
MCF-7: 2.7

(±)
ITP: 25 ± 1
ICB: 54

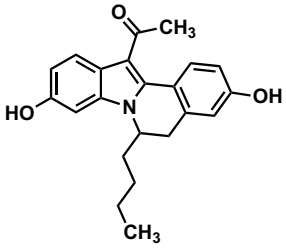

TP: 24
MDA: 2.2
MCF-7: 2.5

Methoxy-Substituted 3-Formyl-2-phenylindoles Inhibit Tubulin Polymerization

Robert Gastpar, Michael Goldbrunner, Doris Marko, and Erwin von Angerer

J. Med. Chem. 1998, 41, 4965-4972

MDA: human breast cancer- μM
MCF: estrogen-sensitive breast- μM
tubulin: μM

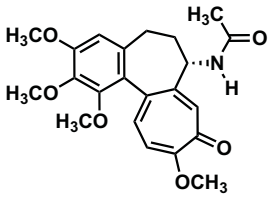

MDA: 0.03 ± 0.01
MCF: nd
tubulin: 1.9

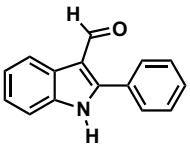

MDA: 0.42 ± 0.07
MCF: 0.65 ± 0.08

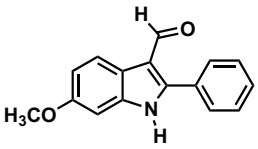

MDA: 0.24 ± 0.02
MCF: 0.19 ± 0.08

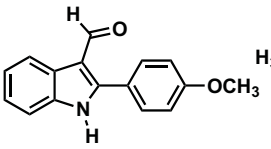

MDA: 0.47 ± 0.02
MCF: 0.18 ± 0.04
tubulin: 3.3

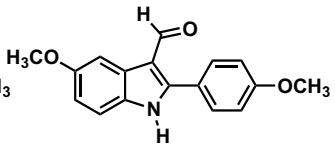

MDA: 0.26 ± 0.03
MCF: 0.18 ± 0.07
tubulin: 4.0

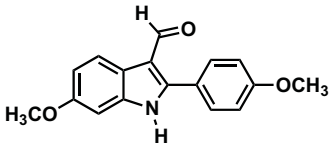

MDA: 0.035 ± 0.004
MCF: 0.16 ± 0.03
tubulin: 1.5

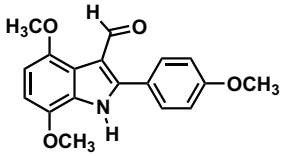

MDA: >10
MCF: 6.6 ± 0.3

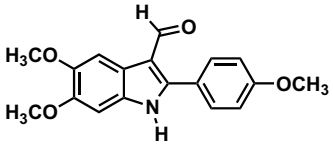

MDA: 0.22 ± 0.05
MCF: 0.23 ± 0.01

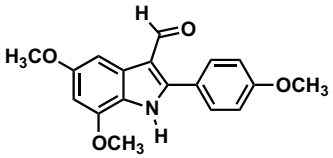

MDA: 2.8 ± 0.2
MCF: 1.7 ± 0.1

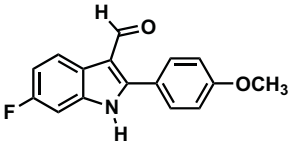

MDA: 0.049 ± 0.006
MCF: 0.043 ± 0.009
tubulin: 1.8

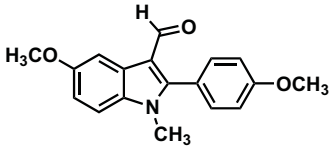

MDA: >10
MCF: >10

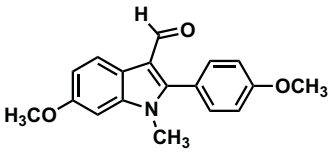

MDA: 2.4 ± 0.2
MCF: 5.4 ± 0.1

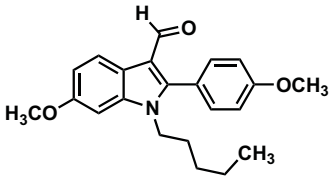

MDA: 3.3 ± 0.2
MCF: 2.4 ± 0.2

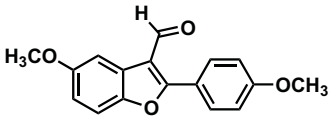

MDA: 8.4 ± 1.6
MCF: >10

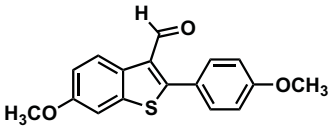

MDA: 0.99 ± 0.12
MCF: 0.23 ± 0.03
tubulin: 1.8

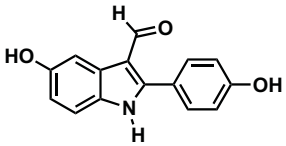

MDA: 2.5 ± 0.4
MCF: 6.7 ± 0.2

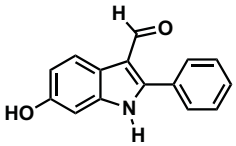

MDA: 7.9 ± 0.4
MCF: 3.3 ± 0.1

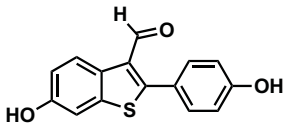

MDA: 9.3 ± 0.2
MCF: >10

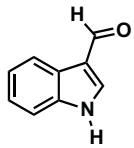

MDA: >10
MCF: >10

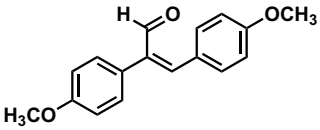

MDA: 7.9 ± 0.4
MCF: 7.0 ± 0.1

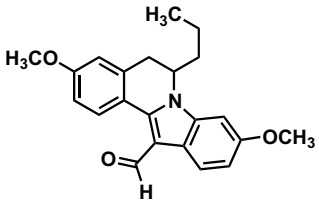

MDA: >10
MCF: nd

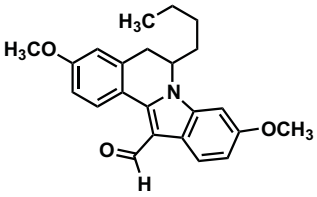

MDA: 8.7
MCF: nd

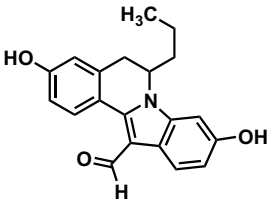

MDA: 0.3
MCF: 0.29
tubulin: 19

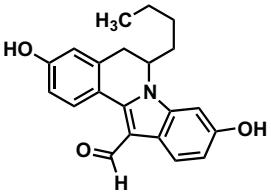

MDA: 1.4
MCF: 0.22
tubulin: 8.9

Molecule Tubulin Inhibitors 2-Aroylindoles, a Novel Class of Potent, Orally Active Small

Thomas Beckers, Thomas Reissmann, Mathias Schmidt, Angelika M. Burger, Heinz H. Fiebig, Udo Vanhoefer, Herwig Pongratz, Harald Hufsky, Jorg Hockemeyer, Markus Frieser, and Siavosh Mahboobi

CANCER RESEARCH 62, 3113–3119, June 1, 2002

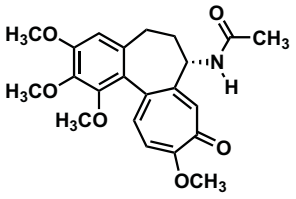

colchicine

MDA-MB 231: 25
Hec1A: >1000
A431: 19
SKOV3: 20
HeLa/KB: 23
HT 29: 23
A549: 56
PC-3: 19
AsPC-1: >1000
Cal27: 21
U 87: 16
Saos-2: 11
Renca: 33
T24: 24

MDR1
L1210: 0.051
$L1210^{VCR}$: 5.48
MDR1
MCF-7: nd
MCF-7/adr: nd
MDR1
A2780: nd
A2780/Dx5: nd
MRP
HT1080: nd
HT1080/DR4: nd

5-FU
HT29: nd
5-FU Bolus
HT29/R1: nd
5-FU Continous
HT29/R24: nd
Raltitrexed
HT29/ICID: nd
Topoisomerase I
HCT-8: nd
HCT-8/SN-38: nd

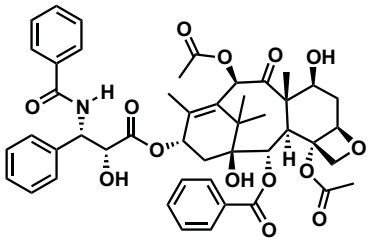

paclitaxel

RKO p21: >10
RKO: 0.006
G_2-M arrest: 0.025
MDA-MB 231: 11
Hec1A: >1000
A431: 3.3
SKOV3: 7.0
HeLa/KB: 7.0
HT 29: 10
A549: 13
PC-3: 12
AsPC-1: 12
Cal27: 8.9
U 87: 13
Saos-2: 8.8
Renca: 14
T24: 10

MDR1
L1210: 0.140
$L1210^{VCR}$: 15.3
MDR1
MCF-7: 0.003
MCF-7/adr: 2.1
MDR1
A2780: 0.005
A2780/Dx5: 0.145
MRP
HT1080: 0.003
HT1080/DR4: 0.005

5-FU
HT29: 0.007
5-FU Bolus
HT29/R1: 0.006
5-FU Continous
HT29/R24: 0.006
Raltitrexed
HT29/ICID: 0.016
Topoisomerase I
HCT-8: 0.033
HCT-8/SN-38: 0.133

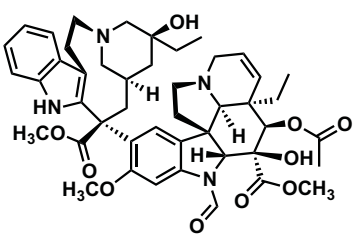

vincristine

RKO p21: >10
RKO: 0.001
G_2-M arrest: 0.002
MDA-MB 231: 8.0
Hec1A: >1000
A431: 1.0
SKOV3: 2.0
HeLa/KB: 1.0
HT 29: 5.0
A549: 27
PC-3: 4.0
AsPC-1: 17
Cal27: 1.9
U 87: 3.0
Saos-2: 4.2
Renca: 1.0
T24: 5.3

MDR1
L1210: 0.021
$L1210^{VCR}$: 1.46
MDR1
MCF-7: 0.001
MCF-7/adr: 1.2
MDR1
A2780: 0.0006
A2780/Dx5: 0.024
MRP
HT1080: 0.0008
HT1080/DR4: 0.018

5-FU
HT29: 0.003
5-FU Bolus
HT29/R1: 0.002
5-FU Continous
HT29/R24: 0.003
Raltitrexed
HT29/ICID: 0.006
Topoisomerase I
HCT-8: 0.013
HCT-8/SN-38: 0.02

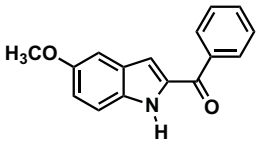

HeLa/KB: 0.074
U373: 0.074
tubulin: 0.53
colchocine: 0.51

RKO p21: >10
RKO: 0.042
G_2-M arrest: 0.092
MDA-MB 231: 62
Hec1A: >1000
A431: 48
SKOV3: 24
HeLa/KB: 48
HT 29: 37
A549: 63
PC-3: 56
AsPC-1: >1000
Cal27: 65
U 87: 88
Saos-2: 42
Renca: 144
T24: 63

MDR1
L1210: 0.102
$L1210^{VCR}$: 0.077
MDR1
MCF-7: 0.04
MCF-7/adr: 0.06
MDR1
A2780: 0.024
A2780/Dx5: 0.02
MRP
HT1080: 0.027
HT1080/DR4: 0.02

5-FU
HT29: 0.055
5-FU Bolus
HT29/R1: 0.076
5-FU Continous
HT29/R24: 0.058
Raltitrexed
HT29/ICID: 0.093
Topoisomerase I
HCT-8: 0.028
HCT-8/SN-38: 0.038

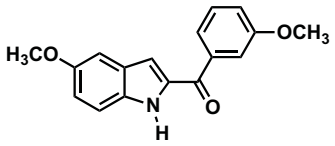

HeLa/KB: 0.027
U373: 0.028
tubulin: 0.53
colchocine: 0.28

RKO p21: >10
RKO: 0.018
G_2-M arrest: 0.028
MDA-MB 231: 25
Hec1A: >1000
A431: 19
SKOV3: 11
HeLa/KB: 29
HT 29: 22
A549: 28
PC-3: 25
AsPC-1: >1000
Cal27: 19
U 87: 31
Saos-2: 18
Renca: 37
T24: 27

MDR1
L1210: 0.027
$L1210^{VCR}$: 0.045
MDR1
MCF-7: nd
MCF-7/adr: nd
MDR1
A2780: nd
A2780/Dx5: nd
MRP
HT1080: nd
HT1080/DR4: nd

5-FU
HT29: nd
5-FU Bolus
HT29/R1: nd
5-FU Continous
HT29/R24: nd
Raltitrexed
HT29/ICID: nd
Topoisomerase I
HCT-8: nd
HCT-8/SN-38: nd

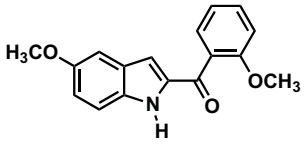

RKO p21: >10
RKO: 0.082
G_2-M arrest: nd
HeLa/KB: 0.106
U373: 0.121
tubulin: 1.29
colchocine: 0.80

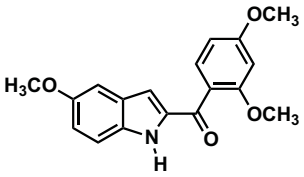

RKO p21: >10
RKO: 0.246
G_2-M arrest: nd
HeLa/KB: 0.25
U373: 0.362
tubulin: 5.60
colchocine: 2.50

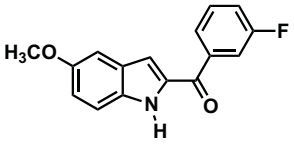

RKO p21: >10
RKO: 0.017
G_2-M arrest: 0.039
HeLa/KB: 0.020
U373: 0.024
tubulin: 0.39
colchocine: 0.14

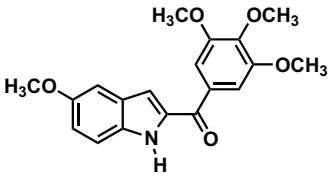

RKO p21: >10
RKO: 0.05
G_2-M arrest: nd
HeLa/KB: 0.082
U373: 0.073
tubulin: 0.99
colchocine: 0.29

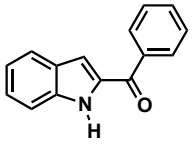

RKO p21: nd
RKO: nd
G_2-M arrest: nd
HeLa/KB: >10
U373: >10
tubulin: >10
colchocine: >10

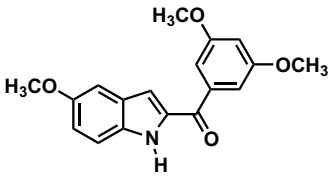

RKO p21: >10
RKO: 0.019
G_2-M arrest: 0.030
HeLa/KB: 0.019
U373: 0.018
tubulin: 0.81
colchocine: 0.27

RKO p21: antiproliferative activity IC_{50} colon with $p21^{waf1}$ expression-μM
RKO: antiproliferative activity IC_{50} colon without-μM
G_2-M arrest: HeLa/KB cervial cells-flow cytomerty-μM
MDA-MB 231: GI_{50} breast-nM
Hec1A: GI_{50} endometrium-nM
A431: GI_{50} vulva-nM
SKOV3: GI_{50} ovary-nM
HeLa/KB: GI_{50} cervix-nM
HT 29: GI_{50} colon-nM
A549: GI_{50} lung-nM
PC-3: GI_{50} prostate-nM
AsPC-1: GI_{50} pancreas-nM
Cal27: GI_{50}tongue-nM
U 87: GI_{50} brain-nM
Saos-2: GI_{50} bone-nM
Renca: GI_{50} kidney-nM
T24: GI_{50} bladder-nM

Cytotoxicity
HeLa/KB: cervical-μM
U373: astrocytoma-μM
tubulin: inhibition-μM
colchocine: binding-μM

antiproliferative activity IC_{50} of resistance phenotypes-μM

MDR1
L1210:
$L1210^{VCR}$:
MDR1
MCF-7:
MCF-7/adr:
MDR1
A2780:
A2780/Dx5
MRP
HT1080:
HT1080/DR4:

5-FU
HT29:
5-FU Bolus
HT29/R1:
5-FU Continous
HT29/R24:
Raltitrexed
HT29/ICID:
Topoisomerase I
HCT-8:
HCT-8/SN-38:

New Arylthioindoles: Potent Inhibitors of Tubulin Polymerization. 2. Structure-Activity Relationships and Molecular Modeling Studies

Gabriella De Martino, Michael C. Edler, Giuseppe La Regina, Antonio Coluccia, Maria Chiara Barbera, Denise Barrow, Robert I. Nicholson, Gabriela Chiosis, Andrea Brancale, Ernest Hamel, Marino Artico, and Romano Silvestri

J. Med. Chem. 2006, 49, 947-954

tubulin: μM
MCF: nM-human breast
col inh: %
SCLC: nM- small cell lung

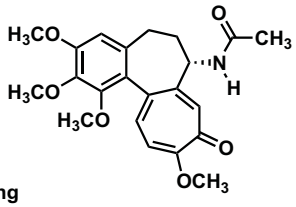

tubulin: 3.2 ± 0.4
MCF: 13 ± 3
col inh: nd
SCLC: nd

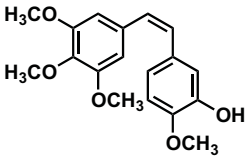

tubulin: 2.2 ± 0.2
MCF: 17 ± 10
col inh: 97 ± 10
SCLC: nd

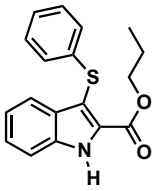

tubulin: >40
MCF: >2.5
col inh: nd
SCLC: nd

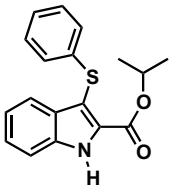

tubulin: 18 ± 2
MCF: >2.5
col inh: nd
SCLC: nd

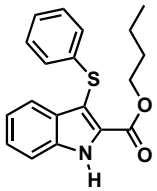

tubulin: >40
MCF: >2.5
col inh: nd
SCLC: nd

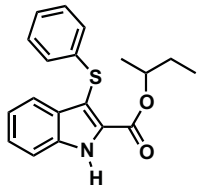

tubulin: >40
MCF: >2.5
col inh: nd
SCLC: nd

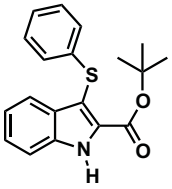

tubulin: >40
MCF: >2.5
col inh: nd
SCLC: nd

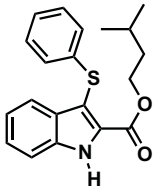

tubulin: >40
MCF: >2.5
col inh: nd
SCLC: nd

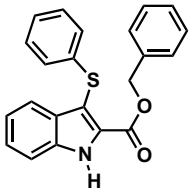

tubulin: >40
MCF: >2.5
col inh: nd
SCLC: nd

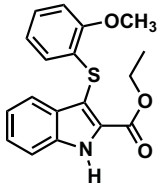

tubulin: 12 ± 2
MCF: >2.5
col inh: nd
SCLC: nd

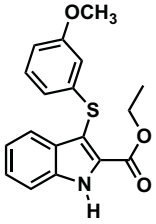

tubulin: 2.9 ± 0.3
MCF: 150 ± 90
col inh: 48 ± 7
SCLC: 585 ± 50

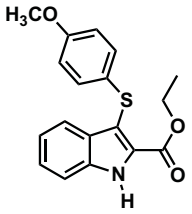

tubulin: >40
MCF: >2.5
col inh: nd
SCLC: nd

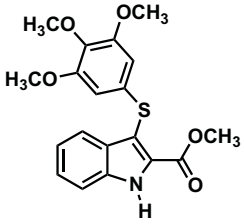

tubulin: 2.9 ± 0.1
MCF: 25 ± 1
col inh: 74 ± 2
SCLC: 52 ± 3

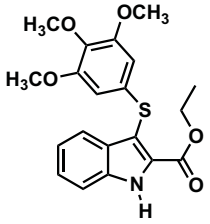

tubulin: 2.9 ± 0.2
MCF: 40 ± 2
col inh: 51 ± 3
SCLC: 84 ± 5

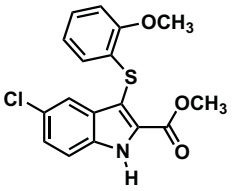

tubulin: 4.2 ± 0.6
MCF: 1300 ± 400
col inh: 34 ± 6
SCLC: 7000 ± 300

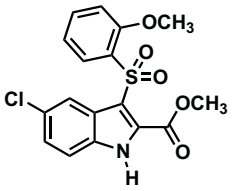

tubulin: >40
MCF: >2.5
col inh: nd
SCLC: nd

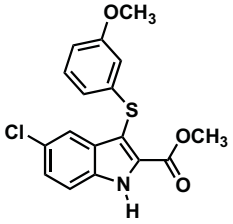

tubulin: 1.8 ± 0.2
MCF: 330 ± 40
col inh: 53 ± 4
SCLC: 3200 ± 800

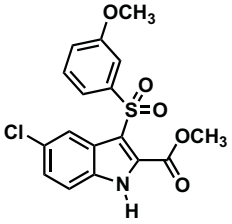

tubulin: 31 ± 4
MCF: >2.5
col inh: nd
SCLC: >10000

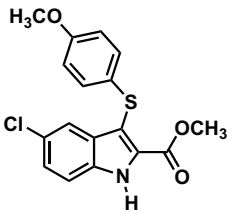

tubulin: >40
MCF: >2.5
col inh: nd
SCLC: >10000

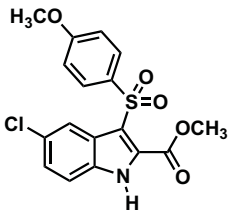

tubulin: >40
MCF: >2.5
col inh: nd
SCLC: nd

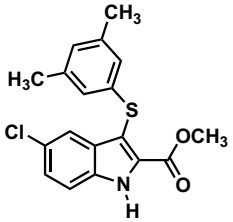

tubulin: >40
MCF: >2.5
col inh: nd
SCLC: nd

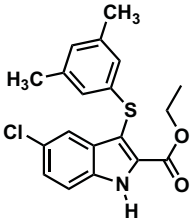

tubulin: >40
MCF: 1200 ± 200
col inh: nd
SCLC: nd

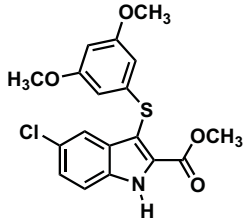

tubulin: 2.2 ± 0.2
MCF: 34 ± 10
col inh: 82 ± 2
SCLC: 18 ± 1

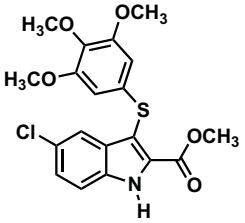

tubulin: 2.5 ± 0.3
MCF: 42 ± 10
col inh: 57 ± 2
SCLC: 216 ± 17

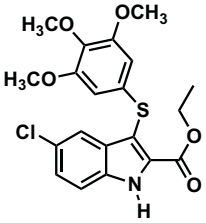

tubulin: 2.2 ± 0.2
MCF: 110 ± 20
col inh: 53 ± 6
SCLC: 93 ± 10

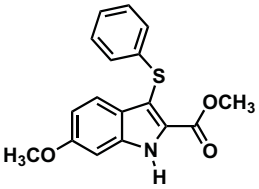

tubulin: >40
MCF: >2.5
col inh: nd
SCLC: nd

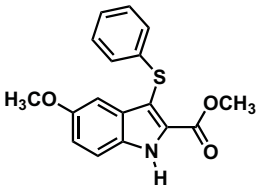

tubulin: 6.2 ± 0.3
MCF: >2.5
col inh: 30 ± 6
SCLC: nd

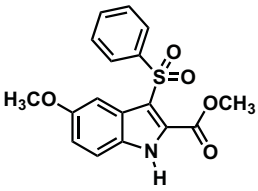

tubulin: >40
MCF: >2.5
col inh: nd
SCLC: nd

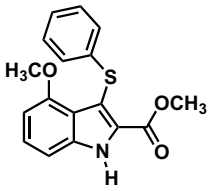

tubulin: >40
MCF: >2.5
col inh: nd
SCLC: nd

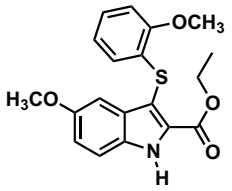

tubulin: 16 ± 0.5
MCF: 350 ± 60
col inh: nd
SCLC: 220 ± 200

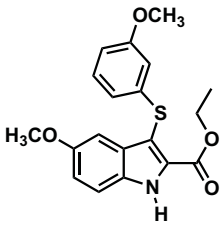

tubulin: 3.1 ± 0.2
MCF: 280 ± 100
col inh: 39 ± 3
SCLC: 584 ± 40

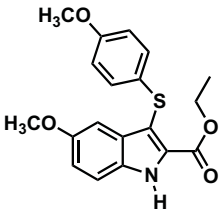

tubulin: >40
MCF: >2.5
col inh: nd
SCLC: >10000

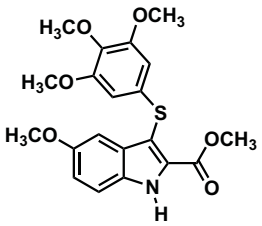

tubulin: 2.0 ± 0.2
MCF: 13 ± 3
col inh: 90 ± 1
SCLC: 47 ± 2

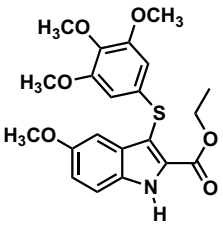

tubulin: 2.4 ± 0.2
MCF: 46 ± 3
col inh: 71 ± 2
SCLC: nd

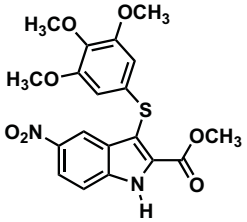

tubulin: 4.5 ± 0.1
MCF: 120 ± 40
col inh: 32 ± 2
SCLC: nd

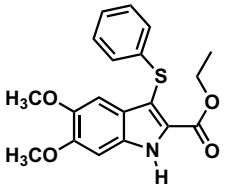

tubulin: 14 ± 1
MCF: >2.5
col inh: nd
SCLC: nd

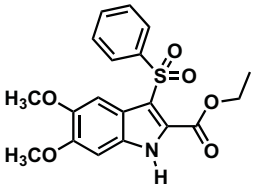

tubulin: >40
MCF: >2.5
col inh: nd
SCLC: nd

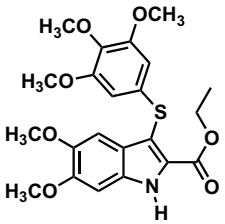

tubulin: 22 ± 0.7
MCF: 1000 ± 200
col inh: nd
SCLC: nd

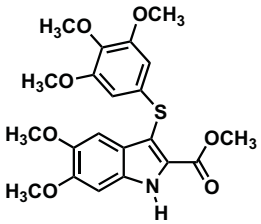

tubulin: >40
MCF: 1600 ± 400
col inh: nd
SCLC: nd

Novel potent antimitotic heterocyclic ketones: Synthesis, antiproliferative activity, and structure–activity relationships

Laixing Hu, Jian-dong Jiang, Jinrong Qu, Yan Li, Jie Jin, Zhuo-rong Li,
and David W. Boykina

Bioorganic & Medicinal Chemistry Letters 17 (2007) 3613–3617

CEM: T-cell leukemia-nM
Molt-3: T-cell leukemia-nM
Bel-7402: heptoma-nM
MCF-7: breast cancer-nM
DU-145: prostate-nM
PC-3: prostate-nM
DND-1: melanoma-nM

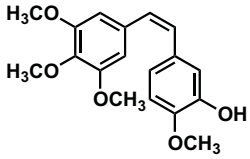

CEM: 1.9
Molt-3: 9.3
Bel-7402: 10
MCF-7: 12
DU-145: 9.3
PC-3: 2.8
DND-1: 2.5

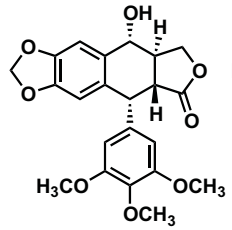

podophyllotoxin

CEM: 7.2 **Molt-3: 14**
Bel-7402: 9.1 **MCF-7: 15**
DU-145: 52 **PC-3: 10**
DND-1: 12

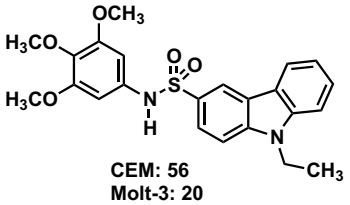

CEM: 56
Molt-3: 20
Bel-7402: 201
MCF-7: 89
DU-145: 603
PC-3: 201
DND-1: 89

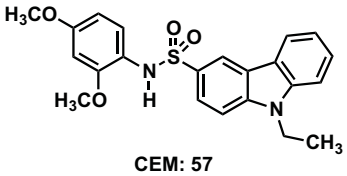

CEM: 57

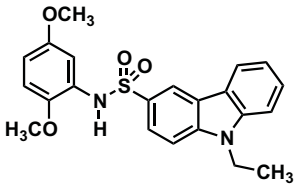

CEM: 61

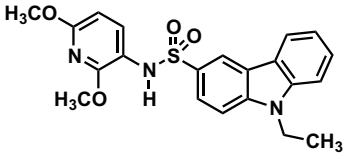

CEM: 122

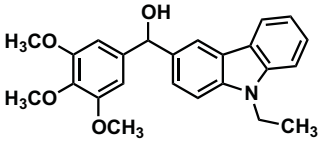

CEM: 192

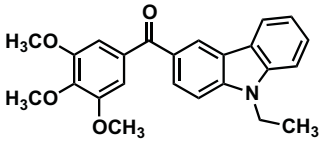

CEM: 90
Molt-3: 51
Bel-7402: 90
MCF-7: 26
DU-145: 39
PC-3: 103
DND-1: 21
tubulin: 3.4 μM

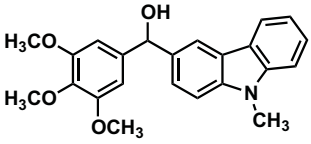

CEM: 59
Molt-3: 38
Bel-7402: 88
MCF-7: 44
DU-145: 103
PC-3: 117
DND-1: 59

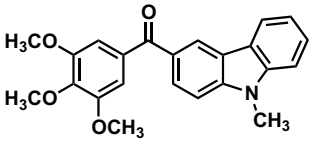

CEM: 18
Molt-3: 18
Bel-7402: 21
MCF-7: 9.2
DU-145: 26
PC-3: 25
DND-1: 15

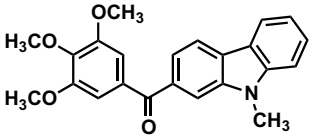

CEM: 30
Molt-3: 18
Bel-7402: 27
MCF-7: 24
DU-145: 75
PC-3: 75
DND-1: 27

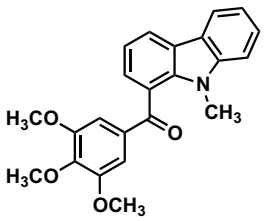

CEM: 307

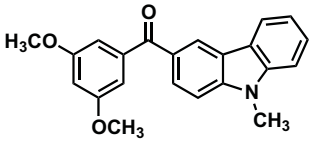

CEM: 1693

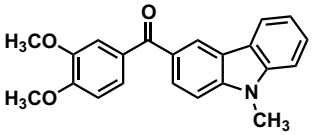

CEM: 1693

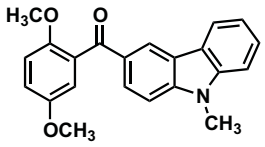

CEM: 2370

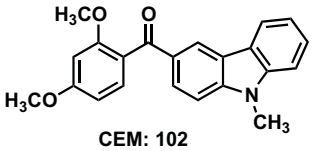

CEM: 102
Molt-3: 24
Bel-7402: 44
MCF-7: 85
DU-145: 34
PC-3: 203
DND-1: 118

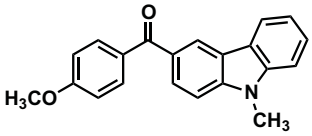

CEM: 1131

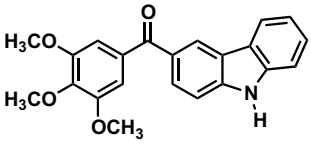

CEM: 225

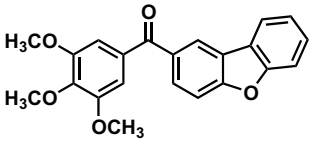

CEM: 288

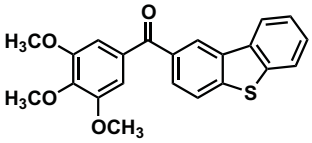

CEM: 303

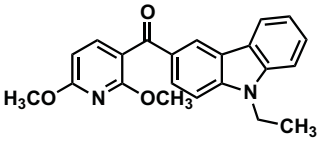

CEM: 555

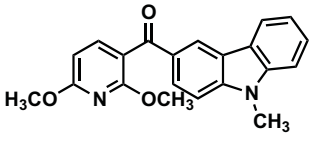

CEM: 1012

One-Pot Synthesis of Benzo[b]furan and Indole Inhibitors of Tubulin Polymerization

Bernard L. Flynn, Ernest Hamel, and M. Katherine Jung

J. Med. Chem. 2002, 45, 2670-2673

Tubulin: μM

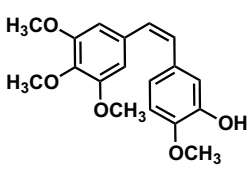

Tubulin: 2.1± 0.1

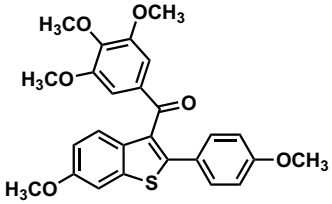

Tubulin: >40

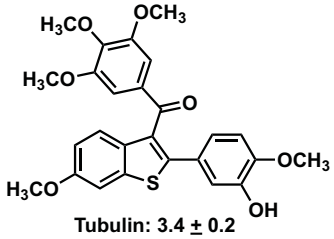

Tubulin: 3.4 ± 0.2

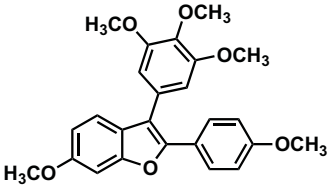

Tubulin: >40

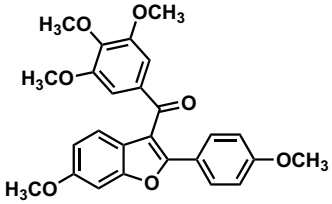

Tubulin: 0.41± 0.1

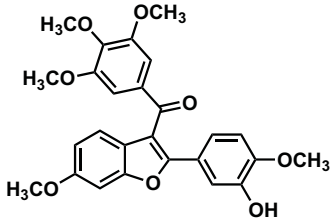

Tubulin: 1.3 ± 0.2

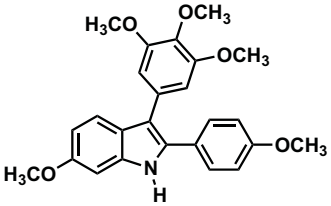

Tubulin: >40

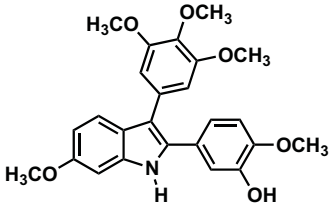

Tubulin: 4.1± 0.6

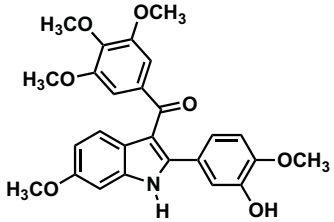

Tubulin: 1.6

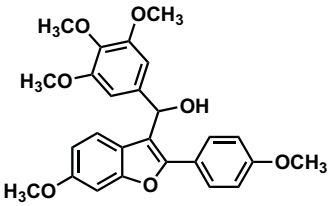

Tubulin: >40

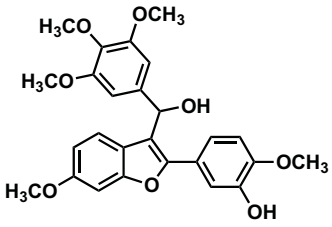

Tubulin: 8.8 ± 1.4

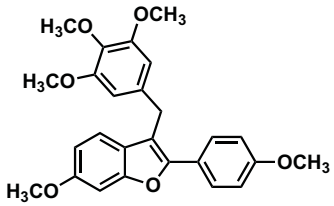

Tubulin: 2.5 ± 0.3

Scaffold-Hopping Strategy: Synthesis and Biological Evaluation of 5,6-Fused Bicyclic Heteroaromatics To Identify Orally Bioavailable Anticancer Agents

Yen-Shih Tung, Mohane Selvaraj Coumar, Yu-Shan Wu, Hui-Yi Shiao, Jang-Yang Chang, Jing-Ping Liou, Paritosh Shukla, Chun-Wei Chang, Chi-Yen Chang, Ching-Chuan Kuo, Teng-Kuang Yeh, Chin-Yu Lin, Jian-Sung Wu, Su-Ying Wu, Chun-Chen Liao, and Hsing-Pang Hsieh

J. Med. Chem. 2011, 54, 3076–3080

KB: cervical-nM
MKN-45: gastric carcinoma-nM
metabolic stability: % compound remaining after 30 min incubation with human liver microsome

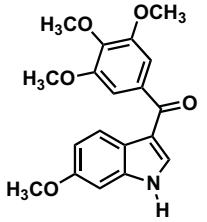

BPR0L075

KB: 6
MKN-45: 5
metabolic stability: 54.1

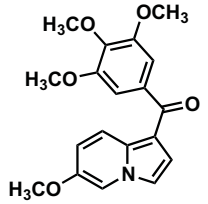

KB: 284
MKN-45: 80
metabolic stability: nd

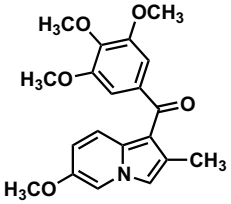

KB: 31
MKN-45: 26
metabolic stability: 35.4

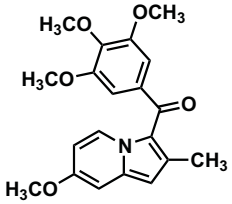

KB: >1000
MKN-45: 354
metabolic stability: nd

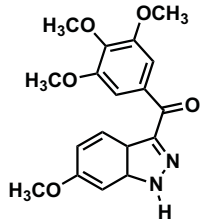

KB: 70
MKN-45: 95
metabolic stability: nd

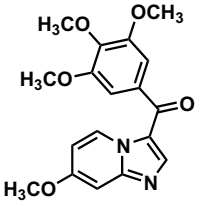

KB: 770
MKN-45: 730
metabolic stability: nd

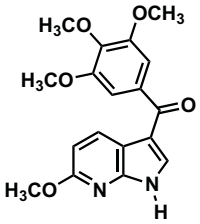

KB: 20
MKN-45: 16
metabolic stability: 88.3

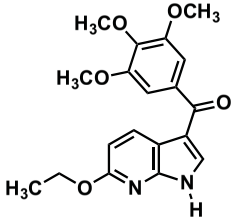

KB: 12
MKN-45: 14
metabolic stability: 96.4

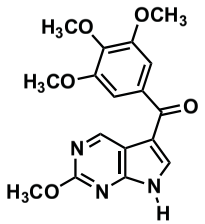

KB: 284
MKN-45: 80
metabolic stability: nd

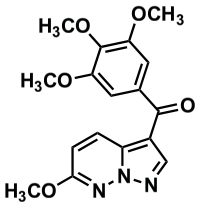

KB: >1000
MKN-45: >1000
metabolic stability: 99.6

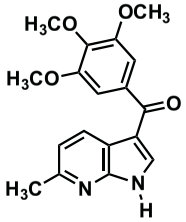

KB: 23
MKN-45: 22
metabolic stability: 86.7

Structure-activity relationships of indole compounds derived from combretastatin A4: Synthesis and biological screening of 5-phenylpyrrolo[3,4-a] carbazole-1,3-diones as potential antivascular agents

Nancy Ty, Grégory Dupeyre, Guy G. Chabot, Johanne Seguin, Lionel Quentin, Angèle Chiaroni, François Tillequin, Daniel Scherman, Sylvie Michel, Xavier Cachet

European Journal of Medicinal Chemistry 45 (2010) 3726e3739

B16: murine melanoma-μM
Morph: lowest conc. that casues rounding up of HUVEC after 2 h exposure-μM
na- not active

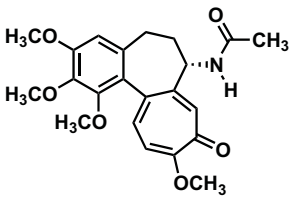

B16: 0.031 ± 0.003
Morph: 0.003

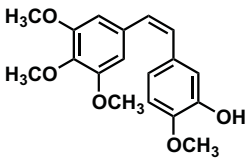

B16: 0.003 ± 0.001
Morph: 0.008

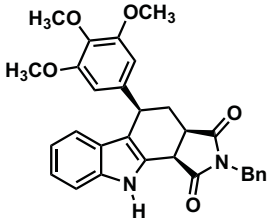

B16: 3.7 ± 0.1
Morph: 50

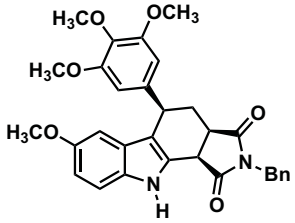

B16: >80
Morph: na

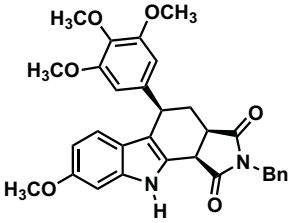

B16: >80
Morph: 2.5

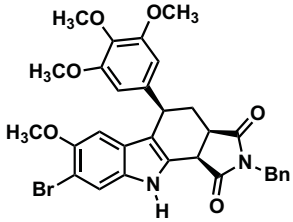

B16: >40
Morph: na

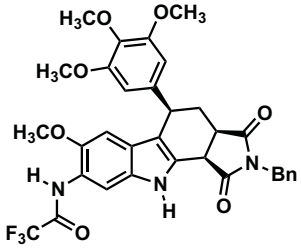

B16: 20.0 ± 5.3
Morph: 20

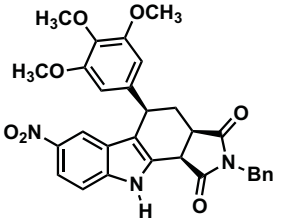

B16: >40
Morph: na

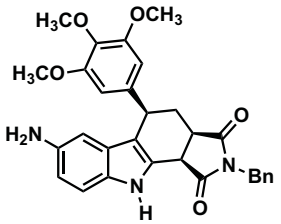

B16: 16.6 ± 2.8
Morph: 10

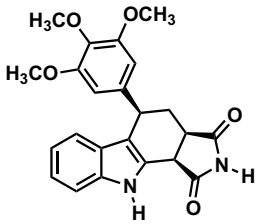

B16: >40
Morph: 1.3

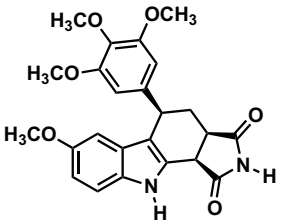

B16: >80
Morph: na

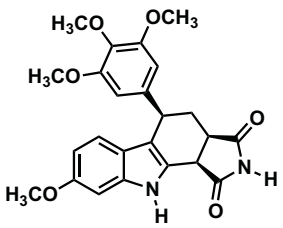

B16: 2.6 ± 1.5
Morph: 0.3

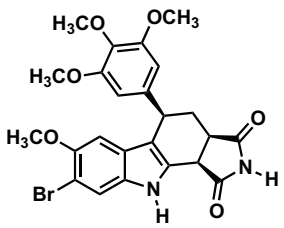

B16: 60.9 ± 4.3
Morph: 50

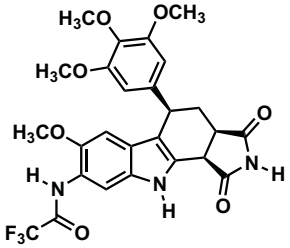

B16: 23.1 ± 4.2
Morph: na

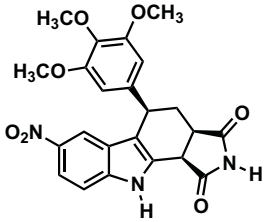

B16: >50
Morph: na

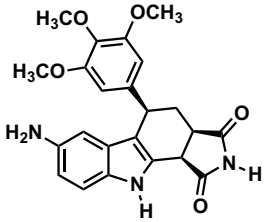

B16: >100
Morph: 100

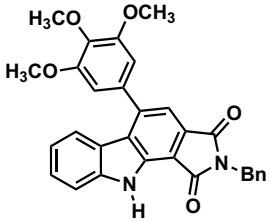

B16: 3.3 ± 2.0
Morph: na

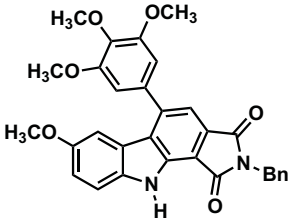

B16: 12.8 ± 4.9
Morph: 100

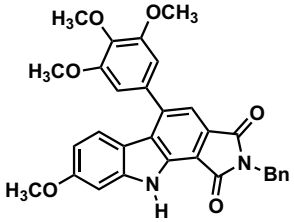

B16: 3.9 ± 1.3
Morph: 100

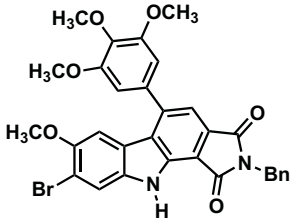

B16: >100
Morph: na

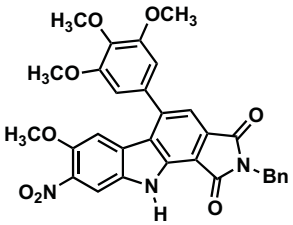

B16: >50
Morph: na

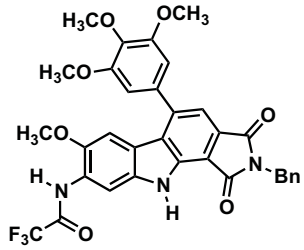

B16: >100
Morph: na

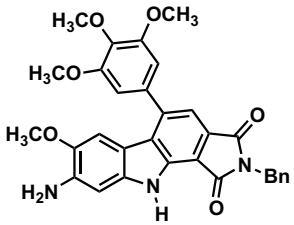

B16: >50
Morph: na

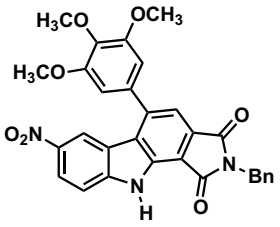

B16: >25
Morph: na

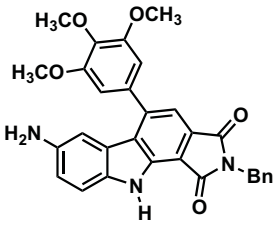

B16: 4.1 ± 0.8
Morph: na

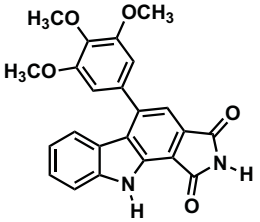

B16: >100
Morph: 100

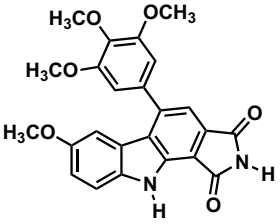

B16: >100
Morph: 100

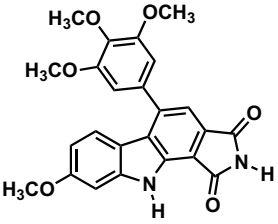

B16: 0.6 ± 0.1
Morph: 0.025

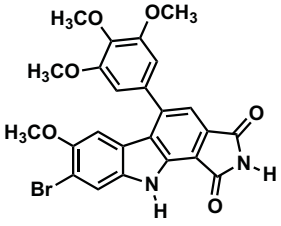

B16: 13.5
Morph: 100

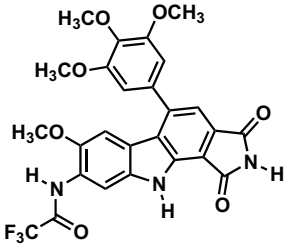

B16: 43.9 ± 4.0
Morph: na

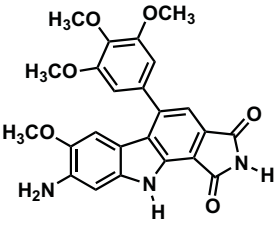

B16: 16.8 ± 0.2
Morph: 100

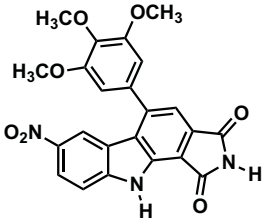

B16: >50
Morph: na

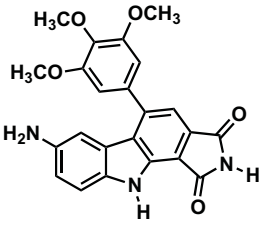

B16: 12.8 ± 2.9
Morph: na

Synthesis and antineoplastic activity of combretastatin analogues: Heterocombretastatins

Manuel Medarde, Angel Ramos, Esther Caballero, Rafael Pelaez-Lamamie de Clairac, Jose Luis Lopez, Dolores Garcia Gravalos, Arturo San Feliciano

Eur. J. Med. Chem. 33 (1998) 71-77

P-388: lymphoid neoplasm -μM
A-549: human lung -μM
HT-29: human colon -μM
MEL-28: human melanoma -μM

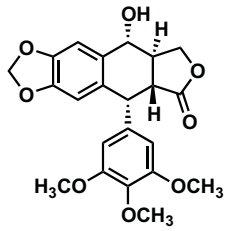

podophyllotoxin

P-388: 0.05
A-549: 0.05
HT-29: 0.05
MEL-28: 0.06

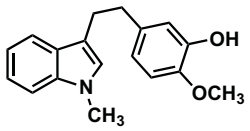

P-388: 3.6
A-549: 3.6
HT-29: 8.9
MEL-28: 3.6

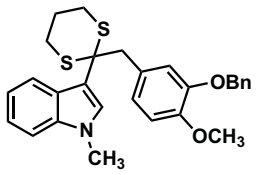

P-388: 5.3
A-549: 10.5
HT-29: 21.1
MEL-28: 10.5

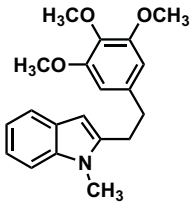

P-388: 15.4
A-549: 15.4
HT-29: 15.4
MEL-28: 15.4

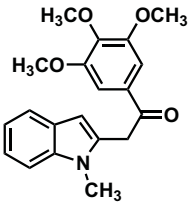

P-388: 0.6
A-549: 0.6
HT-29: 0.6
MEL-28: 0.3

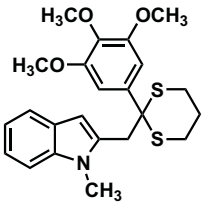

P-388: 5.8
A-549: 5.8
HT-29: 11.6
MEL-28: 11.6

Synthesis and biological evaluation of (3,4,5-trimethoxyphenyl)indol-3-ylmethane derivatives as potential antivascular agents

Gregory Dupeyre, Guy G. Chabot, Sylviane Thoret, Xavier Cachet, Johanne Seguin, Daniel Guenard, Francois Tillequin, Daniel Scherman, Michel Kocha and Sylvie Michel

Bioorganic & Medicinal Chemistry 14 (2006) 4410–4426

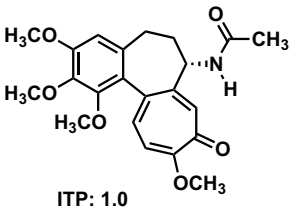

ITP: 1.0
SEM: 0.031 ± 0.003
MA: 3+

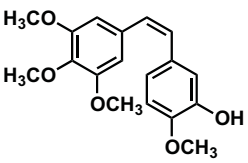

ITP: 0.7
SEM: 0.003 ± 0.001
MA: 5+

ITP: inhibition of tubulin polymerization ($IC_{50}/IC_{50colchicine}$)
SEM: B16 melanoma cell line- μM
MA: morphological activity-HUVEC-lowest concentration at which cell rounding was observed after 2h incubation

1+ = 25 μg/mL 2+ = 2.5 μg/mL
3+ = 0.25 μg/mL 4+ = 0.025 μg/mL
5+ = 0.0025 μg/mL

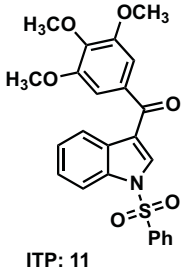

ITP: 11
SEM: 8.4 ± 0.9
MA: 1+

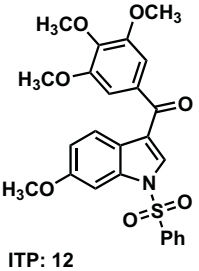

ITP: 12
SEM: 0.211 ± 0.040
MA: 4+

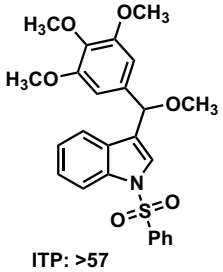

ITP: >57
SEM: 20.9 ± 6.7
MA: no rounding

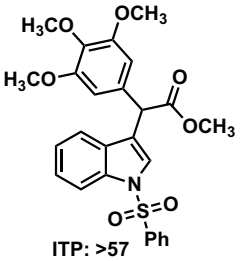

ITP: >57
SEM: 7.5 ± 1.2
MA: 2+

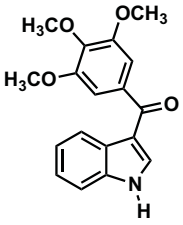

ITP: 57
SEM: 5.0 ± 1.0
MA: 2+

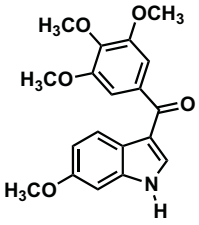

ITP: 0.4
SEM: 0.013 ± 0.004
MA: 5+

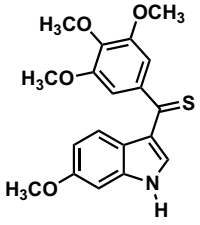

ITP: 0.2
SEM: 0.024 ± 0.007
MA: 5+

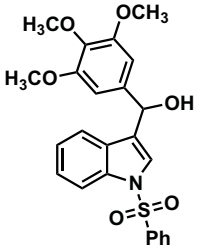

ITP: 9
SEM: 16.2 ± 0.8
MA: 1+

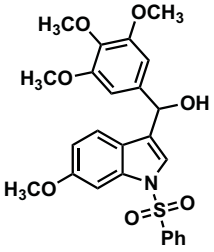

ITP: 13
SEM: >51.70
MA: 1+

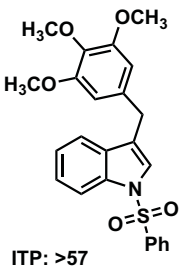

ITP: >57
SEM: 6.1 ± 0.7
MA: no rounding

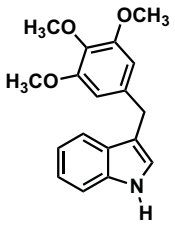

ITP: >57
SEM: 6.1 ± 1.0
MA: 2+

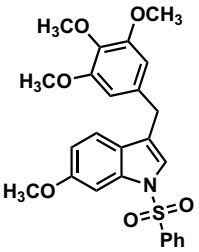

ITP: 4
SEM: 7.0 ± 0.4
MA: 2+

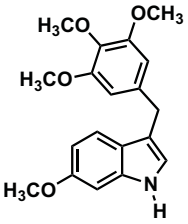

ITP: 0.2
SEM: 0.045 ± 0.006
MA: 4+

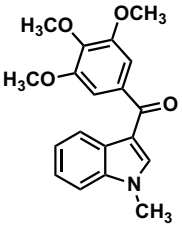

ITP: 40
SEM: 7.0 ± 1.6
MA: 1+

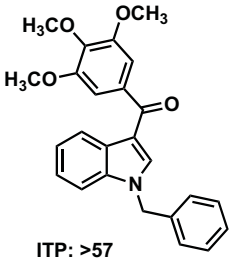

ITP: >57
SEM: 22.7 ± 1.9
MA: no rounding

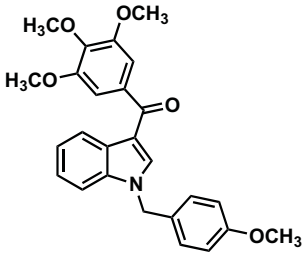

ITP: 41
SEM: 36.0 ± 5.2
MA: no rounding

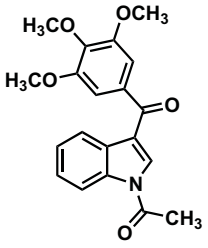

ITP: 35
SEM: 7.3 ± 3.2
MA: 2+

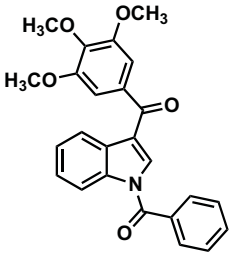

ITP: 31
SEM: 3.5 ± 0.7
MA: 2+

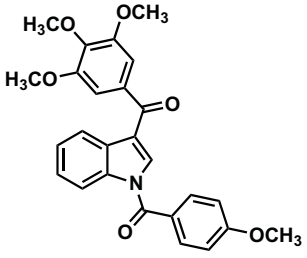

ITP: 24
SEM: 5.3 ± 1.1
MA: 1+

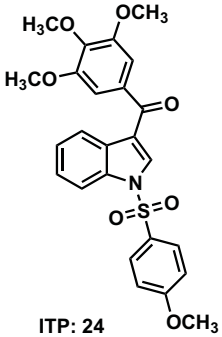

ITP: 24
SEM: 23.9 ± 4.7
MA: 1+

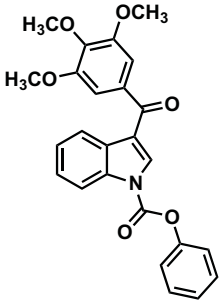

ITP: 5
SEM: 5.2 ± 2.2
MA: 1+

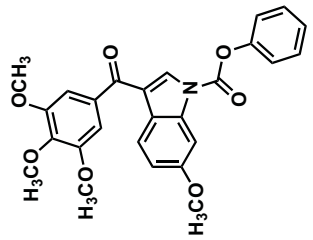

ITP: 0.2
SEM: 0.023 ± 0.010
MA: 5+

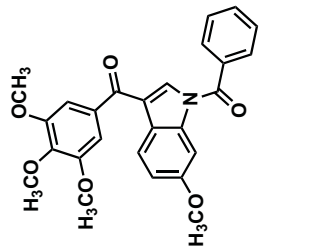

ITP: 11
SEM: 0.035 ± 0.022
MA: 3+

Synthesis and biological evaluation of 1-(4-Indolyl and 6-Quinolinyl) indoles as a new class of potent anticancer agents

Mei-Jung Lai, Jang-Yang Chang, Hsueh-Yun Lee, Ching-Chuan Kuo, Mei-Hsiang Lin, Hsing-Pang Hsieh, Chi-Yen Chang, Jian-Sung Wu, Su-Ying Wu, Kuang-Shing Shey, Jing-Ping Liou

European Journal of Medicinal Chemistry 46 (2011) 3623e3629

Cells: nM
Tubulin: μM

KB: cervical
KB-VIN10: MDR1-positive
H460: non small lung
HT29: colon
MKN45: stomach

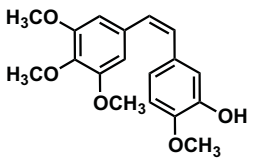

KB: 2 ± 0.4
KB-VIN10: 0.7 ± 0.4
H460: 2.3 ± 0.9
HT29: 94 ± 26
MKN45: 4.8 ± 0.8
Tubulin: 1.8 ± 0.2

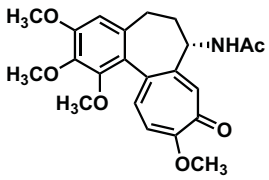

KB: 10 ± 1
KB-VIN10: 121 ± 10
H460: 20 ± 0.1
HT29: 15 ± 0.5
MKN45: 12 ± 2
Tubulin: 4.1 ± 0.5

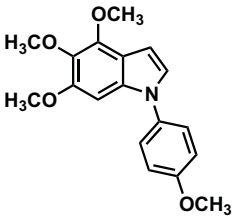

KB: 186 ± 14
KB-VIN10: 135 ± 22
H460: 198 ± 19
HT29: 179 ± 12
MKN45: 145 ± 7

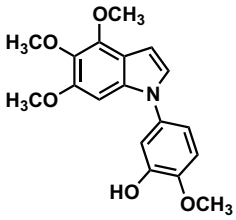

KB: 131 ± 53
KB-VIN10: 68 ± 11
H460: 737 ± 64
HT29: 6395 ± 1160
MKN45: 5899 ± 760

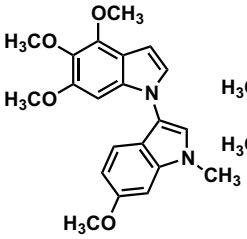

KB: 148 ± 33
KB-VIN10: 63 ± 8
H460: 172 ± 27
HT29: 148 ± 33
MKN45: 105 ± 21

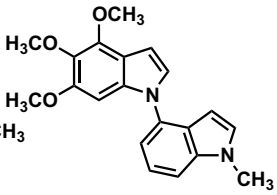

KB: 32 ± 5
KB-VIN10: 25 ± 5
H460: 49 ± 26
HT29: 44 ± 23
MKN45: 40 ± 32
Tubulin: 1.7 ± 0.1

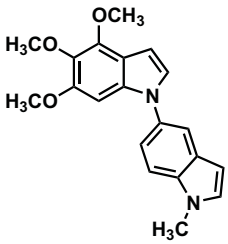

KB: 73 ± 20
KB-VIN10: 53 ± 9
H460: 76 ± 4
HT29: 74 ± 2
MKN45: 40 ± 9
Tubulin: 2.7 ± 0.5

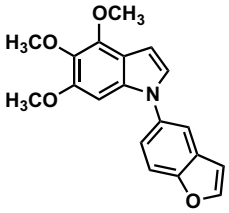

KB: 537 ± 50
KB-VIN10: 265 ± 24
H460: 690 ± 106
HT29: 646 ± 110
MKN45: 322 ± 106

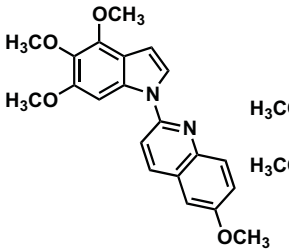

KB: 7369 ± 820
KB-VIN10: 9114 ± 824
H460: 6170 ± 472
HT29: 3652 ± 1247
MKN45: 11482 ± 1075

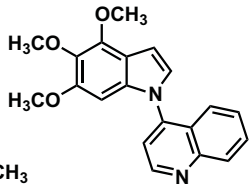

KB: 216 ± 23
KB-VIN10: 130 ± 9
H460: 318 ± 99
HT29: 329 ± 63
MKN45: 197 ± 44

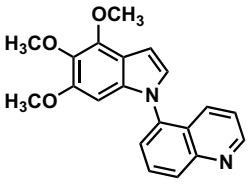

KB: 900 ± 8
KB-VIN10: 535 ± 71
H460: 955 ± 101
HT29: 921 ± 108
MKN45: 682 ± 223

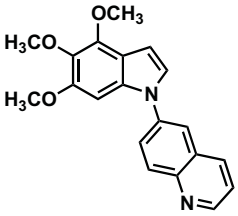

KB: 18 ± 2
KB-VIN10: 11 ± 4
H460: 31 ± 12
HT29: 34 ± 5
MKN45: 24 ± 7
Tubulin: 2.7 ± 0.2

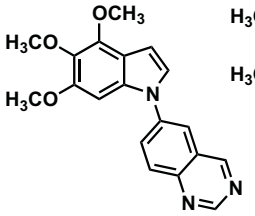

KB: 7950 ± 636
KB-VIN10: 3449 ± 1153
H460: 7515 ± 200
HT29: 8136 ± 371
MKN45: 4309 ± 144

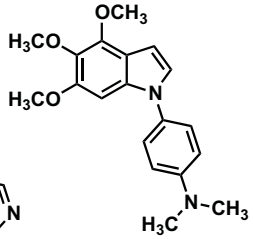

KB: 148 ± 33
KB-VIN10: 63 ± 8
H460: 172 ± 27
HT29: 148 ± 33
MKN45: 105 ± 21

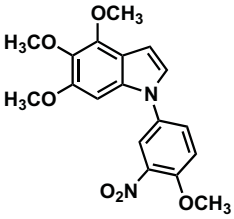

not tested

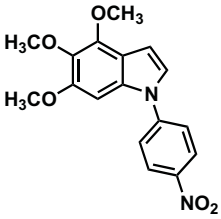

not tested

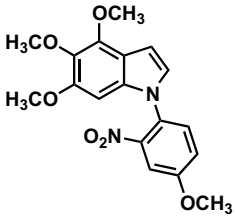

not tested

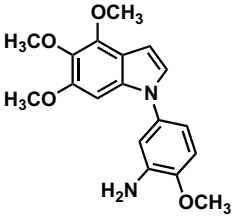

KB: 3250 ± 212
KB-VIN10: 1378 ± 180
H460: 2393 ± 13
HT29: 4146 ± 75
MKN45: 1544 ± 19

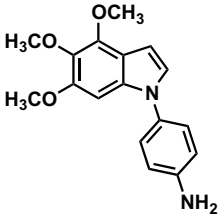

KB: 216 ± 23
KB-VIN10: 130 ± 9
H460: 318 ± 99
HT29: 329 ± 63
MKN45: 197 ± 44

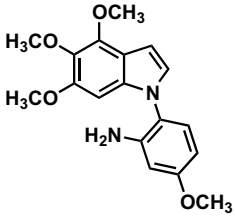

KB: 102 ± 12
KB-VIN10: 50 ± 2
H460: 96 ± 10
HT29: 101 ± 16
MKN45: 49 ± 15
Tubulin: 4.7 ± 0.5

Synthesis and Biological Evaluation of 1-Arylsulfonyl-5-(Nhydroxyacrylamide) indoles as Potent Histone Deacetylase Inhibitors with Antitumor Activity in Vivo

Mei-Jung Lai, Han-Li Huang, Shiow-Lin Pan, Yi-Min Liu, Chieh-Yu Peng, Hsueh-Yun Lee, Teng-Kuang Yeh, Po-Hsien Huang, Che-Ming Teng, Ching-Shih Chen, Hsun-Yueh Chuang, and Jing Ping Liou

J. Med. Chem. 2012, 55, 3777-3791

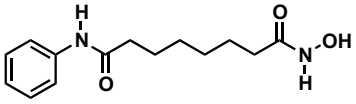

SAHA
Hep3B: 0.69 ± 0.2
MDA-MB-231: 0.97 ± 0.2
PC-3: 1.21 ± 0.3
A549: 1.85 ± 0.3

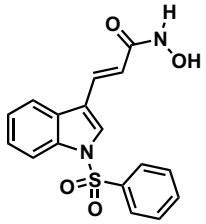

Hep3B: 8.87 ± 0.2
MDA-MB-231: 8.14 ± 0.7
PC-3: 5.77 ± 0.5
A549: 7.06 ± 0.1

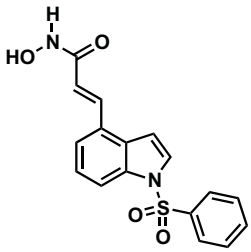

Hep3B: 4.32 ± 0.1
MDA-MB-231: 4.16 ± 0.3
PC-3: 3.67 ± 0.3
A549: 6.70 ± 0.2

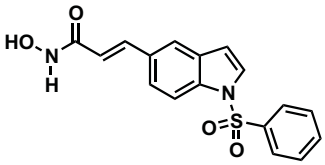

Hep3B: 0.41 ± 0.1
MDA-MB-231: 0.48 ± 0.1
PC-3: 0.62 ± 0.2
A549: 1.02 ± 0.2

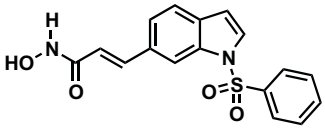

Hep3B: 2.12 ± 0.1
MDA-MB-231: 2.41 ± 0.3
PC-3: 2.40 ± 0.3
A549: 5.30 ± 0.7

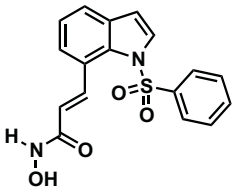

Hep3B: 3.82 ± 0.4
MDA-MB-231: 7.71 ± 0.6
PC-3: 4.75 ± 0.4
A549: 5.50 ± 0.4

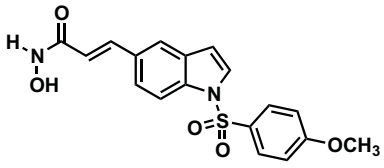

Hep3B: 0.55 ± 0.1
MDA-MB-231: 0.75 ± 0.1
PC-3: 0.80 ± 0.2
A549: 1.18 ± 0.2

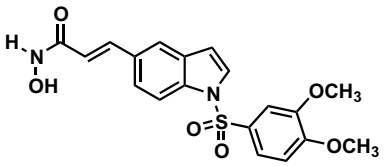

Hep3B: 0.36 ± 0.1
MDA-MB-231: 0.37 ± 0.1
PC-3: 0.93 ± 0.3
A549: 0.56 ± 0.1

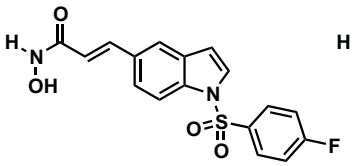

Hep3B: 0.64 ± 0.1
MDA-MB-231: 0.66 ± 0.2
PC-3: 0.39 ± 0.1
A549: 0.75 ± 0.7

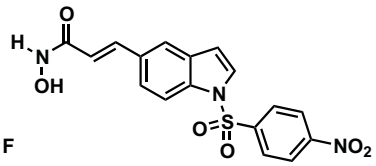

Hep3B: 0.56 ± 0.1
MDA-MB-231: 0.75 ± 0.2
PC-3: 0.85 ± 0.2
A549: 1.21 ± 0.2

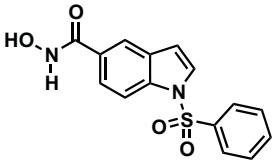

Hep3B: >10
MDA-MB-231: 5.68 ± 0.3
PC-3: 7.26 ± 0.6
A549: >10

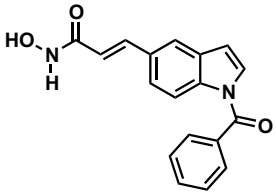

Hep3B: 2.40 ± 0.3
MDA-MB-231: 3.18 ± 0.4
PC-3: 2.32 ± 0.2
A549: 5.80 ± 0.8

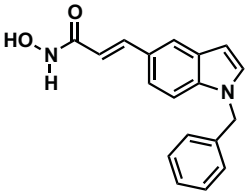

Hep3B: 0.86 ± 0.1
MDA-MB-231: 1.18 ± 0.2
PC-3: 1.23 ± 0.2
A549: 2.37 ± 0.1

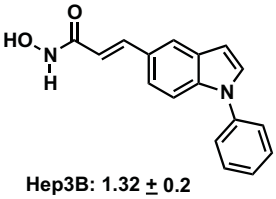

Hep3B: 1.32 ± 0.2
MDA-MB-231: 1.73 ± 0.1
PC-3: 1.54 ± 0.2
A549: 2.85 ± 0.8

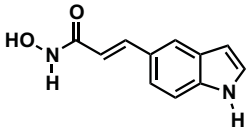

Hep3B: 3.65 ± 0.4
MDA-MB-231: 4.37 ± 0.5
PC-3: 4.80 ± 0.1
A549: 9.07 ± 0.9

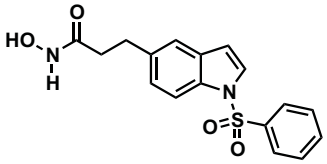

Hep3B: 2.56 ± 0.3
MDA-MB-231: 2.21 ± 0.4
PC-3: 2.07 ± 0.1
A549: 4.04 ± 0.2

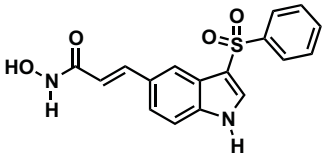

Hep3B: 1.27 ± 0.1
MDA-MB-231: 1.25 ± 0.1
PC-3: 1.26 ± 0.1
A549: 3.33 ± 0.2

Synthesis and Biological Evaluation of 1-Methyl-2-(3',4',5'-trimethoxybenzoyl)-3-aminoindoles as a New Class of Antimitotic Agents and Tubulin Inhibitors

Romeo Romagnoli, Pier Giovanni Baraldi, Taradas Sarkar, Maria Dora Carrion, Carlota Lopez Cara, Olga Cruz-Lopez, Delia Preti, Mojgan Aghazadeh Tabrizi, Manlio Tolomeo, Stefania Grimaudo, Antonella Di Cristina, Nicola Zonta, Jan Balzarini, Andrea Brancale, Hsing-Pang Hsieh, and Ernest Hamel

J. Med. Chem. 2008, 51, 1464–1468

L1210: murine leukemia-nM
FM3A: murine mammary-nM
Molt4/C8: human T-lymphocyte-nM
CEM: human T-lymphocyte-nM
tubulin: μM
colch-inbit: % inhibition

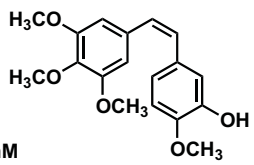

L1210: 2.8 ± 1.1
FM3A: 42 ± 6
Molt4/C8: 1.6 ± 1.4
CEM: 1.9 ± 1.6
tubulin: 1.2 ± 0.1
colch-inbit: 86 ± 3

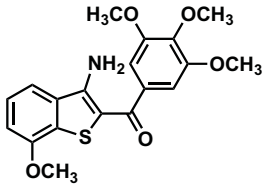

L1210: 33 ± 29
FM3A: 27 ± 13
Molt4/C8: 8.5 ± 1.4
CEM: 8.9 ± 2.0
tubulin: 2.1 ± 0.3
colch-inbit: 39 ± 1

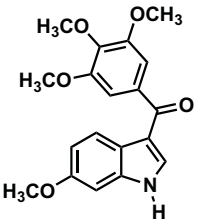

BPR0L075

L1210: 3.5 ± 1
FM3A: 3.7 ± 0.2
Molt4/C8: 3.4 ± 0.0
CEM: 3.6 ± 1
tubulin: 2.9 ± 0.1
colch-inbit: 84 ± 0.7

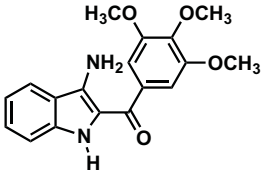

L1210: >10000
FM3A: >10000
Molt4/C8: >10000
CEM: >10000
tubulin: nd
colch-inbit: nd

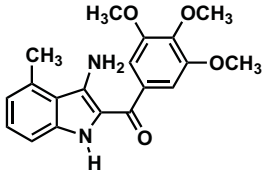

L1210: >10000
FM3A: >10000
Molt4/C8: >10000
CEM: >10000
tubulin: nd
colch-inbit: nd

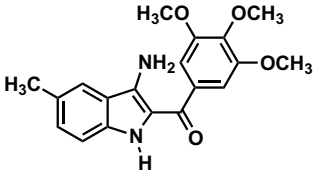

L1210: >10000
FM3A: >10000
Molt4/C8: >10000
CEM: >10000
tubulin: nd
colch-inbit: nd

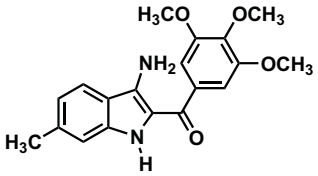

L1210: 3500 ± 150
FM3A: >10000
Molt4/C8: 1400 ± 80
CEM: 2600 ± 0
tubulin: nd
colch-inbit: nd

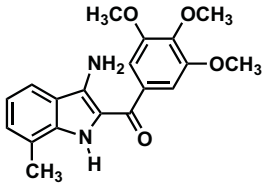

L1210: >10000
FM3A: >10000
Molt4/C8: >10000
CEM: >10000
tubulin: nd
colch-inbit: nd

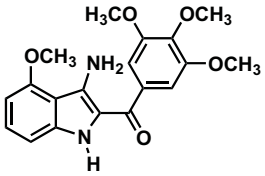

L1210: >10000
FM3A: >10000
Molt4/C8: >10000
CEM: >10000
tubulin: nd
colch-inbit: nd

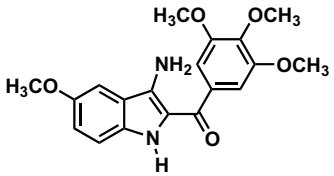

L1210: 9700 ± 0
FM3A: 9900 ± 30
Molt4/C8: 6900 ± 190
CEM: 8600 ± 30
tubulin: nd
colch-inbit: nd

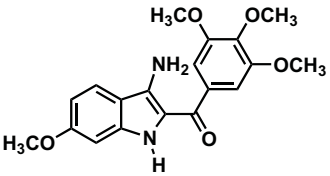

L1210: 970 ± 24
FM3A: 1600 ± 30
Molt4/C8: 630 ± 10
CEM: 320 ± 90
tubulin: >40
colch-inbit: nd

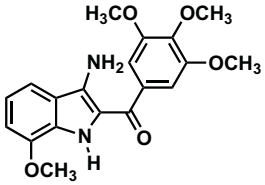

L1210: >10000
FM3A: >10000
Molt4/C8: 640 ± 260
CEM: 630 ± 10
tubulin: nd
colch-inbit: nd

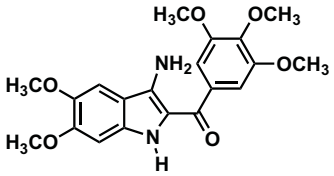

L1210: >10000
FM3A: >10000
Molt4/C8: 8600 ± 110
CEM: 9500 ± 0
tubulin: nd
colch-inbit: nd

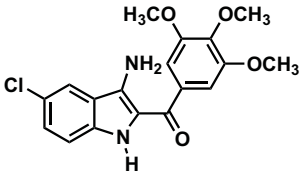

L1210: >10000
FM3A: >10000
Molt4/C8: >10000
CEM: >10000
tubulin: nd
colch-inbit: nd

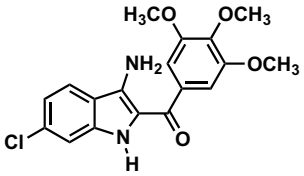

L1210: >10000
FM3A: >10000
Molt4/C8: 9200 ± 60
CEM: >10000
tubulin: nd
colch-inbit: nd

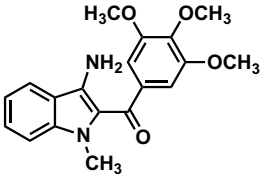

L1210: 8100 ± 37
FM3A: >10000
Molt4/C8: 2100 ± 0.0
CEM: 6800 ± 80
tubulin: nd
colch-inbit: nd

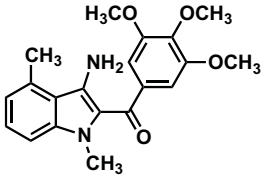

L1210: >10000
FM3A: >10000
Molt4/C8: >10000
CEM: >10000
tubulin: nd
colch-inbit: nd

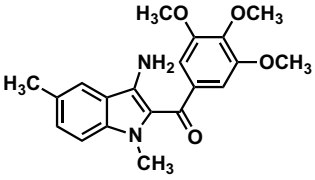

L1210: 1900 ± 300
FM3A: 1600 ± 200
Molt4/C8: 1700 ± 100
CEM: 1700 ± 200
tubulin: 10 ± 0.2
colch-inbit: nd

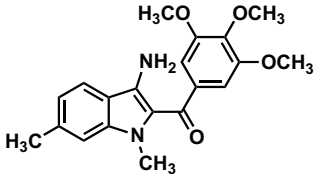

L1210: 1900 ± 150
FM3A: 1500 ± 90
Molt4/C8: 110 ± 30
CEM: 400 ± 110
tubulin: 6.4 ± 0.07
colch-inbit: nd

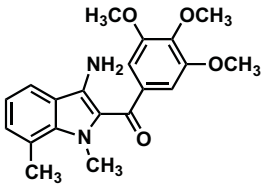

L1210: 1800 ± 120
FM3A: 1400 ± 110
Molt4/C8: 270 ± 90
CEM: 1200 ± 400
tubulin: 8.4 ± 0.1
colch-inbit: nd

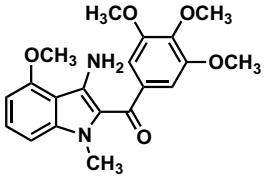

L1210: >10000
FM3A: >10000
Molt4/C8: >10000
CEM: >10000
tubulin: nd
colch-inbit: nd

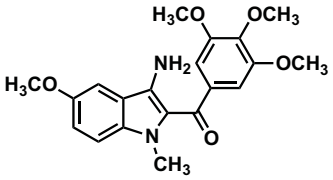

L1210: 4200 ± 110
FM3A: 5200 ± 90
Molt4/C8: 2100 ± 0
CEM: 3900 ± 100
tubulin: 15 ± 2
colch-inbit: nd

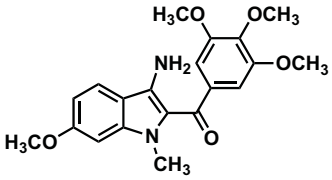

L1210: 69 ± 37
FM3A: 97 ± 3
Molt4/C8: 57 ± 7
CEM: 71 ± 5
tubulin: 4.6 ± 0.07
colch-inbit: 38 ± 5

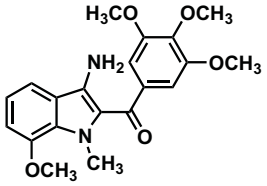

L1210: 15 ± 4
FM3A: 15 ± 0
Molt4/C8: 3.8 ± 0.6
CEM: 8.8 ± 1
tubulin: 1.4 ± 0.07
colch-inbit: 76 ± 5

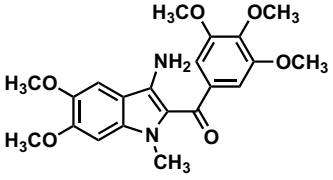

L1210: 5400 ± 270
FM3A: 5000 ± 430
Molt4/C8: 5000 ± 440
CEM: 5000 ± 260
tubulin: 18 ± 1
colch-inbit: nd

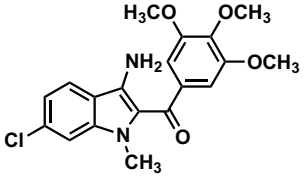

L1210: 1100 ± 60
FM3A: 970 ± 75
Molt4/C8: 480 ± 0
CEM: 1000 ± 60
tubulin: 7.1 ± 0.3
colch-inbit: nd

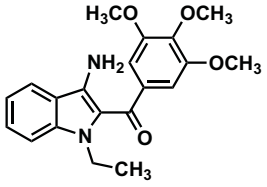

L1210: >10000
FM3A: >10000
Molt4/C8: >10000
CEM: >10000
tubulin: nd
colch-inbit: nd

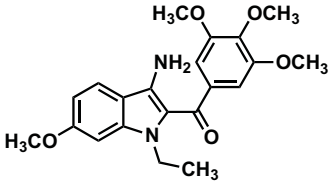

L1210: >10000
FM3A: >10000
Molt4/C8: >10000
CEM: >10000
tubulin: nd
colch-inbit: nd

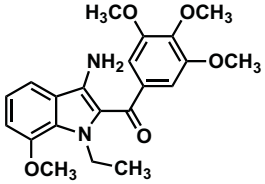

L1210: >10000
FM3A: >10000
Molt4/C8: 9100 ± 210
CEM: >10000
tubulin: nd
colch-inbit: nd

Synthesis and biological evaluation of new disubstituted analogues of 6-methoxy-3 (3,4,5-trimethoxybenzoyl)-1H-indole (BPR0L075), as potential antivascular agents

Nancy Ty, Grégory Dupeyre, Guy G. Chabot, Johanne Seguin, François Tillequin, Daniel Scherman, Sylvie Michel, Xavier Cachet

Bioorganic & Medicinal Chemistry 16 (2008) 7494–7503

ITP: IC_{50} tubulin inhibiton / IC_{50} colchicine
B16: melanoma (μM)

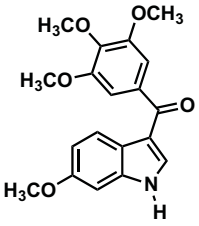

BPR0L075

ITP: 0.4
B16: 0.013 ± 0.004

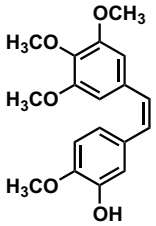

CA-4

ITP: 0.7
B16: 0.003 + 0.001

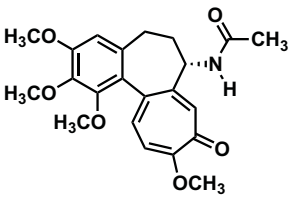

colchicine

ITP: 1.0
B16: 0.031 + 0.003

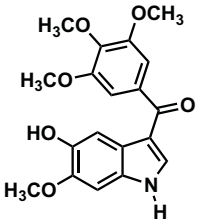

ITP: 31
B16: 12.18 + 5.06

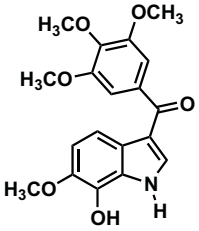

ITP: 1.3
B16: 0.24 + 0.14

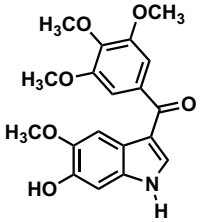

ITP: 12
B16: 5.07 + 0.91

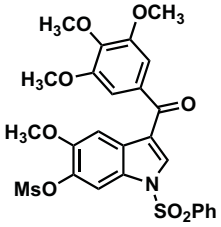

ITP: 18
B16: 3.14 + 2.17

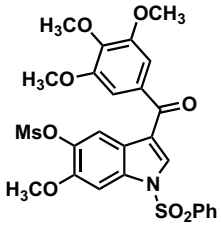

ITP: 15
B16: 3.29 + 1.15

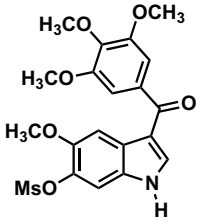

ITP: >40
B16: 32.42 + 2.24

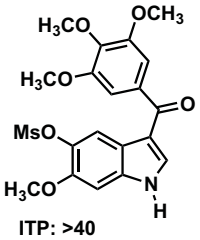

ITP: >40
B16: 13.67 + 1.40

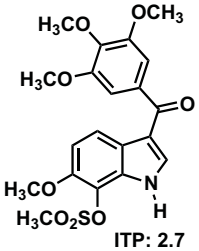

ITP: 2.7
B16: 0.17 + 0.05

SYNTHESIS AND PHARMACOLOGICAL ACTIVITY OF DIARYLINDOLE DERIVATIVES. CYTOTOXIC AGENTS BASED ON COMBRETASTATINS

Manuel Medarde, Angel C. Ramos, Esther Caballero, Rafael Pelaez-Lamamie de Clairac, Jose Luis Lopez, Dolores G Gravalos and Arturo San Feliciano

Bioorganic & Medicinal Chemistry Letters 9 (1999) 2303-2308

Log_{10} GI_{50}: cytostatic
Log_{10} LC_{50}: cytotoxic
HL-60: leukemia
RPMI-8226: leukemia
NCI-H522: non-small lung
COLO 205: colon
HTC-116: colon
SF-295: CNS
SF-539: CNS
SNB-19: CNS
SK-MEL-5: melanoma
OVCAR-3: ovarian

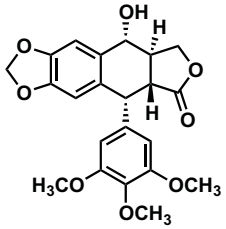

podophyllotoxin

Log_{10} IC_{50} = -7.22 M tubulin inhinition

P-388: 0.05 μM
A-549: 0.05 μM
HT-29: 0.05 μM
MEL-28: 0.06 μM

Log_{10} IC_{50} M
P-388: lymphoid neoplasm
A-549: human lung
HT-29: human colon
MEL-28: human melanoma

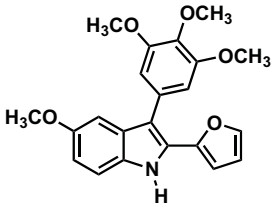

P-388: -6.15
A-549: -5.88
HT-29: -5.88
MEL-28: -5.88

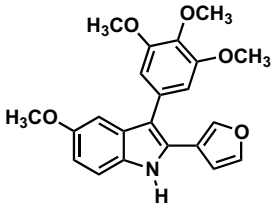

P-388: -5.49
A-549: -5.49
HT-29: -5.49
MEL-28: -5.49

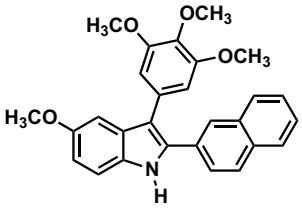

P-388: -5.95
A-549: -5.95
HT-29: -5.95
MEL-28: -5.95

Cell line: Log_{10} GI_{50} ; Log_{10} LC_{50}
HL-60: -7.29; >-4.0
RPMI-8226: -7.04; -4.12
NCI-H522: -7.12; -5.47
COLO 205: -6.73; -6.17
HTC-116: -6.86; -5.60
SF-295: -6.86; -4.63
SF-539: -6.93; -6.03
SNB-19: -7.64; -6.01
SK-MEL-5: -6.61; -4.54
OVCAR-3: -6.77; -5.14

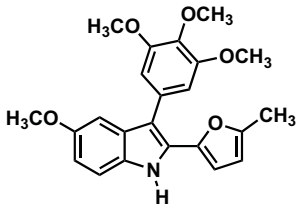

P-388: -5.29
A-549: -5.29
HT-29: -5.19
MEL-28: -5.29

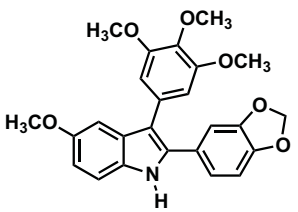

P-388: -5.64
A-549: -5.20
HT-29: -5.20
MEL-28: -5.20

Synthesis and structure–activity relationships of N-aryl(indol-3-yl)glyoxamides as antitumor agents

Pascal Marchand, Maud Antoine, Guillaume Le Baut, Michael Czech, Silke Baasner, Eckhard Günther

Bioorganic & Medicinal Chemistry 17 (2009) 6715–6727

Hela/KB: human cervix-nM
L1210: murine leukemia-nM
SKOV3: human ovarian-nM

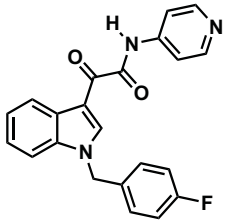

D-24241

Hela/KB: 54 ± 6
L1210: 455 ± 22
SKOV3: 455 ± 32

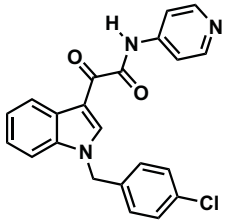

D-24851

Hela/KB: 44 ± 7
L1210: 44 ± 5
SKOV3: 77 ± 8

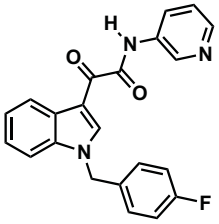

Hela/KB: 4687 ± 490
L1210: 4687 ± 520
SKOV3: 4687 ± 540

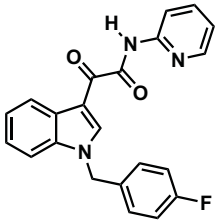

Hela/KB: >10000
L1210: 8302 ± 350
SKOV3: >10000

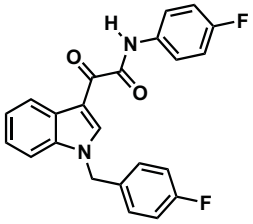

Hela/KB: 7941 ± 350
L1210: 4483 ± 310
SKOV3: >10000

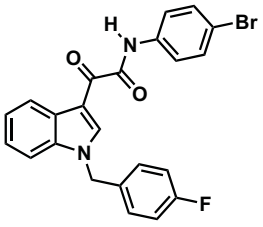

Hela/KB: 3878 ± 390
L1210: 3878 ± 410
SKOV3: 3878 ± 420

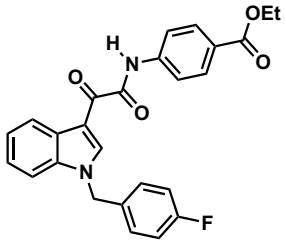

Hela/KB: 3937 ± 310
L1210: 3937 ± 360
SKOV3: 3937 ± 380

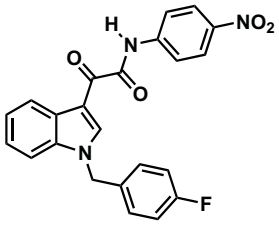

Hela/KB: >10000
L1210: >10000
SKOV3: >10000

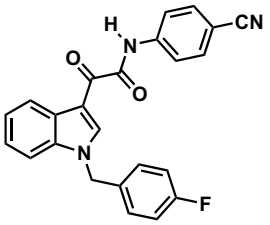

Hela/KB: >10000
L1210: >10000
SKOV3: >10000

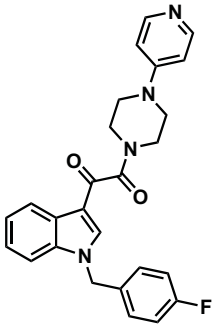

Hela/KB: >10000
L1210: 3955 ± 270
SKOV3: >10000

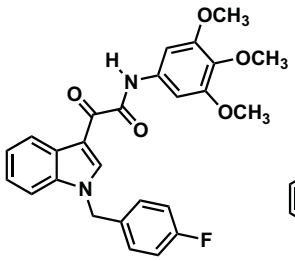

Hela/KB: 378 ± 31
L1210: 378 ± 42
SKOV3: 3784 ± 390

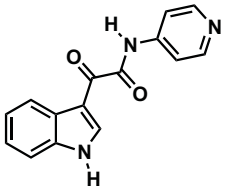

Hela/KB: >10000
L1210: >10000
SKOV3: >10000

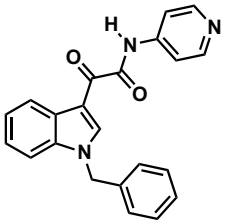

Hela/KB: 141 ± 15
L1210: 253 ± 34
SKOV3: 4924 ± 390

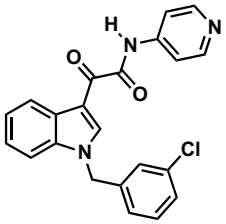

Hela/KB: 4489 ± 290
L1210: 4489 ± 310
SKOV3: 4489 ± 350

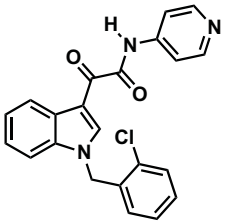

Hela/KB: 4489 ± 340
L1210: 4489 ± 350
SKOV3: 6618 ± 590

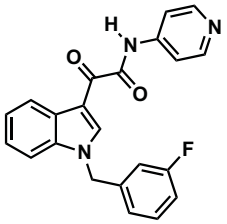

Hela/KB: 469 ± 26
L1210: 469 ± 31
SKOV3: 469 ± 37

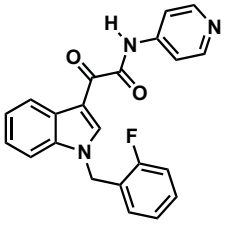

Hela/KB: 4687 ± 320
L1210: 3687 ± 340
SKOV3: >10000

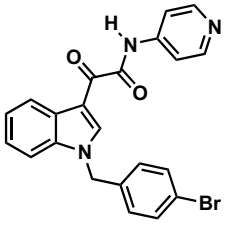

Hela/KB: 403 ± 22
L1210: 403 ± 27
SKOV3: 403 ± 34

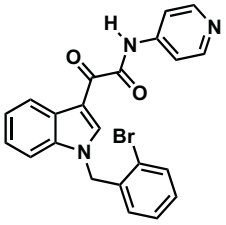

Hela/KB: 4029 ± 310
L1210: >10000
SKOV3: >10000

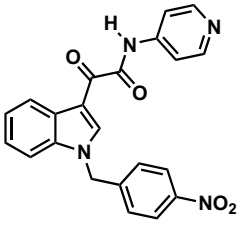

Hela/KB: >10000
L1210: >10000
SKOV3: >10000

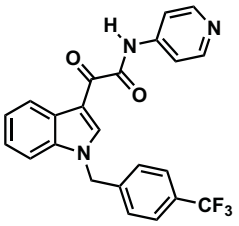

Hela/KB: 7464 ± 610
L1210: 7464 ± 650
SKOV3: 7464 ± 670

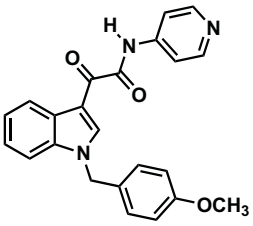

Hela/KB: 4541 ± 310
L1210: 454 ± 36
SKOV3: 4541 ± 340

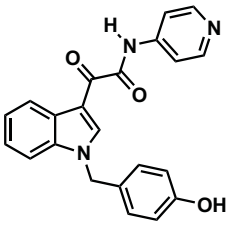

Hela/KB: >10000
L1210: >10000
SKOV3: >10000

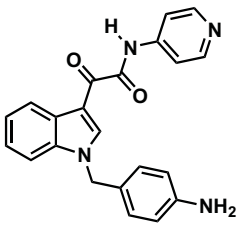

Hela/KB: >10000
L1210: 3510 ± 190
SKOV3: >10000

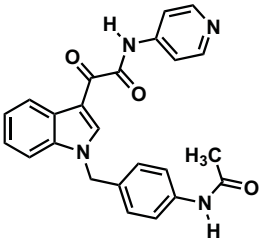

Hela/KB: >10000
L1210: >10000
SKOV3: >10000

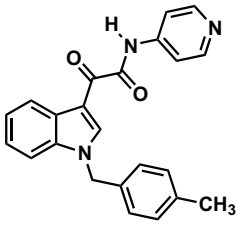

Hela/KB: 474 ± 42
L1210: 474 ± 48
SKOV3: 471 ± 54

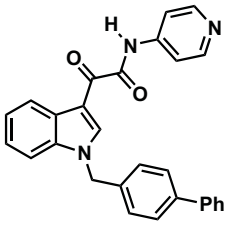

Hela/KB: >10000
L1210: >10000
SKOV3: >10000

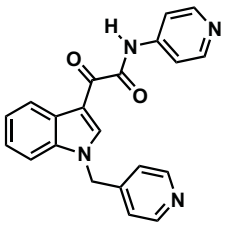

Hela/KB: >10000
L1210: 6580 ± 560
SKOV3: >10000

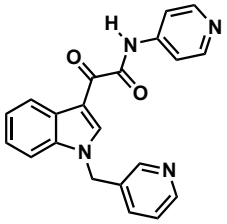

Hela/KB: >10000
L1210: 4910 ± 430
SKOV3: >10000

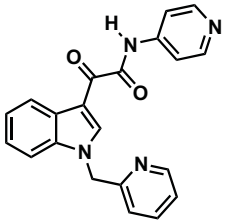

Hela/KB: 4910 ± 460
L1210: >10000
SKOV3: >10000

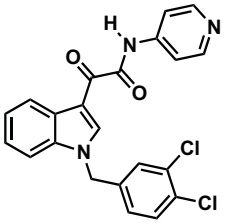

Hela/KB: >10000
L1210: >10000
SKOV3: >10000

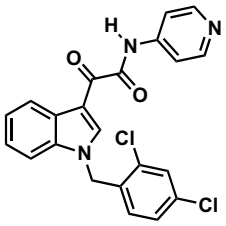

Hela/KB: 7448 ± 670
L1210: 7448 ± 680
SKOV3: 7448 ± 690

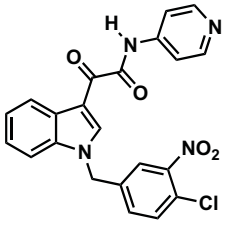

Hela/KB: 39 ± 4
L1210: 51 ± 8
SKOV3: 11 ± 2

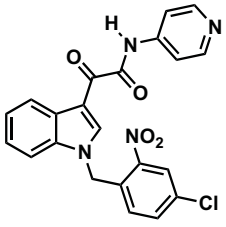

Hela/KB: >10000
L1210: >10000
SKOV3: >10000

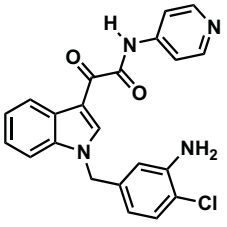

Hela/KB: 701 ± 55
L1210: 706 ± 64
SKOV3: 1213 ± 120

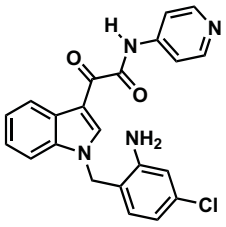

Hela/KB: 462 ± 47
L1210: 574 ± 52
SKOV3: 338 ± 34

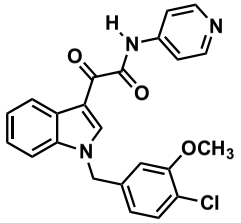

Hela/KB: 3132 ± 160
L1210: 6145 ± 510
SKOV3: 2451 ± 260

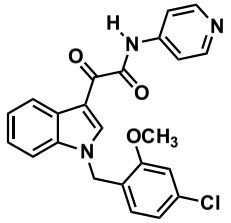

Hela/KB: 4023 ± 440
L1210: 6154 ± 580
SKOV3: 5340 ± 510

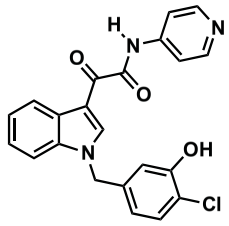

Hela/KB: 729 ± 97
L1210: >10000
SKOV3: 6111 ± 580

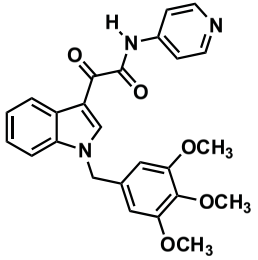

Hela/KB: >10000
L1210: >10000
SKOV3: >10000

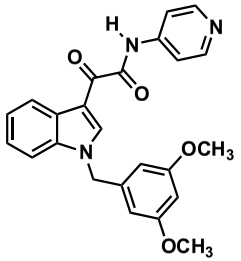

Hela/KB: >10000
L1210: >10000
SKOV3: >10000

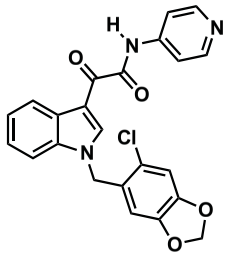

Hela/KB: 7284 ± 650
L1210: 7284 ± 670
SKOV3: 7284 ± 690

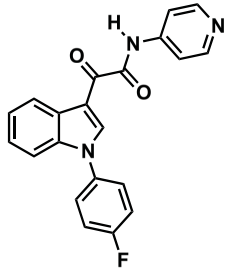

Hela/KB: >10000
L1210: >10000
SKOV3: >10000

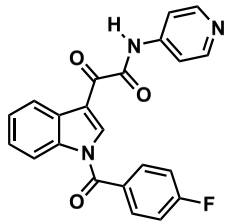

Hela/KB: >10000
L1210: >10000
SKOV3: >10000

Synthetic 2-Aroylindole Derivatives as a New Class of Potent Tubulin-Inhibitory, Antimitotic Agents

Siavosh Mahboobi, Herwig Pongratz, Harald Hufsky, Jorg Hockemeyer, Markus Frieser, Alexei Lyssenko, Dietrich H. Paper, Jutta Burgermeister, Frank-D. Bohmer, Heinz-Herbert Fiebig, Angelika M. Burger, Silke Baasner, and Thomas Beckers

J. Med. Chem. 2001, 44, 4535-4553

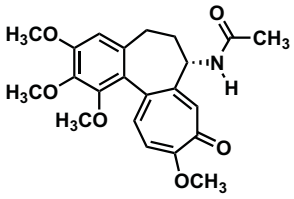

HeLa/KB: 0.023
SK-OV-3: 0.020

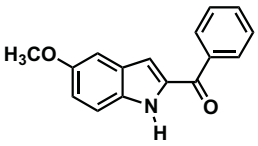

ITP: 0.53
HeLa/KB: 0.068
SK-OV-3: 0.68

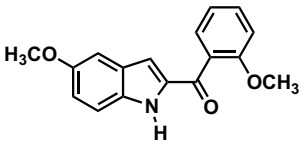

ITP: 1.29
HeLa/KB: 0.036
SK-OV-3: 0.11

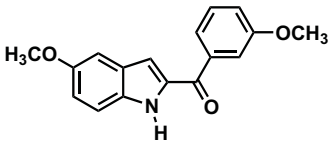

ITP: 0.53
HeLa/KB: 0.011
SK-OV-3: 0.011

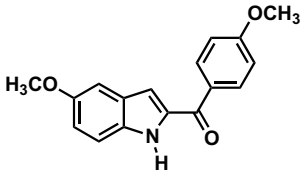

ITP: no effect
HeLa/KB: 11.4
SK-OV-3: 11.4

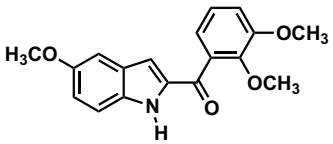

ITP: >10
HeLa/KB: 6.4
SK-OV-3: 3.2

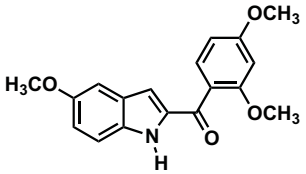

ITP: 5.6
HeLa/KB: 0.10
SK-OV-3: 1.03

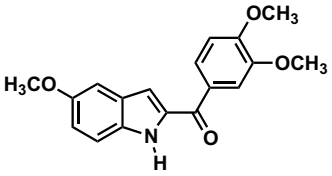

ITP: 0.81
HeLa/KB: 1.32
SK-OV-3: 1.64

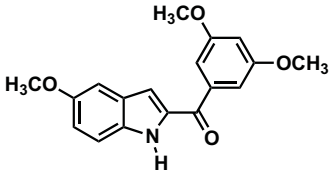

ITP: 0.81
HeLa/KB: 0.019
SK-OV-3: 0.019

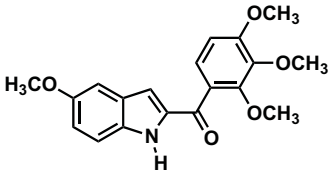

ITP: ≥10
HeLa/KB: 0.059
SK-OV-3: 0.088

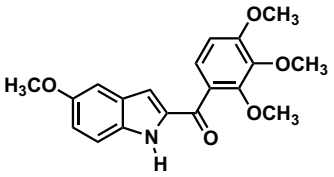

ITP: ≥ 10
HeLa/KB: 0.059
SK-OV-3: 0.088

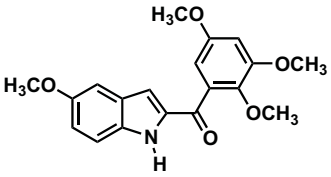

ITP: no effect
HeLa/KB: 8.79
SK-OV-3: 9.37

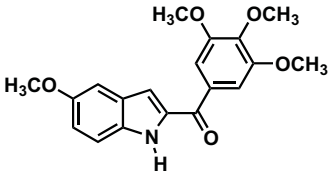

ITP: 0.99
HeLa/KB: 0.029
SK-OV-3: 0.058

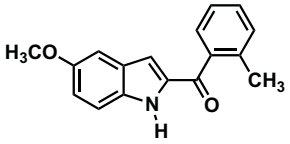

ITP: 4.8
HeLa/KB: 1.21
SK-OV-3: 0.38

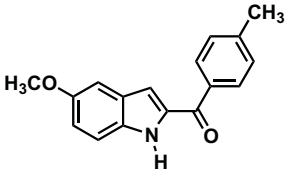

ITP: 1.5
HeLa/KB: 0.38
SK-OV-3: 1.88

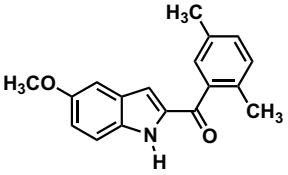

ITP: 5.2
HeLa/KB: 0.72
SK-OV-3: 0.72

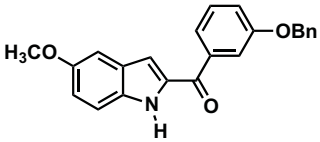

ITP: no effect
HeLa/KB: >8.6
SK-OV-3: >8.6

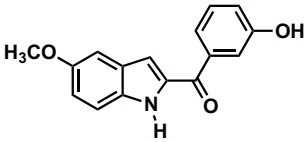

ITP: 0.66
HeLa/KB: 0.22
SK-OV-3: 0.22

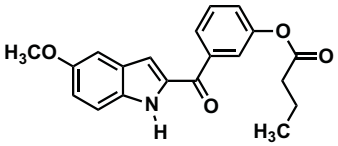

ITP: 0.85
HeLa/KB: 0.27
SK-OV-3: 0.24

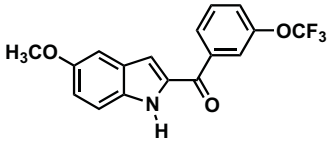

ITP: 1.7
HeLa/KB: 0.27
SK-OV-3: 0.21

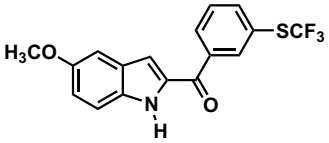

ITP: 1.29
HeLa/KB: 0.036
SK-OV-3: 0.11

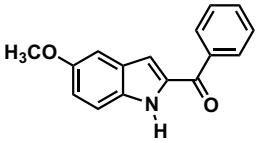

ITP: ≥ 10
HeLa/KB: 0.88
SK-OV-3: 0.63

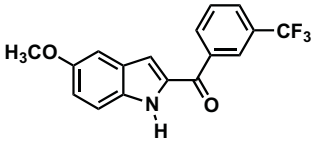

ITP: 1.5
HeLa/KB: 0.03
SK-OV-3: 0.03

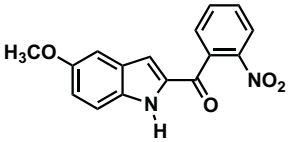

ITP: >10
HeLa/KB: >10.8
SK-OV-3: >10.8

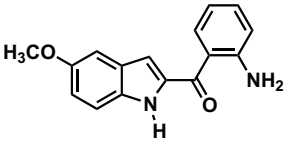

ITP: 6.7
HeLa/KB: 3.76
SK-OV-3: 3.76

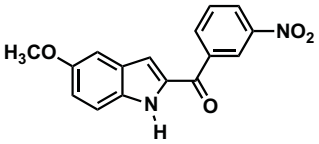

ITP: 0.85
HeLa/KB: 0.10
SK-OV-3: 0.10

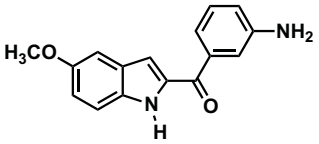

ITP: 0.99
HeLa/KB: 0.34
SK-OV-3: 0.23

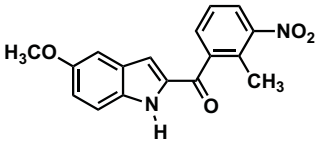

ITP: >10
HeLa/KB: >10.3
SK-OV-3: >10.3

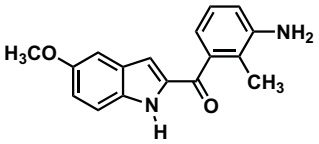

ITP: >10
HeLa/KB: 11.4
SK-OV-3: 11.4

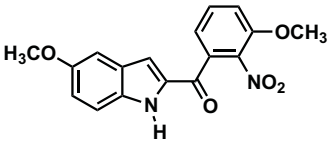

ITP: >10
HeLa/KB: >9.8
SK-OV-3: >9.8

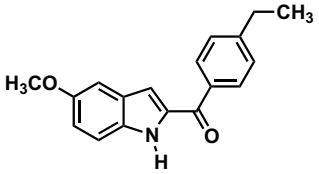

ITP: ≥ 10
HeLa/KB: 8.9
SK-OV-3: 11.5

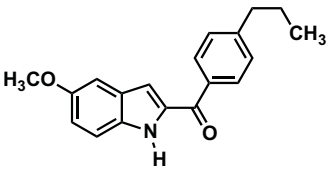

ITP: >10
HeLa/KB: >10.9
SK-OV-3: >10.9

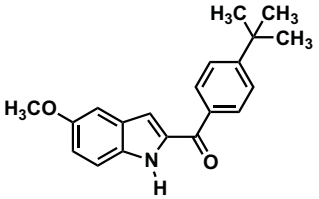

ITP: no effect
HeLa/KB: >10.4
SK-OV-3: >10.4

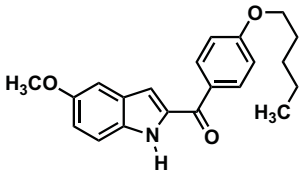

ITP: no effect
HeLa/KB: >9.5
SK-OV-3: >9.5

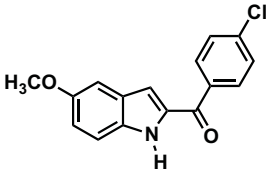

ITP: 5.0
HeLa/KB: 3.50
SK-OV-3: 1.75

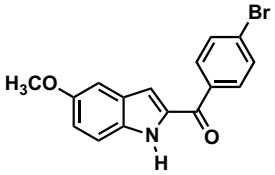

ITP: 4.3
HeLa/KB: 0.91
SK-OV-3: 0.91

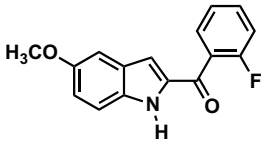

ITP: 1.0
HeLa/KB: 0.37
SK-OV-3: 0.74

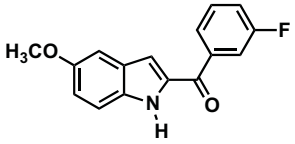

ITP: 0.39
HeLa/KB: 0.026
SK-OV-3: 0.015

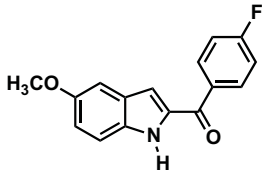

ITP: not determined
HeLa/KB: 5.57
SK-OV-3: 7.43

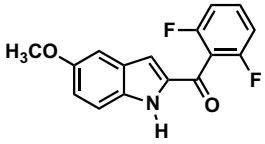

ITP: no effect
HeLa/KB: 6.96
SK-OV-3: 8.70

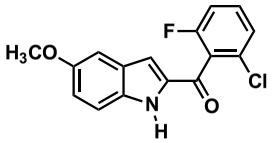

ITP: >10
HeLa/KB: >10.5
SK-OV-3: >10.5

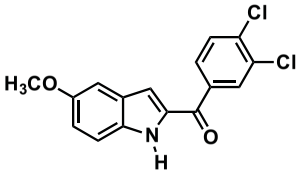

ITP: 2.5
HeLa/KB: 0.10
SK-OV-3: 0.10

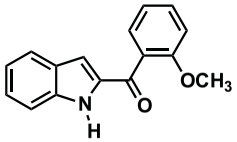

ITP: >10
HeLa/KB: >12.7
SK-OV-3: >12.7

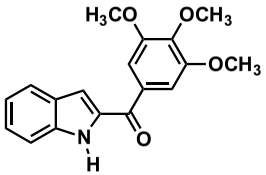

ITP: no effect
HeLa/KB: 6.42
SK-OV-3: 9.64

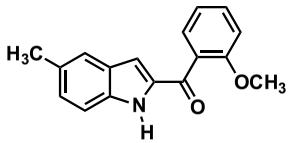

ITP: 3.5
HeLa/KB: 0.38
SK-OV-3: 0.75

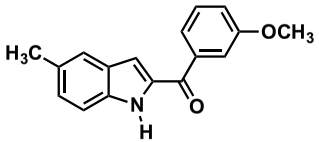

ITP: >10
HeLa/KB: >12.1
SK-OV-3: >12.1

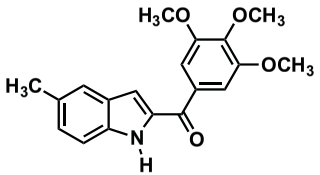

ITP: 0.86
HeLa/KB: 0.03
SK-OV-3: 0.03

Tandem Heck–Suzuki–Miyaura reaction: Application to the synthesis of constrained analogues of combretastatin A-4

Martin Arthuis, Rene´e Pontikis and Jean-Claude Florent

Tetrahedron Letters 48 (2007) 6397–6400

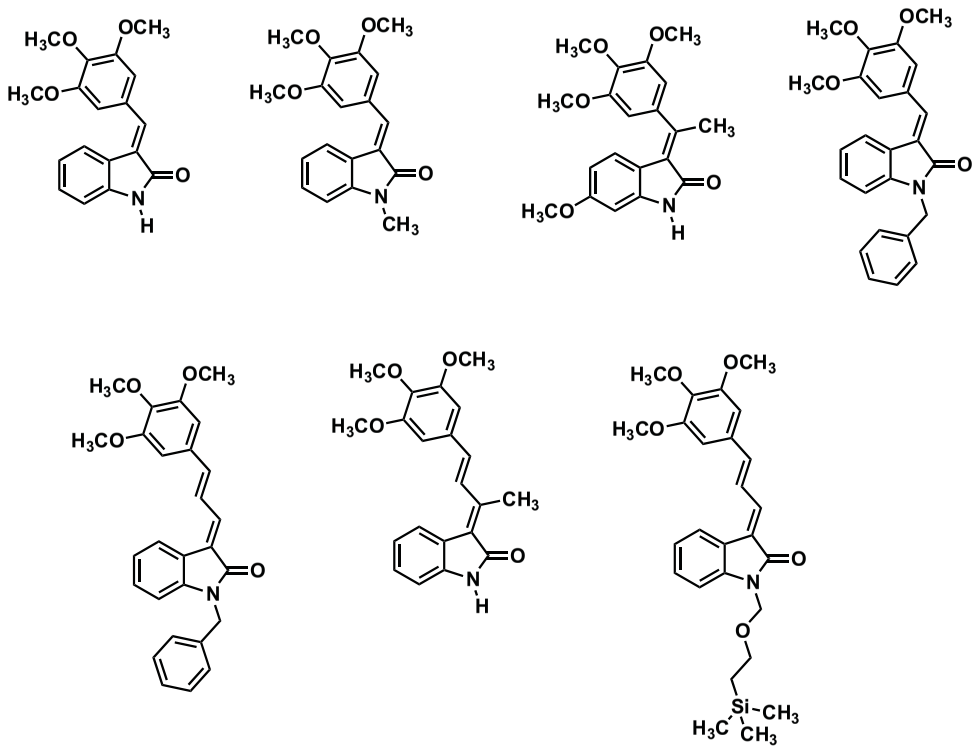

APPENDIX B

Supporting Information: Synthesis of a 2-Aryl-3-Aroyl-Indole Salt (OXi8007) Resembling Combretastatin A-4 with Application as a Vascular Disrupting Agent

This appendix published as supporting information: Hadimani, M. B.; MacDonough, M. T.; Strecker, T. E.; Lopez, R.; Sriram, M.; Nguyen, B. L.; Kessler, R. J.; Ghatak, A.; Shirali, A. R.; Liu, L.; Garner, C. M.; Pettie, G. R.; Hamel, E.; Chaplin, D. J.; Mason, R. P.; Trawick, M. L.; Pinney, K. G. Synthesis of a 2-Aryl-3-Aroyl-Indole Salt (OXi8007) Resembling Combretastatin A-4 with Application as a Vascular Disrupting Agent. *J. Nat. Prod.* **2013**, http://dx.doi.org/10.1021/np400374w.

The author M. T. MacDonough contributed to this manuscript through the synthesis of two of the final four compounds including full characterization analysis of both in addition to the synthesis and characterization of two key intermediates en route to the other two final compounds. Furthermore, M. T. MacDonough played a significant role in the preparation of the manuscript including writing and editing.

Supporting Information

Synthesis of a 2-Aryl-3-Aroyl-Indole Salt (OXi8007) Resembling Combretastatin A-4 with Application as a Vascular Disrupting Agent

Mallinath B. Hadimani,[†] Matthew T. MacDonough,[†] Tracy E. Strecker,[†] Ramona Lopez,[‡] Madhavi Sriram,[†] Benson L. Nguyen,[†] Raymond J. Kessler,[†] Anjan Ghatak,[†▽] Anupama R. Shirali,[†] Li Liu, [‡] Charles M. Garner,[†] George R. Pettit,[§] Ernest Hamel,[⊥] David J. Chaplin,[‖] Ralph P. Mason,[‡] Mary Lynn Trawick,[†] and Kevin G. Pinney[†]*

[†] Department of Chemistry and Biochemistry, Baylor University, One Bear Place #97348, Waco, Texas, 76798-7348, USA

[‡] Department of Radiology, The University of Texas Southwestern Medical Center, 5323 Harry Hines Boulevard, Dallas, Texas, 75390-9058, USA

[§] Department of Chemistry and Biochemistry, Arizona State University, Tempe, Arizona, 85287-1604, USA

[⊥] Screening Technologies Branch, Developmental Therapeutics Program, Division of Cancer Treatment and Diagnosis, National Caner Institute, Frederick National Laboratory for Cancer Research, National Institutes of Health, Frederick, Maryland, 21702, USA

[‖] Oxigene Inc., 701 Gateway Boulevard, Suite 210, South San Francisco, California, 94080, USA

[▽] Dedicated to the memory of Dr. Anjan Ghatak, who passed away on July 22, 2003

[*]Corresponding Author: Kevin G. Pinney
Telephone: 1-254-710-4117
Fax: 1-254-710-4272
Email: Kevin_Pinney@baylor.edu

Table of Contents

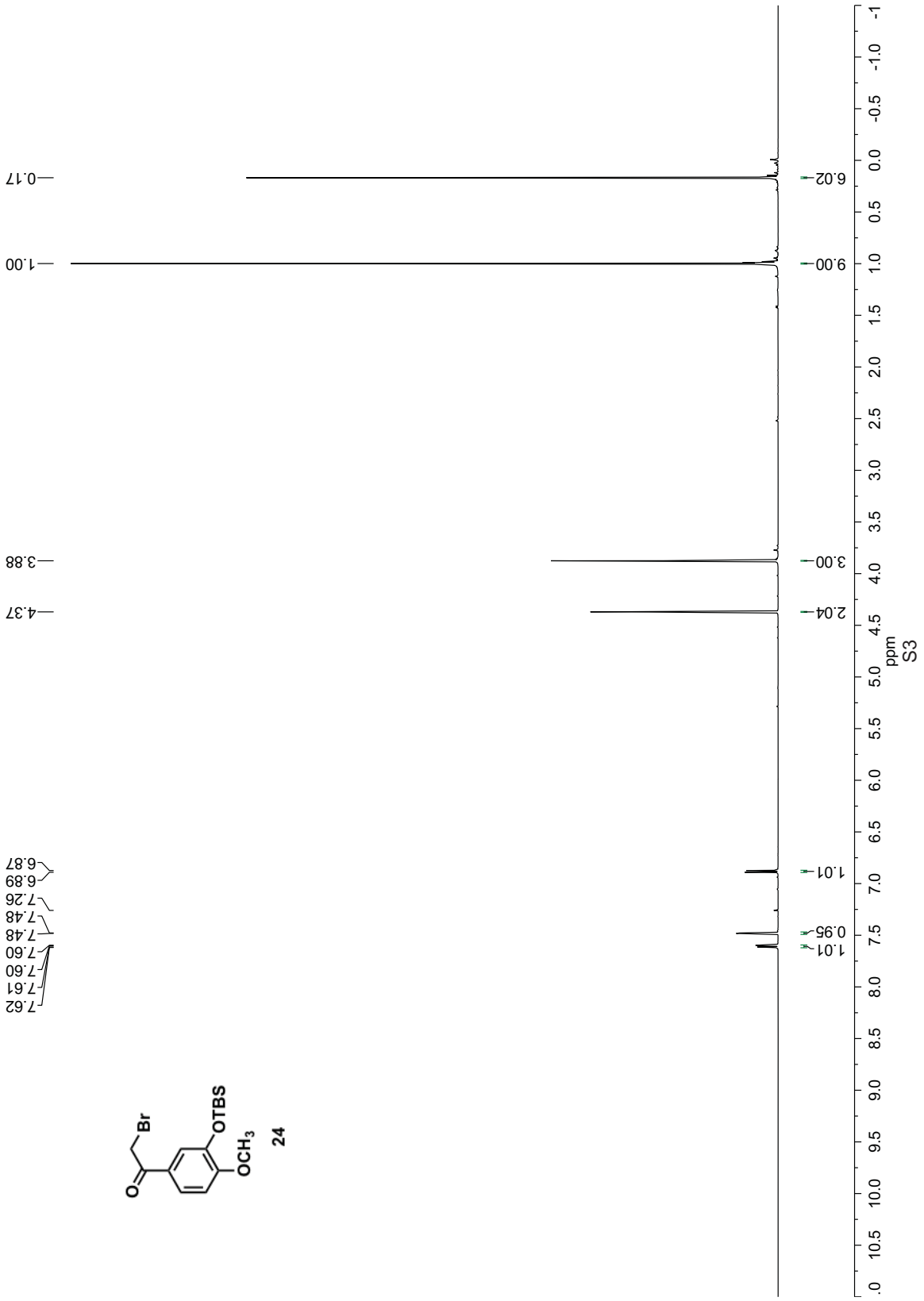
Br
O
OTBS
OCH3
24
7.62
7.61
7.60
7.60
7.48
7.48
7.26
6.89
6.87
4.37
3.88
1.00
0.17
1.01
0.95
1.01
2.04
3.00
9.00
6.02
ppm
S3

190.01
156.21
145.23
127.22
124.34
121.19
111.12
77.41
77.16
76.91
55.67
30.86
25.78
18.55
-4.49
Br
O
OTBS
OCH3
24
ppm
S4

Data File C:\CHEM32\1\DATA\MATT MAC\BROMO-2000006.D
Sample Name: run1

HPLC traces of compound **24**

```
==========================================================================
Acq. Operator   : Matt Mac
Acq. Instrument : Instrument 1                    Location :   -
Injection Date  : 4/19/2013 2:40:41 PM
Acq. Method     : C:\CHEM32\1\METHODS\MASTERMETHOD.M
Last changed    : 4/19/2013 2:38:56 PM by Matt Mac
Analysis Method : C:\CHEM32\1\DATA\MATT MAC\BROMO-2000006.D\DA.M (MASTERMETHOD.M)
Last changed    : 4/19/2013 4:40:04 PM by Matt Mac
```

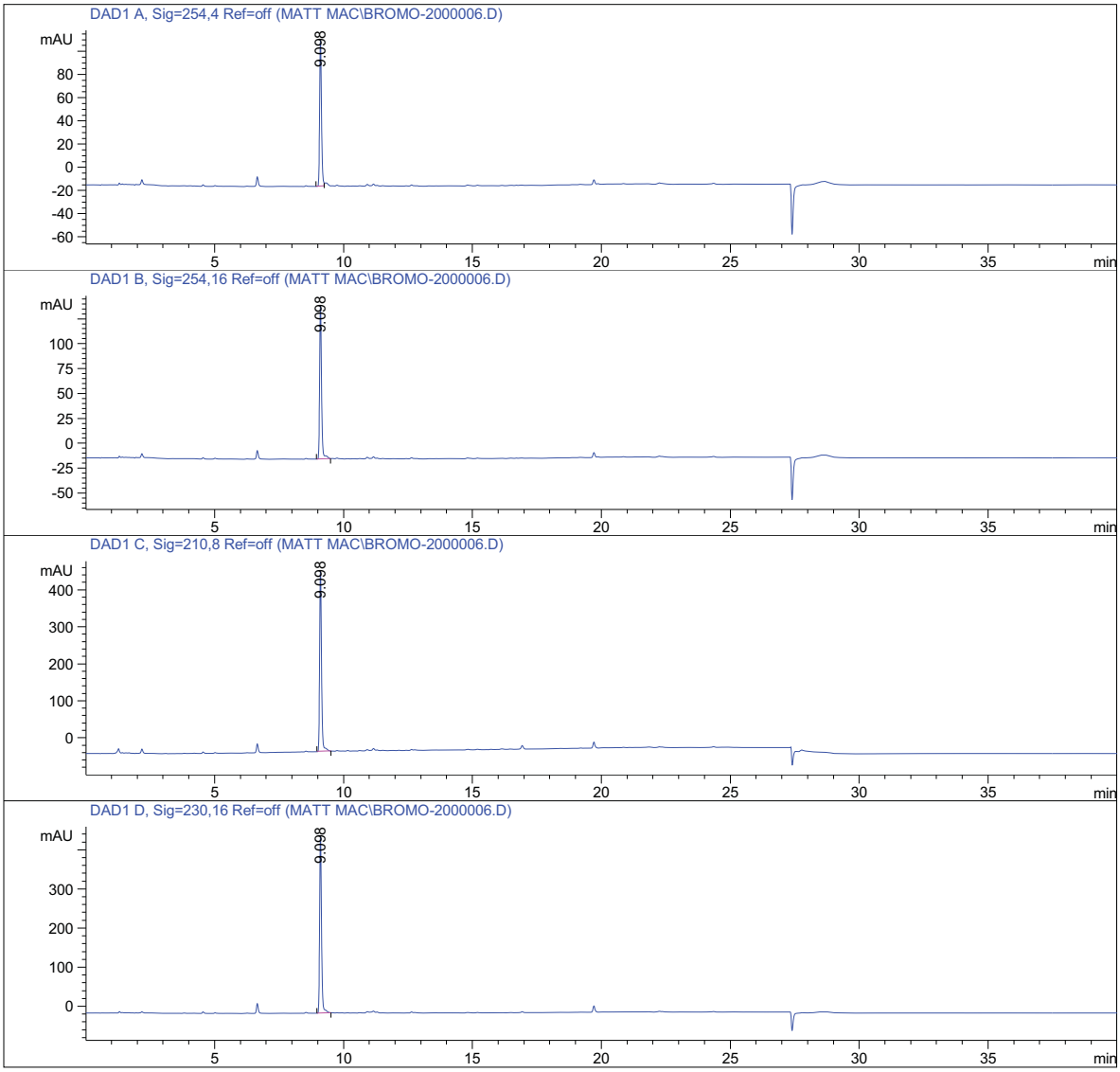

Data File C:\CHEM32\1\DATA\MATT MAC\BROMO-2000006.D
Sample Name: run1

HPLC traces of compound **24**

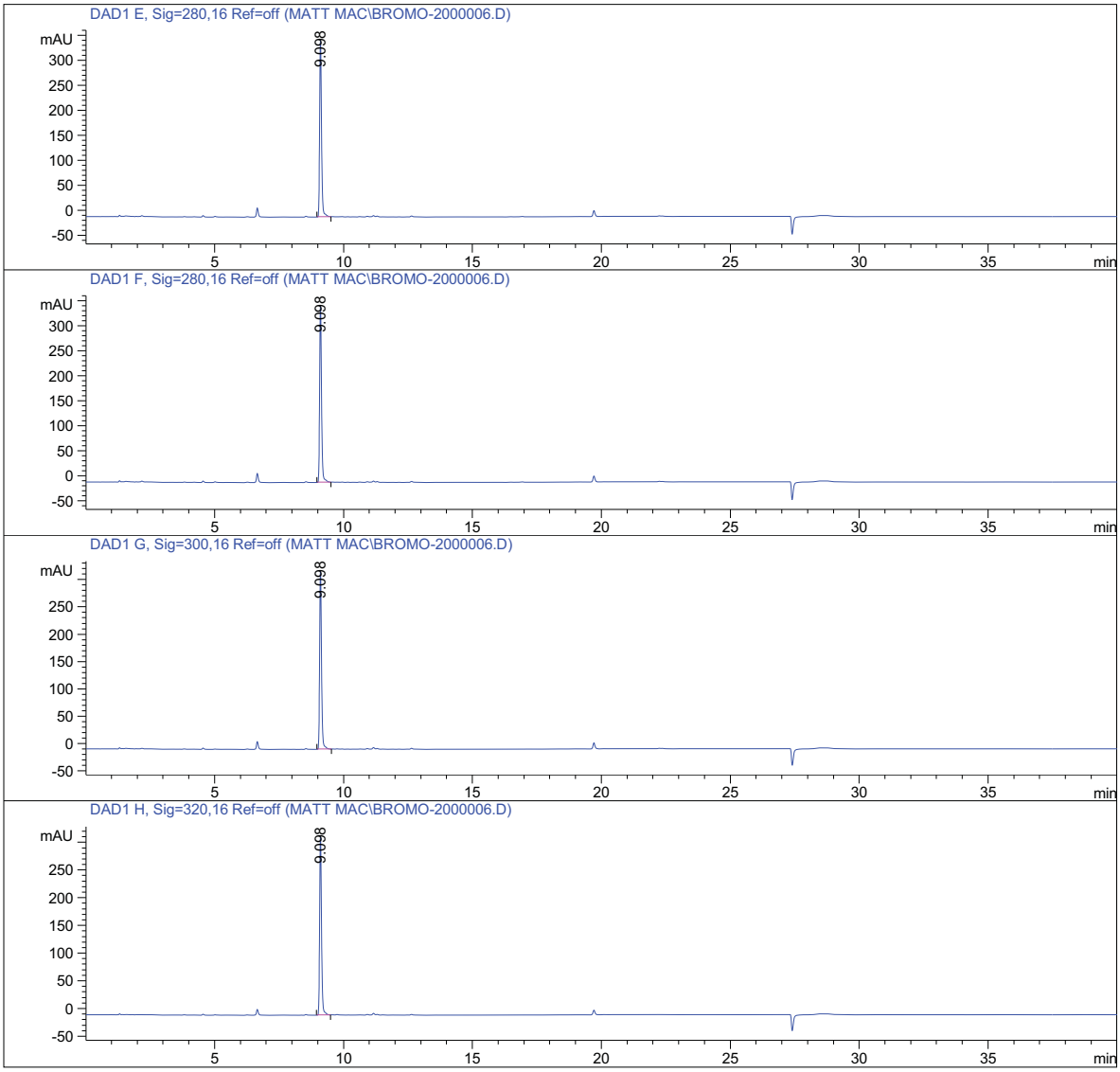

==========

Area Percent Report

==========

Sorted By : Signal
Multiplier : 1.0000
Dilution : 1.0000
Use Multiplier & Dilution Factor with ISTDs

Instrument 1 4/19/2013 4:59:48 PM Matt Mac

Data File C:\CHEM32\1\DATA\MATT MAC\BROMO-2000006.D
Sample Name: run1

HPLC traces of compound **24**

Signal 1: DAD1 A, Sig=254,4 Ref=off

Peak #	RetTime [min]	Type	Width [min]	Area [mAU*s]	Height [mAU]	Area %
1	9.098	BV	0.0764	631.17712	126.04517	100.0000
Totals :				631.17712	126.04517	

Signal 2: DAD1 B, Sig=254,16 Ref=off

Peak #	RetTime [min]	Type	Width [min]	Area [mAU*s]	Height [mAU]	Area %
1	9.098	BB	0.0782	795.44574	154.09218	100.0000
Totals :				795.44574	154.09218	

Signal 3: DAD1 C, Sig=210,8 Ref=off

Peak #	RetTime [min]	Type	Width [min]	Area [mAU*s]	Height [mAU]	Area %
1	9.098	BB	0.0779	2506.93262	488.09872	100.0000
Totals :				2506.93262	488.09872	

Signal 4: DAD1 D, Sig=230,16 Ref=off

Peak #	RetTime [min]	Type	Width [min]	Area [mAU*s]	Height [mAU]	Area %
1	9.098	BB	0.0777	2310.07349	451.59116	100.0000
Totals :				2310.07349	451.59116	

Signal 5: DAD1 E, Sig=280,16 Ref=off

Peak #	RetTime [min]	Type	Width [min]	Area [mAU*s]	Height [mAU]	Area %
1	9.098	BB	0.0774	1806.34863	354.52115	100.0000
Totals :				1806.34863	354.52115	

Data File C:\CHEM32\1\DATA\MATT MAC\BROMO-2000006.D
Sample Name: run1

HPLC traces of compound **24**

Signal 6: DAD1 F, Sig=280,16 Ref=off

Peak #	RetTime [min]	Type	Width [min]	Area [mAU*s]	Height [mAU]	Area %
1	9.098	BB	0.0774	1806.34863	354.52115	100.0000
Totals :				1806.34863	354.52115	

Signal 7: DAD1 G, Sig=300,16 Ref=off

Peak #	RetTime [min]	Type	Width [min]	Area [mAU*s]	Height [mAU]	Area %
1	9.098	BB	0.0773	1658.41321	326.37286	100.0000
Totals :				1658.41321	326.37286	

Signal 8: DAD1 H, Sig=320,16 Ref=off

Peak #	RetTime [min]	Type	Width [min]	Area [mAU*s]	Height [mAU]	Area %
1	9.098	BB	0.0773	1638.77759	322.66156	100.0000
Totals :				1638.77759	322.66156	

*** End of Report ***

HRMS of compound **24**

bromoacetophenone_130417210932 4/17/2013 9:26:32 PM bromoacetophenone

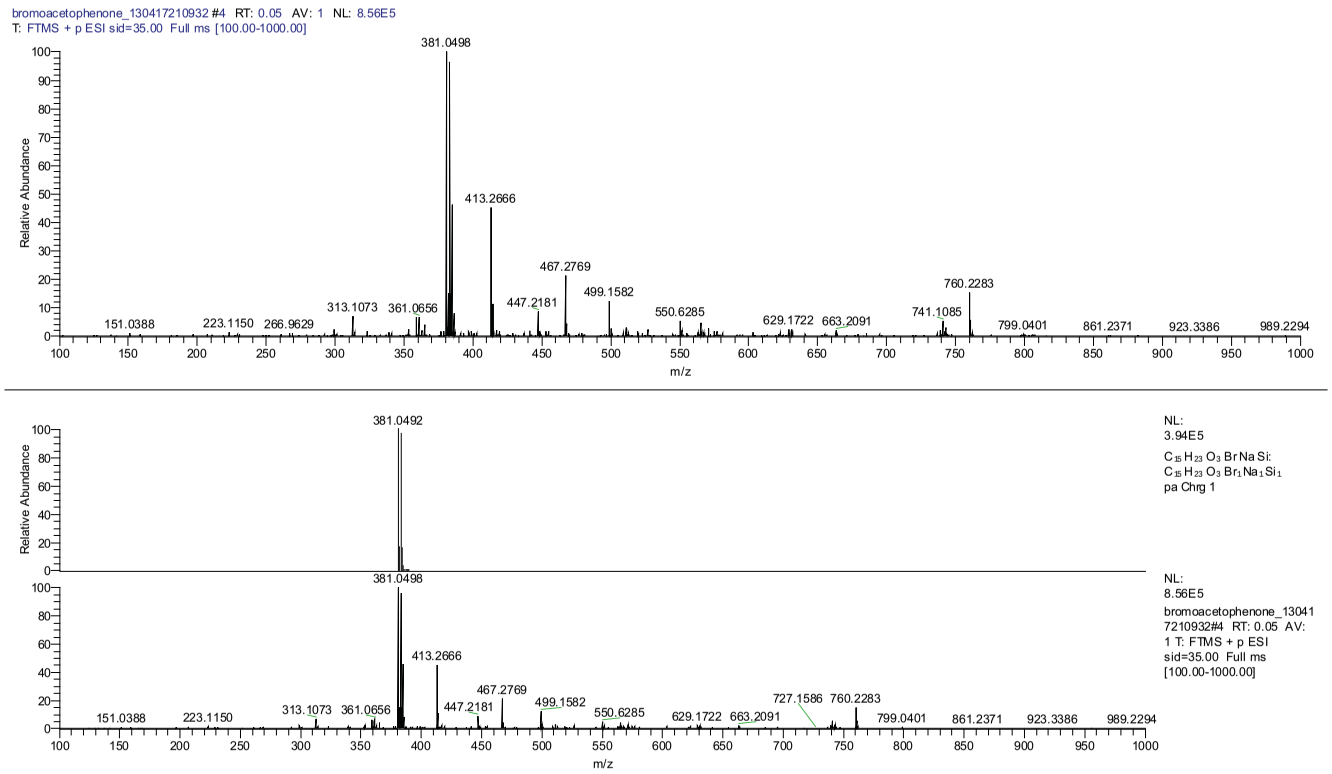

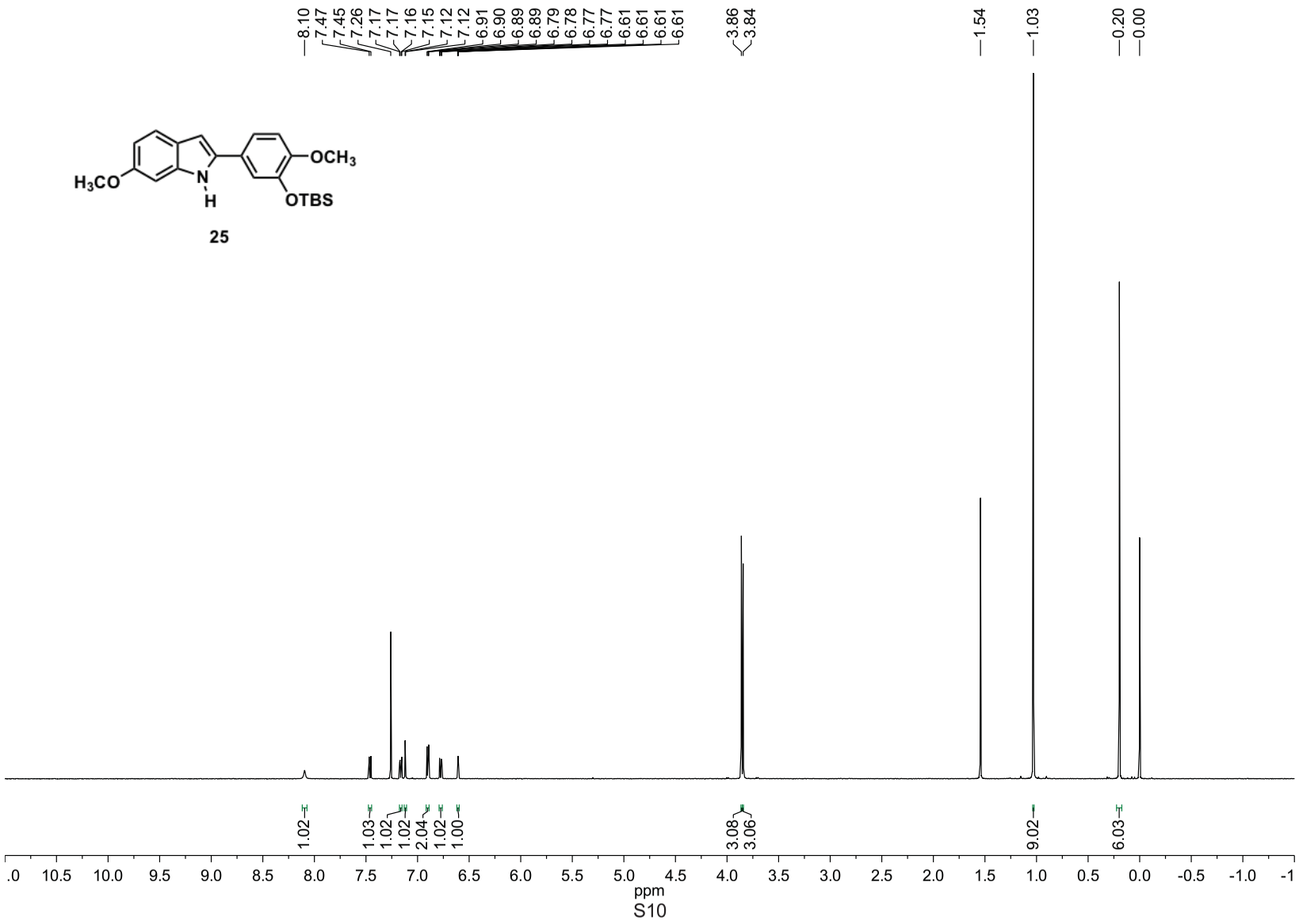
8.10
7.47
7.45
7.26
7.17
7.17
7.16
7.15
7.12
7.12
6.91
6.90
6.89
6.89
6.79
6.78
6.77
6.77
6.61
6.61
6.61
6.61
3.86
3.84
1.54
1.03
0.20
0.00
H3CO
N
H
OCH3
OTBS
25
1.02
1.03
1.02
1.02
2.04
1.02
1.00
3.08
3.06
9.02
6.03
.0 10.5 10.0 9.5 9.0 8.5 8.0 7.5 7.0 6.5 6.0 5.5 5.0 4.5 4.0 3.5 3.0 2.5 2.0 1.5 1.0 0.5 0.0 -0.5 -1.0 -1
ppm

OCH3
OTBS
H3CO
N
H
25
156.37
150.62
145.44
137.58
137.03
125.87
123.83
120.96
118.29
117.93
112.47
110.06
98.69
94.70
77.41
77.16
76.91
55.70
55.53
25.88
18.60
-4.45
ppm
S11

Data File C:\CHEM32\1\DATA\MATT MAC\TBS-INDOLE00016.D
Sample Name: run1

HPLC traces of compound **25**

```
==========================================================================
Acq. Operator   : Matt Mac
Acq. Instrument : Instrument 1                    Location :   -
Injection Date  : 4/23/2013 12:56:40 PM
Acq. Method     : C:\CHEM32\1\METHODS\MASTERMETHOD.M
Last changed    : 4/23/2013 12:54:20 PM by Matt Mac
Analysis Method : C:\CHEM32\1\DATA\MATT MAC\TBS-INDOLE00016.D\DA.M (MASTERMETHOD.M)
Last changed    : 4/23/2013 1:46:54 PM by Matt Mac
```

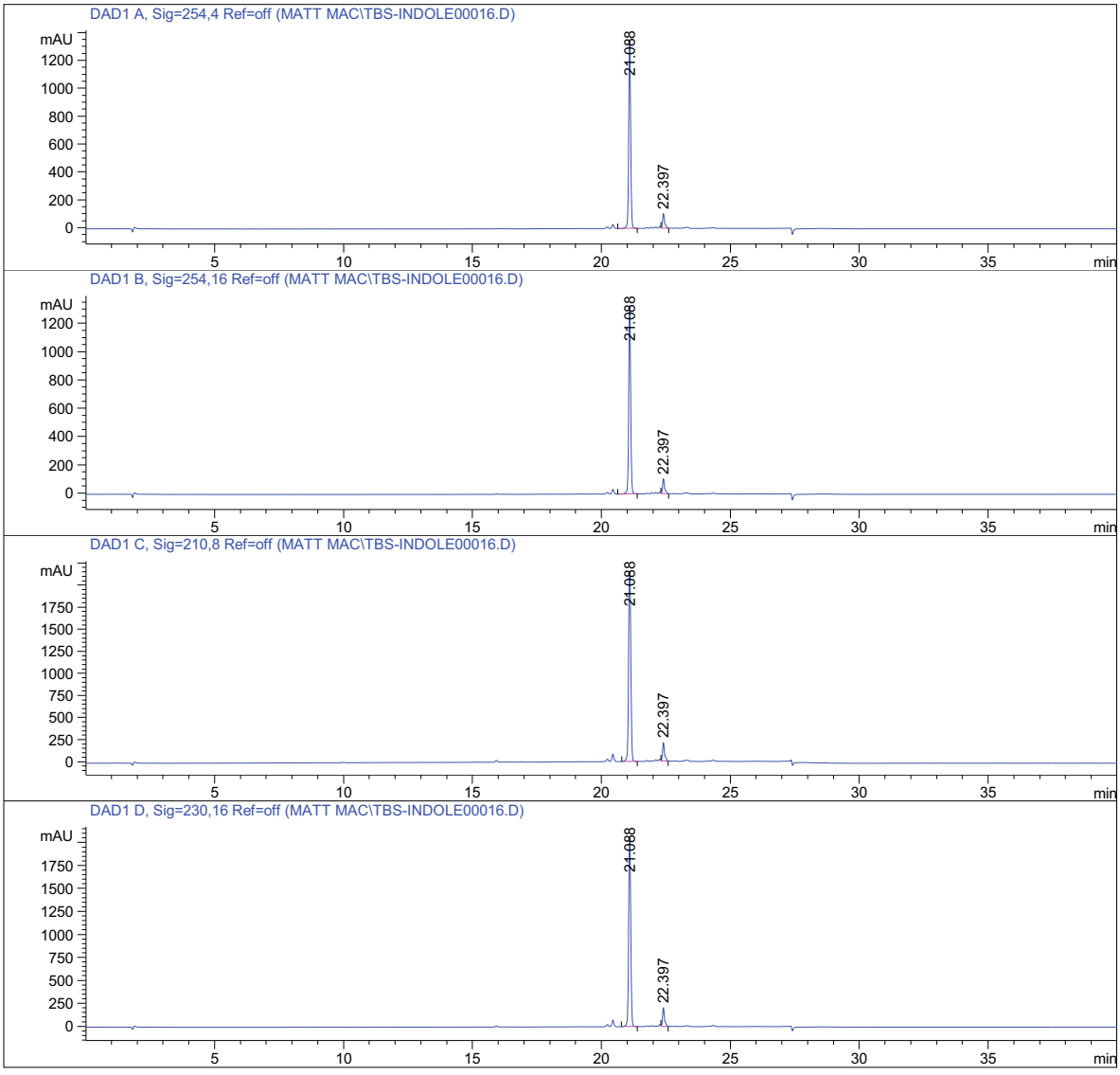

Data File C:\CHEM32\1\DATA\MATT MAC\TBS-INDOLE00016.D
Sample Name: run1

HPLC traces of compound **25**

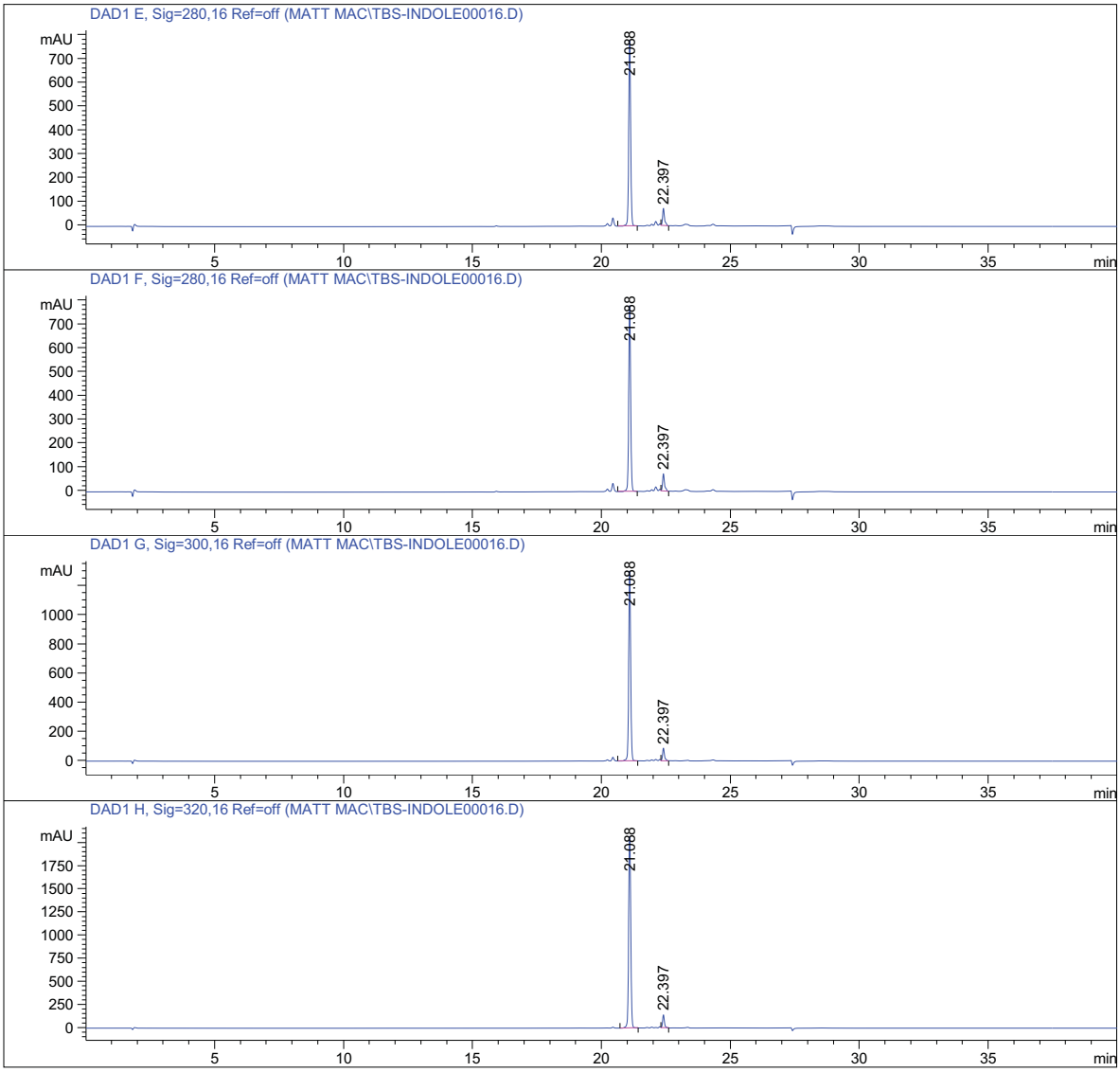

==========

Area Percent Report

==========

Sorted By : Signal
Multiplier : 1.0000
Dilution : 1.0000
Use Multiplier & Dilution Factor with ISTDs

Instrument 1 4/23/2013 2:28:57 PM Matt Mac

Data File C:\CHEM32\1\DATA\MATT MAC\TBS-INDOLE00016.D
Sample Name: run1

HPLC traces of compound **25**

Signal 1: DAD1 A, Sig=254,4 Ref=off

Peak #	RetTime [min]	Type	Width [min]	Area [mAU*s]	Height [mAU]	Area %
1	21.088	BV	0.0808	7048.01367	1353.30042	92.2446
2	22.397	VB	0.0813	592.55328	105.83783	7.7554
Totals :				7640.56696	1459.13824	

Signal 2: DAD1 B, Sig=254,16 Ref=off

Peak #	RetTime [min]	Type	Width [min]	Area [mAU*s]	Height [mAU]	Area %
1	21.088	BV	0.0807	6934.87109	1332.94495	92.1334
2	22.397	VB	0.0809	592.11774	106.44548	7.8666
Totals :				7526.98883	1439.39043	

Signal 3: DAD1 C, Sig=210,8 Ref=off

Peak #	RetTime [min]	Type	Width [min]	Area [mAU*s]	Height [mAU]	Area %
1	21.088	BV	0.0989	1.31208e4	2159.70190	91.7169
2	22.397	VB	0.0810	1184.95386	212.75230	8.2831
Totals :				1.43057e4	2372.45421	

Signal 4: DAD1 D, Sig=230,16 Ref=off

Peak #	RetTime [min]	Type	Width [min]	Area [mAU*s]	Height [mAU]	Area %
1	21.088	BV	0.0899	1.17001e4	2071.15112	91.2732
2	22.397	VB	0.0817	1118.66235	204.91919	8.7268
Totals :				1.28188e4	2276.07031	

Data File C:\CHEM32\1\DATA\MATT MAC\TBS-INDOLE00016.D
Sample Name: run1

HPLC traces of compound **25**

Signal 5: DAD1 E, Sig=280,16 Ref=off

Peak #	RetTime [min]	Type	Width [min]	Area [mAU*s]	Height [mAU]	Area %
1	21.088	BB	0.0803	4049.49487	782.92035	91.0860
2	22.397	VB	0.0817	396.29663	72.56457	8.9140
Totals :				4445.79150	855.48492	

Signal 6: DAD1 F, Sig=280,16 Ref=off

Peak #	RetTime [min]	Type	Width [min]	Area [mAU*s]	Height [mAU]	Area %
1	21.088	BB	0.0803	4049.49487	782.92035	91.0860
2	22.397	VB	0.0817	396.29663	72.56457	8.9140
Totals :				4445.79150	855.48492	

Signal 7: DAD1 G, Sig=300,16 Ref=off

Peak #	RetTime [min]	Type	Width [min]	Area [mAU*s]	Height [mAU]	Area %
1	21.088	BB	0.0811	6833.25537	1304.07190	93.7372
2	22.397	VB	0.0796	456.54562	86.49632	6.2628
Totals :				7289.80099	1390.56821	

Signal 8: DAD1 H, Sig=320,16 Ref=off

Peak #	RetTime [min]	Type	Width [min]	Area [mAU*s]	Height [mAU]	Area %
1	21.088	BB	0.0904	1.18015e4	2073.40820	94.4001
2	22.397	VB	0.0763	700.07214	140.10805	5.5999
Totals :				1.25016e4	2213.51625	

*** End of Report ***

Instrument 1 4/23/2013 2:28:57 PM Matt Mac

HRMS of compound **25**

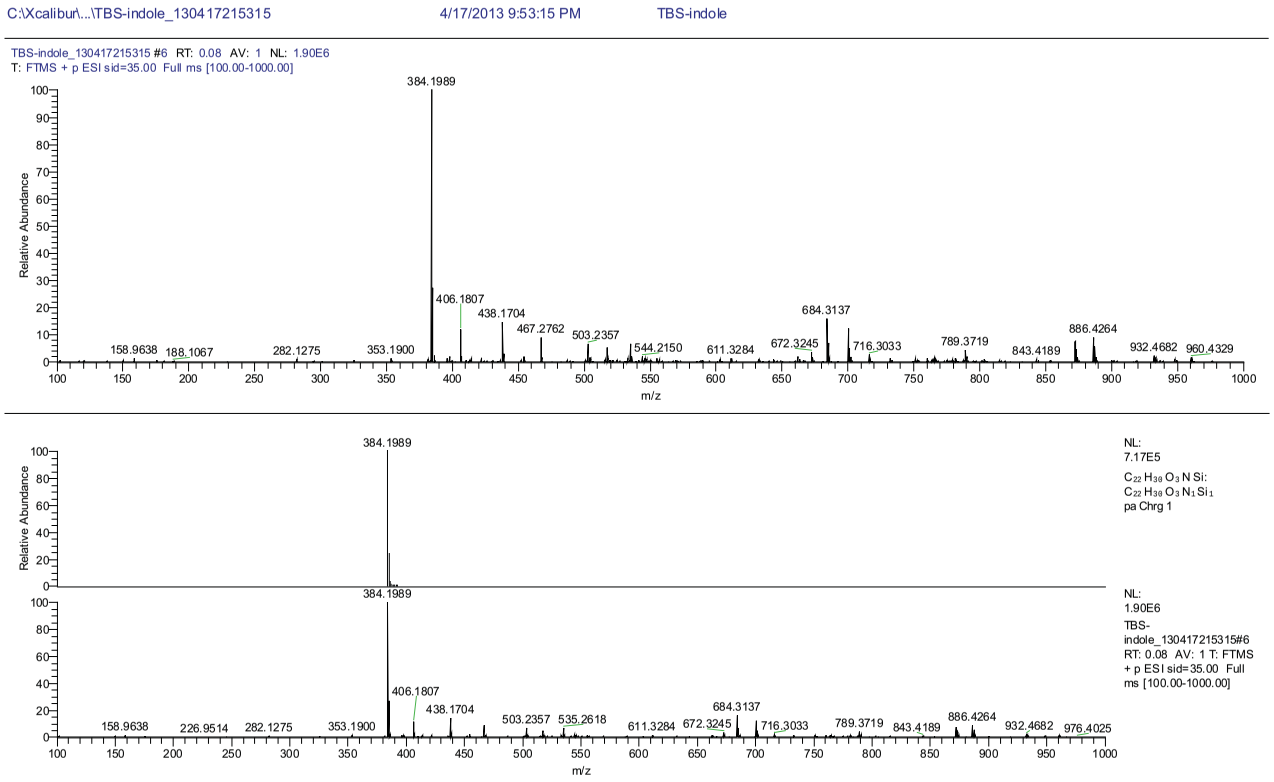

9.22
7.79
7.78
7.34
7.27
7.27
7.27
7.27
7.26
6.94
6.91
6.90
6.88
6.86
6.55
6.53
5.18
5.16
3.84
3.79
3.65
3.57
1.74
0.00
1.03
1.08
9.77
1.09
1.19
2.00
1.04
1.17
1.15
2.14
3.04
6.03
3.04
ppm
S17
31

192.08
157.27
152.67
141.29
141.15
136.74
134.95
128.84
128.78
128.12
127.84
123.05
122.30
112.81
112.02
111.70
107.42
94.86
70.29
70.24
60.94
56.15
55.78
55.72
ppm
S18
31

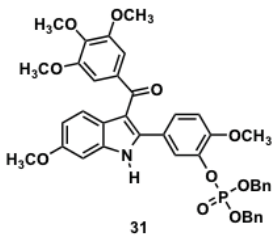
H3CO
OCH3
H3CO
O
OCH3
H3CO
N
H
O
O
P
OBn
OBn

31

-6.14
100
95
90
85
80
75
70
65
60
55
50
45
40
35
30
25
20
15
10
5
0
-5
-10
-15
-20
-25
-30
ppm

Data File C:\CHEM32\1\DATA\MATT MAC\MBH-IV-12300001.D
Sample Name: run1

HPLC traces of compound **31**

```
==========================================================================
Acq. Operator   : Matt Mac
Acq. Instrument : Instrument 1                    Location :   -
Injection Date  : 4/19/2013 10:12:02 AM
Acq. Method     : C:\CHEM32\1\METHODS\MASTERMETHOD.M
Last changed    : 4/19/2013 10:10:42 AM by Matt Mac
Analysis Method : C:\CHEM32\1\DATA\MATT MAC\MBH-IV-12300001.D\DA.M (MASTERMETHOD.M)
Last changed    : 4/19/2013 11:02:16 AM by Matt Mac
```

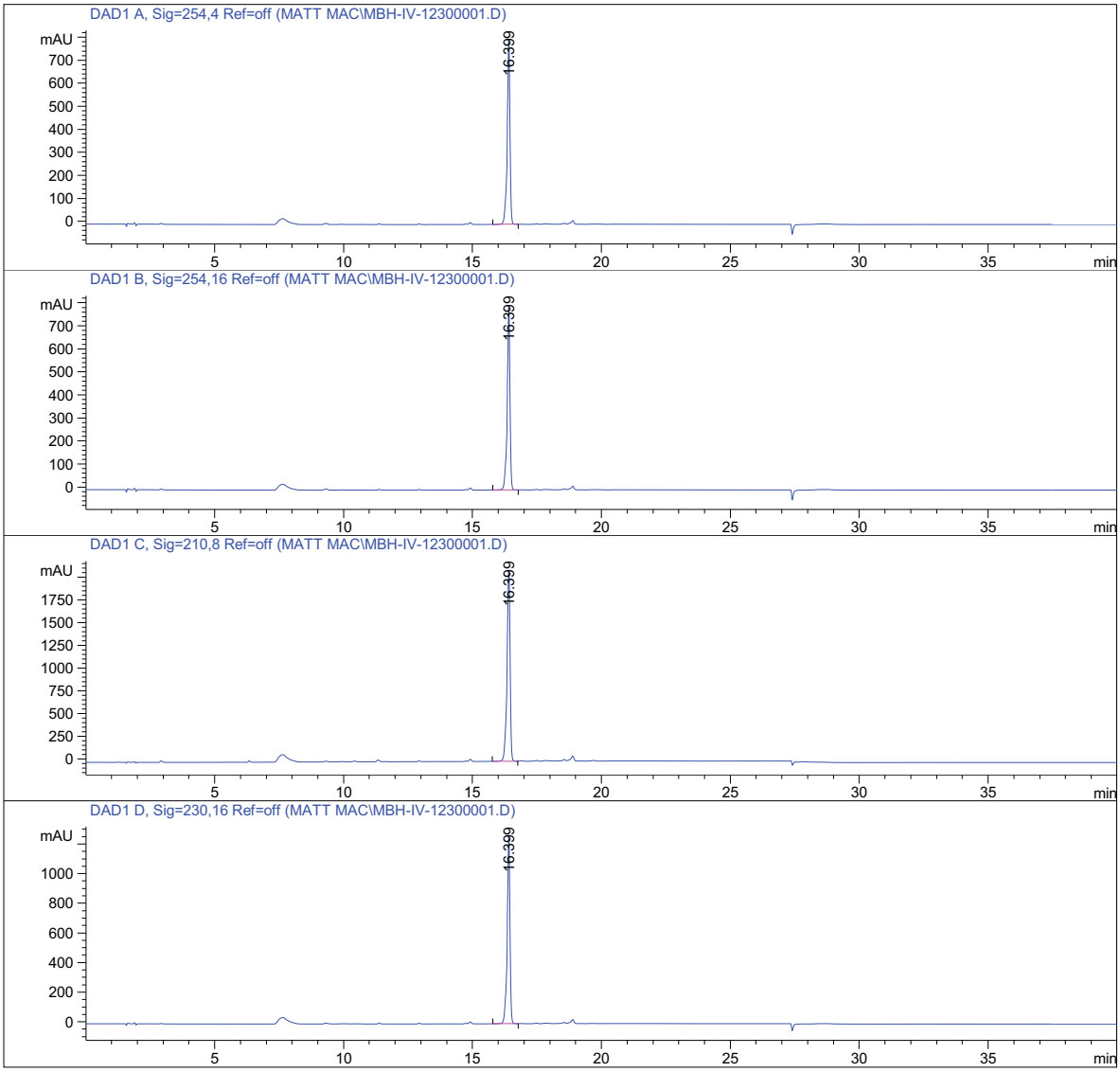

Data File C:\CHEM32\1\DATA\MATT MAC\MBH-IV-12300001.D
Sample Name: run1

HPLC traces of compound **31**

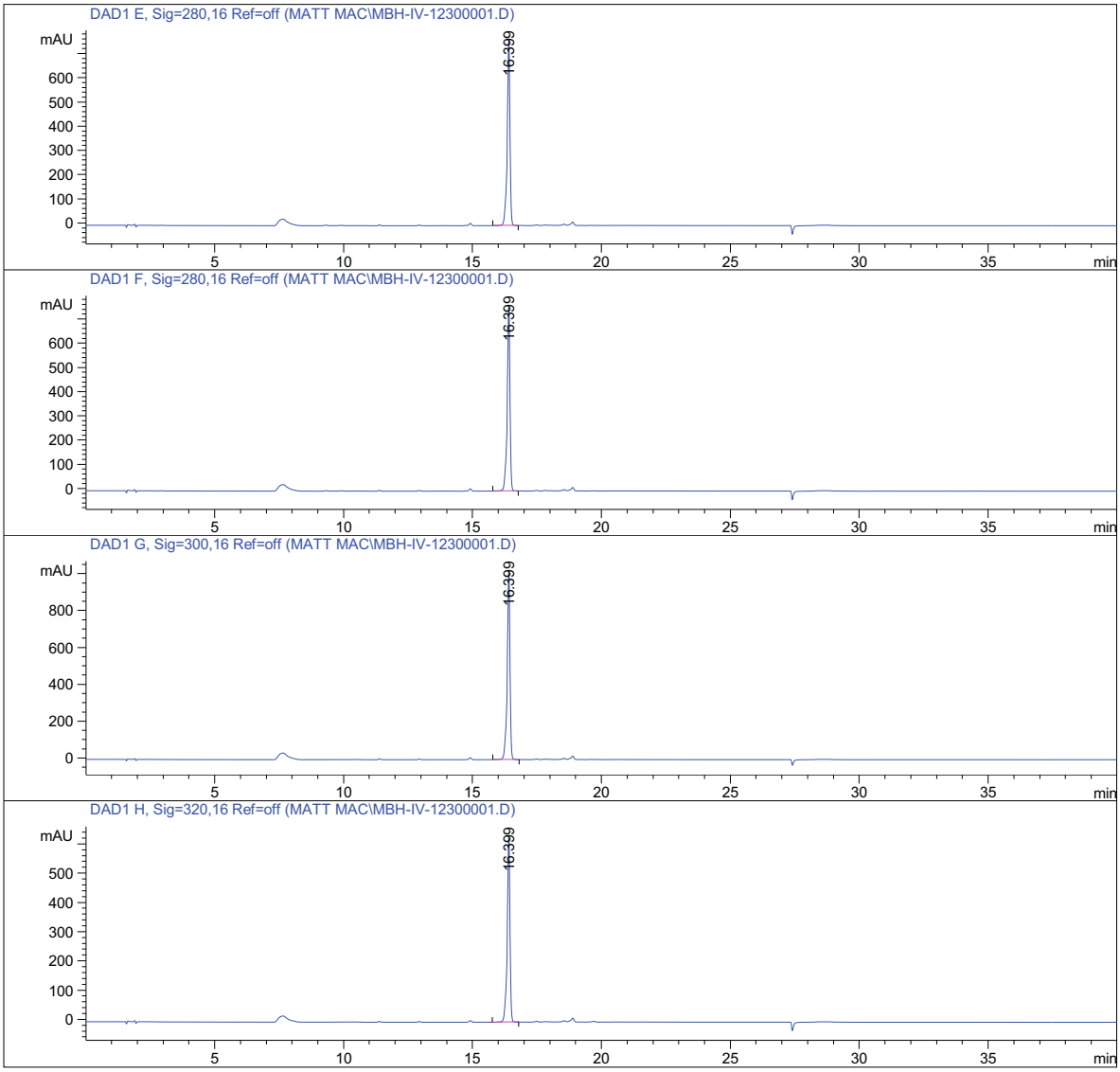

==========

Area Percent Report

==========

Sorted By : Signal
Multiplier : 1.0000
Dilution : 1.0000
Use Multiplier & Dilution Factor with ISTDs

Data File C:\CHEM32\1\DATA\MATT MAC\MBH-IV-12300001.D
Sample Name: run1

HPLC traces of compound **31**

Signal 1: DAD1 A, Sig=254,4 Ref=off

Peak #	RetTime [min]	Type	Width [min]	Area [mAU*s]	Height [mAU]	Area %
1	16.399	BB	0.1077	5895.92139	802.57043	100.0000
Totals :				5895.92139	802.57043	

Signal 2: DAD1 B, Sig=254,16 Ref=off

Peak #	RetTime [min]	Type	Width [min]	Area [mAU*s]	Height [mAU]	Area %
1	16.399	BB	0.1077	5895.67969	802.37427	100.0000
Totals :				5895.67969	802.37427	

Signal 3: DAD1 C, Sig=210,8 Ref=off

Peak #	RetTime [min]	Type	Width [min]	Area [mAU*s]	Height [mAU]	Area %
1	16.399	BV	0.1254	1.75157e4	2098.39795	100.0000
Totals :				1.75157e4	2098.39795	

Signal 4: DAD1 D, Sig=230,16 Ref=off

Peak #	RetTime [min]	Type	Width [min]	Area [mAU*s]	Height [mAU]	Area %
1	16.399	BV	0.1089	9433.00391	1266.84875	100.0000
Totals :				9433.00391	1266.84875	

Signal 5: DAD1 E, Sig=280,16 Ref=off

Peak #	RetTime [min]	Type	Width [min]	Area [mAU*s]	Height [mAU]	Area %
1	16.399	BV	0.1078	5649.78125	768.28760	100.0000
Totals :				5649.78125	768.28760	

Data File C:\CHEM32\1\DATA\MATT MAC\MBH-IV-12300001.D
Sample Name: run1

HPLC traces of compound **31**

Signal 6: DAD1 F, Sig=280,16 Ref=off

Peak #	RetTime [min]	Type	Width [min]	Area [mAU*s]	Height [mAU]	Area %
1	16.399	BV	0.1078	5649.78125	768.28760	100.0000
Totals :				5649.78125	768.28760	

Signal 7: DAD1 G, Sig=300,16 Ref=off

Peak #	RetTime [min]	Type	Width [min]	Area [mAU*s]	Height [mAU]	Area %
1	16.399	BB	0.1080	7557.41553	1024.94617	100.0000
Totals :				7557.41553	1024.94617	

Signal 8: DAD1 H, Sig=320,16 Ref=off

Peak #	RetTime [min]	Type	Width [min]	Area [mAU*s]	Height [mAU]	Area %
1	16.399	BB	0.1077	4676.26318	636.32965	100.0000
Totals :				4676.26318	636.32965	

*** End of Report ***

HRMS of compound **31**

C:\Xcalibur\...\MBH-VI-123_130417220746 4/17/2013 10:37:49 PM MBH-VI-123

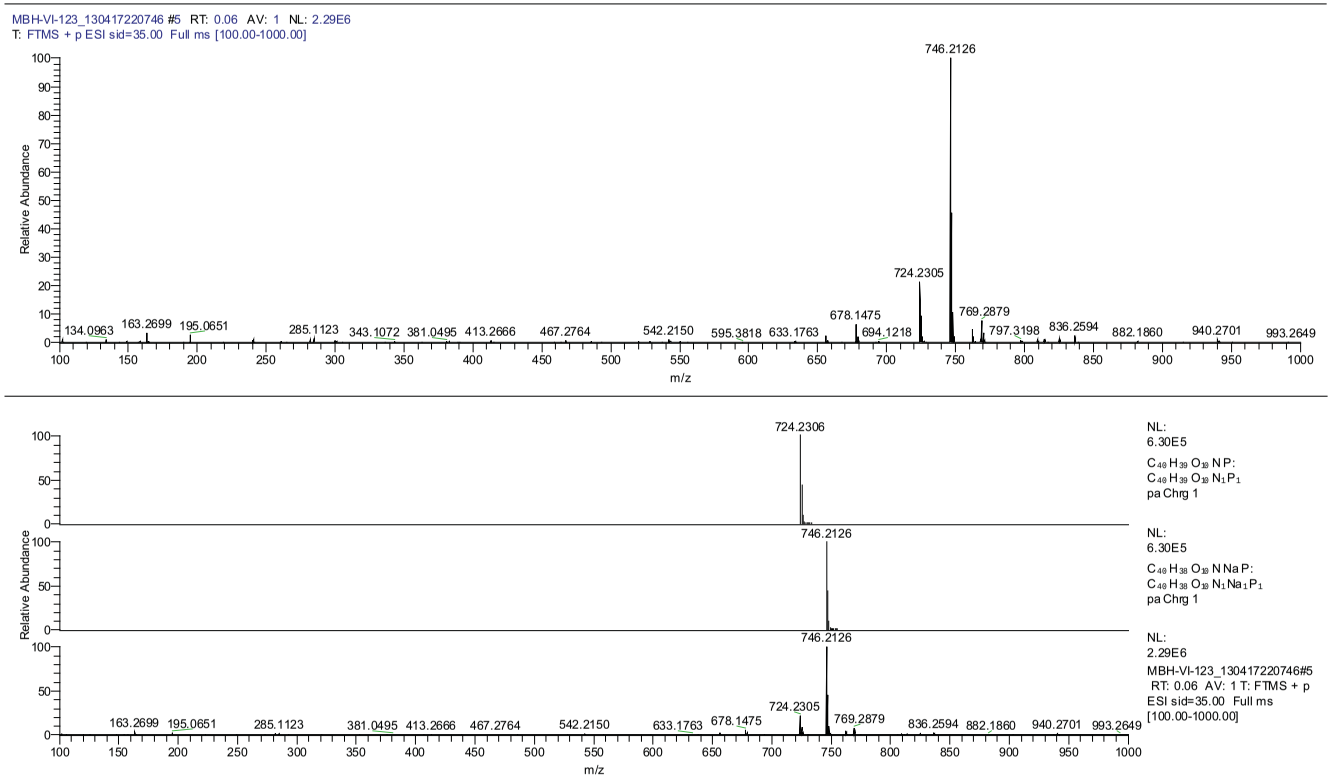

8 (OXi8006)
8.47
7.92
7.90
7.26
6.95
6.93
6.92
6.92
6.90
6.76
6.76
6.75
6.74
6.62
6.60
5.57
3.87
3.81
3.79
3.70
0.00
1.00
1.04
1.98
2.99
1.05
1.07
1.03
3.05
3.09
3.08
6.09
ppm
S25

192.70
157.08
152.48
147.01
145.32
143.30
141.04
136.57
135.02
125.07
122.98
122.11
121.48
115.10
112.58
111.64
110.27
107.36
94.79
77.41
77.16
76.91
60.81
56.02
55.82
55.63
8 (OXi8006)
ppm
S26

Data File C:\CHEM32\1\DATA\MATT MAC\OXI8006000029.D
Sample Name: run1

HPLC traces of compound **8** (OXi8006)

```
==========================================================================
Acq. Operator   : Matt Mac
Acq. Instrument : Instrument 1                    Location :   -
Injection Date  : 8/31/2012 11:53:26 AM
Acq. Method     : C:\CHEM32\1\METHODS\MASTERMETHOD.M
Last changed    : 8/31/2012 11:42:10 AM by Matt Mac
                  (modified after loading)
Analysis Method : C:\CHEM32\1\DATA\MATT MAC\OXI8006000029.D\DA.M (MASTERMETHOD.M)
Last changed    : 8/31/2012 12:43:41 PM by Matt Mac
Sample Info     :
```

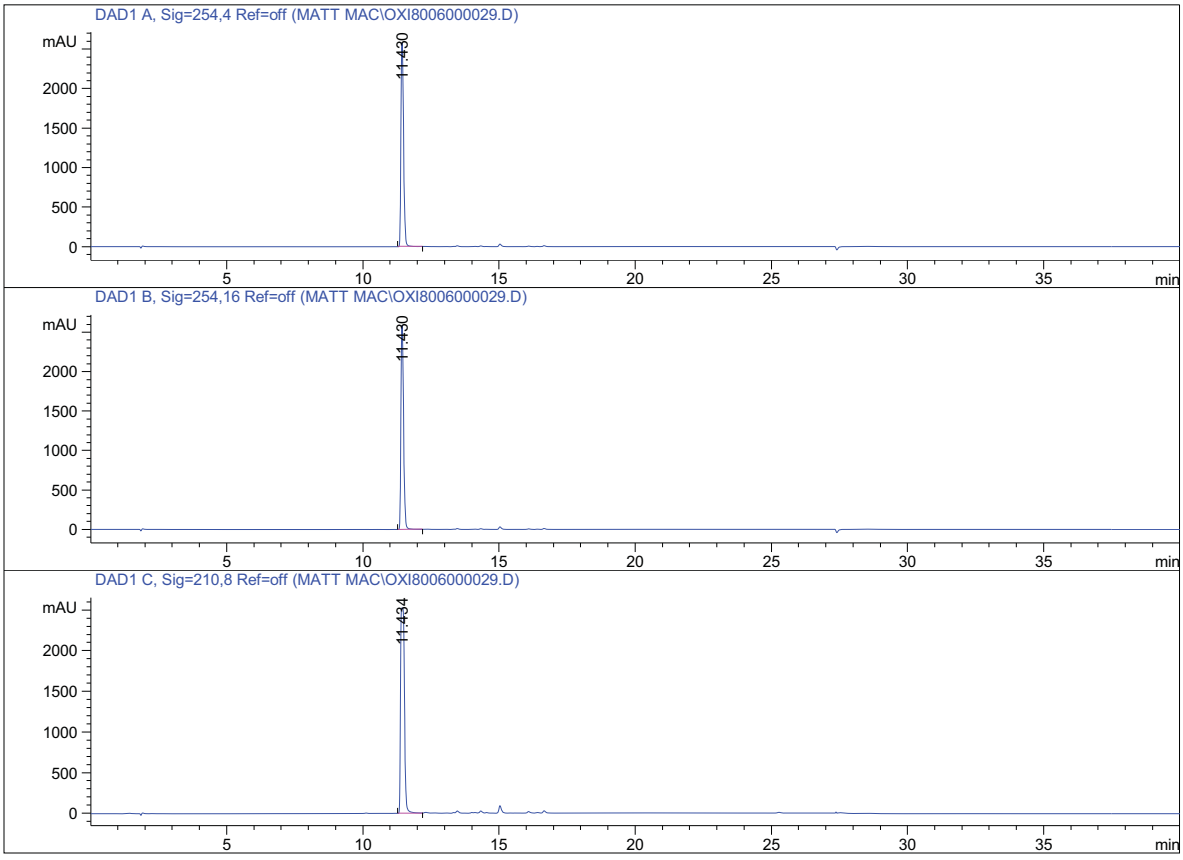

Instrument 1 4/23/2013 3:02:43 PM Matt Mac

Data File C:\CHEM32\1\DATA\MATT MAC\OXI8006000029.D
Sample Name: run1

HPLC traces of compound **8** (OXi8006)

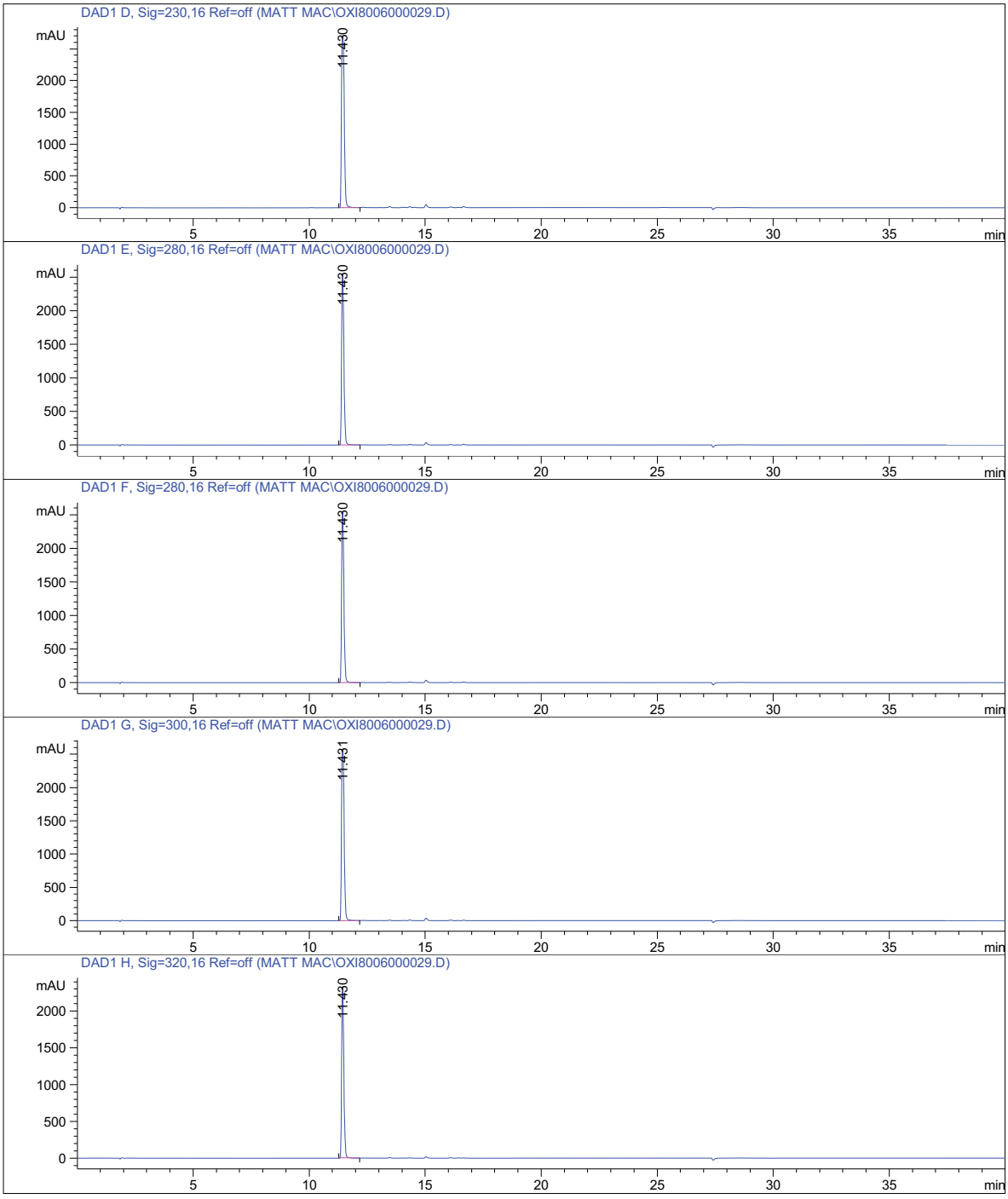

Instrument 1 4/23/2013 3:02:43 PM Matt Mac

Data File C:\CHEM32\1\DATA\MATT MAC\OXI8006000029.D
Sample Name: run1

HPLC traces of compound **8** (OXi8006)

```
================================================================================
                          Area Percent Report
================================================================================

Sorted By             :      Signal
Multiplier            :      1.0000
Dilution              :      1.0000
Use Multiplier & Dilution Factor with ISTDs


Signal 1: DAD1 A, Sig=254,4 Ref=off

Peak RetTime Type  Width     Area      Height     Area
  #   [min]        [min]   [mAU*s]     [mAU]        %
----|-------|----|-------|----------|----------|--------|
   1  11.430 BV    0.1062 1.73226e4  2584.75806 100.0000

Totals :                  1.73226e4  2584.75806



Signal 2: DAD1 B, Sig=254,16 Ref=off

Peak RetTime Type  Width     Area      Height     Area
  #   [min]        [min]   [mAU*s]     [mAU]        %
----|-------|----|-------|----------|----------|--------|
   1  11.430 BV    0.1062 1.73567e4  2590.07788 100.0000

Totals :                  1.73567e4  2590.07788



Signal 3: DAD1 C, Sig=210,8 Ref=off

Peak RetTime Type  Width     Area      Height     Area
  #   [min]        [min]   [mAU*s]     [mAU]        %
----|-------|----|-------|----------|----------|--------|
   1  11.434 BV    0.1610 2.48943e4  2525.35937 100.0000

Totals :                  2.48943e4  2525.35937



Signal 4: DAD1 D, Sig=230,16 Ref=off

Peak RetTime Type  Width     Area      Height     Area
  #   [min]        [min]   [mAU*s]     [mAU]        %
----|-------|----|-------|----------|----------|--------|
   1  11.430 BV    0.1358 2.26553e4  2702.47852 100.0000

Totals :                  2.26553e4  2702.47852
```

Data File C:\CHEM32\1\DATA\MATT MAC\OXI8006000029.D
Sample Name: run1

HPLC traces of compound **8** (OXi8006)

Signal 5: DAD1 E, Sig=280,16 Ref=off

Peak #	RetTime [min]	Type	Width [min]	Area [mAU*s]	Height [mAU]	Area %
1	11.430	BV	0.1071	1.73240e4	2554.55151	100.0000
Totals :				1.73240e4	2554.55151	

Signal 6: DAD1 F, Sig=280,16 Ref=off

Peak #	RetTime [min]	Type	Width [min]	Area [mAU*s]	Height [mAU]	Area %
1	11.430	BV	0.1071	1.73240e4	2554.55151	100.0000
Totals :				1.73240e4	2554.55151	

Signal 7: DAD1 G, Sig=300,16 Ref=off

Peak #	RetTime [min]	Type	Width [min]	Area [mAU*s]	Height [mAU]	Area %
1	11.431	BV	0.1254	2.02066e4	2579.51099	100.0000
Totals :				2.02066e4	2579.51099	

Signal 8: DAD1 H, Sig=320,16 Ref=off

Peak #	RetTime [min]	Type	Width [min]	Area [mAU*s]	Height [mAU]	Area %
1	11.430	BV	0.1019	1.51963e4	2336.06787	100.0000
Totals :				1.51963e4	2336.06787	

*** End of Report ***

Instrument 1 4/23/2013 3:02:43 PM Matt Mac

HRMS compound **8** (OXi8006)

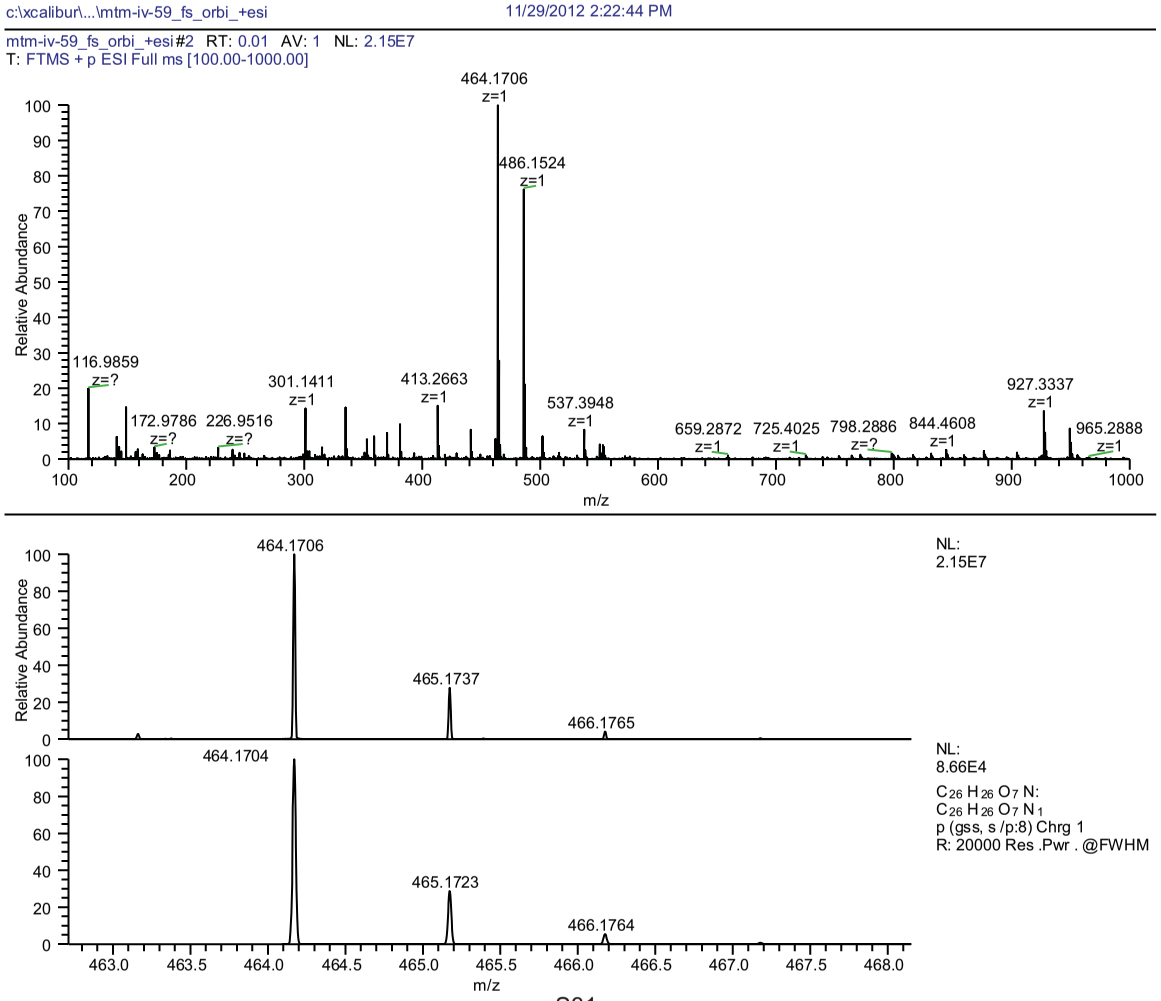

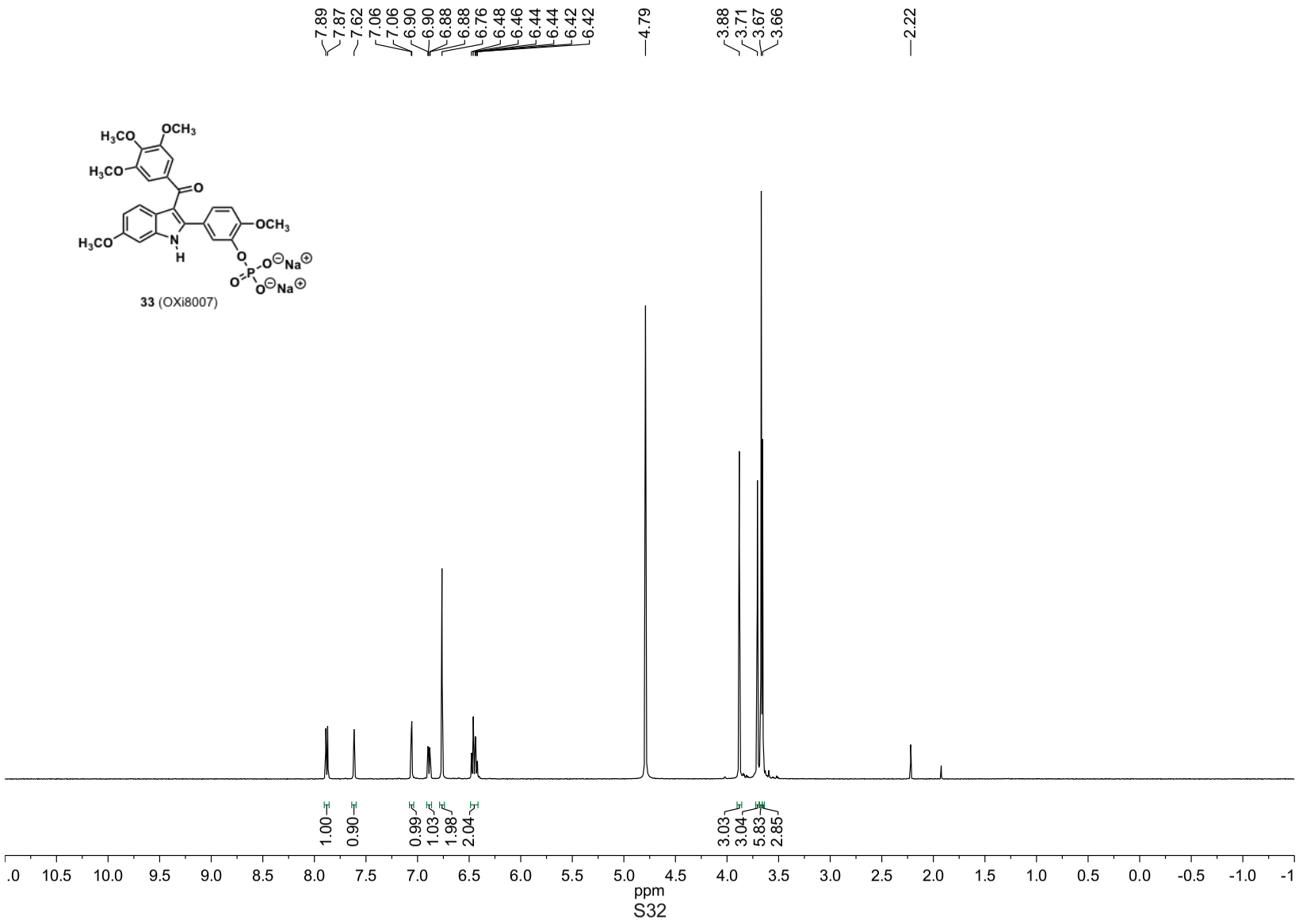
7.89
7.87
7.62
7.06
7.06
6.90
6.90
6.88
6.88
6.76
6.48
6.46
6.44
6.44
6.42
6.42
4.79
3.88
3.71
3.67
3.66
2.22
33 (OXi8007)
1.00
0.90
0.99
1.03
1.98
2.04
3.03
3.04
5.83
2.85
ppm

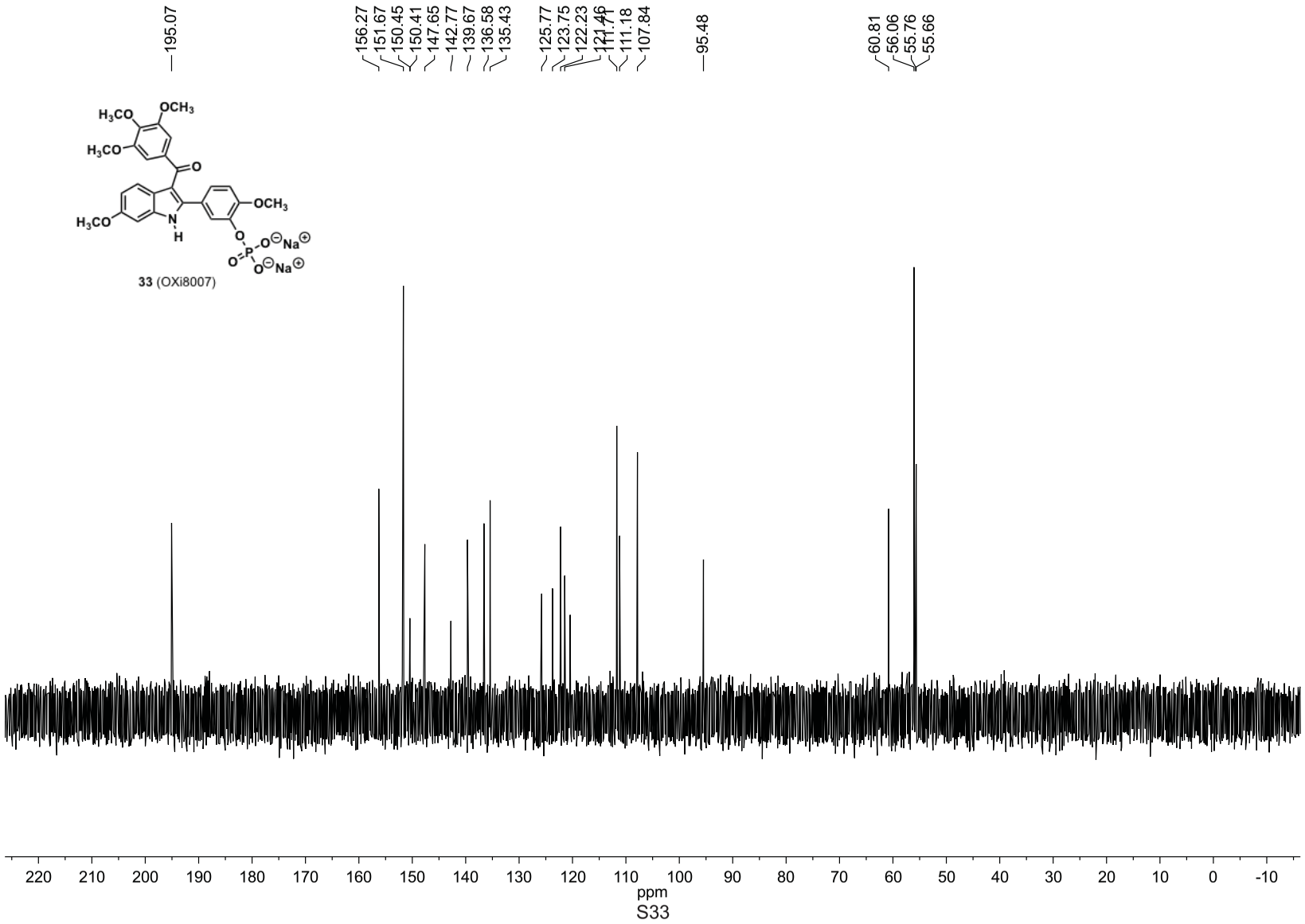
195.07
156.27
151.67
150.45
150.41
147.65
142.77
139.67
136.58
135.43
125.77
123.75
122.23
121.46
111.71
111.18
107.84
95.48
60.81
56.06
55.76
55.66
33 (OXi8007)
220
210
200
190
180
170
160
150
140
130
120
110
100
90
80
70
60
50
40
30
20
10
0
-10
ppm

S33

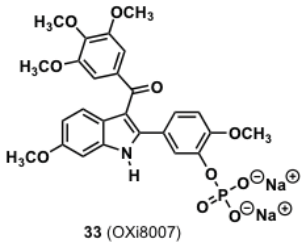
H3CO
OCH3
H3CO
O
OCH3
H3CO
N
H
O
O
P
O
Na
O
Na

33 (OXi8007)

0.58
100
95
90
85
80
75
70
65
60
55
50
45
40
35
30
25
20
15
10
5
0
-5
-10
-15
-20
-25
-30
ppm

Data File C:\CHEM32\1\DATA\MATT MAC\8007000037.D
Sample Name: 8007

HPLC traces of compound **33** (OXi8007)

```
==========================================================================
Acq. Operator   : Matt Mac
Acq. Instrument : Instrument 1                    Location :   -
Injection Date  : 5/4/2012 10:23:02 AM
Acq. Method     : C:\CHEM32\1\METHODS\MASTERMETHOD.M
Last changed    : 5/4/2012 10:16:05 AM by Matt Mac
                  (modified after loading)
Analysis Method : C:\CHEM32\1\DATA\MATT MAC\8007000037.D\DA.M (MASTERMETHOD.M)
Last changed    : 4/19/2013 10:08:53 AM by Matt Mac
                  (modified after loading)
Sample Info     :  8007 (0.1% TFA in H2O)
```

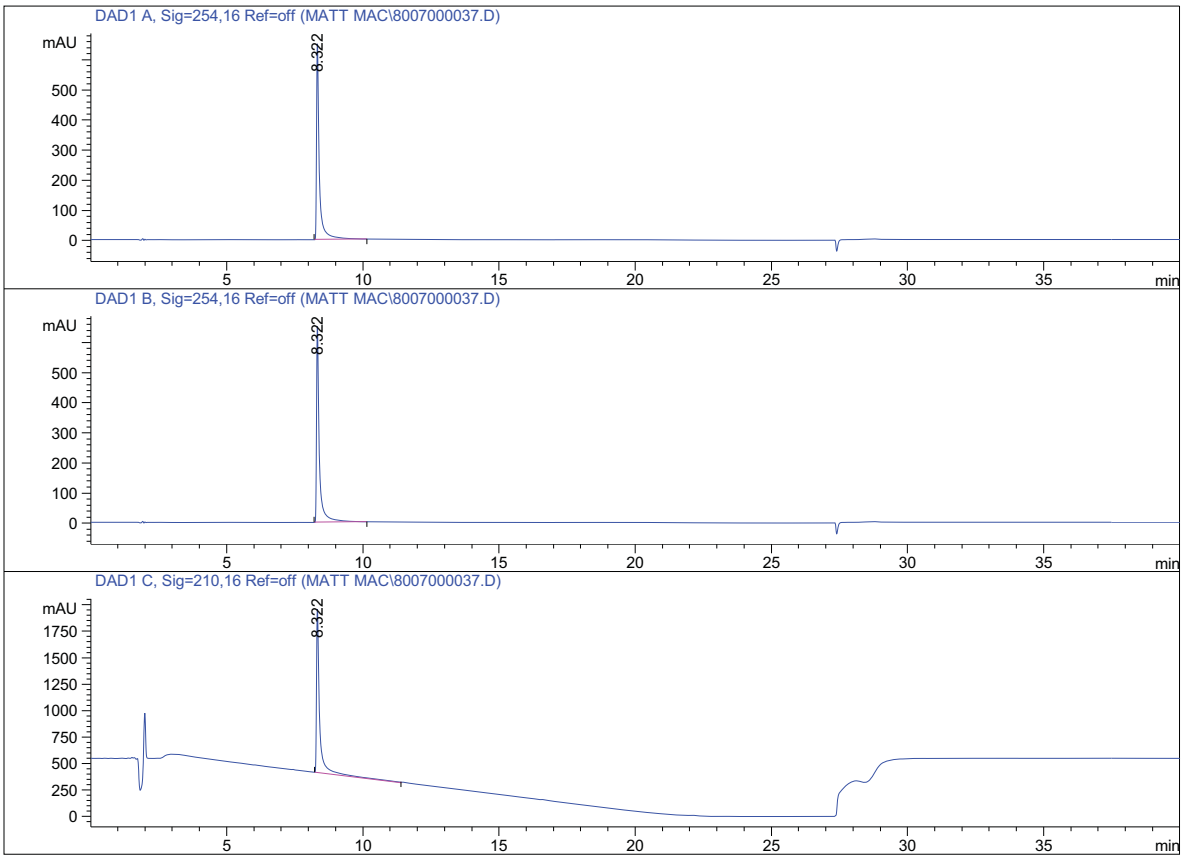

Data File C:\CHEM32\1\DATA\MATT MAC\8007000037.D
Sample Name: 8007

HPLC traces of compound **33** (OXi8007)

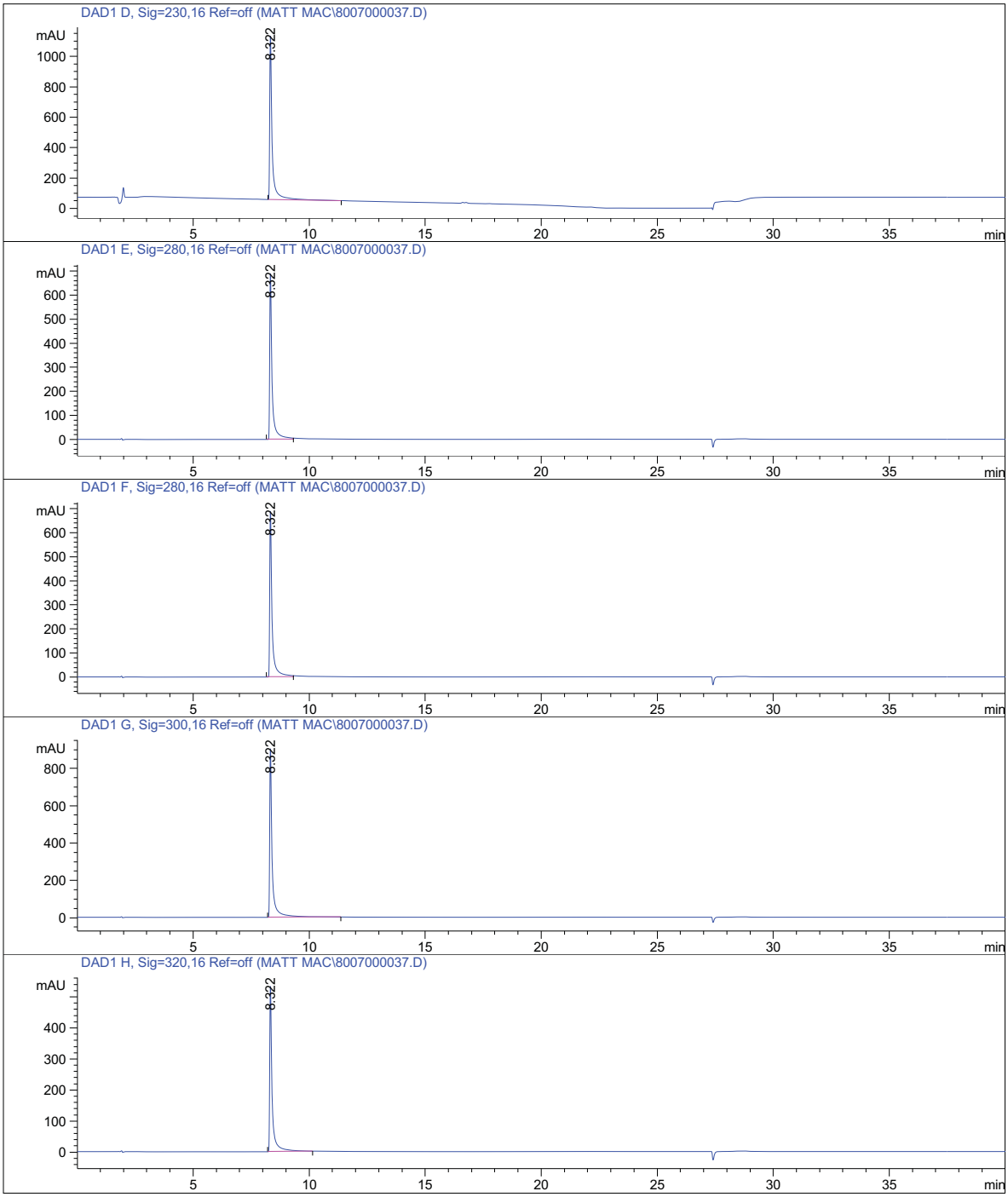

Instrument 1 4/19/2013 10:11:17 AM Matt Mac Page 2 of 4

Data File C:\CHEM32\1\DATA\MATT MAC\8007000037.D
Sample Name: 8007

HPLC traces of compound **33** (OXi8007)

```
=====================================================================
                        Area Percent Report
=====================================================================

Sorted By             :      Signal
Multiplier            :      1.0000
Dilution              :      1.0000
Use Multiplier & Dilution Factor with ISTDs


Signal 1: DAD1 A, Sig=254,16 Ref=off

Peak RetTime Type  Width     Area      Height     Area
  #   [min]        [min]   [mAU*s]     [mAU]        %
----|-------|----|-------|----------|----------|--------|
   1   8.322 BB    0.1027 4736.21777  651.99268 100.0000

Totals :                  4736.21777  651.99268



Signal 2: DAD1 B, Sig=254,16 Ref=off

Peak RetTime Type  Width     Area      Height     Area
  #   [min]        [min]   [mAU*s]     [mAU]        %
----|-------|----|-------|----------|----------|--------|
   1   8.322 BB    0.1027 4736.21777  651.99268 100.0000

Totals :                  4736.21777  651.99268



Signal 3: DAD1 C, Sig=210,16 Ref=off

Peak RetTime Type  Width     Area      Height     Area
  #   [min]        [min]   [mAU*s]     [mAU]        %
----|-------|----|-------|----------|----------|--------|
   1   8.322 BV    0.1171 1.28711e4  1547.13928 100.0000

Totals :                  1.28711e4  1547.13928



Signal 4: DAD1 D, Sig=230,16 Ref=off

Peak RetTime Type  Width     Area      Height     Area
  #   [min]        [min]   [mAU*s]     [mAU]        %
----|-------|----|-------|----------|----------|--------|
   1   8.322 BV    0.1074 8262.35937 1078.22693 100.0000

Totals :                  8262.35937 1078.22693
```

HPLC traces of compound **33** (OXi8007)

Signal 5: DAD1 E, Sig=280,16 Ref=off

Peak #	RetTime [min]	Type	Width [min]	Area [mAU*s]	Height [mAU]	Area %
1	8.322	BV	0.1020	4969.80322	690.56696	100.0000
Totals :				4969.80322	690.56696	

Signal 6: DAD1 F, Sig=280,16 Ref=off

Peak #	RetTime [min]	Type	Width [min]	Area [mAU*s]	Height [mAU]	Area %
1	8.322	BV	0.1020	4969.80322	690.56696	100.0000
Totals :				4969.80322	690.56696	

Signal 7: DAD1 G, Sig=300,16 Ref=off

Peak #	RetTime [min]	Type	Width [min]	Area [mAU*s]	Height [mAU]	Area %
1	8.322	BB	0.1056	6794.81299	904.99524	100.0000
Totals :				6794.81299	904.99524	

Signal 8: DAD1 H, Sig=320,16 Ref=off

Peak #	RetTime [min]	Type	Width [min]	Area [mAU*s]	Height [mAU]	Area %
1	8.322	BB	0.1029	3886.76294	533.83514	100.0000
Totals :				3886.76294	533.83514	

*** End of Report ***

HRMS of compound **33** (OXi8007)

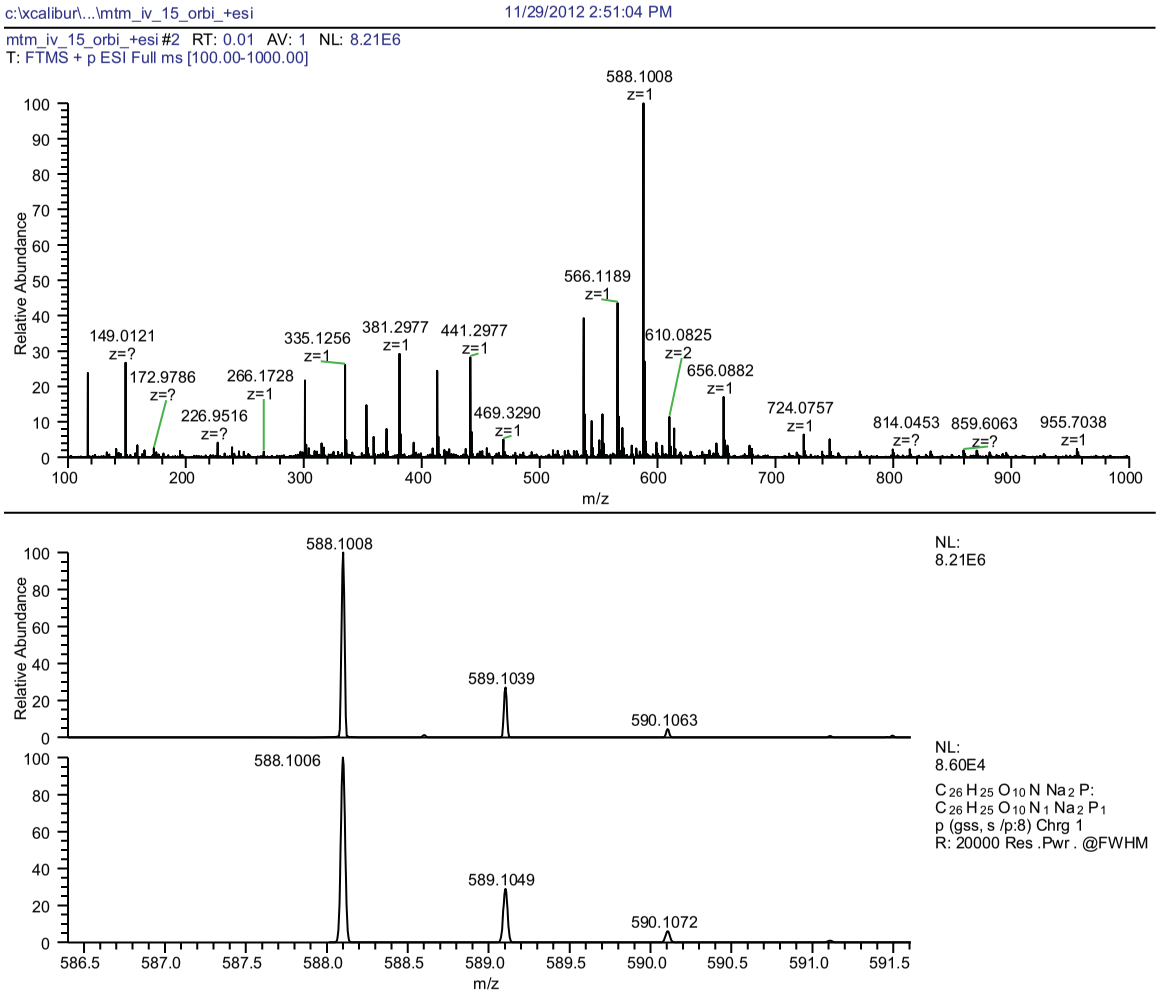

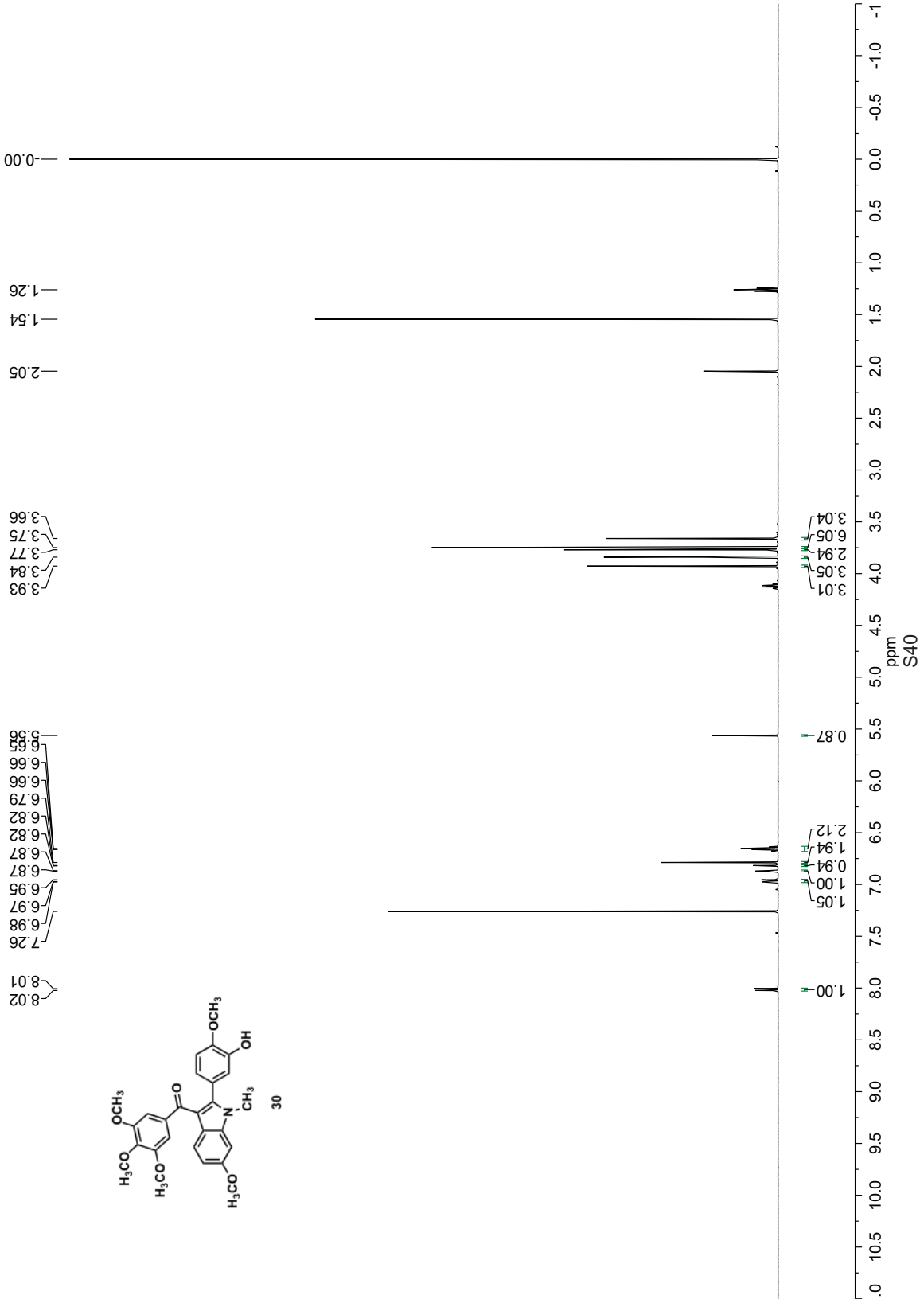
8.02
8.01
7.26
6.98
6.97
6.95
6.87
6.87
6.82
6.82
6.79
6.66
6.66
6.65
5.56
3.93
3.84
3.77
3.75
3.66
2.05
1.54
1.26
0.00
1.00
0.87
3.01
3.05
2.94
6.05
3.04
1.05
1.00
0.94
1.94
2.12
ppm
S40
30

192.19
157.31
152.30
147.00
145.44
145.18
140.24
138.19
135.83
123.95
123.55
122.72
121.88
116.97
114.35
111.67
110.22
106.63
93.69
77.58
77.16
76.74
60.75
56.08
56.02
55.88
31.45
OCH3
OH
O
N
CH3
H3CO
H3CO
H3CO
30
ppm
S41

Data File C:\CHEM32\1\DATA\MATT MAC\MBH-V-123000017.D
Sample Name: run1

HPLC traces of compound **30**

```
==================================================================
Acq. Operator   : Matt Mac
Acq. Instrument : Instrument 1                    Location :   -
Injection Date  : 4/23/2013 2:41:13 PM
Acq. Method     : C:\CHEM32\1\METHODS\MASTERMETHOD.M
Last changed    : 4/23/2013 1:46:54 PM by Matt Mac
Analysis Method : C:\CHEM32\1\DATA\MATT MAC\MBH-V-123000017.D\DA.M (MASTERMETHOD.M)
Last changed    : 4/23/2013 3:33:35 PM by Matt Mac
```

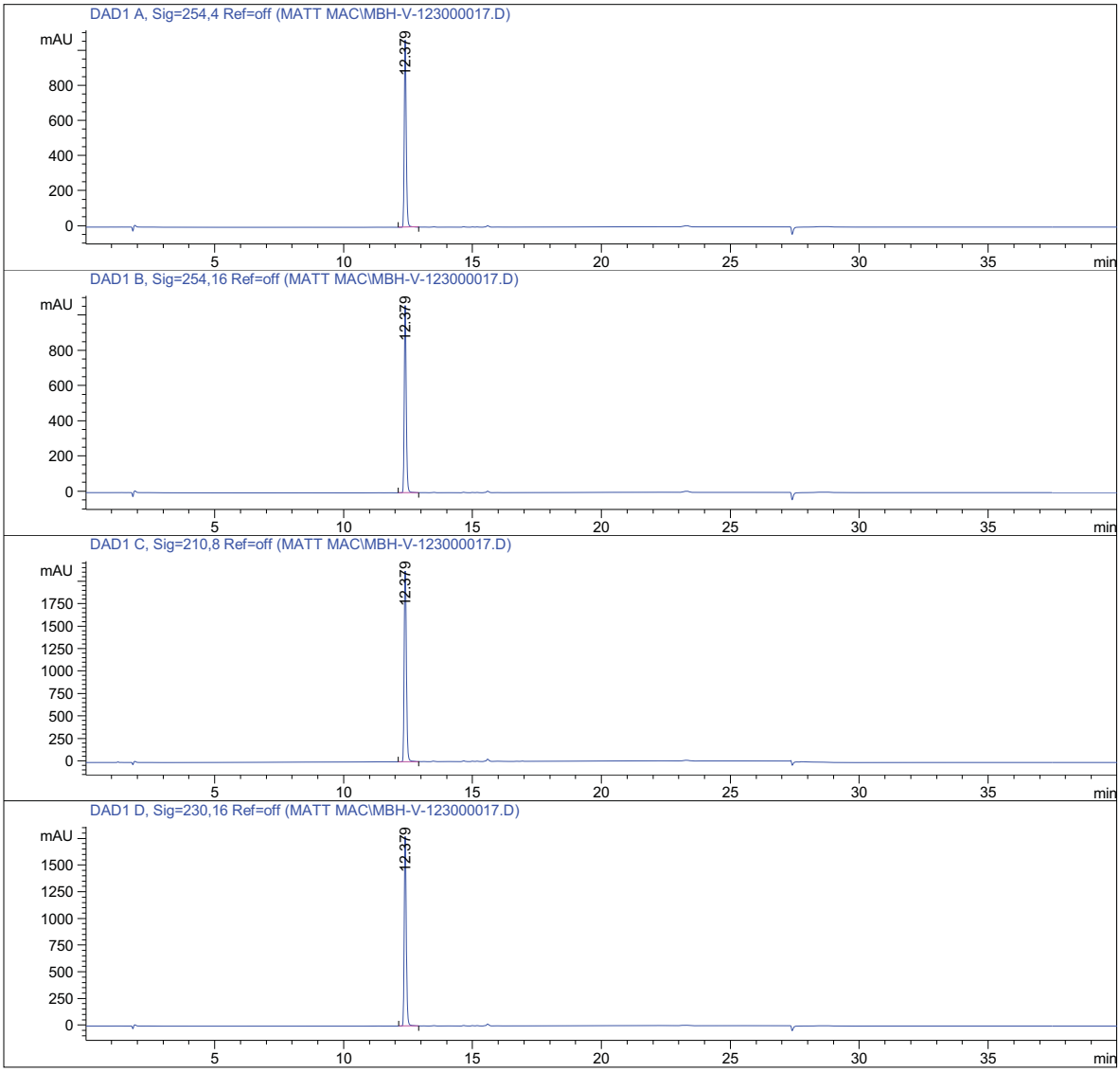

Data File C:\CHEM32\1\DATA\MATT MAC\MBH-V-123000017.D
Sample Name: run1

HPLC traces of compound **30**

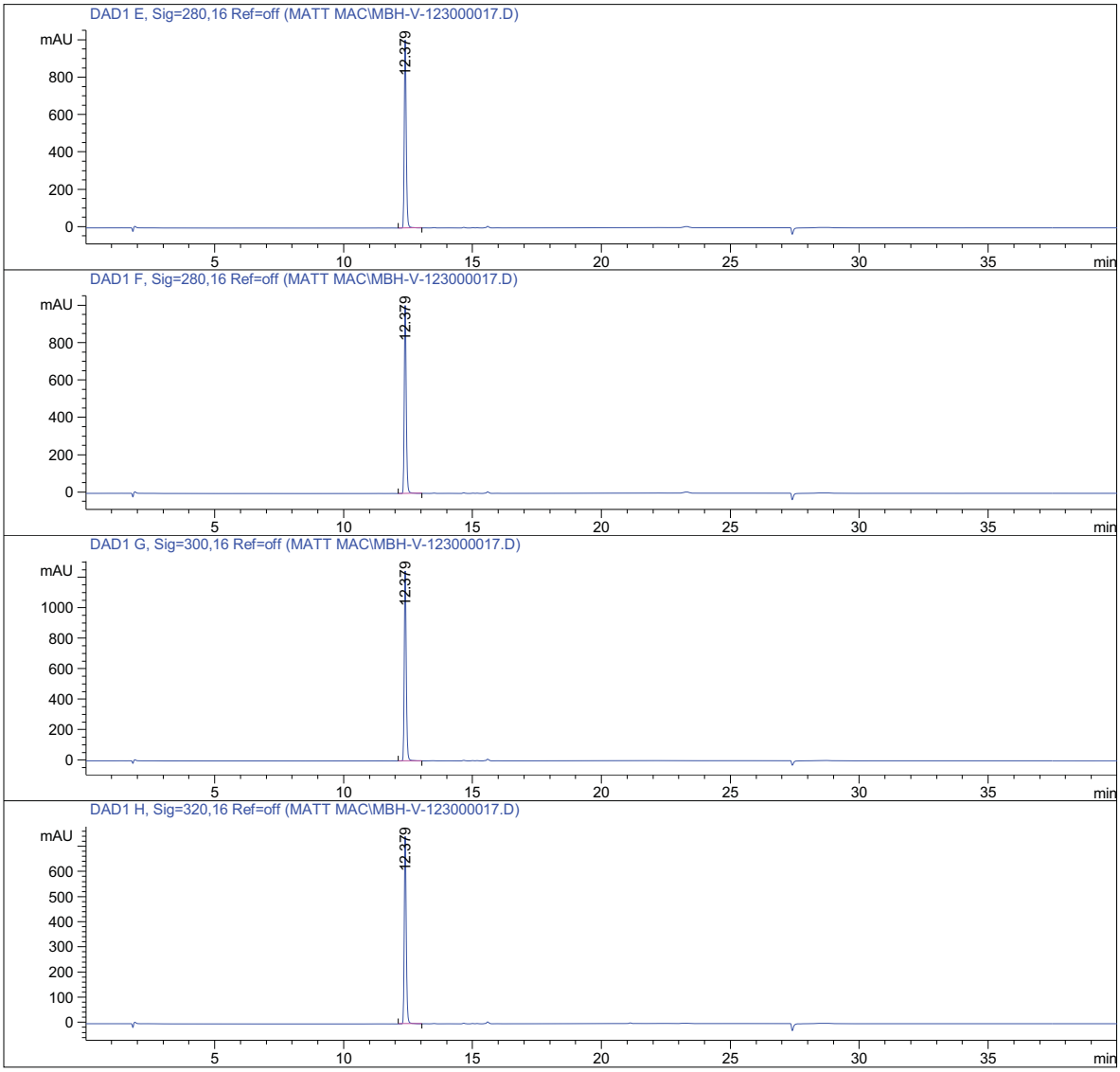

==========

Area Percent Report

==========

Sorted By : Signal
Multiplier : 1.0000
Dilution : 1.0000
Use Multiplier & Dilution Factor with ISTDs

Instrument 1 4/23/2013 3:34:07 PM Matt Mac

Data File C:\CHEM32\1\DATA\MATT MAC\MBH-V-123000017.D
Sample Name: run1

HPLC traces of compound **30**

Signal 1: DAD1 A, Sig=254,4 Ref=off

Peak #	RetTime [min]	Type	Width [min]	Area [mAU*s]	Height [mAU]	Area %
1	12.379	BB	0.0824	5719.47656	1068.60681	100.0000
Totals :				5719.47656	1068.60681	

Signal 2: DAD1 B, Sig=254,16 Ref=off

Peak #	RetTime [min]	Type	Width [min]	Area [mAU*s]	Height [mAU]	Area %
1	12.379	BB	0.0824	5699.11182	1064.78992	100.0000
Totals :				5699.11182	1064.78992	

Signal 3: DAD1 C, Sig=210,8 Ref=off

Peak #	RetTime [min]	Type	Width [min]	Area [mAU*s]	Height [mAU]	Area %
1	12.379	BV	0.0972	1.29636e4	2125.26245	100.0000
Totals :				1.29636e4	2125.26245	

Signal 4: DAD1 D, Sig=230,16 Ref=off

Peak #	RetTime [min]	Type	Width [min]	Area [mAU*s]	Height [mAU]	Area %
1	12.379	BB	0.0869	9904.25781	1779.95203	100.0000
Totals :				9904.25781	1779.95203	

Signal 5: DAD1 E, Sig=280,16 Ref=off

Peak #	RetTime [min]	Type	Width [min]	Area [mAU*s]	Height [mAU]	Area %
1	12.379	BV	0.0826	5410.01904	1008.05243	100.0000
Totals :				5410.01904	1008.05243	

HPLC traces of compound **30**

Signal 6: DAD1 F, Sig=280,16 Ref=off

Peak #	RetTime [min]	Type	Width [min]	Area [mAU*s]	Height [mAU]	Area %
1	12.379	BV	0.0826	5410.01904	1008.05243	100.0000
Totals :				5410.01904	1008.05243	

Signal 7: DAD1 G, Sig=300,16 Ref=off

Peak #	RetTime [min]	Type	Width [min]	Area [mAU*s]	Height [mAU]	Area %
1	12.379	BV	0.0829	6736.20020	1249.14526	100.0000
Totals :				6736.20020	1249.14526	

Signal 8: DAD1 H, Sig=320,16 Ref=off

Peak #	RetTime [min]	Type	Width [min]	Area [mAU*s]	Height [mAU]	Area %
1	12.379	BB	0.0825	3998.25464	746.37738	100.0000
Totals :				3998.25464	746.37738	

*** End of Report ***

HRMS of compound **30**

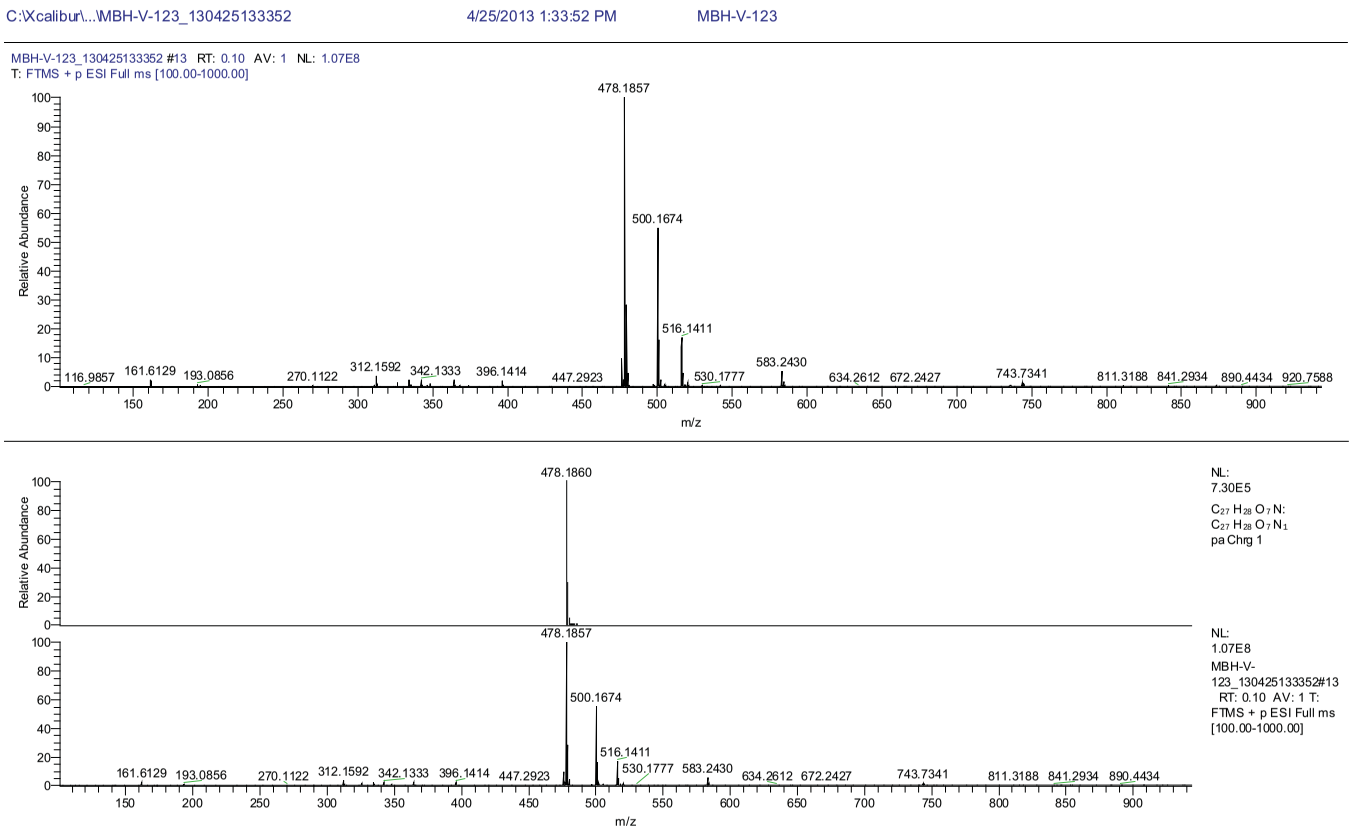

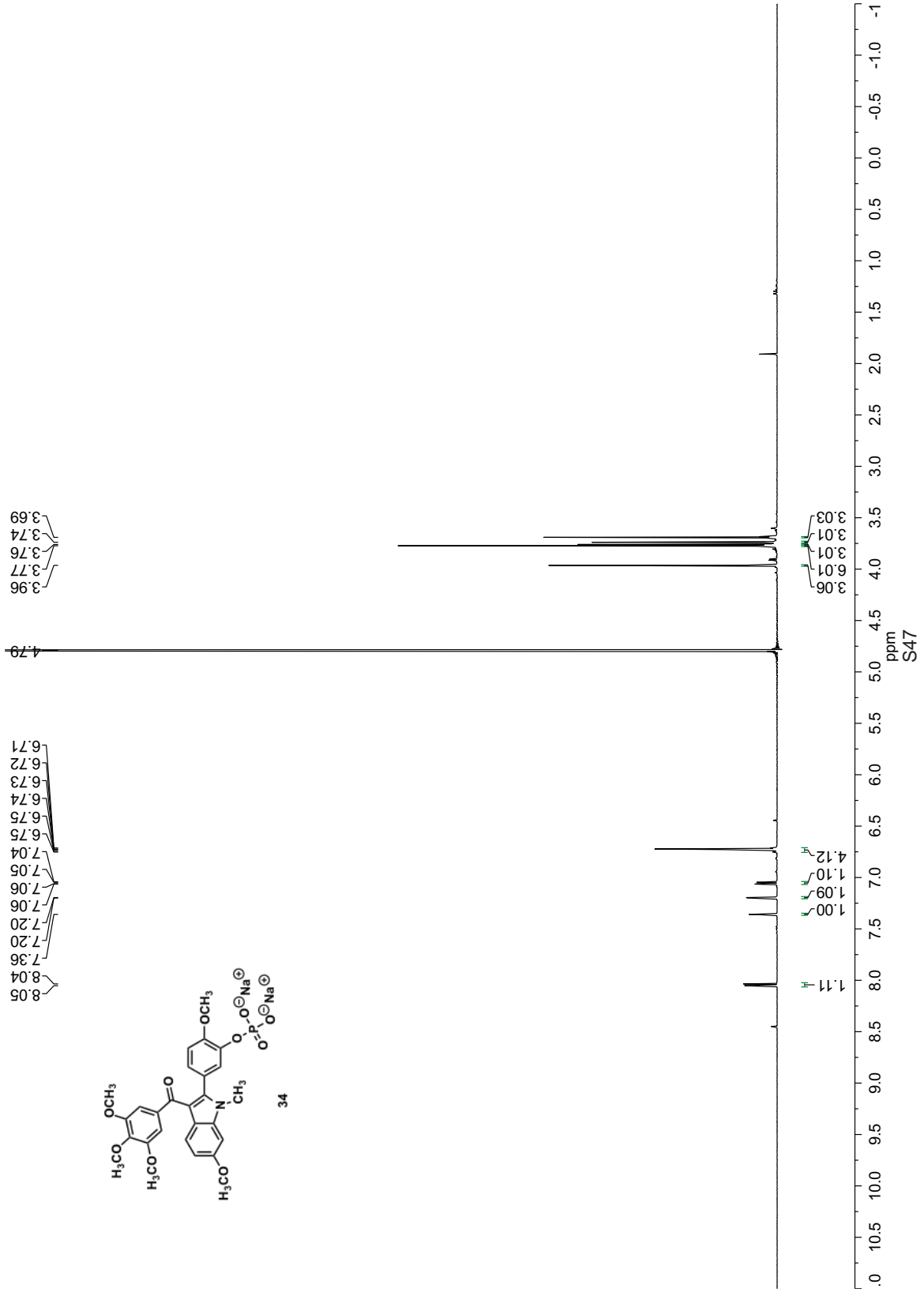
8.05
8.04
7.36
7.20
7.20
7.06
7.06
7.05
7.04
6.75
6.75
6.74
6.73
6.72
6.71
4.79
3.96
3.77
3.76
3.74
3.69
1.11
4.12
1.10
1.09
1.00
6.01
3.01
3.01
3.06
3.03
ppm
S47
34

32.32
48.15
48.43
48.72
49.00
49.28
49.57
49.85
56.10
56.57
56.79
61.04
94.70
107.92
112.54
112.81
114.51
123.11
123.94
124.26
126.41
137.31
139.87
141.47
145.50
145.58
148.81
152.19
153.67
158.75
194.89
OCH3
H3CO
H3CO
H3CO
O
N
CH3
O
P
O
Na
Na
34
ppm
S48

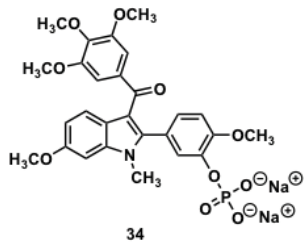
H3CO
OCH3
H3CO
O
OCH3
H3CO
N
CH3
O
O
Na
P
O
Na

34

1.84
140
120
100
80
60
40
20
0
-10
-30
-50
-70
-90
-110
-140
-170
-200
-230
ppm

250

Data File C:\CHEM32\1\DATA\MATT MAC\MBH-V-127000046.D
Sample Name: run2

HPLC traces of compound **34**

```
==========================================================================
Acq. Operator   : Matt Mac
Acq. Instrument : Instrument 1                    Location :   -
Injection Date  : 9/6/2012 10:27:00 AM
Acq. Method     : C:\CHEM32\1\METHODS\MASTERMETHOD.M
Last changed    : 9/6/2012 10:15:31 AM by Matt Mac
                  (modified after loading)
Analysis Method : C:\CHEM32\1\DATA\MATT MAC\MBH-V-127000046.D\DA.M (MASTERMETHOD.M)
Last changed    : 4/19/2013 11:09:00 AM by Matt Mac
Sample Info     :
```

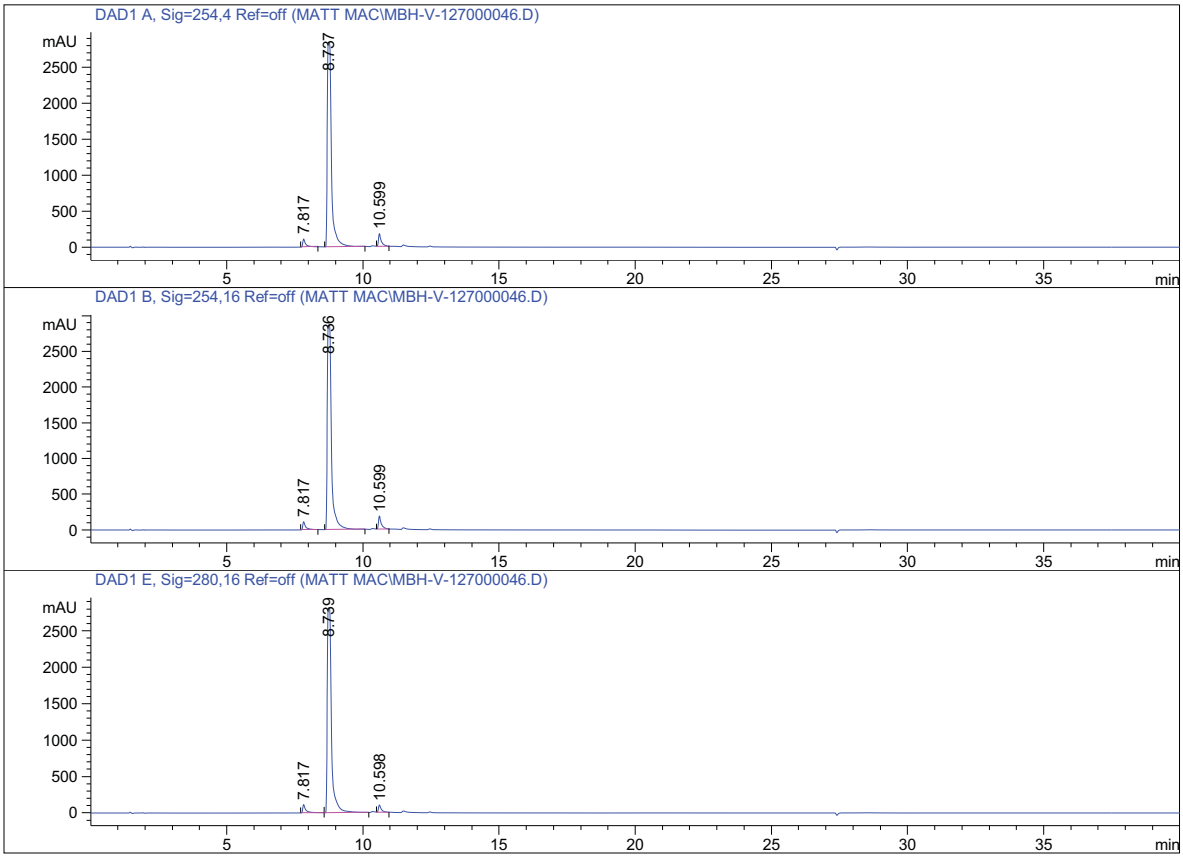

Data File C:\CHEM32\1\DATA\MATT MAC\MBH-V-127000046.D
Sample Name: run2

HPLC traces of compound **34**

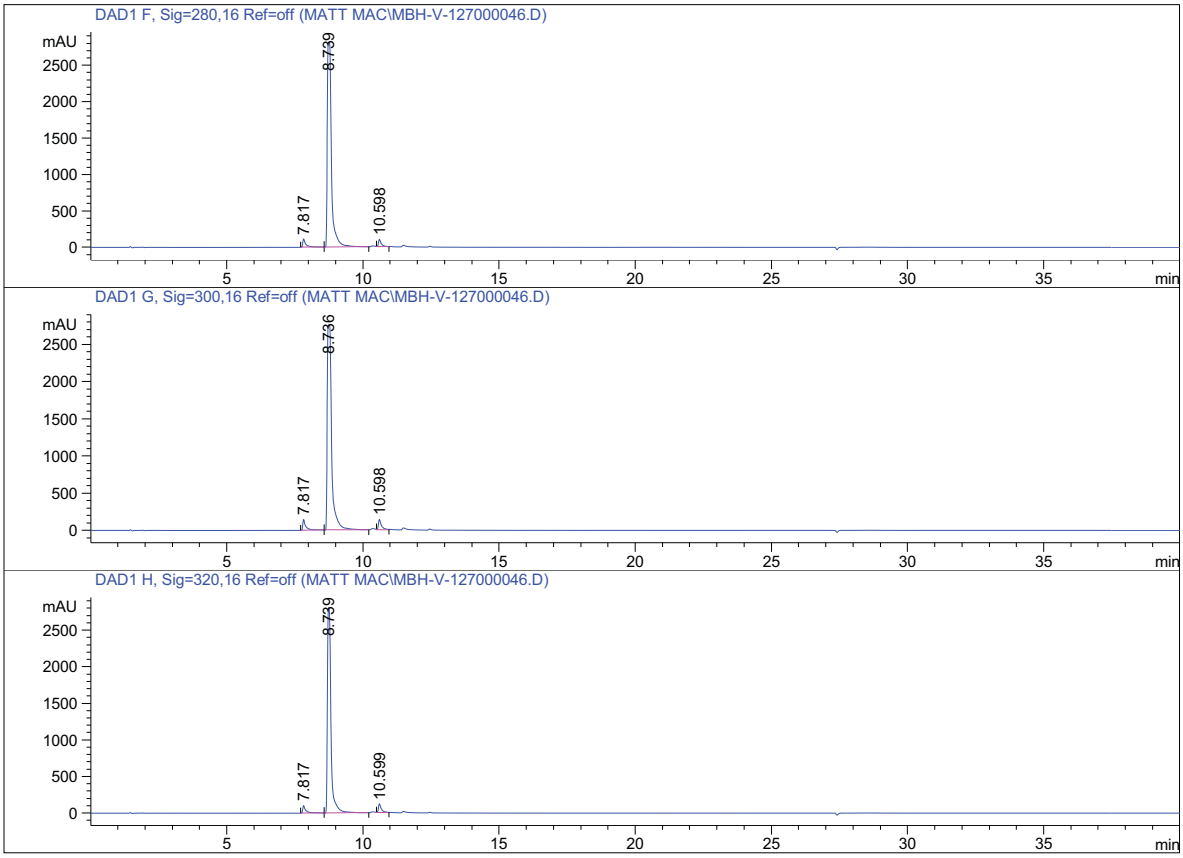


```
=====================================================================
                      Area Percent Report
=====================================================================

Sorted By             :      Signal
Multiplier            :      1.0000
Dilution              :      1.0000
Use Multiplier & Dilution Factor with ISTDs


Signal 1: DAD1 A, Sig=254,4 Ref=off

Peak RetTime Type  Width     Area      Height     Area
  #   [min]        [min]   [mAU*s]     [mAU]       %
----|-------|----|-------|----------|----------|--------|
   1   7.817 BB    0.1052  832.67535  111.45625   2.5651
   2   8.737 BV    0.1642 3.02329e4  2840.07813  93.1333
   3  10.599 VV    0.1089 1396.39478  179.13266   4.3016

Totals :                  3.24620e4  3130.66704
```

Data File C:\CHEM32\1\DATA\MATT MAC\MBH-V-127000046.D
Sample Name: run2

HPLC traces of compound **34**

Signal 2: DAD1 B, Sig=254,16 Ref=off

Peak #	RetTime [min]	Type	Width [min]	Area [mAU*s]	Height [mAU]	Area %
1	7.817	BB	0.1052	847.97809	113.49478	2.5929
2	8.736	BV	0.1639	3.03989e4	2863.14014	92.9509
3	10.599	VV	0.1089	1457.37646	186.94902	4.4562
Totals :				3.27043e4	3163.58394	

Signal 3: DAD1 E, Sig=280,16 Ref=off

Peak #	RetTime [min]	Type	Width [min]	Area [mAU*s]	Height [mAU]	Area %
1	7.817	BV	0.1156	954.00940	113.99458	3.0209
2	8.739	VB	0.1637	2.98201e4	2812.08154	94.4265
3	10.598	VV	0.1121	806.10425	102.11512	2.5526
Totals :				3.15802e4	3028.19125	

Signal 4: DAD1 F, Sig=280,16 Ref=off

Peak #	RetTime [min]	Type	Width [min]	Area [mAU*s]	Height [mAU]	Area %
1	7.817	BV	0.1156	954.00940	113.99458	3.0209
2	8.739	VB	0.1637	2.98201e4	2812.08154	94.4265
3	10.598	VV	0.1121	806.10425	102.11512	2.5526
Totals :				3.15802e4	3028.19125	

Signal 5: DAD1 G, Sig=300,16 Ref=off

Peak #	RetTime [min]	Type	Width [min]	Area [mAU*s]	Height [mAU]	Area %
1	7.817	BV	0.1147	1202.43677	145.03081	3.6154
2	8.736	VB	0.1731	3.09650e4	2755.52661	93.1029
3	10.598	VV	0.1101	1091.45081	138.21220	3.2817
Totals :				3.32588e4	3038.76962	

Data File C:\CHEM32\1\DATA\MATT MAC\MBH-V-127000046.D
Sample Name: run2

HPLC traces of compound **34**

Signal 6: DAD1 H, Sig=320,16 Ref=off

Peak #	RetTime [min]	Type	Width [min]	Area [mAU*s]	Height [mAU]	Area %
1	7.817	BV	0.1145	843.73242	101.98655	3.0931
2	8.739	VB	0.1400	2.54740e4	2803.70117	93.3866
3	10.599	VV	0.1101	960.27112	121.60765	3.5203
Totals :				2.72780e4	3027.29537	

*** End of Report ***

HRMS of compound **34**

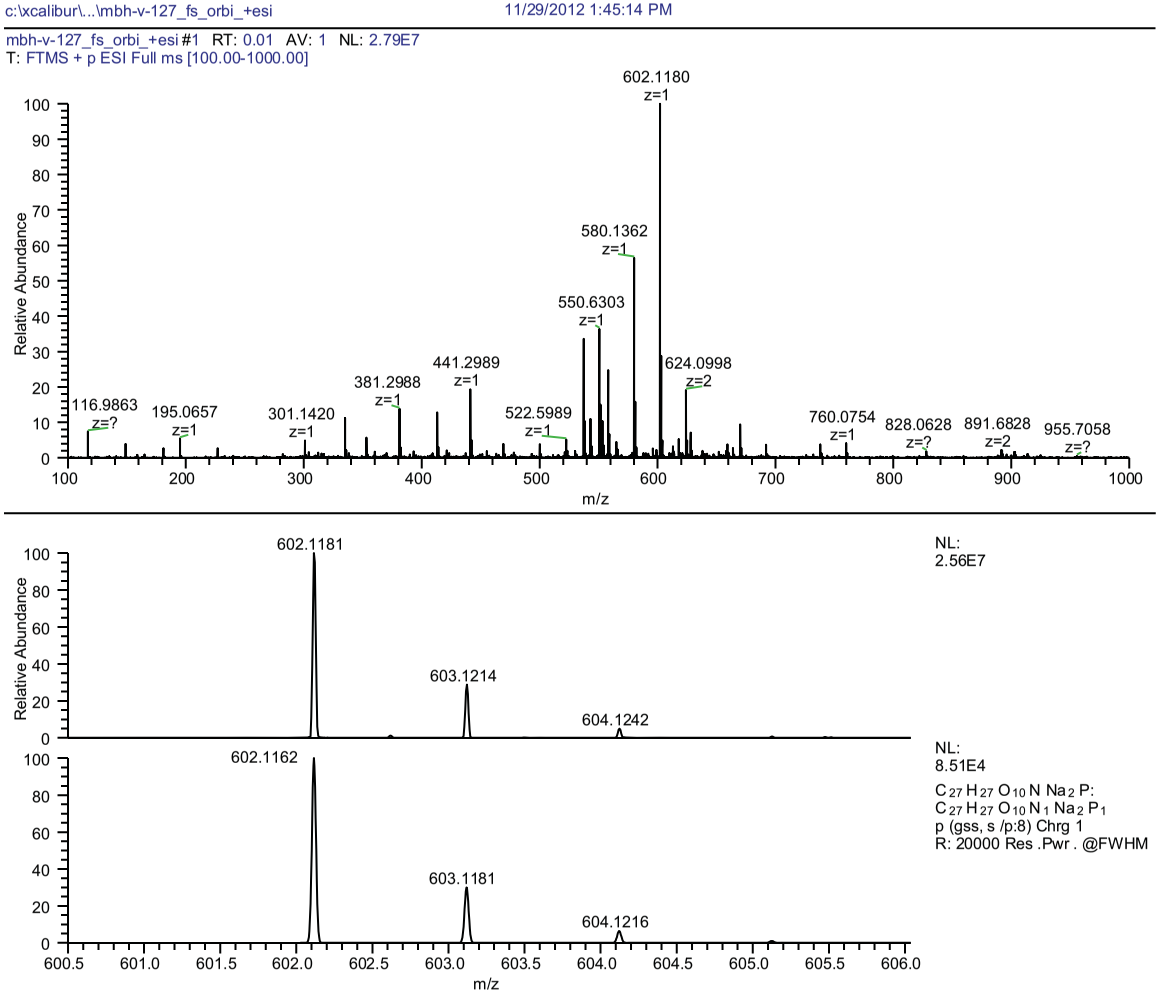

APPENDIX C

Supplementary Data: Synthesis and Biological Evaluation of Indole-based, Anti-cancer Agents Inspired by the Vascular Disrupting Agent 2-(3′-Hydroxy-4′-methoxyphenyl)-3-(3′′, 4′′, 5′′-trimethoxybenzoyl)-6-methoxyindole (OXi8006)

This appendix published as supplementary Data: MacDonough, M. T.; Strecker, T. E.; Hamel, E.; Hall, J. J.; Chaplin, D. J.; Trawick, M. L.; Pinney, K. G. Synthesis and Biological Evaluation of Indole-based, Anti-cancer Agents Inspired by the Vascular Disrupting Agent 2-(3′-Hydroxy-4′-methoxyphenyl)-3-(3′′, 4′′, 5′′-trimethoxybenzoyl)-6-methoxyindole (OXi8006). *Bioorg. Med. Chem.* **2013**, http://dx.doi.org/10.1016/j.bmc.2013.07.028.

Supplementary Data

Synthesis and Biological Evaluation of Indole-based, Anti-cancer Agents Inspired by the Vascular Disrupting Agent 2-(3′-Hydroxy-4′-methoxyphenyl)-3-(3′′,4′′,5′′-trimethoxybenzoyl)-6-methoxyindole (OXi8006)

Matthew T. MacDonough,[a] Tracy E. Strecker,[a] Ernest Hamel,[b] John J. Hall,[a] David J. Chaplin,[c] Mary Lynn Trawick,[a] and Kevin G. Pinney[a*]

[a] Department of Chemistry and Biochemistry, Baylor University, One Bear Place #97348, Waco, Texas, 76798-7348, USA

[b] Screening Technologies Branch, Developmental Therapeutics Program, Division of Cancer Treatment and Diagnosis, National Caner Institute, Frederick National Laboratory for Cancer Research, National Institutes of Health, Frederick, Maryland, 21702, USA

[c] Oxigene Inc., 701 Gateway Boulevard, Suite 210, South San Francisco, California, 94080, USA

[*]Corresponding Author: Kevin G. Pinney

Telephone: 1-254-710-4117

Fax: 1-254-710-4272

Email: Kevin_Pinney@baylor.edu

Table of Contents

12.21
9.06
8.68
8.68
8.67
8.41
8.40
8.06
8.05
6.97
6.97
6.93
6.93
6.91
6.91
6.72
6.71
6.70
6.70
6.68
6.67
6.54
6.54
3.83
3.65
3.32
2.50
2.50
2.50
0.97
3.03
3.01
1.00
2.06
0.98
0.96
0.90
0.84
1.72
0.97
ppm
S3
25

186.67
156.84
148.23
147.08
146.68
146.13
142.76
136.72
128.48
123.26
121.75
121.75
121.70
119.26
117.15
111.95
111.73
111.14
95.02
55.67
55.34
40.02
39.85
39.69
39.52
39.35
39.19
39.02
ppm
S4
25

Data File C:\CHEM32\1\DATA\MATT MAC\RH-I-05000001.D
Sample Name: run1

HPLC traces of compound **25**

```
==========================================================================
Acq. Operator   : Matt Mac
Acq. Instrument : Instrument 1                    Location :   -
Injection Date  : 1/9/2013 5:48:17 PM
Acq. Method     : C:\CHEM32\1\METHODS\MASTERMETHOD.M
Last changed    : 1/9/2013 5:30:58 PM by Matt Mac
Analysis Method : C:\CHEM32\1\METHODS\MASTERMETHOD.M
Last changed    : 1/9/2013 2:04:11 PM by Matt Mac
                  (modified after loading)
```

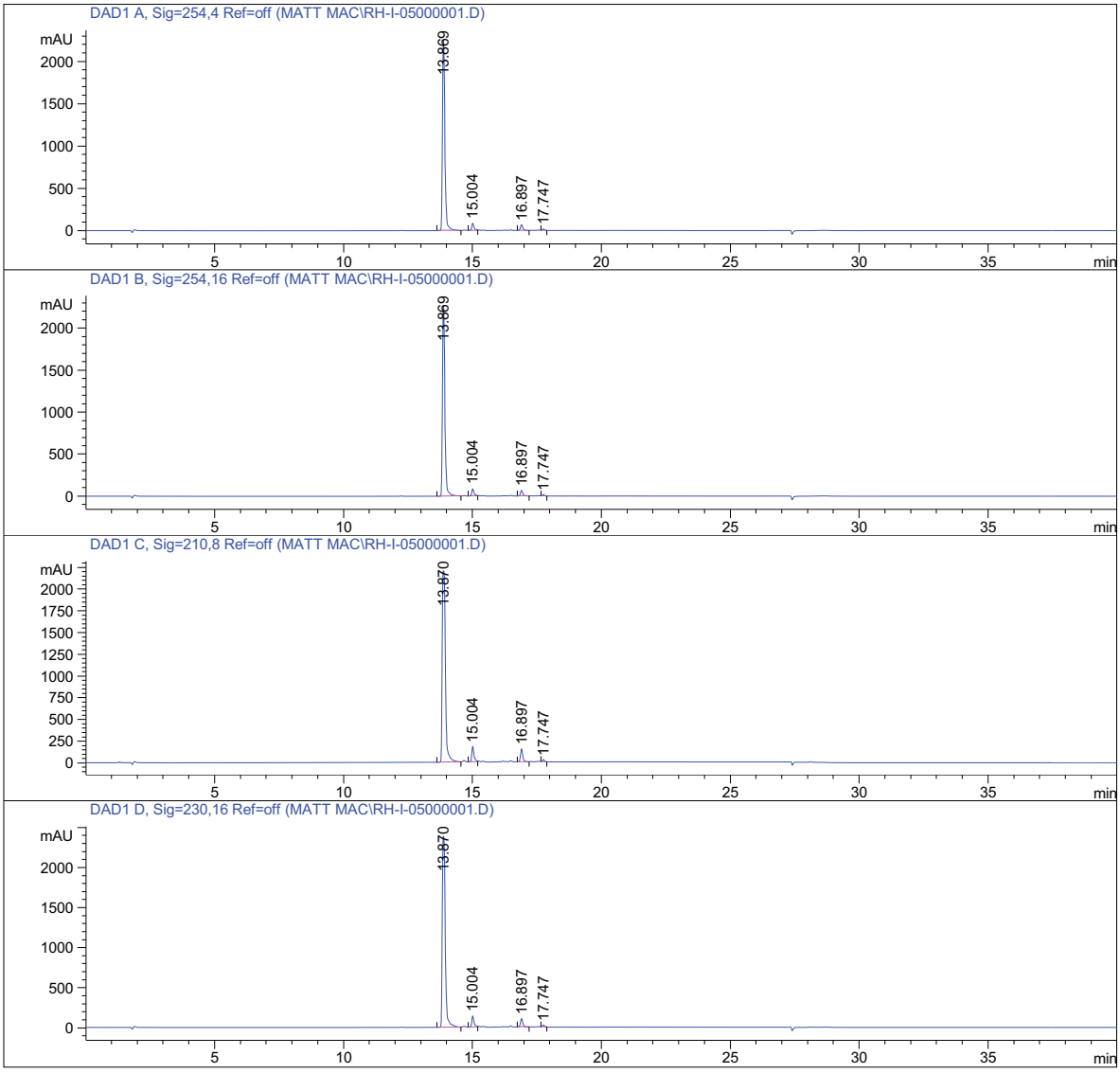

Data File C:\CHEM32\1\DATA\MATT MAC\RH-I-05000001.D
Sample Name: run1

HPLC traces of compound **25**

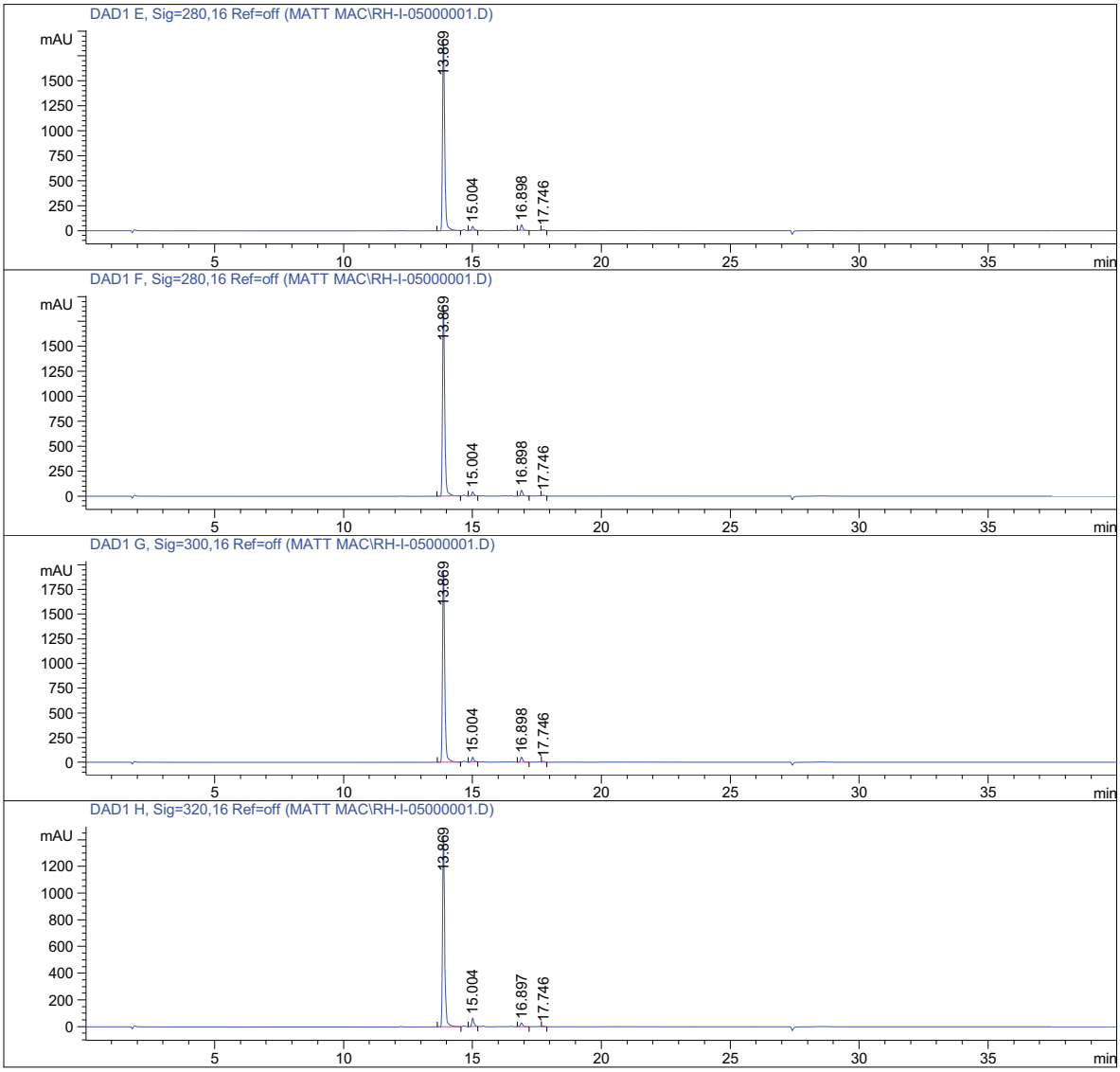

==========

Area Percent Report

==========

Sorted By : Signal
Multiplier : 1.0000
Dilution : 1.0000
Use Multiplier & Dilution Factor with ISTDs

Data File C:\CHEM32\1\DATA\MATT MAC\RH-I-05000001.D
Sample Name: run1

HPLC traces of compound **25**

Signal 1: DAD1 A, Sig=254,4 Ref=off

Peak #	RetTime [min]	Type	Width [min]	Area [mAU*s]	Height [mAU]	Area %
1	13.869	BV	0.0999	1.47072e4	2260.91943	93.3598
2	15.004	BV	0.0927	533.26215	85.62164	3.3851
3	16.897	BB	0.0934	422.24030	67.12388	2.6803
4	17.747	VB	0.0792	90.54961	17.25830	0.5748
Totals :				1.57532e4	2430.92325	

Signal 2: DAD1 B, Sig=254,16 Ref=off

Peak #	RetTime [min]	Type	Width [min]	Area [mAU*s]	Height [mAU]	Area %
1	13.869	BV	0.0999	1.48180e4	2276.77466	93.4310
2	15.004	BV	0.0925	527.65247	84.90611	3.3270
3	16.897	BB	0.0934	423.42865	67.28013	2.6698
4	17.747	VB	0.0792	90.75919	17.31082	0.5723
Totals :				1.58598e4	2446.27172	

Signal 3: DAD1 C, Sig=210,8 Ref=off

Peak #	RetTime [min]	Type	Width [min]	Area [mAU*s]	Height [mAU]	Area %
1	13.870	BV	0.1375	1.91453e4	2200.73096	89.8328
2	15.004	BV	0.0924	1104.12341	177.90869	5.1807
3	16.897	BV	0.0923	923.61694	148.94827	4.3337
4	17.747	VB	0.0799	139.10408	26.22550	0.6527
Totals :				2.13122e4	2553.81342	

Signal 4: DAD1 D, Sig=230,16 Ref=off

Peak #	RetTime [min]	Type	Width [min]	Area [mAU*s]	Height [mAU]	Area %
1	13.870	BV	0.1274	1.90738e4	2383.21851	92.0747
2	15.004	BV	0.0912	840.35529	137.73363	4.0566
3	16.897	BB	0.0935	663.92902	105.42035	3.2050
4	17.747	VB	0.0790	137.49413	26.29313	0.6637

HPLC traces of compound **25**

Totals :			2.07156e4	2652.66561		

Signal 5: DAD1 E, Sig=280,16 Ref=off

Peak #	RetTime [min]	Type	Width [min]	Area [mAU*s]	Height [mAU]	Area %
1	13.869	BV	0.0915	1.14248e4	1918.42883	94.3685
2	15.004	BV	0.0925	267.09799	42.97807	2.2062
3	16.898	BB	0.0918	361.20950	58.69957	2.9836
4	17.746	VB	0.0793	53.48040	10.17261	0.4417
Totals :				1.21066e4	2030.27908	

Signal 6: DAD1 F, Sig=280,16 Ref=off

Peak #	RetTime [min]	Type	Width [min]	Area [mAU*s]	Height [mAU]	Area %
1	13.869	BV	0.0915	1.14248e4	1918.42883	94.3685
2	15.004	BV	0.0925	267.09799	42.97807	2.2062
3	16.898	BB	0.0918	361.20950	58.69957	2.9836
4	17.746	VB	0.0793	53.48040	10.17261	0.4417
Totals :				1.21066e4	2030.27908	

Signal 7: DAD1 G, Sig=300,16 Ref=off

Peak #	RetTime [min]	Type	Width [min]	Area [mAU*s]	Height [mAU]	Area %
1	13.869	BV	0.0926	1.17744e4	1945.19104	94.6889
2	15.004	BV	0.0924	307.58649	49.56367	2.4736
3	16.898	BB	0.0924	309.97372	49.95343	2.4928
4	17.746	VB	0.0794	42.87123	8.13978	0.3448
Totals :				1.24348e4	2052.84792	

Signal 8: DAD1 H, Sig=320,16 Ref=off

Peak #	RetTime [min]	Type	Width [min]	Area [mAU*s]	Height [mAU]	Area %
1	13.869	BV	0.0868	8205.55176	1432.52271	93.2305
2	15.004	BV	0.0903	388.63116	64.46502	4.4156

Data File C:\CHEM32\1\DATA\MATT MAC\RH-I-05000001.D
Sample Name: run1

HPLC traces of compound **25**

Peak #	RetTime [min]	Type	Width [min]	Area [mAU*s]	Height [mAU]	Area %
3	16.897	BB	0.0936	179.76132	28.50370	2.0424
4	17.746	VB	0.0795	27.41720	5.20166	0.3115
Totals :				8801.36144	1530.69308	

*** End of Report ***

HRMS of compound **25**

C:\Xcalibur\...\Matt\2-10-2013\RH-I-05 2/10/2013 5:57:30 PM RH-I-05

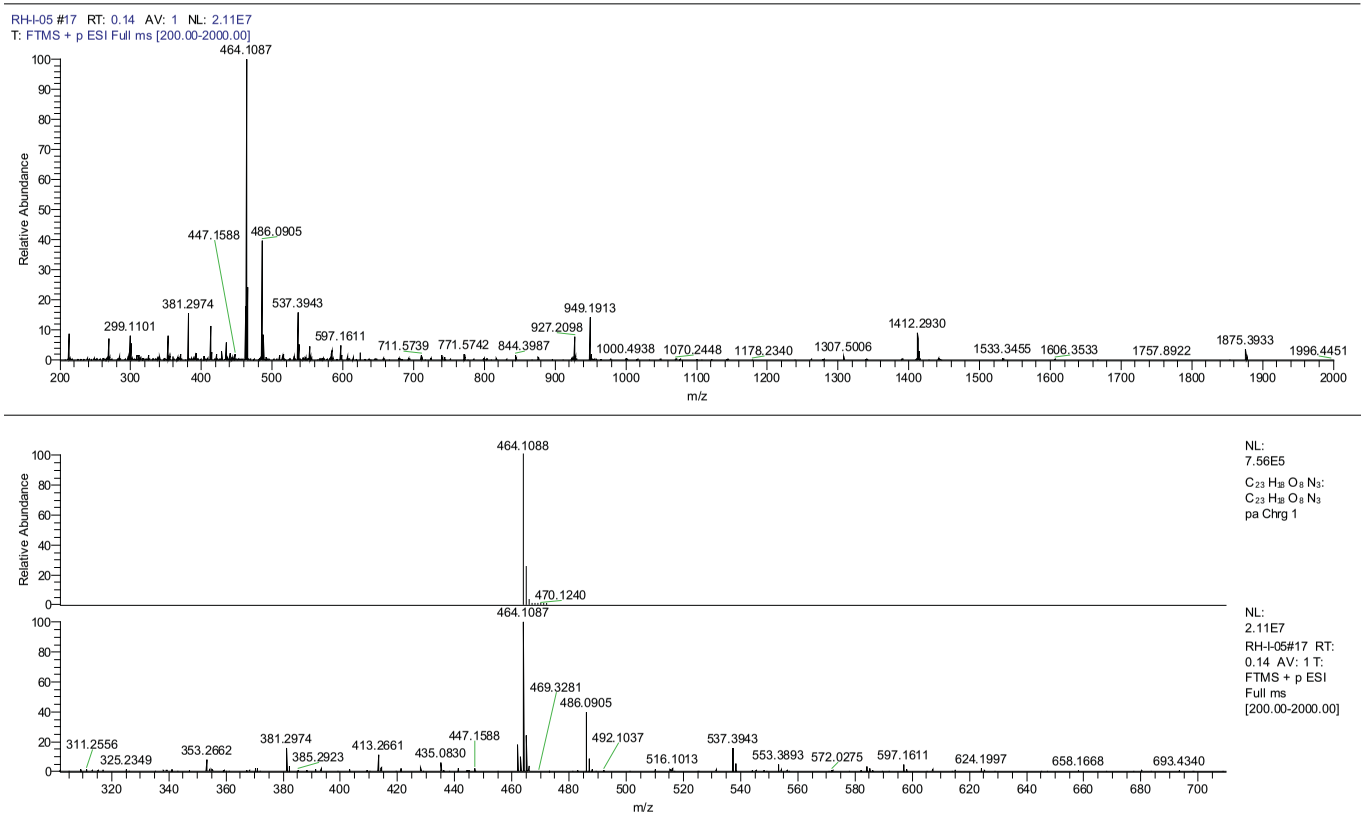

12.04
9.05
7.98
7.97
7.84
7.82
7.62
7.60
6.95
6.95
6.86
6.86
6.85
6.84
6.72
6.71
6.68
6.67
6.64
6.62
3.81
3.65
3.32
2.50
1.04
0.98
2.01
1.00
1.92
1.03
1.09
0.94
1.05
1.01
3.03
3.02
ppm
S11
26

190.09
156.56
148.26
148.00
146.07
145.98
136.63
129.79
123.86
122.59
121.96
121.47
116.83
111.62
111.55
94.87
55.72
55.30
40.02
39.85
39.69
39.64
39.52
39.35
39.19
39.02
ppm
S12
OCH3
OH
O
N
H
O2N
H3CO
26

Data File C:\CHEM32\1\DATA\MATT MAC\MTM-IV-54000001.D
Sample Name: run1

HPLC traces of compound **26**

```
==========================================================================
Acq. Operator   : Matt Mac
Acq. Instrument : Instrument 1                    Location :   -
Injection Date  : 1/9/2013 7:50:53 PM
Acq. Method     : C:\CHEM32\1\METHODS\MASTERMETHOD.M
Last changed    : 1/9/2013 7:39:41 PM by Matt Mac
Analysis Method : C:\CHEM32\1\METHODS\MASTERMETHOD.M
Last changed    : 1/9/2013 2:04:11 PM by Matt Mac
                  (modified after loading)
```

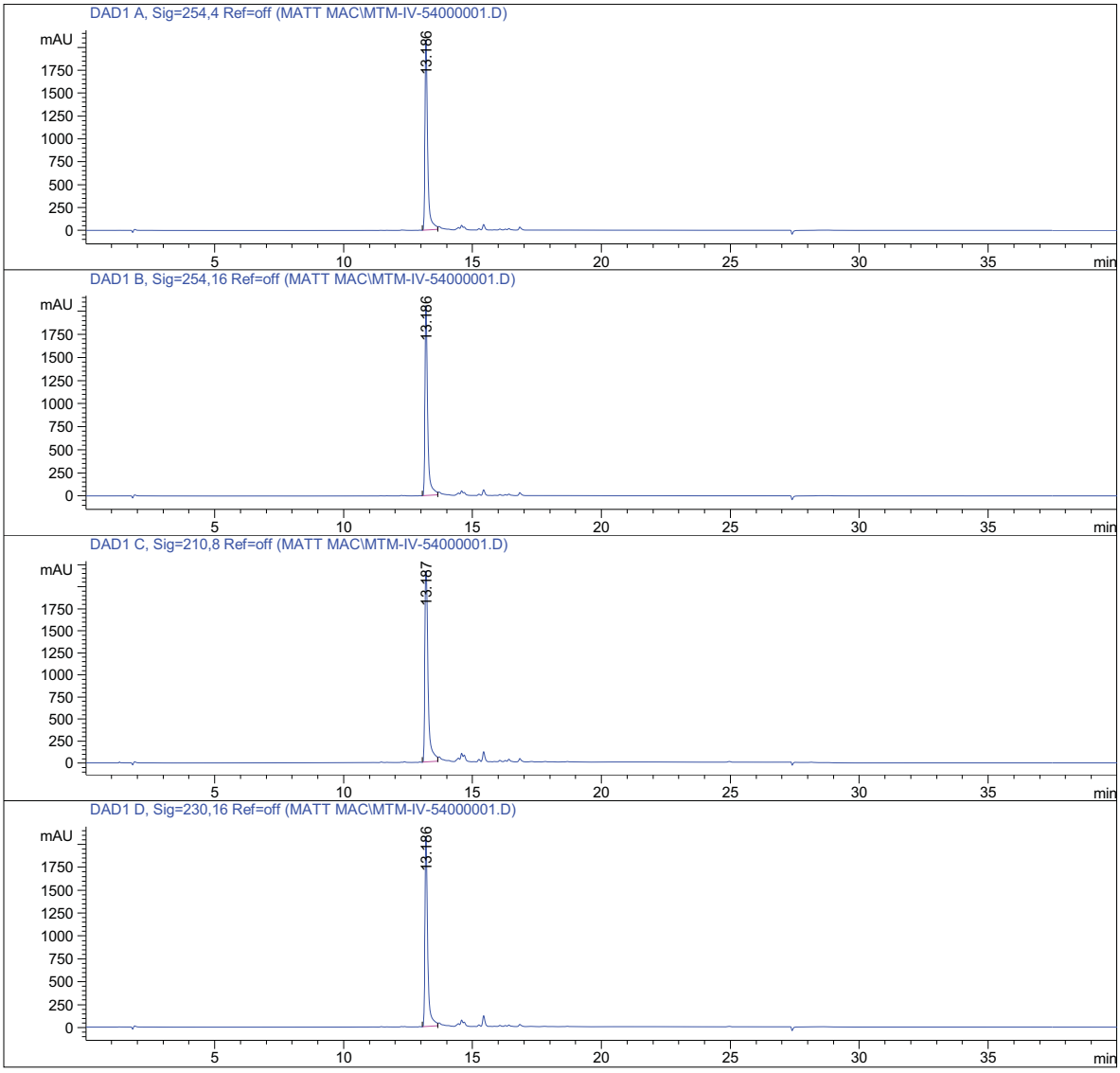

Data File C:\CHEM32\1\DATA\MATT MAC\MTM-IV-54000001.D
Sample Name: run1

HPLC traces of compound **26**

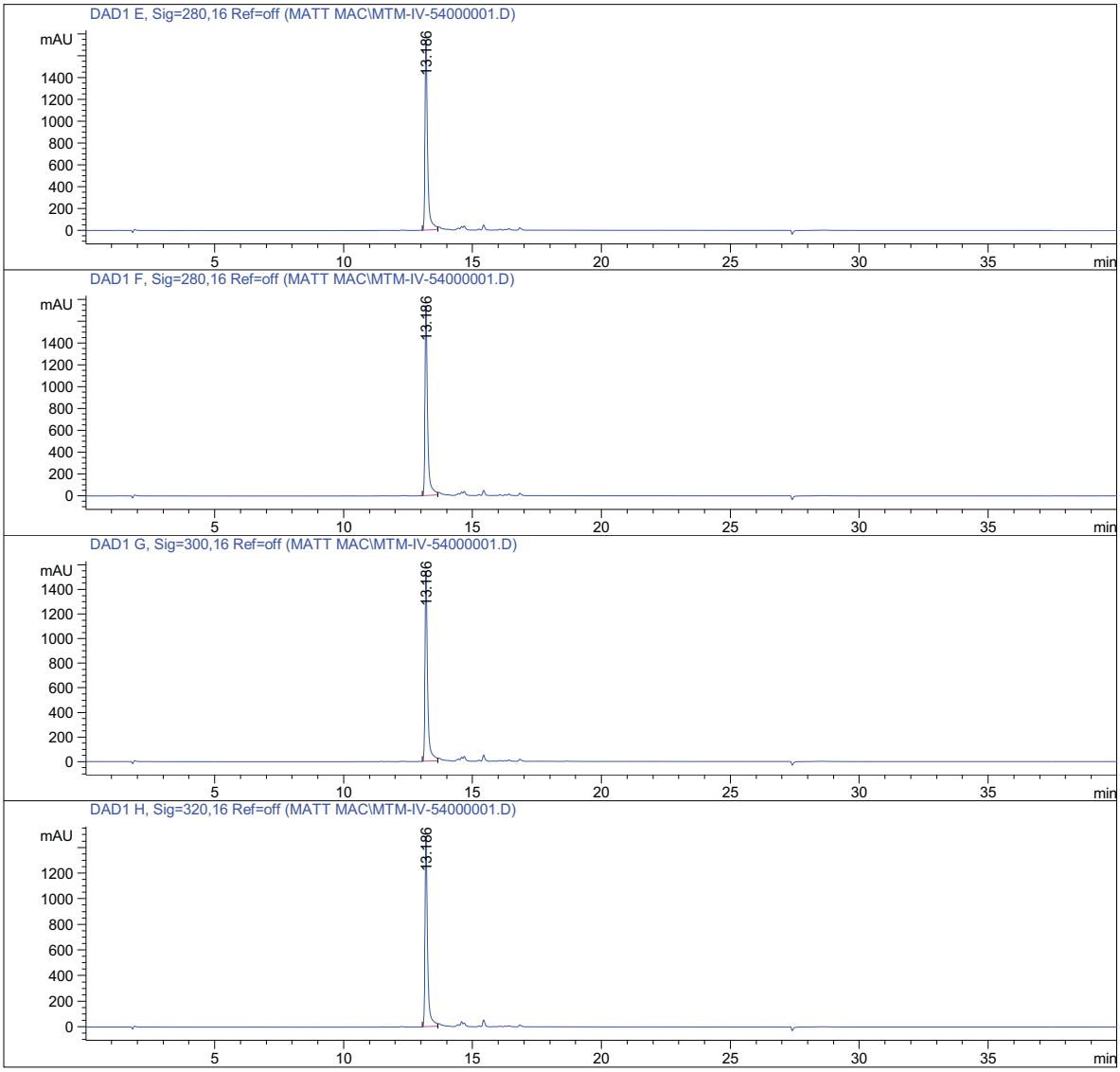

==========

Area Percent Report

==========

Sorted By : Signal
Multiplier : 1.0000
Dilution : 1.0000
Use Multiplier & Dilution Factor with ISTDs

Data File C:\CHEM32\1\DATA\MATT MAC\MTM-IV-54000001.D
Sample Name: run1

HPLC traces of compound **26**

Signal 1: DAD1 A, Sig=254,4 Ref=off

Peak #	RetTime [min]	Type	Width [min]	Area [mAU*s]	Height [mAU]	Area %
1	13.186	BV	0.1094	1.52234e4	2080.05469	100.0000
Totals :				1.52234e4	2080.05469	

Signal 2: DAD1 B, Sig=254,16 Ref=off

Peak #	RetTime [min]	Type	Width [min]	Area [mAU*s]	Height [mAU]	Area %
1	13.186	BV	0.1089	1.50116e4	2063.30054	100.0000
Totals :				1.50116e4	2063.30054	

Signal 3: DAD1 C, Sig=210,8 Ref=off

Peak #	RetTime [min]	Type	Width [min]	Area [mAU*s]	Height [mAU]	Area %
1	13.187	BV	0.1346	1.90632e4	2167.22290	100.0000
Totals :				1.90632e4	2167.22290	

Signal 4: DAD1 D, Sig=230,16 Ref=off

Peak #	RetTime [min]	Type	Width [min]	Area [mAU*s]	Height [mAU]	Area %
1	13.186	BV	0.1104	1.54060e4	2079.89819	100.0000
Totals :				1.54060e4	2079.89819	

Signal 5: DAD1 E, Sig=280,16 Ref=off

Peak #	RetTime [min]	Type	Width [min]	Area [mAU*s]	Height [mAU]	Area %
1	13.186	BV	0.1036	1.22133e4	1745.71863	100.0000
Totals :				1.22133e4	1745.71863	

Data File C:\CHEM32\1\DATA\MATT MAC\MTM-IV-54000001.D
Sample Name: run1

HPLC traces of compound **26**

Signal 6: DAD1 F, Sig=280,16 Ref=off

Peak #	RetTime [min]	Type	Width [min]	Area [mAU*s]	Height [mAU]	Area %
1	13.186	BV	0.1036	1.22133e4	1745.71863	100.0000
Totals :				1.22133e4	1745.71863	

Signal 7: DAD1 G, Sig=300,16 Ref=off

Peak #	RetTime [min]	Type	Width [min]	Area [mAU*s]	Height [mAU]	Area %
1	13.186	BV	0.1009	1.07514e4	1549.86780	100.0000
Totals :				1.07514e4	1549.86780	

Signal 8: DAD1 H, Sig=320,16 Ref=off

Peak #	RetTime [min]	Type	Width [min]	Area [mAU*s]	Height [mAU]	Area %
1	13.186	BV	0.1004	1.02645e4	1488.61096	100.0000
Totals :				1.02645e4	1488.61096	

*** End of Report ***

HRMS of compound **26**

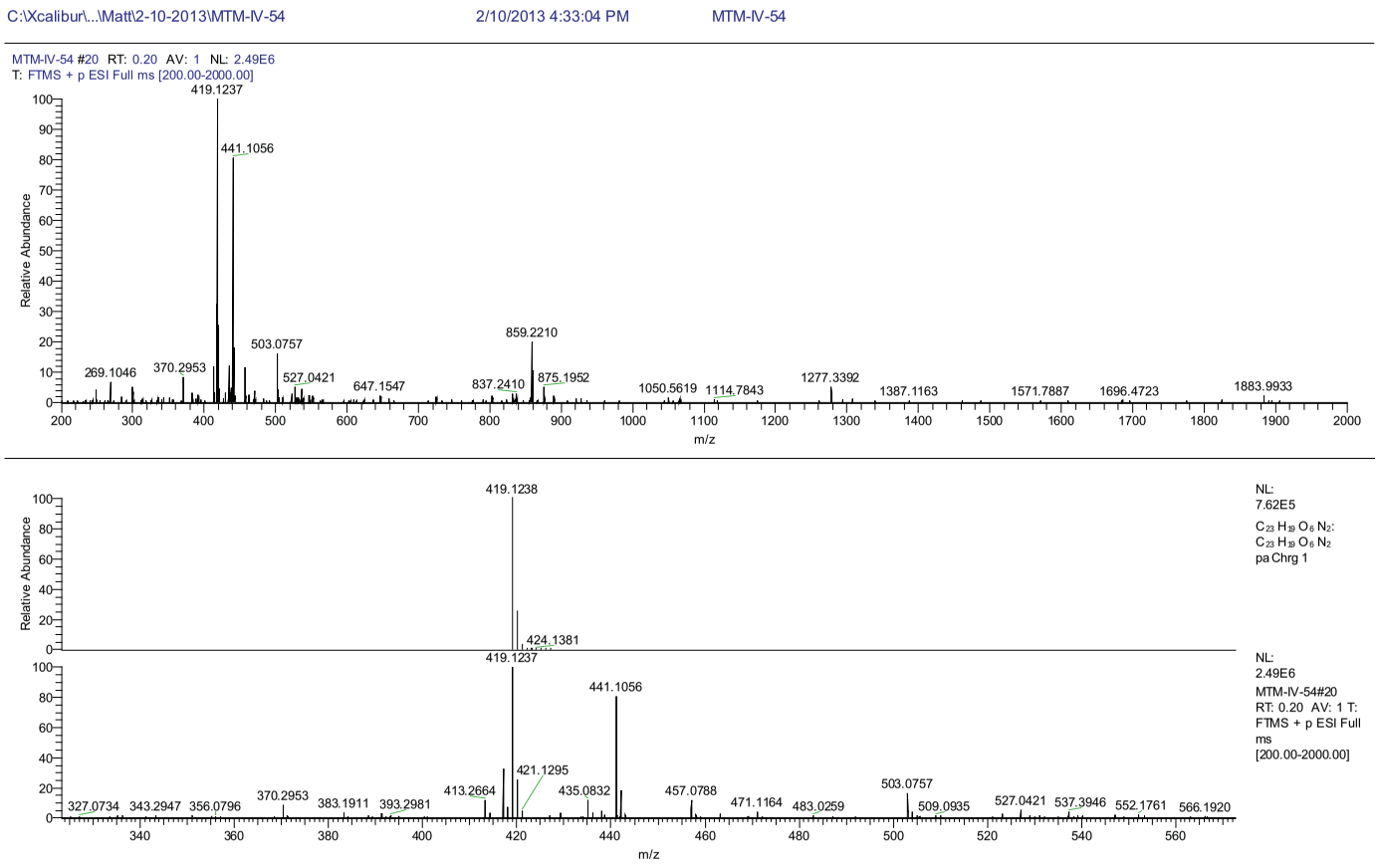

10.95
8.25
8.25
8.25
8.14
8.13
8.13
8.03
8.01
7.94
7.93
7.92
7.92
7.92
7.69
7.50
7.49
7.47
7.06
7.06
6.92
6.92
6.90
6.90
6.81
6.81
6.79
6.78
6.77
6.73
6.72
3.86
3.75
2.81
2.06
2.05
2.05
2.04
0.92
3.12
3.12
0.86
1.00
1.00
1.03
0.90
1.20
1.00
1.05
0.93
1.10
1.12
ppm
S18
27

206.42
206.27
206.26
206.25
206.25
206.10
190.51
158.52
149.15
147.40
145.95
143.10
138.04
135.88
130.11
125.82
125.69
124.84
123.73
123.04
122.91
117.53
113.02
112.73
112.25
95.75
56.48
55.97
30.46
30.31
30.15
29.84
29.69
29.54
ppm
S19
27

Data File C:\CHEM32\1\DATA\MATT MAC\MTM-III-8900002.D
Sample Name: run1

HPLC traces of compound **27**

```
==========================================================================
Acq. Operator   : Matt Mac
Acq. Instrument : Instrument 1                    Location :   -
Injection Date  : 1/8/2013 7:19:42 PM
Acq. Method     : C:\CHEM32\1\METHODS\MASTERMETHOD.M
Last changed    : 1/8/2013 7:13:43 PM by Matt Mac
Analysis Method : C:\CHEM32\1\METHODS\MASTERMETHOD.M
Last changed    : 1/8/2013 8:58:30 AM by Matt Mac
                  (modified after loading)
```

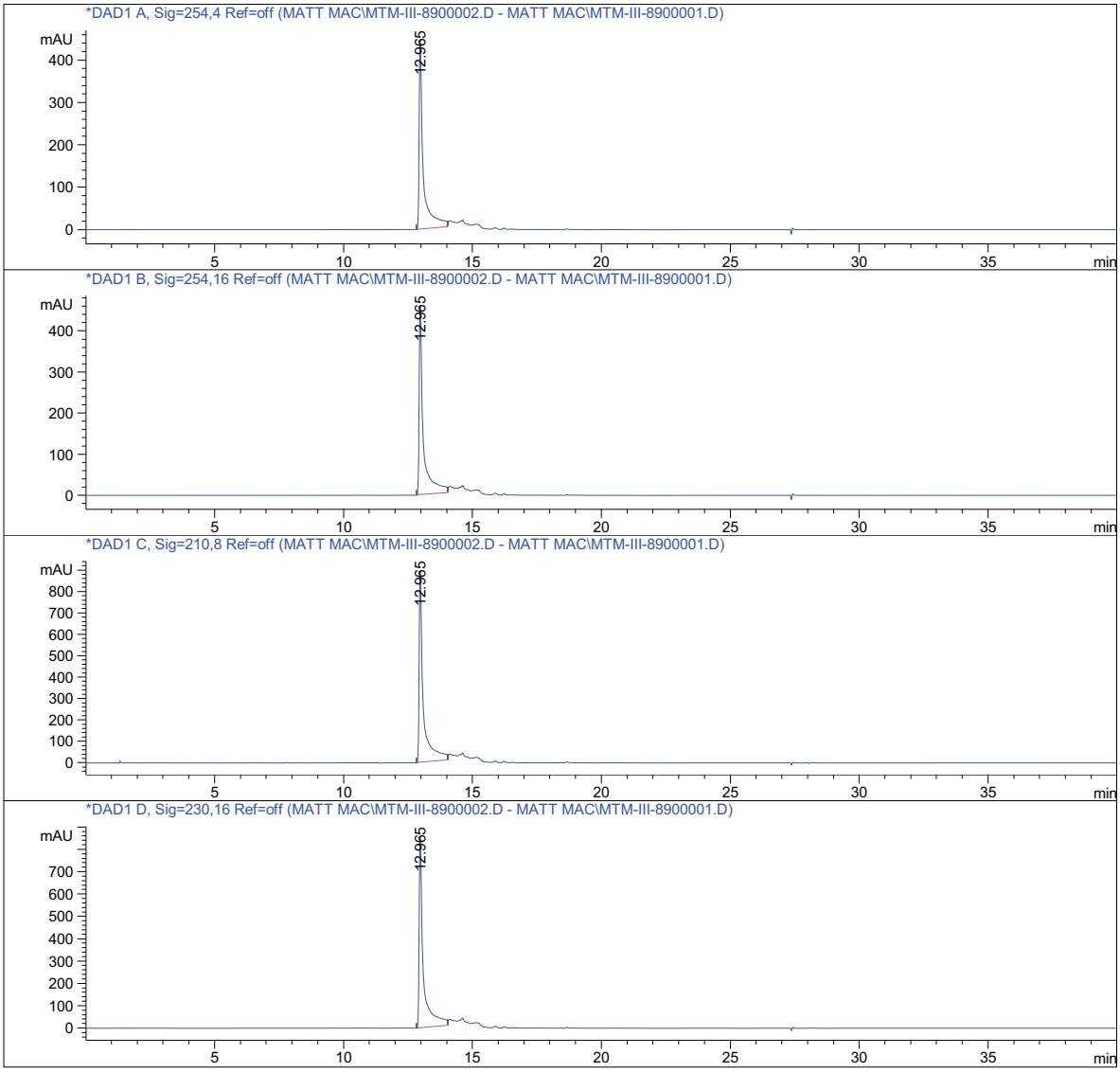

Data File C:\CHEM32\1\DATA\MATT MAC\MTM-III-8900002.D
Sample Name: run1

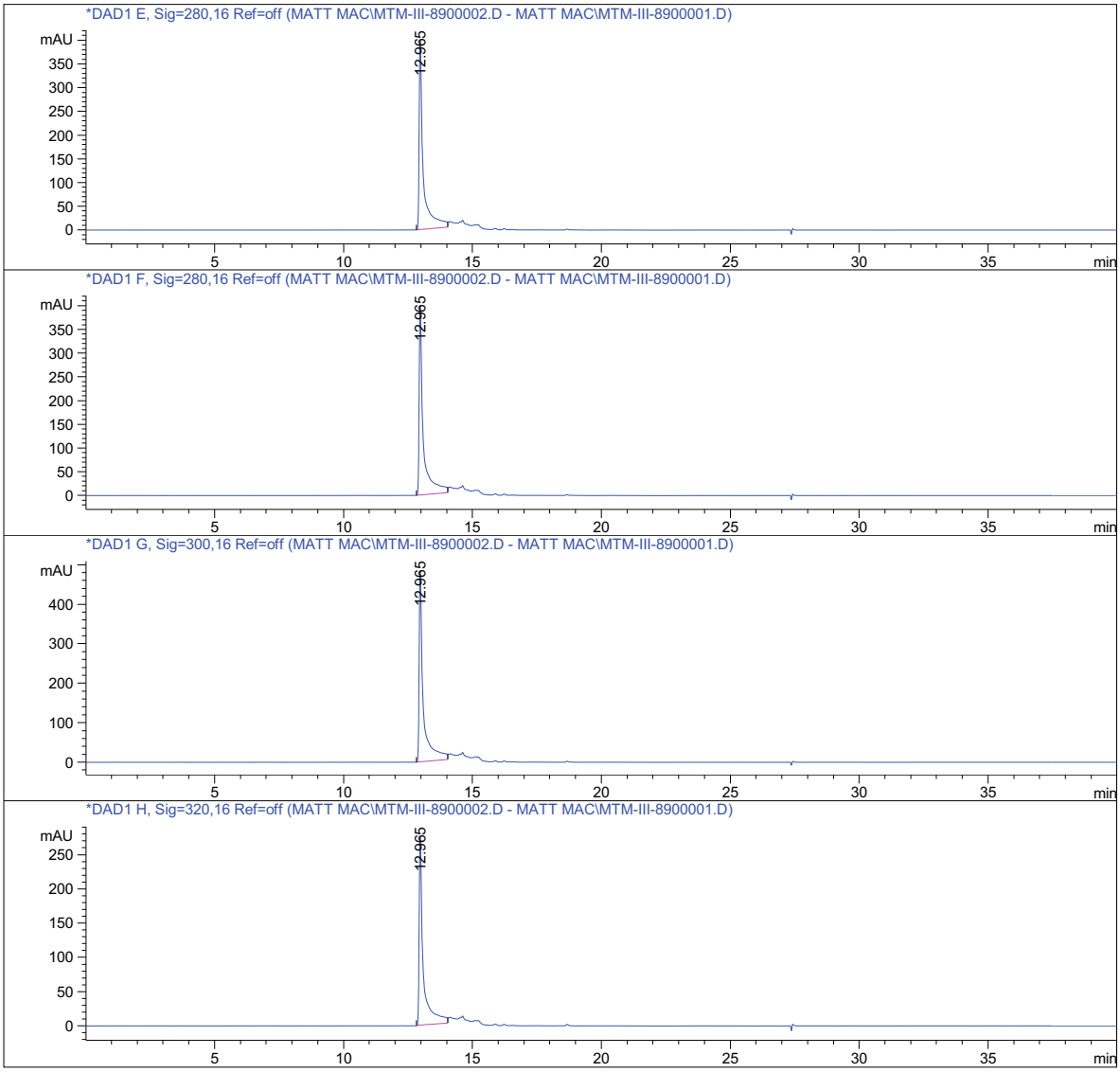

==========

Area Percent Report

==========

Sorted By : Signal
Multiplier : 1.0000
Dilution : 1.0000
Use Multiplier & Dilution Factor with ISTDs

Data File C:\CHEM32\1\DATA\MATT MAC\MTM-III-8900002.D
Sample Name: run1

HPLC traces of compound **27**

Signal 1: DAD1 A, Sig=254,4 Ref=off
Signal has been modified after loading from rawdata file!

Peak #	RetTime [min]	Type	Width [min]	Area [mAU*s]	Height [mAU]	Area %
1	12.965	BV	0.1527	5005.44141	446.85699	100.0000
Totals :				5005.44141	446.85699	

Signal 2: DAD1 B, Sig=254,16 Ref=off
Signal has been modified after loading from rawdata file!

Peak #	RetTime [min]	Type	Width [min]	Area [mAU*s]	Height [mAU]	Area %
1	12.965	BV	0.1526	5166.09326	461.32089	100.0000
Totals :				5166.09326	461.32089	

Signal 3: DAD1 C, Sig=210,8 Ref=off
Signal has been modified after loading from rawdata file!

Peak #	RetTime [min]	Type	Width [min]	Area [mAU*s]	Height [mAU]	Area %
1	12.965	BV	0.1532	1.00692e4	895.34930	100.0000
Totals :				1.00692e4	895.34930	

Signal 4: DAD1 D, Sig=230,16 Ref=off
Signal has been modified after loading from rawdata file!

Peak #	RetTime [min]	Type	Width [min]	Area [mAU*s]	Height [mAU]	Area %
1	12.965	BV	0.1531	9635.51758	857.25806	100.0000
Totals :				9635.51758	857.25806	

Data File C:\CHEM32\1\DATA\MATT MAC\MTM-III-8900002.D
Sample Name: run1

HPLC traces of compound **27**

Signal 5: DAD1 E, Sig=280,16 Ref=off
Signal has been modified after loading from rawdata file!

Peak #	RetTime [min]	Type	Width [min]	Area [mAU*s]	Height [mAU]	Area %
1	12.965	BV	0.1523	4463.91895	399.77322	100.0000
Totals :				4463.91895	399.77322	

Signal 6: DAD1 F, Sig=280,16 Ref=off
Signal has been modified after loading from rawdata file!

Peak #	RetTime [min]	Type	Width [min]	Area [mAU*s]	Height [mAU]	Area %
1	12.965	BV	0.1523	4463.91895	399.77322	100.0000
Totals :				4463.91895	399.77322	

Signal 7: DAD1 G, Sig=300,16 Ref=off
Signal has been modified after loading from rawdata file!

Peak #	RetTime [min]	Type	Width [min]	Area [mAU*s]	Height [mAU]	Area %
1	12.965	BV	0.1524	5404.95215	483.64343	100.0000
Totals :				5404.95215	483.64343	

Signal 8: DAD1 H, Sig=320,16 Ref=off
Signal has been modified after loading from rawdata file!

Peak #	RetTime [min]	Type	Width [min]	Area [mAU*s]	Height [mAU]	Area %
1	12.965	BV	0.1526	3091.80371	276.23389	100.0000
Totals :				3091.80371	276.23389	

==========

*** End of Report ***

HPLC traces of compound **27**

C:\Xcalibur\...\2-10-2013\MTM-III-89 2/10/2013 6:58:21 PM MTM-III-89

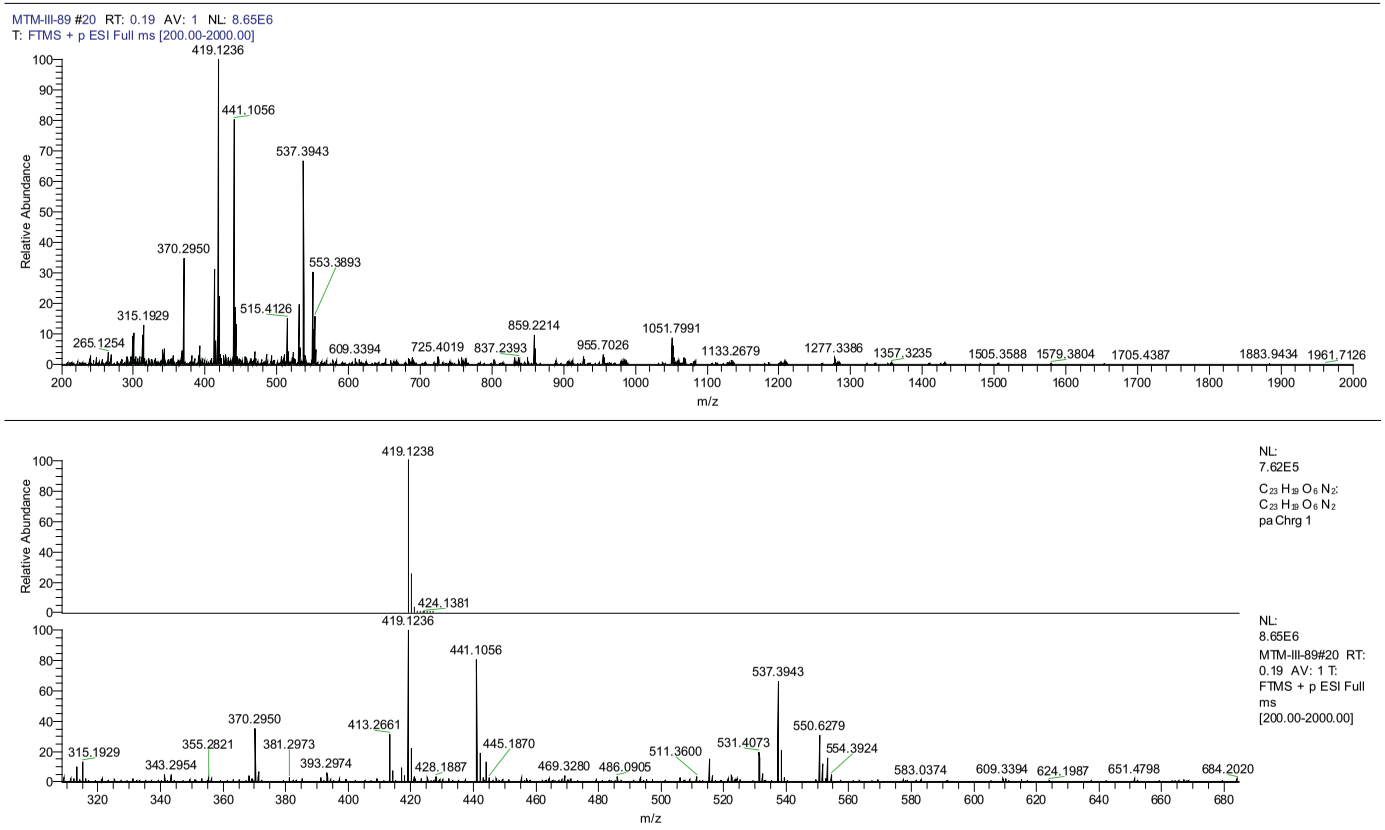

12.02
9.12
7.86
7.84
7.30
7.28
7.27
6.94
6.87
6.86
6.85
6.84
6.81
6.80
6.71
6.70
6.69
3.81
3.73
3.32
2.50
2.08
1.00
1.06
1.15
2.30
1.17
1.24
1.26
1.05
1.16
3.06
3.15
ppm
S25
28

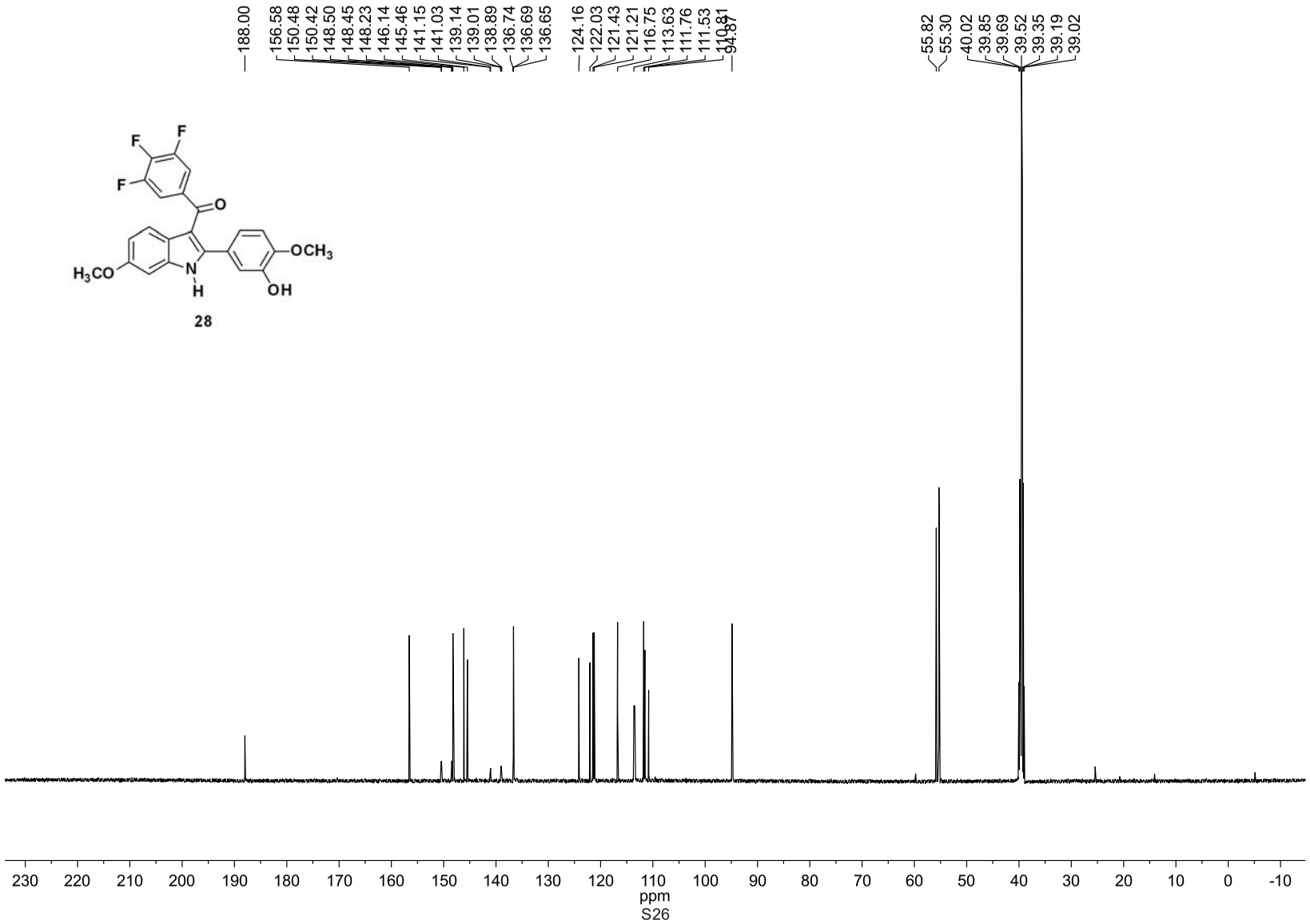
188.00
156.58
150.48
150.42
148.50
148.45
148.23
146.14
145.46
141.15
141.03
139.14
139.01
138.89
136.74
136.69
136.65
124.16
122.03
121.43
121.21
116.75
113.63
111.76
111.53
110.81
94.87
55.82
55.30
40.02
39.85
39.69
39.52
39.35
39.19
39.02
F
F
F
O
OCH3
H3CO
N
H
OH
28
230
220
210
200
190
180
170
160
150
140
130
120
110
100
90
80
70
60
50
40
30
20
10
0
-10
ppm
S26

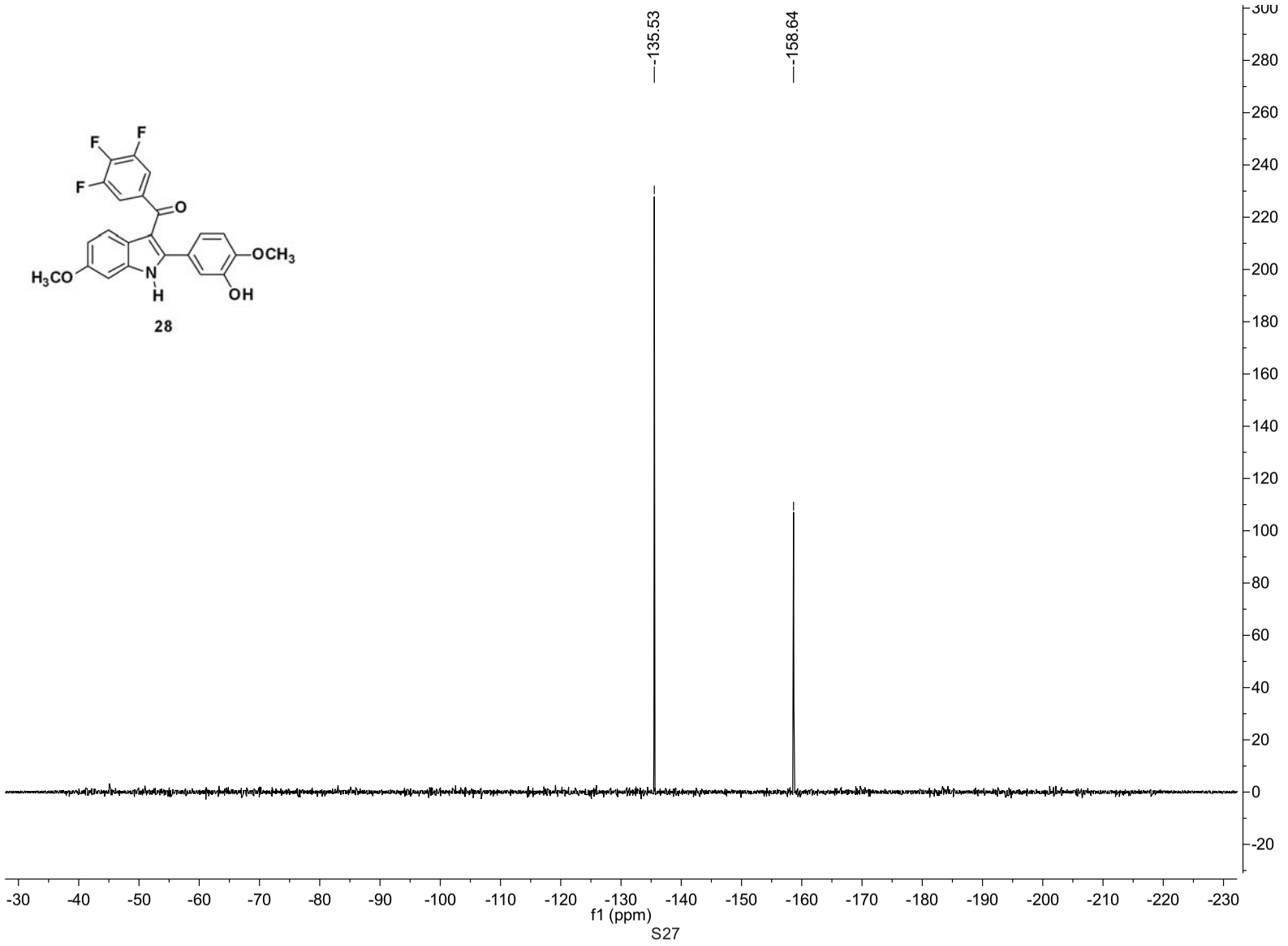
-135.53
-158.64
F
F
F
O
OCH3
H3CO
N
H
OH
28
f1 (ppm)
S27

Data File C:\CHEM32\1\DATA\MATT MAC\SA-I-06000001.D
Sample Name: run1

HPLC traces of compound **28**

```
==========================================================================
Acq. Operator   : Matt Mac
Acq. Instrument : Instrument 1                    Location :   -
Injection Date  : 1/9/2013 2:09:32 PM
Acq. Method     : C:\CHEM32\1\METHODS\MASTERMETHOD.M
Last changed    : 1/9/2013 2:01:45 PM by Matt Mac
Analysis Method : C:\CHEM32\1\METHODS\MASTERMETHOD.M
Last changed    : 1/9/2013 2:04:11 PM by Matt Mac
                  (modified after loading)
```

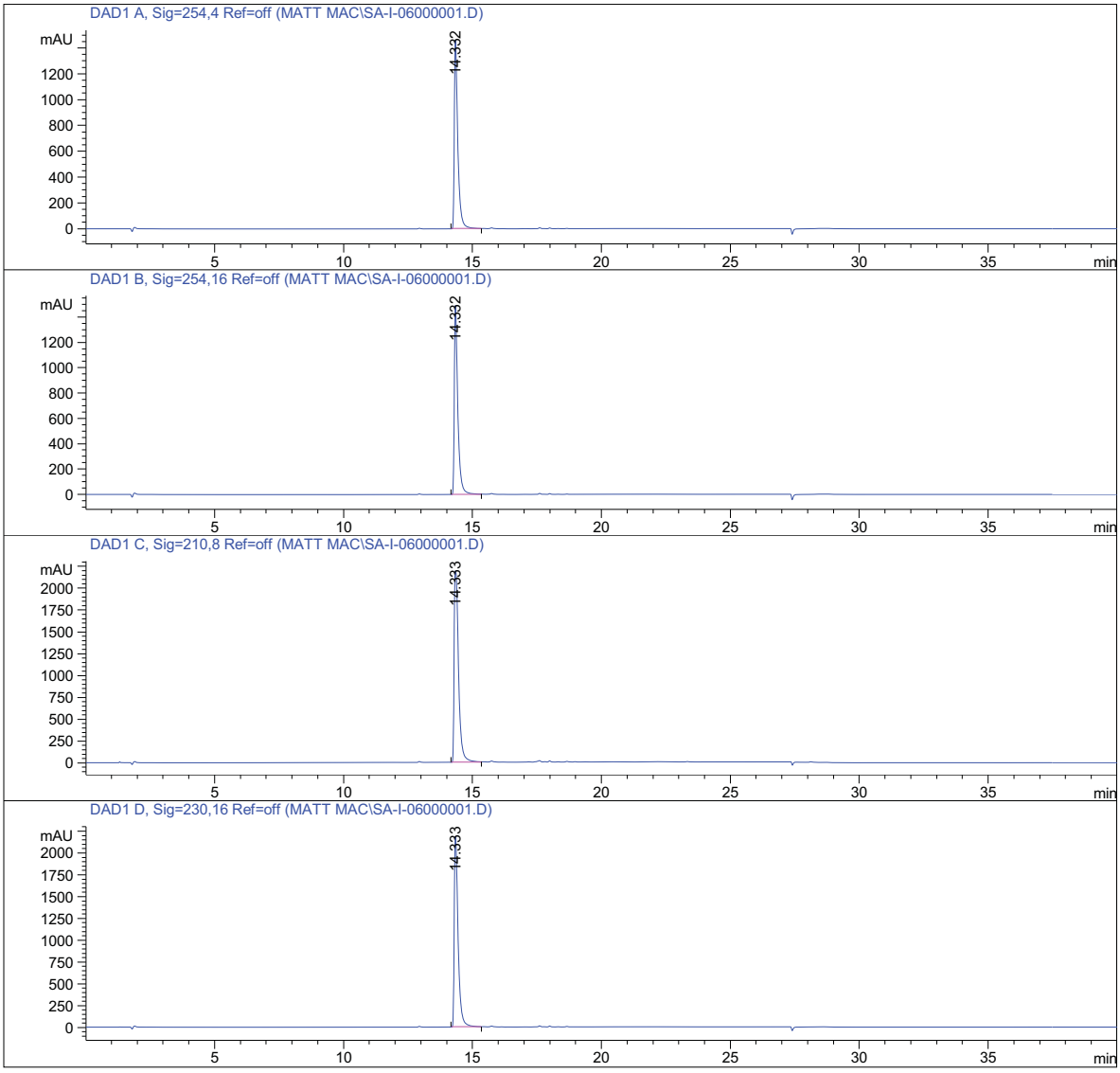

Data File C:\CHEM32\1\DATA\MATT MAC\SA-I-06000001.D
Sample Name: run1

HPLC traces of compound **28**

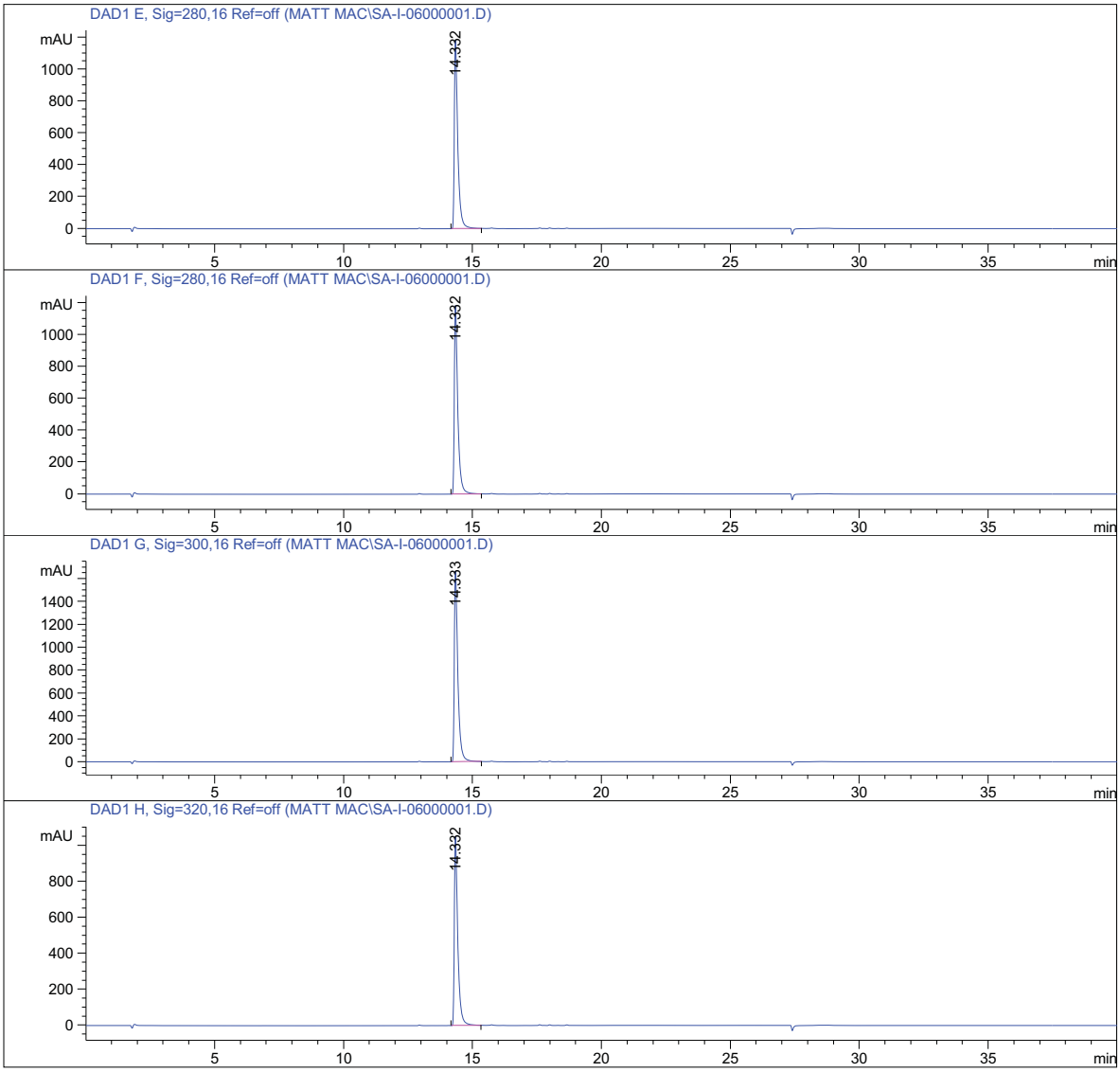

==========

Area Percent Report

==========

Sorted By : Signal
Multiplier : 1.0000
Dilution : 1.0000
Use Multiplier & Dilution Factor with ISTDs

Data File C:\CHEM32\1\DATA\MATT MAC\SA-I-06000001.D
Sample Name: run1

HPLC traces of compound **28**

Signal 1: DAD1 A, Sig=254,4 Ref=off

Peak #	RetTime [min]	Type	Width [min]	Area [mAU*s]	Height [mAU]	Area %
1	14.332	BV	0.1353	1.37124e4	1463.69946	100.0000
Totals :				1.37124e4	1463.69946	

Signal 2: DAD1 B, Sig=254,16 Ref=off

Peak #	RetTime [min]	Type	Width [min]	Area [mAU*s]	Height [mAU]	Area %
1	14.332	BV	0.1354	1.39932e4	1492.83130	100.0000
Totals :				1.39932e4	1492.83130	

Signal 3: DAD1 C, Sig=210,8 Ref=off

Peak #	RetTime [min]	Type	Width [min]	Area [mAU*s]	Height [mAU]	Area %
1	14.333	BV	0.1830	2.61008e4	2190.66382	100.0000
Totals :				2.61008e4	2190.66382	

Signal 4: DAD1 D, Sig=230,16 Ref=off

Peak #	RetTime [min]	Type	Width [min]	Area [mAU*s]	Height [mAU]	Area %
1	14.333	BV	0.1573	2.27137e4	2185.28418	100.0000
Totals :				2.27137e4	2185.28418	

Signal 5: DAD1 E, Sig=280,16 Ref=off

Peak #	RetTime [min]	Type	Width [min]	Area [mAU*s]	Height [mAU]	Area %
1	14.332	BV	0.1345	1.10130e4	1183.79114	100.0000
Totals :				1.10130e4	1183.79114	

Data File C:\CHEM32\1\DATA\MATT MAC\SA-I-06000001.D
Sample Name: run1

HPLC traces of compound **28**

Signal 6: DAD1 F, Sig=280,16 Ref=off

Peak #	RetTime [min]	Type	Width [min]	Area [mAU*s]	Height [mAU]	Area %
1	14.332	BV	0.1345	1.10130e4	1183.79114	100.0000
Totals :				1.10130e4	1183.79114	

Signal 7: DAD1 G, Sig=300,16 Ref=off

Peak #	RetTime [min]	Type	Width [min]	Area [mAU*s]	Height [mAU]	Area %
1	14.333	BB	0.1388	1.58261e4	1666.54199	100.0000
Totals :				1.58261e4	1666.54199	

Signal 8: DAD1 H, Sig=320,16 Ref=off

Peak #	RetTime [min]	Type	Width [min]	Area [mAU*s]	Height [mAU]	Area %
1	14.332	BV	0.1344	9783.57031	1052.70361	100.0000
Totals :				9783.57031	1052.70361	

*** End of Report ***

HRMS of compound **28**

C:\Xcalibur\...\Matt\2-10-2013\SA-I-06 2/10/2013 5:04:20 PM SA-I-06

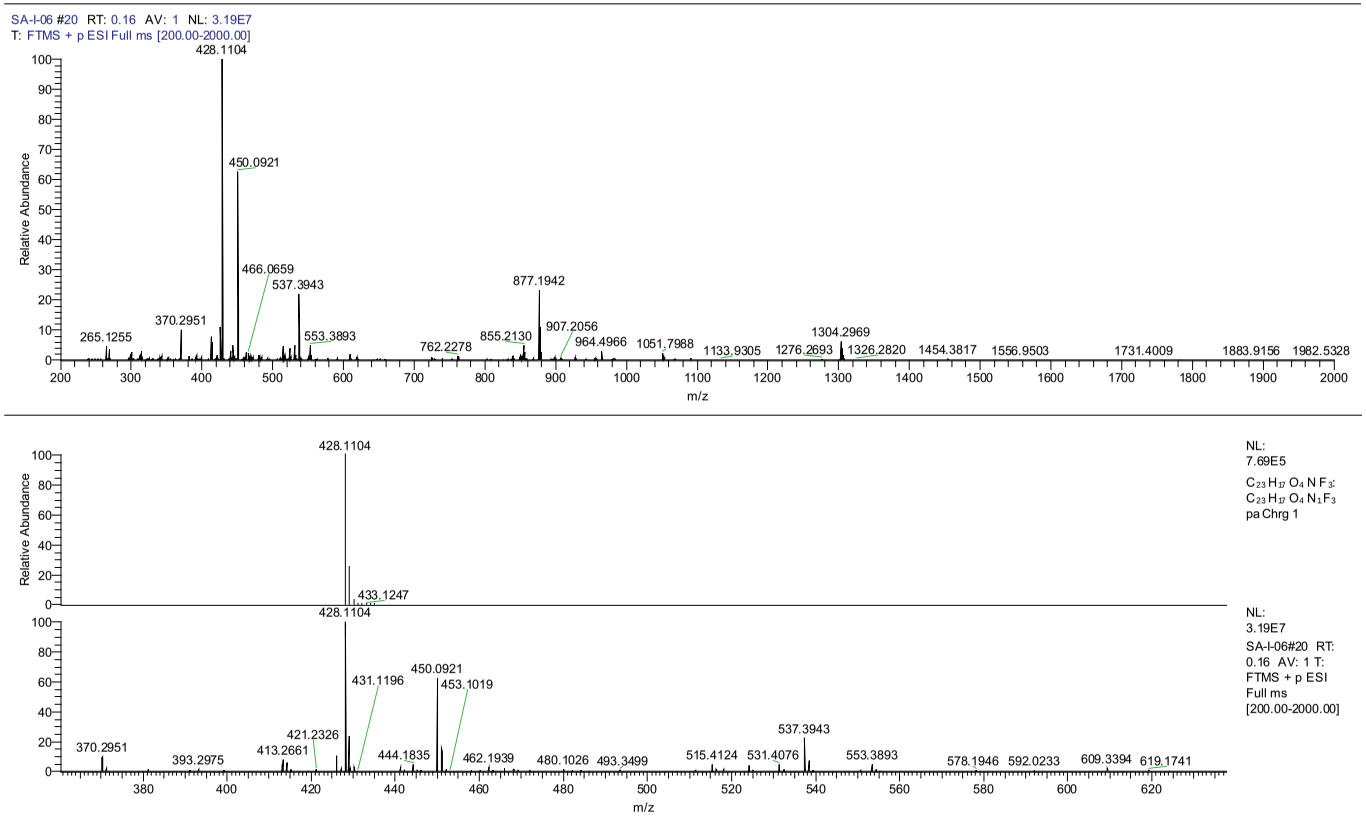

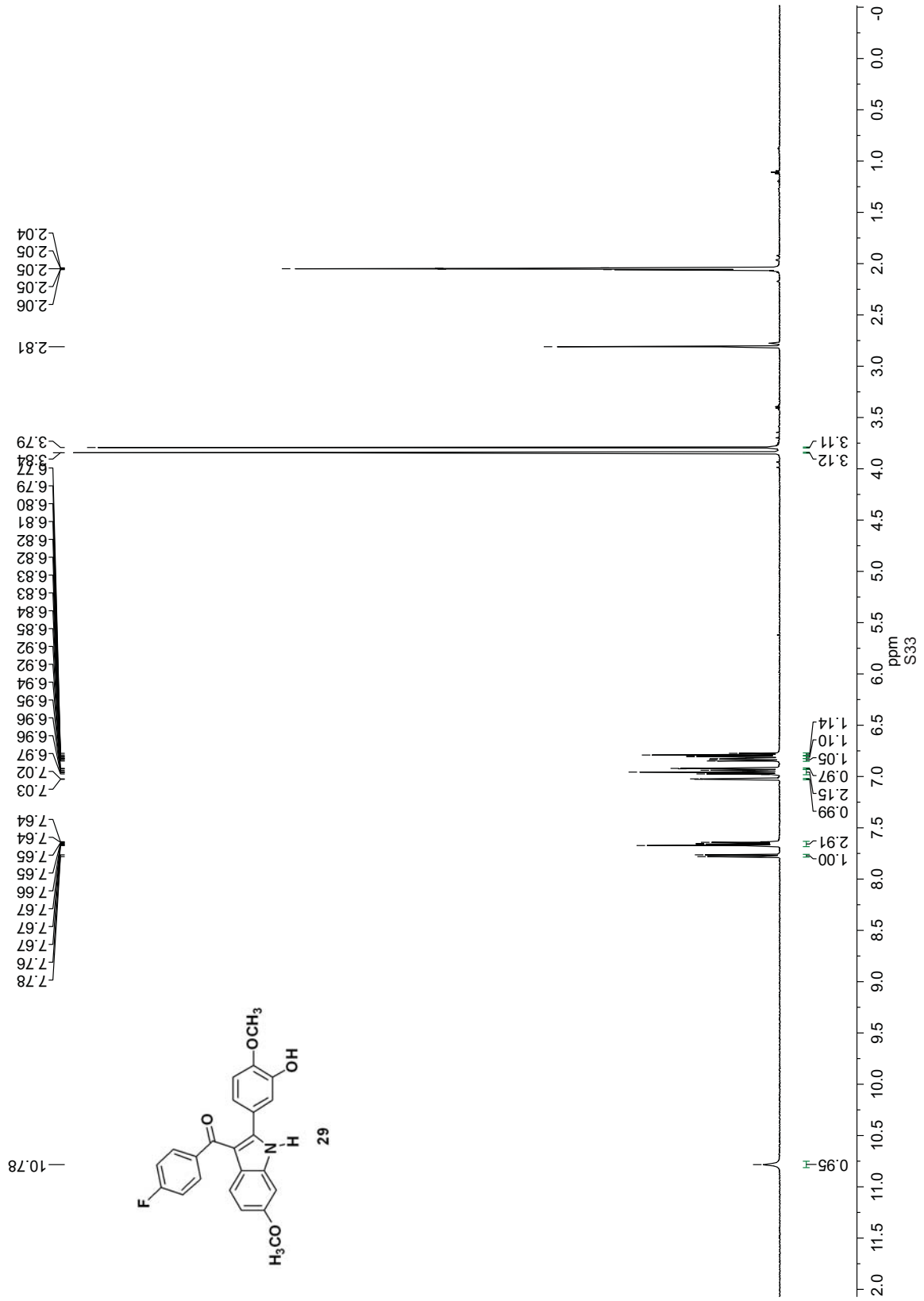
29
S33
ppm

190.57
165.29
163.31
157.16
147.91
146.33
143.04
136.98
136.85
131.84
131.77
125.07
122.98
121.65
121.45
116.04
114.44
114.27
112.19
111.17
111.15
94.49
55.41
54.86
OCH3
OH
O
F
N
H
H3CO
29
ppm
S34

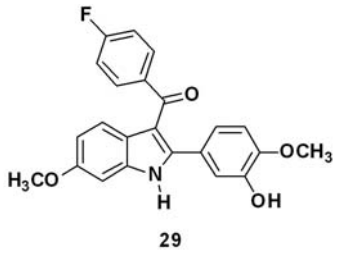
F
O
OCH3
H3CO
N
H
OH

29

-110.75
-30
-40
-50
-60
-70
-80
-90
-100
-110
-120
-130
ppm
-140
-150
-160
-170
-180
-190
-200
-210
-220
-230

S35

Data File C:\CHEM32\1\DATA\MATT MAC\MTM-III-9000006.D
Sample Name: run1

HPLC traces of compound **29**

```
==========================================================================
Acq. Operator   : Matt Mac
Acq. Instrument : Instrument 1                    Location :   -
Injection Date  : 1/8/2013 3:01:17 PM
Acq. Method     : C:\CHEM32\1\METHODS\MASTERMETHOD.M
Last changed    : 1/8/2013 2:20:25 PM by Matt Mac
Analysis Method : C:\CHEM32\1\METHODS\MASTERMETHOD.M
Last changed    : 1/8/2013 8:58:30 AM by Matt Mac
                  (modified after loading)
```

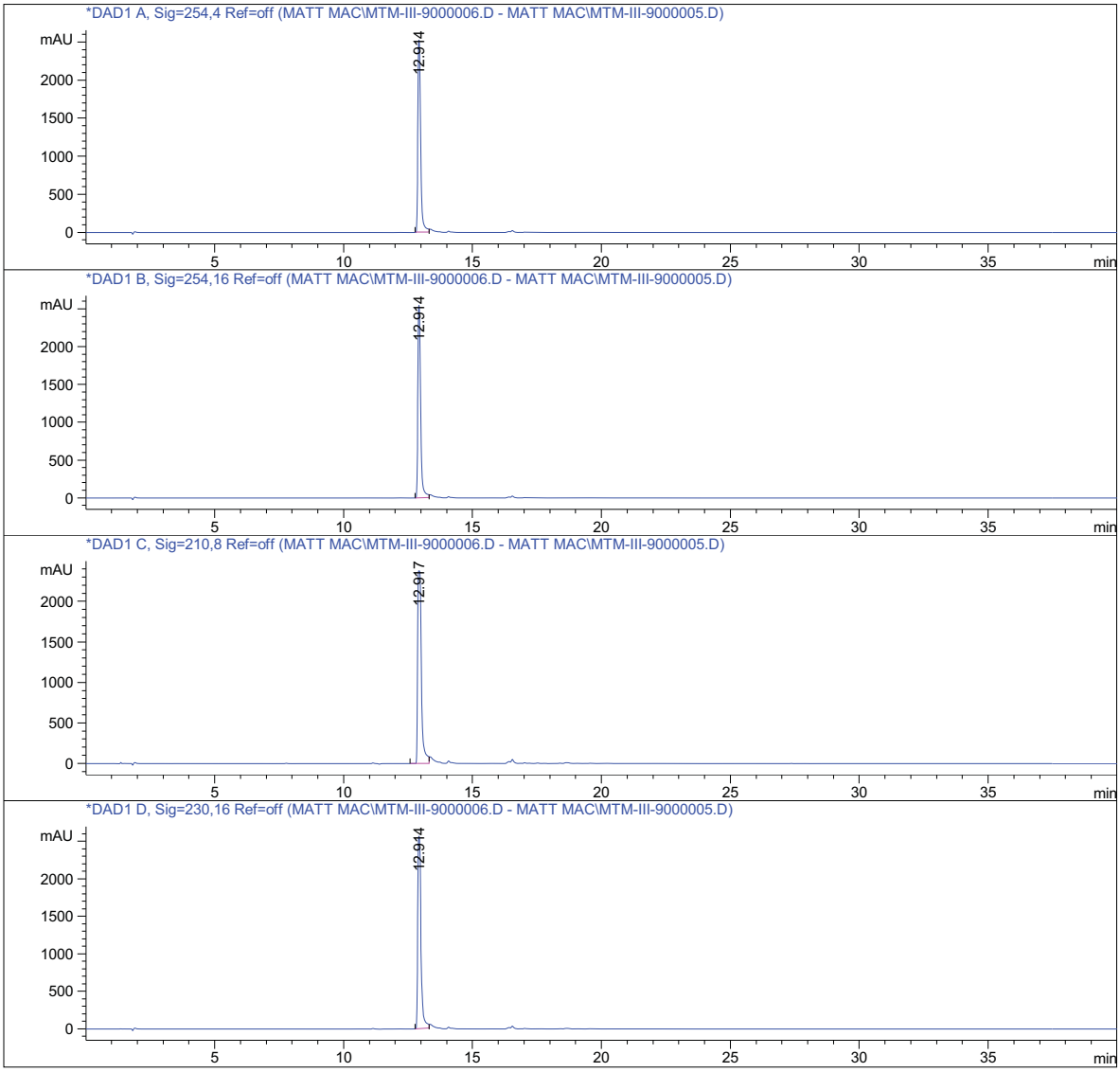

Data File C:\CHEM32\1\DATA\MATT MAC\MTM-III-9000006.D
Sample Name: run1

HPLC traces of compound **29**

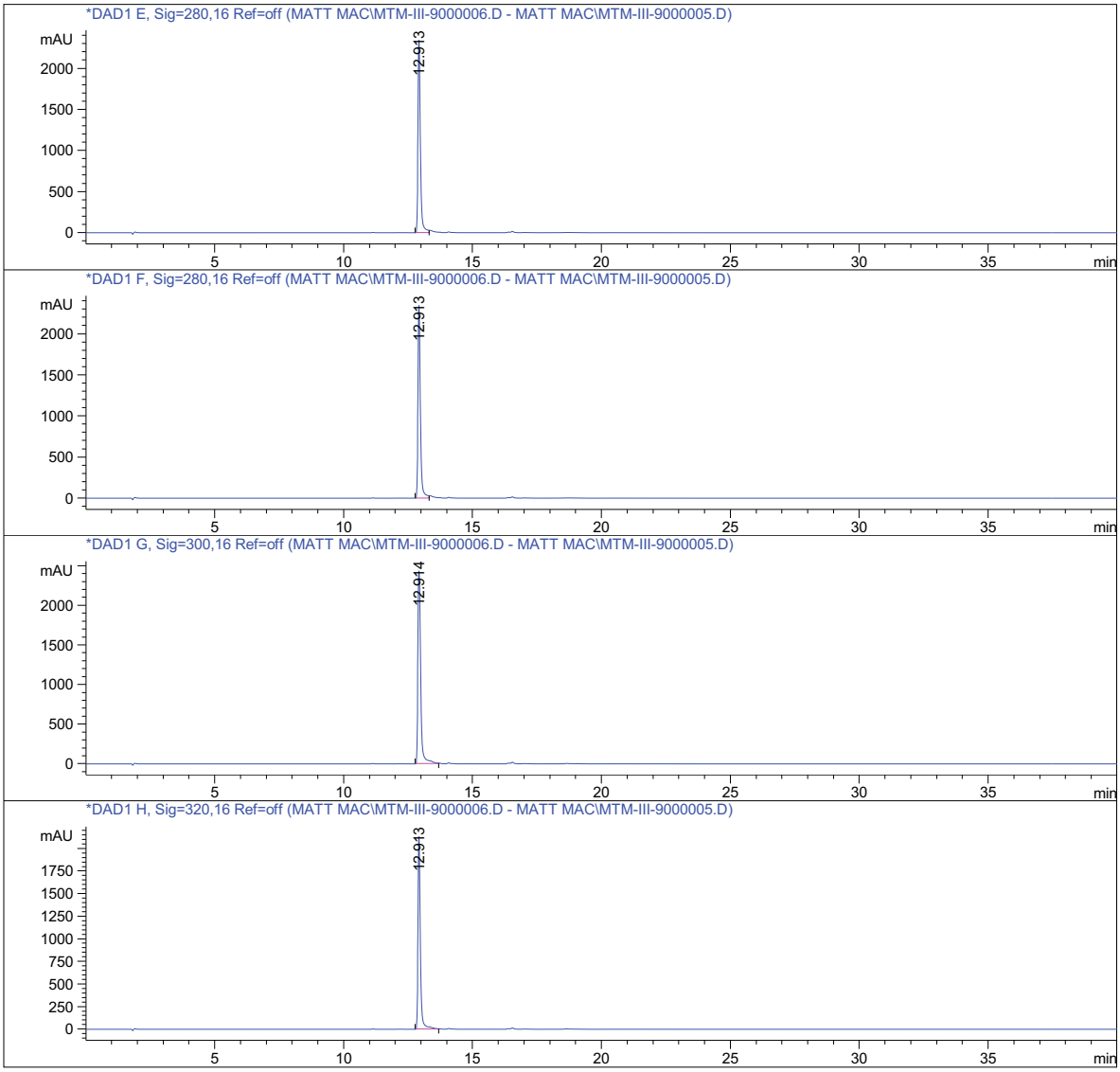

==========

Area Percent Report

==========

Sorted By : Signal
Multiplier : 1.0000
Dilution : 1.0000
Use Multiplier & Dilution Factor with ISTDs

Data File C:\CHEM32\1\DATA\MATT MAC\MTM-III-9000006.D
Sample Name: run1

HPLC traces of compound **29**

Signal 1: DAD1 A, Sig=254,4 Ref=off
Signal has been modified after loading from rawdata file!

Peak #	RetTime [min]	Type	Width [min]	Area [mAU*s]	Height [mAU]	Area %
1	12.914	BV	0.1192	1.93264e4	2528.52637	100.0000
Totals :				1.93264e4	2528.52637	

Signal 2: DAD1 B, Sig=254,16 Ref=off
Signal has been modified after loading from rawdata file!

Peak #	RetTime [min]	Type	Width [min]	Area [mAU*s]	Height [mAU]	Area %
1	12.914	BV	0.1185	1.93178e4	2547.96143	100.0000
Totals :				1.93178e4	2547.96143	

Signal 3: DAD1 C, Sig=210,8 Ref=off
Signal has been modified after loading from rawdata file!

Peak #	RetTime [min]	Type	Width [min]	Area [mAU*s]	Height [mAU]	Area %
1	12.917	BV	0.1595	2.43604e4	2378.69629	100.0000
Totals :				2.43604e4	2378.69629	

Signal 4: DAD1 D, Sig=230,16 Ref=off
Signal has been modified after loading from rawdata file!

Peak #	RetTime [min]	Type	Width [min]	Area [mAU*s]	Height [mAU]	Area %
1	12.914	BV	0.1364	2.25143e4	2565.28882	100.0000
Totals :				2.25143e4	2565.28882	

HPLC traces of compound **29**

Signal 5: DAD1 E, Sig=280,16 Ref=off
Signal has been modified after loading from rawdata file!

Peak #	RetTime [min]	Type	Width [min]	Area [mAU*s]	Height [mAU]	Area %
1	12.913	BV	0.1006	1.53996e4	2346.69971	100.0000
Totals :				1.53996e4	2346.69971	

Signal 6: DAD1 F, Sig=280,16 Ref=off
Signal has been modified after loading from rawdata file!

Peak #	RetTime [min]	Type	Width [min]	Area [mAU*s]	Height [mAU]	Area %
1	12.913	BV	0.1006	1.53996e4	2346.69971	100.0000
Totals :				1.53996e4	2346.69971	

Signal 7: DAD1 G, Sig=300,16 Ref=off
Signal has been modified after loading from rawdata file!

Peak #	RetTime [min]	Type	Width [min]	Area [mAU*s]	Height [mAU]	Area %
1	12.914	BV	0.1206	1.89096e4	2435.48779	100.0000
Totals :				1.89096e4	2435.48779	

Signal 8: DAD1 H, Sig=320,16 Ref=off
Signal has been modified after loading from rawdata file!

Peak #	RetTime [min]	Type	Width [min]	Area [mAU*s]	Height [mAU]	Area %
1	12.913	BV	0.0976	1.38327e4	2135.87988	100.0000
Totals :				1.38327e4	2135.87988	

*** End of Report ***

HRMS of compound **29**

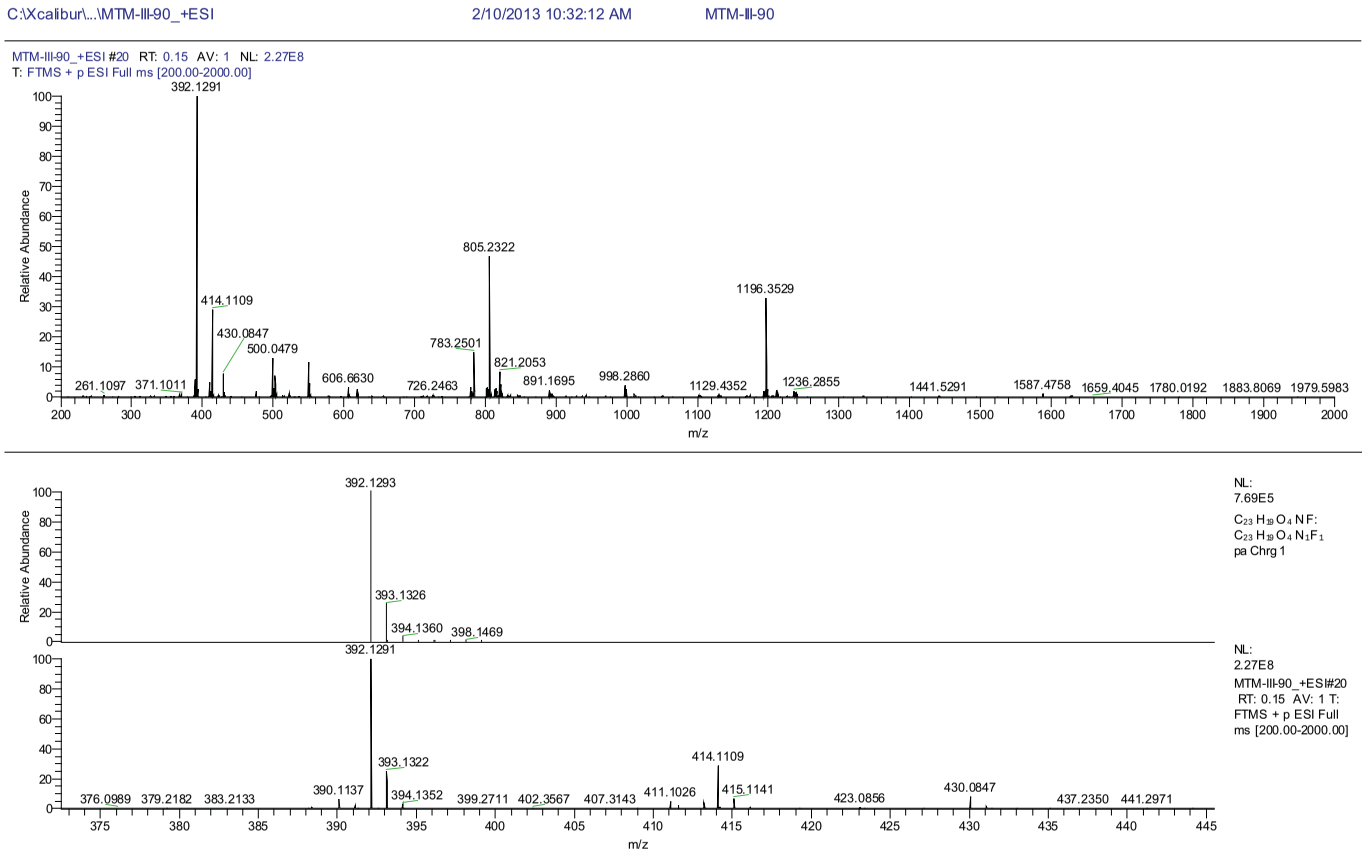

12.10
9.00
8.00
7.98
7.90
6.96
6.96
6.91
6.90
6.89
6.88
6.64
6.63
3.82
3.66
3.32
2.50
2.50
2.50
0.98
3.02
1.00
1.00
1.94
1.98
0.99
3.03
3.08
ppm
S41
30

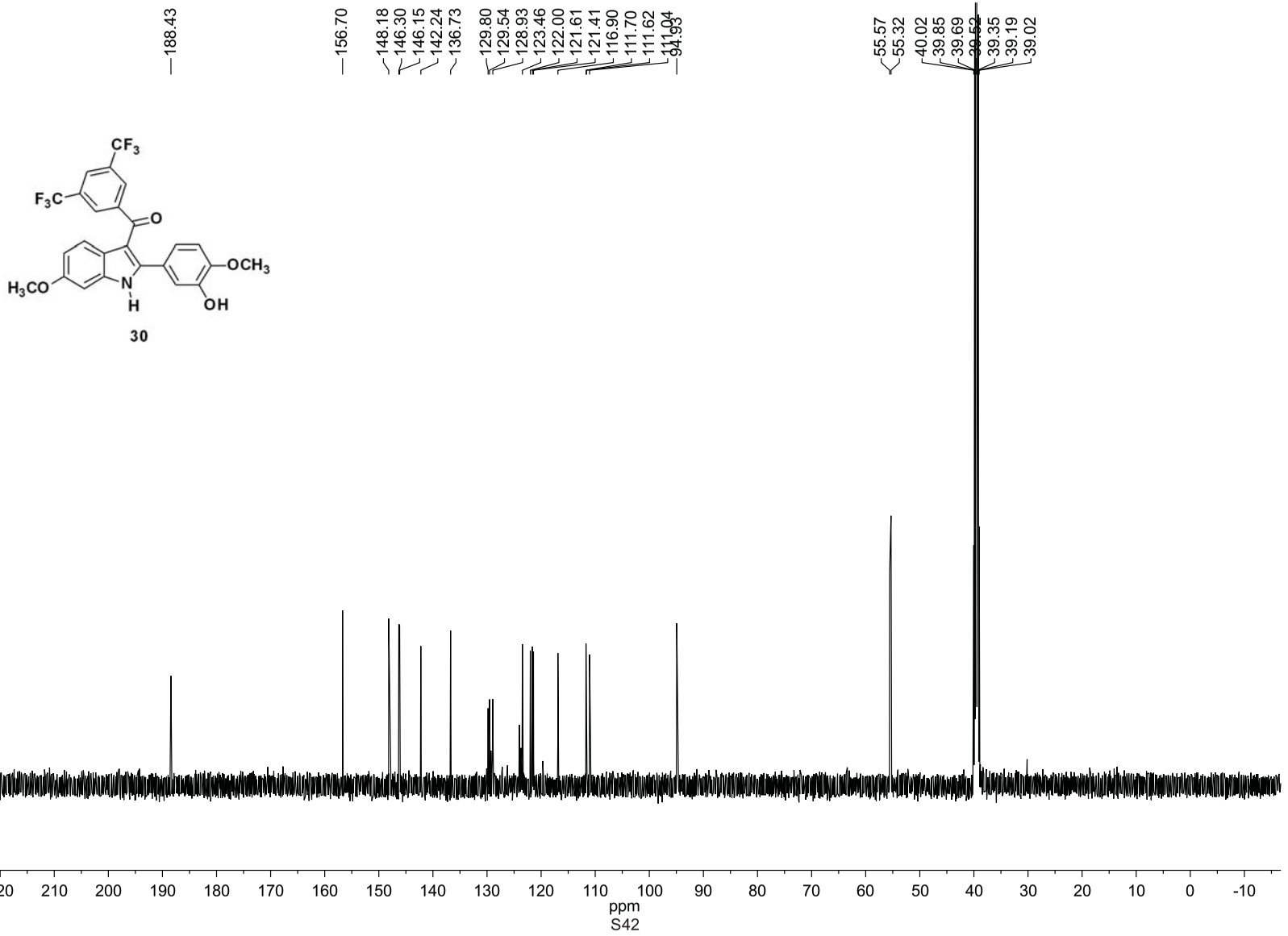
188.43
156.70
148.18
146.30
146.15
142.24
136.73
129.80
129.54
128.93
123.46
122.00
121.61
121.41
116.90
111.70
111.62
111.04
94.93
55.57
55.32
40.02
39.85
39.69
39.52
39.35
39.19
39.02
CF3
F3C
O
OCH3
H3CO
N
H
OH
30
220
210
200
190
180
170
160
150
140
130
120
110
100
90
80
70
60
50
40
30
20
10
0
-10
ppm
S42

-61.41
CF3
F3C
O
N
H
OCH3
OH
H3CO
30
-30
-40
-50
-60
-70
-80
-90
-100
-110
-120
-130
-140
-150
-160
-170
-180
-190
-200
-210
-220
-230
ppm
S43

Data File C:\CHEM32\1\DATA\MATT MAC\RH-I-06000001.D
Sample Name: run1

HPLC traces of compound **30**

```
==========================================================================
Acq. Operator   : Matt Mac
Acq. Instrument : Instrument 1                    Location :   -
Injection Date  : 1/9/2013 3:45:45 PM
Acq. Method     : C:\CHEM32\1\METHODS\MASTERMETHOD.M
Last changed    : 1/9/2013 2:59:47 PM by Matt Mac
Analysis Method : C:\CHEM32\1\METHODS\MASTERMETHOD.M
Last changed    : 1/9/2013 2:04:11 PM by Matt Mac
                  (modified after loading)
```

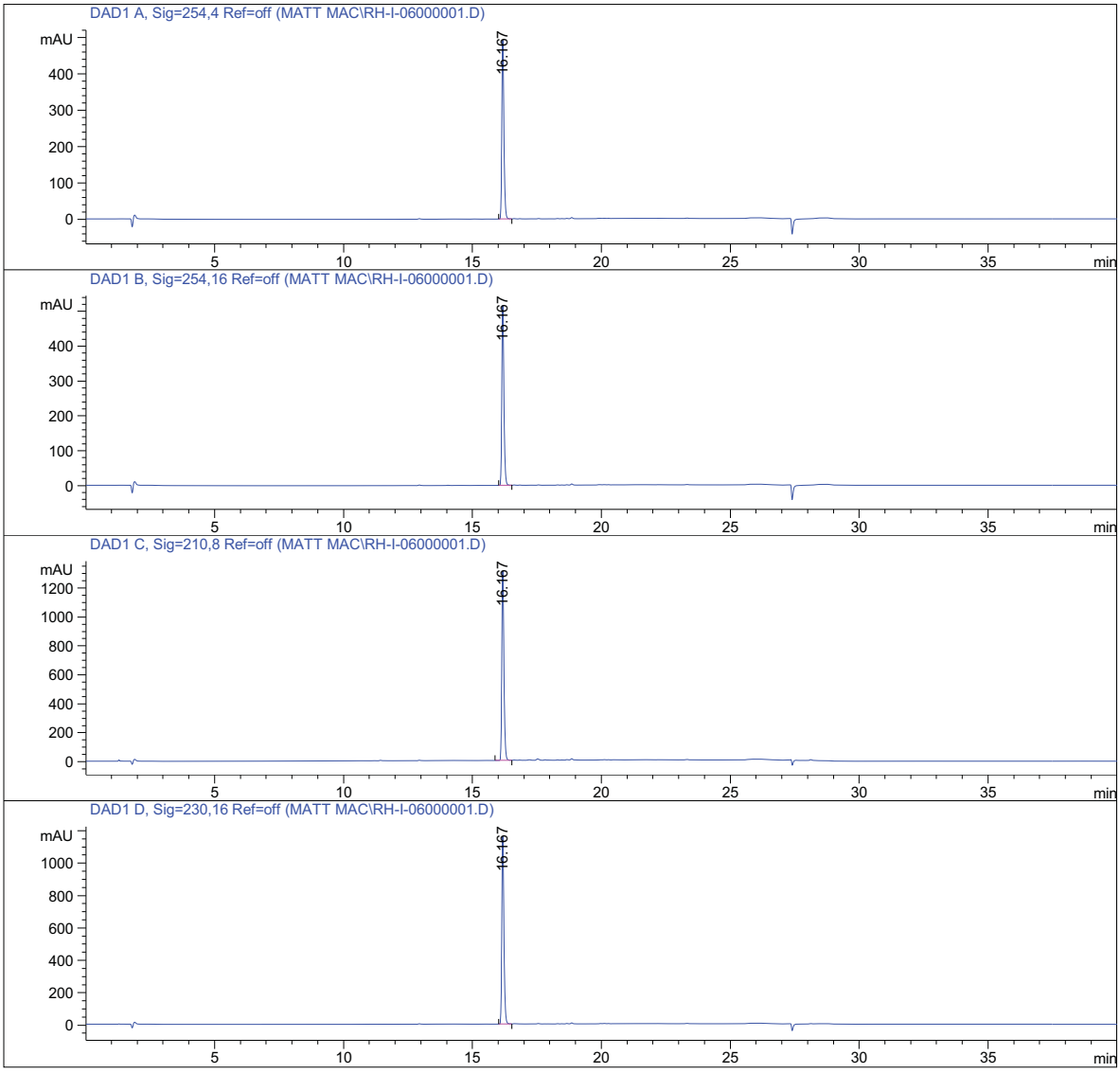

Data File C:\CHEM32\1\DATA\MATT MAC\RH-I-06000001.D
Sample Name: run1

HPLC traces of compound **30**

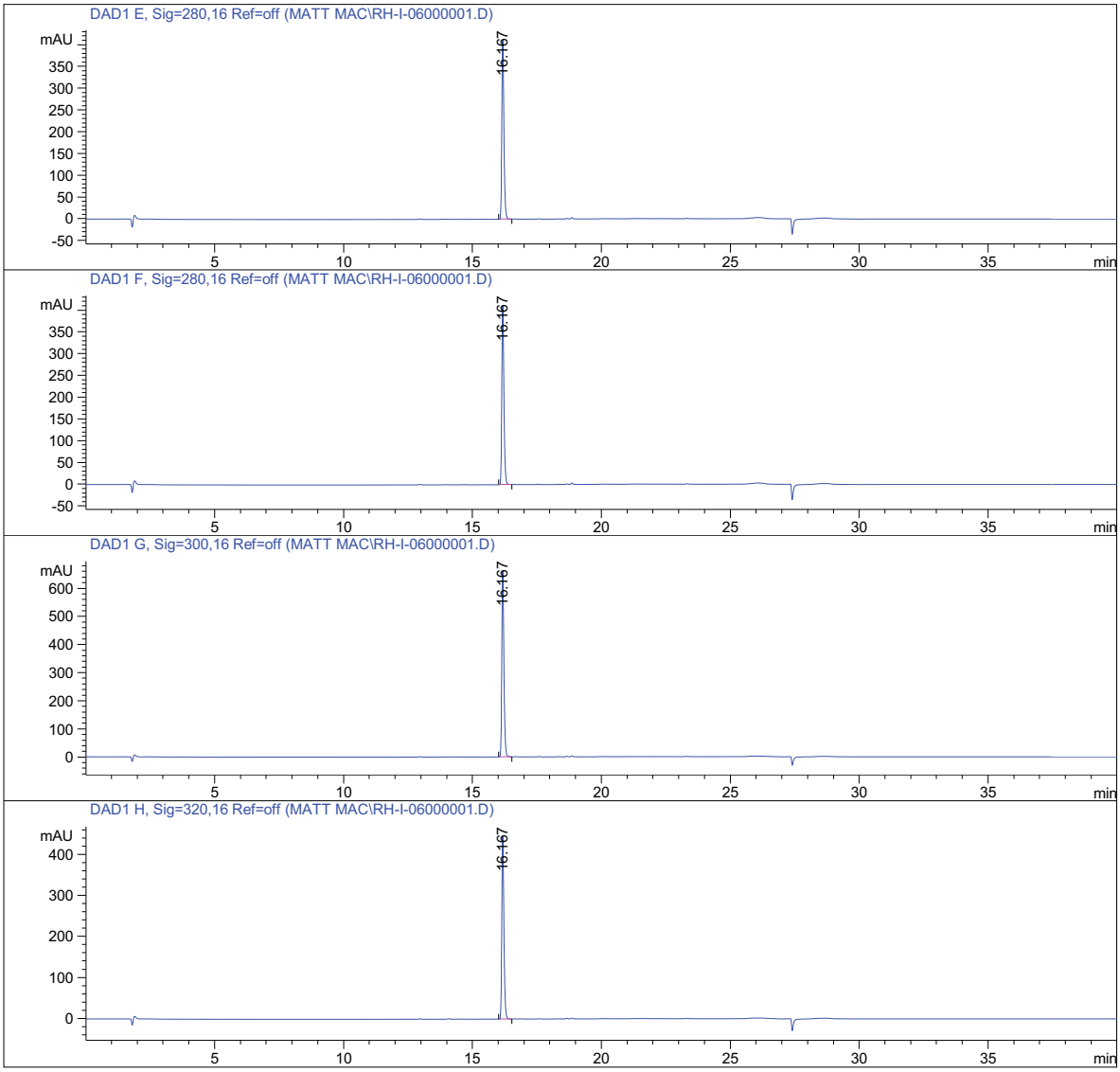

==========

Area Percent Report

==========

Sorted By : Signal
Multiplier : 1.0000
Dilution : 1.0000
Use Multiplier & Dilution Factor with ISTDs

Data File C:\CHEM32\1\DATA\MATT MAC\RH-I-06000001.D
Sample Name: run1

HPLC traces of compound **30**

Signal 1: DAD1 A, Sig=254,4 Ref=off

Peak #	RetTime [min]	Type	Width [min]	Area [mAU*s]	Height [mAU]	Area %
1	16.167	BV	0.0852	2759.49121	493.87103	100.0000
Totals :				2759.49121	493.87103	

Signal 2: DAD1 B, Sig=254,16 Ref=off

Peak #	RetTime [min]	Type	Width [min]	Area [mAU*s]	Height [mAU]	Area %
1	16.167	BV	0.0852	2894.88745	518.10498	100.0000
Totals :				2894.88745	518.10498	

Signal 3: DAD1 C, Sig=210,8 Ref=off

Peak #	RetTime [min]	Type	Width [min]	Area [mAU*s]	Height [mAU]	Area %
1	16.167	BV	0.0860	7422.78369	1312.45374	100.0000
Totals :				7422.78369	1312.45374	

Signal 4: DAD1 D, Sig=230,16 Ref=off

Peak #	RetTime [min]	Type	Width [min]	Area [mAU*s]	Height [mAU]	Area %
1	16.167	BV	0.0856	6530.87451	1161.71985	100.0000
Totals :				6530.87451	1161.71985	

Signal 5: DAD1 E, Sig=280,16 Ref=off

Peak #	RetTime [min]	Type	Width [min]	Area [mAU*s]	Height [mAU]	Area %
1	16.167	BV	0.0851	2305.04321	413.06256	100.0000
Totals :				2305.04321	413.06256	

Data File C:\CHEM32\1\DATA\MATT MAC\RH-I-06000001.D
Sample Name: run1

HPLC traces of compound **30**

Signal 6: DAD1 F, Sig=280,16 Ref=off

Peak #	RetTime [min]	Type	Width [min]	Area [mAU*s]	Height [mAU]	Area %
1	16.167	BV	0.0851	2305.04321	413.06256	100.0000
Totals :				2305.04321	413.06256	

Signal 7: DAD1 G, Sig=300,16 Ref=off

Peak #	RetTime [min]	Type	Width [min]	Area [mAU*s]	Height [mAU]	Area %
1	16.167	BV	0.0852	3709.70337	663.46100	100.0000
Totals :				3709.70337	663.46100	

Signal 8: DAD1 H, Sig=320,16 Ref=off

Peak #	RetTime [min]	Type	Width [min]	Area [mAU*s]	Height [mAU]	Area %
1	16.167	BV	0.0852	2500.62109	447.69040	100.0000
Totals :				2500.62109	447.69040	

*** End of Report ***

HRMS of compound **30**

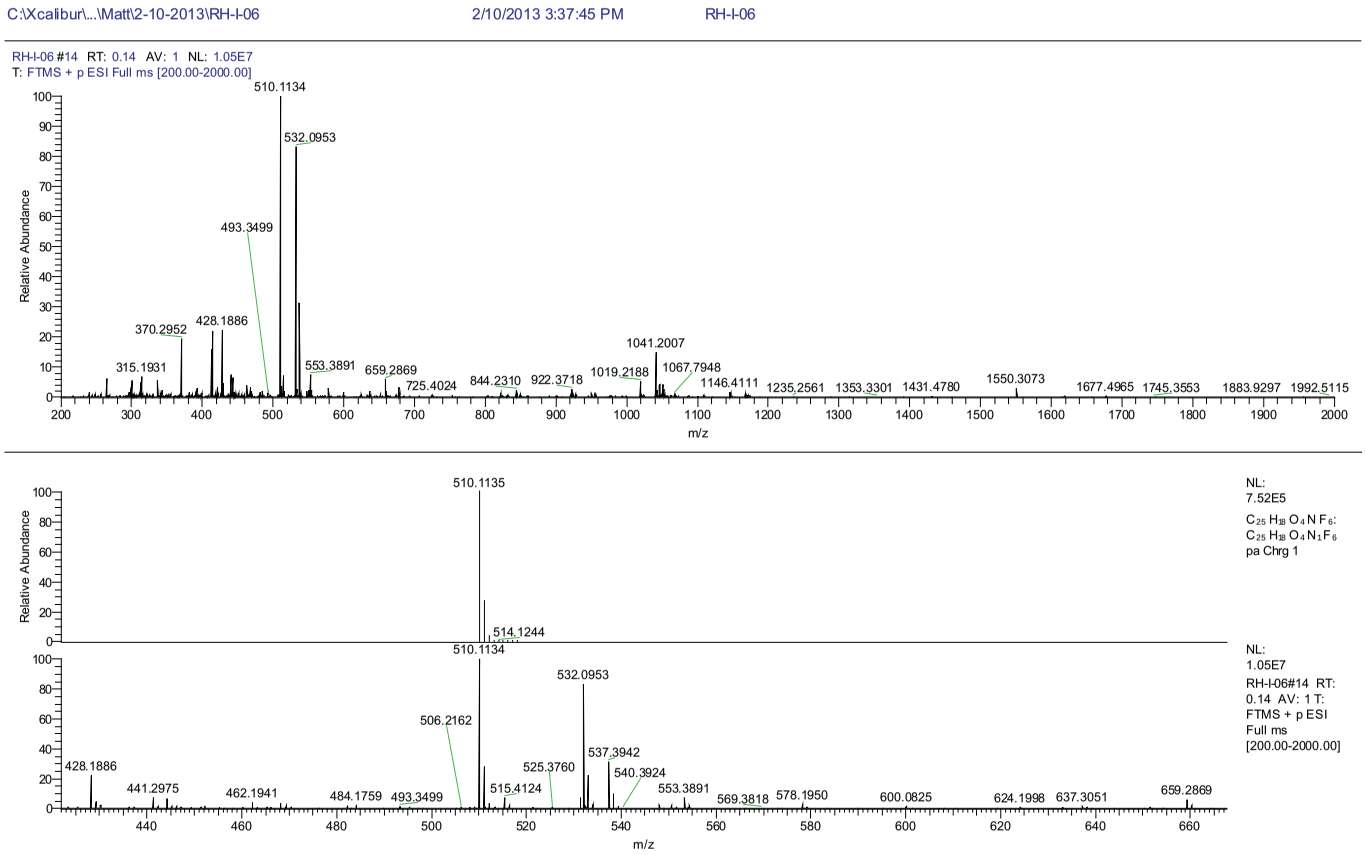

10.89
7.90
7.88
7.72
7.55
7.54
7.47
7.32
7.30
7.29
7.27
7.25
7.04
7.04
6.93
6.93
6.89
6.88
6.87
6.86
6.79
6.79
6.77
6.77
6.73
6.71
3.84
3.76
3.03
2.06
2.05
2.05
2.04
0.94
3.00
1.01
1.00
1.00
0.99
1.06
0.99
1.00
0.99
1.02
1.02
0.99
ppm
S49
31

206.46
191.43
158.14
149.41
149.40
148.91
147.24
143.75
137.84
130.31
128.85
125.59
123.94
122.63
122.59
122.16
116.92
112.33
111.95
95.55
56.20
55.76
30.30
30.15
29.99
29.84
29.69
29.53
29.38
OCH3
OH
O
N
H
F3CO
H3CO
31
ppm
S50

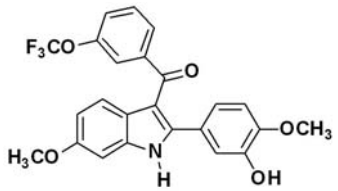
F3CO
O
OCH3
H3CO
N
H
OH

31

-58.50
0
5
0
-5
-10
-15
-20
-25
-30
-35
-40
-45
-50
-55
-60
-65
-70
-75
-80
-85
-90
-95
-100
-10
ppm

S51

Data File C:\CHEM32\1\DATA\MATT MAC\MTM-V-33000001.D
Sample Name: run1

HPLC traces of compound **31**

```
==========================================================================
Acq. Operator   : Matt Mac
Acq. Instrument : Instrument 1                    Location :   -
Injection Date  : 1/10/2013 10:51:03 AM
Acq. Method     : C:\CHEM32\1\METHODS\MASTERMETHOD.M
Last changed    : 1/10/2013 10:04:38 AM by Matt Mac
                  (modified after loading)
Analysis Method : C:\CHEM32\1\METHODS\MASTERMETHOD.M
Last changed    : 1/10/2013 10:52:42 AM by Matt Mac
                  (modified after loading)
```

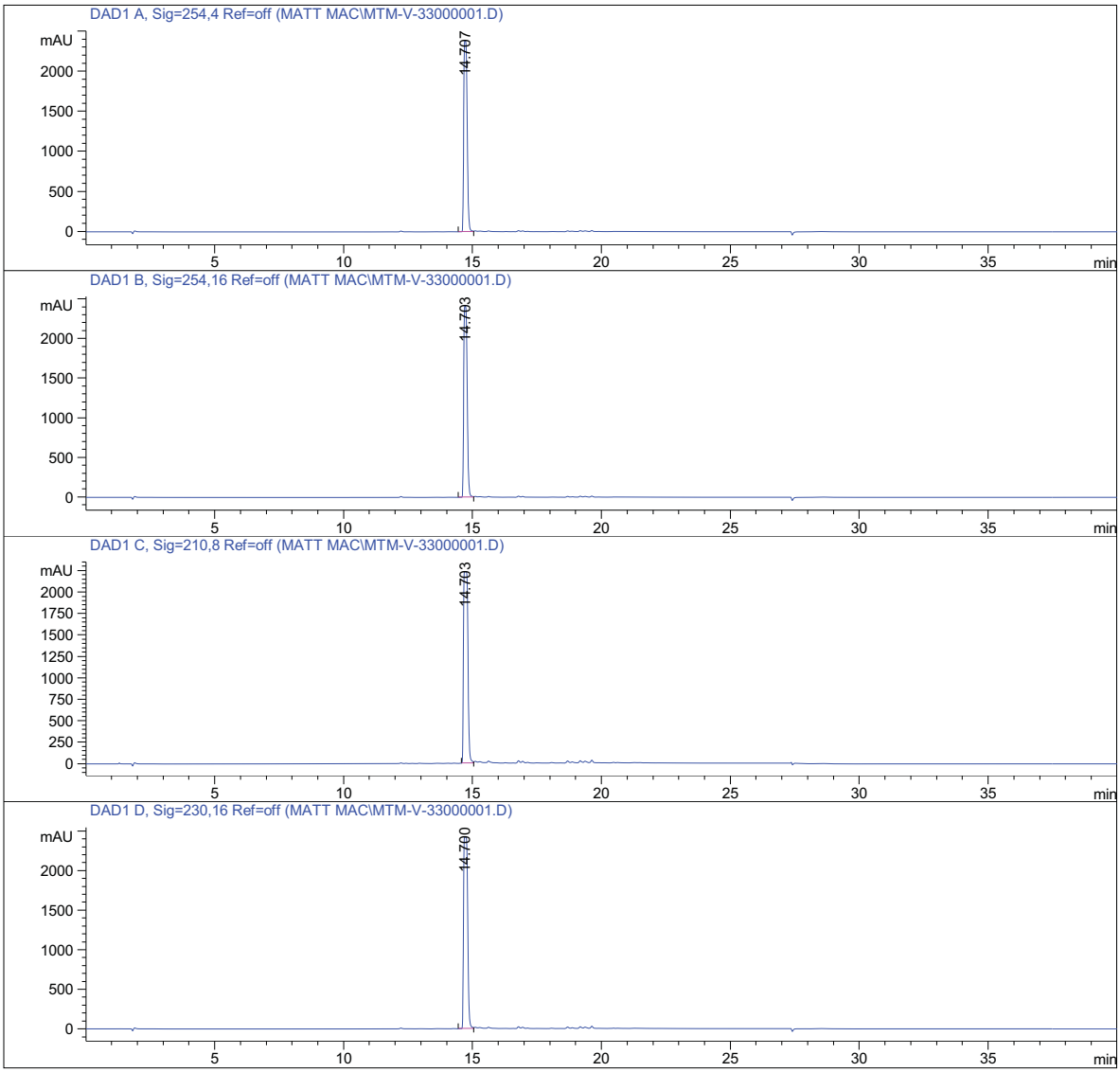

Data File C:\CHEM32\1\DATA\MATT MAC\MTM-V-33000001.D
Sample Name: run1

HPLC traces of compound **31**

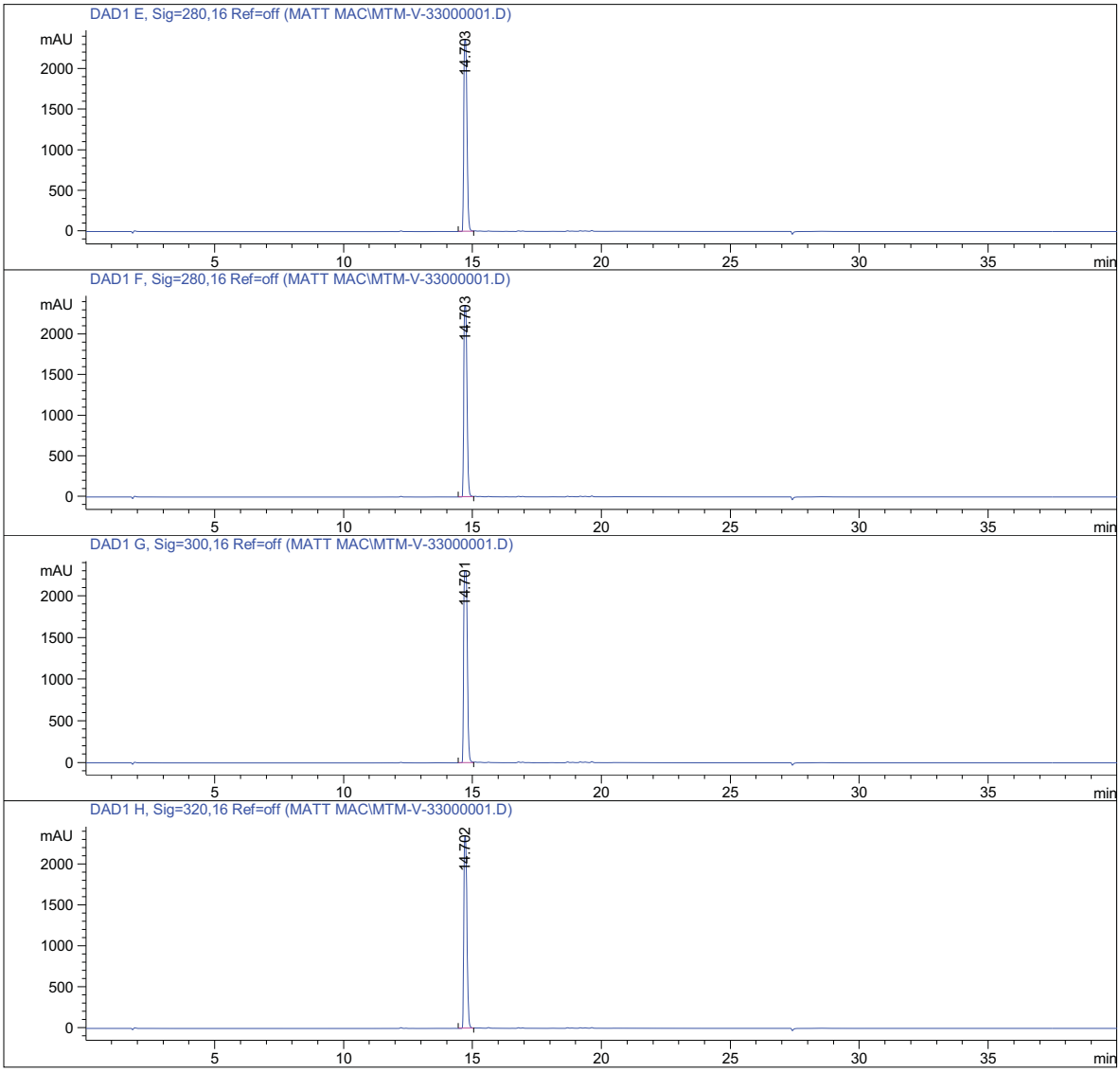

==========

Area Percent Report

==========

Sorted By : Signal
Multiplier : 1.0000
Dilution : 1.0000
Use Multiplier & Dilution Factor with ISTDs

Data File C:\CHEM32\1\DATA\MATT MAC\MTM-V-33000001.D
Sample Name: run1

HPLC traces of compound **31**

Signal 1: DAD1 A, Sig=254,4 Ref=off

Peak #	RetTime [min]	Type	Width [min]	Area [mAU*s]	Height [mAU]	Area %
1	14.707	BV	0.1464	2.17409e4	2383.37598	100.0000
Totals :				2.17409e4	2383.37598	

Signal 2: DAD1 B, Sig=254,16 Ref=off

Peak #	RetTime [min]	Type	Width [min]	Area [mAU*s]	Height [mAU]	Area %
1	14.703	BV	0.1489	2.21007e4	2411.10132	100.0000
Totals :				2.21008e4	2411.10132	

Signal 3: DAD1 C, Sig=210,8 Ref=off

Peak #	RetTime [min]	Type	Width [min]	Area [mAU*s]	Height [mAU]	Area %
1	14.703	BV	0.1598	2.59557e4	2230.39380	100.0000
Totals :				2.59557e4	2230.39380	

Signal 4: DAD1 D, Sig=230,16 Ref=off

Peak #	RetTime [min]	Type	Width [min]	Area [mAU*s]	Height [mAU]	Area %
1	14.700	BV	0.1769	2.63170e4	2418.76001	100.0000
Totals :				2.63170e4	2418.76001	

Signal 5: DAD1 E, Sig=280,16 Ref=off

Peak #	RetTime [min]	Type	Width [min]	Area [mAU*s]	Height [mAU]	Area %
1	14.703	BV	0.1372	2.00450e4	2357.87817	100.0000
Totals :				2.00450e4	2357.87817	

Data File C:\CHEM32\1\DATA\MATT MAC\MTM-V-33000001.D
Sample Name: run1

HPLC traces of compound **31**

Signal 6: DAD1 F, Sig=280,16 Ref=off

Peak #	RetTime [min]	Type	Width [min]	Area [mAU*s]	Height [mAU]	Area %
1	14.703	BV	0.1372	2.00450e4	2357.87817	100.0000
Totals :				2.00450e4	2357.87817	

Signal 7: DAD1 G, Sig=300,16 Ref=off

Peak #	RetTime [min]	Type	Width [min]	Area [mAU*s]	Height [mAU]	Area %
1	14.701	BV	0.1575	2.24037e4	2303.29663	100.0000
Totals :				2.24037e4	2303.29663	

Signal 8: DAD1 H, Sig=320,16 Ref=off

Peak #	RetTime [min]	Type	Width [min]	Area [mAU*s]	Height [mAU]	Area %
1	14.702	BV	0.1321	1.93282e4	2345.59521	100.0000
Totals :				1.93282e4	2345.59521	

*** End of Report ***

HRMS of compound **31**

C:\Xcalibur\...\Matt\2-10-2013\MTM-V-33 2/10/2013 12:38:13 PM MTM-V-33

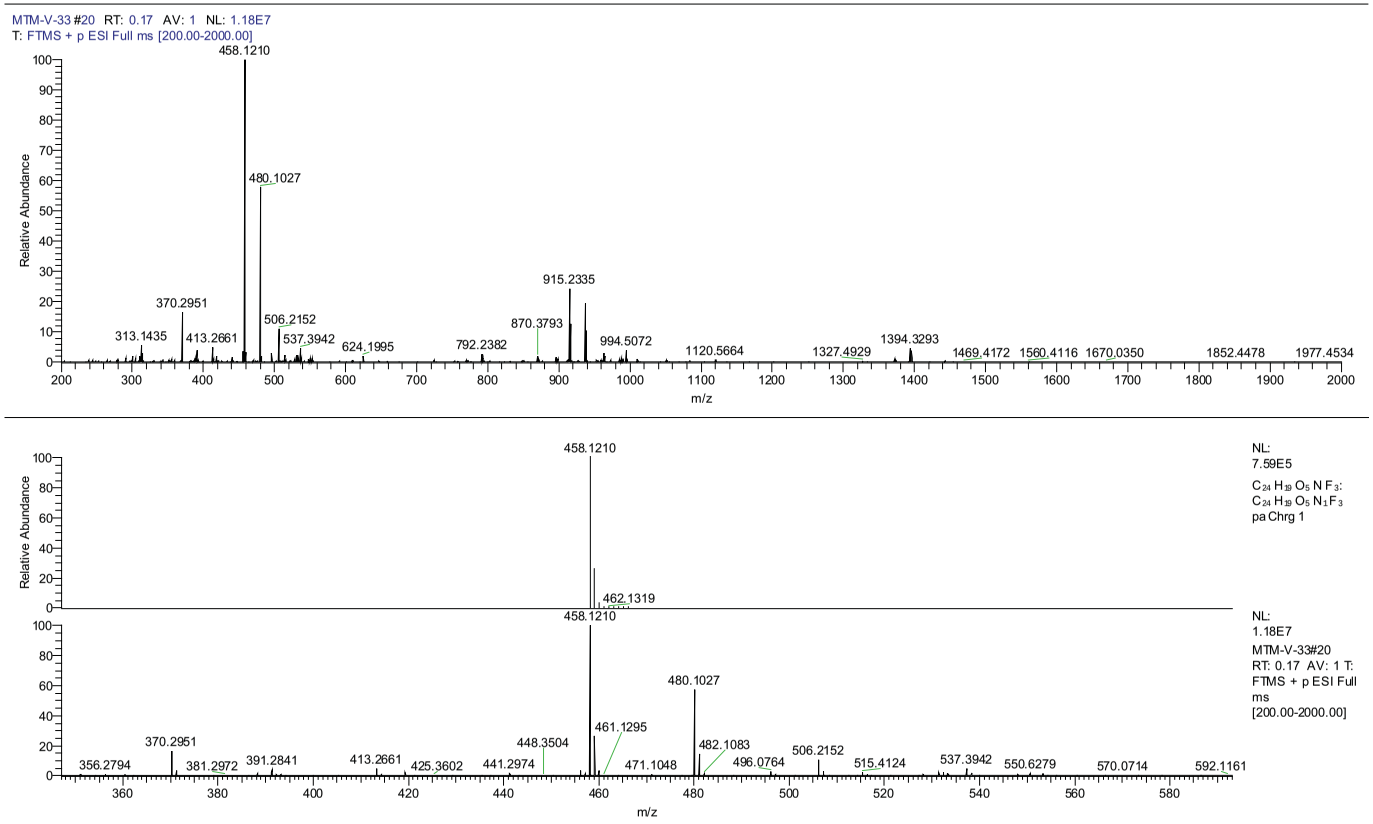

10.86
7.92
7.90
7.69
7.66
7.64
7.11
7.09
7.04
7.03
6.90
6.88
6.88
6.86
6.71
3.84
3.77
2.94
2.06
2.05
2.05
2.04
0.90
1.00
0.97
1.97
2.01
1.00
0.98
1.03
2.01
3.00
3.01
ppm
S57
32

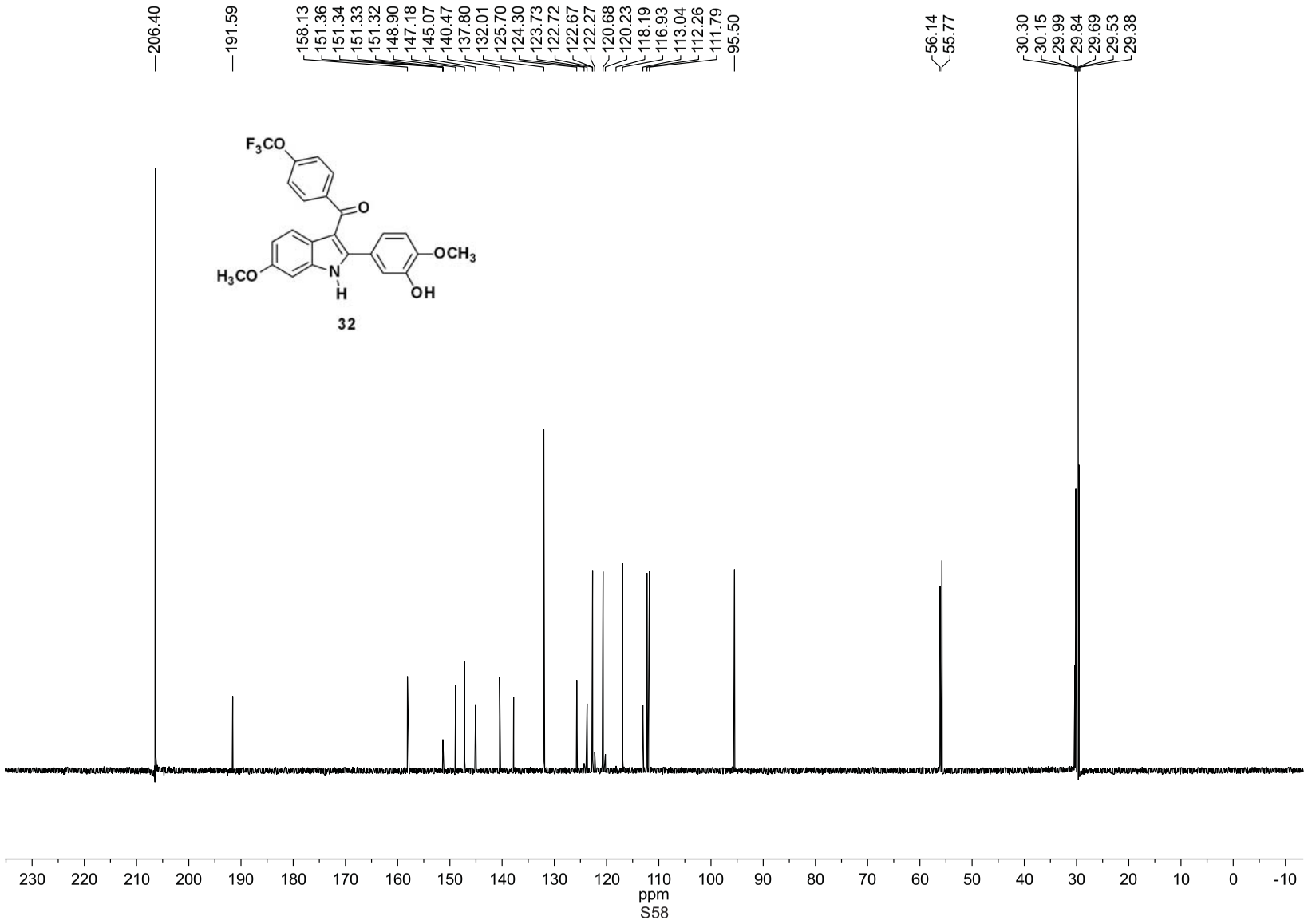
206.40
191.59
158.13
151.36
151.34
151.33
151.32
148.90
147.18
145.07
140.47
137.80
132.01
125.70
124.30
123.73
122.72
122.67
122.27
120.68
120.23
118.19
116.93
113.04
112.26
111.79
95.50
56.14
55.77
30.30
30.15
29.99
29.84
29.69
29.53
29.38
F3CO
O
OCH3
H3CO
N
H
OH
32
230
220
210
200
190
180
170
160
150
140
130
120
110
100
90
80
70
60
50
40
30
20
10
0
-10
ppm
S58

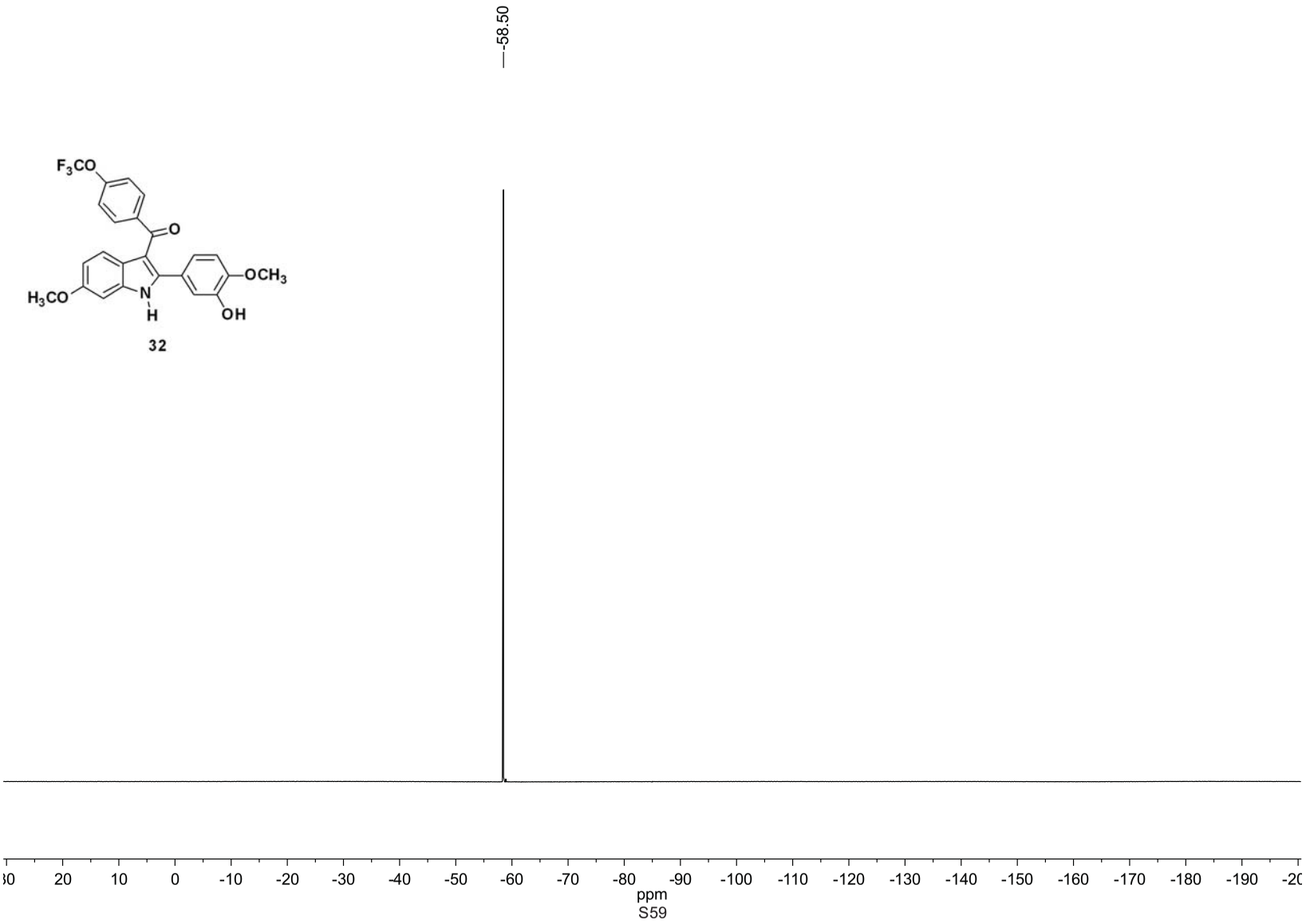
-58.50
F3CO
O
OCH3
H3CO
N
H
OH
32
30
20
10
0
-10
-20
-30
-40
-50
-60
-70
-80
-90
-100
-110
-120
-130
-140
-150
-160
-170
-180
-190
ppm
S59

Data File C:\CHEM32\1\DATA\MATT MAC\MTM-V-32000001.D
Sample Name: run1

HPLC traces of compound **32**

```
==========================================================================
Acq. Operator   : Matt Mac
Acq. Instrument : Instrument 1                    Location :   -
Injection Date  : 1/9/2013 10:48:37 PM
Acq. Method     : C:\CHEM32\1\METHODS\MASTERMETHOD.M
Last changed    : 1/9/2013 10:45:53 PM by Matt Mac
Analysis Method : C:\CHEM32\1\METHODS\MASTERMETHOD.M
Last changed    : 1/9/2013 2:04:11 PM by Matt Mac
                  (modified after loading)
```

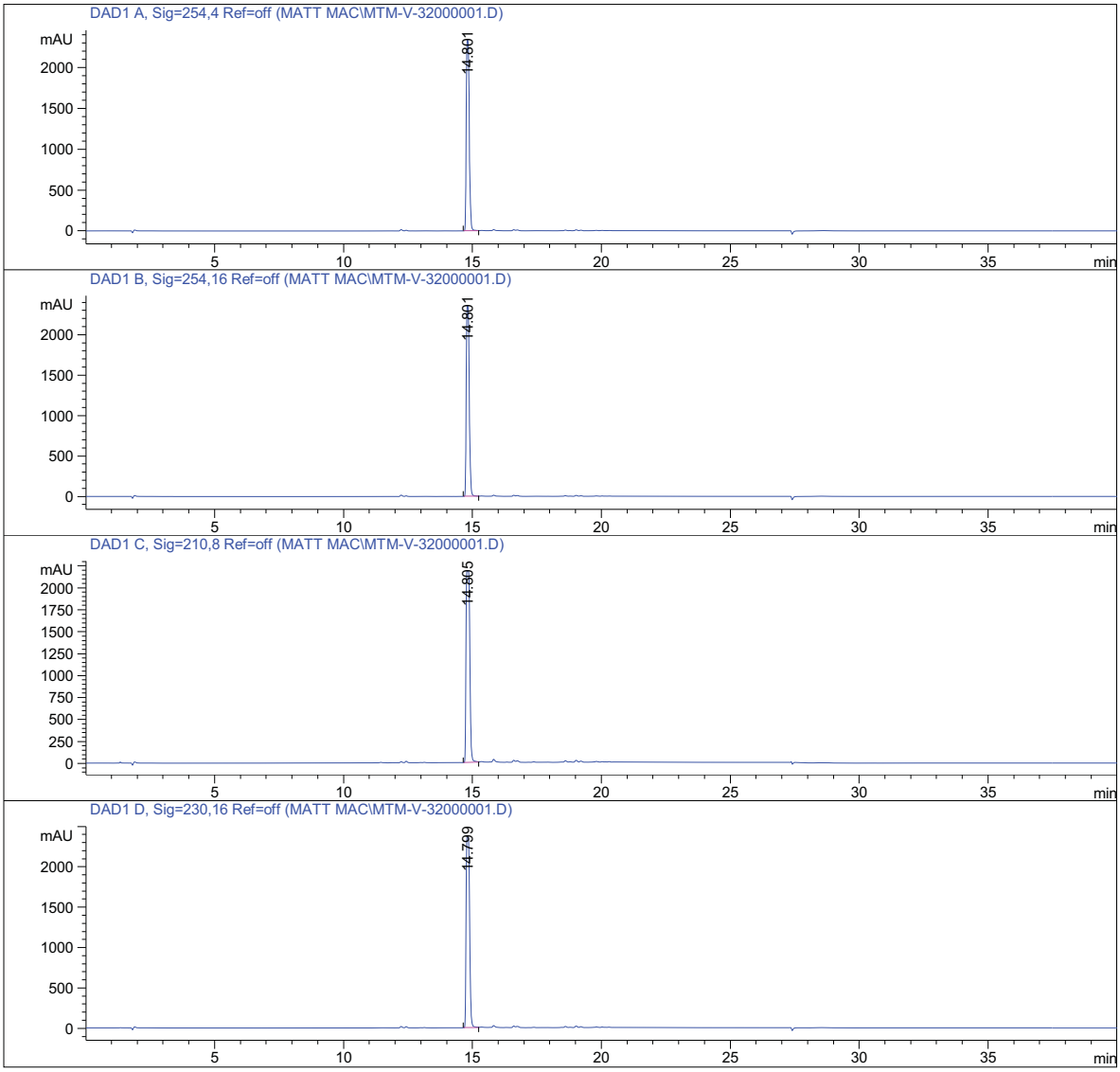

Data File C:\CHEM32\1\DATA\MATT MAC\MTM-V-32000001.D
Sample Name: run1

HPLC traces of compound **32**

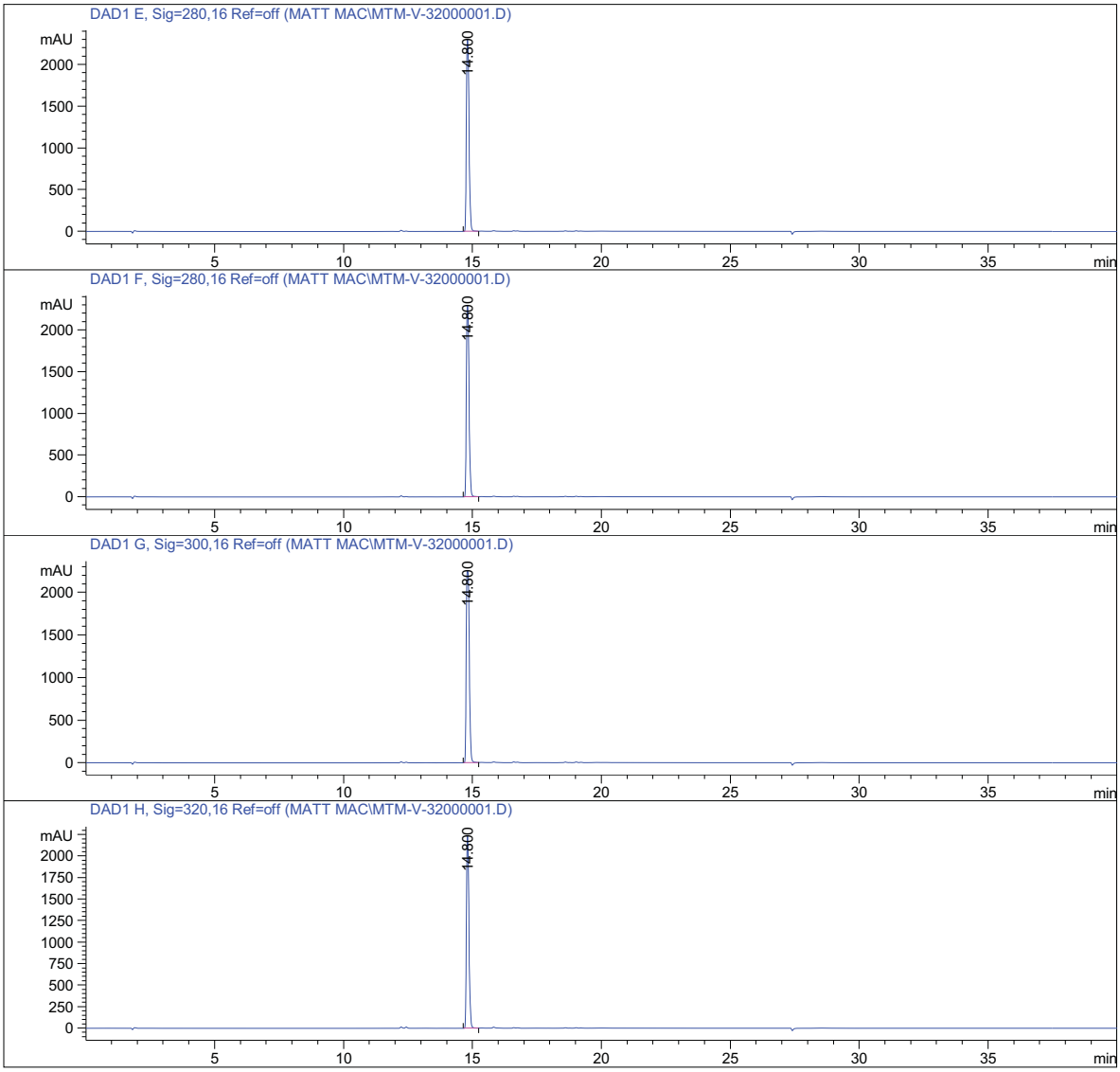

==========

Area Percent Report

==========

Sorted By : Signal
Multiplier : 1.0000
Dilution : 1.0000
Use Multiplier & Dilution Factor with ISTDs

Data File C:\CHEM32\1\DATA\MATT MAC\MTM-V-32000001.D
Sample Name: run1

HPLC traces of compound **32**

Signal 1: DAD1 A, Sig=254,4 Ref=off

Peak #	RetTime [min]	Type	Width [min]	Area [mAU*s]	Height [mAU]	Area %
1	14.801	BV	0.1293	1.86964e4	2338.97241	100.0000
Totals :				1.86964e4	2338.97241	

Signal 2: DAD1 B, Sig=254,16 Ref=off

Peak #	RetTime [min]	Type	Width [min]	Area [mAU*s]	Height [mAU]	Area %
1	14.801	BV	0.1292	1.88715e4	2362.03735	100.0000
Totals :				1.88715e4	2362.03735	

Signal 3: DAD1 C, Sig=210,8 Ref=off

Peak #	RetTime [min]	Type	Width [min]	Area [mAU*s]	Height [mAU]	Area %
1	14.805	BV	0.1658	2.20478e4	2183.30298	100.0000
Totals :				2.20478e4	2183.30298	

Signal 4: DAD1 D, Sig=230,16 Ref=off

Peak #	RetTime [min]	Type	Width [min]	Area [mAU*s]	Height [mAU]	Area %
1	14.799	BV	0.1507	2.20887e4	2369.97437	100.0000
Totals :				2.20887e4	2369.97437	

Signal 5: DAD1 E, Sig=280,16 Ref=off

Peak #	RetTime [min]	Type	Width [min]	Area [mAU*s]	Height [mAU]	Area %
1	14.800	BV	0.1131	1.63461e4	2295.18311	100.0000
Totals :				1.63461e4	2295.18311	

Data File C:\CHEM32\1\DATA\MATT MAC\MTM-V-32000001.D
Sample Name: run1

HPLC traces of compound **32**

Signal 6: DAD1 F, Sig=280,16 Ref=off

Peak #	RetTime [min]	Type	Width [min]	Area [mAU*s]	Height [mAU]	Area %
1	14.800	BV	0.1131	1.63461e4	2295.18311	100.0000
Totals :				1.63461e4	2295.18311	

Signal 7: DAD1 G, Sig=300,16 Ref=off

Peak #	RetTime [min]	Type	Width [min]	Area [mAU*s]	Height [mAU]	Area %
1	14.800	BV	0.1317	1.84678e4	2251.13892	100.0000
Totals :				1.84678e4	2251.13892	

Signal 8: DAD1 H, Sig=320,16 Ref=off

Peak #	RetTime [min]	Type	Width [min]	Area [mAU*s]	Height [mAU]	Area %
1	14.800	BV	0.1063	1.49695e4	2231.31665	100.0000
Totals :				1.49695e4	2231.31665	

*** End of Report ***

HRMS of compound **32**

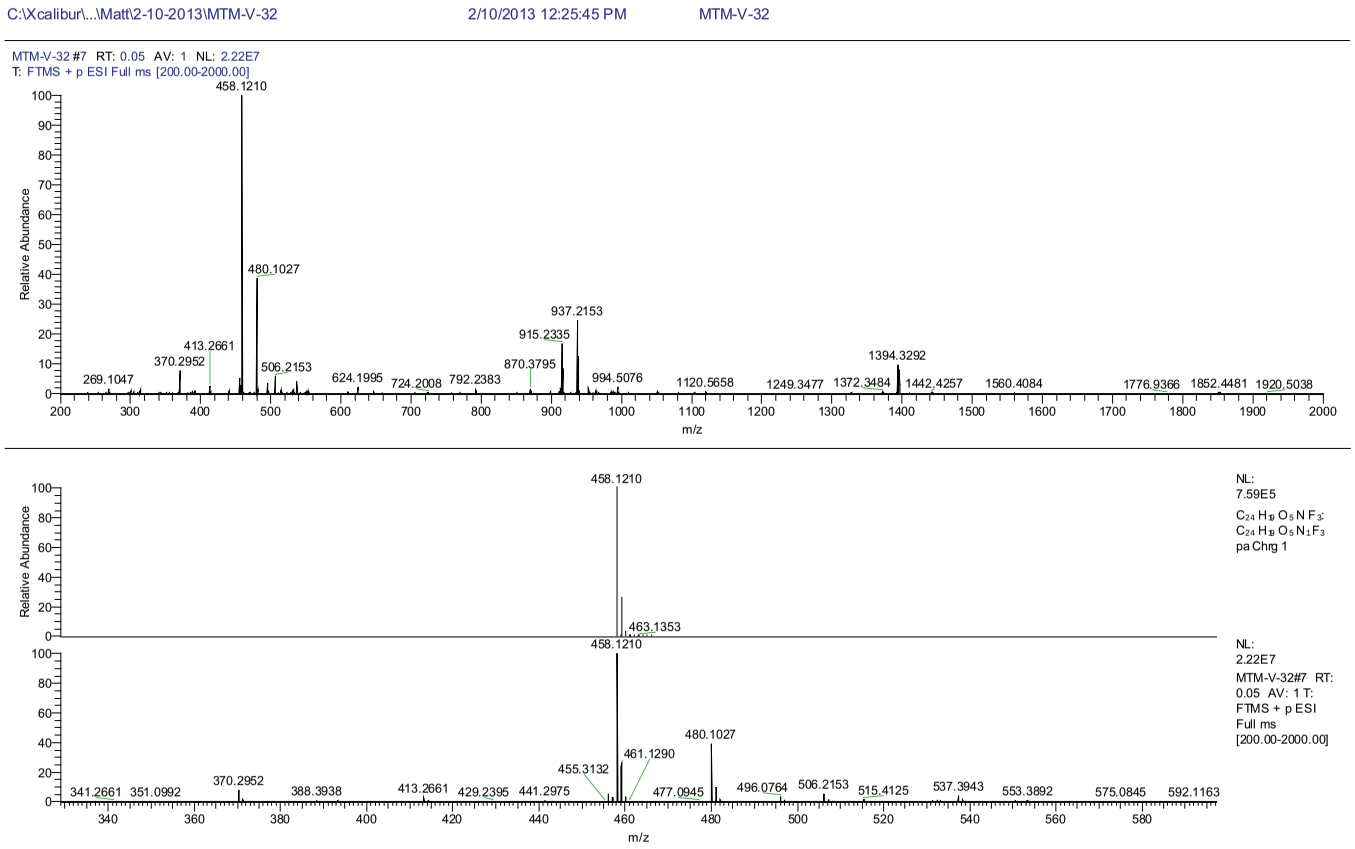

11.62
9.19
9.00
7.67
7.66
6.82
6.81
6.78
6.75
6.75
6.73
6.68
6.67
6.66
6.66
6.65
6.65
3.69
3.61
3.59
3.32
2.50
2.50
2.50
0.98
1.04
1.01
1.00
1.03
2.02
2.13
2.13
3.00
6.04
3.01
ppm
S65
33

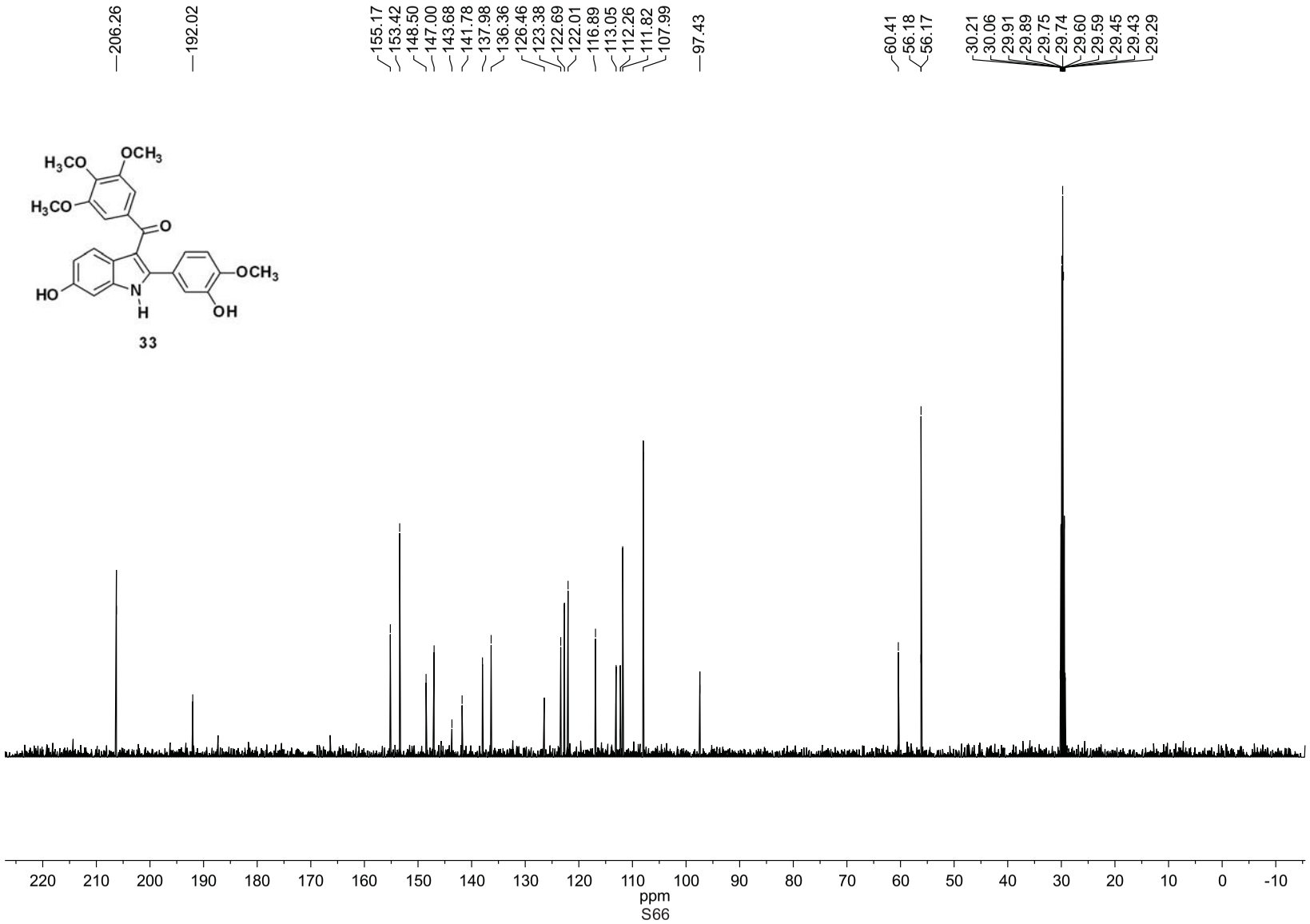
206.26
192.02
155.17
153.42
148.50
147.00
143.68
141.78
137.98
136.36
126.46
123.38
122.69
122.01
116.89
113.05
112.26
111.82
107.99
97.43
60.41
56.18
56.17
30.21
30.06
29.91
29.89
29.75
29.74
29.60
29.59
29.45
29.43
29.29
H3CO
OCH3
H3CO
O
HO
N
H
OCH3
OH
33
220
210
200
190
180
170
160
150
140
130
120
110
100
90
80
70
60
50
40
30
20
10
0
-10
ppm
S66

Data File C:\CHEM32\1\DATA\MATT MAC\PSH-I-48000001.D
Sample Name: run1

HPLC traces of compound **33**

```
==========================================================================
Acq. Operator   : Matt Mac
Acq. Instrument : Instrument 1                    Location :   -
Injection Date  : 1/8/2013 9:52:08 PM
Acq. Method     : C:\CHEM32\1\METHODS\MASTERMETHOD.M
Last changed    : 1/8/2013 9:30:46 PM by Matt Mac
Analysis Method : C:\CHEM32\1\METHODS\MASTERMETHOD.M
Last changed    : 1/3/2013 5:04:04 PM by Laxman
```

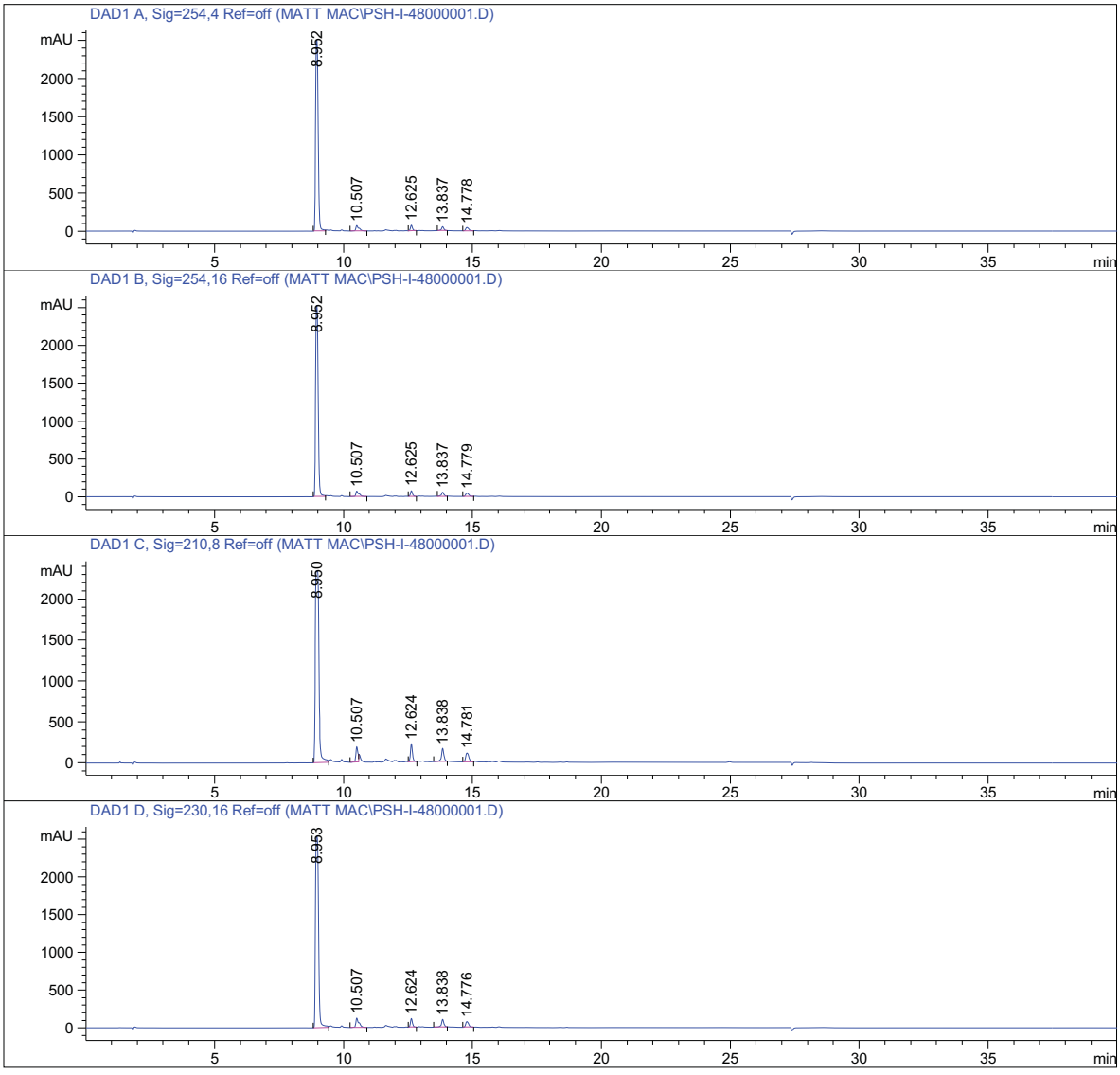

Data File C:\CHEM32\1\DATA\MATT MAC\PSH-I-48000001.D
Sample Name: run1

HPLC traces of compound **33**

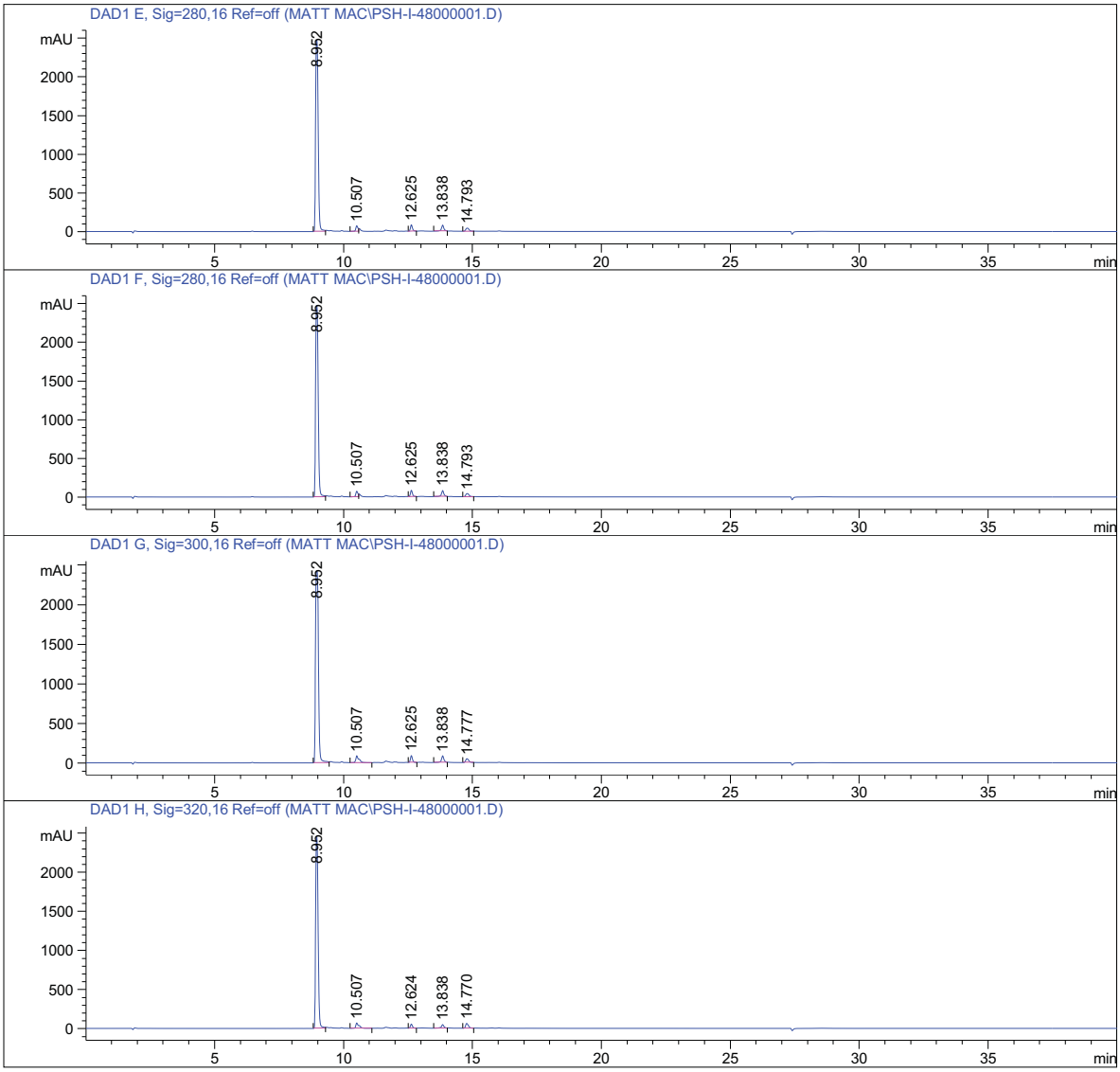

==========

Area Percent Report

==========

Sorted By : Signal
Multiplier : 1.0000
Dilution : 1.0000
Use Multiplier & Dilution Factor with ISTDs

Data File C:\CHEM32\1\DATA\MATT MAC\PSH-I-48000001.D
Sample Name: run1

HPLC traces of compound **33**

Signal 1: DAD1 A, Sig=254,4 Ref=off

Peak #	RetTime [min]	Type	Width [min]	Area [mAU*s]	Height [mAU]	Area %
1	8.952	BV	0.1133	1.74400e4	2503.49414	90.6932
2	10.507	BB	0.1183	610.17493	70.97384	3.1731
3	12.625	VV	0.0842	406.46713	73.85258	2.1138
4	13.837	VV	0.1047	393.10352	54.14516	2.0443
5	14.778	BV	0.1371	379.91687	43.85746	1.9757
Totals :				1.92296e4	2746.32318	

Signal 2: DAD1 B, Sig=254,16 Ref=off

Peak #	RetTime [min]	Type	Width [min]	Area [mAU*s]	Height [mAU]	Area %
1	8.952	BV	0.1130	1.75295e4	2525.12695	90.7013
2	10.507	BB	0.1182	618.83783	72.06956	3.2020
3	12.625	VV	0.0841	405.30692	73.71142	2.0971
4	13.837	VV	0.1050	394.96179	54.20537	2.0436
5	14.779	BV	0.1377	378.02029	43.34686	1.9560
Totals :				1.93266e4	2768.46016	

Signal 3: DAD1 C, Sig=210,8 Ref=off

Peak #	RetTime [min]	Type	Width [min]	Area [mAU*s]	Height [mAU]	Area %
1	8.950	BV	0.1577	2.28634e4	2345.01953	83.7926
2	10.507	BV	0.0861	1096.52075	187.73811	4.0187
3	12.624	VV	0.0843	1212.12024	219.94164	4.4423
4	13.838	BV	0.1033	1167.94214	163.60349	4.2804
5	14.781	BV	0.1384	945.71265	107.69555	3.4660
Totals :				2.72857e4	3023.99831	

Signal 4: DAD1 D, Sig=230,16 Ref=off

Peak #	RetTime [min]	Type	Width [min]	Area [mAU*s]	Height [mAU]	Area %
1	8.953	BV	0.1354	2.11507e4	2534.16040	87.2935
2	10.507	BB	0.1178	1058.27429	123.76330	4.3677

Data File C:\CHEM32\1\DATA\MATT MAC\PSH-I-48000001.D
Sample Name: run1

HPLC traces of compound **33**

Peak #	RetTime [min]	Type	Width [min]	Area [mAU*s]	Height [mAU]	Area %
3	12.624	VV	0.0846	639.06421	115.47739	2.6376
4	13.838	BV	0.1035	740.73499	103.53637	3.0572
5	14.776	BV	0.1350	640.64758	75.48686	2.6441
Totals :				2.42294e4	2952.42432	

Signal 5: DAD1 E, Sig=280,16 Ref=off

Peak #	RetTime [min]	Type	Width [min]	Area [mAU*s]	Height [mAU]	Area %
1	8.952	BV	0.1131	1.71869e4	2472.61279	90.5848
2	10.507	BV	0.0859	419.13235	72.05910	2.2091
3	12.625	VV	0.0840	451.04239	82.25859	2.3773
4	13.838	BV	0.1015	549.10632	78.58857	2.8941
5	14.793	BV	0.1445	367.09229	40.21583	1.9348
Totals :				1.89733e4	2745.73488	

Signal 6: DAD1 F, Sig=280,16 Ref=off

Peak #	RetTime [min]	Type	Width [min]	Area [mAU*s]	Height [mAU]	Area %
1	8.952	BV	0.1131	1.71869e4	2472.61279	90.5848
2	10.507	BV	0.0859	419.13235	72.05910	2.2091
3	12.625	VV	0.0840	451.04239	82.25859	2.3773
4	13.838	BV	0.1015	549.10632	78.58857	2.8941
5	14.793	BV	0.1445	367.09229	40.21583	1.9348
Totals :				1.89733e4	2745.73488	

Signal 7: DAD1 G, Sig=300,16 Ref=off

Peak #	RetTime [min]	Type	Width [min]	Area [mAU*s]	Height [mAU]	Area %
1	8.952	BV	0.1265	1.91870e4	2420.31030	89.6657
2	10.507	BB	0.1181	743.72498	86.64207	3.4756
3	12.625	VB	0.0835	472.35669	86.76642	2.2074
4	13.838	VV	0.1002	582.41565	84.67338	2.7218
5	14.777	BV	0.1360	412.87323	48.15561	1.9295
Totals :				2.13983e4	2726.54778	

Data File C:\CHEM32\1\DATA\MATT MAC\PSH-I-48000001.D
Sample Name: run1

HPLC traces of compound **33**

Signal 8: DAD1 H, Sig=320,16 Ref=off

Peak #	RetTime [min]	Type	Width [min]	Area [mAU*s]	Height [mAU]	Area %
1	8.952	BV	0.1054	1.62748e4	2453.87549	90.6305
2	10.507	BB	0.1190	586.09778	67.68012	3.2638
3	12.624	VV	0.0850	289.21191	51.90499	1.6106
4	13.838	BV	0.1074	337.07236	44.99344	1.8771
5	14.770	BV	0.1219	470.12784	61.00558	2.6180
Totals :				1.79573e4	2679.45962	

*** End of Report ***

HRMS of compound **33**

C:\Xcalibur\...\Matt\2-10-2013\PSH-I-48 2/10/2013 8:21:48 PM PSH-I-48

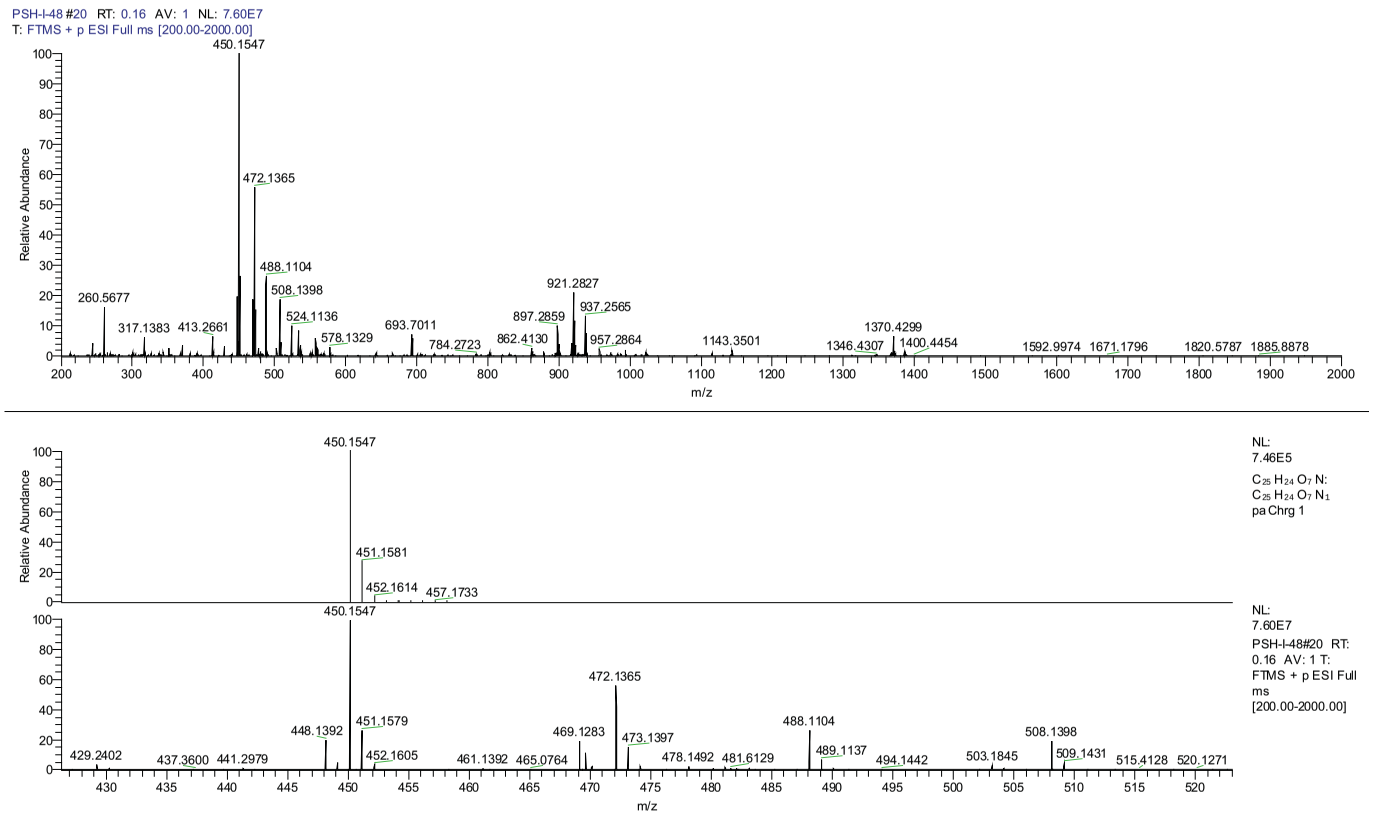

8.30
7.26
7.15
6.99
6.99
6.90
6.90
6.89
6.88
6.71
6.70
6.68
5.62
3.90
3.85
3.84
3.82
3.74
3.69
1.57
0.00
1.00
0.90
2.92
2.74
2.91
2.76
6.01
2.90
1.99
0.97
0.99
1.04
1.05
ppm
S73
34

193.44
152.83
152.16
146.84
146.48
145.84
142.11
137.80
137.04
134.57
132.36
125.14
120.48
116.56
113.68
112.59
110.94
107.50
89.73
77.41
77.16
76.91
61.37
61.00
60.78
56.40
56.33
56.07
ppm
S74
34

Data File C:\CHEM32\1\DATA\MATT MAC\MTM-III-8600002.D
Sample Name: run1

HPLC traces of compound **34**

```
==========================================================================
Acq. Operator   : Matt Mac
Acq. Instrument : Instrument 1                    Location :   -
Injection Date  : 1/7/2013 4:14:42 PM
Acq. Method     : C:\CHEM32\1\METHODS\MASTERMETHOD.M
Last changed    : 1/7/2013 4:13:16 PM by Matt Mac
                  (modified after loading)
Analysis Method : C:\CHEM32\1\METHODS\MASTERMETHOD.M
Last changed    : 1/3/2013 5:04:04 PM by Laxman
```

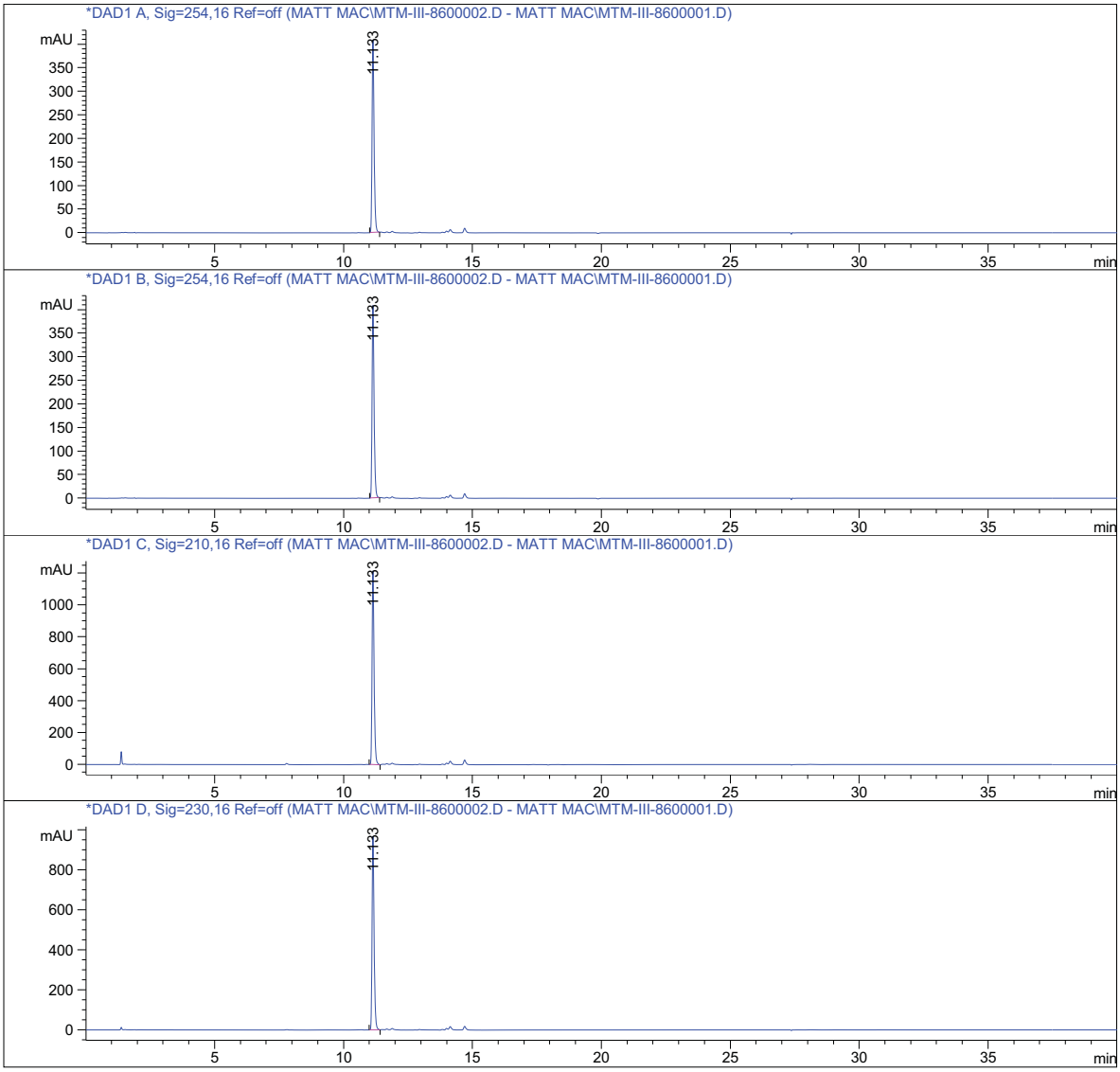

Data File C:\CHEM32\1\DATA\MATT MAC\MTM-III-8600002.D
Sample Name: run1

HPLC traces of compound **34**

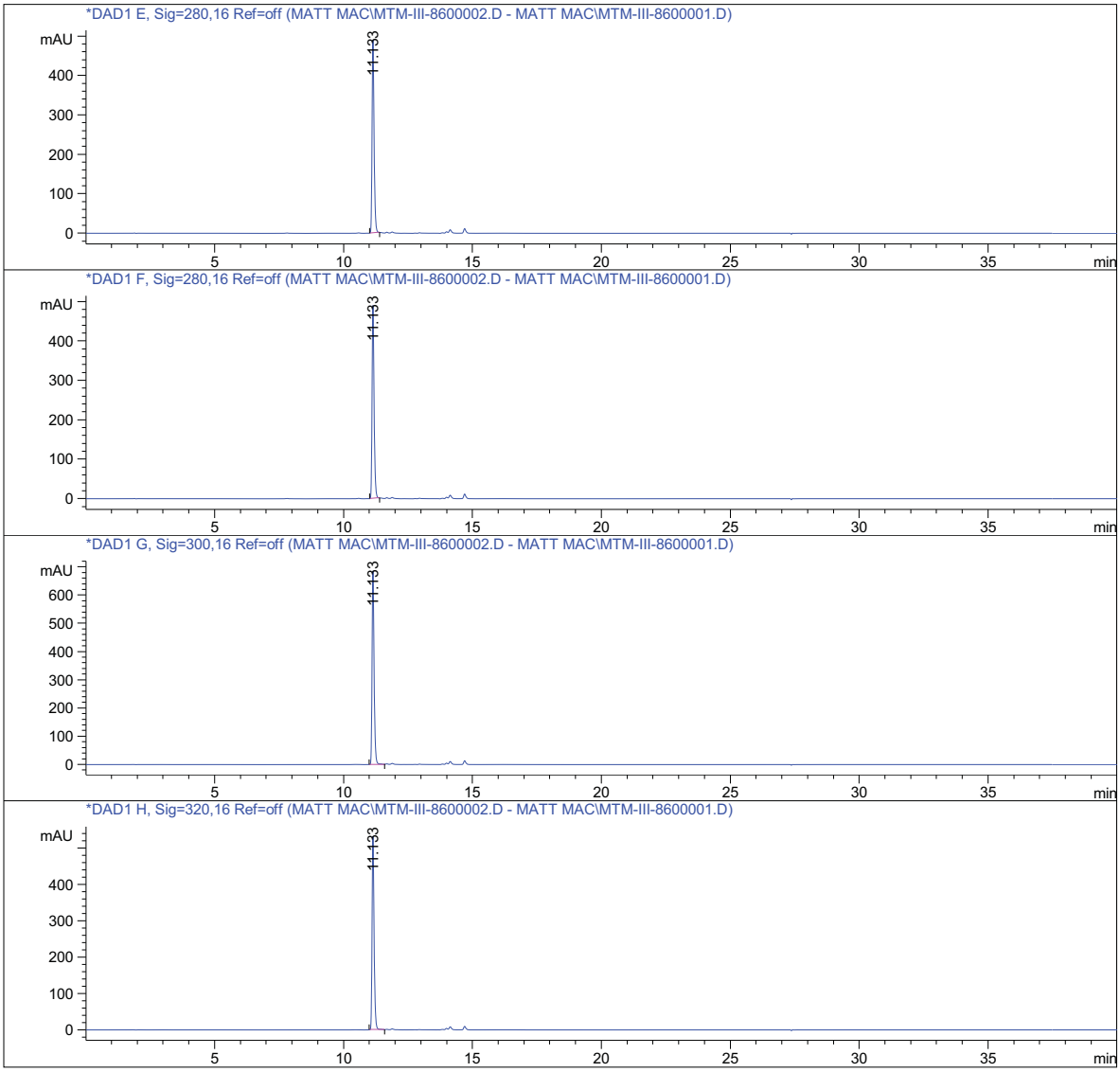

==========

Area Percent Report

==========

Sorted By : Signal
Multiplier : 1.0000
Dilution : 1.0000
Use Multiplier & Dilution Factor with ISTDs

Data File C:\CHEM32\1\DATA\MATT MAC\MTM-III-8600002.D
Sample Name: run1

HPLC traces of compound **34**

Signal 1: DAD1 A, Sig=254,16 Ref=off
Signal has been modified after loading from rawdata file!

Peak #	RetTime [min]	Type	Width [min]	Area [mAU*s]	Height [mAU]	Area %
1	11.133	BB	0.0810	2210.16919	409.56378	100.0000
Totals :				2210.16919	409.56378	

Signal 2: DAD1 B, Sig=254,16 Ref=off
Signal has been modified after loading from rawdata file!

Peak #	RetTime [min]	Type	Width [min]	Area [mAU*s]	Height [mAU]	Area %
1	11.133	BB	0.0810	2210.16919	409.56378	100.0000
Totals :				2210.16919	409.56378	

Signal 3: DAD1 C, Sig=210,16 Ref=off
Signal has been modified after loading from rawdata file!

Peak #	RetTime [min]	Type	Width [min]	Area [mAU*s]	Height [mAU]	Area %
1	11.133	VB	0.0817	6658.21045	1218.85291	100.0000
Totals :				6658.21045	1218.85291	

Signal 4: DAD1 D, Sig=230,16 Ref=off
Signal has been modified after loading from rawdata file!

Peak #	RetTime [min]	Type	Width [min]	Area [mAU*s]	Height [mAU]	Area %
1	11.133	BB	0.0815	5278.77148	970.38177	100.0000
Totals :				5278.77148	970.38177	

HPLC traces of compound **34**

Signal 5: DAD1 E, Sig=280,16 Ref=off
Signal has been modified after loading from rawdata file!

Peak #	RetTime [min]	Type	Width [min]	Area [mAU*s]	Height [mAU]	Area %
1	11.133	BB	0.0809	2644.89453	490.63278	100.0000
Totals :				2644.89453	490.63278	

Signal 6: DAD1 F, Sig=280,16 Ref=off
Signal has been modified after loading from rawdata file!

Peak #	RetTime [min]	Type	Width [min]	Area [mAU*s]	Height [mAU]	Area %
1	11.133	BB	0.0809	2644.89453	490.63278	100.0000
Totals :				2644.89453	490.63278	

Signal 7: DAD1 G, Sig=300,16 Ref=off
Signal has been modified after loading from rawdata file!

Peak #	RetTime [min]	Type	Width [min]	Area [mAU*s]	Height [mAU]	Area %
1	11.133	BV	0.0816	3745.30640	686.99261	100.0000
Totals :				3745.30640	686.99261	

Signal 8: DAD1 H, Sig=320,16 Ref=off
Signal has been modified after loading from rawdata file!

Peak #	RetTime [min]	Type	Width [min]	Area [mAU*s]	Height [mAU]	Area %
1	11.133	BV	0.0815	2904.22461	533.46991	100.0000
Totals :				2904.22461	533.46991	

*** End of Report ***

HRMS of compound **34**

C:\Xcalibur\...\2-10-2013\MTM-III-86 2/10/2013 4:13:03 PM MTM-III-86

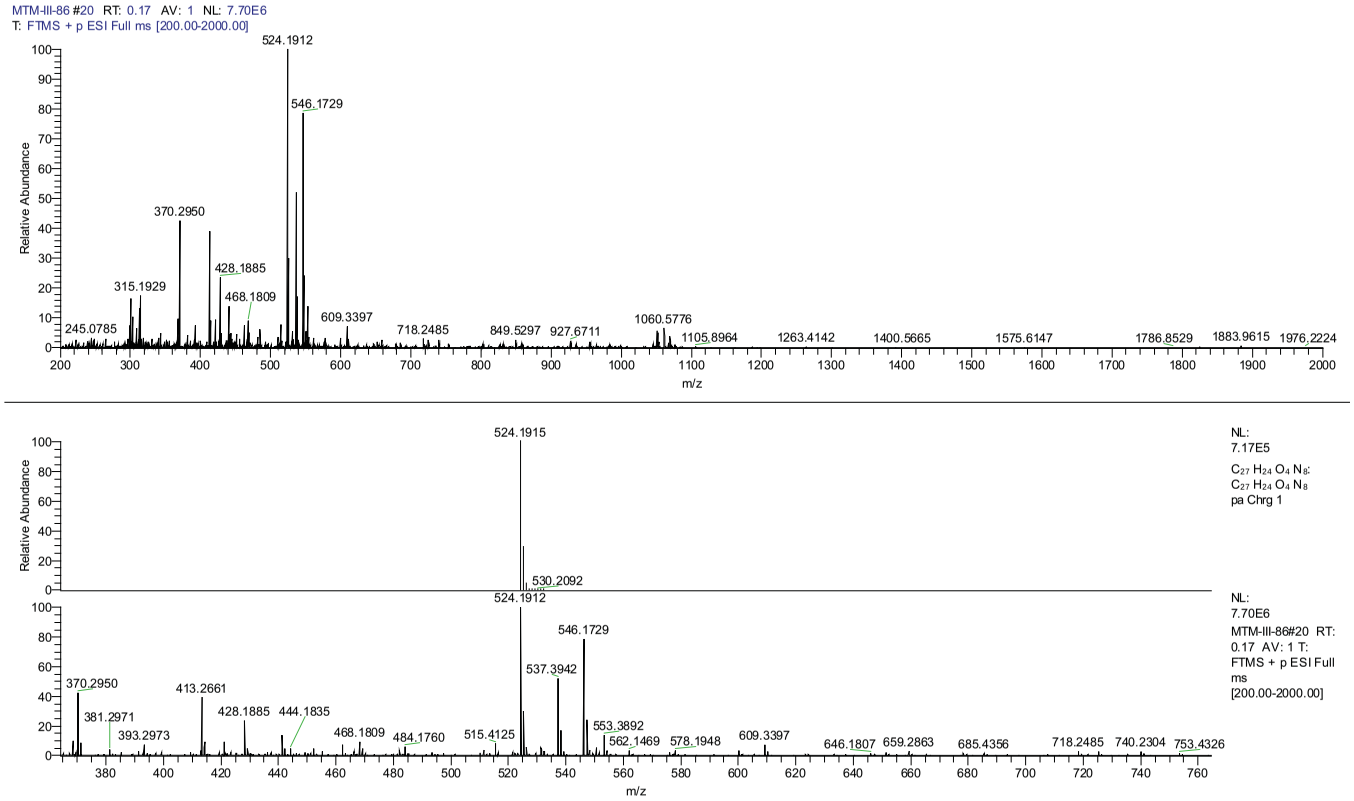

8.57
7.53
7.52
7.29
7.28
7.26
6.95
6.75
6.74
5.76
3.97
3.80
3.75
3.69
1.59
0.00
1.00
2.01
3.00
2.00
0.99
3.00
3.01
3.02
6.00
ppm
S80
OCH3
H3CO
H3CO
O
N
H
OH
H3CO
OCH3
35

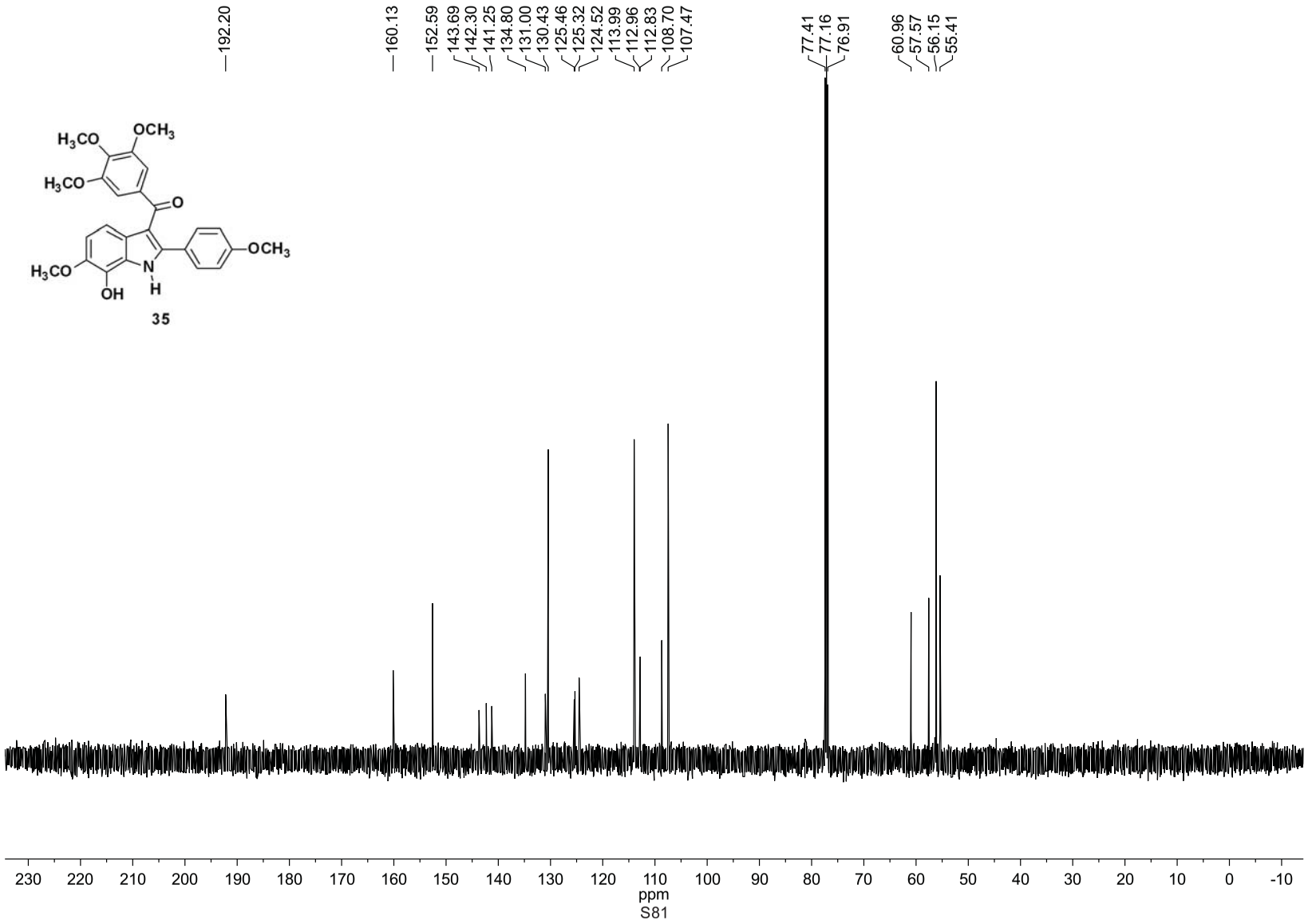
192.20
160.13
152.59
143.69
142.30
141.25
134.80
131.00
130.43
125.46
125.32
124.52
113.99
112.96
112.83
108.70
107.47
77.41
77.16
76.91
60.96
57.57
56.15
55.41
H3CO
OCH3
H3CO
O
H3CO
N
H
OH
OCH3
35
230 220 210 200 190 180 170 160 150 140 130 120 110 100 90 80 70 60 50 40 30 20 10 0 -10
ppm
S81

Data File C:\CHEM32\1\DATA\MATT MAC\MTM-V-58000002.D
Sample Name: run1

HPLC traces of compound **35**

```
==========================================================================
Acq. Operator   : Matt Mac
Acq. Instrument : Instrument 1                    Location :   -
Injection Date  : 1/25/2013 3:29:20 PM
Acq. Method     : C:\CHEM32\1\METHODS\MASTERMETHOD.M
Last changed    : 1/25/2013 3:22:08 PM by Matt Mac
Analysis Method : C:\CHEM32\1\DATA\MATT MAC\MTM-V-58000002.D\DA.M (MASTERMETHOD.M)
Last changed    : 1/25/2013 4:52:52 PM by Matt Mac
Sample Info     :
```

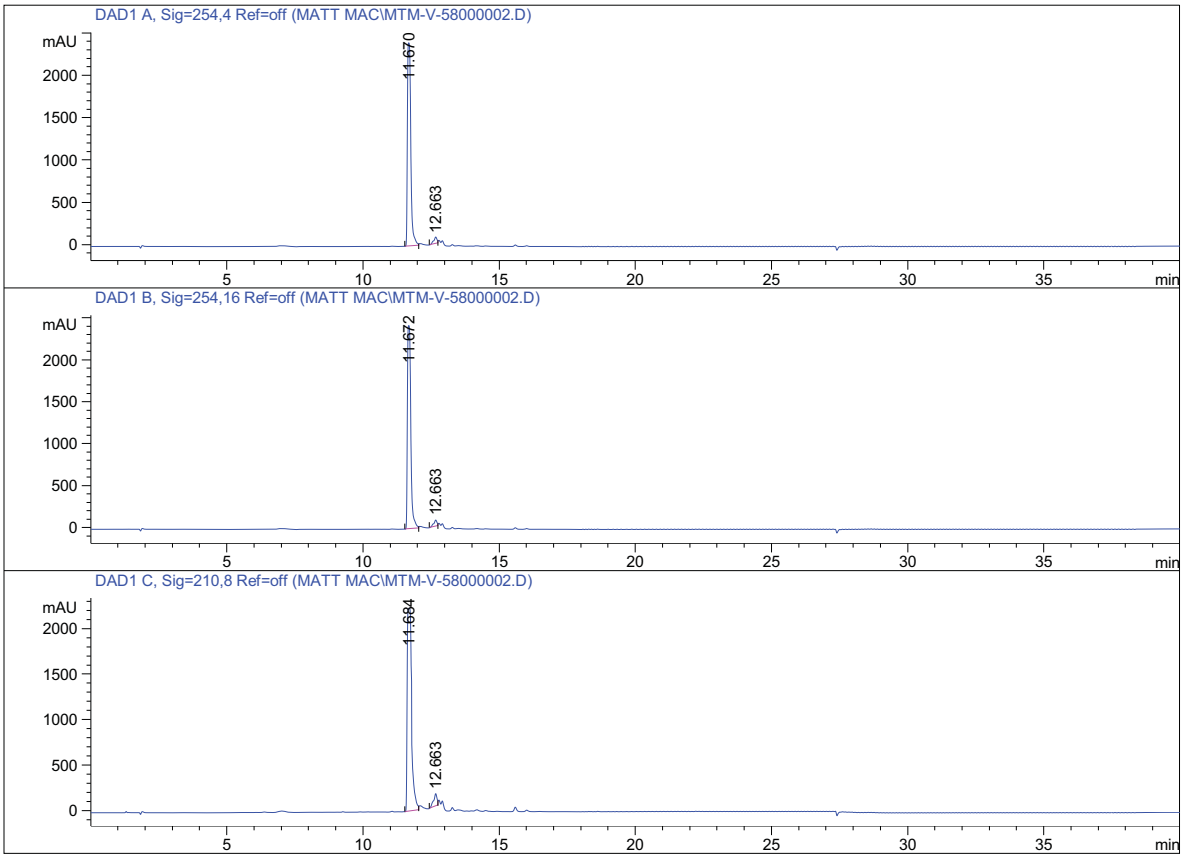

Instrument 1 1/25/2013 4:54:21 PM Matt Mac

Page 1 of 5

Data File C:\CHEM32\1\DATA\MATT MAC\MTM-V-58000002.D
Sample Name: run1

HPLC traces of compound **35**

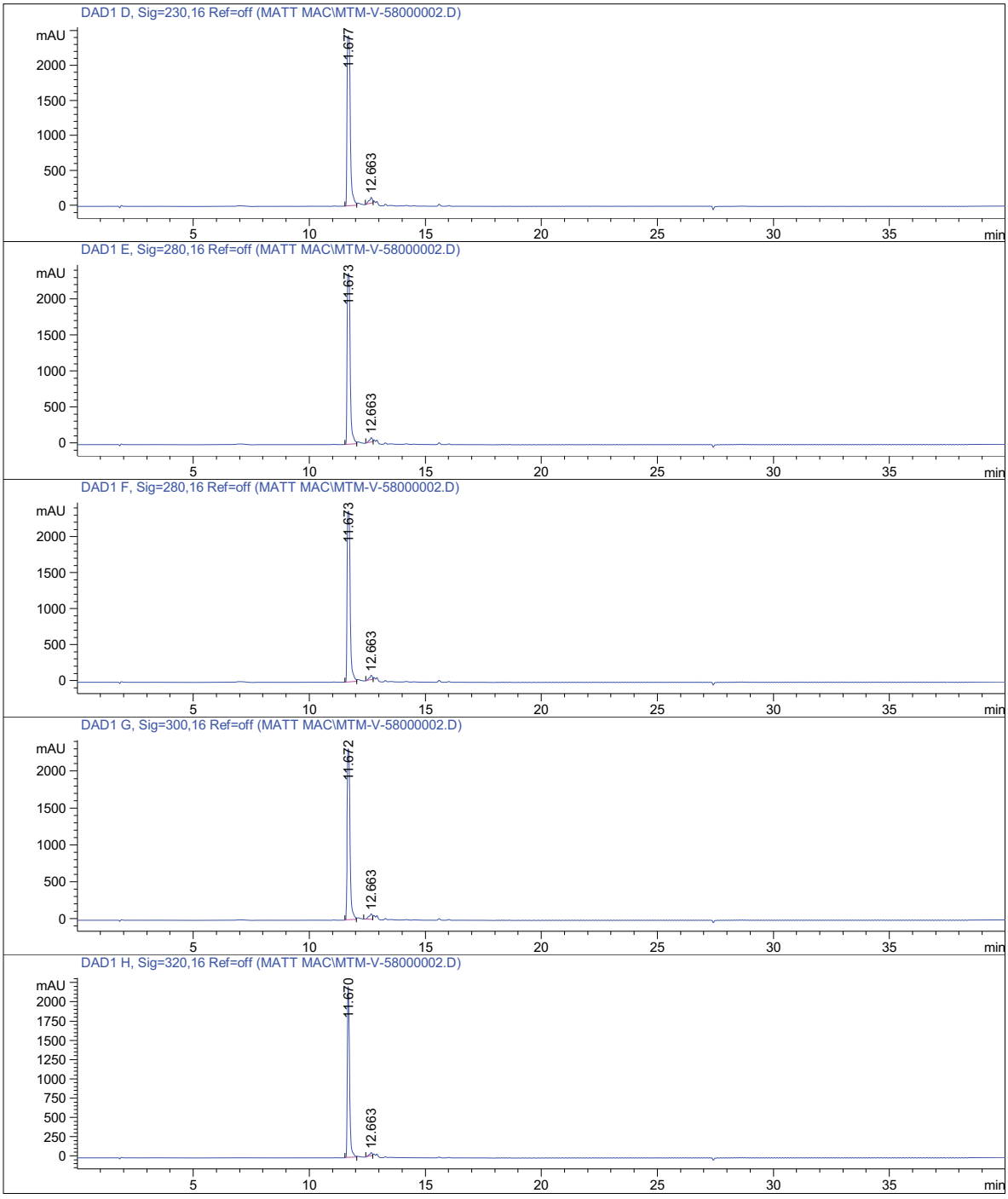

Instrument 1 1/25/2013 4:54:21 PM Matt Mac

Data File C:\CHEM32\1\DATA\MATT MAC\MTM-V-58000002.D
Sample Name: run1

HPLC traces of compound **35**

```
================================================================================
                            Area Percent Report
================================================================================

Sorted By             :      Signal
Multiplier            :      1.0000
Dilution              :      1.0000
Use Multiplier & Dilution Factor with ISTDs


Signal 1: DAD1 A, Sig=254,4 Ref=off

Peak RetTime Type  Width     Area      Height     Area
  #   [min]        [min]   [mAU*s]     [mAU]        %
----|-------|----|-------|----------|----------|--------|
   1  11.670 BV    0.1366 2.06994e4  2400.60474  96.8656
   2  12.663 BV    0.1233  669.79010   77.10614   3.1344

Totals :                  2.13692e4  2477.71088



Signal 2: DAD1 B, Sig=254,16 Ref=off

Peak RetTime Type  Width     Area      Height     Area
  #   [min]        [min]   [mAU*s]     [mAU]        %
----|-------|----|-------|----------|----------|--------|
   1  11.672 BV    0.1390 2.09971e4  2425.36963  96.9310
   2  12.663 BV    0.1241  664.80243   75.93778   3.0690

Totals :                  2.16619e4  2501.30741



Signal 3: DAD1 C, Sig=210,8 Ref=off

Peak RetTime Type  Width     Area      Height     Area
  #   [min]        [min]   [mAU*s]     [mAU]        %
----|-------|----|-------|----------|----------|--------|
   1  11.684 BV    0.1768 2.49809e4  2228.70850  95.3229
   2  12.663 BV    0.1273 1225.71509  135.74158   4.6771

Totals :                  2.62066e4  2364.45007



Signal 4: DAD1 D, Sig=230,16 Ref=off

Peak RetTime Type  Width     Area      Height     Area
  #   [min]        [min]   [mAU*s]     [mAU]        %
----|-------|----|-------|----------|----------|--------|
   1  11.677 BV    0.1549 2.35212e4  2429.63184  96.4298
   2  12.663 BV    0.1388  870.83435   86.97546   3.5702
```

Data File C:\CHEM32\1\DATA\MATT MAC\MTM-V-58000002.D
Sample Name: run1

HPLC traces of compound **35**

Peak #	RetTime [min]	Type	Width [min]	Area [mAU*s]	Height [mAU]	Area %
Totals :				2.43920e4	2516.60730	

Signal 5: DAD1 E, Sig=280,16 Ref=off

Peak #	RetTime [min]	Type	Width [min]	Area [mAU*s]	Height [mAU]	Area %
1	11.673	BV	0.1442	2.16120e4	2373.22510	97.4647
2	12.663	BV	0.1249	562.18378	63.75766	2.5353
Totals :				2.21741e4	2436.98276	

Signal 6: DAD1 F, Sig=280,16 Ref=off

Peak #	RetTime [min]	Type	Width [min]	Area [mAU*s]	Height [mAU]	Area %
1	11.673	BV	0.1442	2.16120e4	2373.22510	97.4647
2	12.663	BV	0.1249	562.18378	63.75766	2.5353
Totals :				2.21741e4	2436.98276	

Signal 7: DAD1 G, Sig=300,16 Ref=off

Peak #	RetTime [min]	Type	Width [min]	Area [mAU*s]	Height [mAU]	Area %
1	11.672	BV	0.1341	1.95065e4	2319.21680	96.0807
2	12.663	BV	0.1414	795.70215	76.45817	3.9193
Totals :				2.03022e4	2395.67496	

Signal 8: DAD1 H, Sig=320,16 Ref=off

Peak #	RetTime [min]	Type	Width [min]	Area [mAU*s]	Height [mAU]	Area %
1	11.670	BV	0.1026	1.46092e4	2224.54712	97.2378
2	12.663	BV	0.1257	415.00085	45.78540	2.7622
Totals :				1.50242e4	2270.33252	

Instrument 1 1/25/2013 4:54:21 PM Matt Mac

Data File C:\CHEM32\1\DATA\MATT MAC\MTM-V-58000002.D
Sample Name: run1

HPLC traces of compound **35**

==========

*** End of Report ***

HRMS of compound **35**

C:\Xcalibur\...\Matt\2-10-2013\MTM-V-58 2/10/2013 4:22:35 PM MTM-V-58

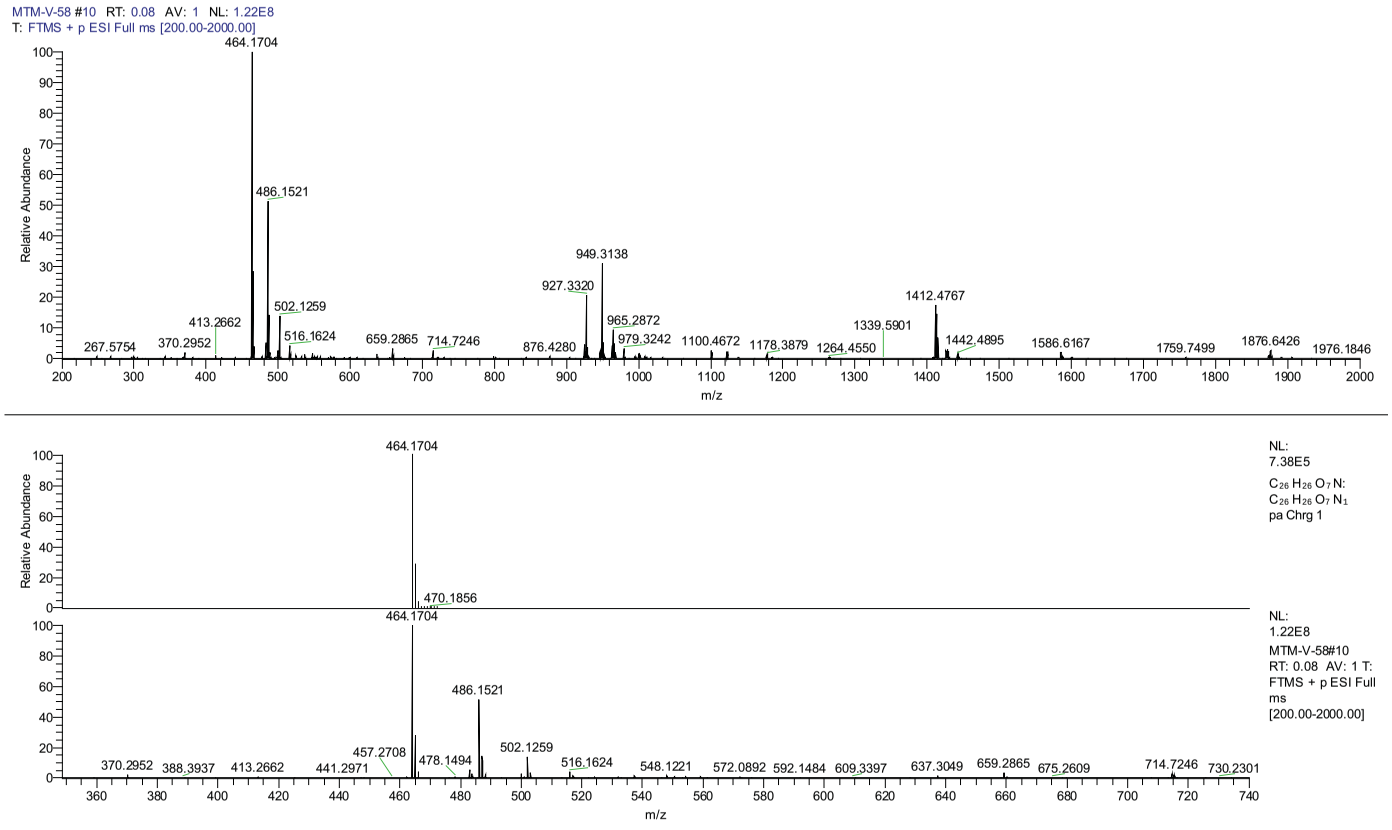

8.57
7.71
7.70
7.26
6.98
6.97
6.97
6.96
6.94
6.80
6.79
6.78
6.78
6.65
6.63
5.63
4.06
3.96
3.83
3.79
3.71
2.04
1.58
1.00
0.92
1.00
1.01
1.04
2.01
1.00
1.00
3.00
3.02
3.00
3.00
6.02
ppm
S88
OCH3
H3CO
H3CO
O
N
H
OCH3
H3CO
OCH3
OH
36

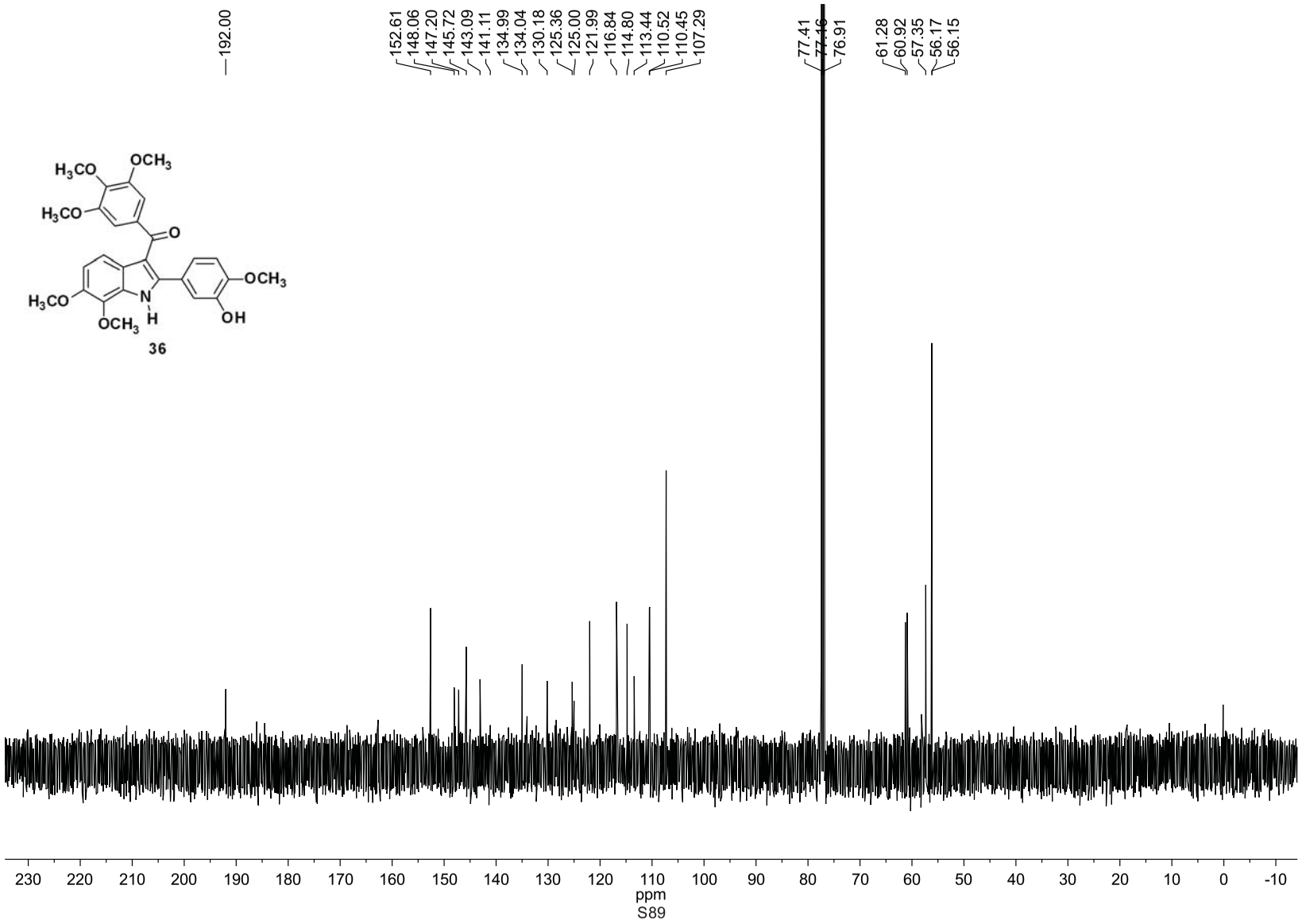
192.00
152.61
148.06
147.20
145.72
143.09
141.11
134.99
134.04
130.18
125.36
125.00
121.99
116.84
114.80
113.44
110.52
110.45
107.29
77.41
77.16
76.91
61.28
60.92
57.35
56.17
56.15
H3CO
OCH3
H3CO
O
H3CO
N
H
OCH3
OCH3
OH
36
230 220 210 200 190 180 170 160 150 140 130 120 110 100 90 80 70 60 50 40 30 20 10 0 -10
ppm
S89

Data File C:\CHEM32\1\DATA\MATT MAC\MTM-V-63000003.D
Sample Name: run1

HPLC traces of compound **36**

```
==========================================================================
Acq. Operator   : Matt Mac
Acq. Instrument : Instrument 1                    Location :   -
Injection Date  : 3/4/2013 1:27:41 PM
Acq. Method     : C:\CHEM32\1\METHODS\MASTERMETHOD.M
Last changed    : 3/4/2013 12:54:38 PM by Matt Mac
Analysis Method : C:\CHEM32\1\DATA\MATT MAC\MTM-V-63000003.D\DA.M (MASTERMETHOD.M)
Last changed    : 3/4/2013 2:17:56 PM by Matt Mac
```

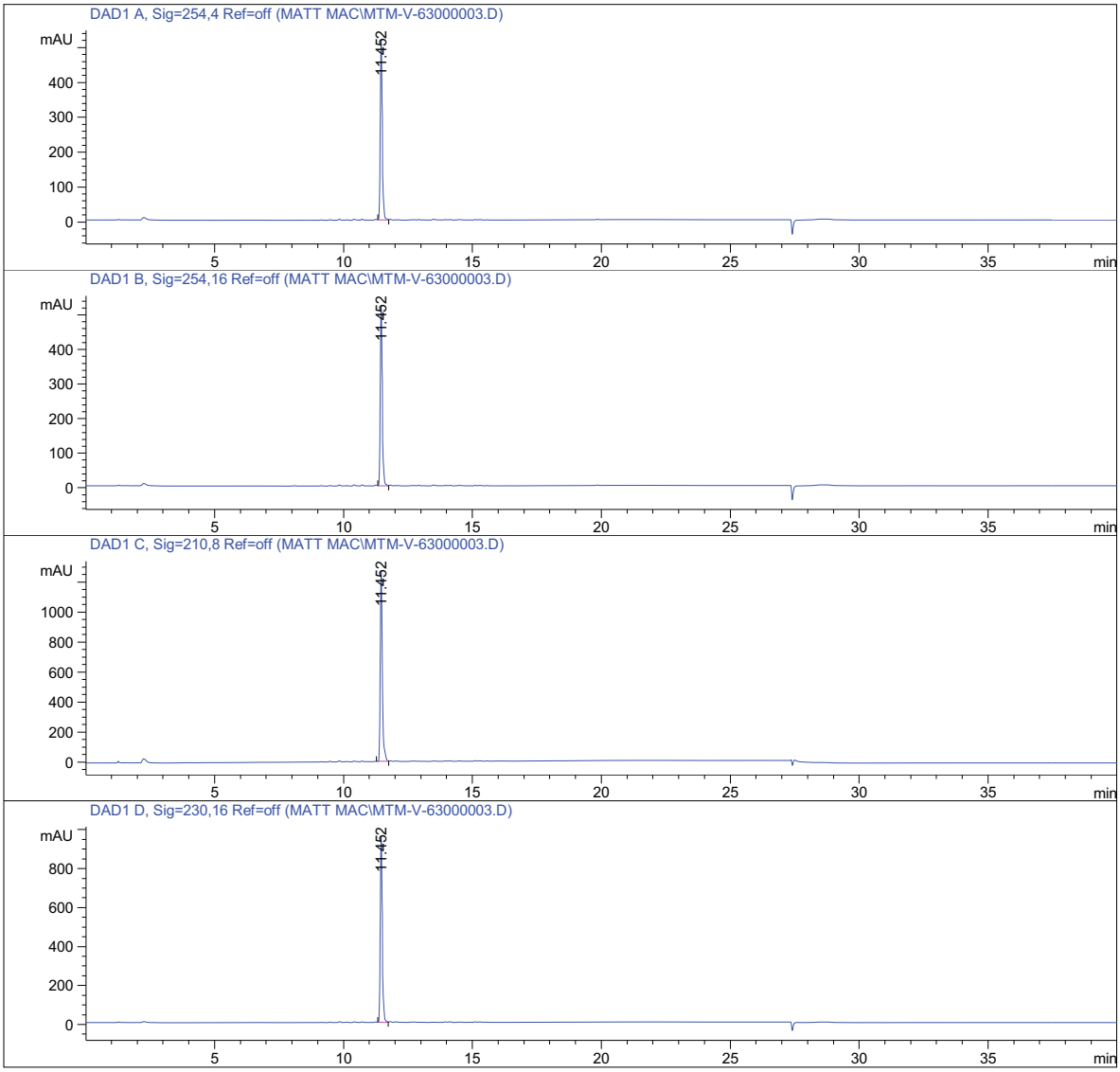

Data File C:\CHEM32\1\DATA\MATT MAC\MTM-V-63000003.D
Sample Name: run1

HPLC traces of compound **36**

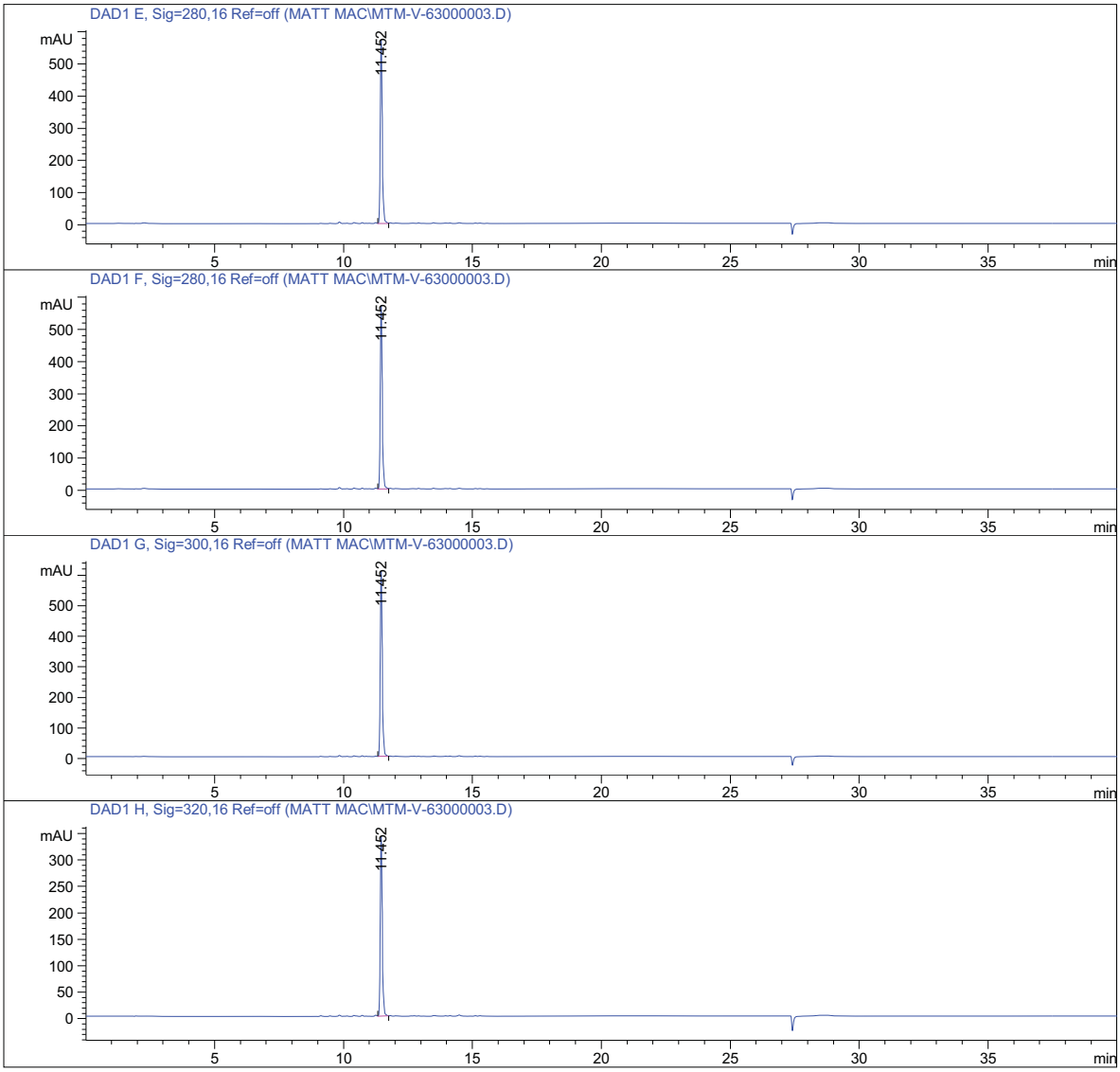

==========

Area Percent Report

==========

Sorted By : Signal
Multiplier : 1.0000
Dilution : 1.0000
Use Multiplier & Dilution Factor with ISTDs

Data File C:\CHEM32\1\DATA\MATT MAC\MTM-V-63000003.D
Sample Name: run1

HPLC traces of compound **36**

Signal 1: DAD1 A, Sig=254,4 Ref=off

Peak #	RetTime [min]	Type	Width [min]	Area [mAU*s]	Height [mAU]	Area %
1	11.452	VV	0.0809	2782.00977	516.37561	100.0000
Totals :				2782.00977	516.37561	

Signal 2: DAD1 B, Sig=254,16 Ref=off

Peak #	RetTime [min]	Type	Width [min]	Area [mAU*s]	Height [mAU]	Area %
1	11.452	VV	0.0809	2812.19629	521.91907	100.0000
Totals :				2812.19629	521.91907	

Signal 3: DAD1 C, Sig=210,8 Ref=off

Peak #	RetTime [min]	Type	Width [min]	Area [mAU*s]	Height [mAU]	Area %
1	11.452	BV	0.0858	7160.16650	1269.44250	100.0000
Totals :				7160.16650	1269.44250	

Signal 4: DAD1 D, Sig=230,16 Ref=off

Peak #	RetTime [min]	Type	Width [min]	Area [mAU*s]	Height [mAU]	Area %
1	11.452	VV	0.0813	5182.18311	954.98956	100.0000
Totals :				5182.18311	954.98956	

Signal 5: DAD1 E, Sig=280,16 Ref=off

Peak #	RetTime [min]	Type	Width [min]	Area [mAU*s]	Height [mAU]	Area %
1	11.452	VV	0.0809	3076.47729	570.49207	100.0000
Totals :				3076.47729	570.49207	

Data File C:\CHEM32\1\DATA\MATT MAC\MTM-V-63000003.D
Sample Name: run1

HPLC traces of compound **36**

Signal 6: DAD1 F, Sig=280,16 Ref=off

Peak #	RetTime [min]	Type	Width [min]	Area [mAU*s]	Height [mAU]	Area %
1	11.452	VV	0.0809	3076.47729	570.49207	100.0000
Totals :				3076.47729	570.49207	

Signal 7: DAD1 G, Sig=300,16 Ref=off

Peak #	RetTime [min]	Type	Width [min]	Area [mAU*s]	Height [mAU]	Area %
1	11.452	VV	0.0809	3278.34961	607.59808	100.0000
Totals :				3278.34961	607.59808	

Signal 8: DAD1 H, Sig=320,16 Ref=off

Peak #	RetTime [min]	Type	Width [min]	Area [mAU*s]	Height [mAU]	Area %
1	11.452	VV	0.0808	1831.79126	340.07983	100.0000
Totals :				1831.79126	340.07983	

*** End of Report ***

HRMS of compound **36**

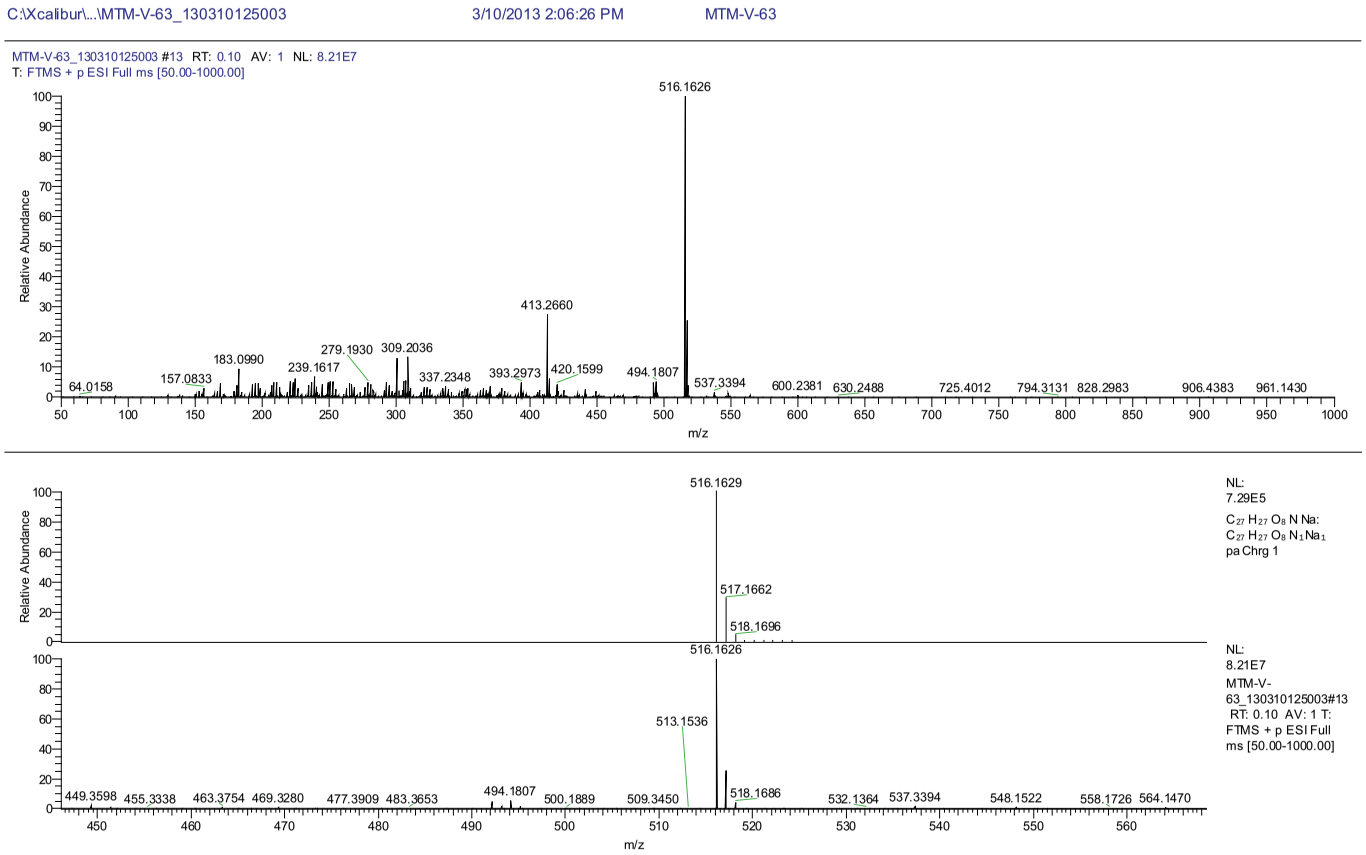

X-ray Crystallographic Analysis:

X-ray crystallographic analysis of compound **10**.[S1] Crystallographic data were collected on a crystal of **10** with dimensions 0.27 x 0.15 x 0.13 mm^3. Data were collected at 110 K on a Bruker X8 Apex using Mo KR radiation (λ = 0.71073 Å). The structure was solved by direct methods after correction of the data using SADABS. Crystallographic data and refinement details for the complex mentioned herein is found in the Supporting Information (Table S1-S4). The thermal ellipsoid plots at 50% probability for compound **10** is displayed in Figure S1. All data were processed using the Bruker AXS SHELXTL software, version 6.10.

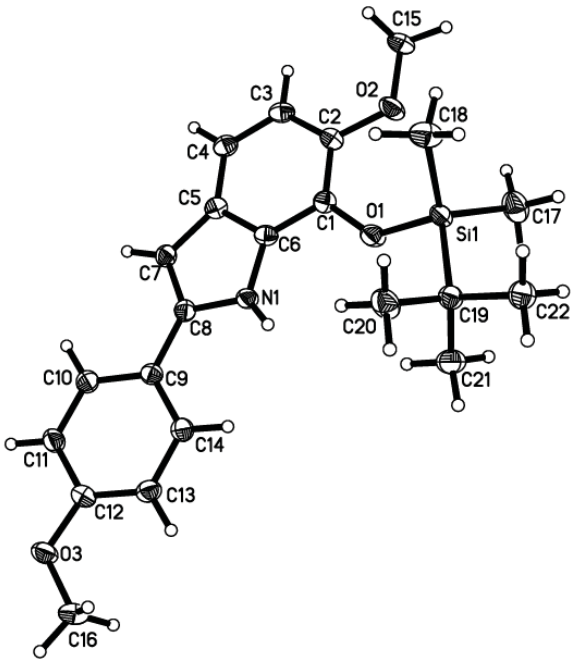

Figure S1. X-ray crystallography of compound **10.**

Table S1. Crystal data and structure refinement for **10**.

Identification code	kp50	
Empirical formula	C22 H29 N O3 Si	
Formula weight	383.55	
Temperature	110(2) K	
Wavelength	0.71073 Å	
Crystal system	Triclinic	
Space group	P-1	
Unit cell dimensions	a = 7.3314(5) Å	□= 97.114(2)°.
	b = 9.6558(5) Å	□= 94.927(2)°.
	c = 15.1609(9) Å	□ = 99.888(2)°.
Volume	1042.84(11) $Å^3$	
Z	2	
Density (calculated)	1.221 Mg/m^3	
Absorption coefficient	0.134 mm^{-1}	
F(000)	412	
Crystal size	0.27 x 0.15 x 0.13 mm^3	
Theta range for data collection	1.36 to 26.37°.	
Index ranges	-9<=h<=9, -8<=k<=12, -18<=l<=18	
Reflections collected	17172	
Independent reflections	4231 [R(int) = 0.0490]	
Completeness to theta = 26.37°	99.2 %	
Absorption correction	Semi-empirical from equivalents	
Max. and min. transmission	0.9823 and 0.9647	
Refinement method	Full-matrix least-squares on F^2	
Data / restraints / parameters	4231 / 0 / 255	
Goodness-of-fit on F^2	1.037	
Final R indices [I>2sigma(I)]	R1 = 0.0427, wR2 = 0.1042	
R indices (all data)	R1 = 0.0564, wR2 = 0.1142	
Largest diff. peak and hole	0.340 and -0.313 $e.Å^{-3}$	

Table S2. Atomic coordinates (x 10^4) and equivalent isotropic displacement parameters ($Å^2$x 10^3) for **10**. U(eq) is defined as one third of the trace of the orthogonalized U^{ij} tensor.

	x	y	z	U(eq)
Si(1)	4713(1)	9097(1)	1851(1)	21(1)
O(1)	4220(2)	7418(1)	2037(1)	26(1)
O(2)	3856(2)	6872(1)	191(1)	28(1)
O(3)	768(2)	2922(1)	6726(1)	28(1)
N(1)	2658(2)	5171(2)	2980(1)	20(1)
C(1)	3300(2)	6151(2)	1571(1)	20(1)
C(2)	3079(2)	5808(2)	644(1)	21(1)
C(3)	2156(2)	4453(2)	238(1)	23(1)
C(4)	1451(2)	3422(2)	740(1)	23(1)
C(5)	1660(2)	3736(2)	1675(1)	20(1)
C(6)	2594(2)	5099(2)	2067(1)	19(1)
C(7)	1117(2)	2997(2)	2405(1)	20(1)
C(8)	1734(2)	3898(2)	3191(1)	20(1)
C(9)	1561(2)	3677(2)	4120(1)	19(1)
C(10)	443(2)	2452(2)	4313(1)	23(1)
C(11)	226(2)	2227(2)	5182(1)	25(1)
C(12)	1118(2)	3234(2)	5895(1)	22(1)
C(13)	2259(2)	4445(2)	5724(1)	25(1)
C(14)	2468(2)	4661(2)	4844(1)	24(1)
C(15)	3613(3)	6623(2)	-762(1)	27(1)
C(16)	1662(3)	3927(2)	7474(1)	29(1)
C(17)	6965(3)	9383(2)	1362(1)	34(1)
C(18)	2779(3)	9591(2)	1155(1)	33(1)
C(19)	4968(2)	10083(2)	3024(1)	23(1)
C(20)	3072(3)	9877(2)	3394(1)	31(1)
C(21)	6344(3)	9509(2)	3636(1)	32(1)
C(22)	5653(3)	11685(2)	3021(1)	28(1)

Table S3. Bond lengths [Å] and angles [°] for **10**.

Si(1)-O(1)	1.6635(12)
Si(1)-C(18)	1.8580(19)
Si(1)-C(17)	1.860(2)
Si(1)-C(19)	1.8879(18)
O(1)-C(1)	1.367(2)
O(2)-C(2)	1.375(2)
O(2)-C(15)	1.426(2)
O(3)-C(12)	1.367(2)
O(3)-C(16)	1.428(2)
N(1)-C(6)	1.374(2)
N(1)-C(8)	1.386(2)
C(1)-C(2)	1.393(2)
C(1)-C(6)	1.393(2)
C(2)-C(3)	1.404(2)
C(3)-C(4)	1.384(2)
C(4)-C(5)	1.403(2)
C(5)-C(6)	1.407(2)
C(5)-C(7)	1.437(2)
C(7)-C(8)	1.377(2)
C(8)-C(9)	1.464(2)
C(9)-C(14)	1.396(2)
C(9)-C(10)	1.396(2)
C(10)-C(11)	1.379(2)
C(11)-C(12)	1.394(2)
C(12)-C(13)	1.382(2)
C(13)-C(14)	1.392(2)
C(19)-C(21)	1.532(2)
C(19)-C(20)	1.534(2)
C(19)-C(22)	1.543(2)
O(1)-Si(1)-C(18)	111.85(8)
O(1)-Si(1)-C(17)	108.82(8)
C(18)-Si(1)-C(17)	113.09(9)
O(1)-Si(1)-C(19)	101.50(7)

C(18)-Si(1)-C(19)	110.31(8)
C(17)-Si(1)-C(19)	110.67(9)
C(1)-O(1)-Si(1)	136.84(11)
C(2)-O(2)-C(15)	118.03(14)
C(12)-O(3)-C(16)	117.14(14)
C(6)-N(1)-C(8)	109.35(14)
O(1)-C(1)-C(2)	125.36(15)
O(1)-C(1)-C(6)	117.24(15)
C(2)-C(1)-C(6)	117.35(15)
O(2)-C(2)-C(1)	114.75(15)
O(2)-C(2)-C(3)	124.85(15)
C(1)-C(2)-C(3)	120.38(16)
C(4)-C(3)-C(2)	121.61(16)
C(3)-C(4)-C(5)	119.27(16)
C(4)-C(5)-C(6)	118.14(16)
C(4)-C(5)-C(7)	135.97(16)
C(6)-C(5)-C(7)	105.88(14)
N(1)-C(6)-C(1)	128.28(15)
N(1)-C(6)-C(5)	108.47(15)
C(1)-C(6)-C(5)	123.25(15)
C(8)-C(7)-C(5)	108.16(15)
C(7)-C(8)-N(1)	108.11(14)
C(7)-C(8)-C(9)	130.51(15)
N(1)-C(8)-C(9)	121.37(15)
C(14)-C(9)-C(10)	117.27(16)
C(14)-C(9)-C(8)	122.51(15)
C(10)-C(9)-C(8)	120.22(15)
C(11)-C(10)-C(9)	121.54(16)
C(10)-C(11)-C(12)	120.31(16)
O(3)-C(12)-C(13)	125.15(16)
O(3)-C(12)-C(11)	115.49(15)
C(13)-C(12)-C(11)	119.35(16)
C(12)-C(13)-C(14)	119.81(16)
C(13)-C(14)-C(9)	121.69(16)
C(21)-C(19)-C(20)	108.49(15)
C(21)-C(19)-C(22)	109.60(15)

C(20)-C(19)-C(22)	108.58(14)
C(21)-C(19)-Si(1)	110.38(12)
C(20)-C(19)-Si(1)	109.42(12)
C(22)-C(19)-Si(1)	110.33(12)

Symmetry transformations used to generate equivalent atoms:

Table S4. Anisotropic displacement parameters ($Å^2 x\ 10^3$) for **10**. The anisotropic displacement factor exponent takes the form: $-2p^2[\ h^2\ a^{*2}U^{11} + ... + 2\ h\ k\ a^*\ b^*\ U^{12}\ ]$

	U^{11}	U^{22}	U^{33}	U^{23}	U^{13}	U^{12}
Si(1)	27(1)	19(1)	17(1)	4(1)	5(1)	3(1)
O(1)	41(1)	18(1)	16(1)	1(1)	1(1)	-1(1)
O(2)	43(1)	25(1)	16(1)	4(1)	6(1)	1(1)
O(3)	38(1)	27(1)	16(1)	2(1)	5(1)	2(1)
N(1)	26(1)	17(1)	16(1)	1(1)	1(1)	1(1)
C(1)	22(1)	18(1)	20(1)	1(1)	2(1)	4(1)
C(2)	24(1)	22(1)	18(1)	4(1)	4(1)	6(1)
C(3)	26(1)	26(1)	16(1)	-1(1)	0(1)	7(1)
C(4)	25(1)	23(1)	20(1)	-2(1)	0(1)	4(1)
C(5)	21(1)	20(1)	20(1)	1(1)	2(1)	5(1)
C(6)	21(1)	21(1)	17(1)	2(1)	2(1)	7(1)
C(7)	22(1)	18(1)	21(1)	2(1)	2(1)	2(1)
C(8)	18(1)	19(1)	22(1)	5(1)	2(1)	4(1)
C(9)	20(1)	20(1)	20(1)	4(1)	1(1)	5(1)
C(10)	26(1)	21(1)	21(1)	0(1)	3(1)	0(1)
C(11)	29(1)	22(1)	22(1)	4(1)	6(1)	0(1)
C(12)	25(1)	24(1)	19(1)	5(1)	5(1)	8(1)
C(13)	28(1)	24(1)	20(1)	0(1)	-1(1)	2(1)
C(14)	28(1)	20(1)	23(1)	5(1)	0(1)	0(1)
C(15)	34(1)	32(1)	15(1)	6(1)	4(1)	8(1)
C(16)	37(1)	33(1)	17(1)	1(1)	1(1)	8(1)
C(17)	39(1)	33(1)	33(1)	6(1)	15(1)	4(1)
C(18)	42(1)	33(1)	23(1)	3(1)	0(1)	11(1)
C(19)	28(1)	19(1)	20(1)	3(1)	2(1)	2(1)
C(20)	39(1)	31(1)	24(1)	2(1)	12(1)	4(1)
C(21)	44(1)	24(1)	24(1)	4(1)	-5(1)	3(1)
C(22)	34(1)	20(1)	28(1)	3(1)	2(1)	4(1)

S1. Crystallographic data for structure **10** (deposition number CCDC 935741) reported in this paper have been deposited with the Cambridge Crystallographic Data Centre. Copies of the data can be obtained, free of charge, on application to the Director, CCDC, 12 Union Road, Cambridge CB2 1EZ, UK (fax: +44-(0) 1223-336033 or e-mail: deposit@ccdc.cam.ac.uk).

APPENDIX D

Indole-based Bioreductively Activatable Prodrug Conjugates

7.72
7.71
6.84
6.84
5.09
5.08
5.06
5.05
3.71
1.54
1.53
0.96
1.00
1.02
0.98
3.04
ppm
OH
CH3
S
O2N

159.94
149.89
129.07
122.20
77.41
77.16
76.90
66.28
25.02
ppm

7.16
7.15
7.15
7.14
6.93
6.92
6.92
6.92
6.91
6.91
6.90
6.90
2.53
1.63
6.00
1.04
1.03
1.00
1.00
ppm

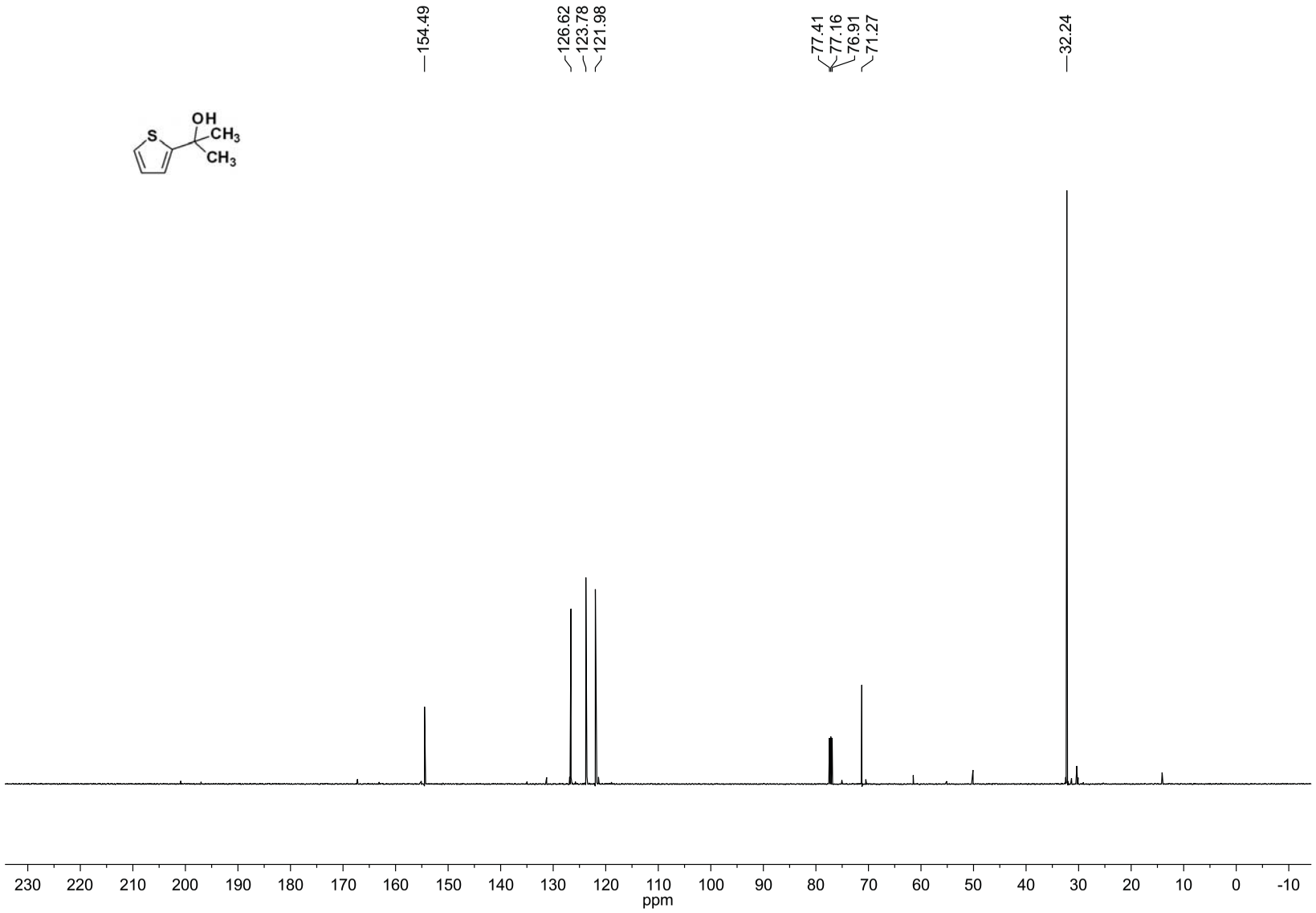
154.49
126.62
123.78
121.98
77.41
77.16
76.91
71.27
32.24
OH
CH3
CH3
S
230 220 210 200 190 180 170 160 150 140 130 120 110 100 90 80 70 60 50 40 30 20 10 0 -10
ppm

1.64
6.02
7.75
7.74
6.85
6.84
0.98
1.00
ppm

164.09
129.05
121.41
77.42
77.16
76.91
71.96
32.02
OH
CH3
CH3
S
O2N
ppm

8.36
7.83
7.81
7.80
7.79
7.26
7.15
7.14
7.13
7.00
6.97
6.96
6.92
6.91
6.90
6.90
6.89
6.88
6.86
4.96
3.88
3.86
3.82
3.69
1.54
0.00
1.00
1.09
0.92
1.19
2.01
1.03
3.13
1.15
2.00
3.12
3.02
3.03
6.01
ppm
OCH3
H3CO
H3CO
O
N
H
H3CO
O
S
NO2

191.95
157.49
152.77
151.84
150.63
148.08
146.97
141.82
141.55
136.47
134.87
128.54
125.08
124.85
123.10
122.86
122.54
117.26
113.00
111.94
111.87
107.49
94.67
77.41
77.16
76.91
66.91
61.06
56.21
56.09
55.78
ppm

Data File C:\CHEM32\1\DATA\MATT MAC\MTM-III-9500035.D
Sample Name: run1

```
    ======================================================================
    Acq. Operator   : Matt Mac
    Acq. Instrument : Instrument 1                    Location :   -
    Injection Date  : 8/31/2012 5:23:34 PM
    Acq. Method     : C:\CHEM32\1\METHODS\MASTERMETHOD.M
    Last changed    : 8/31/2012 5:17:17 PM by Matt Mac
                      (modified after loading)
    Analysis Method : C:\CHEM32\1\DATA\MATT MAC\MTM-III-9500035.D\DA.M (MASTERMETHOD.M)
    Last changed    : 8/31/2012 6:13:49 PM by Matt Mac
    Sample Info     :
```

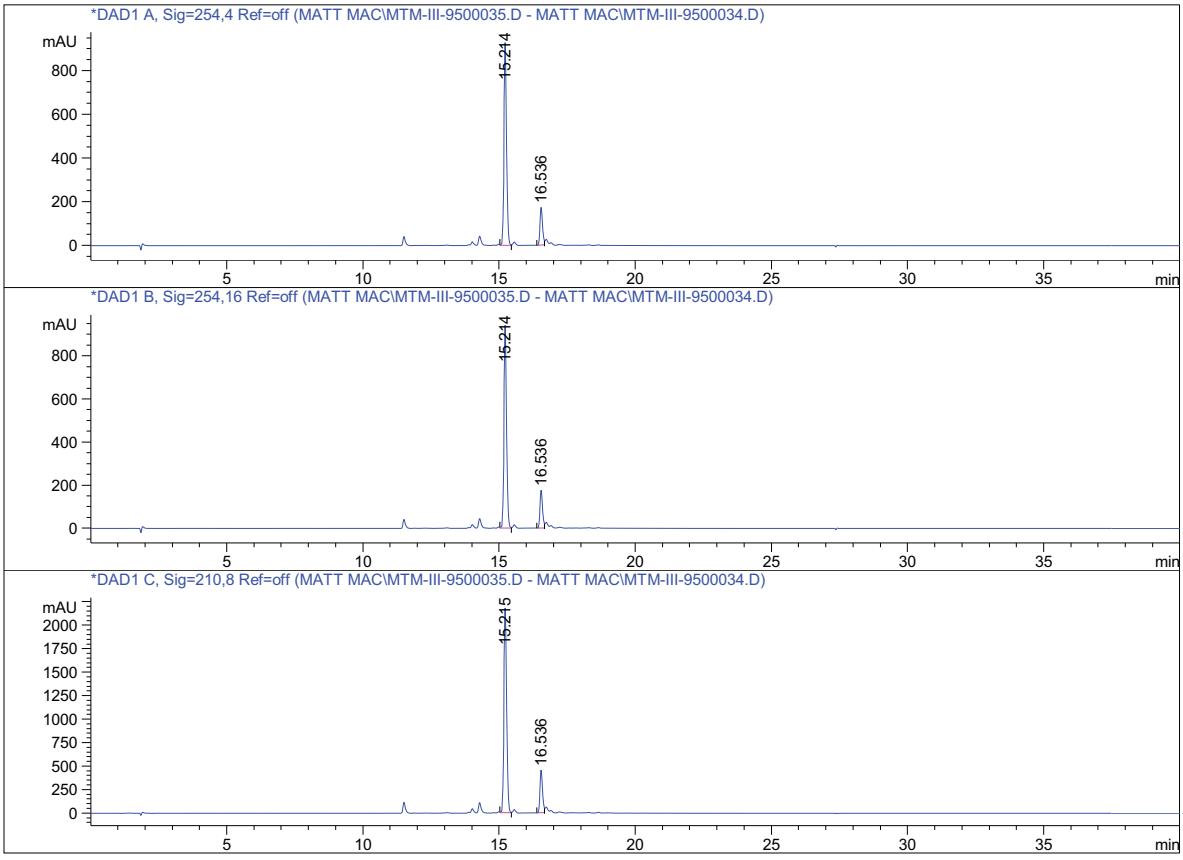

Data File C:\CHEM32\1\DATA\MATT MAC\MTM-III-9500035.D
Sample Name: run1

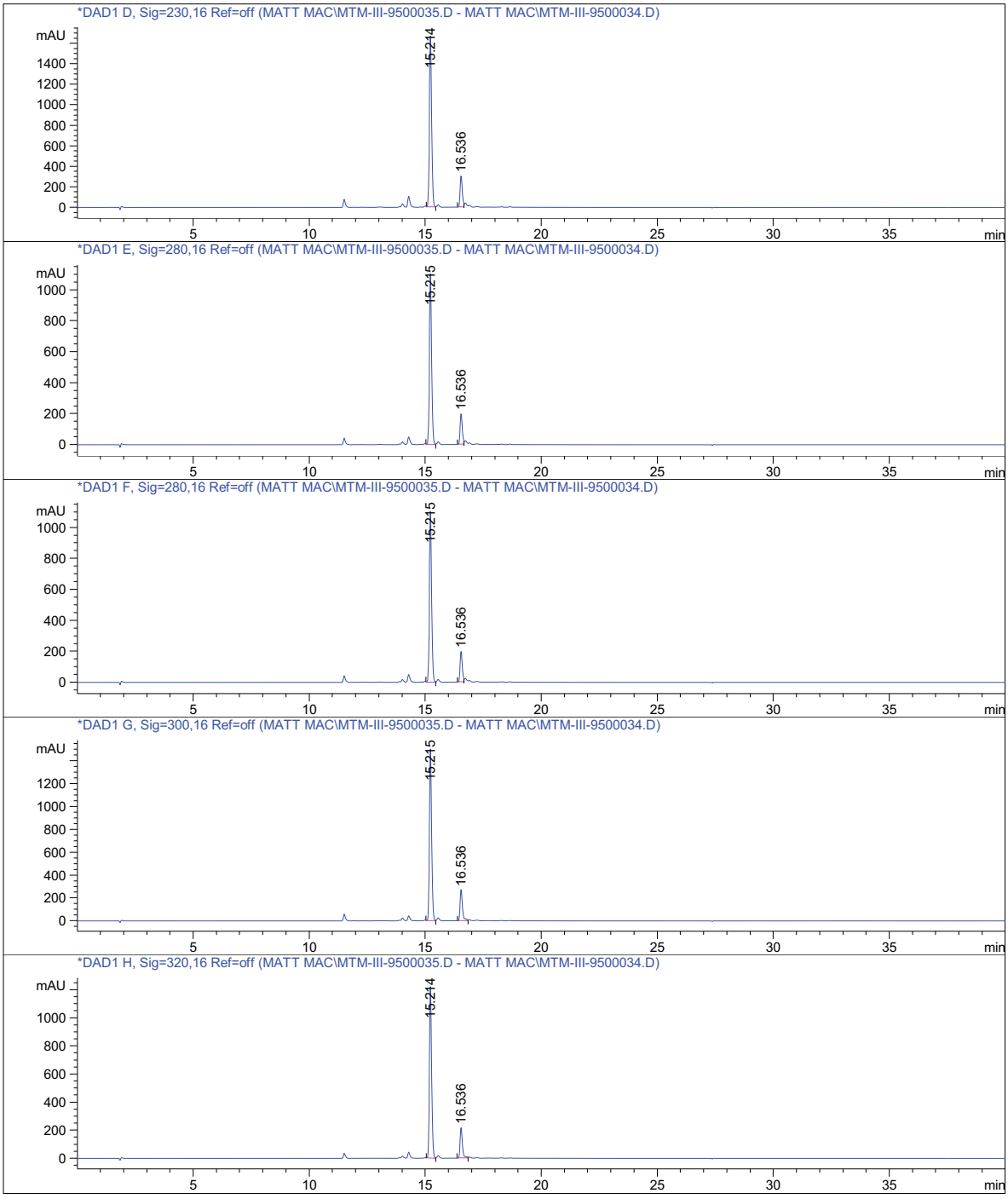

Data File C:\CHEM32\1\DATA\MATT MAC\MTM-III-9500035.D
Sample Name: run1

==========

Area Percent Report

==========

Sorted By : Signal
Multiplier : 1.0000
Dilution : 1.0000
Use Multiplier & Dilution Factor with ISTDs

Signal 1: DAD1 A, Sig=254,4 Ref=off
Signal has been modified after loading from rawdata file!

Peak #	RetTime [min]	Type	Width [min]	Area [mAU*s]	Height [mAU]	Area %
1	15.214	VV	0.1001	6063.56348	929.57355	84.1695
2	16.536	BV	0.1007	1140.43201	173.51051	15.8305
Totals :				7203.99548	1103.08406	

Signal 2: DAD1 B, Sig=254,16 Ref=off
Signal has been modified after loading from rawdata file!

Peak #	RetTime [min]	Type	Width [min]	Area [mAU*s]	Height [mAU]	Area %
1	15.214	VV	0.1001	6153.04248	943.16779	84.2085
2	16.536	BV	0.1008	1153.86731	175.39597	15.7915
Totals :				7306.90979	1118.56375	

Signal 3: DAD1 C, Sig=210,8 Ref=off
Signal has been modified after loading from rawdata file!

Peak #	RetTime [min]	Type	Width [min]	Area [mAU*s]	Height [mAU]	Area %
1	15.215	VV	0.1076	1.52843e4	2184.93066	83.5471
2	16.536	BV	0.1009	3009.93872	456.42361	16.4529
Totals :				1.82942e4	2641.35428	

Data File C:\CHEM32\1\DATA\MATT MAC\MTM-III-9500035.D
Sample Name: run1

Signal 4: DAD1 D, Sig=230,16 Ref=off
Signal has been modified after loading from rawdata file!

Peak #	RetTime [min]	Type	Width [min]	Area [mAU*s]	Height [mAU]	Area %
1	15.214	VV	0.1019	1.11799e4	1674.31799	84.7870
2	16.536	BV	0.1009	2005.96411	304.30643	15.2130
Totals :				1.31859e4	1978.62442	

Signal 5: DAD1 E, Sig=280,16 Ref=off
Signal has been modified after loading from rawdata file!

Peak #	RetTime [min]	Type	Width [min]	Area [mAU*s]	Height [mAU]	Area %
1	15.215	VV	0.1002	7223.75781	1105.92590	84.6893
2	16.536	BV	0.1009	1305.95715	198.03979	15.3107
Totals :				8529.71497	1303.96570	

Signal 6: DAD1 F, Sig=280,16 Ref=off
Signal has been modified after loading from rawdata file!

Peak #	RetTime [min]	Type	Width [min]	Area [mAU*s]	Height [mAU]	Area %
1	15.215	VV	0.1002	7223.75781	1105.92590	84.6893
2	16.536	BV	0.1009	1305.95715	198.03979	15.3107
Totals :				8529.71497	1303.96570	

Signal 7: DAD1 G, Sig=300,16 Ref=off
Signal has been modified after loading from rawdata file!

Peak #	RetTime [min]	Type	Width [min]	Area [mAU*s]	Height [mAU]	Area %
1	15.215	VV	0.1007	9901.29590	1506.61536	83.6760
2	16.536	BV	0.1067	1931.59778	272.64737	16.3240
Totals :				1.18329e4	1779.26273	

Data File C:\CHEM32\1\DATA\MATT MAC\MTM-III-9500035.D
Sample Name: run1

Signal 8: DAD1 H, Sig=320,16 Ref=off
Signal has been modified after loading from rawdata file!

Peak #	RetTime [min]	Type	Width [min]	Area [mAU*s]	Height [mAU]	Area %
1	15.214	VV	0.1001	7991.85156	1224.54712	83.9649
2	16.536	BV	0.1060	1526.23022	217.26747	16.0351
Totals :				9518.08179	1441.81459	

*** End of Report ***

C:\Xcalibur\...\MTM-III-95_+ESI 2/10/2013 10:57:41 AM MTM-III-95

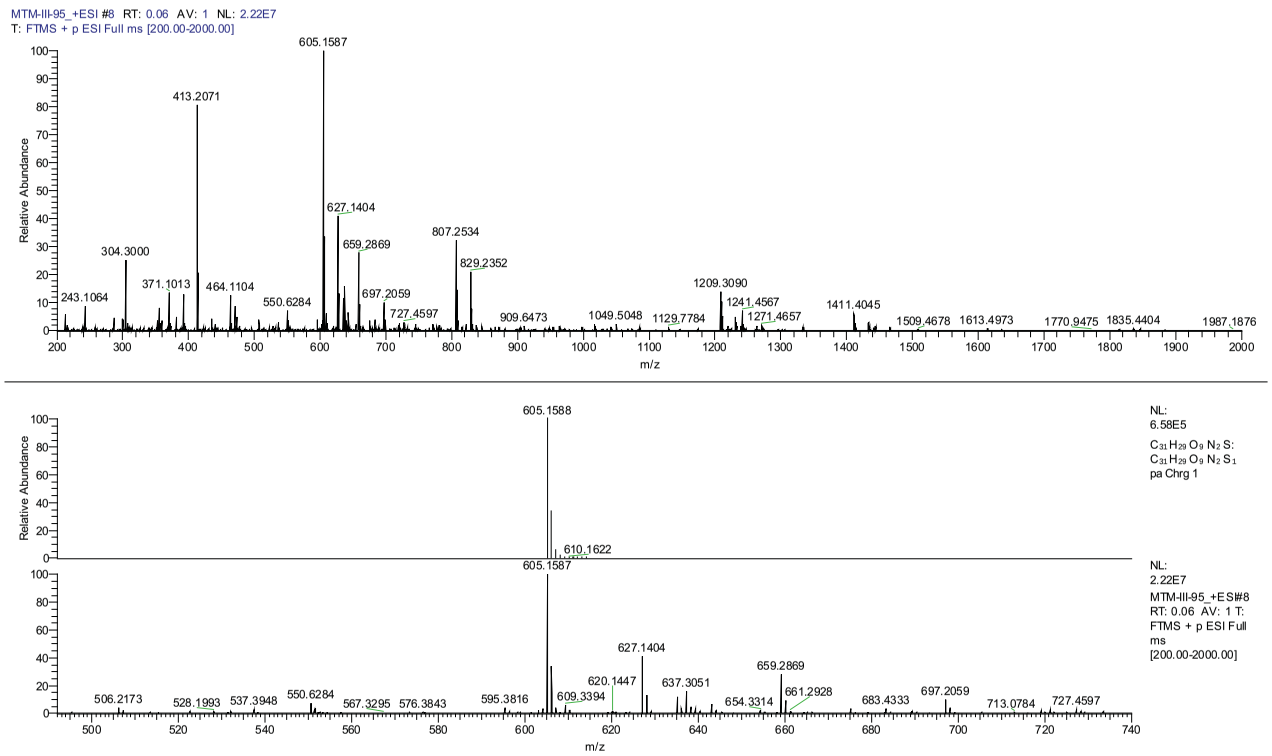

8.97
7.76
7.74
7.69
7.68
7.26
6.99
6.87
6.86
6.85
6.84
6.84
6.84
6.80
6.72
6.70
5.15
5.14
5.13
5.11
3.82
3.80
3.78
3.66
1.54
1.52
0.00
1.01
1.00
0.92
1.00
2.01
1.01
2.02
1.00
1.00
1.10
3.02
3.01
6.01
3.00
ppm
OCH3
H3CO
H3CO
O
N
H
H3CO
OCH3
O
S
NO2
H3C

191.91
157.41
155.30
152.73
151.35
150.94
146.08
141.71
141.51
136.49
134.73
128.57
124.84
123.41
123.13
123.09
122.40
119.70
112.87
112.12
111.83
107.44
94.64
77.41
77.16
76.91
61.01
56.17
56.01
55.74
22.92
ppm

Data File C:\CHEM32\1\DATA\MATT MAC\MTM-IV-74000033.D
Sample Name: run1

```
    ======================================================================
    Acq. Operator   : Matt Mac
    Acq. Instrument : Instrument 1                    Location :   -
    Injection Date  : 8/31/2012 3:34:49 PM
    Acq. Method     : C:\CHEM32\1\METHODS\MASTERMETHOD.M
    Last changed    : 8/31/2012 3:29:16 PM by Matt Mac
                      (modified after loading)
    Analysis Method : C:\CHEM32\1\DATA\MATT MAC\MTM-IV-74000033.D\DA.M (MASTERMETHOD.M)
    Last changed    : 8/31/2012 4:27:39 PM by Matt Mac
    Sample Info     :
```

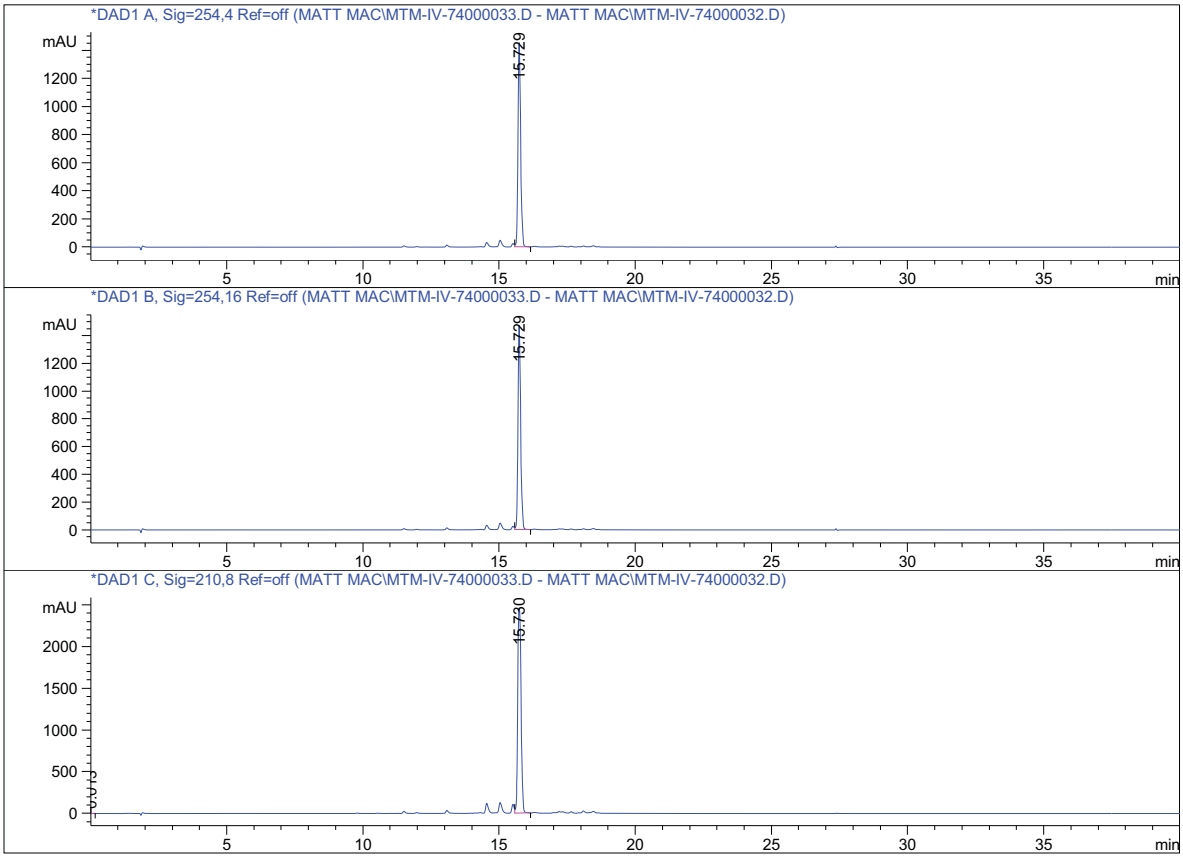

Data File C:\CHEM32\1\DATA\MATT MAC\MTM-IV-74000033.D
Sample Name: run1

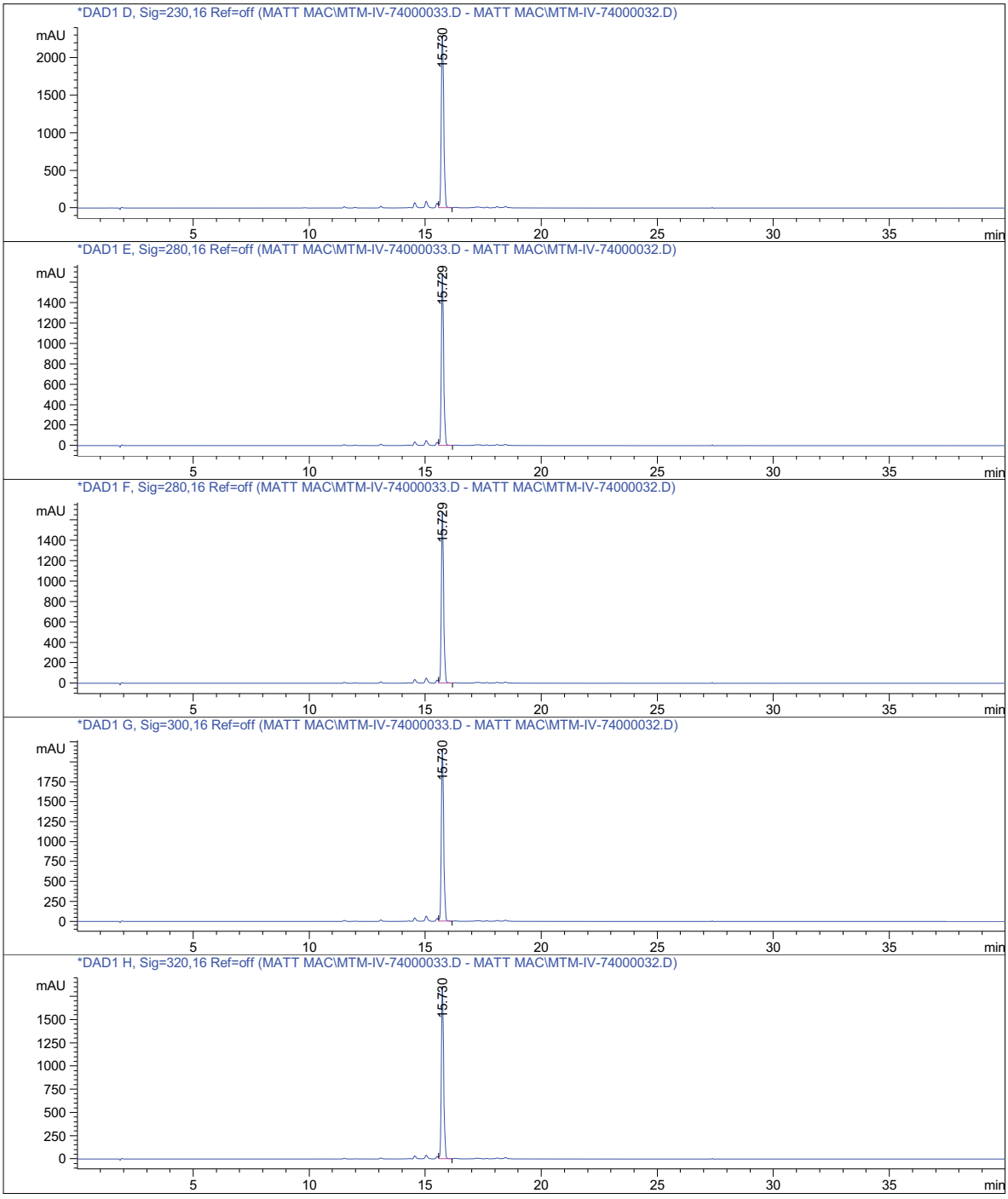

Data File C:\CHEM32\1\DATA\MATT MAC\MTM-IV-74000033.D
Sample Name: run1

==========

Area Percent Report

==========

Sorted By : Signal
Multiplier : 1.0000
Dilution : 1.0000
Use Multiplier & Dilution Factor with ISTDs

Signal 1: DAD1 A, Sig=254,4 Ref=off
Signal has been modified after loading from rawdata file!

Peak #	RetTime [min]	Type	Width [min]	Area [mAU*s]	Height [mAU]	Area %
1	15.729	VB	0.1049	9837.97559	1454.12830	100.0000
Totals :				9837.97559	1454.12830	

Signal 2: DAD1 B, Sig=254,16 Ref=off
Signal has been modified after loading from rawdata file!

Peak #	RetTime [min]	Type	Width [min]	Area [mAU*s]	Height [mAU]	Area %
1	15.729	VV	0.1051	1.00002e4	1474.76697	100.0000
Totals :				1.00002e4	1474.76697	

Signal 3: DAD1 C, Sig=210,8 Ref=off
Signal has been modified after loading from rawdata file!

Peak #	RetTime [min]	Type	Width [min]	Area [mAU*s]	Height [mAU]	Area %
1	0.013	BB	0.0857	11.56789	2.25001	0.0553
2	15.730	VB	0.1372	2.09122e4	2459.61768	99.9447
Totals :				2.09238e4	2461.86769	

Signal 4: DAD1 D, Sig=230,16 Ref=off
Signal has been modified after loading from rawdata file!

Data File C:\CHEM32\1\DATA\MATT MAC\MTM-IV-74000033.D
Sample Name: run1

Peak #	RetTime [min]	Type	Width [min]	Area [mAU*s]	Height [mAU]	Area %
1	15.730	VB	0.1188	1.70194e4	2288.63818	100.0000
Totals :				1.70194e4	2288.63818	

Signal 5: DAD1 E, Sig=280,16 Ref=off
Signal has been modified after loading from rawdata file!

Peak #	RetTime [min]	Type	Width [min]	Area [mAU*s]	Height [mAU]	Area %
1	15.729	VV	0.1056	1.14876e4	1684.72949	100.0000
Totals :				1.14876e4	1684.72949	

Signal 6: DAD1 F, Sig=280,16 Ref=off
Signal has been modified after loading from rawdata file!

Peak #	RetTime [min]	Type	Width [min]	Area [mAU*s]	Height [mAU]	Area %
1	15.729	VV	0.1056	1.14876e4	1684.72949	100.0000
Totals :				1.14876e4	1684.72949	

Signal 7: DAD1 G, Sig=300,16 Ref=off
Signal has been modified after loading from rawdata file!

Peak #	RetTime [min]	Type	Width [min]	Area [mAU*s]	Height [mAU]	Area %
1	15.730	VV	0.1105	1.52888e4	2162.58813	100.0000
Totals :				1.52888e4	2162.58813	

Signal 8: DAD1 H, Sig=320,16 Ref=off
Signal has been modified after loading from rawdata file!

Peak #	RetTime [min]	Type	Width [min]	Area [mAU*s]	Height [mAU]	Area %
1	15.730	VV	0.1062	1.27597e4	1855.55859	100.0000

Data File C:\CHEM32\1\DATA\MATT MAC\MTM-IV-74000033.D
Sample Name: run1

Totals :	1.27597e4	1855.55859

==========

*** End of Report ***

C:\Xcalibur\...\Matt\2-10-2013\MTM-IV-74 2/10/2013 4:43:40 PM MTM-IV-74

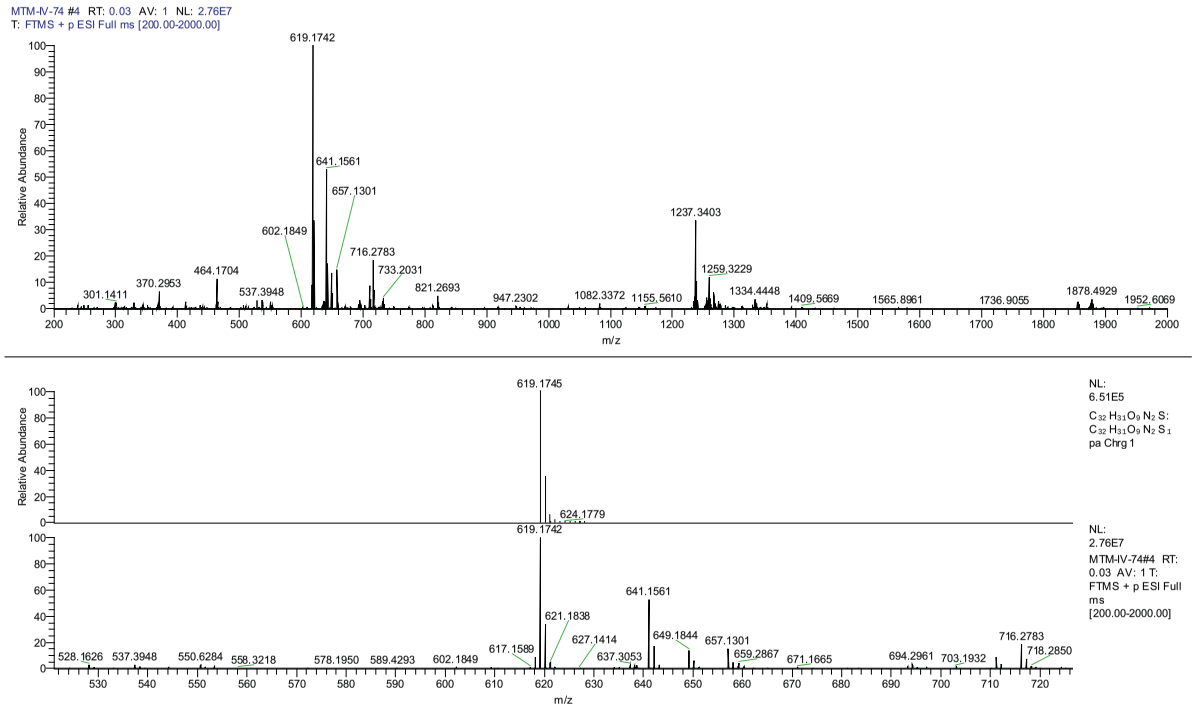

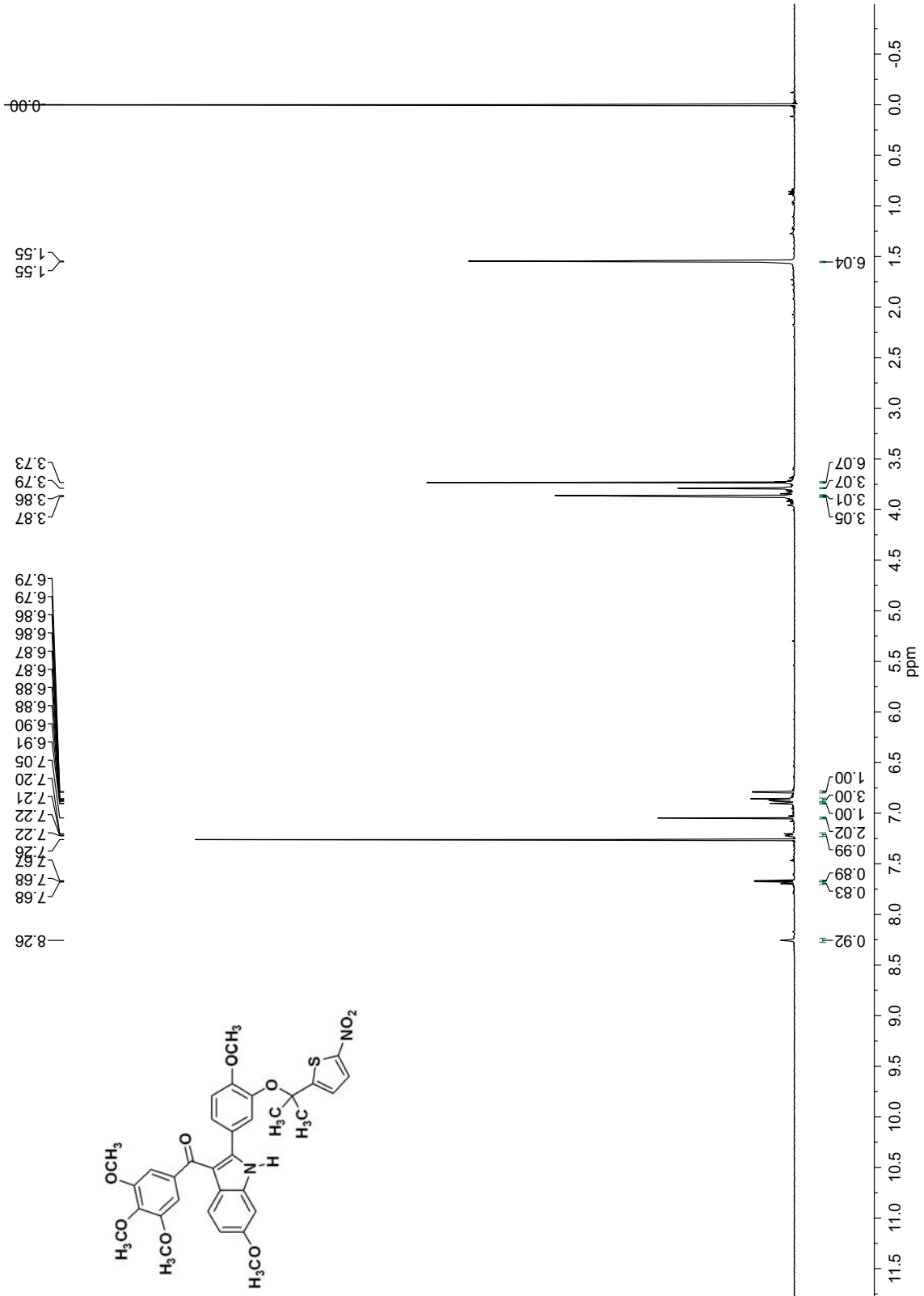
0.00
1.55
3.73
3.79
3.86
3.87
6.79
6.79
6.86
6.86
6.87
6.87
6.88
6.88
6.90
6.91
7.05
7.20
7.21
7.22
7.22
7.26
7.67
7.68
7.68
8.26
0.92
0.83
0.89
0.99
2.02
1.00
3.00
1.00
6.07
3.07
3.01
3.05
6.04
ppm
OCH3
H3CO
H3CO
H3CO
O
N
H
H3C
H3C
O
S
NO2

191.54
161.12
157.38
154.09
152.78
150.74
143.40
141.61
141.27
136.43
134.54
128.44
125.36
124.83
124.76
123.05
122.35
122.18
112.93
112.20
111.75
107.57
94.60
80.66
77.41
77.16
76.91
61.02
56.25
55.84
55.79
28.66
ppm
OCH3
H3CO
H3CO
O
N
H
H3CO
O
H3C
H3C
S
NO2

Data File C:\CHEM32\1\DATA\MATT MAC\MTM-V-23000031.D
Sample Name: run1

```
    ======================================================================
    Acq. Operator   : Matt Mac
    Acq. Instrument : Instrument 1                    Location :   -
    Injection Date  : 8/31/2012 1:46:10 PM
    Acq. Method     : C:\CHEM32\1\METHODS\MASTERMETHOD.M
    Last changed    : 8/31/2012 1:44:19 PM by Matt Mac
                      (modified after loading)
    Analysis Method : C:\CHEM32\1\DATA\MATT MAC\MTM-V-23000031.D\DA.M (MASTERMETHOD.M)
    Last changed    : 8/31/2012 2:39:30 PM by Matt Mac
    Sample Info     :
```

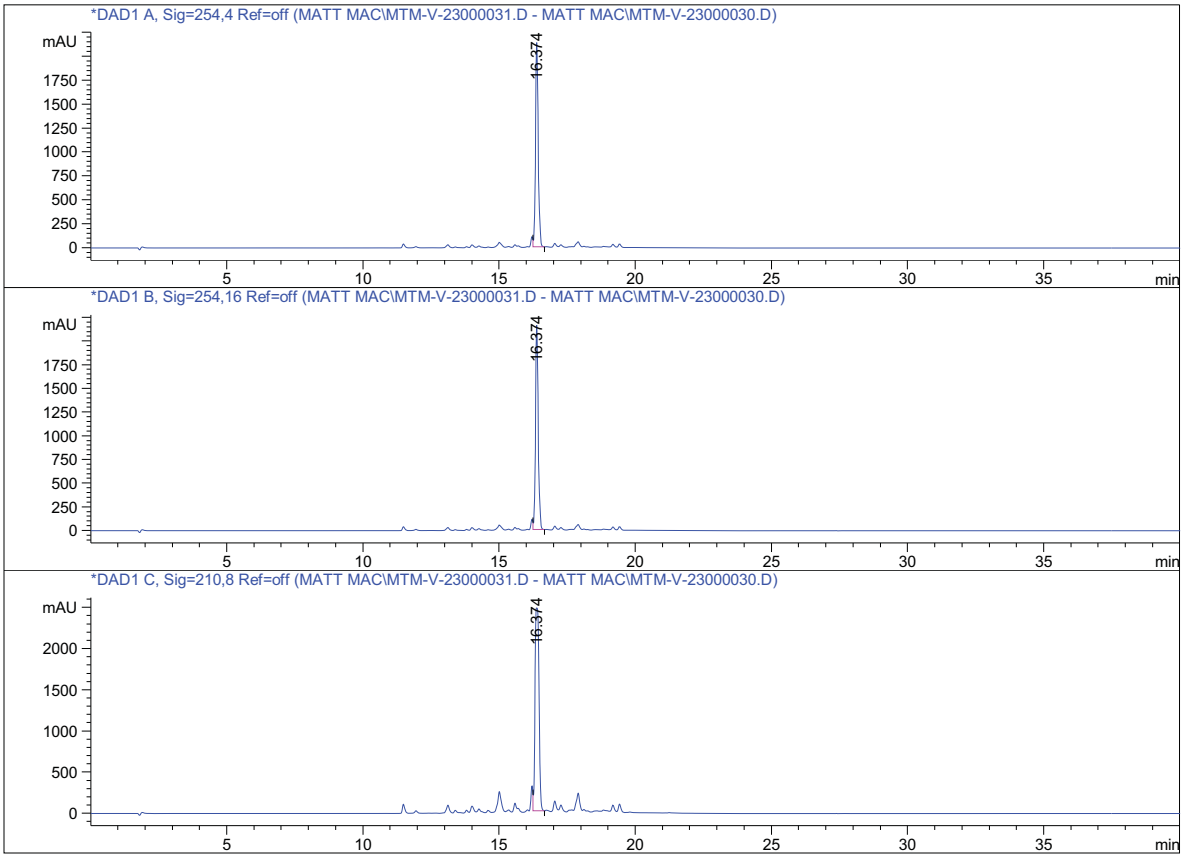

Data File C:\CHEM32\1\DATA\MATT MAC\MTM-V-23000031.D
Sample Name: run1

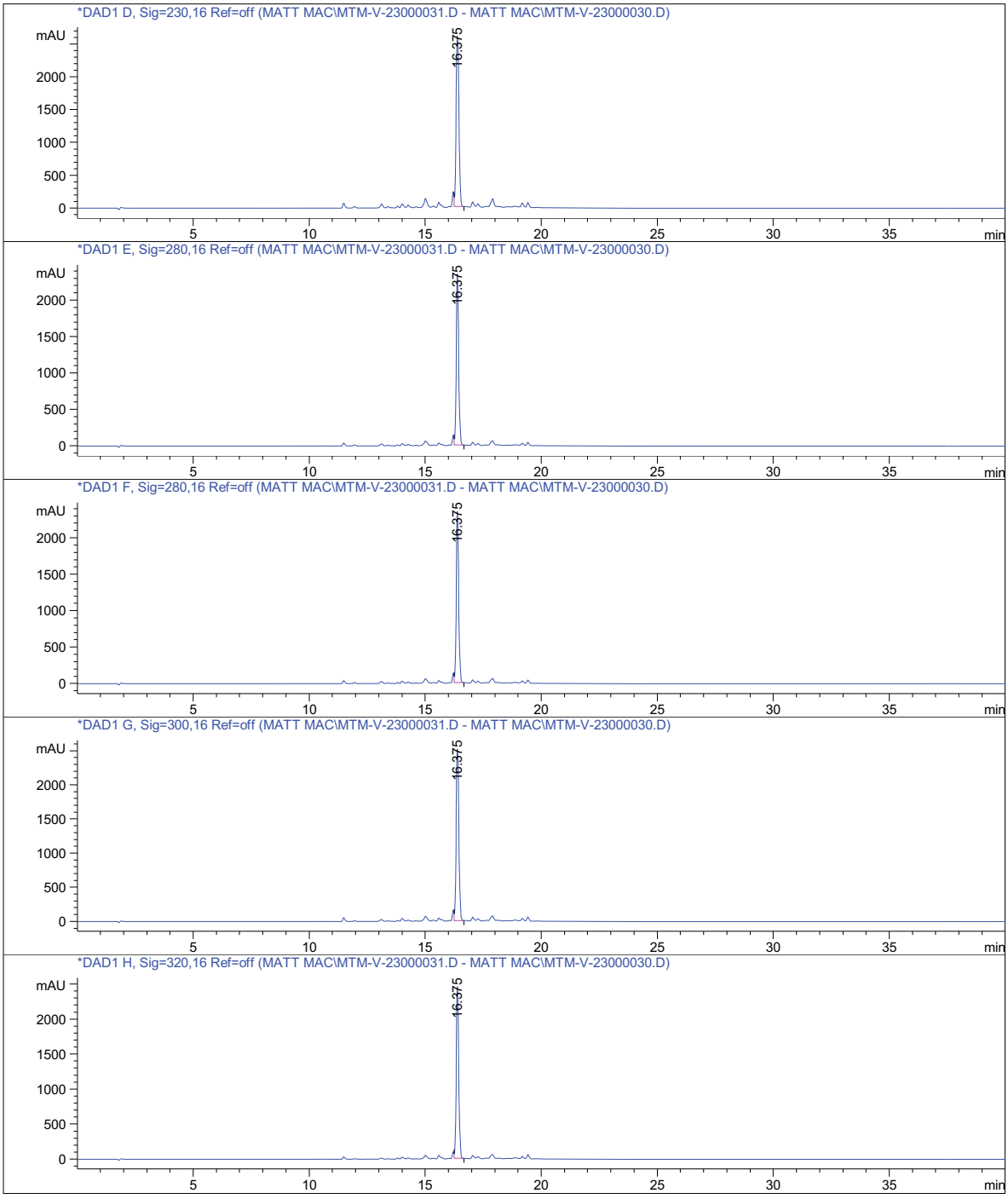

Data File C:\CHEM32\1\DATA\MATT MAC\MTM-V-23000031.D
Sample Name: run1

==========

Area Percent Report

==========

Sorted By : Signal
Multiplier : 1.0000
Dilution : 1.0000
Use Multiplier & Dilution Factor with ISTDs

Signal 1: DAD1 A, Sig=254,4 Ref=off
Signal has been modified after loading from rawdata file!

Peak #	RetTime [min]	Type	Width [min]	Area [mAU*s]	Height [mAU]	Area %
1	16.374	VB	0.1033	1.45361e4	2137.30200	100.0000
Totals :				1.45361e4	2137.30200	

Signal 2: DAD1 B, Sig=254,16 Ref=off
Signal has been modified after loading from rawdata file!

Peak #	RetTime [min]	Type	Width [min]	Area [mAU*s]	Height [mAU]	Area %
1	16.374	VB	0.1036	1.47351e4	2160.42700	100.0000
Totals :				1.47351e4	2160.42700	

Signal 3: DAD1 C, Sig=210,8 Ref=off
Signal has been modified after loading from rawdata file!

Peak #	RetTime [min]	Type	Width [min]	Area [mAU*s]	Height [mAU]	Area %
1	16.374	VB	0.1635	2.48179e4	2463.75830	100.0000
Totals :				2.48179e4	2463.75830	

Signal 4: DAD1 D, Sig=230,16 Ref=off
Signal has been modified after loading from rawdata file!

Data File C:\CHEM32\1\DATA\MATT MAC\MTM-V-23000031.D
Sample Name: run1

Peak #	RetTime [min]	Type	Width [min]	Area [mAU*s]	Height [mAU]	Area %
1	16.375	VB	0.1348	2.20597e4	2606.19116	100.0000
Totals :				2.20597e4	2606.19116	

Signal 5: DAD1 E, Sig=280,16 Ref=off
Signal has been modified after loading from rawdata file!

Peak #	RetTime [min]	Type	Width [min]	Area [mAU*s]	Height [mAU]	Area %
1	16.375	VB	0.1087	1.67091e4	2357.75903	100.0000
Totals :				1.67091e4	2357.75903	

Signal 6: DAD1 F, Sig=280,16 Ref=off
Signal has been modified after loading from rawdata file!

Peak #	RetTime [min]	Type	Width [min]	Area [mAU*s]	Height [mAU]	Area %
1	16.375	VB	0.1087	1.67091e4	2357.75903	100.0000
Totals :				1.67091e4	2357.75903	

Signal 7: DAD1 G, Sig=300,16 Ref=off
Signal has been modified after loading from rawdata file!

Peak #	RetTime [min]	Type	Width [min]	Area [mAU*s]	Height [mAU]	Area %
1	16.375	VB	0.1275	2.01742e4	2516.56909	100.0000
Totals :				2.01742e4	2516.56909	

Signal 8: DAD1 H, Sig=320,16 Ref=off
Signal has been modified after loading from rawdata file!

Peak #	RetTime [min]	Type	Width [min]	Area [mAU*s]	Height [mAU]	Area %
1	16.375	VB	0.1163	1.81833e4	2458.02002	100.0000

Data File C:\CHEM32\1\DATA\MATT MAC\MTM-V-23000031.D
Sample Name: run1

Totals :	1.81833e4	2458.02002

==========

*** End of Report ***

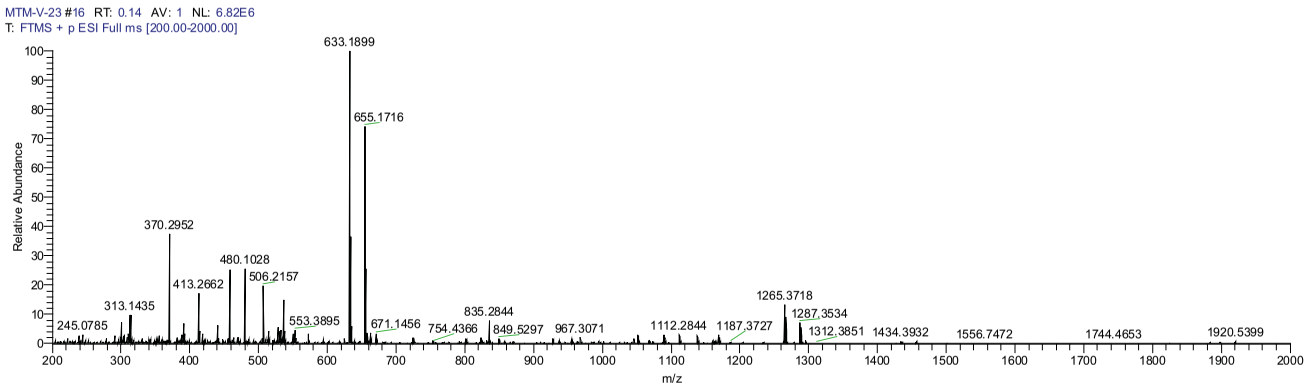
MTM-V-23 #16 RT: 0.14 AV: 1 NL: 6.82E6
T: FTMS + p ESI Full ms [200.00-2000.00]
Relative Abundance
m/z
633.1899
655.1716
370.2952
480.1028
506.2157
413.2662
313.1435
245.0785
553.3895
671.1456
754.4366
835.2844
849.5297
967.3071
1112.2844
1187.3727
1265.3718
1287.3534
1312.3851
1434.3932
1556.7472
1744.4653
1920.5399

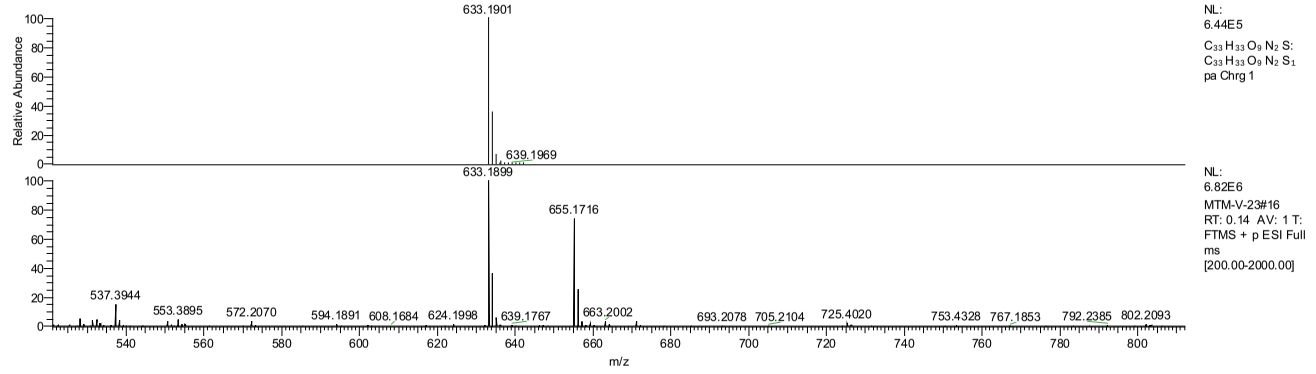
Relative Abundance
m/z
633.1901
639.1969
NL:
6.44E5
C33 H33 O9 N2 S:
C33 H33 O9 N2 S1
pa Chrg 1
633.1899
655.1716
537.3944
553.3895
572.2070
594.1891
608.1684
624.1998
639.1767
663.2002
693.2078
705.2104
725.4020
753.4328
767.1853
792.2385
802.2093
NL:
6.82E6
MTM-V-23#16
RT: 0.14 AV: 1 T:
FTMS + p ESI Full
ms
[200.00-2000.00]

APPENDIX E

Mechanisms of Heterocyclic Ring Formation

9.82
7.48
7.48
7.47
7.46
7.37
7.36
7.26
6.96
6.95
3.89
1.01
0.17
O
H
OTBS
OCH3
0.89
1.00
0.92
1.08
3.01
9.03
6.01
ppm

190.40
156.32
145.33
130.04
126.18
119.56
111.02
77.42
77.16
76.90
55.24
25.45
18.19
-4.86
OTBS
OCH3
H
O
220
210
200
190
180
170
160
150
140
130
120
110
100
90
80
70
60
50
40
30
20
10
0
-10
ppm

HO
CH3
OTBS
OCH3
6.86
6.86
6.85
6.85
6.84
6.77
6.76
6.76
6.75
6.75
4.72
4.72
4.71
4.71
4.70
4.69
4.68
4.68
3.75
2.75
1.52
1.50
1.26
1.25
1.01
0.16
1.98
1.00
1.07
3.00
1.07
5.85
1.61
1.67
8.97
ppm

150.06
144.84
138.87
118.54
118.53
118.27
118.26
111.91
77.42
77.16
76.91
69.77
69.46
55.45
25.74
25.03
18.41
-4.61
-4.62
HO
CH3
OTBS
OCH3
ppm

150.06
144.84
138.87
118.54
118.53
118.27
118.26
111.91
77.42
77.16
76.91
69.77
69.46
55.45
25.74
25.03
18.41
-4.61
-4.62
HO
CH3
OTBS
OCH3
ppm

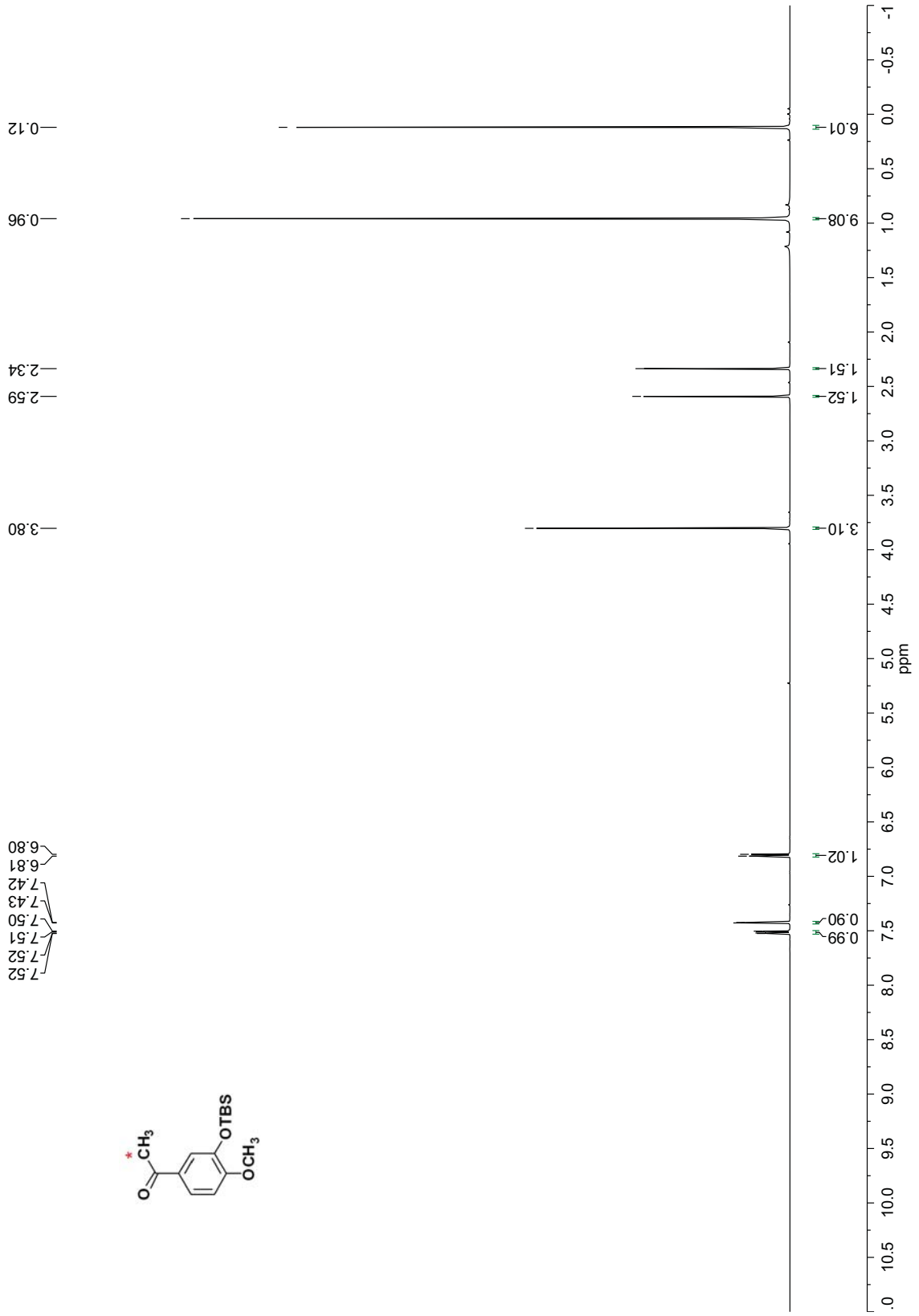
0.12
0.96
2.34
2.59
3.80
6.80
6.81
7.42
7.43
7.50
7.51
7.52
7.52
1.02
0.90
0.99
3.10
1.52
1.51
9.08
6.01
OTBS
OCH3
CH3
O
ppm

196.33
195.99
155.10
144.65
130.45
130.34
123.42
120.10
110.61
77.42
77.16
76.90
55.18
26.00
25.51
18.24
-4.82
OTBS
OCH3
CH3
O
*
ppm

196.33
195.99
155.10
144.65
130.45
130.34
123.42
120.10
110.61
77.42
77.16
76.90
55.18
26.00
25.51
18.24
-4.82
ppm
OTBS
OCH3
CH3
O

TMSO
CH2
OTBS
OCH3
7.23
7.22
7.21
7.21
7.18
7.17
6.83
6.81
4.99
4.98
4.67
4.67
4.54
4.54
4.22
4.22
3.83
1.08
0.32
0.23
1.00
0.93
1.08
3.30
0.53
0.54
0.52
0.51
9.07
9.00
6.01
ppm

TMSO
CH2
OTBS
OCH3
155.71
155.05
151.27
144.58
130.79
130.73
118.92
118.25
118.24
111.51
111.17
89.59
77.41
77.16
76.90
55.48
25.86
18.55
0.17
-4.53
ppm

TMSO
CH2
OTBS
OCH3
155.71
155.05
151.27
144.58
130.79
130.73
118.92
118.25
118.24
111.51
111.17
89.69
77.41
77.16
76.90
55.48
25.86
18.55
0.17
-4.53
ppm

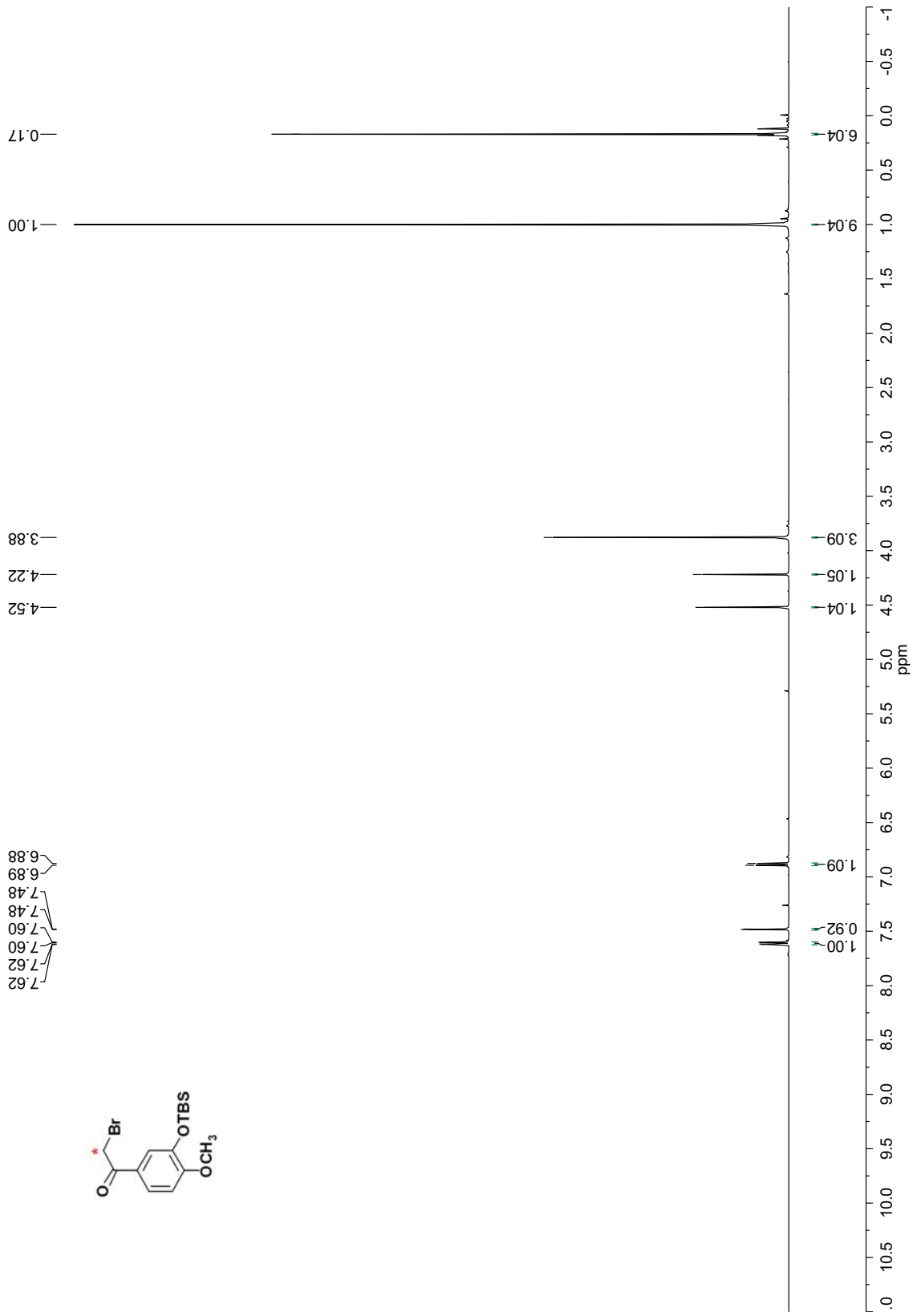
Br
OTBS
OCH3
O
7.62
7.62
7.60
7.60
7.48
7.48
7.60
6.89
6.88
4.52
4.22
3.88
1.00
0.17
1.09
0.92
1.00
1.04
1.05
3.09
9.04
6.04
ppm

190.19
189.85
156.22
145.24
127.30
127.16
124.35
121.21
111.13
77.41
77.16
76.90
55.68
40.00
30.86
19.15
18.56
-4.48
Br
OTBS
OCH3
O
ppm

190.19
189.85
156.22
145.24
127.30
127.16
124.35
121.21
111.13
77.41
77.16
76.90
55.68
40.00
30.86
19.15
18.56
-4.48
Br
OTBS
OCH3
O
ppm

8.13
7.14
7.14
7.13
6.90
6.89
6.88
6.88
6.78
6.45
6.44
6.44
6.44
3.86
3.84
1.04
0.21
1.02
0.53
1.50
2.03
2.03
1.00
3.00
3.00
9.01
5.72
OCH3
OTBS
N
H
H3CO
ppm

156.51
156.51
150.72
145.56
137.30
137.04
136.73
121.05
121.03
118.35
118.33
117.98
117.96
112.55
110.07
98.83
96.22
94.68
94.66
77.41
77.16
76.91
58.71
55.82
55.67
49.96
44.60
25.91
19.98
18.64
-4.42
OCH3
OTBS
H3CO
H
N
*
220
210
200
190
180
170
160
150
140
130
120
110
100
90
80
70
60
50
40
30
20
10
0
-10
ppm

156.51
156.51
150.72
145.56
137.58
137.30
137.04
121.05
121.03
118.35
118.33
117.98
117.96
112.55
110.07
98.83
96.22
94.68
94.66
77.41
77.16
76.91
58.71
55.82
55.67
49.96
44.60
25.91
19.98
18.64
-4.42
OCH3
OTBS
H3CO
N
H
*
ppm

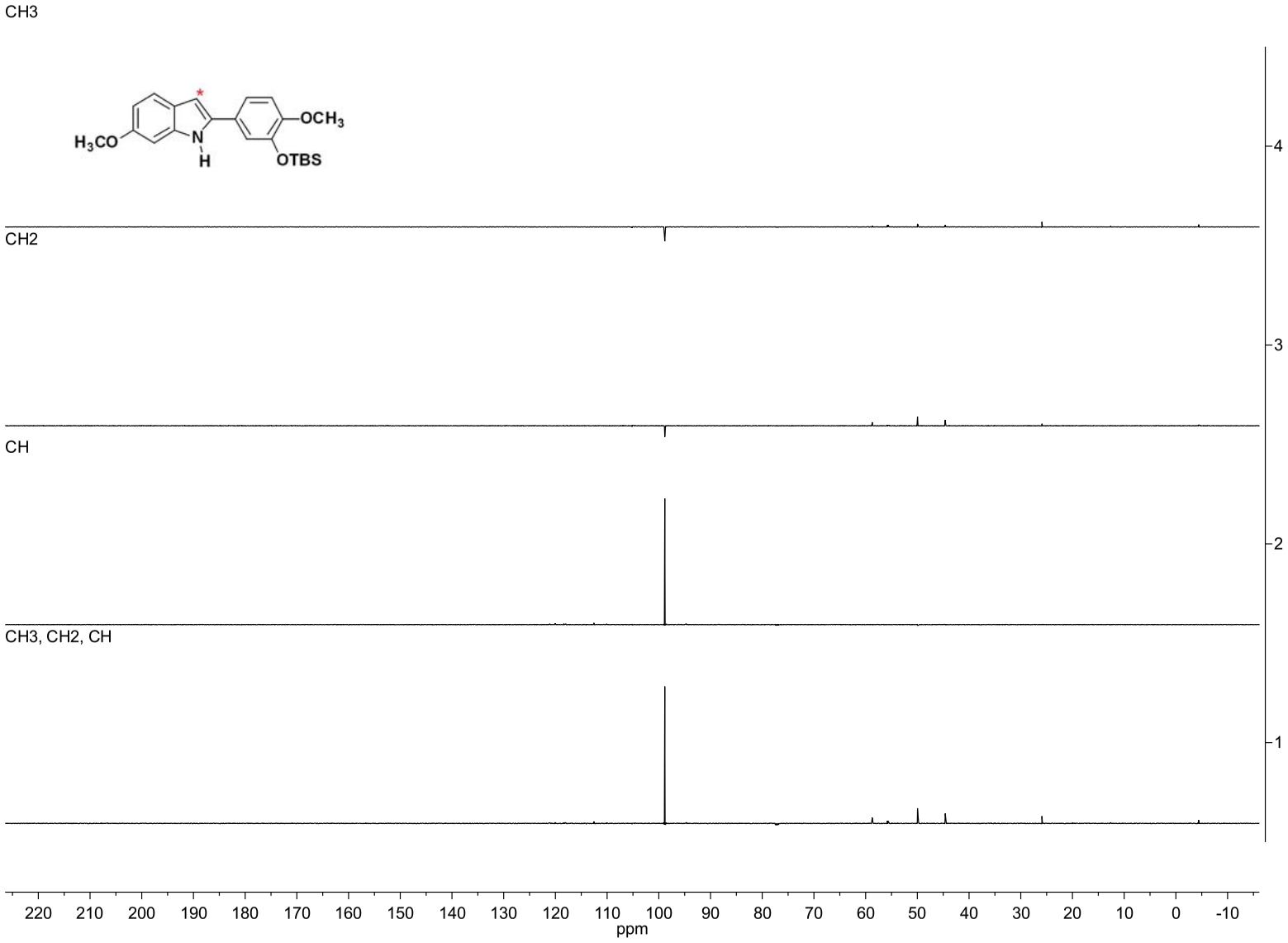
CH3
H3CO
N
H
OCH3
OTBS
CH2
CH
CH3, CH2, CH
4
3
2
1
220 210 200 190 180 170 160 150 140 130 120 110 100 90 80 70 60 50 40 30 20 10 0 -10
ppm

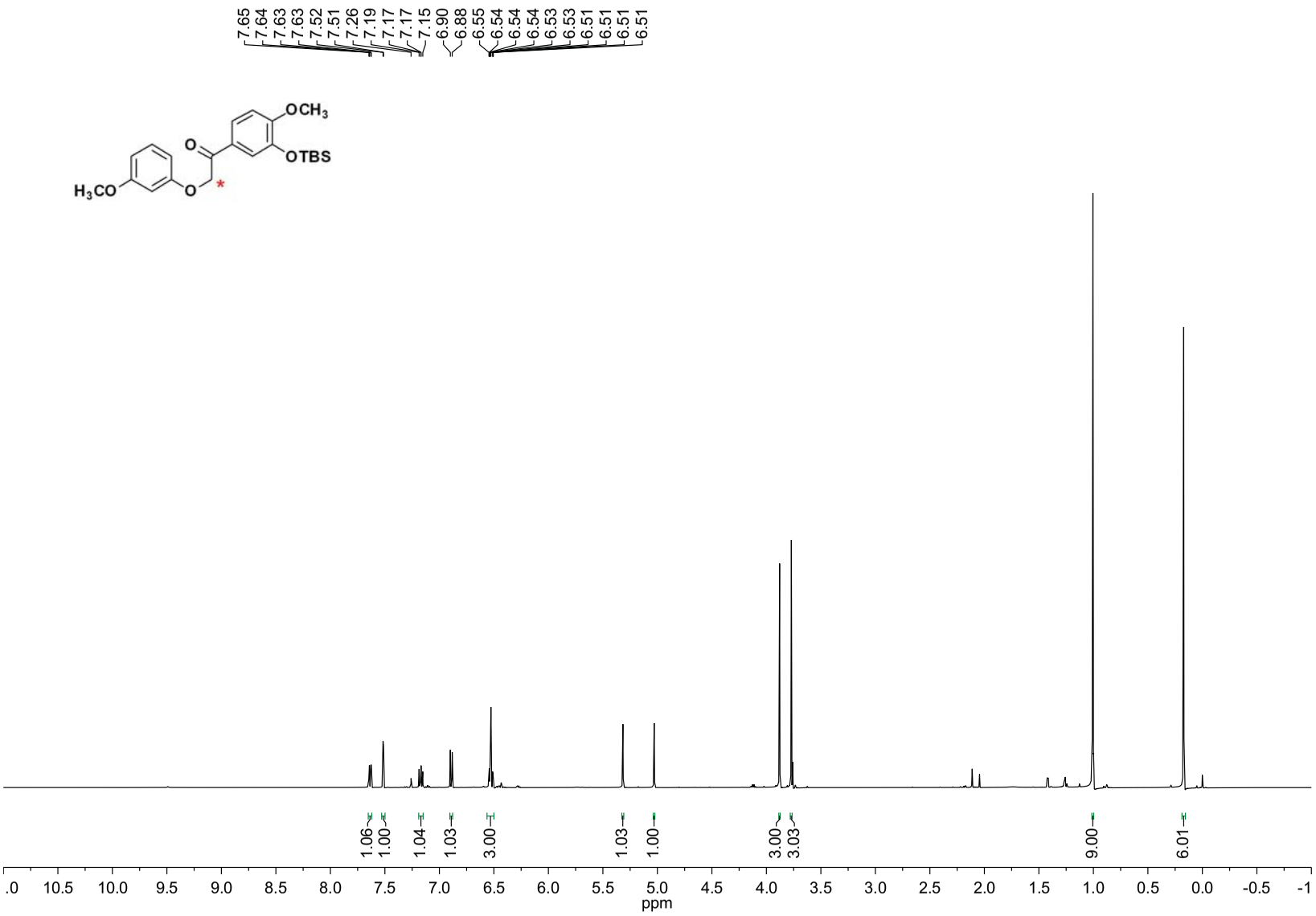
7.65
7.64
7.63
7.63
7.52
7.51
7.26
7.19
7.17
7.17
7.15
6.90
6.88
6.55
6.54
6.54
6.54
6.53
6.53
6.51
6.51
6.51
OCH3
OTBS
O
H3CO
O
*
1.06
1.00
1.04
1.03
3.00
1.03
1.00
3.00
3.03
9.00
6.01
ppm

193.23
192.87
160.92
159.42
156.09
145.21
130.06
127.94
127.81
123.40
120.50
111.12
107.34
106.75
106.72
101.57
101.54
77.41
77.16
76.91
70.75
55.64
55.40
25.78
18.56
-4.49
OCH3
OTBS
O
O
*
H3CO
ppm

193.23
192.87
160.92
159.42
156.09
145.21
130.06
127.94
127.81
123.40
120.50
111.12
107.34
106.75
106.72
101.57
101.54
77.41
77.16
76.91
70.75
55.64
55.40
26.78
18.56
-4.49
OCH3
OTBS
O
O
*
H3CO
ppm

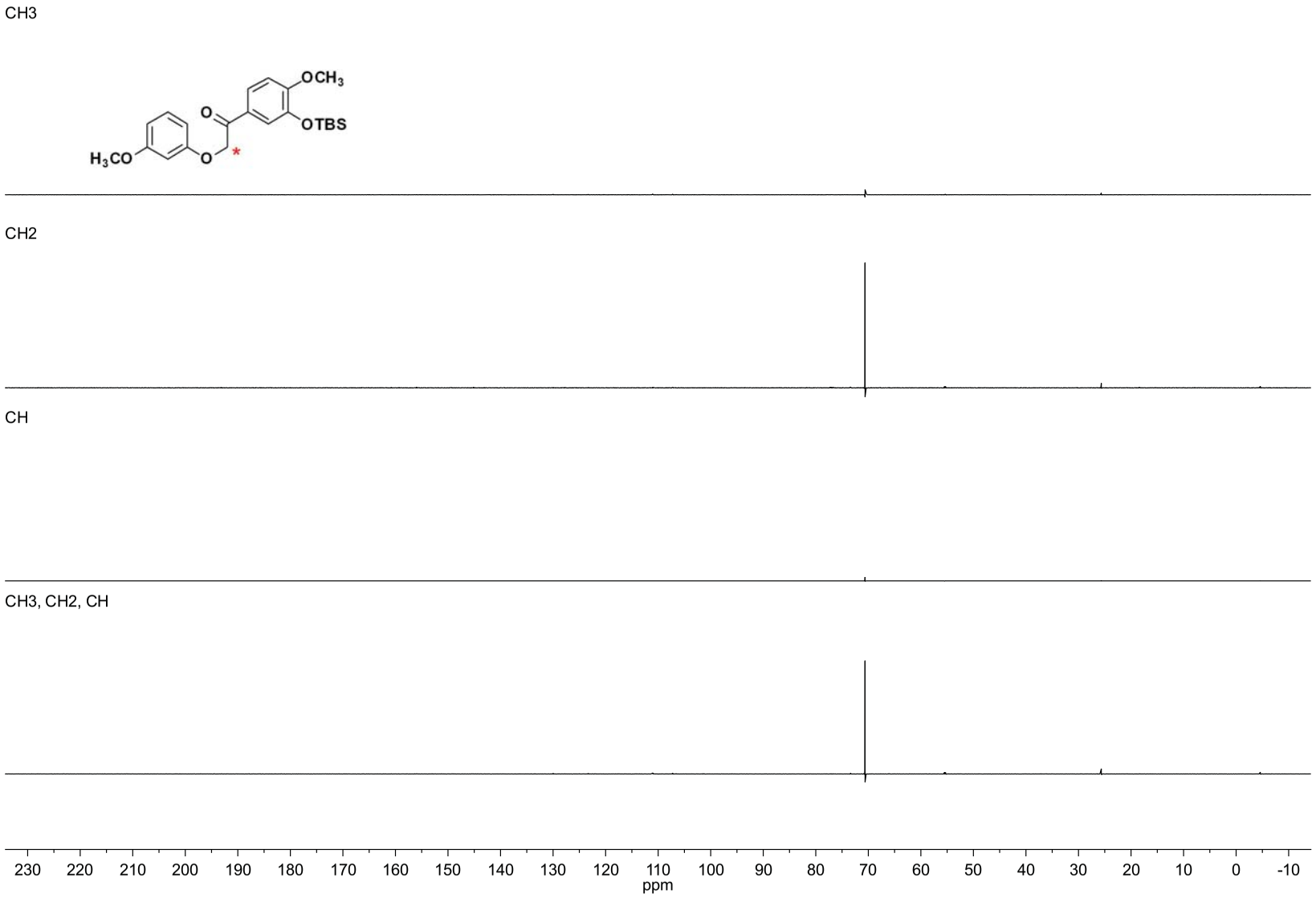
CH3
OCH3
O
OTBS
H3CO
O
*
CH2
CH
CH3, CH2, CH
230 220 210 200 190 180 170 160 150 140 130 120 110 100 90 80 70 60 50 40 30 20 10 0 -10
ppm

7.84
7.65
7.63
7.47
7.46
7.44
7.30
7.26
7.07
7.05
6.94
6.92
3.89
3.87
2.35
1.56
1.25
0.93
0.25
0.00
3.08
3.05
1.11
2.08
0.90
1.75
1.00
0.64
OCH3
OH
O
H3CO
ppm

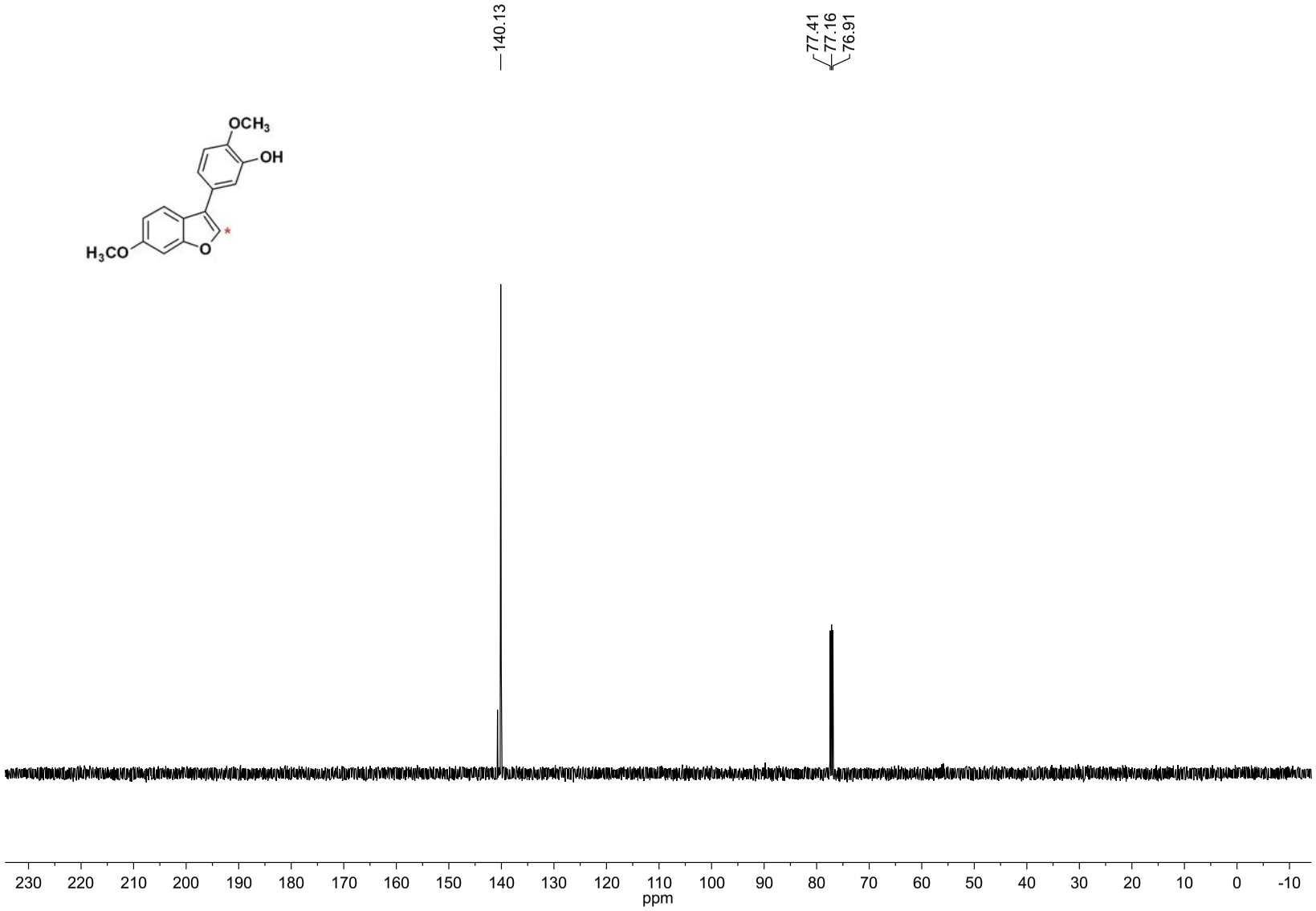
140.13
77.41
77.16
76.91
OCH3
OH
H3CO
O
*
230 220 210 200 190 180 170 160 150 140 130 120 110 100 90 80 70 60 50 40 30 20 10 0 -10
ppm

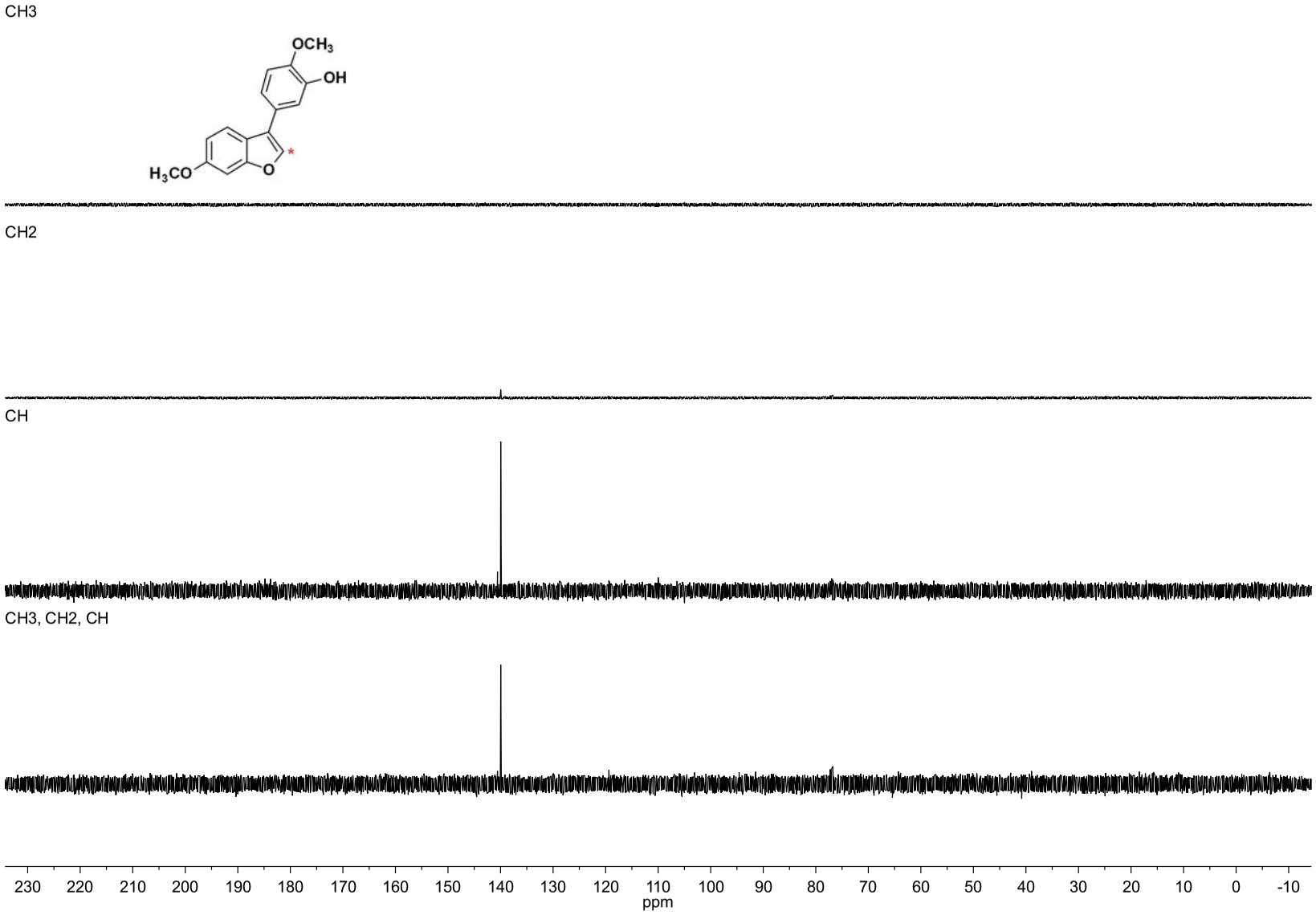
CH3
OCH3
OH
H3CO
O
*
CH2
CH
CH3, CH2, CH
230 220 210 200 190 180 170 160 150 140 130 120 110 100 90 80 70 60 50 40 30 20 10 0 -10
ppm

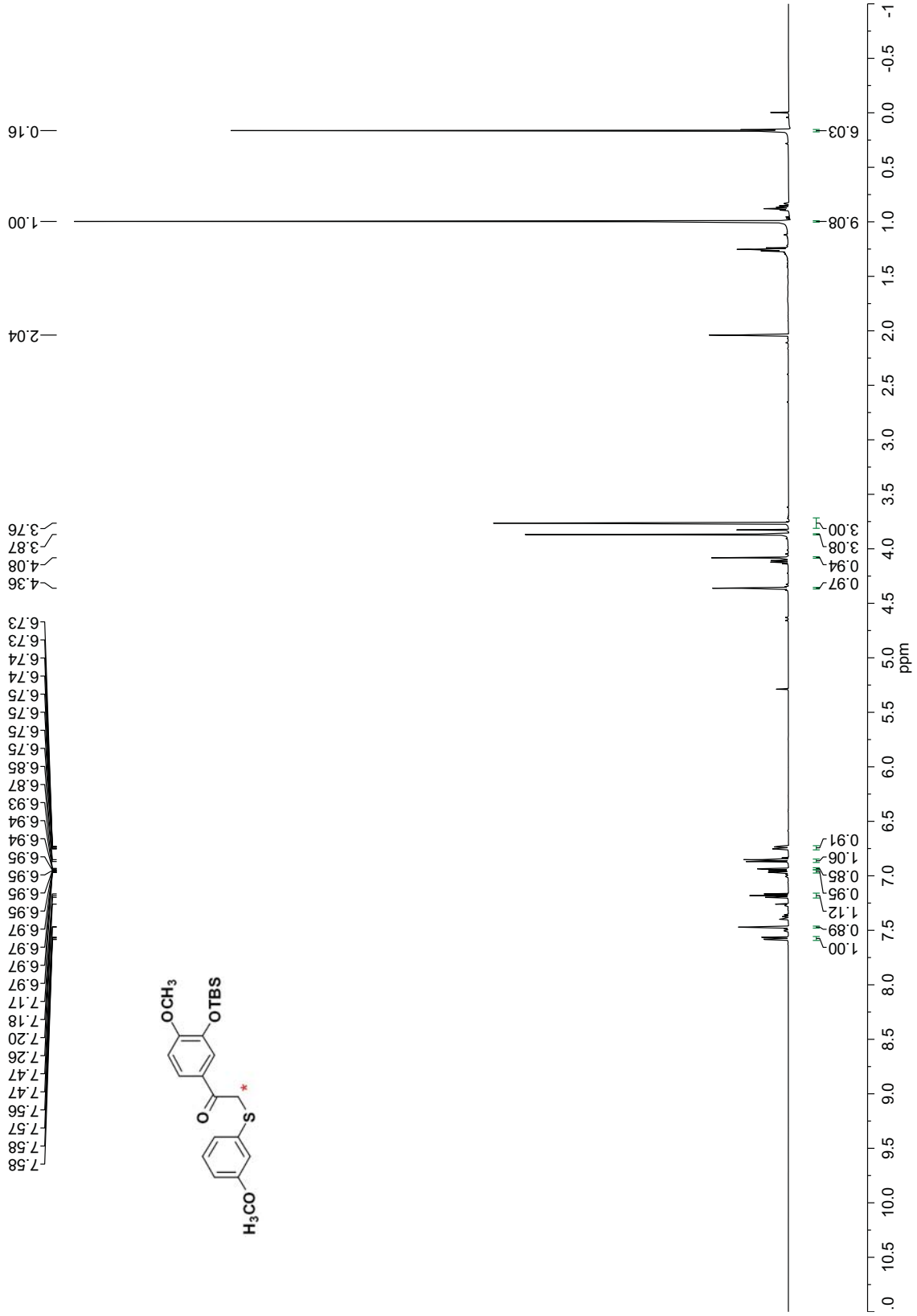
OCH3
OTBS
O
S
*
H3CO
ppm

192.99
192.65
159.90
155.84
145.08
136.63
129.93
128.77
128.65
124.01
122.15
122.13
121.00
115.24
115.22
112.84
110.96
66.20
55.63
55.37
40.82
25.79
18.56
-4.49
OCH3
OTBS
O
S
*
H3CO
ppm

192.99
192.65
159.90
155.84
145.08
136.63
129.93
128.77
128.65
124.01
122.15
122.13
121.00
115.24
115.22
112.84
110.96
66.20
55.63
55.37
40.82
25.79
18.56
-4.49
OCH3
OTBS
O
S
*
H3CO
ppm

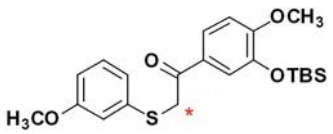
OCH3
O
OTBS
H3CO
S
*

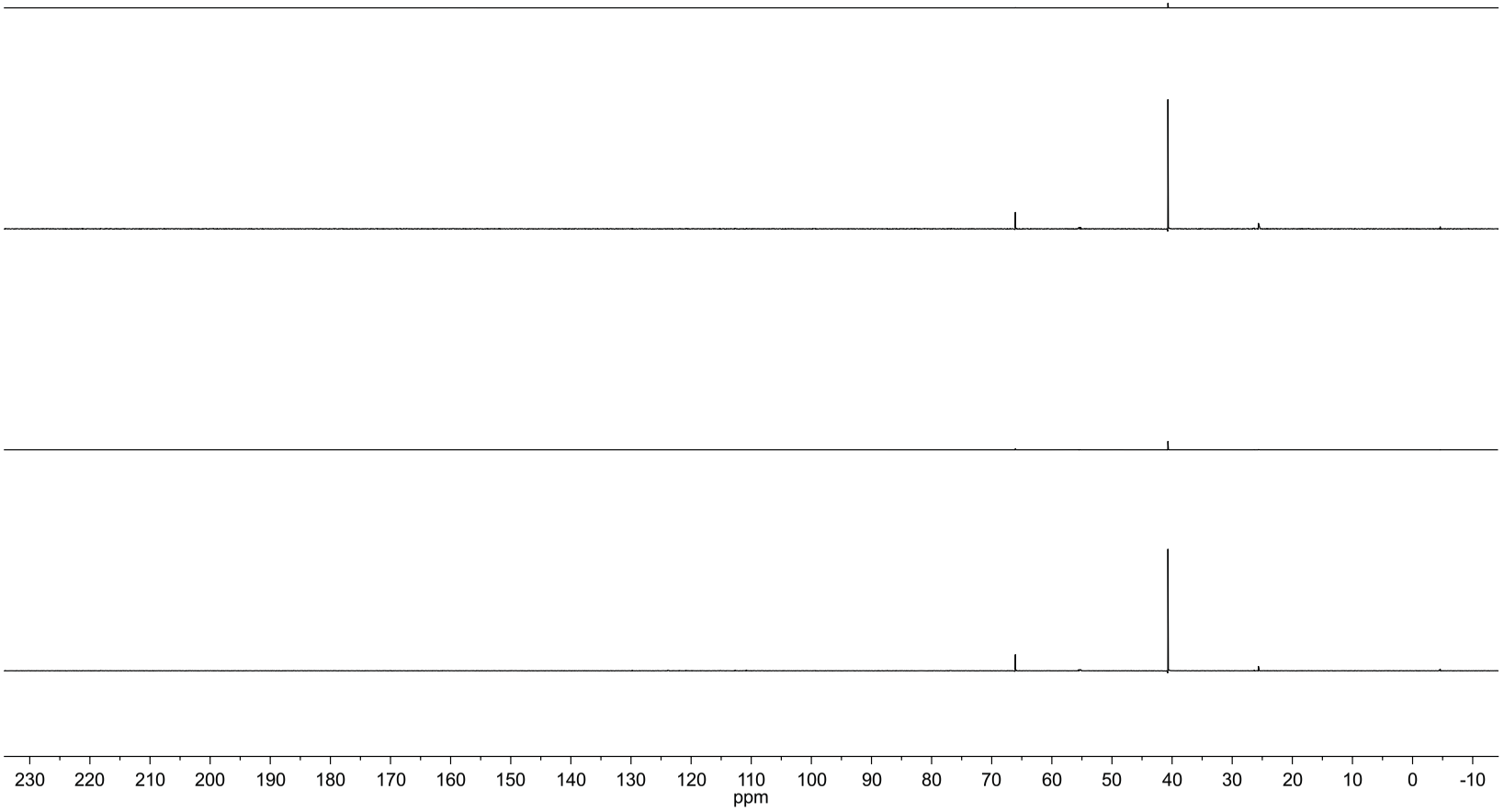
230 220 210 200 190 180 170 160 150 140 130 120 110 100 90 80 70 60 50 40 30 20 10 0 -10
ppm

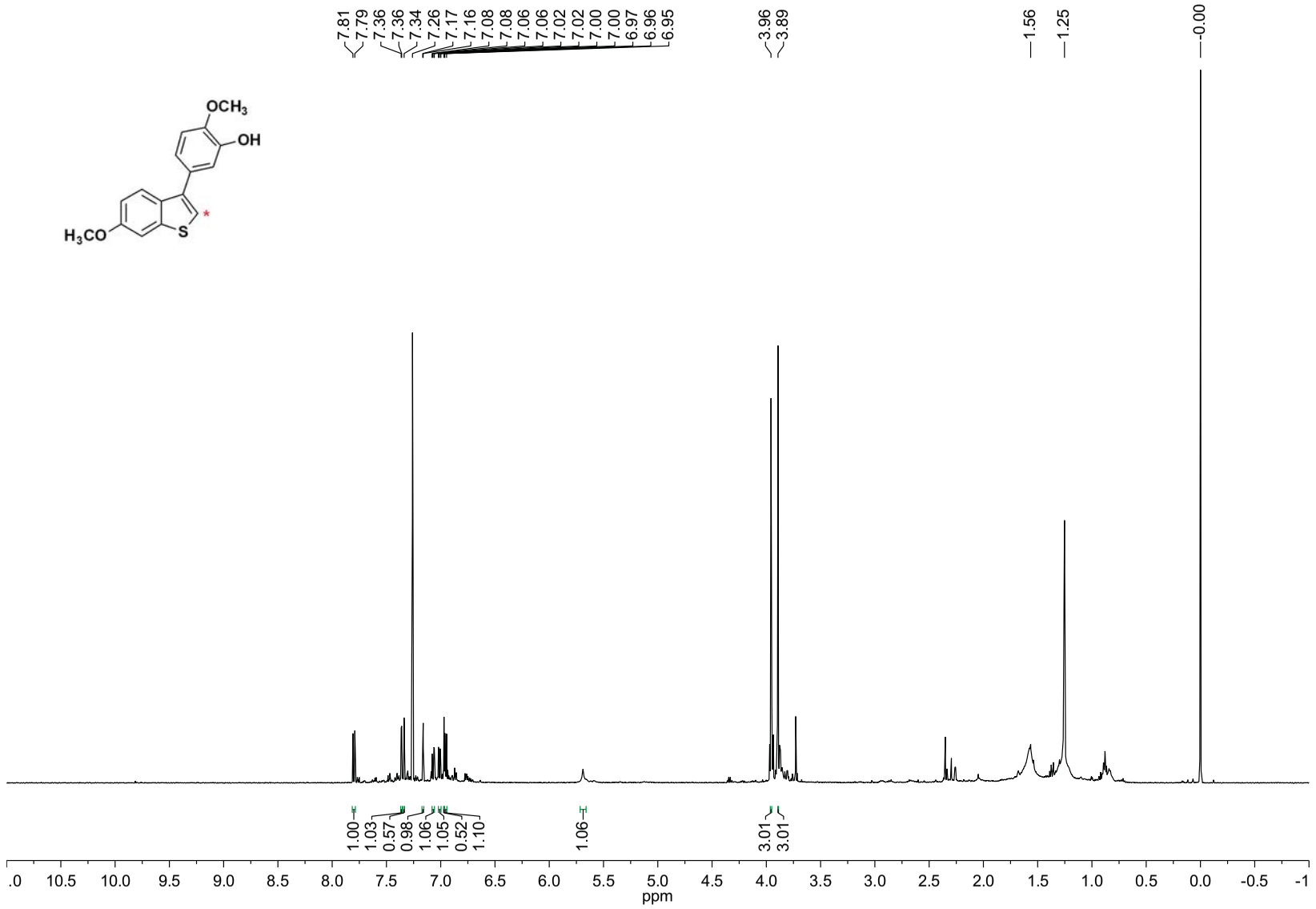
7.81
7.79
7.36
7.36
7.34
7.26
7.17
7.16
7.08
7.08
7.06
7.06
7.02
7.00
7.00
6.97
6.96
6.95
3.96
3.89
1.56
1.25
0.00
OCH3
OH
H3CO
S
*
1.00
1.03
0.57
0.98
1.06
1.05
0.52
1.10
1.06
3.01
3.01
ppm

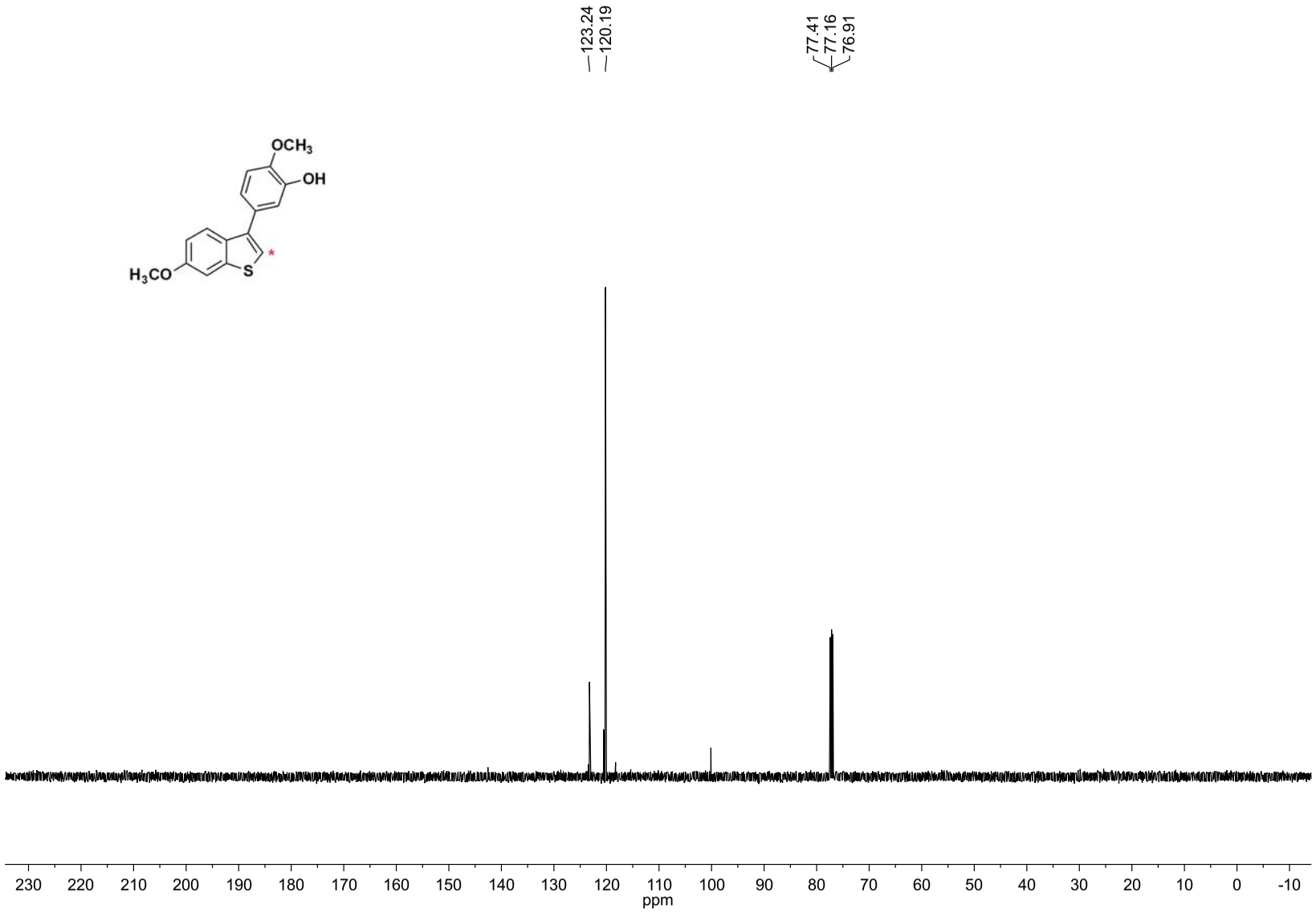
123.24
120.19
77.41
77.16
76.91
OCH3
OH
H3CO
S
*
230 220 210 200 190 180 170 160 150 140 130 120 110 100 90 80 70 60 50 40 30 20 10 0 -10
ppm

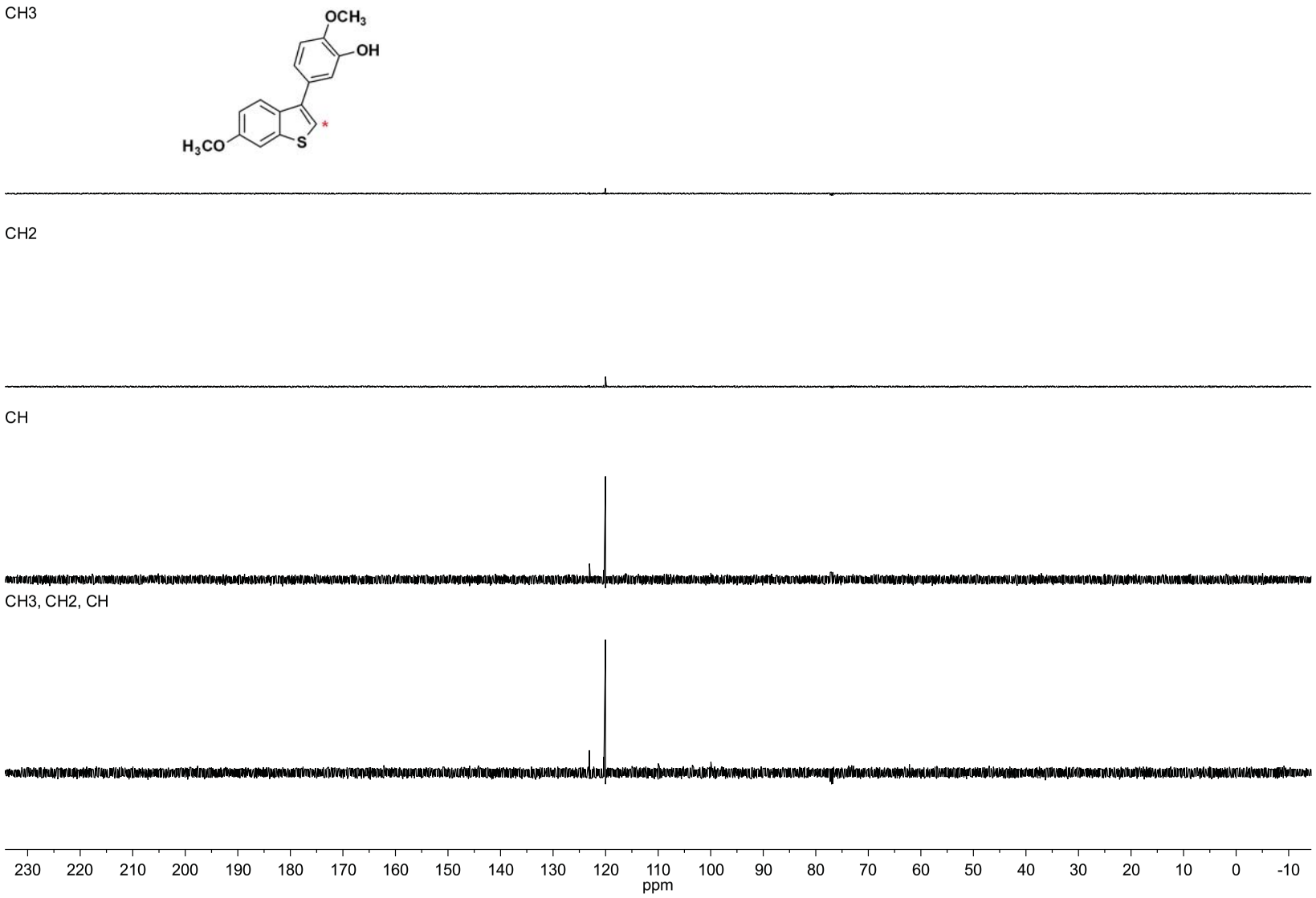
CH3
OCH3
OH
H3CO
S
*
CH2
CH
CH3, CH2, CH
230 220 210 200 190 180 170 160 150 140 130 120 110 100 90 80 70 60 50 40 30 20 10 0 -10
ppm

APPENDIX F

Deuterium Labeled Indole Attempt

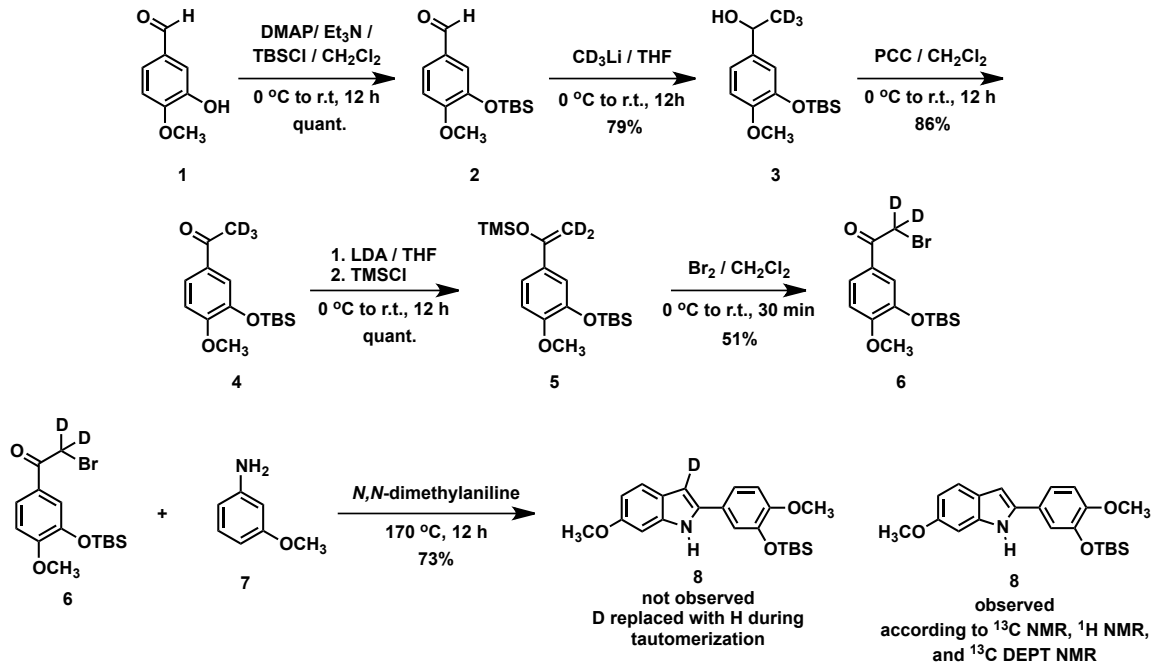

Scheme 1. Synthetic attempt to D-labeled indole **8**.

General Section

CH_2Cl_2, THF, EtOH, and Et_2O were used in their anhydrous forms as obtained from the chemical suppliers. Reactions were performed under an inert atmosphere using nitrogen gas, unless specified otherwise. Thin-layer chromatography (TLC) plates (precoated glass plates with silica gel 60 F254, 0.25 mm thickness) were used to monitor reactions. Purification of intermediates and products was carried out with a flash purification system (Biotage Isolera 1 or 4) using silica gel (200-400 mesh, 60 Å) prepacked columns. Intermediates and products synthesized were characterized on the basis of their ^{1}H NMR (500 MHz), ^{13}C NMR (125 MHz), and DEPT ^{13}C NMR (125 MHz) spectroscopic data using a Varian VNMRS 500 MHz instrument. Spectra were recorded in $CDCl_3$. All of the chemical shifts are expressed in ppm (δ), coupling

constants (*J*) are presented in Hz, and peak patterns are reported as broad (br), singlet (s), doublet (d), double doublet (dd), doublet of quartets (dq), quartet (q), and multiplet (m).

*3-(tert-Butyldimethylsilyloxy)-4-methoxybenzaldehyde **2***

To a clean dry round bottom flask 3-hydroxy-4-methoxybenaldehyde **1** (25.0 g, 164 mmol) was dissolved in CH_2Cl_2 (250 mL). The solution was cooled to 0 ºC and Et_3N (25.2 mL, 181 mmol) was added followed by the addition of *N*,*N*-dimethylaminopyridine (DMAP) (2.01 g, 16.4 mmol). The reaction mixture was stirred for 10 min and *tert*-butyldimethylsilyl chloride (TBSCl) (27.3 g, 181 mmol) was added gradually. The solution was allowed to warm to room temperature and was stirred for 12 hrs. The reaction was diluted with water (150 mL), transferred to a separatory funnel, and was extracted with CH_2Cl_2. The organic extracts were combined, dried over Na_2SO_4, filtered, and concentrated under reduced pressure. The TBS benzaldehyde product **2** (47.1 g, 177 mmol) was isolated quantitatively as a yellow oil and was taken to the next step without further purification.

^{1}H NMR ($CDCl_3$, 500 MHz): δ 9.80 (s, 1H, C<u>H</u>O), 7.45 (dd, *J* = 8.5 Hz, *J* = 2.0 Hz, 1H, Ar<u>H</u>), 7.35 (d, *J* = 2.0 Hz, 1H, Ar<u>H</u>), 6.93 (d, *J* = 8.5 Hz, 1H, Ar<u>H</u>), 3.87 (s, 3H, OC<u>H</u>$_3$), 0.99 (s, 9H, C(C<u>H</u>$_3$)$_3$), 0.16 (s, 6H, Si(C<u>H</u>$_3$)$_2$).

^{13}C NMR ($CDCl_3$, 125 MHz): δ 190.2, 156.2, 145.2, 130.0, 126.0, 119.4, 110.9, 55.1, 25.3, 18.0, -5.0.

*3-tert-Butyldimethylsilyloxy-1-(1'-hydroxyethyl)-4-methoxybenzene **3***

Crude TBS benzaldehyde **2** (2.00 g, 7.52 mmol) was dissolved in dry tetrahydrofuran (50 mL) and was cooled to 0 ºC under nitrogen. Once at 0 ºC, CD_3Li

(19.5 mL, 9.77 mmol) was added dropwise and the solution was then allowed to come to room temperature while stirring for 12 hrs. Upon completion, the reaction was slowly quenched with water and the organic layers were extracted with EtOAc. The extracted layers were then dried over Na_2SO_4, filtered, and concentrated under reduced pressure resulting in alcohol **3** (1.70 g, 5.95 mmol, 79%, R_f = 0.47 (70:30 hexanes:EtOAc)) as a yellow oil which was taken to the next step without further purification.

^{1}H NMR ($CDCl_3$, 500 MHz): δ 6.86 (m, 2H, ArH), 6.78 (m, 1H, ArH), 4.71 (s, 1H, CH), 3.76 (s, 3H, OCH_3), 2.51 (s, 1H, OH), 1.01 (s, 9H, $(CH_3)_3$), 0.16 (s, 6H, $Si(CH_3)_2$).

^{13}C NMR ($CDCl_3$, 125 MHz): δ 150.2, 144.9, 138.8, 118.6, 118.3, 112.0, 69.6, 55.5, 25.8, 18.5, -4.6.

*3-tert-Butyldimethylsilylox)-4-methoxyacetophenone **4***

The crude alcohol **3** (1.50 g, 5.25 mmol) was dissolved in anhydrous CH_2Cl_2 (50 mL). Celite (5 g) was added and the solution was then cooled to 0 ºC in an ice bath under nitrogen. Once at 0 ºC, pyridiniumchlorochromate (PCC) (1.25 g, 5.82 mmol) was added in small increments allowing 10 minutes of stirring between each addition. The reaction was then allowed to warm to room temperature and stirred for 12 hrs. Upon completion the reaction mixture was filtered through through a 50/50 mixture of silica gel/celite rinsing well with CH_2Cl_2. The filtrate was then concentrated under reduced pressure providing the desired acetophenone **4** (1.29 g, 4.54 mmol, 86%) as a pale yellow solid.

^{1}H NMR ($CDCl_3$, 500 MHz): δ 7.58 (dd, *J* = 2.0 Hz, 8.5 Hz, 1H, ArH), 7.49 (d, *J* = 2.5 Hz, 1H, ArH), 6.88 (d, *J* = 8.5 Hz, 1H, ArH), 3. 87 (s, 3H, OCH_3), 1.03 (s, 9H, $C(CH_3)_3$), 0.19 (s, 6H, $Si(CH_3)_2$).

^{13}C NMR ($CDCl_3$, 125 MHz): δ 196.7, 155.3, 144.8, 130.6, 123.5, 120.3, 110.8, 55.4, 25.7, 18.4, -4.7.

*1-(3-tert-Butyldimethylsilyloxy-4-methoxyphenyl)-1-trimethylsilylethene **5***

To a well stirred solution of diisopropylamine (0.9 mL, 6.33 mmol) in dry tetrahydrofuran (50 mL) at 0 °C was added n-butyllithium (2.53 mL, 6.33 mmol) drop wise. The LDA solution was then allowed to stir for 15 min upon which a solution of TBS acetophenone **4** (1.20 g, 4.22 mmol) in dry tetrahydrofuran (5 mL) was added drop wise. The solution was then stirred for 10 min where TMSCl (0.81 mL, 6.33 mmol) was then added drop wise and the reaction was allowed to warm to room temperature. The solution was then stirred for 12 hrs and after completion was quenched using a 10% $NaHCO_3$ (50 mL). The organic layers were then extracted with diethyl ether, dried over Na_2SO_4, and concentrated under reduced pressure resulting in TMS enol ether **5** (1.57 g, 4.42 mmol) quantitatively as a dark yellow oil which was taken to the next step without purification.

^{1}HNMR ($CDCl_3$, 500 MHz): δ 7.20 (dd, *J* = 2.5, Hz, 8.5 Hz, 1H Ar<u>H</u>), 7.15 (d, *J* = 2.5 Hz, 1H, Ar<u>H</u>), 6.81 (d, *J* = 8.5 Hz, 1H, Ar<u>H</u>), 3.82 (s, 3H, OC<u>H</u>$_3$), 1.06 (s, 9H, C(C<u>H</u>$_3$)$_3$), 0.30 (s, 9H, Si(C<u>H</u>$_3$)$_3$), 0.21 (s, 6H, Si(C<u>H</u>$_3$)$_2$).

^{13}C NMR ($CDCl_3$, 125 MHz): δ 155.3, 151.3, 144.6, 130.8, 118.9, 118.3, 111.5, 89.6, 55.5, 25.9, 18.6, 0.2, -4.5.

*3'-(tert-Butyldimethylsilyloxy)-4'-methoxy-2-bromoacetophenone **6***

A solution of crude **5** (1.57 g, 4.42 mmol) in dry CH_2Cl_2 (50 mL) and anhydrous K_2CO_3 (0.03 g, 0.91 mmol) was cooled to 0° C under nitrogen. Bromine (0.14 mL, 2.65

mmol) was added drop wise and the solution was allowed to stir for 30 minutes. The reaction was then quenched using 10 % sodium thiosulfate solution and transferred to separatory funnel where the organic layers were extracted with CH_2Cl_2. The crude solution was then dried over Na_2SO_4 and concentrated under reduced pressure. The crude was then subjected to flash chromatography using a prepacked 50 g silica column [eluents: solvent A, EtOAc, solvent B, hexanes; gradient, 5% A/95% B (4 CV), 5% A/95% B → 10% A/90% B (12 CV), 45% A/55% B (5.7 CV); flow rate, 25 mL/min; monitored at λ's 254 and 280 nm] to yield bromoacetophenone **6** as a tan solid (0.82 g, 2.26 mmol, 51%, R_f 0.29 (80:20 hexanes:EtOAc)).

^{1}H NMR ($CDCl_3$, 500 MHz): δ 7.57 (dd, *J* = 2.5 Hz, 8.5 Hz, 1H, Ar<u>H</u>), 7.46 (d, *J* = 2.0 Hz, 1H, Ar<u>H</u>), 6.85 (d, *J* = 8.5 Hz, 1H, Ar<u>H</u>), 3.84 (s, 3H, OC<u>H</u>$_3$), 0.98 (s, 9H, C(C<u>H</u>$_3$)$_3$), 0.15 (s, 6H, Si(C<u>H</u>$_3$)$_2$).

^{13}C NMR ($CDCl_3$, 125 MHz): δ 189.9, 156.1, 145.1, 127.1, 124.3, 121.0, 111.0, 55.6, 25.7, 18.4, -4.6.

*2-(3'-tert-Butyldimethylsilyloxy-4'-methoxyphenyl)-6-methoxyindole **8***

A solution of *m*-anisidine (0.70 mL, 6.27 mmol) was dissolved in *N*,*N*-dimethylaniline (20 mL) and was heated to reflux at 170 ºC. Then a solution of **6** (0.69 g, 1.90 mmol) in EtOAc (5 mL) was added dropwise. The reaction mixture was then allowed to stir at 170 ºC for 12 hours. Upon completion, water was added, the phases were separated, and the organic layers were extracted with EtOAc (3 x 50 mL). The combined organic layers were dried over Na_2SO_4 and concentrated under reduced pressure. Purification by flash chromatography using a prepacked 25 g silica column

[eluents: solvent A, EtOAc, solvent B, hexanes; gradient, 12% A/88% B (4 CV), 12% A/88% B → 100% A/0% B (10 CV), 100% A/0% B (2.6 CV); flow rate, 25 mL/min; monitored at λ's 254 and 280 nm] resulted in the desired phenylindole **8** (0.54 g, 1.40 mmol, 73%, R_f 0.48 (50:50 hexanes:EtOAc)) as light tan crystals.

^{1}H NMR ($CDCl_3$, 500 MHz): δ 8.18 (br s, 1H, NH), 7.49 (d, *J* = 8.5 Hz, 1H, ArH), 7.16 (d, *J* = 2.0 Hz, 1H, ArH), 7.14 (dd, *J* = 2.5 Hz, 8.0 Hz, 1H, ArH), 6.87 (m, 2H, ArH), 6.81 (dd, *J* = 2.5 Hz, 9.0 Hz, 1H, ArH), 6.63 (d, *J* = 1.5 Hz, 1H, ArH), 3.85 (s, 3H, OCH_3), 3.84 (s, 3H, OCH_3), 1.07 (s, 9H, $C(CH_3)_3$), 0.23 (s, 6H, $Si(CH_3)_2$).

^{13}C NMR ($CDCl_3$, 125 MHz): δ 156.5, 150.7, 145.5, 137.6, 137.0, 125.9, 123.9, 121.0, 118.3, 118.0, 112.5, 110.1, 98.8, 94.7, 55.8, 55.6, 25.9, 18.6, -4.4.

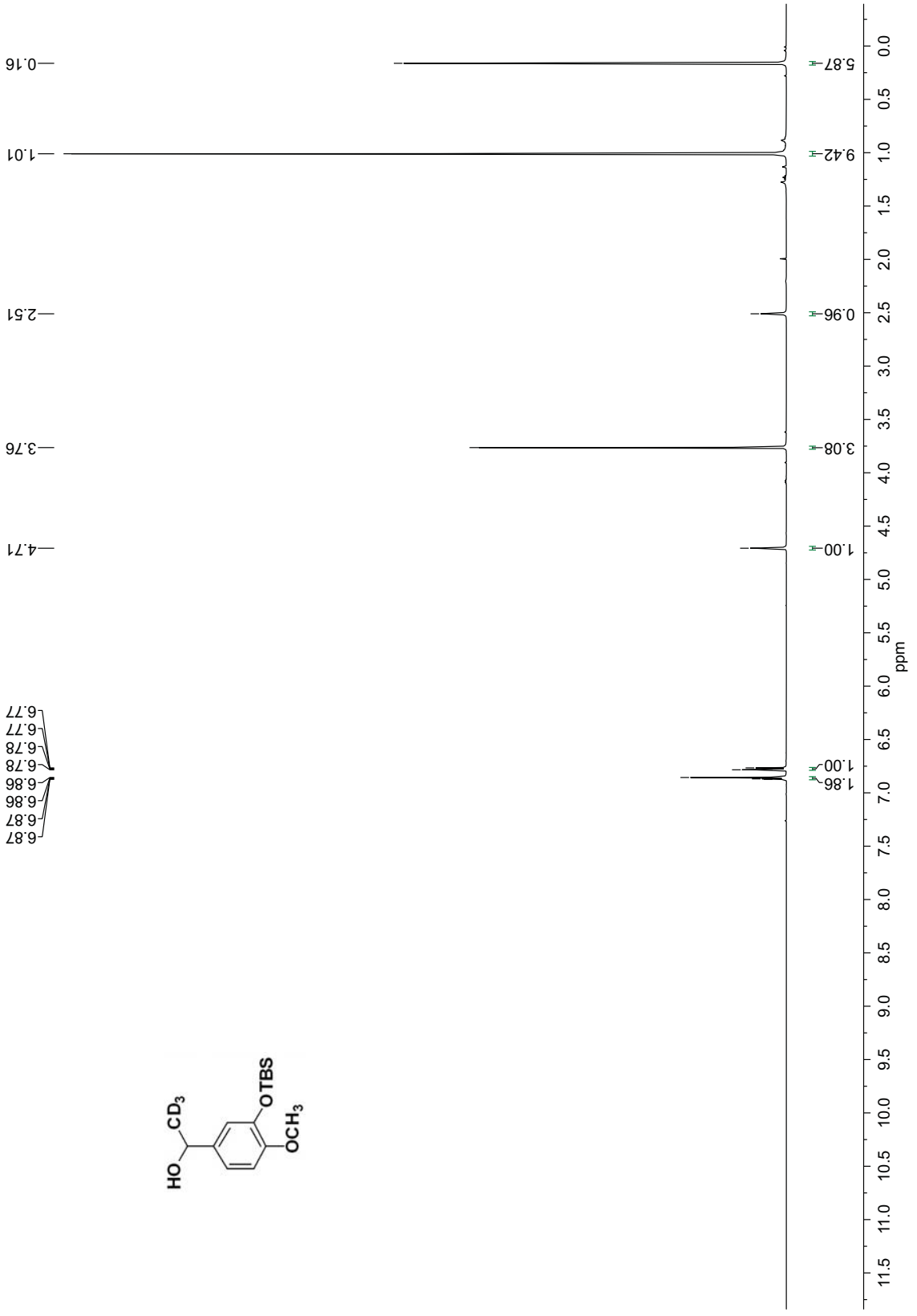
HO
CD3
OTBS
OCH3
6.87
6.87
6.86
6.86
6.78
6.78
6.77
6.77
4.71
3.76
2.51
1.01
0.16
1.00
1.86
1.00
3.08
0.96
9.42
5.87
ppm

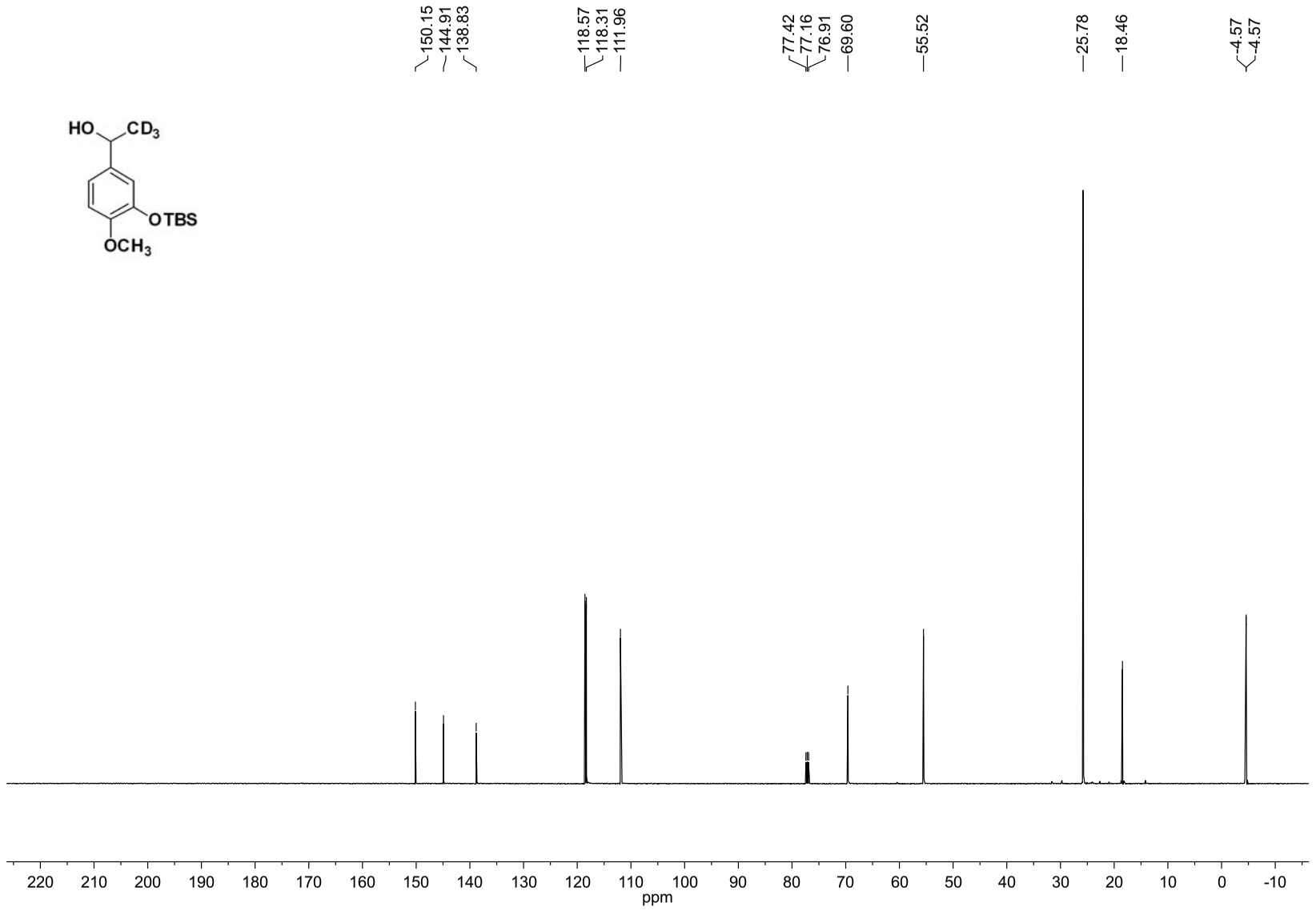
150.15
144.91
138.83
118.57
118.31
111.96
77.42
77.16
76.91
69.60
55.52
25.78
18.46
-4.57
-4.57
HO
CD3
OTBS
OCH3
220
210
200
190
180
170
160
150
140
130
120
110
100
90
80
70
60
50
40
30
20
10
0
-10
ppm

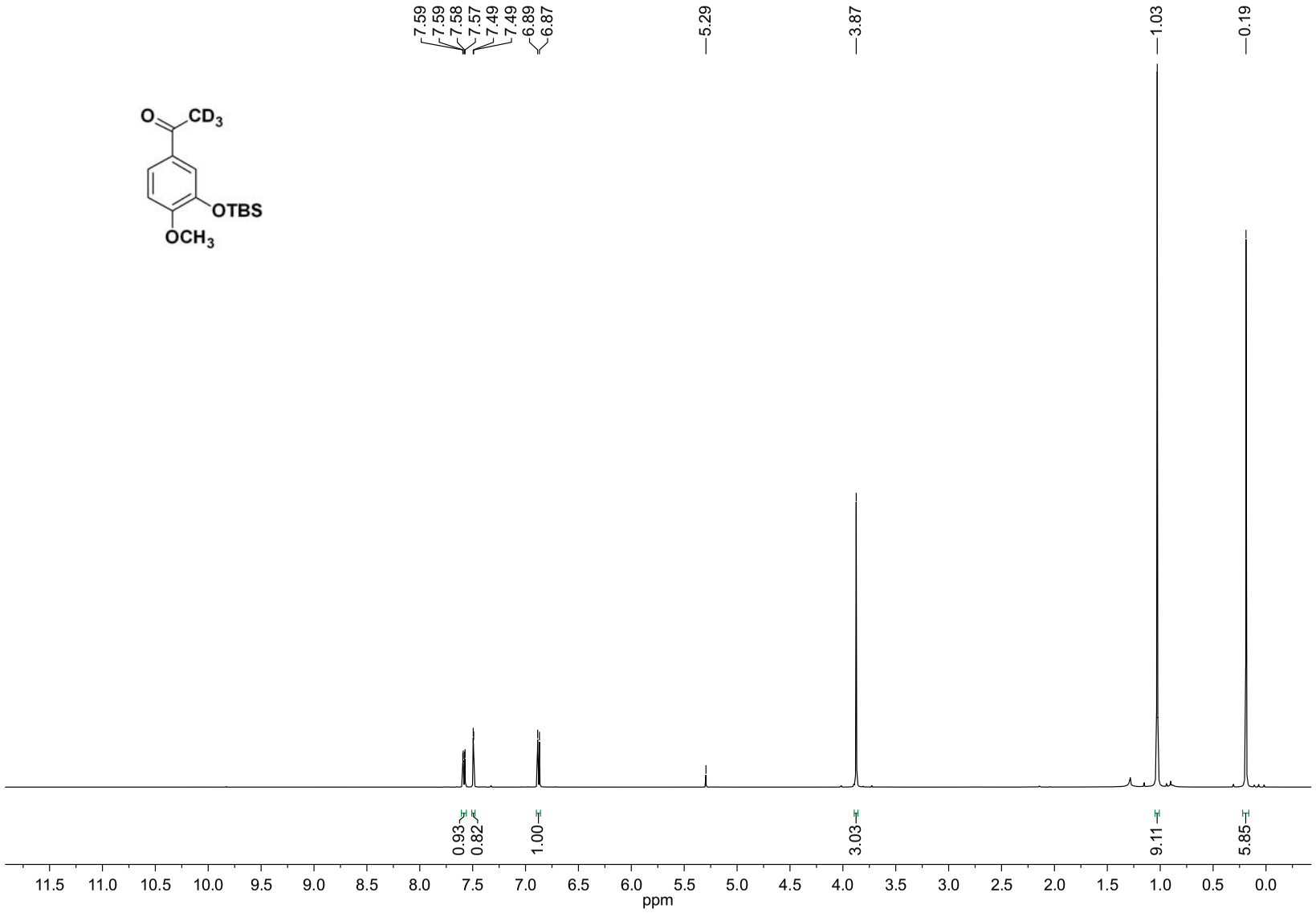
7.59
7.59
7.58
7.57
7.49
7.49
6.89
6.87
5.29
3.87
1.03
0.19
O
CD3
OTBS
OCH3
0.93
0.82
1.00
3.03
9.11
5.85
11.5 11.0 10.5 10.0 9.5 9.0 8.5 8.0 7.5 7.0 6.5 6.0 5.5 5.0 4.5 4.0 3.5 3.0 2.5 2.0 1.5 1.0 0.5 0.0
ppm

196.67
155.29
144.82
130.57
123.54
120.34
110.76
77.41
77.16
76.90
55.40
25.67
18.41
-4.65
OTBS
OCH3
CD3
O
ppm

7.21
7.21
7.19
7.19
7.15
7.15
6.82
6.81
3.82
1.06
0.30
0.21
1.00
0.87
1.11
3.11
9.05
8.77
6.19
ppm
OTMS
OTBS
OCH3
D2C

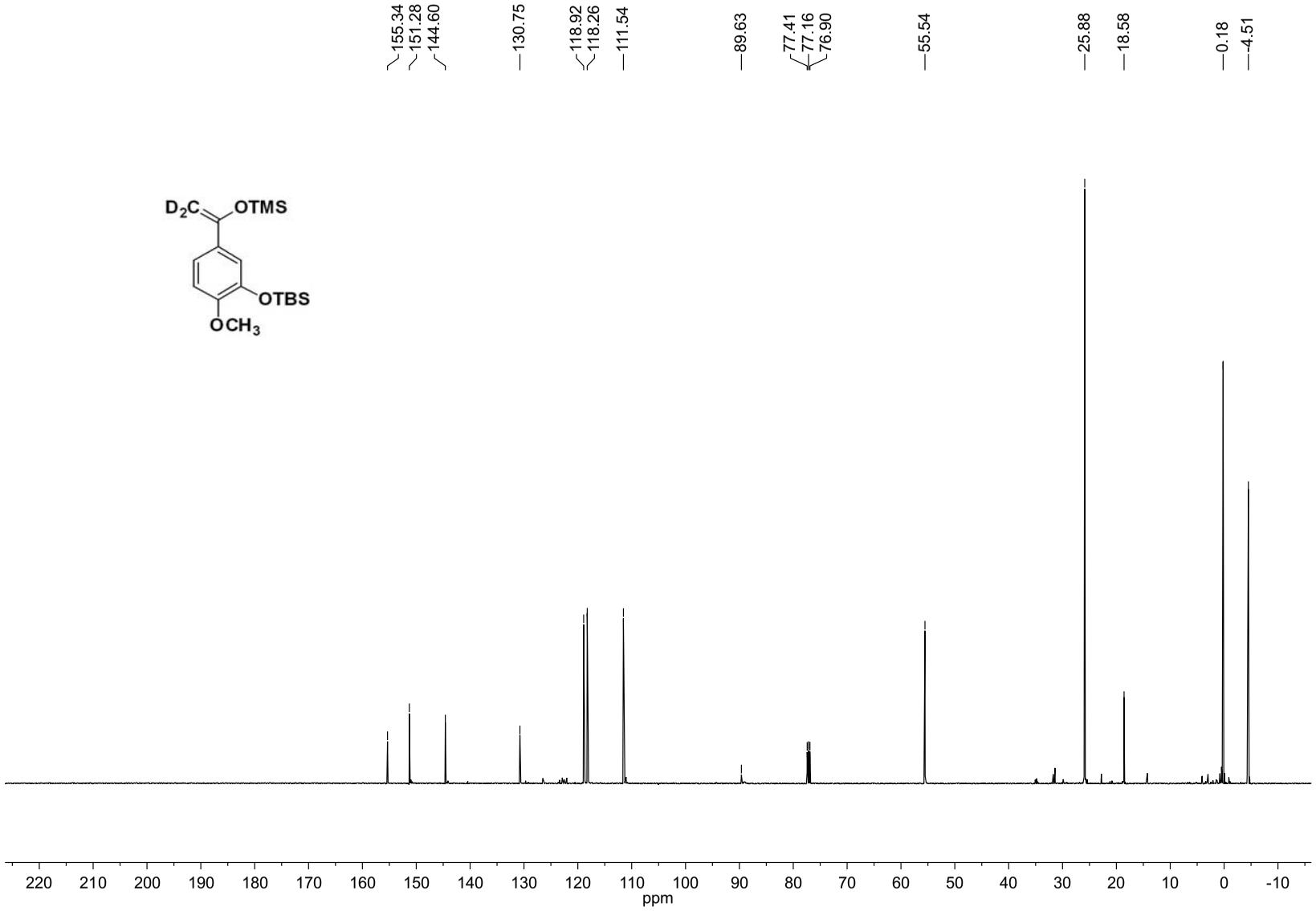
155.34
151.28
144.60
130.75
118.92
118.26
111.54
89.63
77.41
77.16
76.90
55.54
25.88
18.58
0.18
-4.51
D2C
OTMS
OTBS
OCH3
220 210 200 190 180 170 160 150 140 130 120 110 100 90 80 70 60 50 40 30 20 10 0 -10
ppm

7.58
7.58
7.57
7.56
7.46
7.46
7.26
6.86
6.84
5.25
3.84
0.98
0.15
0.97
0.90
1.00
3.02
9.08
6.16
ppm
D
D
Br
O
OTBS
OCH3

189.92
156.09
145.12
127.10
124.27
121.01
111.03
77.41
77.16
76.91
55.55
25.68
18.43
-4.59
D
D
Br
O
OTBS
OCH3
ppm

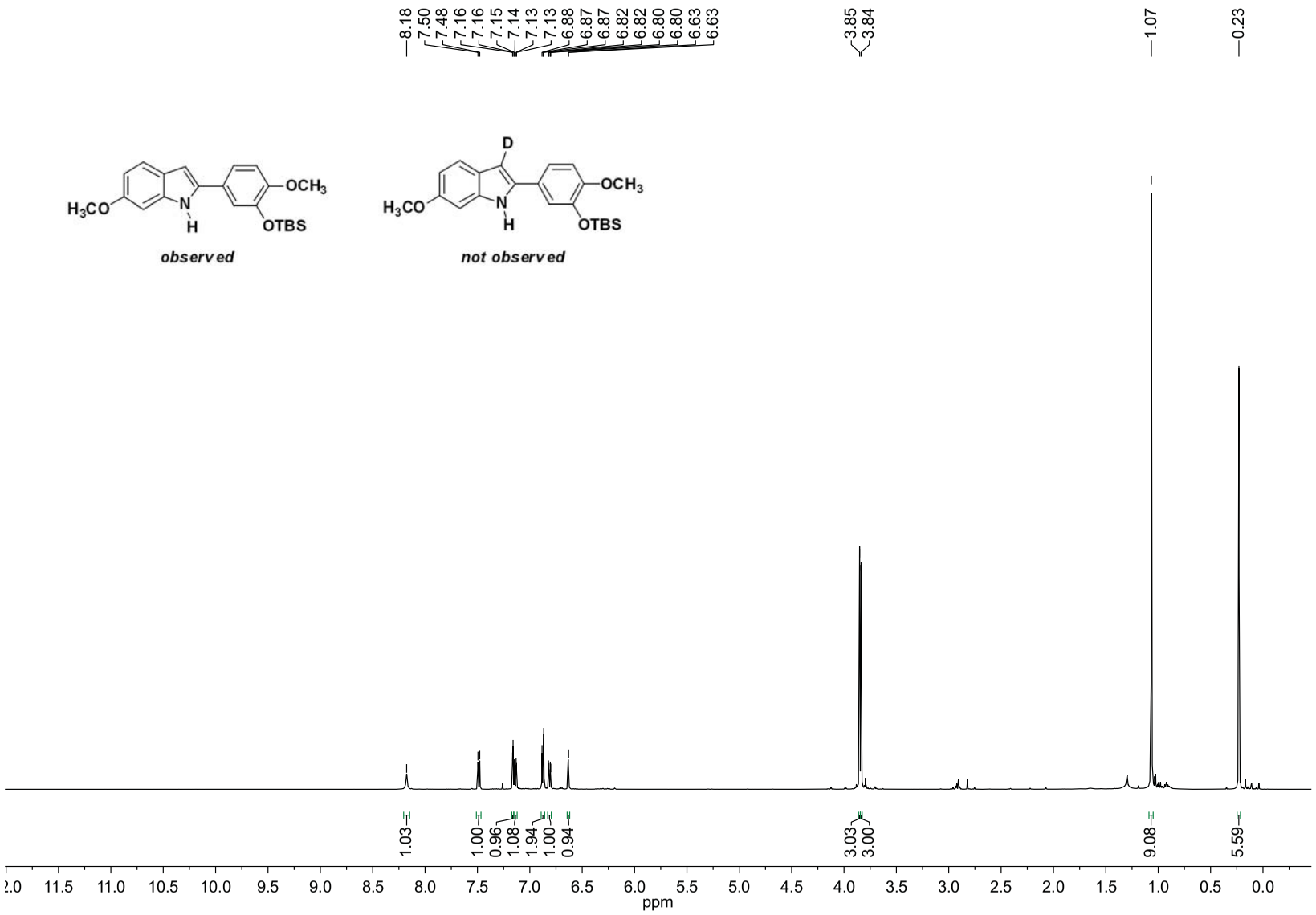
8.18
7.50
7.48
7.16
7.16
7.15
7.14
7.13
7.13
6.88
6.87
6.87
6.82
6.82
6.80
6.80
6.63
6.63
3.85
3.84
1.07
0.23
H3CO
OCH3
N
H
OTBS
observed
D
H3CO
OCH3
N
H
OTBS
not observed
1.03
1.00
0.96
1.08
1.94
1.00
0.94
3.03
3.00
9.08
5.59
ppm

-4.43
18.63
25.90
55.62
55.77
76.91
77.16
77.41
94.68
98.78
110.06
112.52
117.96
118.32
121.01
123.85
125.92
137.03
137.57
145.51
150.69
156.45
OCH3
OTBS
H
N
H3CO
observed
D
not observed
ppm

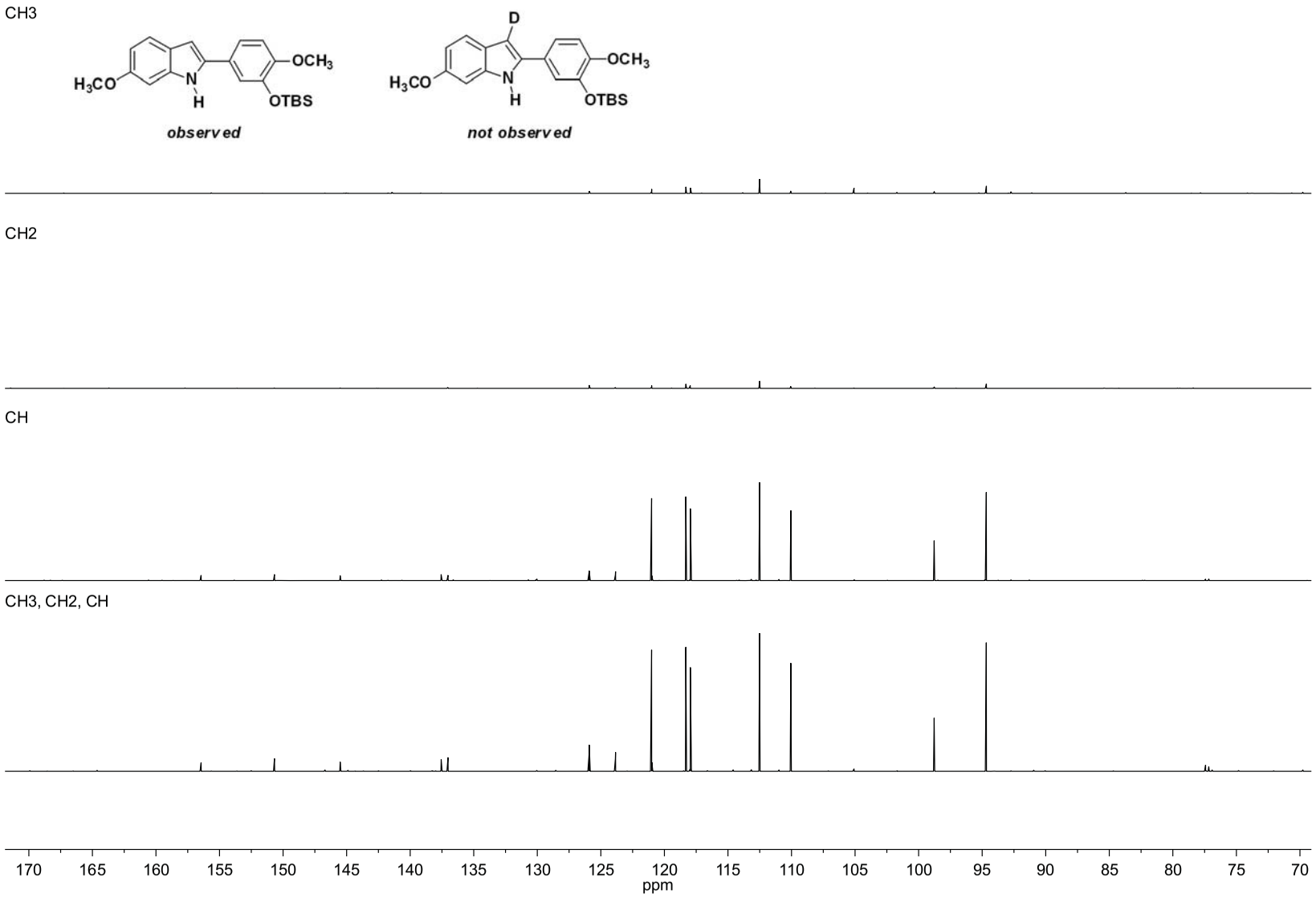
CH3
H3CO
OCH3
N
H
OTBS
observed
D
H3CO
OCH3
N
H
OTBS
not observed
CH2
CH
CH3, CH2, CH
170
165
160
155
150
145
140
135
130
125
120
115
110
105
100
95
90
85
80
75
70
ppm

REFERENCES

Alhasan, M. K.; Liu, L.; Lewis, M. A.; Magnusson, J.; Mason, R. P. Comparison of Optical and Power Doppler Ultrasound Imaging for Non-Invasive Evaluation of Arsenic Trioxide as a Vascular Disrupting Agent in Tumors. *PLoS ONE* **2012**, *7*, e46106.

Bischler, A.; Brion, H. *Chem. Ber.* **1892**, *25*, 2860.

Boehle, A. S.; Sipos, B.; Kliche, U.; Kalthoff, H.; Dohrmann, P. Ann. Thorac. Surg. 2001, 71, 1657-1665.

Boehm, S.; Rothermundt, C.; Hess, D.; Joerger, M. Antiangiogenic Drugs in Oncology: A Focus on Drug Safety and the Elderly- A Mini Review. Gerontology, 2010, 56, 303-309.

Boyland, E.; Boyland, M. E. Studies in Tissue Metabolism: The Action of Colchicine and B. Typhosus Extract. Biochemistry, 1937, 31(3), 454-460.

Brancale, A.; Silvestri, R. Indole, A Core Nucleus for Potent Inhibitors of Tubulin Polymerization. Med. Res. Rev. 2007, 27(2), 209-238.

Brem, S.; Brem, H.; Folkman, J.; Finkelstein, D.; Patz, A. Prolonged Tumor Dormancy by Prevention of Neovascularization in the Vitreous. Cancer Res. 1976, 36, 2807-2812.

Brown, J. M.; SR 4233 (tirapazamine): a new anticancer drug exploiting hypoxia in solid tumours. Br. J. Cancer 1993, 67, 1163–1170.

Carmeliet, P. Angiogenesis in Helath and Disease. *Nat. Med.* **2003**, *9*, 653-660.

Carmeliet, P.; Jain, R. K. Molecular Mechanisms and Clinical Applications of Angiogenesis. Nature, 2011, 473, 298-307.

Carmeliet, P.; Jain, R. K.; Angiogenesis in Cancer and Other Diseases. Nature, 2000, 407, 249-257.

Chamberlain, M. C. Bevacizumab for the Treatment of Recurrent Glioblastoma. Clin. Med. Insights Oncol. 2011, 5, 117-129.

Chaplin, D. J.; Pettit, G. R.; Hill, S. A. Anti-vascular Approaches to Solid Tumour Therapy: Evaluation of Combretastatin A4 Phosphate. Anticancer Res. 1999, 19, 189-195.

Chaudhary, A.; Pandeya, S. N.; Kumar, P.; Sharma, P. P.; Gupta, S.; Soni, N.; Verma, K. K.; Bhardwaj, G. Combretastatin A-4 Analogs as Anticancer Agents. Mini-Rev. Med. Chem. 2007, 7, 1186-1205.

Chowdhury, G.; Junnotula, V.; Daniels, J. S.; Greenberg, M. M.; Gates, K. S. DNA strand damage product analysis provides evidence that the tumor cell specific cytotoxin tirapazamine produces hydroxyl radical and acts as a surrogate for O2. J. Am. Chem. Soc. 2007, 129, 12870–12877.

Cragg, G. M.; Newman, D. J. Plants as a Source of Anti-cancer Agents. J. Ethnopharmacol. 2005, 100, 72-79.

Dalal, S.; Burchill, S. A. Preclinical Evaluation of Vascular-disrupting Agents in Ewing's Sarcoma Family of Tumours. Eur. J. Cancer 2009, 45, 713-722.

Denekamp, J.; Hill, S. A.; Hobson, B. Vascular Occlusion and Tumor Cell Death. Eur. J. Cancer Clin. Oncl. 1983, 19, 271-275.

Dewhirst, M. W.; Kimura, H.; Rehmus, S. W.; Braun, R. D.; Papahadjopoulos, D.; Hong, K.; Secomb, T. W. Microvascular Studies on the Origins of Perfusion-limited Hypoxia. Br. J. Cancer. 1996, 27, S247-S251.

Dougherty, G. J.; Chaplin, D. J. in Vascular Disruptive Agents for the Treatment of Cancer, ed. T. Meyer, Springer, New York, 2010, ch. 1, 1-27.

Dowlati, A.; Robertson, K. Cooney, M.; Petros, W. P.; Stratford, M.; Jesberger, J.; Rafie, N.; Overmoyer, B.; Makkar, V.; Stambler, B.; Taylor, A.; Waas, J.; Lewin, J. S.; McCrae, K. R.; Remick, S. C. A Phase I Pharmacokinetic and Translational Study of the Novel Vascular Targeting Agent Combretastatin A-4 Phosphate on a Single-dose Intravenous Schedule in Patients with Advanced Cancer. Cacner Res. 2002, 62(12), 3408-3416.

Dowlati, A.; Robertson, K.; Cooney, M.; Petros, W. P.; Stratford, M.; Jesberger, J.; Rafie, N.; Overmoyer, B.; Makkar, V.; Stambler, B.; Taylor, A.; Waas, J.; Lewin, J. S.; McCrae, K. R.; Remick, S. C. J. Clin. Oncol. 2003, 62(12), 3408-3416.

El-Zayat, A. A. E.; Degan, D.; Drabek, S. *Anticancer Drugs* **1993**, *4*, 19-25.

Etienne-Manneville, S. *Curr. Opin. Cell Biol.* **2010**, *22*, 104–111.

Ferrara, N. Vascular Endothelial Growth Factor. Arterioscler Thromb. Vasc. Biol. 2009, 29, 789-791.

Flynn, B. L.; Flynn, G. P.; Hamel, E.; Jung, M. K. Bioorg. Med. Chem. Lett. 2001, 11, 2341–2343.

Flynn, B. L.; Gill, G. S.; Grobelny, D. W.; Chaplin, J. H.; Paul, D.; Leske, A. F.; Lavranos, T. C.; Chalmers, D. K.; Charman, S. A.; Kostewicz, E.; Shackleford, D. M.; Morizzi, J.; Hamel, E.; Jung, M. K.; Kremmidiotis, G. Discovery of 7-Hydroxy-6-methoxy-2-methyl-3-(3,4,5-trimethoxybenzoyl)benzo[b]furan (BNC105), a Tubulin Polymerization Inhibitor with Potent Antiproliferative and Tumor Vascular Disrupting Properties. J. Med. Chem. 2011, 54, 6014-6027.

Flynn, B. L.; Hamel, E.; Jung, M. K. One-Pot Synthesis of Benzo[b]furan and Indole Inhibitors of Tubulin Polymerization. J. Med. Chem. 2002, 45, 2670-2673.

Folkman J. Tumor Angiogenesis: Therapeutic Implications. N. Engl. J. Med. 1971, 285, 1182–1186.

Gastpar, R.; Goldbrunner, M.; Marko, D.; von Angerer, E. Methoxy-Substituted 3-Formyl-2-phenylindoles Inhibit Tubulin Polymerization. J. Med. Chem. 1998, 41, 4965-4972.

Gee M. S.; Procopio, W. N.; Makonnen, S.; Feldman, M. D.; Yeilding, N. M.; Lee, W. M. Tumor Vessel Development and Maturation Impose Limits on the Effectiveness of Anti-vascular Therapy. Am. J. Pathol. 2003, 162, 183-193.

Goertz, D. E.; Yu, J. L.; Kerbel, R. S.; Burns, P. N.; Foster, F. S. High-frequency Doppler Ultrasound Monitors the Effects of Antivascular Therapy on Tumor Blood Flow. Cancer Res. 2002, 62, 6371-6375.

Hadimani, M. B.; Kessler, R. J.; Kautz, J. A.; Ghatak, A.; Shirali, A. R.; O'dell, H.; Garner, C. M.; Pinney, K. G. 2-(3-tert-Butyldimethylsiloxy-4-methoxyphenyl)-6-methoxy-3-(3, 4, 5-trimethoxybenzoyl)indole. Acta. Cryst. 2002, C58, 330-332.

Hadimani, M. B.; MacDonough, M. T.; Strecker, T. E.; Lopez, R.; Sriram, M.; Nguyen, B. L.; Kessler, R. J.; Ghatak, A.; Shirali, A. R.; Liu, L.; Garner, C. M.; Pettit, G. R.; Hamel, H.; Chaplin, D. J.; Mason, R. P.; Trawick, M. L.; Pinney, K. G. Manuscript submitted to J. Nat. Prod. (May 9, 2013).

Hall, J. J.; Sriram, M.; Strecker, T. E.; Tidmore, J. K.; Jelinek, C. J.; Kumar, G. D. K.; Hadimani, M. B.; Pettit, G. R.; Chaplin, D. J.; Trawick, M. L.; Pinney, K. G. Bioorg. Med. Chem. Lett. 2008, 18, 5146-5149.

Hamel, E. An Overview of Compounds and their Effects on Microtubule Assembly. In Microtubule Targets in Cancer Therapy, Fojo, A. T., Ed.; Humana Press: Towota, New Jersey, 2008; pp. 1-20.

Hamel, E. Evaluation of Antimitotic Agents by Quantitative Comparisons of Their Effects on the Polymerization of Purified Tubulin. Cell Biochem. Biophys. 2003, 38, 1-21.

Hamel, E.; Lin, C. M. *Biochim. Biophys. Acta*. **1981**, *675*, 226-231.

Hamel, E.; Lin, C. M. Separation of Active Tubulin and Microtubule-associated Proteins by Ultracentrifugation and Isolation of a Component Causing the Formation of Microtubule Bundles. Biochemistry 1984, 23, 4173-4184.

Hamel, E.; Lin, C. M. Stabilization of the Colchicine Binding Activity of Tubulin by Organic Acids. Biochim. Biophys. Acta 1981, 675, 226-231.

Hasani, A.; Leighl, N. Classification and Toxicities of Vascular Disrupting Agents. Clin. Lung Cancer. 2011, 12(1), 18-25.

Heidemann, S. Microtubules, Leukemia, and Cough Syrup. *Blood*, **2006**, *107*, 2216-2217.

Hida, K.; Hida, Y.; Shindoh, M. *Cancer Sci*. **2008**, *99*(3), 459-466.

Horsman, M. R.; Bohn, A. B.; Busk, M. Vascular Targeting Therapy: Potential Benefit Depends of Tumor and Host Related Effects. Exp. Oncol. 2010, 32(3), 143-148.

Jain, R. K. Determinants of Tumor Blood Flow: A Review. Cancer Res. 1988, 48, 2641-2658.

Jain, R. K. Normalization of Tumor Vasculature: An Emerging Concept in Antiangiogenic Therapy. Science, 2005, 307, 58-62.

Jones, C. D.; Jevnikar, M. G.; Pike, A. J.; Peters, M. K.; Black, L. J.; Thompson, A. R.; Falcone, J. F.; Clemens, J. A. Antiestrogens. 2. Structure-Activity Studies in a Series of 3-Aroyl-2-arylbenzo[b]thiophene Derivatives Leading to [6-Hydroxy-2-(4-hydroxyphenyl)benzo[b]thien-3-yl]-[4-[2-(1-piperidinyl)ethoxy]phenyl]methanone Hydrochloride (LY 156758), a Remarkably Effective Estrogen Antagonist with Only Minimal Intrinsic Estrogenicity. J. Med. Chem. 1984, 27, 1057-1066.

Jordan, M. A.; Wilson, L. *Nat. Rev. Cancer* **2004**, *4*, 253–265.

Kanthou, C.; Tozer, G. M. *Exp. Opin. Ther. Targets* **2007**, *11*(11), 1443-1457.

Kaufmann, D.; Pojarova, M.; Vogel, S.; Liebl, R.; Gastpar, R.; Gross, D.; Nishino, T.; Pfaller, T.; von Angerer, E.; Antimitotic Activities of 2-Phenylindole-3-carbaldehydes in Human Breast Cancer Cells. Bioorg. Med. Chem. 2007, 15, 5122-5136.

Kemperman, G. J.; Roeters, T. A.; Hilberink, P. W. *Eur. J. Org. Chem*. **2003**, 1681-1686.

Kerbel, R.; Folkman, J. Clinical Translation of Angiogenesis Inhibitors. Nat. Revs. Cancer, 2002, 2, 727-739.

Kessler, R. J.; Arambula, J. F.; Nguyen, B. L.; Hadimani, M. B.; Pinney, K. G. (Poster). 4th Annual Spring Research Symposium, Department of Chemistry & Biochemistry & The Center for Drug Discovery, Baylor University, Waco, TX, March 2003.

Kessler, R. J.; Hadimani, B.; Pinney, K. G.; Edvardsen, K. (Poster). 38th National Organic Symposium Indiana University, Bloomington IN, June 8-12, 2003.

Konerding, M. A.; Fait, E.; Gaumann, A. 3D Microvascular Architecture of Pre-cancerous Lesions and Invasive Carcinomas of the Colon. Br. J. Cancer. 2001, 84, 1354-1362.

Kremmidiotis, G.; Leske, A. F.; Lavranos, T. C.; Beaumont D.; Hall, A.; O'Callaghan, M.; Matthews, C. A.; Flynn, B. L. Mol. Cancer Ther. 2010, 6, 1562-1573.

Kremmidiotis, G.; Leske, A. F.; Lavranos, T. C.; Beaumont, D.; Gasic, J.; Hall, A.; O'Callaghan, M.; Matthews, C. A.; Flynn, B. BNC105: A Novel Tubulin Polymerization Inhibitor that Selectively Disrupts Tumor Vasculature and Displays Single-Agent Antitumor Efficacy. Mol. Cancer Ther. 2010, 9, 1562-1573.

Kuo, C.-C.; Hsieh, H.-P.; Pan, W.-Y.; Chen, C.-P.; Liou, J.-P.; Lee, S.-J.; Chang, L.-Y.; Chen, L.-T.; Chen, C.-T.; Chang, J.-Y. BPR0L075, A Novel Synthetic Indole Compound with Antimitotic Activity in Human Cancer Cells, Exerts Effective Antitumoral Activity in Vivo. Cancer Res. 2004, 64, 4621-4628.

Kym, P. R.; Anstead, G. M.; Pinney, K. G.; Wilson, S. R.; Katzenellenbogen, J. A. Structural and Computational Modeling Studies on 3-aroyl-2-arylbenzo[b]thiophene Estrogen Receptor Ligands: LY117018 and Aryl Azide Photoaffinity Labeling Analogs; Investigation of Conformational Preferences, Differential Photoreactivity, and Preferential Modes of Binding. J. Med. Chem. 1993, 36, 3910-3922.

La Regina, Bai, R.; Rensen, W. M.; Cesare, E. D.; Coluccia, A.; Piscitelli, F.; Famiglini, V.; Reggio, A.; Nalli, M.; Pelliccia, S.; Pozza, E. D.; Costa, B.; Granata, I.; Porta, A.; Maresca, B.; Soriani, A.; Iannitto, M. L.; Santoni, A.; Li, J.; Cona, M. M.; Chen, F.; Ni, Y.; Brancale, A.; Dondio, G.; Vultaggio, S.; Varasi, M.; Mercurio, C.; Martini, C.; Hamel, E.; Lavia, P.; Novellino, E.; Silvestri, R. J. Med. Chem. 2013, 56, 123-149.

La Regina, G.; Sarkar, T.; Bai, R.; Edler, M. C.; Saletti, R.; Coluccia, A.; Piscitelli, F.; Minelli, L.; Gatti, V.; Mazzoccoli, C.; Palermo, V.; Mazzoni, C.; Falcone, C.; Scovassi, A. I.; Giansanti, V.; Campiglia, P.; Porta, A.; Maresca, B.; Hamel, E.; Brancale, A.; Novellino, E.; Silvestri, R. J. Med. Chem. 2009, 52, 7512-7527.

Lee, H.-Y.; Chang, J.-Y.; Chang, L.-Y.; Lai, W.-Y.; Lai, M.-J.; Shih, K.-H.; Kuo, C.-C.; Chang, C.-Y.; Liou, J.-P. Concise Syntheses of N-Aryl-5,6,7-trimethoxyindoles as Antimitotic and Vascular Disrupting Agents: Application of the Copper-Mediated Ullmann-Type Arylation. Org. Biomol. Chem. 2011, 9, 3154-3157.

Lee, R. M.; Gewirtz, D. A. Colchicine Site Inhibitors of Microtubule Integrity as Vascular Disrupting Agents. Drug Dev. Res. 2008, 69(6), 352-358.

Leu, A. J.; Berk, D. A.; Lymboussaki, A.; Alitalo, K.; Jain, R. K. Absence of Functional Lymphatics Within a Murine Sarcoma: a Molecular and Functional Evaluation. Cancer Res. 2000, 60, 4324-4327.

Lin, C. M.; Ho, H. H.; Pettit, G. R.; Hamel, E. The Antimitotic Natural Products Combretastatin A-2 and Combretastatin A-4: Studies on the Mechanism of Their Inhibition of the Binding of Colchicine to Tubulin. Biochemistry, 1989, 28, 6984-6991.

Liou, J.-P.; Chang, Y.-L.; Kuo, F.-M.; Chang, C.-W.; Tseng, H.-Y.; Wang, C.-C.; Yang, Y.-N.; Chang, J.-Y.; Lee, S.-J.; Hsieh, H.-P. Concise Synthesis and Structure-Activity Relationships of Combretastatin A-4 Analogues, 1-Aroylindoles and 3-Aroylindoles, as Novel Classes of Potent Antitubulin Agents. J. Med. Chem. 2004, 47, 4247-4257.

Liou, J.-P.; Wu, C.-Y.; Hsieh, H.-P.; Chang, C.-Y.; Chen, C.-M.; Kuo, C.-C.; Chang, J.-Y. 4- and 5-Aroylindoles as Novel Classes of Potent Antitubulin Agents. J. Med. Chem. 2007, 50, 4548-4552.

Liou, J.-P.; Wu, Z.-Y.; Kuo, C.-C.; Chang, C.-Y.; Lu, P.-Y.; Chen, C.-M.; Hsieh, H.-P.; Chang, J.-Y. Discovery of 4-Amino and 4-Hydroxy-1-aroylindoles as Potent Tubulin Polymerization Inhibitors. J. Med. Chem. 2008, 51, 4351–4355.

Liu, L.; Beck, H.; Wang, X.; Hsieh, H.-P.; Mason, R. P.; Liu, X. Tubulin-Destabilizing Agent BPR0L075 Induces Vascular-Disruption in Human Breast Cancer Mammary Fat Pad Xenografts. PLoS ONE, published online August 24, 2012; DOI: 10.1371/journal.pone.0043314.

Lopus, M.; Yenjerle, M.; Wilson, L. In Wiley Encyclopedia of Chemical Biology; Begley, T. P.; Eds.; John Wiley and Sons, Inc.: Hoboken, NJ, 2008; 3, 153-160.

Mahboobi, S.; Pongratz, H.; Hufsky, H.; Hockemeyer, J.; Frieser, M.; Lyssenko, A.; Paper, D. H.; Burgermeister, J.; Bohmer, F.-D.; Fiebig, H.-H.; Burger, A. M.; Baasner, S.; Beckers, T. Synthetic 2-Aroylindole Derivatives as a New Class of Potent Tubulin-Inhibitory, Antimitotic Agents. J. Med. Chem. 2001, 44, 4535-4553.

Martino, G. D.; La Regina, G.; Coluccia, A.; Edler, M. C.; Barbera, M. C.; Brancale, A.; Wilcox, E.; Hamel, E.; Artico, M.; Silvestri, R. Arylthioindoles, Potent Inhibitors of Tubulin Polymerization. J. Med. Chem. 2004, 47, 6120-6123.

Mason, R. P.; Zhao, D.; Liu, L.; Trawick, M. L.; Pinney, K. G. A Perspective on Vascular Disrupting Agents that Interact with Tubulin: Preclinical Tumor Imaging and Biological Assessment. Integr. Biol., 2011, 3, 375-387.

McDonald, D.; Choyke, P. Imaging of Agiogenesis: From Microscope to Clinic. Nature Med. 2003, 9, 713-725.

McGowan, A. T.; Fox, B. W. *Cancer Chemother. Pharmacol.* **1990**, *26*, 79-81.

Mohlau, H. *Chem. Ber.* **1881**, *14*, 173.

Monks, A.; Scudiero, D.; Skehan, P.; Shoemaker, R.; Paull, K.; Vistica, D.; Hose, C.; Langley, J.; Cronise, P.; Vaigro-Wolff, A.; Gray-Goodrich, M.; Campbell, H.; Mayo, J.; Boyd, M. Feasibility of a High-flux Anticancer Drug Screen Using a Diverse Panel of Cultured Human Tumor Cell Lines. J. Natl. Cancer Inst. 1991, 83, 757-766.

Mullica, D. F.; Pinney, K. G.; Dingeman, K. M.; Bounds, A. D.; Sappenfield, E. L. X-ray Structures of Two Methoxybenzo[b]thiophenes. J. Chem. Crystallogr. 1996, 26, 801-806.

Mullica, D. F.; Pinney, K. G.; Mocharla, V. P.; Dingeman, K. M.; Bounds, A. D.; Sappenfield, E. L. Characterization and Structural Analyses of Trimethoxy and Triethoxybenzo[b]thiophene. J. Chem. Crystallogr. 1998, 28, 289-295.

Ohno, T.; Kawano, K.; Tahara, K. *Gastroenterology* **2001**, *120*, 2831.

Oshumi, K.; Hatanaka, R.; Nakagawa, R. *Anticancer Drug Des.* **1999**, *14*, 539-548.

Oshumi, K.; Nakagawa, R.; Fukuda, Y. *J. Med. Chem.* **1998**, *41*, 3022-3032.

Owellen, R. J.; Hartke, C. A.; Dickerson, R. M.; Hains, F. O. Inhibition of Tubulin-microtubule Polymerization by Drugs of the Vinca Alkaloid Class. Cancer Res. 1976, 36, 1499-1502.

Padera, T. P.; Kadambi, A.; di Tomaso, E.; Carrerira, C. M.; Brown, E. B.; Boucher, Y.; Choi, N. C.; Mathisen, D.; Wain, J.; Mark, E. J.; Munn, L. L.; Jain, R. K. Lymphatic Metastasis in the Absence of Functional Intratumor Lymphatics. Scicence, 2000, 296, 1883-1886.

Patil, S. A.; Patil, R.; Miller, D. D. Indole Moleceules as Inhibitors of Tubulin Polymerization: Potential New Anitcancer Agents. Future Med. Chem. 2012, 4(16), 2085-2115.

Pettit G. R.; Pinney, K. G. Major Milestones. In American Society of Pharmacognosy History. Cragg, G., Ed.; 2009.

Pettit, G. R.; Cragg, G. M.; Herald, D. L.; Schmidt, J. M.; Lohavanijaya, P. Antineoplastic agents. 84. Isolation and Structure of Combretastatin. Can. J. Chem. 1982, 60, 1374-1376.

Pettit, G. R.; Cragg, G. M.; Singh, S. B. Antineoplastic Agents, 112. Constituents of Combretum Caffrum. J. Nat. Prod. 1987, 50, 386-391.

Pettit, G. R.; Grealish, M. P.; Herald, D. L.; Boyd, M. R.; Hamel, E.; Pettit, R. K. Antineoplastic Agents. 443. Synthesis of the Cancer Cell Growth Inhibitor Hydroxyphenstatin and Its Sodium Diphosphate Prodrug. J. Med. Chem. 2000, 43, 2731-2737.

Pettit, G. R.; Lippert, J. W. III. *Anticancer Drug Des*. **2000**, *15*, 203-216.

Pettit, G. R.; Minardi, M. D.; Boyd, M. R.; Pettit, R. K. Anticancer Drug Des. 2000, 15, 397-403.

Pettit, G. R.; Moser, B. R.; Boyd, M. R. *Anticancer Drug Des*. **2001**, *16*, 185-193.

Pettit, G. R.; Rhodes, M. R. Antineoplastic Agents 389. New Syntheses of the Combretastatin A-4 Prodrug. Anticancer Drug. Des. 1998, 13, 183-191.

Pettit, G. R.; Rosenberg, H. J.; Dixon, R.; Knight, J. C.; Hamel, E.; Chapuis, J.-C.; Pettit, R. K.; Hogan, F.; Sumner, B.; Ain, K. B.; Trickey-Platt, B. Antineoplastic Agents. 548. Synthesis of Iodo- and Diiodocombstatin Phosphate Prodrugs. J. Nat. Prod. 2012, 75, 385-393.

Pettit, G. R.; Singh, S. B.; Boyd, M. R. *J. Med. Chem*. **1995**, *38*, 1666-1672.

Pettit, G. R.; Singh, S. B.; Hamel, E.; Lin, C. M.; Alberts, D. S.; Garcia-Kendall, D. Experientia 1989, 45(2), 209-211.

Pettit, G. R.; Singh, S. B.; Niven, M. L.; Hamel, E.; Schmidt, J. M. J. Nat. Prod. 1987, 50(1), 119-131.

Pinney, K. G. in Vascular-Targeted Therapies in Oncolgy, ed. Siemann, D. John Wiley & Sons, London, UK, 2006, ch. 6, 95-121.

Pinney, K. G.; Bounds, A. D.; Dingeman, K. M.; Mocharla, V. P.; Pettit, G. R.; Bai, R.; Hamel, E. A New Anti-tubulin Agent Containing the Benzo[b]thiophene Ring System. Bioorg. Med. Chem. Lett. 1999, 9, 1081-1086.

Pinney, K. G.; Mocharla, V. P.; Chen, Z.; Garner, C. M.; Ghatak, A.; Hadimani, M.; Kessler, J.; Dorsey, J. Tubulin Binding Ligands and Corresponding Prodrug Constructs. US6593374 B2, 2003.

Pinney, K. G.; Mocharla, V. P.; Chen, Z.; Garner, C. M.; Ghatak, A.; Hadimani, M.; Kessler, J.; Dorsey, J. M. Preparation of Trimethoxyphenyl-containing Tubulin Binding Ligands and Corresponding Prodrug Constructs as Inhibitors of Tubulin Polymerization and Antimitotic Agents. From PCT Int. Appl. 2001, WO 2001068654 A2 20010920.

Pinney, K. G.; Pettie, G. R.; Mocharla, V. P.; Pilar, M.; Shirali, A. Description Anti-mitotic Agents Which Inhibit Tubulin Polymerization. US6350777 B2, 2002.

Pinney, K. G.; Pettit, G. R.; Trawick, M. L.; Jelinek, C.; Chaplin, D. J. The Discovery and Development of the Combretastatins. In Antitumor Agents from Natural Products, 2nd ed.; Kingston, D., Newman, D., Cragg, G., Eds.; CRC Press, Taylor and Francis Group: Boca Raton, Florida, 2011; pp 27-64.

Pinney, K. G.; Pilar, M.; Mocharla, V. P.; Shirali, A.; Pettie, G. R. Anti-mitotic Agents Which Inhibit Tubulin Polymerization. US06162930, 2000.

Pinney, K. G.; Sriram, M. Combretastatin Analogs with Tubulin Binding Activity. US8394859 B2, 2013.

Pinney, K. G.; Wang, F.; Del Pilar Mejia, M. Preparation of Indole-containing and Combretastatin-related Anti-mitotic and Anti-tubulin Polymerization Agents. From PCT Int. Appl. 2001, WO 2001019794 A2 20010322.

Pinney, K. G.; Wang, F.; Hadimani, M. B. Indole-containing and Combretastatin-related Anti-mitotic and Anti-tubulin Polymerization Agents. US6849656 B1, 2005.

Pinney, K.; Wang, F.; Hadimani, M.; Del Pilar Mejia, M.; Preparation of Trimethoxyphenyl-substituted Indoles with Anti-tubulin and Vascular Targeting Activity for Treatment of Cancer. From PCT Int. Appl. 2004, WO 2004099139 A1 20041118.

Reck, M.; von Pawel, J.; Zatloukal, P.; Ramlau, R.; Gorbounova, V.; Hirsh, V.; Leighl, N.; Mezger, J.; Archer, V.; Moore, N.; Manegold, C. Phase III of Cisplatin Plus Gemcitabine with Either Placebo or Bevacizumab as First-line Therapy For Nonsquamous Non-small-cell Lung Cacner: AVAiL. J. Clin. Oncol. 2009, 27(8), 1227-1234.

Regina, G. L.; Bai, R.; Rensen, W.; Coluccia, A.; Piscitelli, F.; Gatti, V.; Bolognesi, A.; Lavecchia, A.; Granata, I.; Porta, A.; Maresca, B.; Soriani, A.; Iannitto, M. L.; Mariani, M.; Santoni, A.; Brancale, A.; Ferlini, C.; Dondio, G.; Varasi, M.; Mercurio, C.; Hamel, E.; Lavia, P.; Novellino, E.; Silvestri, R. Design and Synthesis of 2-Heterocyclyl-3-arylthio-1H-indoles as Potent Tubulin Polymerization and Cell Growth Inhibitors with Improved Metabolic Stability. J. Med. Chem. 2011, 54, 8394-8406.

Rini, B. I. Vascular Endothelial Growth Factor-targeted Therapy in Renal Cell Carcinoma: Current Status and Future Directions. Clin. Cancer Res. 2007, 13, 1098-1106.

Romagnoli, R.; Baraldi, P. G.; Sarkar, T.; Carrion, M. D.; Cara, C. L.; Cruz-Lopez, O.; Preti, D.; Tabrizi, M. A.; Tolomeo, M.; Grimaudo, S.; Cristina, A. D.; Zonta, N.; Balzarini, J.; Brancale, A.; Hsieh, H.-P.; Hamel, E. Synthesis and Biological Evaluation of 1-Methyl-2-(3',4',5'-trimethoxybenzoyl)-3-aminoindoles as a New Class of Antimitotic Agents and Tubulin Inhibitors. J. Med. Chem. 2008, 51, 1464–1468.

Roughley, S. D.; Jordan, A. M. The Medicinal Chemist's Toolbox: An Analysis of Reactions Used in the Pursuit of Drug Candidates. J. Med. Chem. 2011, 54, 3451-3479.

Rustin, G. J.; Galbraith, S. M.; Anderson, H.; Stratford, M.; Folkes, L. K.; Sena, L.; Gumbrell, L.; Price, P. M. Phase I Clinical Trial of Weekly Combretastatin A-4 Phosphate: Clinical and Pharmacokinetic Results. J. Clin. Oncol. 2003, 21(15), 2815-2822.

Sandler, A.; Gray, R.; Perry, M. C.; Brahmer, J.; Schiller, J. H.; Dowiati, A.; Lilenbaum, R.; Johnson, D. H. Paclitaxel-carboplatin Alone or with Bevacizumab for Non-small-cell Lung Cancer. N. Engl. J. Med. 2006, 355(24), 2542-2550.

Shinde, S. S.; Hay, M. P.; Patterson, A. V.; Denny, W. A.; Anderson, R. F. Spin trapping of radicals other than the *OH radical upon reduction of the anticancer agent tirapazamine by cytochrome P450 reductase. J. Am. Chem. Soc. 2009, 131, 14220–14221.

Siemann, D. W. in Vascular-Targeted Therapies in Oncology, ed. Siemann, D. John Wiley & Sons, London, UK, 2006, ch. 1, 1-8.

Siemann, D. W. The Unique Characteristics of Tumor Vasculature and Preclinical Evidence for its Selective Disruption by Tumor-Vascular Disrupting Agents. Cancer Treatment Reviews. 2011, 37, 63-74.

Siemann, D. W.; Bibby, M. C.; Dark, G. G.; Dicker, A. P.; Eskens, F. A. L. M.; Horsman, M. R.; Marme, D.; LoRusso, P. M. Differentiation and Definition of Vascular-Targeting Therapies. Clin. Cancer Res. 2005, 11, 416-420.

Siemann, D. W.; Warrington, K. H.; Horsman, M. R. Targeting Tumor Blood Vessels: An Adjuvant Strategy for Radiation Therapy. Radiother. Oncol. 2000, 57, 5-12.

Siles, R.; Ackley, J. F.; Hadimani, M. B.; Hall, J. J.; Mugabe, B. E.; Guddneppanavar, R.; Monk, K. A.; Chapuis, J.; Pettit, G. R.; Chaplin, D. J.; Edvardsen, K.; Trawick, M. L.; Garner, C. M.; Pinney, K. G. Combretastatin Dinitrogen-substituted Stilbene Analogues as Tubulin-binding and Vascular-disrupting Agents. J. Nat. Prod. 2008, 71, 313-320.

Sriram, M.; Hall, J. J.; Grohmann, N. C.; Strecker, T. E.; Wootton, T.; Franken, A.; Trawick, M. L.; Pinney, K. G. Design, Synthesis, and Biological Evaluation of Dihydronaphthalene and Benzosuberene Analogs of Combretastatins as Inhibitors of Tubulin Polymerization in Cancer Chemotherapy. Bioorg. Med. Chem. 2008, 16(17), 8161-8171.

Stanton, R. A.; Gernert, K. M.; Nettles, J. H.; Aneja, R. Drugs that Target Dynamic Microtubules: A New Molecular Perspective. Med. Res. Rev. 2011, 31(3), 443-481.

Tanpure, R. P.; Harkrider, A. R.; Strecker, T. E.; Hamel, E.; Trawick, M. L.; Pinney, K. G. Application of the McMurry Coupling Reaction in the Synthesis of Tri- and Tetra-arylethylene Analogues as Potential Cancer Chemotherapeutic Agents. Bioorg. Med. Chem. 2009, 17, 6993-7001.

Tapure, R. P.; George, C. S.; Sriram, M.; Strecker, T.; Tidmore, J. K.; Hamel, E.; Charlton-Sevcik, A. K.; Chaplin, D. J.; Trawick, M. L.; Pinney, K. G.; Med. Chem. Comm. 2012, 3, 720-724.

Thompson, P.; Naylor, M. A.; Everett, S. A.; Stratford, M. R. L.; Lewis, G.; Hill, S.; Patel, K. B.; Wardman, P.; Davis, P. D. Synthesis and Biological Properties of Bioreductively Targeted Nitrothienyl Prodrugs of Combretastatin A-4. Mol. Cancer Ther. 2006, 5(11), 2886-2894.

Tong, R. T.; Boucher, Y.; Kozin, S. V.; Winkler, F.; Hicklin, D. J.; Jain, R. K. Vascular Normalization by Vascular Endothelial Growth Factor Receptor 2 Blockade Induces a Pressure Gradient Across the Vasculature and Improves Drug Penetration in Tumors. Cancer Res. 2004, 64, 3731-3736.

Tozer, G. M.; Kanthou, C.; Baguley, B. C. Disrupting Tumour Blood Vessels. Nat. Rev. Cancer 2005, 5, 423-435.

Ty, N.; Dupeyre, G.; Chabot, G. G.; Seguin, J.; Tillequin, F.; Scherman, D.; Michel, S.; Cachet, X. Synthesis and Biological Evaluation of New Disubstituted Analogues of 6-Methoxy-3-(3,4,5-trimethoxybenzoyl)-1H-indole (BPR0L075), as Potential Antivascular Agents. Bioorg. Med. Chem. 2008, 16, 7494–7503.

Ty, N.; Dupeyre, G.; Chabot, G. G.; Seguin, J.; Tillequin, F.; Scherman, D.; Michel, S.; Cachet, X. Bioorg. Med. Chem. 2008, 16(15), 7494-7503.

Valiron, O.; Caudron, N.; Job, D. *Cell. Mol. Life Sci.* **2001**, *58*, 2069–2084.

Vara, Y.; Aldaba, E.; Arrieta, A.; Pizarro, J. L.; Arriortua, M. I.; Cossio, F. P. Regiochemistry of the Microwave-assisted Reaction Between Aromatic Amines and a-Bromoketones to Yield Substituted 1H-indoles. Org. Biomol. Chem. 2008, 6, 1763-1772.

Vaupel, P.; Fortmeyer, H. P.; Runkel, S.; Kallinowski, F. Blood Flow, Oxygen Consumption, and Tissue Oxygenation of Human Breast Cancer Xenografts in Nude Rats. Cancer Res. 1987, 47, 3496-3503.

Vaupel, P.; Hockel, M. Blood Supply, Oxygenation Status and Metabolic Mircomilieu of Breast Cancers: Characterization and Therapeutic Relevance. Int. J. Oncol. 2000, 17, 869-879.

Vaupel, P.; Schlenger, K.; Knoop, C.; Hockel, M. Oxygenation of Human Tumors: Evaluation of Tissue Oxygen Distribution in Breast Cancers by Computerized O2 Tension Measurements. Cancer Res. 1991, 51(12), 3316-3322.

Verdier-Pinard, P.; Lai, J. Y.; Yoo, H. D.; Yu, J.; Marquez, B.; Nagle, D. G.; Nambu, M.; White, J. D.; Falck, J. R.; Gerwick, W. H.; Day, B. W.; Hamel, E. Structure-activity Analysis of the Interaction of Curacin A, The Potent Colchicine Site Antimitotic Agent, with Tubulin and Effects of Analogs on the Growth of MCF-7 Breast Cancer Cells. Mol. Pharmacol. 1998, 53, 62-76.

Vichai, V.; Kirtikara, K. Sulforhodamine B Colorimetric Assay for Cytotoxicity Screening. Nat. Protocols 2006, 1, 1112-1116.

Vogelstein, B.; Kinzler, K. W.; Cancer Genes and the Pathways They Control. Nat. Med. 2004, 10, 789-799.

von Angerer, E.; Prekajac, J.; Strohmeier, J. 2-Phenylindoles. Relationship between Structure, Estrogen Receptor Affinity, and Mammary Tumor Inhibiting Activity in the Rat. J. Med. Chem. 1984, 27, 1439-1447.

Wade, R. H. *Mol. Biotechnol.* **2009**, *43*, 177–191.

Walker, R. A.; O'Brien, E. T.; Pryer, N. K.; Soboeiro, M. F.; Voter, W. A.; Erickson, H. P.; Salmon, E. D. Dynamic Instability of Individual Microtubules Analyzed by Video Light Microscopy: Rate Constants and Transition Frequencies. J. Cell Biol. 1988, 107, 1437-1448.

Weisenberg, R. C.; Borisy, G. G.; Taylor, W. *Biochemistry* **1968**, *7*, 4466-4477.

Wilson, W. P.; Hay, M. P. Targeting Hypoxia in Cancer Therapy. Nature Reviews. 2011, 11, 393-410.

Wu, J. M.; Staton, C. A. Anti-angiogenic Drug Discovery: Lessons From the Past and Thoughts for the Furture. Expert Opin. Drug Discov. 2012, 7(8), 723-743.

Yang, J. C.; Haworth, L.; Sherry, R. M.; Hwu, P.; Schwartzentruber, D. J.; Topalian, S. L.; Steinberg, S. M.; Chen, H. X.; Rosenberg, S. A. A Randomized Trial of Bevacizumab, An Anti-vascular Endothelial Growth Factor Antibody, for Metastatic Renal Cancer. N. Engl. J. Med. 2003, 349(5), 427-434.

Zhao, D.-G.; Chen, J. J.; Du, Y.-R.; Ma, Y.-Y.; Chen, Y.-X.; Gao, K.; Hu, B.-R. Synthesis and Structure-Activity Relationships of N-Methyl-5,6,7-trimethoxyindoles as Novel Antimitotic and Vascular Disrupting Agents. J. Med. Chem. 2013, 56, 1467-1477.